

THE 67TH INTERNATIONAL



OPEN READINGS

CONFERENCE FOR STUDENTS OF PHYSICS AND NATURAL SCIENCES

**BOOK OF
ABSTRACTS**

2024



Vilnius
University

VILNIUS UNIVERSITY PRESS

Editors:

Martynas Keršys
Rimantas Naina
Vincentas Adomaitis
Emilijus Maskvytis

Cover and Interior Design:

Goda Grybauskaitė

Vilnius University Press
9 Saulėtekio Av., III Building, LT-10222 Vilnius
info@leidykla.vu.lt, www.leidykla.vu.lt/en/
www.knygynas.vu.lt, www.journals.vu.lt

Bibliographic information is available
on the Lithuanian Integral Library Information System (LIBIS) portal www.ibiblioteka.lt
ISBN 978-609-07-1051-7 (PDF)

© Vilnius University, 2024

Dear Participant,

Welcome to the 67th International Conference for Students of Physics and Natural Sciences 'Open Readings 2024'!

The 'Open Readings 2024' organizing committee is proud to welcome not only students, but also accomplished scientists worldwide, creating an exceptional platform for you to grow as a researcher by sharing your work, exchanging ideas and connecting with fellow scientists.

Offering an exciting programme of world-renowned scientist lectures spanning a wide array of topics and presentations by enthusiastic young researchers like yourselves, the conference promises an enriching memorable experience. We encourage you to approach this opportunity with curiosity and creativity and this way contribute to fostering collaboration in pushing the boundaries of knowledge, leading the world towards a brighter future.

We wish you the best of luck in your scientific journey! May 'Open Readings 2024' inspire you to maintain curiosity and innovation all throughout your life and scientific career.

Sincerely,

The Open Readings Organizing Committee



Conference Chair:

Šarūnas Mickus, *Faculty of Physics, Vilnius University, SPIE Chapter of Vilnius University, OPTICA Chapter of Vilnius University*

Organizing Committee:

Domantas Klumbys, *Faculty of Physics, Vilnius University, OPTICA Chapter of Vilnius University*

Lukas Naimovičius, *Department of Chemistry and Biochemistry, University of California San Diego*

Erikas Atkočaitis, *Faculty of Physics, Vilnius University, SPIE Chapter of Vilnius University, OPTICA Chapter of Vilnius University*

Goda Mažeikaitė, *Faculty of Physics, Vilnius University*

Goda Grybauskaitė, *Faculty of Physics, Vilnius University*

Eimantas Urniežius, *Faculty of Physics, Vilnius University*

Martynas Keršys, *Faculty of Physics, Vilnius University*

Giedrius Puidokas, *Faculty of Physics, Vilnius University*

Povilas Užtupys, *Faculty of Physics, Vilnius University*

Džiugas Krencius, *Faculty of Physics, Vilnius University*

Aidas Mikalauskas, *Faculty of Physics, Vilnius University*

Patricija Strumilaitė, *Faculty of Physics, Vilnius University*

Laura Grizickaitė, *Faculty of Philology, Vilnius University*

Deimantė Vაžinskytė, *Faculty of Communication, Vilnius University*

Justas Norkus, *Faculty of Physics, Vilnius University*

Ignas Dailidėnas, *Faculty of Physics, Vilnius University*

Kristupas Bagdonas, *Faculty of Physics, Vilnius University*

Teresė Kreišmontaitė, *Faculty of Physics, Vilnius University*

Mykolas Vaitilas, *Faculty of Physics, Vilnius University*

Viktorija Milko, *Faculty of Philology, Vilnius University*

Mykolas Žemaitis, *Faculty of Physics, Vilnius University*

Vincentas Adomaitis, *Faculty of Physics, Vilnius University*

Rimantas Naina, *Faculty of Physics, Vilnius University, SPIE Chapter of Vilnius University*

Emilijus Maskvytis, *Faculty of Physics, Vilnius University*

Deividas Rūškys, *Faculty of Physics, Vilnius University*

Justas Lebedevas, *Faculty of Physics, Vilnius University*

Programme Committee:

Dr. Agnė Kalnaitytė-Vengeliėnė, *Laser Research Center, Faculty of Physics, Vilnius University*

Dr. Aidas Matijošius, *Faculty of Physics, Vilnius University*

Dr. Aldona Balčiūnaitė, *Department of Optoelectronics, Center for Physical Sciences and Technology*

Dr. Algirdas Mikalkėnas, *Institute of Biosciences, Life Sciences Centre, Vilnius University*

Dr. Andrius Gelžinis, *Institute of Chemical Physics, Faculty of Physics, Vilnius University*

Dr. Andrius Źemaitis, *Department of Laser Technologies, Center for Physical Sciences and Technology*

Dr. Brigita Abakevičienė, *Institute of Materials Science, Faculty of Mathematics and Natural Sciences, Kaunas University of Technology*

Dr. Dalia Kaškelytė, *Laser Research Center, Faculty of Physics, Vilnius University*

Dr. Danielis Rutkauskas, *Department of Molecular Compound Physics, Center for Physical Sciences and Technology*

Dr. Darius Gailevičius, *Laser Research Center, Faculty of Physics, Vilnius University*

Dr. Dovydas Banevičius, *Institute of Photonics and Nanotechnology, Faculty of Physics, Vilnius University*

Dr. Edvinas Orentas, *Department of Organic Chemistry, Faculty of Chemistry and Geosciences, Vilnius University*

Dr. Edvinas Radiunas, *Institute of Photonics and Nanotechnology, Faculty of Physics, Vilnius University*

Enrika Celitan, *Department of Biochemistry and Molecular Biology, Life Sciences Center, Vilnius University*

Dr. Gintaras Valušis, *Department of Optoelectronics, Center for Physical Sciences and Technology*

Dr. Ieva Matulaitienė, *Department of Organic Chemistry, Center for Physical Sciences and Technology*

Dr. Ieva Uogintė, *Department of Environmental Research, SRI Center for Physical Sciences and Technology*

Dr. Ilja Ignatjev, *Department of Organic Chemistry, Center for Physical Sciences and Technology*

Dr. Irena Nedveckytė, *Institute of Biosciences, Life Sciences Centre, Vilnius University*

Dr. Julius Vengelis, *Laser Research Center, Faculty of Physics, Vilnius University*

Dr. Jurga Būdienė, *Department of Organic Chemistry, Center for Physical Sciences and Technology*

Dr. Jurga Juodkazytė, *Department of Chemical Engineering and Technology, Center for Physical Sciences and Technology*

Dr. Justinas Čėponkus, *Institute of Chemical Physics, Faculty of Physics, Vilnius University*

Dr. Kristijonas Genevičius, *Department of Solid State Electronics, Vilnius University*

Dr. Laimonas Deveikis, *Institute of Photonics and Nanotechnology, Faculty of Physics, Vilnius University*

Dr. Linas Vilčiauskas, *Department of Chemical Engineering and Technology, Center for Physical Sciences and Technology*

Dr. Mažėna Mackoit-Sinkevičienė, *Institute of Theoretical Physics and Astronomy, Vilnius University*

Dr. Mindaugas Kamarauskas, *Institute of Chemical Physics, Faculty of Physics, Vilnius University*

Dr. Nina Urbelienė, *Institute of Biochemistry, Life Sciences Center, Vilnius University*

Dr. Paulius Baronas, *Department of Superconducting Materials and Nanostructure at Large Scale, Institute of Materials Science of Barcelona*

Dr. Renata Butkutė, *Optoelectronics Department, Center for Physical Sciences and Technology*

Dr. Sergėjus Balčiūnas, *Institute of Applied Electrodynamics and Telecommunications, Faculty of Physics, Vilnius University*

Dr. Steponas Raišys, *Institute of Photonics and Nanotechnology, Faculty of Physics, Vilnius University*

Dr. Tadas Malinauskas, *Institute of Photonics and Nanotechnology, Faculty of Physics, Vilnius University*

Dr. Tomas Čeponis, *Institute of Photonics and Nanotechnology, Faculty of Physics, Vilnius University*

Dr. Tomas Serevičius, *Institute of Photonics and Nanotechnology, Faculty of Physics, Vilnius University*

Dr. Tomas Šalkus, *Institute of Applied Electrodynamics and Telecommunications, Faculty of Physics, Vilnius University*

Dr. Tomas Tamulevičius, *Institute of Materials Science, Faculty of Mathematics and Natural Sciences, Kaunas University of Technology*

Dr. Virginija Kalcienė, *Institute of Biosciences, Life Sciences Centre, Vilnius University*

Dr. Vytautas Jakštas, *Department of Physical Technologies, Center for Physical Sciences and Technology*

Dr. Vytautas Klimavičius, *Institute of Chemical Physics, Faculty of Physics, Vilnius University*

Chairmen:

Dr. Agnė Kalnaitytė-Vengeliene, *Laser Research Center, Faculty of Physics, Vilnius University*

Dr. Aistė Zentelytė, *Department of Molecular Cell Biology, Institute of Biochemistry, Life Sciences Center, Vilnius University*

Dr. Aldona Balčiūnaitė, *Department of Catalysis, Center for Physical Sciences and Technology*

Aliona Klimovich, *Department of Organic Chemistry, Center for Physical Sciences and Technology*

Dr. Anton Popov, *Institute of Chemistry, Faculty of Chemistry and Geosciences, Vilnius University*

Dr. Balys Momgaudis, *Laser Research Center, Faculty of Physics, Vilnius University*

Dr. Darius Abramavičius, *Institute of Chemical Physics, Faculty of Physics, Vilnius University*

Dr. Darius Šulskis, *Institute of Biotechnology, Life Sciences Center, Vilnius University*

Dr. Darius Gailevičius, *Laser Research Center, Faculty of Physics, Vilnius University*

Dr. Dovydas Banevičius, *Institute of Photonics and Nanotechnology, Faculty of Physics, Vilnius University*

Dr. Edvinas Orentas, *Department of Organic Chemistry, Faculty of Chemistry and Geosciences, Vilnius University*

Dr. Gytis Šliaužys, *Institute of Chemical Physics, Faculty of Physics, Vilnius University*

Dr. Gražina Petraitytė, *Department of Organic Chemistry, Faculty of Chemistry and Geosciences, Vilnius University*

Dr. Ieva Žutautė, *Department of Organic Chemistry, Faculty of Chemistry and Geosciences, Vilnius University*

Ignas Lukošius, *Laser Research Center, Faculty of Physics, Vilnius University*

Dr. Julija Armalytė, *Department of Biochemistry and Molecular Biology, Institute of Biosciences, Life Science Centre, Vilnius University*

Dr. Julius Vengelis, *Laser Research Center, Faculty of Physics, Vilnius University*

Dr. Jurga Būdienė, *Department of Organic Chemistry, Center for Physical Sciences and Technology*

Dr. Karolis Kazlauskas, *Institute of Photonics and Nanotechnology, Faculty of Physics, Vilnius University*

University

Dr. Kastytis Zubovas, *Institute of Theoretical Physics and Astronomy, Vilnius University*

Dr. Laurita Klimkaitė, *Institute of Biosciences, Life Sciences Centre, Vilnius University*

Dr. Lina Aitmanaitė, *LSC-EMBL Institute for Genome Editing Technologies, Vilnius University*

Lukas Naimovičius, *Department of Chemistry and Biochemistry, University of California, San Diego*

Martynas Malikėnas, *Department of Organic Chemistry, Center for Physical Sciences and Technology*

Dr. Mažena Mackoit-Sinkevičienė, *Institute of Theoretical Physics and Astronomy, Vilnius University*

Dr. Mikas Vengris, *Laser Research Center, Faculty of Physics, Vilnius University*

Dr. Mindaugas Šarpis, *Institute of Photonics and Nanotechnology, Faculty of Physics, Vilnius University/University of Manchester*

Dr. Nina Urbelienė, *Institute of Biochemistry, Life Sciences Center, Vilnius University*

Dr. Rimantė Bandzevičiūtė, *Institute of Chemical Physics, Faculty of Physics, Vilnius University*

Dr. Rytis Butkus, *Laser Research Center, Faculty of Physics, Vilnius University*

Dr. Rūta Kananavičiūtė, *Department of Microbiology and Biotechnology, Life Sciences Centre, Vilnius University*

Dr. Steponas Raišys, *Institute of Photonics and Nanotechnology, Faculty of Physics, Vilnius University*

Dr. Tadas Malinauskas, *Institute of Photonics and Nanotechnology, Faculty of Physics, Vilnius University*

Dr. Tatjana Kirteklienė, *Department of Microbiology and Biotechnology, Institute of Biosciences, Life Sciences Center, Vilnius University*

Dr. Tomas Šalkus, *Institute of Applied Electrodynamics and Telecommunications, Faculty of Physics, Vilnius University*

Tomas Paškevičius, *Department of Organic Chemistry, Center for Physical Sciences and Technology*

Dr. Tomas Čeponis, *Institute of Photonics and Nanotechnology, Faculty of Physics, Vilnius University*

Dr. Viktorija Glembockytė, *Department of Chemistry, Ludwig Maximilian University of Munich*

Dr. Vytautas Klimavičius, *Institute of Chemical Physics, Faculty of Physics, Vilnius University*

Dr. Vytautas Jukna, *Laser Research Center, Faculty of Physics, Vilnius University*

Vladislovas Čižas, *Department of Optoelectronics, Center for Physical Sciences and Technology*

Karolis Neimontas, *Light Conversion*

Linas Giniūnas, *Light Conversion*

Tomas Žukauskas, *BROLIS*

OPEN READINGS 2024

CONFERENCE FOR STUDENTS OF PHYSICS AND NATURAL SCIENCES



CONFERENCE PROGRAMME DAY 1 (2024-04-23)

Room: A101	Opening Ceremony		9:00-9:15
Room: A101	 Ursula Keller PLENARY TALK Chair: Rytis Butkus	25 Years After the Frequency Comb Revolution: Transforming Industries with Dual-Comb Lasers	9:15-10:15
Room: A101	LIGHT CONVERSION		10:15-10:30
Break			10:30-11:00
Room: A101	ORAL SESSION: O1 Laser Physics and Optical Technologies 11:00 Edvinas Aleksandravičius: SUPPRESSION OF FILAMENTATION BY PHOTONIC CRYSTALS 11:15 Matas Štovas: SPECTRAL BROADENING AND POST-COMPRESSION OF FEMTOSECOND PULSES IN ZnS AND KGW CRYSTALS AT 76 MHz REPETITION RATE 11:30 DIMITRA LADIKA: PHOTSENSITIZED AND NON-PHOTSENSITIZED MATERIALS FOR MULTIPHOTON LITHOGRAPHY 11:45 Eulalia Puig Vilardell: 3D GRADIENT PERIOD PHOTONIC CRYSTALS FABRICATED VIA ULTRAFAST LASER LITHOGRAPHY Session Chair: Vytautas Jukna	Room: D401 ORAL SESSION: O2 Material Science and Modern Technologies 11:00 Aivaras Špokas: GaAsBi BASED NIR EMITTERS FOR BLOOD ANALYTE MONITORING 11:15 Petras Lapukas: THE GROWTH OF GaN(0001) ON Sc2O3(111)/Si(111) TEMPLATE VIA MOVPE METHOD 11:30 Mantas Migauskas: PEAK LUMINESCENCE SHIFT OF InGaN DEFECT VICINITIES USING SEM-CL MICROSCOPY 11:45 Monika Jokubauskaitė: INFLUENCE OF AlGaAs BARRIER DESIGN ON PHOTOLUMINESCENCE OF GaAsBi QUANTUM STRUCTURES Session Chair: Tomas Grinys	11:00-12:00
Lunch			12:00-13:00
Room: A101	ORAL SESSION: O3 Laser Physics and Optical Technologies 13:00 Augustė Bielevičiūtė: COMPARATIVE ANALYSIS OF BEAM FOCUSING ABILITIES OF METASURFACE BASED 250GHZ LENSES 13:15 Austėja Trečiokaite: FULL-FIELD OPTICAL COHERENCE TOMOGRAPHY WITH DIGITAL DEFOCUS CORRECTION 13:30 Florian Dötzer: INVESTIGATING MECHANICAL VIBRATIONS AT THE (SUB-)NANOSCALE - ADVANCES IN DIGITAL HOLOGRAPHIC VIBROMETRY 13:45 Mateusz Kaluza: TERAHERTZ DIFFRACTIVE OPTICAL ELEMENTS REALIZING MIMO SYSTEM Session Chair: Balys Momgaudis	Room: D401 ORAL SESSION: O4 Laser Physics and Optical Technologies 13:00 Kipras Čepaitis: FS - LASER ABLATION AND MODIFICATION OF THIN METAL FOR PERIODIC PLASMONIC ARRAYS 13:15 Augustė Černekytė: HIGH-EFFICIENCY MID-IR OPCPA WITH 2.5 mJ 25 fs OUTPUT PULSES 13:30 Julianija Nikitina: INVESTIGATION OF PERIODICALLY STRUCTURED THIN FILMS POLARIZERS 13:45 Martynas Keršys: REFINING LIDT EVALUATION THROUGH MONTE CARLO SIMULATIONS: A PATH TO ISO EXCELLENCE Session Chair: Ignas Lukošiusnas	13:00-14:00
Break			14:00-14:30
Room: A101	EKSPLA		14:30-14:45
Room: A101	 Jens Biegert PLENARY TALK Chair: Mikas Vengris	Attosecond Quantum Dynamics	14:45-15:45
Break			15:45-16:15
Main hall	POSTER SESSION: P1 Laser Physics and Optical Technologies; Spectroscopy and Imaging; Material Science and Modern Technologies; Theoretical Physics and Astrophysics	16:15-18:00	
Room: A101	PANEL DISCUSSION Career Crossroads: Academia or Industry Participants: prof. Ursula Keller, dr. Simona Liukaitytė-Suszczynska, dr. Lina Grinevičiūtė, Eulalia Puig Vilardell Discussion Chair: Arnoldas Solovjovas	16:30-18:15	

OPEN READINGS 2024



CONFERENCE FOR STUDENTS OF PHYSICS AND NATURAL SCIENCES

CONFERENCE PROGRAMME DAY 2 (2024-04-24)

Room: A101 Chair: Jonas Žmuidzinas	 Charles Elachi PLENARY TALK	Space: Exploration and Utilization	9:00-10:00
Room: A101	VISORIAI TECHNOLOGY PARK (VITP)		10:00-10:15
Break			10:15-10:45
Room: A101 ORAL SESSION: O5 Astrophysics and Theoretical Physics 10:45 Karolis Daugevičius: THE LIMITS OF STAR CLUSTER APERTURE PHOTOMETRY IN THE LOCAL UNIVERSE 11:00 Eimantas Kriščiūnas: STAR CLUSTERS AND SPIRAL ARMS OF THE M31 GALAXY 11:15 Wojciech Marciniak: LAMMPS AS A LIBRARY FOR THE THEORETICAL STUDY OF THE ROLE OF PHONONS IN ULTRAFAST DEMAGNETIZATION 11:30 Kotryna Šiškauskaitė: THEORETICAL INVESTIGATION OF ENERGY LEVELS FOR BA VI 11:45 Barkha Yakub Bale: THE STUDY OF THE ATMOSPHERES AND MIXING PROCESSES OF MAGNETICALLY ACTIVE RS CVN GIANTS Session Chair: Kastytis Zubovas	Room: D401 ORAL SESSION: O6 Spectroscopy and Imaging 10:45 Gediminas Usevičius: EPR SPECTROSCOPY OF STRUCTURAL PHASE TRANSITION IN CH ₃ NH ₃ PbCl ₃ HYBRID PEROVSKITE 11:00 Kamilė Tulaitė: PHOTOPHYSICAL STUDY OF PURINE BASED METAL ION SENSORS 11:15 Jonas Haist: CMOS CAMERA SENSOR FOR DETECTION AND IMAGING OF PARTICLES OF IONIZING RADIATION 11:30 Artūras Polita: FLUORESCENT VISCOSITY PROBES AS DIAGNOSTIC TOOLS FOR CANCER DETECTION 11:45 Rokas Lemežis: SOLID STATE NMR STUDY OF HYBRID CALCIUM PHOSPHATES Session Chair: Vytautas Klimavičius		10:45-12:15 10:45-12:00
Lunch			12:15-13:00
Room: A101 ORAL SESSION: O7 Astrophysics and Theoretical Physics 13:00 Joanna Marciniak: BEYOND RARE EARTH: INVESTIGATING FECO ALLOYS UNDER STRAIN FOR PERMANENT MAGNETS 13:15 Nikolajus Elkana Eimutis: INVESTIGATION OF Z ₀ BOSON USING CERN LHCb OPEN DATA 13:30 Nojus Danyla: NIELSEN IDENTITIES IN THE STANDARD MODEL 13:45 Aneta Bień: EXTRACTING DIFFRACTIVE PROTONS AND BACKGROUND ANALYSIS FROM ATLAS FORWARD PROTON DETECTORS 14:00 Lukas Stakela: NORMAL MODES OF SOLID-STATE PLASMA IN CONDITIONS OF BLOCH GAIN Session Chair: Mažena Mackoit-Sinkevičienė	Room: D401 ORAL SESSION: O8 Material Science and Modern Technologies 13:00 Krzysztof Gadomski: TOWARDS HIGHLY CONDUCTIVE NANOCRYSTALLISED VANADATE-PHOSPHATE GLASSES 13:15 Lukas Šiaulyš: CARRIER DYNAMICS IN Ga-POLAR AND N-POLAR InGaN QUANTUM WELL STRUCTURES 13:30 Adam Puchalski: THERMAL CONDUCTIVITY AND STRUCTURAL CHANGES IN ULTRA-HIGH PRESSURE TREATED SILICA GLASS – A MOLECULAR DYNAMICS STUDY 13:45 Maria Skrodzka: PRINTABILITY OF MUCOADHESIVE SODIUM ALGINATE/CHITOSAN GELS DELIVERING PHOTOSENSITIZER IN PHOTODYNAMIC THERAPY 14:00 Elena Mirabela Soare: A MECHANOCHEMICAL PROCESS FOR IMPROVING RESVERATROL PROPERTIES BY CO-CRYSTALLIZATION Session Chair: Tadas Malinauskas	Room: B336 WORKSHOP Bridging Science and Business in Lithuania: Founder Perspectives on Company Creation Dr. Linas Jonušausas, Vital 3D Technologies Dr. Simonas Kičas, OPTOMAN Only 20 spots available. Ask at the registration desk.	13:00-14:15 13:00-14:15 13:00-14:45
Room: A101 Chair: Mindaugas Šarpis	 Chris Parkes PLENARY TALK	Antimatter Matters: the Large Hadron Collider Beauty Experiment at CERN	14:45-15:45
Room: A101	LITHUANIAN CONSORTIUM FOR PARTICLE PHYSICS		15:45-16:00
Break			16:00-16:15
Room: A101	SPECIAL EVENT Green Chemistry: Towards Sustainable Future Participants: dr. Makeda Tekle-Smith, dr. Andrew B. Pun, Pamela Rivera Event Chair: Lukas Naimovičius		16:15-18:00

OPEN READINGS 2024

CONFERENCE FOR STUDENTS OF PHYSICS AND NATURAL SCIENCES



CONFERENCE PROGRAMME DAY 3 (2024-04-25)

Room: A101 Chair: Ieva Žutautė	 Makeda Tekle-Smith PLENARY TALK	Feedstock Alkynes as a Platform for Multi-functionalisation via Radical Cascade Reactions	9:00-10:00
Break			10:00-10:30
Room: A101 Chair: Aldona Balčiūnaitė	ORAL SESSION: O9 Chemistry and Chemical Physics	10:30-11:45	
<p>10:30 Pijus Domantas Valentukevičius: SOLVENT-FREE MECHANOCHEMICAL SYNTHESIS OF CSPBBR3 QUANTUM DOTS WITH SURFACE-PASSIVATING LIGANDS</p> <p>10:45 Vilius Petraška: SYNTHESIS OF 3-(24-DIHYDROXY-5-BENZYL)ALKYL CARBOXYLIC ACIDS AND THEIR DERIVATIVES</p> <p>11:00 Karolis Sarka: CALCULATION OF HIGH-RESOLUTION UV SPECTRA OF DIATOMIC MOLECULES</p> <p>11:15 Andrius Merkys: DETECTING ATOMIC INTERACTIONS IN SMALL-MOLECULE CRYSTAL STRUCTURES</p> <p>11:30 Guoda Pranaitytė: SYNTHESIS OF 1-(2,4-DIFLUORPHENYL)-5-OXOPYRROLIDINE-3-CARBOXYLIC ACID DERIVATIVES AND INVESTIGATION OF THEIR ANTICANCER ACTIVITY</p>			
Room: D401 Chair: Dovydas Banevičius	ORAL SESSION: O10 Nanomaterials and Nanotechnology	10:30-11:45	
<p>10:30 Kernius Vilkevičius: FS-LASER MICROPROCESSING FOR SERS SUBSTRATES OF PERIODIC METALLIC STRUCTURES</p> <p>10:45 Vita Petrikaitė: KCL CONCENTRATION EFFECTS ON THE FORMATION, STABILITY, AND SERS SIGNAL STRENGTH OF LASER-GENERATED GOLD, SILVER, AND HYBRID NANOPARTICLES</p> <p>11:00 Daniel Doveiko: IMPACT OF THE CRYSTAL STRUCTURE OF SILICA NANOPARTICLES ON RHODAMINE 6G ADSORPTION</p> <p>11:15 Ilya Navitski: MXENE-BASED ELECTROCHEMICAL SENSOR FOR PRECISE AND SELECTIVE DETECTION OF LEAD IONS IN AQUEOUS SOLUTIONS</p> <p>11:30 Gintarė Rimkutė: INVESTIGATION OF GRAPHENE/POLYPYRROLE COMPOSITES AND THEIR APPLICATION IN ELECTROCHEMICAL DOPAMINE SENSORS</p>			
Lunch			11:45-12:45
Room: A101 Chair: Steponas Raišys	ORAL SESSION: O11 Chemistry and Chemical Physics	12:45-14:00	
<p>12:45 Cindy Close: DOCKING SITE-MEDIATED PHOTOSTABILIZATION FOR SINGLE-MOLECULE AND SUPER-RESOLUTION IMAGING</p> <p>13:00 Maximilian Aspect: GREEN TO DEEP-UV LIGHT: PUSHING THE ANTI STOKES SHIFT IN PHOTON UPCONVERSION BY BREAKING KASHAS RULE</p> <p>13:15 Jonas Žurauskas: DEVELOPMENT OF A NEW SUPER-OXIDIZING PHOTOCATALYSTS AND THEIR APPLICATIONS IN C-H ACTIVATION REACTIONS VIA IDIOSYNCRATIC MECHANISTIC MODES</p> <p>13:30 Lukas Naimovicius: NEAR-INFRARED SENSITIZED DEEP TISSUE PHOTOACTIVATION OF AZOBENZENE IN BIOMIMETIC CONDITIONS AT LOW PHOTON FLUENCES</p> <p>13:45 Justas Lekavičius: STATISTICAL PROBABILITY OF SINGLET EXCITON GENERATION THROUGH TRIPLET-TRIPLET ANNIHILATION IN TES-ADT ANNIHILATOR</p>			
Room: D401 Chair: Jurga Būdienė	ORAL SESSION: O12 Chemistry and Chemical Physics	12:45-14:00	
<p>12:45 Younes Bourenane Cherif: SYNERGISTIC ENHANCEMENT OF THERMOELECTRIC PERFORMANCE THROUGH ONE DIMENSIONAL HYBRID NANOCOMPOSITES WRAPPED NICKEL OXIDE DECORATED MULTI WALLED CARBON NANOTUBES WITH POLYPYRROLE</p> <p>13:00 Silvija Jučiūtė: STUDY OF SARS-CoV2-S WILD-TYPE SPIKE PROTEIN INTERACTION WITH RANDOMLY AND ORIENTED ANTIBODIES BY QUARTZ CRYSTAL MICROBALANCE</p> <p>13:15 Raminta Bajarunaite: MXENE BASED COLORIMETRIC SENSOR FOR SILVER ION DETECTION IN WATER</p> <p>13:30 Austėja Burbulytė: STUDY OF DIFFERENT PARAMETERS IMPACT TO MICROPLASTIC REMOVAL FROM WATER USING LIGNIN-MAGNETITE NANOSORBENT</p> <p>13:45 Volodymyr Yaremenko: DISSOLUTION ENHANCEMENT OF MEFENAMIC ACID USING SOLID DISPERSIONS OBTAINED BY WET GRANULATION TECHNIQUE</p>			
Break			14:00-14:30
Room: A101 Chair: Karolis Kazlauskas	 Andrew B. Pun PLENARY TALK	New Applications of Upconversion via Exploration of Novel Annihilators	14:30-15:30
Break			15:30-15:45
Main hall	POSTER SESSION: P2 Chemistry and Chemical Physics; Nanomaterials and Nanotechnology		15:45-17:45
SOCIAL EVENING Offsite Location: Artistai Pub, šv. Kazimiero g. 3, Vilnius			19:00-23:30

OPEN READINGS 2024

CONFERENCE FOR STUDENTS OF PHYSICS AND NATURAL SCIENCES



CONFERENCE PROGRAMME DAY 4 (2024-04-26)

Room: A101  Viktorija Glembockytė PLENARY TALK Chair: Edvinas Orentas	Nanoscale Tools for Sensing and Imaging Single Molecules	9:00-10:00
Break		10:00-10:30
Room: D401 ORAL SESSION: O13 10:30-11:45 Biochemistry, Biophysics and Biotechnology 10:30 Julia Niegowska: DEVELOPMENT OF AN INNOVATIVE SCAFFOLD MADE FROM DECELLULARIZED HORSE BONE FOR BONE DEFECTS IN HORSES 10:45 Aida Šermukšnytė: DESIGN AND INVESTIGATION OF 1,2,4-TRIAZOLE-3-YL THIOACETOHYDRAZIDES BEARING GALDIMINE MOIETY AS BIOLOGICALLY ACTIVE AGENTS 11:00 Lukas Volodka: INVESTIGATION OF A NOVEL TRICOMPONENT BACTERIAL ANTIPHAGE DEFENCE SYSTEM 11:15 Vestina Steigvilaitė: IDENTIFICATION OF PHYTIC MICROORGANISMS FROM CRANBERRY AND LINGONBERRY FRUITS BY SURFACE-ENHANCED RAMAN SPECTROSCOPY 11:30 Aivaras Vilutis: TOWARDS A NOVEL MODEL TO STUDY NUCLEAR AGING: BIOPHYSICAL CHARACTERIZATION OF AGE-TUNED MEMBRANES Chair: Aistė Zentelytė	Room: A101 ORAL SESSION: O14 10:30-12:00 Biology, Genetics and Biomedical Sciences 10:30 Justin Stivins: PHARMACOKINETIC EVALUATION OF CEFAZOLIN ANTIMICROBIAL PROPHYLAXIS IN SPINAL SURGERY 10:45 Indrė Krastinaitė: THERAPEUTIC POTENTIAL OF T CELLS FOR PREMATURE OVARIAN INSUFFICIENCY TREATMENT IN MOUSE MODEL 11:00 Agnė Bučaitė: CONSEQUENCES OF LONG TERM EXPOSURE TO MICROPLASTICS AND EFFECTS ON CYTOGENETIC AND ANTIOXIDANT BIOMARKERS IN FISH 11:15 Margarita Kazak: BLOODSUCKING BITING MIDGES - NEGLECTED THREAT FOR WILD BIRDS 11:30 Radvilė Drevinskaitė: ANALYSIS OF VIRULENCE FACTORS IN ISOLATES OF OPPORTUNISTIC PATHOGEN STENOTROPHOMONAS MALTOPHILIA 11:45 Raminta Skipitytė: INVESTIGATION OF THE INTERACTIONS BETWEEN THE SOYBEAN PLANTS AND MICROORGANISMS USING STABLE ISOTOPES Chair: Gytis Dudas	
Lunch		12:00-12:30
Room: D401 ORAL SESSION: O15 12:30-13:30 Biochemistry, Biophysics and Biotechnology 12:30 Paulius Buidovas: CARBON SUPPORTED METAL CATALYST FROM SEAWEED-DERIVED BIO-CHAR PREPARATION AND CHARACTERIZATION VIA CHEMISORPTION 12:45 Agnė Veršulienė: STABLE ISOTOPES AS A TOOL TO TRACK C AND N PATHWAYS IN THE ROOT SYSTEMS 13:00 Joris Dambrauskas: INVESTIGATING THE IMPACT OF ELAVL1 INHIBITION ON PANCREATIC CANCER CELL VIABILITY 13:15 Igor Nagula: INTRINSIC FIRING PROPERTIES OF THE MOUSE HIPPOCAMPAL PYRAMIDAL CA1 NEURONS DURING THE POSTNATAL DEVELOPMENT Chair: Wanessa De Cassia Martins Antunes De Melo	Room: A101 ORAL SESSION: O16 12:30-14:00 Biology, Genetics and Biomedical Sciences 12:30 Paulina Kazlauskaitė: NOTCH SIGNALING PATHWAY COMPONENTS AS POTENTIAL BIOMARKERS FOR THE DIAGNOSIS OF OVARIAN CANCER 12:45 Eglė Žymantaitė: THE ESTABLISHMENT OF THREE NEW OVARIAN CANCER CELL LINES OPENS NEW AVENUE OF RESEARCH INTO TUMOR HETEROGENEITY AND CELL EVOLUTION 13:00 Roberta Pocevičiūtė: DEVELOPMENT OF A DNA OLIGO-CAPTURE METHOD TO STUDY CANCER CELL METASTASIS IN ANIMAL MODELS 13:15 Rugilė Gineikaitė: METHYLATION PROFILING OF HOMEOTIC AND CHROMATIN REMODELING GENES IN CANCEROUS OVARIAN TISSUE 13:30 Mėta Mackevičiūtė: PLANT-DERIVED NANOVESICLES DISPLAY WOUND HEALING PROPERTIES 13:45 Alėja Marija Daugėlaitė: UPCONVERTING NANOCOMPLEX DELIVERY TO DISTINCT PHENOTYPES OF CANCER BY MESENCHYMAL STEM CELLS Chair: Rūta Kananavičiūtė	
Break		14:00-14:15
Main hall	POSTER SESSION: P3 Biochemistry, Biophysics and Biotechnology; Biology, Genetics and Biomedical Sciences	14:15-16:15
Break		16:15-16:30
Room: A101	Closing Ceremony & Awards	16:30-17:00

Contents

Invited Speakers

25 YEARS AFTER THE FREQUENCY COMB REVOLUTION: TRANSFORMING INDUSTRIES WITH DUAL-COMB LASERS	40
Ursula Keller	
ATTOSECOND QUANTUM DYNAMICS	41
Jens Biegert	
SPACE EXPLORATION AND UTILIZATION	42
Charles Elachi	
ANTIMATTER MATTERS: THE LARGE HADRON COLLIDER BEAUTY EXPERIMENT AT CERN	43
Chris Parkes	
FEEDSTOCK ALKYNES AS A PLATFORM FOR MULTI-FUNCTIONALISATION VIA RADICAL CASCADE REACTIONS	44
Makeda Tekle-Smith	
NEW APPLICATIONS OF UPCONVERSION VIA EXPLORATION OF NOVEL ANNIHILATORS	45
Andrew B. Pun	
NANOSCALE TOOLS FOR SENSING AND IMAGING SINGLE MOLECULES	46
Viktorija Glembockytė	

O1: Laser Physics and Optical Technologies

SUPPRESSION OF FILAMENTATION BY PHOTONIC CRYSTALS	47
Edvinas Aleksandravičius, Darius Gailevičius, Audrius Dubietis, Kęstutis Staliūnas	
SPECTRAL BROADENING AND POST-COMPRESSION OF FEMTOSECOND PULSES IN ZnS AND KGW CRYSTALS AT 76 MHz REPETITION RATE	48
Matas Šutovas, Vaida Marčiulionytė, Jonas Banys, Julius Vengelis, Gintaras Tamošauskas, Audrius Dubietis	
PHOTOSENSITIZED AND NON-PHOTOSENSITIZED MATERIALS FOR MULTIPHOTON LITHOGRAPHY	49
Dimitra Ladika, Antanas Butkus, Michalis Stavrou, Gordon Zyla, Vasileia Melissinaki, Edvinas Skliutas, Elmina Kabouraki, Frederic Dumur, David Gray, Saulius Juodkazis, Maria Farsari, Mangirdas Malinauskas	
3D GRADIENT PERIOD PHOTONIC CRYSTALS FABRICATED VIA ULTRAFAST LASER LITHOGRAPHY 50	
Eulàlia Puig Vilardell, Darius Gailevičius, Mangirdas Malinauskas	

O2: Material Science and Modern Technologies

GaAsBi BASED NIR EMITTERS FOR BLOOD ANALYTE MONITORING	51
Aivaras Špokas, Andrea Zelioli, Andrius Bičiūnas, Aurimas Čerškus, Bronislovas Čechavičius, Augustas Vaitkevičius, Evelina Dudutienė, Mindaugas Kamarauskas, Renata Butkutė	

THE GROWTH OF GaN(0001) ON Sc₂O₃(111)/Si(111) TEMPLATE VIA MOVPE METHOD 52
Petras Lapukas, Tomas Grinys, Tadas Malinauskas, Domantas Berenis, Arūnas Kadys

PEAK LUMINESCENCE SHIFT OF InGaN DEFECT VICINITIES USING SEM-CL MICROSCOPY 53
Mantas Migauskas, Viktorija Mickūnaitė, Žydrūnas Podlipskas

INFLUENCE OF AlGaAs BARRIER DESIGN ON PHOTOLUMINESCENCE OF GaAsBi QUANTUM STRUCTURES 54
Monika Jokubauskaitė, Aistė Butkutė, Aivaras Špokas, Andrea Zelioli, Evelina Dudutienė, Bronislovas Čechavičius, Renata Butkutė

O3: Laser Physics and Optical Technologies

COMPARATIVE ANALYSIS OF BEAM FOCUSING ABILITIES OF METASURFACE BASED 250GHZ LENSES 55
Augustė Bielevičiūtė, Karolis Redeckas, Kasparas Stanaitis, Ernestas Nacius, Vladislovas Čižas, Linas Minkevičius

FULL-FIELD OPTICAL COHERENCE TOMOGRAPHY WITH DIGITAL DEFOCUS CORRECTION 56
Austėja Trečiokaitė, Karolis Adomavičius, Egidijus Auksorius

INVESTIGATING MECHANICAL VIBRATIONS AT THE (SUB-)NANOSCALE - ADVANCES IN DIGITAL HOLOGRAPHIC VIBROMETRY 57
Florian Dötzer, Johannes May, Stefan Sinzinger

TERAHERTZ DIFFRACTIVE OPTICAL ELEMENTS REALIZING MIMO SYSTEM 58
Mateusz Kaluza, Paweł Komorowski, Adrianna Nieradka, Mateusz Surma, Przemysław Zagrajek, Agnieszka Siemion

O4: Laser Physics and Optical Technologies

FS - LASER ABLATION AND MODIFICATION OF THIN METAL FOR PERIODIC PLASMONIC ARRAYS 59
Kipras Čepaitis, Kernius Vilkevičius, Evaldas Stankevičius

HIGH-EFFICIENCY MID-IR OPCPA WITH 2.5 mJ 25 fs OUTPUT PULSES 60
Augustė Černeckytė, Augustinas Petrulėnas, Paulius Mackonis, Aleksėj M Rodin

INVESTIGATION OF PERIODICALLY STRUCTURED THIN FILMS POLARIZERS 61
Julianija Nikitina, Rytis Buzelis, Kęstutis Staliūnas, Lina Grinevičiūtė

REFINING LIDT EVALUATION THROUGH MONTE CARLO SIMULATIONS: A PATH TO ISO EXCELLENCE 62
Martynas Keršys, Andrius Melninkaitis

O5: Astrophysics and Theoretical Physics

THE LIMITS OF STAR CLUSTER APERTURE PHOTOMETRY IN THE LOCAL UNIVERSE 63
Karolis Daugevičius, Eimantas Kriščiūnas, Erikas Cicėnas, Rima Stonkutė, Vladas Vansevičius

STAR CLUSTERS AND SPIRAL ARMS OF THE M31 GALAXY	64
Eimantas Kriščiūnas, Karolis Daugevičius, Erikas Cicėnas, Rima Stonkutė, Vladas Vansevičius	
LAMMPS AS A LIBRARY FOR THE THEORETICAL STUDY OF THE ROLE OF PHONONS IN ULTRAFAST DEMAGNETIZATION	65
Wojciech Marciniak, Joanna Marciniak, Jan Ruzs	
THEORETICAL INVESTIGATION OF ENERGY LEVELS FOR BA VI	66
Kotryna Šiškauskaitė, Gediminas Gaigalas, Pavel Rynkun, Laima Kitovienė	
THE STUDY OF THE ATMOSPHERES AND MIXING PROCESSES OF MAGNETICALLY ACTIVE RED DWARF STARS	67
Barkha Bale, Grazina Tautvaisiene, Renata Minkeviciute, Arnas Drazdauskas, Edita Stonkute, Sarunas Mikolaitis	
DEEP LEARNING FOR STAR CLUSTER DETECTION IN GALAXIES	68
Erikas Cicėnas, Karolis Daugevičius, Eimantas Kriščiūnas, Rima Stonkutė, Vladas Vansevičius	
O6: Spectroscopy and Imaging	
EPR SPECTROSCOPY OF STRUCTURAL PHASE TRANSITION IN CH₃NH₃PbCl₃ HYBRID PEROVSKITE	69
Gediminas Usevičius, Michael A Hope, Justinas Turčak, Jūras Banys, Mantas Šimėnas	
PHOTOPHYSICAL STUDY OF PURINE BASED METAL ION SENSORS	70
Kamile Tulaite, Justina Jovaisaite, Irina Novosjolova, Maris Turks, Gediminas Jonusauskas, Saulius Jursenas	
CMOS CAMERA SENSOR FOR DETECTION AND IMAGING OF PARTICLES OF IONIZING RADIATION	71
Jonas Jeffrey Haist, Anton Koroliov, Artūras Plukis	
FLUORESCENT VISCOSITY PROBES AS DIAGNOSTIC TOOLS FOR CANCER DETECTION	72
Artūras Polita	
SOLID STATE NMR STUDY OF HYBRID CALCIUM PHOSPHATES	73
Rokas Lemežis, Vytautas Klimavičius	
O7: Astrophysics and Theoretical Physics	
BEYOND RARE EARTH: INVESTIGATING FECO ALLOYS UNDER STRAIN FOR PERMANENT MAGNETS	74
Wojciech Marciniak, Joanna Marciniak, José Ángel Castellanos-Reyes, Mirosław Werwiński	
INVESTIGATION OF Z⁰ BOSON USING CERN LHCb OPEN DATA	75
Nikolajus Elkana Eimutis, Marijus Ambrozas, Mindaugas Šarpis	
NIELSEN IDENTITIES IN THE STANDARD MODEL	76
Nojus Danyla, Simonas Draukšas	
EXTRACTING DIFFRACTIVE PROTONS AND BACKGROUND ANALYSIS FROM ATLAS FORWARD PROTON DETECTORS	77
Aneta Bień	

NORMAL MODES OF SOLID-STATE PLASMA IN CONDITIONS OF BLOCH GAIN	78
Lukas Stakėla, Kirill N Alekseev	

O8: Material Science and Modern Technologies

TOWARDS HIGHLY CONDUCTIVE NANOCRYSTALLISED VANADATE-PHOSPHATE GLASSES	79
K Gadomski, T K Pietrzak, Sz Starzonek, S J Rzoska, J E Garbarczyk	

CARRIER DYNAMICS IN Ga-POLAR AND N-POLAR InGaN QUANTUM WELL STRUCTURES	80
Lukas Šiaulyš, Monika Gudaitytė, Kazimieras Nomeika	

THERMAL CONDUCTIVITY AND STRUCTURAL CHANGES IN ULTRA-HIGH PRESSURE TREATED SILICA GLASS – A MOLECULAR DYNAMICS STUDY	81
Adam Puchalski, Anton Hul, Jihui Nie, Tomasz K Pietrzak, Paweł Keblinski	

PRINTABILITY OF MUCOADHESIVE SODIUM ALGINATE/CHITOSAN GELS DELIVERING PHOTO-SENSITIZER IN PHOTODYNAMIC THERAPY	82
Maria Skrodzka, Jerzy Detyna, Katarzyna Matczyszyn	

A MECHANOCHEMICAL PROCESS FOR IMPROVING RESVERATROL PROPERTIES BY CO-CRYSTALLIZATION	83
Elena Mirabela Soare, Raul Augustin Mitran, Daniel Lincu, Irina Atkinson, Simona Ioniță, Adriana Rusu, Jeanina Pandeale Cusu, Coca Iordache, Victor Fruth	

O9: Chemistry and Chemical Physics

SOLVENT-FREE MECHANOCHEMICAL SYNTHESIS OF CSPBBR₃ QUANTUM DOTS WITH SURFACE-PASSIVATING LIGANDS	84
Pijus Domantas Valentukevičius, Simas Šakirzanovas	

SYNTHESIS OF 3-(24-DIHYDROXY-5-BENZYL)ALKYL CARBOXYLIC ACIDS AND THEIR DERIVATIVES	85
Vilius Petraška, Ieva Žutautė, Algirdas Brukštus	

CALCULATION OF HIGH-RESOLUTION UV SPECTRA OF DIATOMIC MOLECULES	86
Karolis Sarka	

DETECTING ATOMIC INTERACTIONS IN SMALL-MOLECULE CRYSTAL STRUCTURES	87
Andrius Merkys, Eglė Šidlauskaitė, Antanas Vaitkus	

SYNTHESIS OF 1-(2,4-DIFLUOROPHENYL)-5-OXOPYRROLIDINE-3-CARBOXYLIC ACID DERIVATIVES AND INVESTIGATION OF THEIR ANTICANCER ACTIVITY	88
Guoda Pranaitytė, Birutė Grybaitė, Vytautas Mickevičius, Vilma Petrikaitė, Ugnė Endriulaitytė	

O10: Nanomaterials and Nanotechnology

FS-LASER MICROPROCESSING FOR SERS SUBSTRATES OF PERIODIC METALLIC STRUCTURES	89
Kernius Vilkevičius, Ilja Ignatjev, Evaldas Stankevičius	

KCL CONCENTRATION EFFECTS ON THE FORMATION, STABILITY, AND SERS SIGNAL STRENGTH OF LASER-GENERATED GOLD, SILVER, AND HYBRID NANOPARTICLES	90
Vita Petrikaitė, Evaldas Stankevičius	
IMPACT OF THE CRYSTAL STRUCTURE OF SILICA NANOPARTICLES ON RHODAMINE 6G ADSORPTION	91
Daniel Doveiko, Karina Kubiak-Ossowska, Yu Chen	
MXENE-BASED ELECTROCHEMICAL SENSOR FOR PRECISE AND SELECTIVE DETECTION OF LEAD IONS IN AQUEOUS SOLUTIONS	92
Ilya Navitski, Šarūnas Žukauskas, Alma Ručinskienė, Arūnas Ramanavičius	
INVESTIGATION OF GRAPHENE/POLYPYRROLE COMPOSITES AND THEIR APPLICATION IN ELECTROCHEMICAL DOPAMINE SENSORS	93
Gintarė Rimkutė, Rasa Pauliukaitė, Gediminas Niaura, Jurgis Barkauskas, Justina Gaidukevič	

O11: Chemistry and Chemical Physics

DOCKING SITE-MEDIATED PHOTOSTABILIZATION FOR SINGLE-MOLECULE AND SUPER-RESOLUTION IMAGING	94
Cindy Close, Michael Scheckenbach, Alan Szalai, Julian Bauer, Lennart Grabenhorst, Fiona Cole, Thorben Cordes, Philip Tinnefeld, Viktorija Glembockyte	
DEVELOPMENT OF A NEW SUPER-OXIDIZING PHOTOCATALYSTS AND THEIR APPLICATIONS IN C-H ACTIVATION REACTIONS VIA IDIOSYNCRATIC MECHANISTIC MODES	95
Jonas Žurauskas, Gustautas Snarskis, Barbara Chatinovska, Paulius Vaickūnas, Gediminas Kreiza, Kęstutis Zakarauskas, Edvinas Orentas	
NEAR-INFRARED SENSITIZED DEEP TISSUE PHOTOACTIVATION OF AZOBENZENE IN BIOMIMETIC CONDITIONS AT LOW PHOTON FLUENCES	96
Lukas Naimovicus, Ekin Opar, Justas Lekavicius, Edvinas Radiunas, Helen Holzel, Edvinas Orentas, Karolis Kazlauskas, Pau Gorostiza, Pankaj Bharmoria, Kasper Moth-Poulsen	
STATISTICAL PROBABILITY OF SINGLET EXCITON GENERATION THROUGH TRIPLET-TRIPLET ANNIHILATION IN TES-ADT ANNIHILATOR	97
Justas Lekavičius, Edvinas Radiunas, Karolis Kazlauskas	

O12: Chemistry and Chemical Physics

STUDY OF SARS-CoV2-S WILD-TYPE SPIKE PROTEIN INTERACTION WITH RANDOMLY AND ORIENTED ANTIBODIES BY QUARTZ CRYSTAL MICROBALANCE	98
Silvija Juciutė, Beatričė Urbaitė, Vincentas Mačiulis, Ieva Plikusienė	
MXENE BASED COLORIMETRIC SENSOR FOR SILVER ION DETECTION IN WATER	99
Raminta Bajarunaite, Simonas Ramanavicius, Martynas Talaikis, Anton Popov, Gediminas Niaura, Almira Ramanaviciene	
DISSOLUTION ENHANCEMENT OF MEFENAMIC ACID USING SOLID DISPERSIONS OBTAINED BY WET GRANULATION TECHNIQUE	100
Volodymyr Yaremenko, Volodymyr Fedorenko, Svitlana Gureeva, Olena Ishchenko, Viktoriia Plavan, Volodymyr Bessarabov	

STUDY OF DIFFERENT PARAMETERS IMPACT TO MICROPLASTIC REMOVAL FROM WATER USING LIGNIN-MAGNETITE NANOSORBENT	101
Austėja Burbulytė, Ieva Uogintė, Vaidas Pudžaitis	

O11: Biochemistry, Biophysics and Biotechnology

DEVELOPMENT OF AN INNOVATIVE SCAFFOLD MADE FROM DECELLULARIZED HORSE BONE FOR BONE DEFECTS IN HORSES	102
Julia Niegowska, Łukasz Młynarski, Maciej Janeczek, Tomasz Gębarowski	

DESIGN AND INVESTIGATION OF 1,2,4-TRIAZOLE-3-YL THIOACETOHYDRAZIDES BEARING ALDIMINE MOIETY AS BIOLOGICALLY ACTIVE AGENTS	103
Aida Šermukšnytė, Vilma Petrikaitė, Kristina Kantminienė, Ilona Jonuškienė, Ingrida Tumosienė	

INVESTIGATION OF A NOVEL TRICOMPONENT BACTERIAL ANTIPHAGE DEFENCE SYSTEM ..	104
Lukas Volodka, Inga Songailiene	

TOWARDS A NOVEL MODEL TO STUDY NUCLEAR AGING: BIOPHYSICAL CHARACTERIZATION OF AGE-TUNED MEMBRANES	105
Aivaras Vilitis, Nuno C Santos, Maria J Sarmento	

O14: Biology, Genetics and Biomedical Sciences

PHARMACOKINETIC EVALUATION OF CEFAZOLIN ANTIMICROBIAL PROPHYLAXIS IN SPINAL SURGERY	106
Justin Stivrins, Sigita Kazune	

THERAPEUTIC POTENTIAL OF T CELLS FOR PREMATURE OVARIAN INSUFFICIENCY TREATMENT IN MOUSE MODEL	107
Indrė Krastinaitė, Greta Tamulaitytė, Veronika Viktorija Borutinskaitė	

CONSEQUENCES OF LONG TERM EXPOSURE TO MICROPLASTICS AND EFFECTS ON CYTOGENETIC AND ANTIOXIDANT BIOMARKERS IN FISH	108
Agnė Bučaitė, Gintarė Sauliūtė, Milda Stankevičiūtė	

BLOODSUCKING BITING MIDGES - NEGLECTED THREAT FOR WILD BIRDS	109
Margarita Kazak, Rasa Bernotienė	

ANALYSIS OF VIRULENCE FACTORS IN ISOLATES OF OPPORTUNISTIC PATHOGEN STENOTROPHOMONAS MALTOPHILIA	110
Radvilė Drevinskaitė, Laurita Klimkaitė, Jūratė Skerniškytė, Julija Armalytė	

INVESTIGATION OF THE INTERACTIONS BETWEEN THE SOYBEAN PLANTS AND MICROORGANISMS USING STABLE ISOTOPES	111
Raminta Skipitytė, Rūta Barisevičiūtė, Monika Toleikienė	

O15: Biochemistry, Biophysics and Biotechnology

CARBON SUPPORTED METAL CATALYST FROM SEAWEED-DERIVED BIO-CHAR PREPARATION AND CHARACTERIZATION VIA CHEMISORPTION	112
Paulius Buidovas, Justas Eimontas, Raminta Skvorčinskienė	

STABLE ISOTOPES AS A TOOL TO TRACK C AND N PATHWAYS IN THE ROOT SYSTEMS 113
Agnė Veršulienė, Andrius Garbaras

INVESTIGATING THE IMPACT OF ELAVL1 INHIBITION ON PANCREATIC CANCER CELL VIABILITY
. 114
Joris Dambrauskas, Darius Stukas

**INTRINSIC FIRING PROPERTIES OF THE MOUSE HIPPOCAMPAL PYRAMIDAL CA1 NEURONS
DURING THE POSTNATAL DEVELOPMENT** 115
Igor Nagula, Emilija Kavalnytė, Kornelija Vitkutė, Daiva Dabkevičienė, Urtė Neniškytė, Aidas Alaburda

O16: Biology, Genetics and Biomedical Sciences

**THE ESTABLISHMENT OF THREE NEW OVARIAN CANCER CELL LINES OPENS NEW AVENUE
OF RESEARCH INTO TUMOR HETEROGENEITY AND CELL EVOLUTION** 116
Eglė Žymantaitė, Agata Mlynska, Neringa Dobrovolskienė, Birutė Intaitė, Vita Pašukonienė

**DEVELOPMENT OF A DNA OLIGO-CAPTURE METHOD TO STUDY CANCER CELL METASTASIS
IN ANIMAL MODELS** 117
Roberta Pocevičiūtė, Šarūnas Tumas, Anna Malkova, Michael Sherman

**METHYLATION PROFILING OF HOMEOTIC AND CHROMATIN REMODELING GENES IN CANCER-
OUS OVARIAN TISSUE** 118
Rugilė Gineikaitė, Ieva Vaicekauskaitė, Rūta Čiurlienė, Rasa Sabaliauskaitė

**NOTCH SIGNALING PATHWAY COMPONENTS AS POTENTIAL BIOMARKERS FOR THE DIAGNO-
SIS OF OVARIAN CANCER** 119
Paulina Kazlauskaitė, Ieva Vaicekauskaitė, Rūta Čiurlienė, Rasa Sabaliauskaitė

**UPCONVERTING NANOCOMPLEX DELIVERY TO DISTINCT PHENOTYPES OF CANCER BY MES-
ENCHYMAL STEM CELLS** 120
Alėja Marija Daugėlaitė, Greta Butkienė, Simona Steponkienė, Vaidas Klimkevičius, Vilius Poderys, Ilona Uzielienė, Vitalijus Karabanovas, Ričardas Rotomskis

PLANT-DERIVED NANOVESICLES DISPLAY WOUND HEALING PROPERTIES 121
Mėta Mackevičiūtė, Aistė Jekabsone, Zbigniev Balion

P1: Laser Physics and Optical Technologies; Spectroscopy and Imaging; Material Science and Modern Technologies; Theoretical Physics and Astrophysics

**APPLICATION OF THE HIGH THROUGHPUT DARK-FIELD FULL-FIELD OPTICAL COHERENCE
TOMOGRAPHY SYSTEM** 122
Karolis Adomavičius, Austėja Trečiokaitė, Erikas Tarvydas, Danielis Rutkauskas, Egidijus Aukorius

**INVESTIGATION OF SUPERCONTINUUM GENERATION IN PHOTONIC CRYSTAL FIBERS WITH
DIFFERENT CHARACTERISTICS USING FEMTOSECOND PUMP PULSES** 123
Ieva Baltrukonytė, Jokūbas Pimpė, Julius Vengelis

PROCESSING OF THZ IMAGES USING DIFFERENT NEURAL NETWORK MODELS 124
Ugnė Šilingaitė, Ignas Grigelionis

PICOSECOND LASER WELDING OF SODA-LIME GLASS WITH MHZ BURSTS	125
Neda Mažeikytė, Edgaras Markauskas	
DEBRIS REMOVAL TECHNIQUES FOR PICOSECOND LASER BOTTOM-UP MILLING OF FUSED SILICA	126
Aleksandras Kondratas, Miglė Mackevičiūtė, Juozas Dudutis, Paulius Gečys	
INVESTIGATION OF AN OPTICAL PARAMETRIC AMPLIFIER WITH SUBNANOSECOND PULSES BASED ON FAN-OUT GRATING DESIGN MgO:PPLN CRYSTAL USING CONTINUUM SEED	127
Simona Armalytė, Jonas Banys, Julius Vengelis	
NANO-PROCESSING BY FS-UVINTERFERENCE METHOD	128
Tadas Latvys, Darius Gailevičius, Dominyka Stonytė, Domas Paipulas, Vytautas Jukna	
OPTIMIZING PHOTOVOLTAIC DEVICES THROUGH GALVANOMETRIC MIRROR-ASSISTED LASER ANNEALING	129
Gustas Mickevičius, Miglė Lenkauskaitė, Rokas Kondrotas, Marius Franckevičius	
SUMMARY OF 2D PHOTONIC CRYSTALS	130
Andrius Zinkevičius, Ignas Lukošius	
SPECTRAL BROADENING AND POST-COMPRESSION OF FEMTOSECOND YB:KGW OSCILLATOR PULSES	131
Titas Tamošauskas, Vaida Marčiulionytė, Jonas Banys, Gintaras Tamošauskas, Julius Vengelis, Audrius Dubietis	
FEMTOSECOND ULTRAVIOLET LASER MODIFICATION OF GALLIUM NITRIDE THIN-FILM COATINGS	132
Paulius Zakarauskas, Dominyka Stonytė, Arūnas Kadys, Darius Gailevičius, Domas Paipulas	
THZ METALENSESWITH DIFFERENT SPLIT RING RESONATOR GEOMETRIES	133
Karolis Redeckas, Kasparas Stanaitis, Vladislovas Čižas, Linas Minkevičius	
HOMODYNE IMAGING SET UP OPTIMIZATION: BEAM ENGINEERING OF ILLUMINATION AND COLLECTION USING HIPS BASED LENSES	134
Kasparas Stanaitis, Karolis Redeckas, Augustė Bielevičiūtė, Linas Minkevičius	
MICROSTRUCTURING OF HIGH BANDGAP MATERIALS USING FEMTOSECOND UV LASER PULSES FOR MULTI-LEVEL DIFFRACTIVE OPTICAL ELEMENTS	135
Vitalija Smirnovaitė, Dominyka Stonytė, Domas Paipulas	
FOUR PASS DUAL CELL SBS-PCM AMPLIFIER	136
Domantas Klumbys, Paulius Mackonis, Augustė Černekytė, Augustinas Petrulėnas, Aleksej M Rodin	
INVESTIGATION OF PUMP DEPLETION IN SUBNANOSECOND OPTICAL PARAMETRIC GENERATOR BASED ON PPLN CRYSTAL	137
Tomas Latvys, Viktorija Tamulienė	

DEVELOPMENT OF INTEGRATION TECHNOLOGY OF DIFFRACTIVE STRUCTURES INTO PLASTIC SURFACE OF THE PRODUCTS	138
Erika Rajackaitė, Indrė Danisevičienė, Andrius Žutautas, Pranas Narmontas	
DEVELOPMENT AND OPTIMIZATION OF A SUBNANOSECOND OPTICAL PARAMETRIC GENERATOR BASED ON COMBINED PPLN CRYSTAL STAGES	139
Augustė Stravinskiatė, Jonas Banys, Julius Vengelis	
ACRYLIC RESINS FOR LASER 3D LITHOGRAPHY OF HIGHLY-POROUS MICROSTRUCTURES . . .	140
Saulė Petrauskaitė, Ioanna Angeliki Petsi, Arūnas Čiburys, Antanas Butkus, Karolis Galvanauskas, Mangirdas Malinauskas	
LASER TWO-PHOTON PRINTING OF LOW-DENSITY 3D MICROSTRUCTURES OF ACRYLATE MATERIALS	141
Ioanna Angeliki Petsi, Saulė Petrauskaitė, Eulàlia Puig Vilardell, Antanas Butkus, Karolis Galvanauskas, Darius Gailevičius, Mangirdas Malinauskas	
CREATING 3D MODELS OF NATURAL OBJECTS FROM 2D IMAGES USING MACHINE LEARNING	142
Andrius Jedik, Donatas Narbutis	
EPR OF NEUTRON-RADIATION-INDUCED DEFECTS IN GGG	143
Jekabs Cirulis, Uldis Rogulis, Andris Antuzevics	
DISCRIMINATION OF PATHOGENIC YEAST AND BACTERIA BY MEANS OF ATR IR SPECTROSCOPY	144
Gerda Anužienė, Irmantas Arūnas Čiužas, Eglė Lastauskienė, Justinas Čeponkus	
WATER VAPOR INTERACTION WITH LIQUID ETHANOL WAS INVESTIGATED USING THE TERAHERTZ TIME-DOMAIN SPECTROSCOPY TECHNIQUE.	145
Ihor Krapivin, dr Ramūnas Adomavičius	
STRUCTURE OF VALERIC ACID MONOMERS AND DIMERS. MATRIX ISOLATION INFRARED SPECTROSCOPY STUDY	146
Jogile Macyte, Rasa Platakyte, Joanna Stocka, Valdas Sablinskas	
APPLICATION OF TERAHERTZ TIME-DOMAIN SPECTROSCOPY TO STUDY THE CURING PROCESSES OF EPOXY RESINS	147
Mykolas Šikas, Ramūnas Adomavičius	
RAMAN ASSISTED STUDY OF THE IMPACT OF ANNEALING TEMPERATURE FOR THE FORMATION AND STRUCTURE CHANGES FOR TIN SULFIDE FILMS	148
Boldizsár Zsiros, Ieva Barauskiene, Attila Farkas, Ingrida Ancutiene, Asta Bronusiene	
MICROWAVE COUPLING OF A NOVEL SUPERCONDUCTING EPR MICRORESONATOR	149
Ignas Pocius, Gediminas Usevičius, Paulina Vertbaitytė, Jūras Banys, Mantas Šimėnas	
CATHODOLUMINESCENCE IN NEW GENERATION NITRIDE COMPOUNDS	150
Gabija Soltanaitė, Žydrūnas Podlipskas, Viktorija Mickūnaitė	

TERAHERTZ IMAGING USING PHASE CONTRAST METHOD	151
Adrianna Nieradka, Mateusz Kałuża, Mateusz Surma, Paweł Komorowski, Agnieszka Siemion	
INVESTIGATING THE OPTICAL ATTRIBUTES OF SELAGIBENZOPHENONES AND THEIR COM- PLEXES WITH GRAPHENE QUANTUM DOTS	152
Vilius Čirgelis, Ringailė Lapinskaitė, Andrej Dementjev, Karolina Maleckaitė, Linas Labanauskas, Renata Karpicz	
EPR SPECTROMETER WITH ARBITRARY WAVEFORM GENERATION	153
Justinas Turčak, Jūras Banys, Vidmantas Kalendra, Mantas Šimėnas	
INFLUENCE OF SHORT- AND LONG-RANGE ORDER ON STRUCTURAL AND MAGNETIC PROP- ERTIES OF Fe-Co-C ALLOYS WITH A TETRAGONAL DEFORMATION: A FIRST-PRINCIPLES STUDY	154
Wojciech Marciniak, Mirosław Werwiński	
COMPETING DYNAMICS IN COMPARTMENTAL VOTER MODEL	155
Justas Kvedaravičius, Aleksejus Kononovičius	
CHALLENGES IN NEURAL QUANTUM STATE PERFORMANCE: INSIGHTS FROM THE BOSE- HUBBARD MODEL WITH MAGNETIC FIELD	156
Eimantas Ledinauskas, Egidijus Anisimovas	
NON-PHOTOCHEMICAL QUENCHING IN PHOTOSYNTHETIC ANTENNA	157
Dominykas Borodinas, Jevgenij Chmeliov	
HIGH-FREQUENCY APPROXIMATION FOR PERIODICALLY DRIVEN QUANTUM SYSTEMS IN THE VICINITY OF RESONANCES	158
Yakov Braver, Egidijus Anisimovas	
STRONG LONG-RANGE INTERACTIONS AND GEOMETRICAL FRUSTRATION IN SUBWAVE- LENGTH RAMAN LATTICES	159
Domantas Burba, Gediminas Juzeliunas, Ian B Spielman, Luca Barbiero	
EVALUATING METHODS FOR ESTIMATING THE HURST EXPONENT IN TIME SERIES A COMPAR- ATIVE ANALYSIS OF ACCURACY AND APPLICATION	160
Danielius Kundrotas, Rytis Kazakevičius	
NANO ZEOLITES AS ELECTROCATALYSTS FOR OER IN ALKALINE MEDIA	161
Jadranka Milikić, Sara Knežević, Kristina Radinović, Ana Nastasić, Aleksandar Jović, Aldona Balčiūnaitė, Radmila Hercigonja, Biljana Šljukić	
AB INITIO STUDY OF VIBRATIONAL PROPERTIES OF DIVACANCY DEFECTS IN 4H-SiC	162
Vytautas Žalandauskas, Rokas Silkinis, Lasse Vines, Lukas Razinkovas, Marianne Etzelmüller Bathen	
ANALYSIS OF GNSS LOCALIZATION ACCURACY IN URBAN AREA USING RAY TRACING	163
Karolis Stankevičius, Rimvydas Aleksiejūnas	

OPTICAL PROPERTIES OF CERIUM DOPED MULTICOMPONENT GARNET TYPE SCINTILLATORS GROWN BY LIQUID PHASE EPITAXY	164
Mikas Iršėnas, Augustas Vaitkevičius, Saulius Nargėlas, Arnoldas Solovjovas, Vitaliy Gorbenko, Yuriy Zorenko, Gintautas Tamulaitis	
CONTACT CHARACTERISTICS OF P-TYPE GaN GROWN USING INDIUM SURFACTANT	165
K German, M Vaičiulis, M Biveinytė, V Rumbauskas, K Nomeika, Y Talochka, A Kadys	
THE EFFECT OF MONOATOMIC OXYGEN ON CARBON-SPUTTERED QUARTZ CRYSTALS	166
Eivydas Trioška, Mindaugas Viliūnas, Greta Merkininkaitė, Simas Šakirzanovas	
INVESTIGATION OF SCINTILLATING CHARACTERISTICS IN MOCVD GaN STRUCTURES WITH CHEMICALLY MODIFIED SURFACES	167
Giedrius Juškevičius, Tomas Čeponis, Jevgenij Pavlov	
COMPARISON OF SPECTRAL PROPERTIES OF SEMICONDUCTOR STRUCTURES EQUIPPED WITH METALLIC (Ti/Au) OR N-TYPE GaAs METASURFACES	168
Barbora Škėlaitė, Vladislovas Čižas, Kęstutis Ikamas, Vytautas Jakštas, Domas Jokubauskis, Andrius Bičiūnas, Andrzej Urbanowicz, Marius Treideris, Renata Butkutė, Linas Minkevičius, Ignas Grigelionis	
COMPOSITE ALLOY FORMATION BY LASER METAL 3D PRINTING	169
Karolis Stravinskas	
ADDITIVE MANUFACTURING OF LAB-ON-CHIP PLATFORMS SUPPORTED BY HYDROGEL MATRIX FOR IN VITRO STUDIES	170
Adrianna Cieślak, Agnieszka Krakos, Julita Kulbacka, Jerzy Detyna	
THE IMPACT OF A MIXED-HOST EMISSIVE LAYER FOR HIGH-EFFICIENCY BLUE TADF OLED STABILITY	171
Goda Grybauskaitė, Kristupas Bagdonas, Gediminas Kreiza, Edvinas Orentas, Saulius Juršėnas, Karolis Kazlauskas, Dovydas Banevičius	
NATURAL GRAPHITE AND IRON SULFIDE USED AS NEGATIVE ELECTRODE MATERIALS FOR SODIUM-ION BATTERIES	172
Eglė Ūsovienė, Egidijus Griškonis	
2,5-DIPHENILOXAZOLE (PPO) APPLICATION FOR PHOTON UPCONVERSION FROM VISIBLE TO UV REGION	173
Naglis Vasarevičius, Manvydas Dapkevičius, Justas Lekavičius, Džiugas Krencius, Steponas Raišys, Karolis Kazlauskas	
EXPLORING PHENOTHIAZINE AND ITS DERIVATIVES: HTMS FOR EFFICIENT DOPING FREE FLUORESCENT AND MULTIPLE-RESONANCE TADF OLEDs	174
Melika Ghasemi, Ramakant Gavale, Faizal Khan, Dmytro Volyniuk, Juozas Vidas Grazulevicius, Rajneesh Misra	
3D LASER STRUCTURIZATION OF LUMINESCENT MATERIALS	175
Artūr Harnik, Ugnė Usaitė, Simas Šakirzanovas, Greta Merkininkaitė, Mangirdas Malinauskas	

TRI/TETRAPHENYLETHENYL COUPLED PHENOXAZINE AND PHENOTHIAZINE BASED HIGHLY FLUORESCENT MATERIALS SHOWING A IEE FOR OLEDs	176
Ehsan Ullah Rashid, Monika Cekaviciute, Jurate Simokaitiene, Juozas Vidas Grazulevicius, Dmytro Volyniuk, Khrystyna Ivanyuk, Pavlo Stakhira	
STUDY OF TIMING RESOLUTION OF PROTON IRRADIATED SILICON LOW GAIN AVALANCHE DETECTORS	177
Margarita Biveinytė, Tomas Čeponis, Laimonas Deveikis	
LASER-ANNEALING FOR ANTIMONY SELENIDE (SB₂SE₃) DEFECT PASSIVATION AND IMPROVEMENT OF SB₂SE₃ THIN-FILM SOLAR CELL PARAMETERS	178
Rokas Kondrotas, Miglė Lenkauskaitė, Gustas Mickevičius, Marius Franckevičius, Vidas Pakštas	
CHARGE CARRIER MOBILITY IN Si IRRADIATED WITH FAST ELECTRONS	179
Paula Baltaševičiūtė, Algirdas Mekys, Leonid Makarenko, Šarūnas Vaitekūnis, Juozas Vidmantis Vaitkus	
TRIPHENYLAMINE-BASED MONOLAYERS FOR OPTOELECTRONIC DEVICES	180
Aida Drevilkaukaitė, Artiom Magomedov, Vytautas Getautis	
BROMOQUINOXALINE DERIVATIVES AS ORGANIC ROOM TEMPERATURE PHOSPHORESCENCE; SYNTHESIS AND INVESTIGATION	181
Mohamed Hassan Saad Abdella, Jurate Simokaitiene, Juozas Vidas Grazulevicius	
3-(N,N-DIPHENYLAMINO)CARBAZOLE DONOR CONTAINING BIPOLAR DERIVATIVES WITH VERY HIGH GLASS TRANSITION TEMPERATURES AS POTENTIAL TADF EMITTERS FOR OLEDs	182
Daiva Tavgeniene, Raminta Beresneviute, Gintare Krucaite, Sujith Sudheendran Swayamprabha, Jwo-Huei Jou, Saulius Grigalevicius	
AMBIPOLAR HOSTS FOR BLUE TADF OLEDs: ASSESSMENT OF THE DEVICE PERFORMANCE AND LIFETIME	183
Kristupas Bagdonas, Goda Grybauskaitė, Gediminas Kreiza, Edvinas Orentas, Saulius Juršėnas, Karolis Kazlauskas, Dovydas Banevičius	
PLASMON-ENHANCED VISIBLE LIGHT ABSORPTION FOR PHOTOCATALYTIC WATER SPLITTING	184
Klaudijus Midveris, Tomas Klinavičius, Andrius Vasiliauskas, Šarūnas Meškis, Muhammad Haris, Asta Tamulevičienė, Tomas Tamulevičius	
NEW BIPOLAR DERIVATIVES WITH DIPHENYLSULFONE OR DIPHENYLPHENONE AS TADF BASED EMITTERS OLEDs	185
Gintare Krucaite, Daiva Tavgeniene, Saulius Grigalevicius, Yi-Ting Chen, Yu-Hsuan Chen, Chih-Hao Chang, Raminta Beresneviute	
SYNTHESIS AND CHARACTERIZATION OF NITROGEN MODIFIED REDUCED GRAPHENE OXIDE	186
Rūta Aukštakojytė, Rasa Pauliukaitė, Justina Gaidukevič	
DEPOSITION OF NICKEL-ION COATINGS USING MORPHOLINE BORANE AS A REDUCING AGENT	187
Dmytro Shyshkin, Zita Sukackienė, Jūratė Vaičiūnienė, Loreta Tamašauskaitė-Tamašiūnaitė, Eugenijus Norkus	

AN ENHANCED HYDROGEN EVOLUTION REACTION PERFORMANCE BY NICKEL-MANGANESE BIMETALLIC ELECTROCATALYSTS TOWARDS ALKALINE NATURAL SEAWATER AND SIMULATED SEAWATER SPLITTING	188
Sukomol Barua, Aldona Balčiūnaitė, Jūratė Vaičiūnienė, Loreta Tamašauskaitė-Tamašiūnaitė, Eugenijus Norkus	
TERNARY NICKEL-IRON-PHOSPHOROUS ELECTROCATALYSTS FOR ALKALINE HYDROGEN EVOLUTION REACTION	189
Raminta Šakickaitė, Zita Sukackienė, Aldona Balčiūnaitė, Loreta Tamašauskaitė-Tamašiūnaitė, Eugenijus Norkus	
TIPS-NPH AND IRIIDIUM COMPLEX SYSTEM FOR PHOTON UPCONVERSION FROM VISIBLE LIGHT TO UV	190
Džiugas Krencius, Naglis Vasarevičius, Manvydas Dapkevičius, Justas Lekavičius, Steponas Raišys, Karolis Kazlauskas	
IRON AND CERIUM ION EXCHANGE ON ZEOLITE AS BIFUNCTIONAL ELECTROCATALYST FOR OER AND ORR IN ALKALINE MEDIA	191
Ana Nastasić, Jadranka Milikić, Kristina Radinović, Aldona Balčiūnaitė, Vladislav Rac, Biljana Šljukić	
INTEGRATION OF SILVER NANOPARTICLE POLYMER NANOCOMPOSITES AND 3D PRINTING TECHNOLOGIES FOR DURABLE ANTIMICROBIAL COVERS	192
Mindaugas Illickas, Asta Guobienė, Karolis Gedvilas, Mantvydas Merkis, Brigita Abakevičienė	
IMPROVING THE STABILITY OF PEROVSKITE FILMS IN AMBIENT CONDITIONS	193
Ilija Filipas, Mantas Marčinskas, Artiom Magomedov, Matas Steponaitis	
INVESTIGATION OF THE SMARTPHONE CAMERA WITH SOLID-STATE ILLUMINATION FOR HYPERSPECTRAL IMAGING	194
Agnė Urbonaitė, Pranciškus Vitta	
STUDY OF CARRAGEENAN FERRIC OXIDE TENSION SENSORS	195
Elena Deneb Casas Borregón, Jūratė Jolanta Petronienė, Vytautas Bučinskas	
SYNTHESIS AND INVESTIGATION OF VANILLIN-BASED VITRIMERS	196
Brigita Kazlauskaitė, Sigita Grauzėlienė, Jolita Ostrauskaitė	
SYNTHESIS, CHARACTERIZATION, AND APPLICATION OF POLYVINYLPIRROLIDONE (PVP)/MnFe COMPOSITE FOR WATER SPLITTING	197
Karina Vjūnova, Huma Amber, Jūratė Vaičiūnienė, Loreta Tamašauskaitė-Tamašiūnaitė	
SPECTROSCOPIC ANALYSIS OF FIVE RV TAURI TYPE STARS WITH NO IR EXCESS	198
Karina Korenika, Kārlis Puķītis	
CHEMICAL ANALYSIS OF SOLAR TWIN AND ANALOGUE STARS	199
Ugnė Jonauskaitė, Edita Stonkutė	
INVESTIGATING THE CONNECTION BETWEEN GALACTIC OUTFLOW AND GALAXY PROPERTIES	200
Milda Valytė, Kastytis Zubovas	

ANALYSIS OF SPECTRAL LINES FOR STARS VIA SYNTHETIC SPECTRA	201
Dzmitry Viarbitski, Markus Ambrosch	
ACHIEVING LONG-LASTING ROOM TEMPERATURE PHOSPHORESCENCE IN PHENOTHIAZINE CRYSTALS	202
Vilius Stankevičius, Jonas Žurauskas, Paulius Vaickūnas, Steponas Raišys, Edvinas Orentas, Karolis Kazlauskas	
P2: Chemistry and Chemical physics; Nanomaterials and Nanotechnologies	
Functionalization and Properties Investigations of Benzothiophene Derivatives	203
Arnas Kovševič, Indrė Jaglinskaitė, Vilija Kederienė	
HYDROGELS WITH THE ADDITION OF MODIFIED STARCH AND CLAY OF THE MONTMORILLONITE TYPE	204
Anastasiia Godunko, Irina Liashok, Viktoriia Plavan, Olena Ishchenko, Viacheslav Shvets	
PROPELLANT SELECTION FOR ENHANCED DRUG DELIVERY IN WOUND-HEALING TOPICAL AEROSOLS	205
Mariia Popova, Olena Saliy	
OPTIMIZATION OF THE COMPOSITION OF A SOLID DISPERSED SYSTEM OF NIMESULIDE OBTAINED BY CENTRIFUGAL FIBER FORMATION	206
Viktoriia Lyzhniuk, Viktor Kostyuk, Vadym Lisovyi, Andriy Goy, Galina Kuzmina, Volodymyr Bessarabov	
UV TO NIR EMITTING UPCONVERTING NANOPARTICLES FOR APPLICATIONS IN THERANOSTICS	207
Egle Ezerskyte, Greta Butkiene, Arturas Katelnikovas, Vaidas Klimkevicius	
RESISTIVITY AND LOW FREQUENCY NOISE OF HYBRID COMPOSITES WITH CARBON NANOTUBES AND IRON NANOINCLUSIONS	208
Frydrichas Mireckas	
STRUCTURE OF CAPROIC ACID MONOMERS AND HYDROGEN BOND COMPLEXES. MATRIX ISOLATION IR SPECTROSCOPY STUDY	209
Simona Bučinskaitė, Redas Kazlauskas, Jogilė Mačytė	
INVESTIGATION OF SARS-COV-2 OMIKRON SPIKE PROTEIN REAL-TIME INTERACTIONS WITH SPECIFIC MONOCLONAL ANTIBODIES	210
Justina Liesyte, Silvija Juciute, Vincentas Maciulis, Ieva Plikusiene	
INVESTIGATION OF MXENES ADSORPTION POTENTIAL FOR AZURE A AND METHYLENE BLUE DYES pH-RESPONSIVE BEHAVIOR AND ADSORPTION KINETICS	211
Anton Popov, Martynas Talaikis, Germantė Paulikaitė, Simonas Ramanavicius, Gediminas Niaura	
OPTICAL SECOND HARMONIC GENERATION IN GaN WAVEGUIDE STRUCTURE	212
Ignas Dailidėnas, Roland Tomašiūnas	

SYNTHESIS OF LaMnO₃ NANOPARTICLES AND INVESTIGATION OF THEIR STRUCTURAL, MORPHOLOGICAL AND MAGNETIC PROPERTIES	213
Evaldas Lugauskas, Dovydas Karoblis, Gediminas Niaura, Dominika Zakutna, Aivaras Kareiva	
OPTIMIZATION OF SYNTHESIS PARAMETERS FOR WELL-DEFINED UPCONVERTING NANOPARTICLES	214
Viktorija Vrubliauskaitė, Eglė Ežerskytė, Vaidas Klimkevičius	
THE DEVELOPMENT OF GLUCOSE BIOSENSOR BASED ON DENDRITIC GOLD NANOSTRUCTURES MODIFIED BY CONDUCTING POLYMERS	215
Natalija German, Anton Popov, Arunas Ramanavicius, Almira Ramanaviciene	
INTERNAL QUANTUM EFFICIENCY OF GaAsBi/GaAs QUANTUM WELLS	216
Aistė Butkutė, Aivaras Špokas, Andrea Zelioli, Bronislovas Čechavičius, Sandra Stanionytė, Augustas Vaitkevičius, Evelina Dudutienė, Renata Butkutė	
INFLUENCE OF SI ADDITIVES ON THE STRUCTURE OF NANOCRYSTALLISED Na₂VFe₂(PO₄)₃ ALLUAUDITE-LIKE GLASSES	217
Martyna Jankowska, Krzysztof Gadomski, Maciej Nowagiel, Tomasz K Pietrzak, Linda F Nazar	
INVESTIGATION OF THE USE OF AlGaAs/InGaAs QUANTUM WELL FOR NIR EMITTERS	218
Andrea Zelioli, Aivaras Špokas, Gustas Petrusevičius, Bronislovas Čechavičius, Evelina Dudutienė, Renata Butkutė	
MOCVD GaN SENSORS WITH CHEMICALLY ETCHED SURFACES	219
Gertrūda Pociūtė, Tomas Čeponis, Jevgenij Pavlov	
CATHODOLUMINESCENCE AT THE VICINITY OF DEFECTS IN III-NITRIDES	220
Viktorija Mickūnaitė, Mantas Migauskas, Žydrūnas Podlipskas	
ELECTROCHEMICAL IMMUNOSENSOR BASED ON GOLD NANOSTRUCTURES FOR THE DETECTION OF ANTIBODIES AGAINST SARS-COV-2 SPIKE PROTEIN	221
Kristina Sobol, Katazyna Blazevic, Benediktas Brasiunas, Almira Ramanaviciene	
CONSIDERATION OF THE STABILITY OF A MOLECULARLY IMPRINTED POLYMER LAYER CONCERNING ITS THICKNESS	222
Greta Pilvenytė, Raimonda Bogužaitė, Vilma Ratautaitė, Arūnas Ramanavičius	
APPLICATION OF GOLD NANORODS TOWARDS THE DEVELOPMENT OF ELECTROCHEMICAL BIOSENSORS	223
Marina Šapauskienė, Viktorija Lisyte, Almira Ramanaviciene, Anton Popov	
LUMINESCENT POLYMER COATINGS: ENCAPSULATING PEROVSKITE QUANTUM DOTS ON GLASS SURFACE	224
Živilė Stanionytė, Vaidas Klimkevičius	
EXTENDED REALITY IN NANOTECHNOLOGY	225
Šarūnas Ščefanavičius, Raman Levoshka, Ilse-Christine Gebeshuber	

ANALYSIS OF SILVER NANOPARTICLE LAYER FORMATION ON LASER-INDUCED PERIODIC SURFACE STRUCTURES	226
Mantas Mikalkevičius, Nadzeya Khinevich, Tomas Tamulevičius, Asta Tamulevičienė	
SIZE-DEPENDENT PROPERTIES OF YTTERBIUM DOPED CESIUM LEAD HALIDE PEROVSKITE PARTICLES	227
Daniel Rodz, Simona Streckaitė, Vidmantas Gulbinas	
STABILIZATION OF DELTA-Bi₂O₃ PHASE AT ROOM TEMPERATURE BY THERMAL NANOCRYSTALLIZATION OF BISMUTH OXIDE GLASSES	228
Maciej Nowagiel, Julien Trébosc, Olivier Lafon, Tomasz Płociński, Marek Wasiucioneck, Jerzy E Garbarczyk, Tomasz K Pietrzak	
DESIGN AND SYNTHESIS OF MOLECULAR BUILDING BLOCKS FOR MODULAR SUPRAMOLECULAR CAVITANDS	229
Nojus Radzevičius, Edvinas Orentas	
ELECTROCHEMICAL SENSOR DEVELOPMENT FOR MELAMINE DETECTION	230
Ernestas Brazys, Vilma Ratautaitė, Arūnas Ramanavičius	
ANTIOXIDANT CONTENT OF FOOD PACKAGES MADE FROM POLYETHYLENE	231
Toma Petrulionienė, Tomas Murauskas	
DISSOLUTION-PRECIPIATION SYNTHESIS OF MAGNESIUM WHITLOCKITE FROM AMORPHOUS CALCIUM PHOSPHATE	232
Gabrielė Eglė Budžytė, Rūta Raišeliėnė, Inga Grigoravičiūtė, Aivaras Kareiva, Aleksej Žarkov	
ANALYSIS OF WATER SORPTION OF FILMS BASED ON MODIFIED STARCH	233
Olena Ishchenko, Daria Kuchynska, Irina Liashok, Maria Kuchynska	
AN ATTEMPT TO SYNTHESIZE MESOPOROUS SILICA BY A DIFFERENT SILICA PRECURSORS AND POROGENS	234
Gerardas Laurinavičius, Vilius Poškus	
HYDROGEN GENERATION ON CoFe CoFeMn AND CoFeMo COATINGS DEPOSITED ON Ni FOAM VIA ELCTEROLESS METAL PLATING	235
Huma Amber, Karina Vjunova, Zita Sukackienė, Dijana Šimkūnaitė, Juratė Vaiciuniene, Loreta Tamasauskaite-Tamasiunaite, Eugenijus Norkus	
ELECTRON-POOR ACRIDONES AND ACRIDINIUMS AS SUPER PHOTOOXIDANTS INMOLECULARPHOTOELECTROCHEMISTRY BY UNUSUAL MECHANISMS	236
Jonas Žurauskas, Edvinas Orentas, Paulius Vaickūnas, Soňa Boháčová, Shangze Wu, Valeria Butera, Simon Schmid, Michał Domański, Tomáš Slanina, Joshua P Barham	
ASSEMBLY AND RESEARCH OF ARTIFICIAL ROOT SYSTEM	237
Ernestas Svirbutavičius, Šarūnas Žukauskas, Arūnas Ramanavičius	
SYNTHESIS OF NEW 3-(2-OXOBENZODOXAZOL-3(2H)-YL)PROPANOIC ACID DERIVATIVES ..	238
Birutė Grybaitė, Birutė Sapijanskaitė-Banevič, Rita Vaickelionienė, Kazimieras Anusevičius, Vytautas Mickevičius	

DEVELOPMENT OF ORALLY DISINTEGRATING FILMS BASED ON BIOPOLYMERS AND PLANT EXTRACTS	239
Emilija Galkauskaite, Ramune Rutkaite, Vaida Kitryte-Syrpa, Dovile Liudvinaviciute, Michail Syrpas	
SILVER-TIN OXIDE NANOPARTICLES FOR SHELL ISOLATED NANOPARTICLE ENHANCED RAMAN SPECTROSCOPY	240
Vytautas Taurelė, Tatjana Charkova	
APPLICATION OF COMPUTATIONAL METHODS IN THE DESIGN OF MOLECULARLY IMPRINTED POLYMERS	241
Enayat Mohsenzadeh, Vilma Ratautaite, Arunas Ramanavicius	
PHOTOCATALYTIC DEGRADATION OF LOW-DENSITY POLYETHYLENE IN AQUEOUS SOLUTION USING TiO₂ NANOPARTICLES DEPOSITED ON CLAY KAOLINITE	242
Sonata Pleskytė, Ieva Uogintė, Steigvilė Byčenkienė	
PREPARATION AND INVESTIGATION OF MULTI-LAYERED ORALLY DISINTEGRATING FILMS ..	243
Dovile Liudvinaviciute, Emilija Galkauskaite, Vesta Navikaitė-Šnipaitienė, Vaida Kitryte-Syrpa, Michail Syrpas, Ramune Rutkaite	
BLACK CURRANT SEEDS A SOURCE OF BIOACTIVE COMPOUNDS WITH PROFOUND HEALTH BENEFITS	244
Indrė Pocevičienė, Laura Jūrienė, Audrius Pukalskas, Renata Baranauskienė, Petras Rimantas Venskutonis	
ISOTOPIC COMPOSITION OF CARBONACEOUS AEROSOLS FOR SEASONAL OBSERVATION ..	245
Durre Nayab Habib, Andrius Garbaras, Inga Garbarienė, Agne Mašalaitė	
DI-TERT-ALKYLPHOSPHINE SYNTHESIS AND INVESTIGATION OF CHEMOENZYMATIC SYNTHESIS OF THEIR PRECURSORS - TERTIARYACETATES	246
Jonas Paukštys, Tomas Paškevičius, Ringailė Lapinskaitė, Nina Urbelienė, Linas Labanauskas, Rolandas Meškys	
FABRICATION OF 3D BORON CARBIDE BY COMBINING STEREOLITHOGRAPHY AND PYROLYSIS	247
Robertas Virkėtis, Greta Merkininkaitė, Vaidas Klimkevičius, Simas Šakirzanovas	
MANGANESE DOPING EFFECT ON CRYSTAL STRUCTURE AND MAGNETIC PROPERTIES OF LUTETIUM FERRITE	248
Andrius Pakalniškis, Gediminas Niaura, Ramūnas Skaudžius, Aivaras Kareiva	
SYNTHESIS OF 6-(5-ARYL-1,2,3-THIADIAZOL-4-YL)-(4-BENZYL)BENZENE-1,3-DIOLS AS POTENTIAL HSP 90 INHIBITORS	249
Gabija Griškonytė, Algirdas Brukštus, Ieva Žutautė	
NMR STUDY OF BIOACTIVE IONIC LIQUIDS	250
Lukas Mikalauskas, Vytautas Klimavičius	
NICKEL CATALYSTS FOR HYDROGEN GENERATION	251
Gitana Valeckytė, Zita Sukackienė, Virginija Kepenienė, Irena Stalnionienė, Vitalija Jasulaitienė, Jūratė Vaičiūnienė, Loreta Tamašauskaitė Tamašiūnaitė, Giedrius Stalnionis, Eugenijus Norkus	

SYNTHESIS AND LUMINESCENT PROPERTIES OF EU-DOPED $\text{Ca}_2\text{PO}_4\text{Cl}$	252
Paulina Pažerauskaitė, Artūras Katelnikovas, Aleksej Žarkov	
TUNABLE THERMO-RESPONSIVE COPOLYMERS VIA RAFT POLYMERIZATION: EFFECTS OF COMPOSITION ON PHASE TRANSITION IN AQUEOUS SOLUTIONS	253
Kristina Bolgova, Vaidas Klimkevičius	
PM₁ CHARACTERIZATION FOR CONNECTED-FLOW EVENTS OVER THE BALTIC SEA BETWEEN HYLTEMOSSA AND PREILA	254
Agnė Minderytė, Axel Eriksson, Erik Ahlberg, Steigvilė Byčenkienė, Adam Kristensson, Julija Pauraitė	
BISMUTH DOPED LASER-INDUCED (Bi-LIG) GRAPHENE ELECTROCHEMICAL SENSOR FOR THE DETECTION OF HEAVY METALS	255
Pamela Rivera, Aivaras Sartanavičius, Romualdas Trusovas, Rasa Pauliukaite	
REDOX CONTROLLED BREATHING OF SUPRAMOLECULAR CAPSULE	256
Gabija Sergejevaitė, Domantas Valčekas, Edvinas Orentas	
MULTILAYER CAPACITOR AS AN ELECTROCHEMICAL SENSOR FOR MEASURING HYDROGEN PEROXIDE	257
Alvydas Radžius, Šarūnas Žukauskas, Arūnas Ramanavičius	
SACCHAROMYCES CEREVISIAE CELL MODIFICATION WITH NICKEL AND FERRIC HEXACYANO-FERRATES FOR THE APPLICATION IN BIO-FUEL CELL CONSTRUCTION	258
Gabija Adomaitė, Aušra Valiūnienė	
HYBRID NASICON TYPE BATTERIES MATERIALS SOLID-STATE NMR RESEARCH	259
Matas Manionis, Vytautas Klimavicius	
SYNTHESIS AND OPTICAL PROPERTIES OF CR-SUBSTITUTED BETA-TRICALCIUM PHOSPHATE	260
Jonas Stadulis, Sapargali Pazylbek, Arturas Katelnikovas, Aleksej Zarkov	
SYNTHESIS OF FUNCTIONALISED M-TERPHENYLS AND CHEMOENZYMATIC SEPARATION OF ATROPISOMER	261
Kristupas Volbikas, Tomas Paškevičius, Ringailė Lapinskaitė, Nina Urbelienė, Linas Labanauskas, Rolandas Meškys	
CHARACTERIZATION OF TRANS-STILBENE NANOCRYSTALS IN POLYSTERENE FILMS BY CARS AND AFM MICROSCOPY AND OPTICAL SPECTROSCOPY	262
Ivan Halimski, Renata Karpicz, Andrej Dementjev, Marija Jankunec, Jevgenij Chmeliov, Mindaugas Macernis, Darius Abramavicius, Leonas Valkunas	
EVALUATING THE ROLE OF GREEN INFRASTRUCTURE IN REDUCING TRANSPORT-RELATED MICROPLASTICS FOR STRENGTHENING URBAN ENVIRONMENTAL HEALTH	263
Abdullah Khan, Valda Araminienė, Ieva Uogintė, Lina Davulienė, Iveta Varnagirytė-Kabašinskienė, Valda Gudynaitė-Franckevičienė, Algis Džiugys, Edgaras Misiulis, Steigvilė Byčenkienė	
SYNTHESIS AND LUMINESCENT CHARACTERIZATION OF DOPED $\text{Na}_{1-x}\text{AlGe}_{1-0.5x}\text{O}_4\text{:X}$ PHOSPHORS	264
Gabija Janusauskaite, Martynas Misevicius	

MODELLING OF PORPHINE NANOTUBE ABSORPTION SPECTRA	265
Eimantas Urniežius, Darius Abramavičius	
SYNTHESIS OF CARBAZOLE-BASED MATERIAL WITH ACCEPTOR MOIETIES FOR PEROVSKITE SOLAR CELL TECHNOLOGY	266
Guostė Kaleininkaitė, Aida Drevilkauskaitė, Vytautas Getautis, Artiom Magomedov	
INVESTIGATION OF HOLE TRANSPORT IN SMALLMOLECULE - POLYMER BLENDS	267
Danielius Sakavicius	
LARGE AMOUNT SYNTHESIS OF MAGNESIUM WHITLOCKITE NANOPOWDERS FROM AN ENVIRONMENTALLY FRIENDLY INITIAL REACTANT	268
Rūta Raišeliėnė, Greta Linkaitė, Aleksej Žarkov, Aivaras Kareiva, Monika Skruodienė, Inga Grigoravičiūtė	
BENZOPHENONE-BASED TWISTED DONOR-ACCEPTOR-DONOR DERIVATIVES AS BLUE EMITTERS FOR HIGHLY EFFICIENT FLUORESCENT OLEDs	269
Dovydas Blazevičius, Iram Siddiqui, Prakalp Gautam, Gintare Krucaite, Daiva Tavgeniene, Mangey Ram Nagar, Krishan Kumar, Subrata Banik, Jwo-Huei Jou, Saulius Grigalevičius	
NEW 4H-BONDING MOTIF	270
Vladyslava Romadina, Nojus Radzevičius, Edvinas Orentas	
RESPONSIVE BEHAVIOR OF GRAFT COPOLYMERS BASED ON CHITOSAN	271
Migle Savicke, Ramune Rutkaite	
THIANTHRENE-BASED COMPOUNDS FOR OXYGEN SENSING APPLICATIONS	272
Lukas Dvylys, Rasa Keruckienė, Matas Gužauskas, Melika Ghasemi, Juozas Vidas Gražulevičius	
NAPHTALIMIDE-BASED DERIVATIVES ENABLING HIGH-EFFICIENCY OLEDs	273
Raminta Beresnevičiute, Prakalp Gautam, Mangey Ram Nagar, Gintare Krucaite, Daiva Tavgeniene, Jwo-Huei Jou, Saulius Grigalevičius	
IMPACT OF TERTIARY AMINO LINKAGES ON THE PROPERTIES OF ELECTROACTIVE PHENOTHIAZINYL-BASED COMPOUNDS	274
Domantas Lekavičius, Rasa Keruckienė, Matas Gužauskas, Juozas V Gražulevičius	
MODIFICATION OF METAL OXIDE SURFACES WITH REGENERABLE PHOSPHOLIPID BILAYERS FOR THE DEVELOPMENT OF REUSABLE BIOSENSORS	275
Anastasija Aleksandrovič, Inga Gabriūnaitė, Aušra Valiūnienė	
SYNTHESIS OF BIPHASIC CALCIUM PHOSPHATE GRANULES UNDER STATIC AND ROTATING CONDITIONS FROM ENVIRONMENTALLY BENIGN PRECURSOR - GYPSUM	276
Greta Linkaitė, Rūta Raišeliėnė, Aivaras Kareiva, Monika Skruodienė, Inga Grigoravičiūtė	
SOLID PHASE EXTRACTION BASED ON CATION EXCHANGE SORBENTS FOLLOWED BY FAST GAS CHROMATOGRAPHY TECHNIQUE TO DETERMINE PSYCHOACTIVE SUBSTANCES	277
Nerijus Karlonas	

EVALUATION OF AEGOPODIUM PODAGRARIA ANTIOXIDANT AND ANTIMICROBIAL ACTIVITY USING DIFFERENT EXTRACTION SOLVENTS	278
Ugnė Gabrytė, Rūta Mickienė, Audrius Sigitas Maruška	
PHYSICAL AND CHEMICAL CHARACTERISTICS OF MICROPLASTIC PARTICLES IN LITHUANIAN RIVERS	279
Tomas Stonkus	
ENVIRONMENT-DEPENDENT CHLOROPHYLL-CHLOROPHYLL CHARGE TRANSFER STATES IN Lhca4 PIGMENT-PROTEIN COMPLEX	280
Gabrielė Rankelytė, Jevgenij Chmeliov, Andrius Gelzinis, Leonas Valkunas	
ELECTRONIC EXCITED STATES OF PHTHALOCYANINES	281
Darius Likandrovas, Andrius Gelzinis, Jevgenij Chmeliov, Leonas Valkunas	
THERMOPLASTIC CELLULOSE ACETATE COMPOSITES WITH INORGANIC FILLERS	282
Rokas Jakubauskas, Ramunė Rutkaitė, Dovilė Liudvinavičiūtė, Laura Pečiulytė, Joana Bendoraitienė, Kęstutis Baltakys, Andrius Gineika	
SYNTHESIS AND INVESTIGATION OF NATURAL OIL-BASED SHAPE-MEMORY PHOTOPOLYMERS	283
Viltė Šereikaitė, Auksė Navaruckienė, Jolita Ostrauskaitė	
MAGICAL MANDRAGORA OFFICINARUM L.: UNLOCKING THE SECRETS OF PHYTOCHEMISTRY AND BIOACTIVITIES	284
Goda Jašinskaitė, Petras Rimantas Venskutonis, Ona Ragažinskienė	
SYNTHESIS AND CHARACTERIZATION OF ALKALINE EARTH METALS SUBSTITUTED LANTHANUM MOLYBDATE	285
Giedrė Gaidamavičienė, Artūras Žalga	
DICYANOISOPHORONE BASED SOLID STATE EMITTERS FOR ORGANIC LIGHT EMITTING DIODES	286
Khushdeep Kaur, Asta Dabulienė, Juozas Vidas Grazulevičius	
SYNTHESIS AND CHARACTERIZATION OF ELECTROCONDUCTIVE POLYMERS FOR THE PRODUCTION OF A SARS-COV-2 ANTIBODY SENSOR	287
Felix Lücke, Šarūnas Žukauskas, Arūnas Ramanavičius	
SYNTHESIS OF NEW COMPOSITION PRASEODYMIUM DOPED LUTETIUM AND GADOLINIUM ALUMINUM GARNETS MODIFIED BY SCANDIUM AND BORON ELEMENTS TO IMPROVE LUMINESCENCE PROPERTIES	288
Greta Inkrataite, Jan-Niklas Keil, Thomas Jüstel, Agnė Kizalaite, Ramūnas Skaudzius	
SEARCH AND CHARACTERISATION OF BINDERS FOR AQUEOUS SODIUM ION BATTERIES	289
Adolfas Žukauskas, Nadežda Traškina, Jurgis Pilipavičius, Linas Vilčiauskas	
MOLECULAR DYNAMICS SIMULATIONS OF 1-BUTYL-3-METHYLIMIDAZOLIUM TETRAFLUOROBORATE IONIC LIQUID	290
Gvidas Ropė, Kęstutis Aidas	

FORMATION AND INVESTIGATION OF BIPOLAR AQUEOUS SODIUM ION BATTERIES	291
Dovilė Škarnulytė, Milda Petrulevičienė, Jurga Juodkazytė, Linas Vilčiauskas	
SYNTHESIS AND LUMINESCENT PROPERTIES OF EU-DOPED STRONTIUM CHLORAPATITE	292
Simona Bendziute, Inga Grigoraviciute, Arturas Katelnikovas, Aleksej Zarkov	
STRUCTURAL AND NMR PROPERTIES OF SUPRAMOLECULAR COMPLEXES OF DRUG MOLECULES	293
Benjaminas Malmiga, Kęstutis Aidas	
SYNTHESIS OF TARGETED CONDENSED THIOIMIDAZOLES	294
Martyna Paulauskaitė, Gintarė Sapežinskaitė, Indrė Misiūnaitė, Ieva Žutautė	
P3: Biochemistry, Biophysics and Biotechnology; Biology, Genetics and Biomedical Sciences	
CAPDROP: A NOVEL METHOD FOR PERIPHERAL BLOOD scRNA-seq	295
Emilė Pranauskaitė, Linas Mažutis	
COMPARATIVE STUDIES OF THE ANTIOXIDANT PROPERTIES OF DIOSMIN AND QUERCETIN IN THE MODEL SYSTEM OF DOPAMINE OXIDATION	296
Iryna Povshedna, Vladyslav Udovytskyi, Iryna Pashchenko, Viktoriia Lyzhniuk, Vadym Lisovyi, Volodymyr Bessarabov, Andriy Goy	
INHIBITION OF PERIODONTAL DISEASES SPECIFIC MIRNAS: NEW THERAPEUTIC APPROACH	297
Gabrielė Židonytė, Benita Buragaitė-Staponkienė, Kristina Šnipaitienė, Adomas Rovas, Alina Purienė, Raminta Vaičiulevičiūtė, Eiva Bernotienė, Sonata Jarmalaitė	
INVESTIGATION OF ANXA4 FUNCTION IN CELL PLASMA MEMBRANE PERMEABILIZATION, RESEALING AND CELL VIABILITY POST-ELECTROPORATION	298
Dominykas Makarovas, Baltramiejus Jakštys, Saulius Šatkauskas	
CREATION OF MUTANT VARIANT K102R OF YEAST SACCHAROMYCES CEREVISIAE GENE SUP35	299
Ieva Jankauskaitė, Justina Versockienė, Eglė Lastauskienė	
MINIMIZING CHEMOTHERAPY SIDE EFFECTS: CALCIUM SONOPORATION	300
Reda Rulinskaitė, Rūta Palepšienė, Saulius Šatkauskas, Renaldas Raišutis, Martynas Maciulevičius	
EXPLORING THE IS200/IS605 FAMILY TRANSPOSABLE ELEMENTS FOR NOVEL GENOME EDITING TOOLS	301
Gytis Druteika, Tautvydas Karvelis	
STRUCTURAL VARIABILITY OF PRION PROTEIN AMYLOID FIBRILS DEPENDS ON AGITATION INTENSITY	302
Kamile Mikalauskaite, Mantas Ziaunys, Vytautas Smirnovas	
CRISPR-CAS9 GENOME ENGINEERING IN <i>KLUYVEROMYCES MARXIANUS</i> FOR ENHANCED SECRETION OF RECOMBINANT ANTIBODIES	303
Justina Žičkutė, Danguolė Žiogienė, Alma Gedvilaitė	

SYNTHESIS AND IN SILICO ANALYSIS OF 3-(1-(3-TOLYL)THIOUREIDO)PROPANOIC ACID DERIVATIVES AS ARACHIDONIC ACID METABOLIC PATHWAY INHIBITORS	304
Simonas Gruodis, Kazimieras Anusevičius, Birutė Grybaitė, Ilona Jonuškienė, Birutė Sapijanskaitė-Banevič, Vytautas Mickevičius	
THERMODYNAMIC AND DIELECTRIC PROPERTIES OF THE IMMUNE COMPLEXES BETWEEN SPECIFIC ANTIBODY AND SARS-CoV-2 B.1.1.529 SPIKE PROTEIN	305
Beatričė Urbaitė, Silvija Jučiūtė, Ieva Plikusienė	
PURIFICATION AND ACTIVITY OF THE CHIMERIC SEPTU ANTI-VIRAL DEFENSE SYSTEM	306
Marija Duchovskytė, Dalia Smalakyte, Gintautas Tamulaitis	
ANALYSIS OF PROBIOTIC BACTERIA <i>EXTITLACTICASEIBACILLUS PARACASEI</i> SMALL RNAs INVOLVED IN STRESS RESPONSE	307
Odilija Safinaitė, Milda Mickutė, Renatas Krasauskas, Giedrius Vilkaitis	
ROLE OF SOLUBLE PD-1 AND PD-L1 IN PROSTATE CANCER	308
Žilvinas Survila, Margarita Žvirblė, Lukas Šimkus, Gintaras Zaleskis, Vita Pašukonienė	
ISOLATION AND EVALUATION OF MICROPLASTICS EXTRACTED FROM SEWAGE SLUDGE	309
Dovilė Motiejauskaitė, Karolina Barčauskaitė	
METAGENOMIC ANALYSIS OF THE MICROBIOME COMPOSITION OF APHIDS ADELGES (APHRAS-TASIA) PECTINATAE (HEMIPTERA: ADELGIDAE)	310
Gustė Tamošiūnaitė, Jekaterina Havelka, Nomeda Kuisienė	
MOLECULAR DETECTION OF <i>BORRELIA</i> SPP. IN RED SQUIRREL (<i>SCIURUS VULGARIS</i>)	311
Ugnė Medikaitė, Indrė Lipatova, Justina Snegiriovaitė, Jana Radzijeuskaja, Algimantas Paulauskas	
STUDY OF SOIL HEAVY METAL POLLUTION IMPACT ON THE ONION (<i>ALLIUM CEPA</i> L.) CIRCA-DIAN RHYTHM	312
Goda Petraitytė, Asta Stapulionytė	
MICRORNA SIGNATURES AS PREDICTIVE TOOLS FOR NEOADJUVANT CHEMOTHERAPY RE-SPONSES IN TNBC	313
Domas Štītīlis, Adomas Vasiliauskas, Linas Kunigėnas, Monika Drobniėnė, Eglė Strainienė, Kęstutis Sužiedėlis	
INVESTIGATION OF CHANGES IN OXIDATIVE STRESS BIOMARKERS: CATALASE ACTIVITY AND METALLOTHIONEIN LEVELS IN THE LIVER OF RAINBOW TROUT (<i>ONCORHYNCHUS MYKISS</i>) AFTER EXPOSURE TO MICROPLASTIC PELLETS	314
Vita Žvynakytė, Janina Pažusienė, Gintarė Sauliūtė, Milda Stankevičiūtė	
URBAN MICROBIOLOGY OF VILNIUS. BACTERIAL DIVERSITY IN STREET GREENERY	315
Viktorija Kalasinskaitė, Nomeda Kuisienė	
THE ROLE OF CAPSULAR POLYSACCHARIDES AND OUTER MEMBRANE VESICLES IN THE PATHOGENESIS OF OPPORTUNISTIC PATHOGEN <i>ACINETOBACTER BAUMANNII</i>	316
Meda Skinkytė, Laurita Klimkaitė, Jūratė Skerniškytė	

ANALYSIS OF PUTATIVE BETA-LACTAMASES FROM OPPORTUNISTIC PATHOGEN STENOTROPHOMONAS MALTOPHILIA	317
Edvard Romanovski, Laurita Klimkaitė, Ignas Ragaišis, Julija Armalytė	
THE IMPACT OF ELECTRIC FIELD-BASED ANTICANCER METHODS ON CELL VIABILITY WHEN 2D AND 3D CELL CULTURE MODELS ARE USED	318
Gabija Andreikė, Neringa Barauskaitė-Šarkinienė, Vitalij Novickij, Paulius Ruzgys	
PHYTOCHEMICAL ANALYSIS OF BEE POLLEN IN IMPACT OF DIFFERENT STORAGE CONDITIONS AND DURATION	319
Rosita Stebuliauskaitė, Sonata Trumbeckaitė, Mindaugas Liaudanskas, Vaidotas Žvikas, Neringa Sutkevičienė	
ESTABLISHMENT AND CHARACTERIZATION OF NEW ENDOMETRIAL CANCER CELL LINES	320
Aistė Avižaitė, Laura Marija Račytė, Veronika Dedonytė, Evelina Šidlovskā, Margarita Montrimaitė, Gediminas Januška, Rūta Čiurlienė, Eglė Žalytė	
THE EFFECT OF MATERNAL HIGH-FAT DIET ON MORPHOLOGY AND INFLAMMATION OF OFF-SPRING RETINA	321
Patricija Čepauskytė, Gintarė Urbonaitė, Neda Ieva Biliūtė, Guoda Laurinavičiūtė, Urtė Neniškytė	
FUNCTIONAL ANALYSIS OF HISTONE METHYLATION REGULATORY GENES IN PROSTATE CANCER CELL LINES	322
Marta Tamosiunaite, Ruta Maleckaite, Kristina Daniunaite	
INVESTIGATION OF MITOCHONDRIAL NETWORK IN KERATINOCYTES WITH PSORIATIC PHENOTYPE	323
Martyna Uldukytė, Gabrielė Kulkovienė, Zbigniew Balion, Ramunė Morkūnienė, Aistė Jekabsone	
OPTIMISATION OF THE EXTRACTION OF PHENOLIC COMPOUNDS FROM PLUM (PRUNUS DOMESTICA L.) FRUIT MESOCARPS USING RESPONSE SURFACE METHODOLOGY	324
Gabrielė Bočkutė, Mindaugas Liaudanskas, Kristina Zymonė, Jonas Viškelis, Juozas Lanauskas	
SYNTHESIS AND CHARACTERISATION OF A MACROPHAGE-DERIVED HYBRID NANOSYSTEM FOR DOXORUBICIN DELIVERY TO GLIOBLASTOMA	325
Girstautė Dabkevičiūtė, Christian Celia, Vilma Petrikaitė	
ANTIMICROBIAL PROPERTIES OF BLACK SOLDIER FLY LARVAE PROTEIN EXTRACTS	326
Guoda Varnelytė, Bazilė Ravoitytė, Stanislavas Tracevičius, Elena Servienė	
THE EFFECTS OF HERBICIDE GLYPHOSATE ON THE NUTRITIONAL ECOLOGY OF CARABID BEETLES	327
Ieva Olechnavičiūtė, Norbertas Noreika	
ANALYSIS OF PAH METABOLITES AND ANTIOXIDANT CAPACITY IN MUSSELS (<i>Unio pictorum</i>) FROM NEMUNAS RIVER (LITHUANIA)	328
Reda Nalivaikienė, Virginija Kalcienė, Aleksandras Rybakovas, Dominykas Musneckis, Laura Butrimavičienė	
R-RAS-2 AS A POTENTIAL PREDICTIVE TARGET IN TRIPLE-NEGATIVE BREAST CANCER	329
Justas Burauskas, Agnė Šeštokaitė, Monika Drobniėnė, Rasa Sabaliauskaitė	

INACTIVATION OF ANTIBIOTIC-RESISTANT OPPORTUNISTIC PATHOGEN STENOTROPHOMONAS MALTOPHILIA BY CHLOROPHYLLIN-BASED ANTIMICROBIAL PHOTODYNAMIC THERAPY	330
Justė Tamulionytė, Irina Buchovec, Edita Sužiedėlienė	
DESIGN AND SYNTHESIS OF MUTANT VARIANTS OF THE ALLERGEN COMPONENT ART V 3 FROM ARTEMISIA VULGARIS	331
Eva Kupetytė, Laima Čepulytė, Rasa PetraitytėBurneikienė	
MORPHOLOGICAL AND METABOLIC CHANGES IN BONE MARROW MESENCHYMAL STEM CELLS INDUCED BY HIF-1 ALPHA INHIBITOR LW6	332
Ignas Lebedis, Jolita Pachaleva, Eiva Bernotienė, Giedrius Kvedaras, Ilona Uzieliene	
COMPARATIVE IMPACT OF β-CYCLODEXTRIN AND MUSTARD EXTRACT ON STABILITY IN RED CLOVER EXTRACT-LOADED MICROCAPSULES	333
Jurga Andreja Kazlauskaitė, Jurga Bernatoniene	
FUNCTIONAL ANALYSIS OF ANTIVIRAL BREX PROTEINS	334
Aistė Petrauskaitė, Tomas Šinkūnas	
ANALYSIS OF IN VITRO CYTOTOXICITY AND GENOTOXICITY OF POLYSTYRENE NANOPARTICLES IN HUMAN HEPATOMA CELL LINE (HEPG2)	335
Emilija Striogaitė, Milda Babonaitė, Juozas Rimantas Lazutka	
THE SYNERGISTIC EFFECT OF TYROSINE KINASE INHIBITORS AND DOXORUBICIN IN TRIPLE-NEGATIVE BREAST CANCER	336
Ugnė Mekionytė, Vilma Petrikaitė	
DETERMINANTS OF INTRACELLULAR LOCALISATION OF NATIVE SACCHAROMYCES CEREVISIAE VIRUSES	337
Aušrinė Jašmontaitė, Gerda Skinderytė, Aleksandras Konovalovas, Saulius Serva	
ASSESSMENT OF PATHOGENIC OOMYCETES IMPACT ON <i>Salmosalar</i> L LARVAE USING OXIDATIVE STRESS BIOMARKERS	338
Eglė Gadeikytė, Gintarė Sauliūtė, Arvydas Markuckas, Milda Stankevičiūtė	
MYOGENIC AND EPITHELIOGENIC DIFFERENTIATION OF ADIPOSE AND BUCCAL MUCOSAL STEM CELLS FOR ARTIFICIAL URETHRA CONSTRUCTION	339
Andrius Buivydas, Povilas Barasa, Egidijus Šimoliūnas, Ieva Rinkūnaitė, Emilija Baltrukonytė, Virginija Bukelskienė	
DI(2-ETHYLHEXYL)PHTHALATE AND DIBUTYLPHTHALATE GENOTOXIC EFFECT ON RAT ERYTHROCYTES	340
Laurynas Orla, Edita Paulikaitė, Violeta Žalgevičienė, Rasa Aukštikalnienė, Vaidotas Valskys, Grita Skujienė	
A MULTIPARAMETRIC ANALYSIS OF HUMAN MONOCYTE-DERIVED MACROPHAGE RESPONSE TO CARBON BLACK PARTICLES IN VITRO	341
Justina Pajarskienė, Ieva Uogintė, Steigvilė Byčenkienė, Rūta Aldonytė	

INVESTIGATION OF THE PHOTOSTABILITY OF MAGNESIUMCHLOROPHYLLIN IN BACTERIAL SUSPENSIONS	342
Loreta Stankevičiūtė, Irina Buchovec	
THE IMPACT OF AMINO AND CARBOXYL FUNCTIONAL GROUPS ON AMPEROMETRIC UREA BIOSENSOR AND POTENTIAL APPLICATIONS FOR AGRICULTURE	343
Gerda Šimėnaitė, Vidutė Gurevičienė, Marius Butkevičius	
TAU PROTEIN AND S100A9 CO-INTERACTION STUDIES	344
Lukas Krasauskas, Andrius Sakalauskas, Mantas Ziaunys, Vytautas Smirnovas	
CHANGES IN ELECTROPHYSIOLOGICAL PROPERTIES OF MOUSE CA1 PYRAMIDAL NEURONS DURING EARLY POSTNATAL DEVELOPMENT	345
Emilija Kavalnytė, Kornelija Vitkutė, Daiva Dabkevičienė, Igor Nagula, Urtė Neniškytė, Aidas Alaburda	
EVALUATION OF BIOFILM FORMATION AND BIOFILM-ASSOCIATED GENES DISTRIBUTION IN CLINICAL ISOLATES OF OPPORTUNISTIC PATHOGEN STENOTROPHOMONAS MALTOPHILIA	346
Dominykas Grigorjevas, Laurita Klimkaitė, Edita Sužiedėlienė, Julija Armalytė	
NEUROPROTECTIVE EFFECT OF PLANT DERIVED NANOVESICLES IN ISCHEMIA MODEL	347
Viktorija Kurmytė, Rokas Nekrošius, Zbigniew Balion	
TOWARDS WHOLE-CELL BIOSENSOR DEVELOPMENT FOR MONITORING NATURALLY OCCURRING PHENOLIC ACIDS	348
Ernesta Augustiniene, Ingrida Kutraite, Ilona Jonuskiene, Naglis Malys	
CALCIUM-INDUCED HETERODIMERIZATION OF S100A8 WITH S100A1 TRIGGERS AMYLOID FIBRILLATION	349
Viktorija Karalkevičiūtė, Ieva Baronaitė, Darius Šulskis, Vytautas Smirnovas	
A COMPARATIVE STUDY OF ELECTROPORATION-INDUCED CELL DEATH IN SUSPENSION AND MONOLAYER CULTURES	350
Aras Rafanavičius, Ingrida Šatkauskienė, Saulius Šatkauskas	
DEVELOPMENT OF AN INNOVATIVE SCAFFOLD MADE FROM DECELLULARIZED CANINE BONE FOR USE IN VETERINARY DENTISTRY	351
Łukasz Młynarski, Julia Niegowska, Tomasz Gębarowski, Maciej Janeczek	
THE SEA BUCKTHORN BERRY POMACE AND LEAF EXTRACTS: INVESTIGATION OF BIOLOGICALLY ACTIVE COMPOUNDS AND ANTIBACTERIAL PROPERTIES	352
Juozas Girtas, Natalja Makštutienė, Karolina Almonaitytė, Antanas Šarkinas	
ADVANCING GGT RESEARCH WITH SECM AND NOVEL ELECTROCHEMICAL PROBES	353
Tomas Mockaitis, Sheng-Tung Huang, Inga Morkvėnaitė-Vilkončienė	
POLYPYRROLE-MODIFIED SACCHAROMYCES CEREVISIAE USED IN MICROBIAL FUEL CELL	354
Domas Pirštelis, Kasparas Kižys, Inga Morkvėnaitė-Vilkončienė	

ADAPTABLE TARGET DNA LIBRARY CONSTRUCTION FOR BENCHMARKING PROGRAMMABLE NUCLEASES	355
Agata Kipran, Urtė Glibauskaitė, Rokas Grigaitis, Stephen Knox Jones Jr, Lina Krikščikaitė	
COMPARATIVE STUDIES OF THE EFFECT OF LORATADINE AND DESLORATADINE ON NOVOCAINE HYDROLYSIS	356
Anastasiia Behdai, Roman Smishko, Vadym Lisovyi, Volodymyr Bessarabov, Galina Kuzmina, Olha Syviuk	
ENGINEERING DNMT1 FOR CATALYTIC ACTIVITY WITH SYNTHETIC ADOMET ANALOGS	357
Karina Račaitė, Aleksandras Čečkauskas, Vaidotas Stankevičius, Saulius Klimašauskas, Liepa Gasiulė	
INHIBITION OF CRISPR-CAS DEFENCE BY ANTI-CRISPR PROTEINS	358
Melita Graužinytė, Tomas Šinkūnas	
THE QUANTITATIVE COMPOSITIONS OF MATRIX METALLOPROTEINASES IN BLOOD PLASMA OF DONOR GROUPS WITH VARIOUS TITERS OF ANTI-SARS-COV-2 IGG	359
Antonina Rachkovska, Vitaliy Karbovskiy, Maryna Kalashnikova	
DEVELOPMENT OF A MOLECULARLY IMPRINTED POLYMER IMMUNOSENSOR FOR THE SEROLOGICAL DETECTION OF SARS-CoV-2 PROTEIN	360
Viktorija Liustrovaitė, Vilma Ratautaitė, Arūnas Ramanavičius	
TRANSGLUTAMINASE APPLICATION FOR CARRIER-FREE ENZYME IMMOBILIZATION BY CLEA METHOD	361
Augustinas Vadeiša, Ieva Ožiūnaitė, Inga Matijošytė	
INVESTIGATION OF LIPASE IMMOBILISATION BY CROSS-LINKED ENZYME AGGREGATE (CLEA) METHOD	362
Kristupas Valaitis, Justinas Babinskas, Inga Matijošytė	
APPLICATION AND OPTIMIZATION OF THE ASPERGILLUS NIGER EXTRACELLULAR ENZYME SYSTEM FOR THE DEGRADATION OF SUGAR BEET PULP (SBP)	363
Žydrūnė Gaižauskaitė, Renata Žvirdauskienė, Daiva Žadeikė	
THE UTILISATION OF JUICE INDUSTRY WASTE FOR THE EXTRACTION OF ASCORBATE OXIDASE	B64
Patrycija Kostiukevič, Yelyzaveta Gushchyna, Jolanta Sereikaitė	
OPTIMISATION OF THE EXTRACTION OF PHENOLIC COMPOUNDS AND ORGANIC ACIDS FROM CONIFEROUS FOREST WASTE AND THEIR MICROBIOLOGICAL CHARACTERISTICS	365
Karolina Almonaitytė, Žydrūnė Gaižauskaitė, Juozas Girtas, Antanas Šarkinas, Sandra Kiseliovienė, Natalja Makštutienė, Alviša Šalaševičienė	
TOTAL INTERNAL REFLECTION ELLIPSOMETRY STUDY OF SARS-COV-2 OMICRON SPIKE PROTEIN AND POLYCLONAL ANTIBODIES INTERACTION	366
Mantvydas Usvaltas, Vincentas Mačiulis, Ieva Plikusienė	
APPLICATION OF SUSTAINABLE TECHNOLOGICAL SOLUTIONS FOR THE DEVELOPMENT OF FERMENTED PLANT PRODUCTS	367
Gabija Steigvilaitė, Lina Vaičiulytė	

CHANGES IN CYSTEINE PROTEASE ACTIVITY FROM ANANAS COMOSUS OVER TIME	368
Taisa Vashkevich, Vilma Kaškonienė, Audrius Sigitas Maruška	
CHARACTERISATION OF FOUR ALPHA-L-FUCOSIDASES FROM ALPACA FECAL MICROBIOME METAGENOMIC LIBRARY	369
Pijus Serapinas, Rūta Stanislauskienė, Rasa Rutkienė, Renata Gasparavičiūtė, Agnė Krupinskaitė, Rolandas Meškys, Jonita Stankevičiūtė	
TRANSMISSION OF ACTION POTENTIALS THROUGH INTERNODAL CELLS OF NITELLOPSIS OBTUSA: INVESTIGATION OF THE EFFECT OF GLUTAMATE	370
Radvilė Janušauskaitė, Vilmantas Pupkis, Vilma Kisnierienė, Indrė Lapeikaitė	
CHARACTERIZATION, DEVELOPMENT, AND APPLICATION OF GENTISIC ACID BIOSENSORS	371
Ingrida Kutraite, Ernesta Augustiniene, Naglis Malys	
STUDY OF NEW ANTI-PHAGE DEFENSE SYSTEMS	372
Viktorija Rainytė, Paulius Toliušis, Mindaugas Zaremba	
COMPARING COPPER AND MAGNESIUM CHLOROPHYLLIN-CHITOSAN COMPLEXES	373
Gabrielė Vasiliauskaitė, Irina Buchovec	
PREPERATION OF WATER-SOLUBLE BETA-CAROTENE-XYLAN COMPLEX	374
Elžbieta Karvovska, Rūta Gruškienė	
SURFACE PLASMON RESONANCE IMMUNOSENSOR FOR ACCURATE DETECTION OF ANTIBODIES AGAINST SARS-COV-2 NUCLEOCAPSID PROTEIN	375
Viktorija Lisyte, Almira Ramanaviciene, Anton Popov	
THE FIRST STEP TOWARDS HUMANIZED RECOMBINANT TAU PROTEIN IN P. PASTORIS YEASTS	376
Airdas Jonušas, Lukas Krasauskas, Vytautas Smirnovas, Justina Versockienė, Eglė Lastauskienė	
INHIBITION OF A BACTERIAL ANTIVIRAL BREX DEFENSE SYSTEM	377
Justė Adomaitytė, Tomas Šinkūnas	
S100A8 PROTEIN INTERACTION WITH LIPID MEMBRANES	378
Rimgailė Tamulytė, Darius Šulskis, Marija Jankunec	
STUDY OF THE OPTICAL AND FLUORESCENCE PROPERTIES OF THE COMPLEX OF CARBON QUANTUM DOTS AND COMPOUNDS WITH ANTICANCER PROPERTIES	379
Martynas Zalieckas, Katsiaryna Charniakova, Renata Karpicz	
DEER SPECTROSCOPY OF S100A9 PROTEIN	380
Aistė Peštenytė, Gediminas Usevičius, Darius Šulskis, Ieva Baronaitė, Vytautas Smirnovas, Jūras Banys, Mantas Šimėnas	
DEVELOPMENT AND OPTIMIZATION OF A MONOCLONAL ANTIBODY-BASED SYSTEM FOR QUANTIFICATION OF hBiP	381
Gabija Klimavičiūtė, Evaldas Čiplys, Rimantas Slibinskas, Aurelija Žvirblienė, Martynas Simanavičius	

PREPARATION AND CHARACTERIZATION OF ENCAPSULATED MICROALGAE EXTRACT FROM ARTHROSPIRA PLATENSIS	382
Vesta Navikaite-Snipaitiene, Emilija Galkauskaite, Dovile Liudvinaviciute, Ramune Rutkaite, Vaida Kitryte-Syrpa, Michail Syrpas	
HYDROLYSIS OF ALKYL FUCOSIDES BY ALPHA-L-FUCOSIDASES	383
Daniel Parvicki, Rūta Stanislauskienė, Rasa Rutkienė, Agnė Krupinskaitė, Jonita Stankevičiūtė, Rolandas Meškys	
TNPB-DNA INTERACTION STUDIES IN VITRO USING SINGLE-MOLECULE FLUORESCENCE MICROSCOPY	384
Monika Roliūtė, Aurimas Kopūstas, Marijonas Tutkus	
DEVELOPMENT OF THE SCREENING SYSTEM FOR TRANSPOSABLE ELEMENTS	385
Bartė Žiliukaitė, Gytis Druteika, Tautvydas Karvelis	
FTIR-ATR ANALYSIS FOR THE OPPORTUNISTIC YEASTS GROWN IN SIMULATED MICROGRAVITY AND RESISTANCE TO PHYSICAL AGENTS	386
Irmantas Čiužas, Gerda Anužienė, Justina Versockienė, Eglė Lastauskienė	
DISINFECTION OF MICROORGANISMS WITH FAR-UVC 222 NM IRRADIATION	387
Simona Jaseliunaite, Dovile Cepukoit, Daiva Burokiene	
CONSTRUCTION OF BACTERIOPHAGES GENOMIC LIBRARY	388
Migle Plioplyte, Jonas Juozapaitis, Giedrius Sasnauskas	
STABILITY OF L-A1 VIRUS-LIKE PARTICLES PURIFIED FROM SACCHAROMYCES CEREVISIAE	389
Kamilė Vaišaitė, Enrika Celitan, Saulius Serva	
FUNCTIONAL ANALYSIS OF CRISPR-CAS TYPE I-D SYSTEM AND WYL DOMAIN-CONTAINING PROTEIN	390
Gabija Naujokaitė, Jonas Juozapaitis, Arūnas Šilanskas, Tomas Šinkūnas, Virginijus Šikšnys, Inga Songailienė	
UPCONVERTING NANOPARTICLES AND PHOTSENSITIZER CHLORIN E6 COMPLEX FOR CANCER THERANOSTICS	391
Emilė Pečiukaiytė, Simona Steponkienė, Eglė Ežerskytė, Vaidas Klimkevičius, Vitalijus Karabanovas	
INTERACTION OF ALKYLPHOSPHOLIPIDS WITH TETHERED BILAYER LIPID MEMBRANES	392
Rūta Bagdonaitė, Artūras Polita	
CHANGES OF PHOTOSYNTHETIC PARAMETERS IN MICROALGAE INDUCED BY PHOTOOXIDATIVE STRESS	393
Rasa Miliukaitė, Agnė Kalnaitytė-Vengeliene	
OPTIMAZING LINKER PEPTIDE FOR EFFECTIVE PRESENTATION OF Aga2 AND A. baumannii B1p1 C-TERMINAL FRAGMENT FUSION PROTEIN ON THE SURFACE OF S. cerevisiae	394
Arūnė Verbickaitė, Ieva Šapronytė, Rasa Petraitytė Burneikienė	

ANTIOXIDANT PROPERTIES OF THE SOLID DISPERSION SYSTEM OF HESPERIDIN OBTAINED BY THE CENTRIFUGAL FIBER FORMATION METHOD	395
Vadym Lisovyi, Viktoriia Lyzhniuk, Volodymyr Bessarabov, Andriy Goy, Galina Kuzmina, Olga Kovalevska	
ACTIVATION AND REGULATION OF THE TYPE-III CRISPR-CAS ASSOCIATED SIGNALING CAS-CADE	396
Dalia Smalakyte, Audrone Ruksenaite, Giedrius Sasnauskas, Giedre Tamulaitiene, Gintautas Tamulaitis	
FTDMP: A FRAMEWORK FOR PROTEIN-PROTEIN, PROTEIN-DNA AND PROTEIN-RNA DOCKING AND SCORING	397
Rita Banciul, Kliment Olechnovič, Justas Dapkūnas, Česlovas Venclovas	
The ASCH domain-containing protein from Thermus thermophilus acts as a tRNA deacetylase	398
Greta Gakaite, R Statkevičiūtė, R Meškys	
QUANTITATIVE AND QUALITATIVE ANALYSIS OF MONOTERPENES AND SESQUITERPENES IN INDUSTRIAL HEMP BIOMASS	399
Algimanta Kundrotaitė, Karolina Barčauskaitė	
MECHANISM OF CRISPR-CAS3 HELICASE USING MAGNETIC TWEEZERS	400
Miglė Šarpilo, Algirdas Toleikis	
ANALYSIS OF FLUORESCENCE SPECTRA OF COPPER CHLOROPHYLLIN SOLUTIONS	401
Laura Kaziūnaitė, Irina Buchovec	
PHOTOSENSITIZER TPPS₄ AGGREGATION AND AGGREGATE TYPE SPECTROSCOPIC STUDIES IN NEUTRAL AND HIGHLY ACIDIC PH ENVIRONMENTS	402
Greta Tamoliūnaitė, Vilius Poderys, Ričardas Rotomskis	
MAMMALIAN CELLS ELECTROPORATION IN THE MICROFLUIDIC CHIP	403
Agne Damarackaitė, Neringa Bakute, Arunas Stirke	

25 YEARS AFTER THE FREQUENCY COMB REVOLUTION: TRANSFORMING INDUSTRIES WITH DUAL-COMB LASERS

Ursula Keller¹

¹Department of Physics, ETH Zurich, Switzerland

Since 1999, the frequency comb revolution has significantly impacted research in frequency metrology, optical clocks, and attosecond science. About ten years ago, the introduction of the single-cavity dual-comb laser opened up many industrial applications in spectroscopy and time-resolved measurements. This keynote will offer an introduction, explain the innovations, and show how they are all connected.

ATTOSECOND QUANTUM DYNAMICS

Jens Biegert^{1,2}

¹ICFO - Institut de Ciències Fòniques, The Barcelona Institute of Science and Technology, 08860 Castelldefels (Barcelona), Spain

²ICREA, Pg. Lluís Companys 23, 08010 Barcelona, Spain

Strong field physics gives rise to a variety of phenomena, ranging from coherent electron diffraction to attosecond soft X-ray emission [1]. We have, over the years, developed intense sources of waveform- controlled mid-IR light [2] to exploit aspects such as the ponderomotive scaling, quantum diffusion, and quasi-static photoemission. I will describe how we generate isolated attosecond pulses in the soft X-ray water window [3] across the oxygen edge up to 600 eV. Furthermore, I will explain how attosecond soft x-ray science can provide an entirely new angle into the quantum many body dynamics in real-time [4]. I will describe two applications, addressing some of the most intricate challenges in contemporary physics pertaining to solids [5] and molecular science [6].

[1] B. Wolter et al. Phys. Rev. X 5, 021034 (2015).

[2] U. Elu et al. Nature Phot. 15, 277-280 (2021).

[3] S. M. Teichmann et al. Nature Commun. 7, 11493 (2016).

[4] T.P.H. Sidiropoulos et al. Nature Comm. 14, 7407 (2023)

[5] T.P.H. Sidiropoulos et al. Phys. Rev. X. 11, 041060 (2021).

[6] S. Severino et al. arxiv:2209.04330.

SPACE EXPLORATION AND UTILIZATION

Charles Elachi¹

¹California Institute of technology, 383 S Hill Ave, Pasadena, CA, USA

We live in a Golden Age of Space Exploration. In the last 25 years we have visited every planet in our solar system, probed deep space and discovered extrasolar planets, landed on Mars and Titan, had rovers continuously roving on Mars, demonstrated powered flight on Mars and continuously had astronauts in Space. With the technological advances in electronics, material, structures, communications, etc. . . we now have affordable space systems imbedded in our day to day life (gps, internet, meteorological prediction, map production . . .) and commercial companies, startups, universities are playing an increasingly larger role in Space utilization.

This talk will give an overview of the last 25 years let achievements and opportunities for the next 25 years.

ANTIMATTER MATTERS: THE LARGE HADRON COLLIDER BEAUTY EXPERIMENT AT CERN

Chris Parkes¹

¹University of Manchester, Department of Physics and Astronomy

The Large Hadron Collider (LHC) at CERN is the world's largest and most powerful particle accelerator. This facility and the physics opportunities it makes available will be outlined. One of the four large experiments at the LHC is the Large Hadron Collider beauty (LHCb) experiment, which has a particular focus on the study of differences between matter and antimatter. Over 700 scientific papers have resulted from its initial operating period (2010-2018), including the discovery of new types of matter antimatter difference and of over 60 new particles. The next era has now started for LHCb, with the Upgrade I experiment installed and taking data. This major upgrade allows a significant increase of data rate and provides a more powerful system for identifying the events to be retained for further study. Beyond this, the collaboration is planning an Upgrade II for the 2030s, an ambitious flavour physics experiment for the High-Luminosity LHC.

FEEDSTOCK ALKYNES AS A PLATFORM FOR MULTI-FUNCTIONALISATION VIA RADICAL CASCADE REACTIONS

Makeda Tekle-Smith¹

¹Department of Chemistry, Columbia University 3000 Broadway New York, NY 10027, USA

Controlling the three-dimensional structure of chemical matter is key to obtaining the desired function of a material. Photoredox catalysis is becoming increasingly important in these processes due to the mild reaction conditions that are generally involved, relative to thermal or chemical oxidative/reductive processes. The use of mild conditions permits the development of chemical transformations that are not only highly selective, but also tolerant of the presence of diverse functionality. Radical cyclisation reactions provide access to highly complex molecules in few synthetic steps. Moreover, the mild reactions conditions commonly employed in radical cascade reactions allow for broad functional-group compatibility and as such, have found numerous applications in natural product synthesis. Here, we describe a photoredox-catalyzed method for achieving 1,3-difunctionalization of unactivated alkanes using alkynes as linchpin radical acceptors and hydrogen atom abstractors. This new synthetic platform holds a promising outlook for advancing our understanding of carbon-to-carbon HAT and selective difunctionalization of alkanes.

NEW APPLICATIONS OF UPCONVERSION VIA EXPLORATION OF NOVEL ANNIHILATORS

Andrew B. Pun¹

¹Department of Chemistry and Biochemistry, University of California, 9500 Gilman Dr, La Jolla, San Diego, CA, US

Upconversion that proceeds via triplet fusion (TF), also known as triplet-triplet annihilation (TTA), has received widespread attention for its potential applications ranging from enhancing photovoltaic efficiency, to anti-counterfeiting, to improved 3D printing. In contrast to other mechanisms, TF upconversion is highly efficient even at sub-solar incident flux.

TF upconversion requires two species, a sensitizer which absorbs low energy photons, and an annihilator which emits high energy photons. Despite the breadth of potential applications of TF upconversion, very few annihilators have been studied.

Herein, I will discuss our work in developing new annihilators for TF upconversion. By focusing on annihilators that are synthesized via common wet chemical synthesis, we can develop libraries of molecules that are easily derivatized. This allows the development of structure-function relationships, to synthesize optimized annihilators for any desired application.

NANOSCALE TOOLS FOR SENSING AND IMAGING SINGLE MOLECULES

Viktorija Glembockytė¹

¹Department of Chemistry and Center for NanoScience (CeNS), Ludwig-Maximilians-University, Butenandtstraße 5–13, 81377 Munich, Germany

Advances in fluorescence imaging and microscopy techniques have provided the ability to detect and monitor biomolecules and the interactions between them at the ultimate sensitivity of a single molecule. In this talk I will discuss how single-molecule fluorescence imaging can be synergistically combined with a technique that allows one to also place and position single molecules on the nanoscale, namely, DNA origami, in the pursuit of building new single-molecule sensors and imaging tools. I will discuss how, using DNA as a building material, we can create light antennas on the nanoscale and amplify fluorescence signals of single molecules by up to few hundred-fold, enabling their detection on a smartphone camera [1]. I will also discuss our work on building modular and tunable sensors with high FRET contrast and single-molecule sensitivity. Utilizing a DNA origami nanostructure as a scaffold to arrange and decouple different sensor components we developed a single molecule sensing platform adaptable to a variety of biomolecular targets, such as nucleic acids, proteins, as well as enzymatic activities. The developed platform also offers mechanisms to tune the dynamic window and specificity of the sensor as well as to implement more complex multiplexed sensing schemes [2]. Finally, I will briefly touch on our efforts to develop strategies to increase the robustness and stability of DNA origami sensors and labels in challenging chemical and biochemical environments [3].

[1] Nat. Commun. 2021, 12, 950; Acc. Chem. Res. 2021, 54, 3338-3348; iScience 2021, 24, 10302; Adv. Mater. Interfaces 2022, 200255; ACS Nano 2023, 17, 1327.

[2] bioRxiv 2023, doi: <https://doi.org/10.1101/2023.11.06.565795>.

[3] Angew. Chem. 2020, 60, 4931; Adv. Mater. 2023, 35, 2212024.

SUPPRESSION OF FILAMENTATION BY PHOTONIC CRYSTALS

Edvinas Aleksandravičius¹, Darius Gailevičius¹, Audrius Dubietis¹, Kęstutis Staliūnas^{1,2,3}

¹Vilnius university

²Catalan Institution for Research and Advanced Studies

³Polytechnic University of Catalonia
edvinas.aleksandravicius@ff.vu.lt

Nonlinear propagation of intense ultrashort laser pulses in transparent materials produces a unique and spectacular phenomenon termed femtosecond filamentation. This leads to a transformation of an ultrashort-pulsed laser beam into a light filament, which possesses an ultra-broadband spectrum, termed supercontinuum. Here we propose and substantiate an alternative idea that photonic crystals can efficiently suppress the emerging filamentation. It is well known that photonic crystals can affect the overall diffraction of the beam. For example, the reduced or increased spatial dispersion curvature corresponds to weakened or strengthened diffraction. Another possibility is obtaining a spatial dispersion curve with a negative curvature corresponding to anti-diffraction. Considering this, we can infer that it is possible to devise a photonic crystal with such a geometry, that results in a spatial dispersion regime that can compensate for the nonlinear Kerr focusing of the beam, thus effectively suppressing filamentation. Numerical simulations were performed using a forward beam propagation method, which approximates the envelope of the beam propagating in a slowly varying medium. The profile of refractive index modulation is chosen to be harmonic in both the transverse X and the longitudinal Z directions. The periodicities in both directions were varied to determine an optimal geometry, with the longitudinal period being tied to the transverse period through the Talbot length. It is convenient to introduce the geometric constant Q which is the inverse of the longitudinal period normalized to the Talbot length. In the general case, for a photonic crystal with constant period and for all values of the geometric constant Q that are close to 1, there are multiple dispersion curves corresponding to different Bloch mode branches. This is often undesirable since it makes it impossible to precisely control the diffraction of the beam, however this issue can be overcome by introducing an adiabatic chirp to the longitudinal period of the photonic crystal. We do this by starting at a longitudinal period corresponding to a geometric constant Q sufficiently far from 1 and slowly approaching the desired Q . From the beam diameter evolutions, we can see that in the homogeneous case the beam diameter first increases, but eventually the beam starts to converge and collapses. Using those same beam parameters but this time in a photonic crystal we can see that the beam diameter again initially increases, however this time the beam does not collapse, instead the beam converges only a little and the beam diameter asymptotically approaches some value for which the diffraction and nonlinear focusing are balanced. The results show that using a photonic crystal with a geometry characterized by a value of Q close to 1 gives the desired result. In addition, using positive and negative chirp, both increased diffraction ($Q > 1$) and anti-diffraction ($Q < 1$) can be achieved.

SPECTRAL BROADENING AND POST-COMPRESSION OF FEMTOSECOND PULSES IN ZnS AND KGW CRYSTALS AT 76 MHz REPETITION RATE

Matas Šutovas¹, Vaida Marčiulionytė¹, Jonas Banys¹, Julius Vengelis¹, Gintaras Tamošauskas¹, Audrius Dubietis¹

¹Laser Research Center, Faculty of Physics, Vilnius University
matas.sutovas@ff.stud.vu.lt

An ongoing objective in laser physics is to attain increasingly shorter light pulses. For this, pulse spectral broadening is required. An extension of optical bandwidth by self-phase modulation in the bulk media, followed by post-compression is a simple and robust method to achieve even shorter light pulses. By using multiple plate approach instead of one continuous nonlinear medium, peak and average power scalability is introduced, leading to no further losses in efficiency [1]. Further investigation of new bulk media with optimal characteristics is necessary to achieve pulse spectral broadening in high repetition rate (tens of MHz) and high average power near-infrared laser systems. Recent studies have demonstrated that zinc sulfide (ZnS) and potassium gadolinium tungstate (KGd(WO₄)₂, KGW) crystals are emerging as potential materials for this purpose due to their relatively high resistance to multipulse optical damage and high nonlinearity compared to commonly used fused silica and sapphire [1-3].

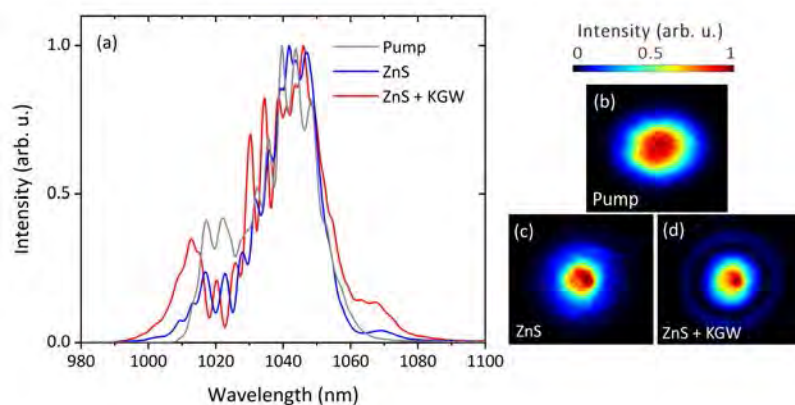


Fig. 1. (a) Comparison of spectral broadening in a single ZnS crystal and the double-pass ZnS+KGW setup. Far-field output beam profiles from pump (b), single ZnS crystal (c) and double-pass ZnS+KGW (d) setups.

In this work, double-pass spectral broadening setup consisting of first ZnS (2 mm) and second KGW (6 mm) crystals was investigated using an Yb:KGW oscillator (FLINT, Light Conversion Ltd.) with a single-pass pre-chip managed (PCMA) rod-type fiber amplifier system, which produced 75 fs pulses with an average power of 15.7 W and a central wavelength of 1038 nm at 76 MHz repetition rate [4]. Symmetric pump pulse spectral broadening due to self-phase modulation in single ZnS and ZnS+KGW setups is shown in Figure 1 (a). Beam profile measurements revealed no significant change in beam quality at the output of the single ZnS crystal setup [Fig.1(b,c)]. The second harmonic frequency-resolved optical gating technique (SHG-FROG) was used for temporal characterization of the pulses after the spectral expansion stage and post-compression stage, which was realized by Gires-Tournois interferometric mirrors. After the first and second stages of spectral broadening, the pump pulses were chirped over 100 fs and over 160 fs, respectively. Pulse compression was limited to 45 fs due to a rapid degradation of the beam quality with the further increase in pulse spectral expansion [Fig.1(d)]. Our results demonstrate a robust and versatile double-pass spectral broadening configuration, offering the potential for advancing the compression of high repetition rate femtosecond pulses which are relevant in the fields of ultrafast spectroscopy and microscopy.

- [1] M. Seidel, G. Arisholm, J. Brons, V. Pervak, O. Pronin, All solid-state spectral broadening: an average and peak power scalable method for compression of ultrashort pulses, *Opt. Express* 24, 9412-9428 (2016).
- [2] V. Marčiulionytė, J. Banys, J. Vengelis, R. Grigutis, G. Tamošauskas, A. Dubietis, Low-threshold supercontinuum generation in a homogeneous bulk material at 76 MHz pulse repetition rate. *Opt. Lett.* 48, 4609-4612 (2023).
- [3] M. Kowalczyk, N. Nagl, P. Steinleitner, N. Karpowicz, V. Pervak, A. Głuszek, A. Hudzikowski, F. Krausz, K. F. Mak, A. Weigel, Ultra-CEP-stable single-cycle pulses at 2.2 μm , *Optica* 10, 801-811 (2023).
- [4] J. Banys, J. Vengelis, Efficient single-pass and double-pass pre-chirp managed Yb-doped rod-type fiber amplifiers using Gires-Tournois interferometric mirrors, *Optik* 249, 168185 (2022).

PHOTOSENSITIZED AND NON-PHOTOSENSITIZED MATERIALS FOR MULTIPHOTON LITHOGRAPHY

Dimitra Ladika^{1,2}, Antanas Butkus², Michalis Stavrou¹, Gordon Zyla¹, Vasileia Melissinaki¹, Edvinas Skliutas², Elmina Kabouraki¹, Frederic Dumur⁵, David Gray¹, Saulius Juodkazis^{2,3,4}, Maria Farsari¹, Mangirdas Malinauskas²

¹Institute of Electronic Structure and Laser, Foundation for Research and Technology-Hellas, 70013 Heraklion, Greece

²Laser Research Center, Faculty of Physics, Vilnius University, Sauletekio Ave. 10, LT-10223 Vilnius, Lithuania

³Optical Sciences Centre and ARC Training Centre in Surface Engineering for Advanced Materials (SEAM), School of Science, Swinburne University of Technology, Melbourne, Australia

⁴WRH Program International Research Frontiers Initiative (IRFI) Tokyo Institute of Technology, Nagatsuta-cho, Midori-ku, Yokohama, Japan

⁵UMR 7273, Aix Marseille Univ., CNRS, ICR, 13397 Marseille, France

dladika@iesl.forth.gr

3D direct laser writing employing Multiphoton lithography (MPL) has emerged as a powerful tool in Additive Manufacturing (AM) at very small scale, both for scientific and industrial applications in various fields, such as micro-optics, tissue engineering and photonics [1]. MPL is based on the phenomenon of multiphoton absorption that is carried out as follows: an ultrafast laser beam is tightly focused inside the volume of a transparent photosensitive material, which typically incorporates a photosensitive molecule, the photoinitiator (PI). The PI absorbs simultaneously two or more photons of the incident light and produces free radicals, which eventually will induce photopolymerization, confined within the beam focus. The choice of a high-performance photoinitiator directly influences the speed, resolution, and quality of the 3D micro/nano structures. Upon this fact, the synthesis of novel photoresists and high-performance PIs for MPL has been the subject of investigation during the last decades [2]. To this end, this work introduces novel PIs [3], named as triphenylamine-based aldehydes, suitable for MPL. In this context, the two-photon absorption cross sections and 3D micro/nanostructures fabricated with the PIs will be shown. Furthermore, a wavelength-independent and non-photosensitized material for MPL is introduced. This is crucial for specific applications due to the two drawbacks of PIs: toxicity and fluorescence. Specifically, wavelengths of 517 nm, 780 nm, and 1035 nm are shown to be suitable for fabricating 300 nm features even at high scanning speeds (up to 100 mm/s) [4]. To conclude, the importance of efficient PIs is highlighted in this work, underlying their potential applications in photonics, optoelectronics etc. On the other hand, the limitations of a PI are minimized by excluding it from the material and studying the material's structuring properties for future applications in bio-scaffolds, tissue engineering, micro-optics etc.

[1] Wang, H. et al. Two-Photon Polymerization Lithography for Optics and Photonics: Fundamentals, Materials, Technologies, and Applications. *Adv Funct Mater* 2214211 (2023)

[2] Wloka, T. et al. From Light to Structure: Photo Initiators for Radical Two-Photon Polymerization. *Chemistry - A European Journal* 28, (2022)

[3] Ladika, D. et al. Synthesis and application of triphenylamine-based aldehydes as photo-initiators for multi-photon lithography. *Applied Physics A* 2022, 128, 1-8 (2022)

[4] Ladika, D. et al. X-photon 3D lithography by fs-oscillators: wavelength-independent and photoinitiator-free. PREPRINT (Version 1) available at Research Square 0-13 (2023)

3D GRADIENT PERIOD PHOTONIC CRYSTALS FABRICATED VIA ULTRAFAST LASER LITHOGRAPHY

Eulàlia Puig Vilardell^{1,2}, Darius Gailevičius², Mangirdas Malinauskas²

¹Erasmus Mundus Joint Master Degree EUROPHOTONICS

²Laser Research Center, Faculty of Physics, Vilnius University, Sauletekio Ave. 10, LT-10223 Vilnius, Lithuania
eulalia.puig@ff.stud.vu.lt

Two photon lithography is a Laser Direct Writing technique (DLW) that allows high precision 3D micro and nano-structures manufacturing with sub-diffraction-limit resolution. Thanks to the advent of femtosecond lasers, nonlinear light-matter interactions are achievable by focusing such high intensity beams into the photo-resins, which due to temporal and spatial overlap can result in two- or even multi-photon absorption inside the volume of the tightly focused laser beam, allowing to polymerize the material in a small confined region, Fig. 1a. This significant advantage makes it a suitable and high desirable technique for the fabrication of micro and nanoscale 3D structures, and it's been widely employed for applications in several fields such as microelectronics, microfluidics, life sciences or photonics.

In this work we explored one of these applications: the fabrication of a 3D photonic crystal, Fig. 1b, able to slow down while spatially separating the frequency components of the light, which results in a localized increase of light intensity chromatically resolved, and thus can be used for application in which enhanced light-matter interaction is required, like optical sensors, solar cells or night vision devices.

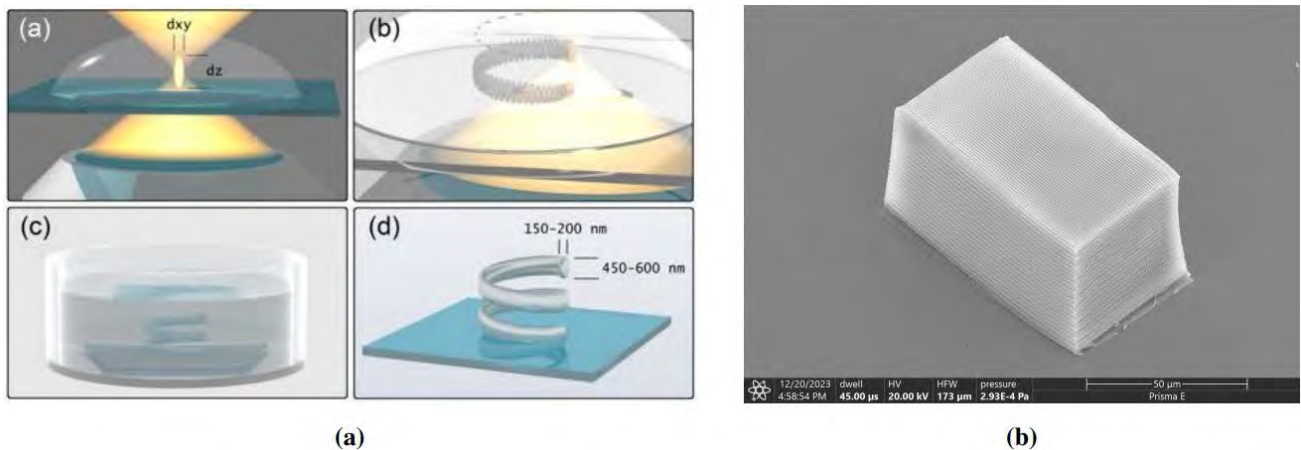


Fig. 1. (a) The principle of direct laser writing 3D nano-lithography, reproduced from [1]. (b) 3D woodpile structure designed for the realization of slow light fabricated via two photon lithography.

After studying how the different fabrication parameters influence the resulting structure, the optimal parameters have been used to fabricate a sample that fulfills the spatial requirements for it to be functional and act as a slowing light photonic crystal.

[1] S. Varapnickas and M. Malinauskas, Processes of Laser Direct Writing 3D Nanolithography (Springer International Publishing, Cham, 2020)

GaAsBi BASED NIR EMITTERS FOR BLOOD ANALYTE MONITORING

Aivaras Špokas¹, Andrea Zelioli¹, Andrius Bičiūnas¹, Aurimas Čerškus¹, Bronislovas Čechavičius¹, Augustas Vaitkevičius^{1,2}, Evelina Dudutienė¹, Mindaugas Kamarauskas³, Renata Butkutė¹

¹Center for Physical Sciences and Technology, Department of Optoelectronics, Saulėtekio av. 3, LT-10257 Vilnius, Lithuania

²Institute of Photonics and Nanotechnology, Faculty of Physics, Vilnius University, Saulėtekio av. 3, LT-10257, Vilnius, Lithuania

³Center for Physical Sciences and Technology, Department of Physical Technologies, Saulėtekio av. 3, LT-10257 Vilnius, Lithuania

aivaras.spokas@ftmc.lt

Pulse oximetry is one of the areas where light emitting diodes (LED) and laser diodes (LD), with emission wavelengths of 660 nm and 940 nm are currently used. Such configuration experiences main drawbacks in reflectance oximetry mode due to the variation of penetration depth into soft tissue. An alternative set of wavelengths (800nm and 1100 nm) is proposed to eliminate the issue of difference in penetration depth, while maintaining an absorption difference for oxyhaemoglobin and non-oxygenated haemoglobin.

In this work we present results of technological development of LEDs and LDs operating in 1 μm – 1.2 μm spectral region. The material chosen for such devices was GaAsBi due to its temperature stability, room temperature (RT) operation, rapid band gap reduction of up to 90 meV/% B_i , and better strain management, when comparing to classical NIR materials.

Optimization of molecular beam epitaxy growth parameters for 3 - 5 GaAsBi rectangular quantum well (RQW) structures was carried out. Two devices on GaAs substrates buffered by an AlAs sacrificial layer were fabricated. GaAsBi RQW based LED with a central emission wavelength of 1070 nm at RT was produced. Moreover, an LD with 3 GaAsBi RQWs was fabricated and room temperature lasing at 1142 nm was recorded. Temperature dependent electroluminescence showed stability of the emission wavelength for both devices.

This work was supported by Research Council of Lithuania under Contract No S-LLT-23-3; project "Development of A3B5-Bi Nanostructure Based Double-Wavelength Microlaser Technology for NIR Sensing Applications".

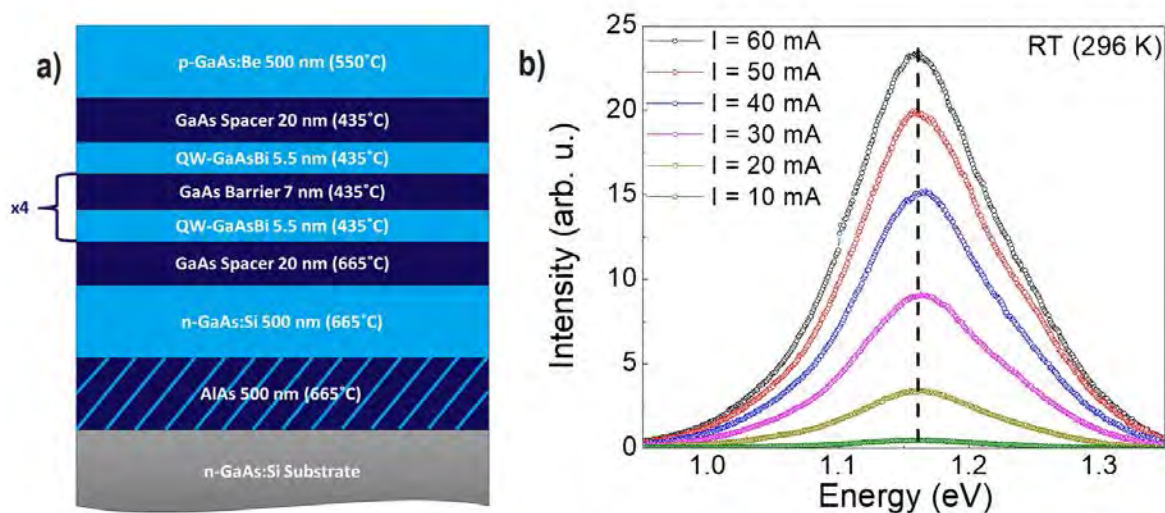


Fig. 1. a) GaAsBi 5xRQW LED structure. Growth temperatures provided from thermocouple readings. b) Excitation dependent RTEL measurement for GaAsBi 5xRQW LED (dashed line serves as eye guide).

THE GROWTH OF GaN(0001) ON Sc₂O₃(111)/Si(111) TEMPLATE VIA MOVPE METHOD

Petras Lapukas¹, Tomas Grinys¹, Tadas Malinauskas¹, Domantas Berenis¹, Arūnas Kadys¹

¹Vilnius University
lapukaspetras@gmail.com

Group III nitride semiconductors are widely used in optoelectronics, high-power and high-frequency electronic devices and have now become critically important in the modern world. To expand their applicability and integrity, researchers are developing various technologies for growing nitride semiconductors on Si, which is widely used in electronics.

This work aims to evaluate the impact of nitrogen and hydrogen atmospheres on the crystallographic and morphological properties of GaN layers grown on Sc₂O₃/Si substrates using the MOVPE method. To achieve this goal we performed several tasks: to grow GaN layers on Sc₂O₃(111)/Si(111) substrates using the MOVPE method in nitrogen and hydrogen atmospheres; to investigate the crystallographic and morphological properties of the grown structures; and to compare the physical properties of GaN layers grown in different atmospheres.

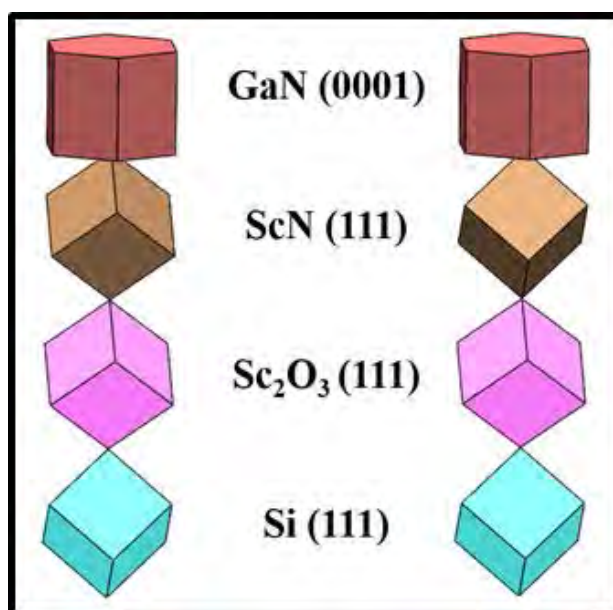


Fig. 1. Schematic view of unit cells, demonstrating the azimuthal orientations of different layers in the sample, where ScN exists in two orientations.

We have presented different layers of our samples and their unit cells azimuthal orientations, using XRD ω - 2θ and ϕ scans. We found that the successful growth of continuous c-axis oriented monocrystalline GaN layer on a Sc₂O₃/Si substrate is possible, despite the formation of a ScN layer composed of twins during the nitridation process of Sc₂O₃. We observed that the strain values along a and c axes calculated from GaN(0002) ω - 2θ scan do not depend on the atmosphere used during the growth. We compared them with strain values based solely on the differences in thermal expansion between GaN and Si. We found that the strain in the GaN layer is a result of a dual-component interaction: lattice mismatch between Si and GaN as well as their different thermal expansion rates. We also showed that controlling the growth atmosphere between N₂ and H₂ during various stages of the GaN growth on Sc₂O₃/Si templates allows to reduce the dislocation densities and enhance the surface morphology of GaN layers.

PEAK LUMINESCENCE SHIFT OF InGaN DEFECT VICINITIES USING SEM-CL MICROSCOPY

Mantas Migauskas¹, Viktorija Mickūnaitė¹, Žydrūnas Podlipskas¹

¹Vilnius university
mantas.migauskas@ff.stud.vu.lt

Researchers have been interested in defects of semiconductor materials for a long time now, because of their strong correlation to the electrical and mechanical properties of a given material. In indium gallium nitride (InGaN) structures, prominent features are V-shaped pits (V-pits), that form due to threading dislocations which propagate to the quantum well layers that are rich in indium. In this work we focus on cathodoluminescence peak wavelength shift of these V-pits and their locale.

To analyze said structures a custom *Python* code was written and used in combination with *Attomap* software. Since we are using hybrid cathodoluminescence and scanning electron microscope (SEM-CL), we get both CL and SEM images of the same area. While SEM lets us see sample topography, CL images each pixel has a whole cathodoluminescence signal spectrum, therefore by fitting Gaussian fit on the main signal peak, we can determine at what wavelength the peak sits. Doing this to all image pixels gives the same image but with each pixel having a peak wavelength associated with it. We call it peak wavelength shift (PWS) map, which lets us see how CL signal peak shifts in a sample.

Secondly, we detected V-pits using *Laplacian of Gaussian* (LoG) filter on SEM images. Since SEM and now generated PWS image areas are the same, we can directly transfer detected V-pits onto PWS image to start the analysis. By knowing the center coordinates and sizes of V-pits in PWS image, we can calculate how the CL peak shifts going outward in a radial pattern from the defect center. Plotting average values of each circle's circumference from V-pit center gave us radial profile of peak wavelength shift. To achieve statistically significant results, we performed this process for all detected V-pits in each image from measured samples and averaged them again across the whole image. An example radial profile of all detected V-pits in an image is shown below.

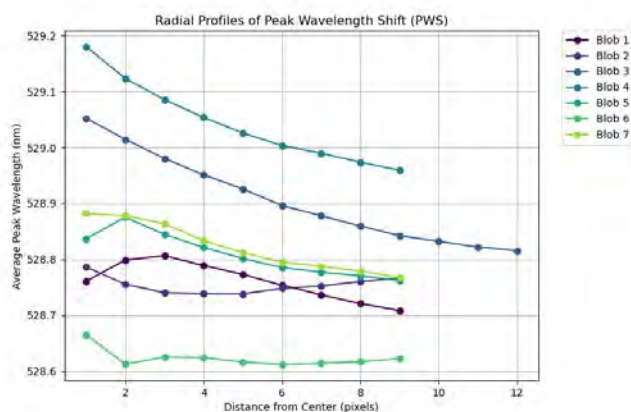


Fig. 1. PWS radial profiles of all detected V-pits in a single image

INFLUENCE OF AlGaAs BARRIER DESIGN ON PHOTOLUMINESCENCE OF GaAsBi QUANTUM STRUCTURES

Monika Jokubauskaitė¹, Aistė Butkutė¹, Aivaras Špokas¹, Andrea Zelioli¹, Evelina Dudutienė¹, Bronislovas Čechavičius¹, Renata Butkutė¹

¹Department of Optoelectronics, Center for Physical Sciences and Technology, Lithuania
monika.jokubauskaite@ftmc.lt

There is a high focus on the task to find a novel light-emitting material, which would serve a purpose of active media in light sources of near-infrared (NIR) range, but would also own superior properties than right now used alloys. One of the potential materials could be GaAsBi. By introducing bismuth atoms into GaAs lattice the bandgap of the alloy is rapidly reduced. Moreover, some unique properties belong to bismides, like large spin-orbit splitting energy and bandgap, less sensitive to temperature. There are already some examples of optoelectronic devices such as light-emitting diodes [1], which work based on GaAsBi. However, the lack of high crystal quality in GaAsBi is reducing the photoluminescence (PL) intensity. Thus, various designs of GaAsBi quantum structures are investigated towards optimization of its optical properties.

Our group [2] already demonstrated GaAsBi quantum wells (QWs) with parabolically graded barriers. Remarkably, a substantial enhancement in PL intensity at room temperature was observed in these structures, exhibiting approximately 50 times greater values than that of rectangular QWs. Moreover, it should be noted that the improved PL intensity was consistently reproducible across various growth conditions in parabolic quantum wells (PQWs). Also, in literature [3] one more design could be found - triangular quantum well (TQW), and its influence on PL was also investigated.

In this work a comparison study between PQW (Fig. 1. (a)) and TQW (Fig. 1. (b)) designs will be done with a goal to look into how barrier design determines carrier trapping and are there any other mechanisms responsible for enhanced PL intensity. Both investigated structures contain single rectangular GaAsBi QW embedded in parabolic or triangular AlGaAs QW. PL and photoluminescence excitation (PLE) techniques along with theoretical calculations will be used to evaluate different barrier design influence on carrier trapping and quality of GaAsBi QW.

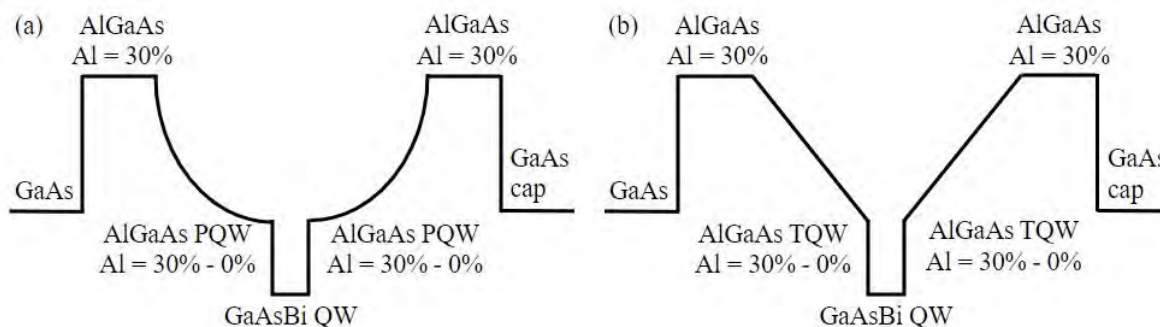


Fig. 1. Schemes of different investigated designs of AlGaAs barrier in GaAsBi quantum well structures: (a) single quantum well embedded in parabolic AlGaAs QW (PQW); (b) single quantum well embedded in triangular AlGaAs QW (TQW).

Acknowledgement

This research was supported by Research Council of Lithuania under the grant No. S-ST-23-199.

- [1] P.K. Patil, E. Luna, T. Matsuda, K. Yamada, K. Kamiya, F. Ishikawa, and S. Shimomura, GaAsBi/GaAs multi-quantum well LED grown by molecular beam epitaxy using a two-substrate-temperature technique, *Nanotechnology* 28, 105702 (2017).
 [2] S. Pūkienė, M. Karaliūnas, A. Jasinskas, E. Dudutienė, B. Čechavičius, J. Devenson, R. Butkutė, A. Udal, and G. Valušis, Enhancement of photoluminescence of GaAsBi quantum wells by parabolic design of AlGaAs barriers, *Nanotechnology* 30, (2019).
 [3] E.O. Göbel, J. Feldmann, and G. Peter, Non-equilibrium Carrier Kinetics in Quantum Wells, *Journal of Modern Optics* 35 (12), 1965-1977 (1988).

COMPARATIVE ANALYSIS OF BEAM FOCUSING ABILITIES OF METASURFACE BASED 250GHZ LENSES

Augustė Bielevičiūtė¹, Karolis Redekas¹, Kasparas Stanaitis¹, Ernestas Nacius¹, Vladislovas Čižas¹, Linas Minkevičius¹

¹Center for physical sciences and technology (FTMC)
auguste.bieleviciute@ftmc.lt

Split-ring resonator (SSR) based metasurface lenses have been a topic of active research in terahertz science [1]. Metasurface lenses offer several advantages over conventional lenses, including compactness, tunability and are employed for terahertz wavefront engineering [2]. In this study, we investigated the beam shaping capabilities of five different SSR designs with varying geometries.

The lenses were fabricated from 25 μm stainless steel foil using laser ablation [3]. Beam profiles were measured along the XZ and XY planes to evaluate the focusing capabilities along the optical axes in a focal plane.

Our results demonstrate that a specific paraxial design with four sub-zones employing two distinct SSR geometries (C03) exhibited best beam focusing performance compared to other lenses, achieving the smallest focus point of FWHM equal to ~ 1.5 mm and highest amplitude ~ 0.14 V at focal point. In contrast, C05 with a two-subzone design, had the poorest focusing performance, with a focal point of FWHM equal to ~ 1.74 mm and the lowest amplitude of ~ 0.063 V. Additionally, C04 had the largest FWHM of ~ 12.70 mm along the z-direction, indicating the broadest beam profile in z-direction among all five designs. C06, a non-paraxial design, demonstrated an amplitude of ~ 0.11 V and an XY plane FWHM of ~ 1.6 mm and was the second best lens for focusing after C03.

Understanding the intricacies of these metasurface lenses is crucial for advancing terahertz technology, opening up avenues for applications that leverage their unique properties, such as enhanced imaging, communication [4,5].

This research has received funding from the Research Council of Lithuania (LMTLT), agreement No [S-MIP-22-76].

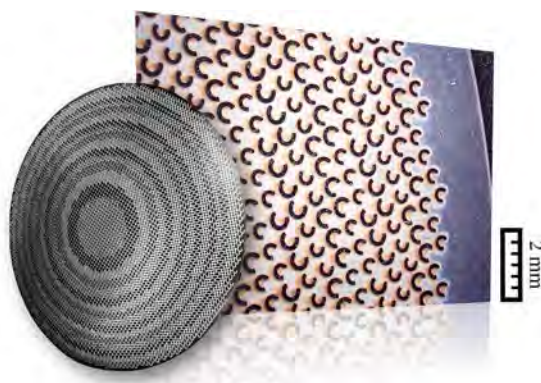


Fig. 1. Split-ring resonator based metasurface lens

-
- [1] R. Ivaškevičiūtė-Povilauskienė et al., (2023) Flexible terahertz optics: light beam profile engineering via C-shaped metallic metasurface
 [2] J. Hu et al., (2021) A Review on Metasurface: From Principle to Smart Metadevices
 [3] L. Minkevičius et al., (2017) Terahertz multilevel phase Fresnel lenses fabricated by laser patterning of silicon
 [4] Q. Yang et al., (2024) Efficient Flat Metasurface Lens for Terahertz Imaging
 [5] H. W. Tian et al., (2020) Terahertz Metasurfaces: Toward Multifunctional and Programmable Wave Manipulation.

FULL-FIELD OPTICAL COHERENCE TOMOGRAPHY WITH DIGITAL DEFOCUS CORRECTION

Austėja Trečiokaite^{1,2}, Karolis Adomavičius¹, Egidijus Auksorius¹

¹State research institute Center for Physical Sciences and Technology

²Vilnius University

austejatreckiokaite@fidi.lt

Full-Field Optical Coherence Tomography (FF-OCT) is a fast, non-invasive/non-destructive interferometric technique for acquiring high-resolution *en face* images at large depths within the sample. In order to avoid as much of the interference noise as possible, a low-coherence light source is used, instead of a laser that is commonly used in holography/interferometry. However, computational aberration/defocus correction, which is possible in Fourier-domain FF-OCT systems using lasers [1][2], is challenging when using incoherent light source, such as LED.

Here we demonstrate a digital defocus correction over a large range of defocus values in FF-OCT employing LEDs. To this end, we show defocus correction on various - reflective and scattering samples.

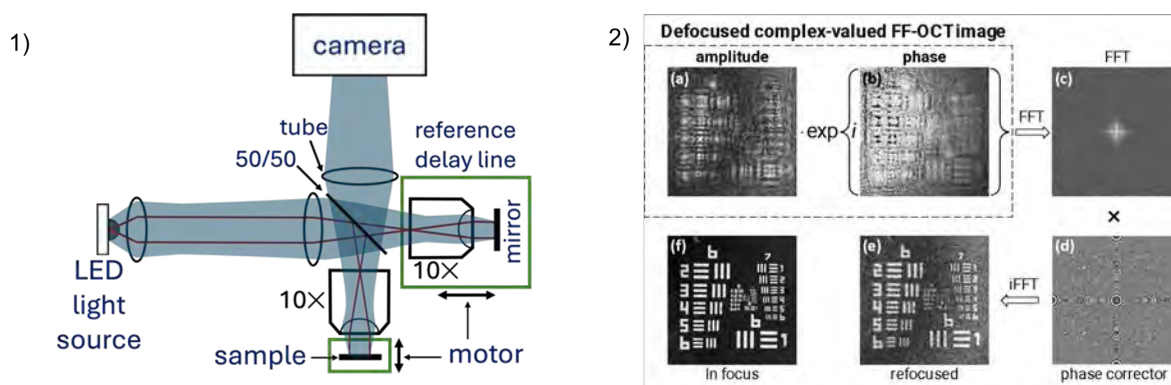


Fig. 1. 1) Principal scheme of FF-OCT system. Dark blue represents spatially incoherent LED illumination path, red – spatially coherent laser. Green boxes indicate translation stages equipped with stepping motors.

2) Digital defocus correction of complex-valued TD-FF-OCT image of USAF target defocused by 1 mm ($u = 676.4$). The complex-valued signal, consisting of amplitude (a) and phase (b), is Fourier-transformed (c), then multiplied by a quadratic phase function (d), and subsequently inverse Fourier-transformed, resulting in a refocused image (e). An in-focus image is provided in (f) for comparison.

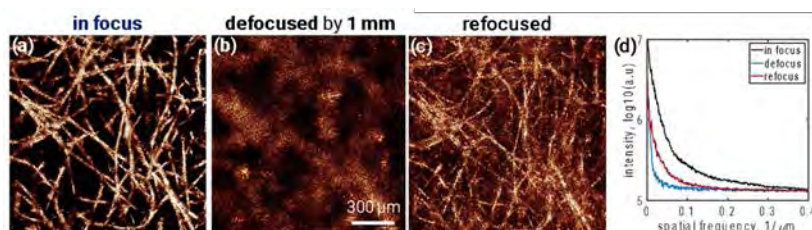


Fig. 2. Digital defocus correction of TD-FF-OCT images acquired 100 μm beneath lens tissue surface. (a) in-focus TD-FF-OCT image, (b) TD-FF-OCT image physically defocused by 500 μm. (c) digitally refocused TD-FF-OCT image. (d) spatial frequency spectra for three images displayed in (a), (b) and (c). The images are normalized whereas curves in (d) are produced from original (non-normalized) TD-FF-OCT images.

Overall, digital defocus correction of images created with TD-FF-OCT systems can be implemented over a much larger range than the Depth of Field (DOF). As DOF with used optics is 10 μm, defocus values up to 1 mm can be negated although with certain spatial resolution and intensity losses. Alongside the use of incoherent light sources, TD-FF-OCT holds an advantage over other holographic microscopy techniques due to reduction in the number of coherent artifacts granting an increase in imaging depth.

[1] A. Dubois et al., "Ultra-high-resolution full-field optical coherence tomography," *Applied Optics*, vol. 43, no. 14, p. 2874, May 2004. doi:10.1364/ao.43.002874

[2] A. Kumar, W. Drexler, and R. A. Leitgeb, "Subaperture correlation based digital adaptive optics for full field optical coherence tomography," *Optics Express*, vol. 21, no. 9, p. 10850, Apr. 2013. doi:10.1364/oe.21.010850

INVESTIGATING MECHANICAL VIBRATIONS AT THE (SUB-)NANOSCALE - ADVANCES IN DIGITAL HOLOGRAPHIC VIBROMETRY

Florian Dötzer¹, Johannes May¹, Stefan Sinzinger¹

¹Optical Engineering Group, Department of Mechanical Engineering, TU Ilmenau, Germany
florian.doetzer@tu-ilmenau.de

Mechanical vibrations are omnipresent in engineering and development, either as a part of an object's functionality or as a parasitic effect. Fast and reliable vibration measurement is an indispensable tool for aiding in the design process and providing quality assurance [1]. Especially challenging is the characterization of micro-electromechanical systems (MEMS) and surface acoustic wave (SAW) devices due to small surface displacements in the (sub-)nanometer range and high frequencies in the MHz to GHz range, often in conjunction with a demand for high lateral spatial resolution.

Interferometric optical techniques offer the required sensitivity, but the installed detector usually either limits it to point measurements (single photodiode) or to low frequencies (camera detector). However, as shown on the left-hand side of Fig. 1, by shifting the laser frequency ω_L in one of the interferometer arms by $\Delta\omega = \omega_{obj} + \omega_b$, static interference (or sufficiently low beat frequencies ω_b) can be obtained even for arbitrarily high vibration frequencies ω_{obj} . This is achieved by a pair of acousto-optic modulators (AOMs) with a frequency difference of $\Delta\omega$ and allows to use camera detectors for vibration frequencies that exceed the frame rate of the camera by several orders of magnitude [2].

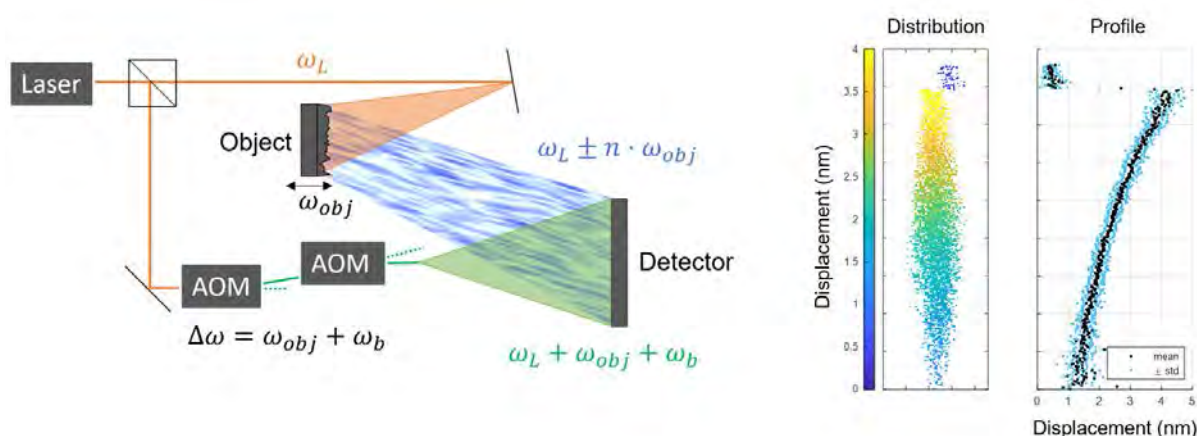


Fig. 1. Interferometer setup (left); Measurement result of an oscillating clarinet reed (right), adapted from [3].

A remaining issue outside controlled laboratory conditions (e.g. production lines) are Doppler frequency shifts arising from a relative motion between the interferometer and the object to be measured. These also shift or even broaden the resulting peak in the frequency spectrum associated to the beat frequency ω_b , such that the desired lock-in detection is no longer possible.

By introducing an additional artificial reference vibration at a frequency close to ω_{obj} , a beat between the two acoustic vibrations results. The properties of the object vibration are now encoded in the temporal variation of the observed vibration amplitude. Because the acoustic frequencies are several orders of magnitude smaller than the optical frequencies, the corresponding absolute Doppler frequency shift of the acoustic beat frequency is negligible for virtually all practical situations. This now allows to perform a lock-in detection and accordingly a highly sensitive measurement even in rough environments. The detection limit and noise levels are currently just below 1 nm (Fig. 1, right hand side), but by using longer lock-in time constants, measurements in the pm range or below are expected to become accessible [4].

-
- [1] S. J. Rothberg et al., An international review of laser Doppler vibrometry: Making light work of vibration measurement, *Optics and Lasers in Engineering*, 99, 11-22 (2017)
 [2] N. Verrier et al., Full Field Holographic Vibrometry at Ultimate Limits, *New Techniques in Digital Holography*, 255-293 (2015)
 [3] F. Dötzer et al., Phase Modulated Frequency Shifted Digital Holographic Vibrometry with Enhanced Robustness, *EPJ Web of Conferences* 287, 09017 (2023)
 [4] K. Hogmoen, O.J. Lokberg, Detection and measurement of small vibrations using electronic speckle pattern interferometry, *Appl. Opt.*, 16, 1869-1875 (1977)

TERAHERTZ DIFFRACTIVE OPTICAL ELEMENTS REALIZING MIMO SYSTEM

Mateusz Kaluza¹, Paweł Komorowski², Adrianna Nieradka¹, Mateusz Surma¹, Przemysław Zagrajek²,
Agnieszka Siemion¹

¹Department of Physics, Warsaw University of Technology, Poland

²Institute of Microelectronics and Optoelectronics, Warsaw University of Technology, Poland
mateusz.kaluza.dokt@pw.edu.pl

One of the prospective applications of terahertz (THz) technologies is in the field of telecommunication. Addressing the current challenge of limited capacity in wireless data distribution, particularly within short-range Wi-Fi technology, the introduction proposes the utilization of THz radiation to increase data transfer ratio and enhance the performance of end-user telecommunication systems. The upcoming generation of telecommunication systems (6G), has already allocated THz bands for potential applications such as Tbps WLANs, WPANs, IAB wireless networks, IoT networks, and THz space communication systems [1]. All these applications necessitate signal multiplexing to improve data transfer ratio. In this study, the implementation of multiplexing functionality is realized through the application of a multiple-input multiple-output (MIMO) system, specifically achieving spatial frequency division multiplexing.

The MIMO system is realized through the incorporation of two diffractive optical elements (DOEs). The first element performs the role of a multiple-input single-output (MISO) system, wherein the DOE combines signals of different frequencies generated by spatially separated radiation sources into a single optical channel. The resultant combined signal beam propagates in free space over a specified distance in the form of a plane wave. Subsequently, the signals are spatially separated by the second DOE, which accomplishes the single-input multiple-output (SIMO) functionality. Consequently, THz signals of varying frequencies can be concurrently gathered by spatially separated detectors.

A crucial aspect of this solution lies in the design of DOEs in the form of kinoform lenses. These appropriately designed structures facilitate arbitrary signal manipulation, resulting in a precisely defined intensity distribution of the output field. The continuous phase profile achieved through kinoform coding ensures a high diffraction efficiency of up to 100% [2]. Fig. 1a and 1b illustrates the phase profiles of the designed MISO and SIMO structures (top image), respectively. The DOEs were manufactured (Fig. 1a and 1b - bottom image) from transparent polymer materials in the THz radiation range using fused deposition modeling (FDM) 3D printing technology. The investigation of optical properties in polymer and composite materials was carried out utilizing THz time-domain spectroscopy (THz TDS) [3], enabling the selection of cyclic olefin copolymer (COC) and styrene-butadiene copolymer (SBC) materials for this specific application. The schematic representation of the functionality of each structure within the THz optical system is depicted in Fig. 1c and 1d.

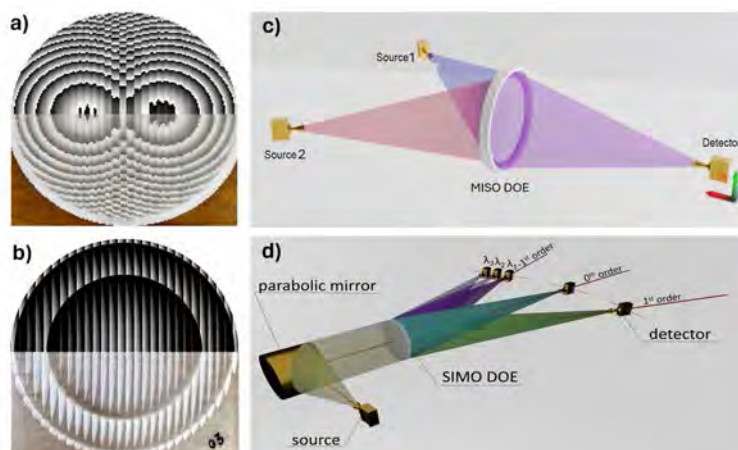


Fig. 1. a) and b) The gray-scale phase maps and 3D printed MISO and SIMO structure, respectively; c) and d) schemes of THz optical systems for MISO and SIMO structures verification.

[1] C. Han, Y. Wu, Z. Chen, and X. Wang, Terahertz communications (teracom): Challenges and impact on 6g wireless systems. (2019). arXiv preprint arXiv:1912.06040

[2] A. Siemion, The magic of optics — an overview of recent advanced terahertz diffractive optical elements, Sensors 21, (2020).

[3] M. Kaluza, M. Surma et al., THz optical properties of different 3d printing polymer materials in relation to FTIR, Raman, and XPS evaluation techniques, 47th International Conference on Infrared 2022, ISSN 2162-2035, Millimeter and Terahertz Waves (IRMMW-THz), IEEE, 2022.

FS - LASER ABLATION AND MODIFICATION OF THIN METAL FOR PERIODIC PLASMONIC ARRAYS

Kipras Čepaitis^{1,2}, Kernius Vilkevičius¹, Evaldas Stankevičius¹

¹Department of Laser Technologies, Center for Physical Sciences and Technology, Lithuania

²Faculty of Physics, Vilnius University, Lithuania

kipras.cepaitis@ftmc.lt

Various precious metals (such as gold, silver, and platinum) are widely studied for their applications in surface-enhanced Raman spectroscopy (SERS) [1], solar panels [2], and biological and chemical sensors [3]. By having metallic nanostructures, the free electron oscillations can be easily excited in these by incident light. The oscillations, known as localized surface plasmons (LSPs), have distinctive optical properties but are localized to the structure. When these are arranged in an orderly manner with a certain characteristic period length, the array of structures acts as a diffraction grating. A surface plasmon polariton is excited and the surface exhibits a hybrid lattice plasmon resonance (HLPR) characterized by its very narrow resonance and high-quality factor along with dispersive properties.

The structures can be formed either by the ablation of the metal, as the non-removed material acts as a plasmonic grating, or by modification as the plasmons are excited in the affected zones. Although nanostructures are usually formed precisely by photolithography [4], such techniques are expensive and difficult to scale up to large-scale production. Direct laser writing (DLW) is an attractive and fast alternative that allows easy fine-tuning of HLPR properties microstructures. The formation mechanism and properties of the structures formed by a focused laser pulse depend on the beam overlapping and pulse energy used [5].

This study investigates the formation of periodic arrays on thin gold film using layer ablation and modification with the third harmonic (343 nm) of a femtosecond laser. The grating properties were compared with respect to their formation mechanism. The ablated structures act as 1D-like grating, while modification enables the formation of both 1D-like and 2D-like arrays. Also, the dependence of HLPR on the polarization and angle of incident light was researched.

[1] J. Langer et al., *ACS Nano*, 14(1), 28-117 (2019).

[2] Q. Duan et al., *Sensors*, 21(16), 5262 (2021)

[3] P.Yu et. al., *Scientific reports*, 7(1), 7696 (2017)

[4] X. Luo and T.Ishihara., *Optics express*, 12(14), 3055-3065, (2004)

[5] E. Stankevičius et al., *Adv. Opt. Mater.* 9(12), 2100027 (2021)

HIGH-EFFICIENCY MID-IR OPCPA WITH 2.5 mJ 25 fs OUTPUT PULSES

Augustė Černekytė¹, Augustinas Petrulėnas¹, Paulius Mackonis¹, Aleksėj M Rodin¹

¹Solid State Lasers laboratory, Center for Physical Sciences and Technology, 231 Savanoriu Ave, 02300 Vilnius, Lithuania
auguste.cernekyte@ftmc.lt

Intense, few-cycle laser sources in the wavelength range 1.5 – 3.0 μm are in demand for generating THz and attosecond X-ray pulses [1]. Invented by Lithuanian scientists from the group of A. Piskarskas, the optical parametric chirped pulse amplification (OPCPA) when operating in degeneracy at $\sim 2 \mu\text{m}$ allows the use of readily available $\sim 1 \mu\text{m}$ driving pulses, while supercontinuum (SC) seed simplifies the design by eliminating the need for active synchronization. We demonstrate a compact, high-efficiency mJ-level mid-IR OPCPA using 1.2 ps pulses from Yb:YAG laser for both pumping and SC generation. Three degenerate OPCPA stages based on BiBO crystals provide output pulses with an energy of $\sim 2.5 \text{ mJ}$ in the wavelength range of $\sim 1.8 - 2.3 \mu\text{m}$. Preliminary results on spectral expansion beyond $\sim 3 \mu\text{m}$ using stimulated rotational Raman scattering (SRRS) in a gas cell will also be reported.

The Yb:YAG chirped pulse amplifier with a grating compressor [2], upgraded by the author of the report, was used as a pump source for both SC and OPCPA allowing 1.5 times better gain (Fig. 1, left). Beam stability was ensured by auto-alignment. The SC seed pulses were generated in a YAG crystal 130 mm long [3]. Compared to the previous implementation the SC seed pulse dispersion has been optimized using an acousto-optic programmable dispersive filter (AOPDF) to provide the best conversion efficiency and ultimate pulse compression.

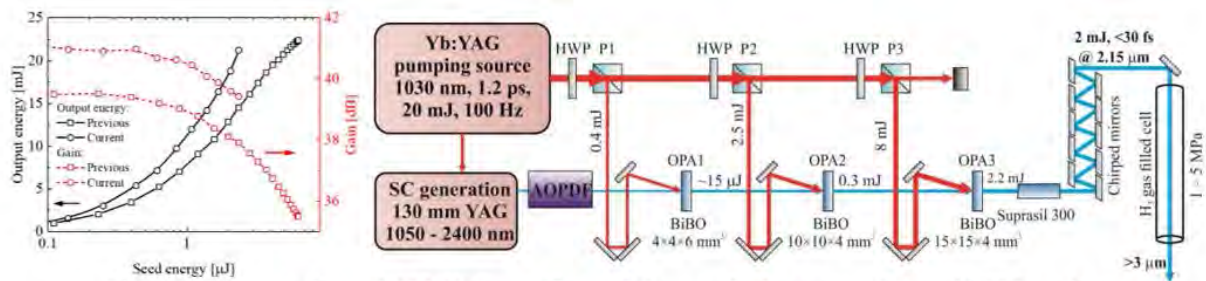


Fig. 1. Performance of upgraded Yb:YAG amplifier – left. Layout of a three-stage OPCPA with SRRS – right.

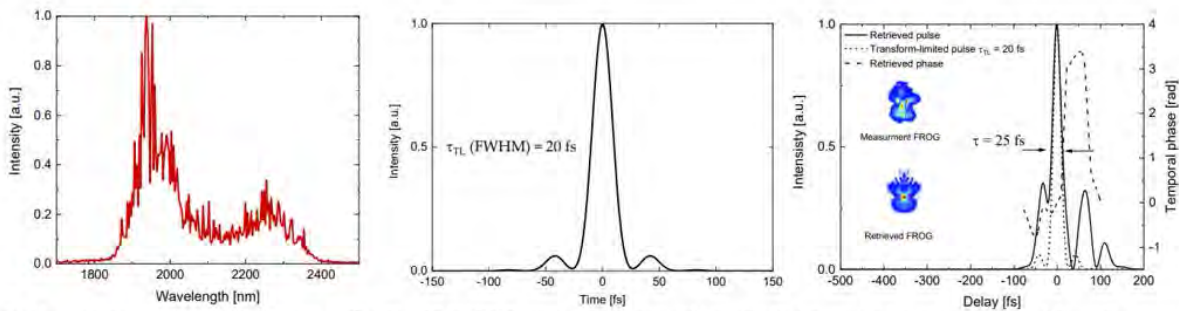


Fig. 2. The spectrum of amplified pulses after the 1st OPCPA stage – left. Transform-limited temporal shape calculated from the measured OPCPA output spectrum – middle. Temporal profile (solid) of the amplified pulse after compression retrieved from the SHG-FROG measurement compared to the transform-limited pulse (dotted) and the retrieved temporal phase (dashed) – right.

The three-stage OPCPA provides $\sim 2.5 \text{ mJ}$, 25 fs output pulses at a center wavelength of $\sim 2150 \text{ nm}$ after compression. In the third OPCPA stage, a conversion efficiency of 27% was achieved. The resulting peak power of $>80 \text{ GW}$ allows for significant spectrum extension beyond $3 \mu\text{m}$ using SRRS in a gas cell. The remaining unused energy of the pump source allows to obtain $\sim 5 \text{ mJ}$ of amplified pulse energy through the use of an additional fourth OPCPA stage.

[1] P. Agostini and L.F. DiMauro, The physics of attosecond light pulses, Rep. Prog. Phys. 67, 813–855 (2004).

[2] P. Mackonis and A.M. Rodin, Laser with 1.2 ps, 20 mJ pulses at 100 Hz based on CPA with a low doping level Yb:YAG rods for seeding and pumping of OPCPA, Opt. Express 28, 1261–1268 (2020).

[3] A. Petrulėnas, P. Mackonis, and A. M. Rodin, High-efficiency bismuth borate-based optical parametric chirped pulse amplifier with approximately 2.1 mJ, 38 fs output pulses at approximately 2150 nm. High Power Laser Sci. 11 (2023).

INVESTIGATION OF PERIODICALLY STRUCTURED THIN FILMS POLARIZERS

Julianija Nikitina¹, Rytis Buzelis¹, Kęstutis Staliūnas^{2,3}, Lina Grinevičiūtė¹

¹Center for Physical Sciences and Technology, Savanorių ave. 231, LT-02300 Vilnius, Lithuania

²ICREA, Passeig Lluis Companys 23, 08010, Barcelona, Spain

³UPC, Rambla Sant Nebridi 22, 08222, Barcelona, Spain

julianija.nikitina@ftmc.lt

Linear polarizers are integral to most laser systems for their role in controlling radiation polarization state. A wide diversity of up-to-date linear polarizers can provide an outstanding polarization extinction ratio. However, many of them come with operational inconveniences: absorptive polarizers suitable for normal incidence have a low laser-induced damage threshold (LIDT), restricting their use in laser applications; birefringent or thin-films polarizers demonstrate a decrease in polarizing efficiency at normal incidence, which becomes concerning as the trend towards miniaturization of laser systems continues. Mentioned limitations of conventional polarizers are becoming more pronounced, underscoring the necessity for alternative solutions.

In the search for high LIDT and efficient polarizing properties at normal incidence, we have focused on periodically modulated dielectric thin films. In the simplest case of single-layer coating, as a high refractive index subwavelength structure surrounded by a lower refractive index media, it features wavelength-selective resonance phenomenon [1]. Moreover, as the structure has modulation only in one direction, its optical response is also polarization-dependent. These features were employed to optimize the architecture of polarizing element for the target wavelength of 1064 nm. Subsequently, the ion beam sputtering technology was used to conformally deposit dielectric coatings on the structured substrate. The potential of fabricated elements for laser applications were evaluated by LIDT 1-on-1 test for nanosecond pulses.

Experimentally demonstrated niobium oxide single-layer polarizing element showed 788:1 polarization ratio for 1064 nm at normal incidence. The LIDT values of periodically modulated single-layer structure have reached 0.7 J/cm² and 3.1 J/cm² for *S*- and *P*- polarizations, that is more than six times smaller values than of planar layer. This difference in optical resistance can be explained with increased electric field intensity in modulated structure, determining damage at relatively low energy densities. To improve optical resistance, wide bandgap dielectrics as hafnium and aluminum oxides were used to create multilayer architecture. Enhanced LIDT values have reached 1.6 J/cm² and 18.5 J/cm² for *S*- and *P*- polarizations, respectively. However, nearly 2 μm thick coating with modulation discrepancies led to optical characteristics distortions which reduced the polarization contrast. The presented results demonstrate the potential possibilities of periodically structured thin-film polarizers and also highlight challenges to be dealt with in the ongoing work.

Acknowledgments: This work was supported by the PerFIN project from the Research Council of Lithuania (LMTLT), agreement No. S-MIP-22-80.

[1] L. Grinevičiūtė, J. Nikitina, C. Babayigit, ir K. Staliūnas, „Fano-like resonances in nanostructured thin films for spatial filtering“, *Appl. Phys. Lett.*, t. 118, nr. 13, 2021, doi: 10.1063/5.0044032.

REFINING LIDT EVALUATION THROUGH MONTE CARLO SIMULATIONS: A PATH TO ISO EXCELLENCE

Martynas Keršys¹, Andrius Melninkaitis^{1,2}

¹Vilnius University, Physics Faculty, Laser Research Center

²UAB Lidaris

martynas.kersys@ff.stud.vu.lt

The assessment of Laser-Induced Damage Threshold (LIDT) plays a pivotal role in ensuring the safety and reliability of laser systems across various scientific and industrial applications. As laser technology is constantly evolving to new irradiation regimes, there is a demand for higher quality optical components, as is to evaluate their damage threshold more accurately and reliably. As a result, there arises a need to revise the current ISO standard for LIDT testing on periodic basis [1]. But to make LIDT standardization efforts more successful and adoptable, there is a need for an easy way to evaluate these methods and show their accuracy under real and different conditions.

This research endeavors to address these challenges by exploring and implementing advanced testing techniques based on Monte Carlo simulations to numerically test and compare different testing approaches. The main goal of our research was to review the accuracy of current ISO standard techniques for LIDT testing ISO 21254:2011 using numerical methods as well as prepare recommendations for the upcoming revision of this standard. For the new revision of this standard, new functional tests, namely R-on-1 and raster scan [2], are intended to be implemented.

In our research, we first compare the classical methods of evaluating the LIDT with our own empirical and experimental insight-based algorithm for 1-on-1 and S-on-1 testing using Monte Carlo simulations. We then go on to evaluate and optimize testing conditions for R-on-1 tests and raster scans, comparing them with the former methods. We do these tests by first generating a virtual sample with randomly distributed sporadic defects on XY plane and by sampling it with a virtual laser beam (Gaussian and a flat top) on our surface to detect them. We introduce a requirement for these tests to cover a certain amount of area $A_{90\%}$ (area where fluence is more than 90% of the peak fluence) to make them comparable with raster scan results.

In our initial findings, by running our simulations with the same initial condition for multiple iterations, we have discovered that by increasing the diameter of our Gaussian beam for roughly the same area irradiated, we decrease the deviation of LIDT values, proving that there is a strong correlation between LIDT test accuracy and the defect density of our surface.

[1] International Organization for Standardization. "ISO 21254-2: Lasers and laser-related equipment -- Test methods for laser-induced damage threshold -- Part 2: Threshold determination." Technical Committee: Optics and Optical Instruments, Subcommittee: Lasers and Laser-Related Equipment, International Standard, International Organization for Standardization, Genève, Switzerland, 2011.

[2] Borden, Michael R., et al. "Improved method for laser damage testing coated optics." Laser-Induced Damage in Optical Materials: 2005. Vol. 5991. SPIE, 2006.

THE LIMITS OF STAR CLUSTER APERTURE PHOTOMETRY IN THE LOCAL UNIVERSE

Karolis Daugevičius¹, Eimantas Kriščiūnas¹, Erikas Cicėnas¹, Rima Stonkutė¹, Vladas Vansevičius¹

¹Center for Physical Sciences and Technology, Saulėtekio av. 3, LT-10257 Vilnius, Lithuania
karolis.daugevicius@ftmc.lt

Star clusters and knowledge of their physical parameters (age, mass, metallicity, extinction) provide an excellent insight into the formation and evolution of their host galaxies, as most of the star formation happens in clusters. A powerful method allowing parameter derivation for a large number of clusters in the Local Universe (≤ 10 Mpc,) is fitting their aperture photometry measurements to stochastic theoretical models [1]. Therefore, it is highly important to understand method's limits in order to not over-interpret the data as we attempt to unravel formation histories of nearby galaxies.

The aim of this study is to estimate maximum possible accuracy of the aperture photometry methods for star cluster studies in the Local Universe. We simulated an extensive (500 nodes) grid of 3D cluster models covering the parameter space of real objects in the Andromeda galaxy (M31). Each node, defined by initial mass, age, and geometric parameters, contains 100 stochastic 3D models. Cluster CCD images were generated in 6 photometric (HST) passbands by taking 100 2D projections of each model, mimicking observations from 100 viewing angles. We modelled clusters to match the real ones in M31 as seen in the PHAT survey [2]. We measured simulated images by using aperture photometry method [3] and ran cluster classification tests [1].

We have demonstrated that using small apertures ($R_{\text{ap}} \leq 0.5$ arcsec) is not advisable as it leads to large physical parameter derivation uncertainties (Fig. 1a-c). This supports an idea suggested in [3, 4] that apertures larger than cluster half-light radii must be used to provide robust results. Aperture-photometry-based classification encounters problems at very young cluster ages (~ 10 Myr), showing large errors (Fig. 1a-c). Using colour-magnitude diagram fitting methods [5] is advised to yield more accurate cluster parameters at ages of ~ 10 Myr. We have shown that there are no significant systematic colour index differences when clusters are measured using smaller apertures (Fig. 1d-e), justifying the adaptive aperture photometry method [3, 4].

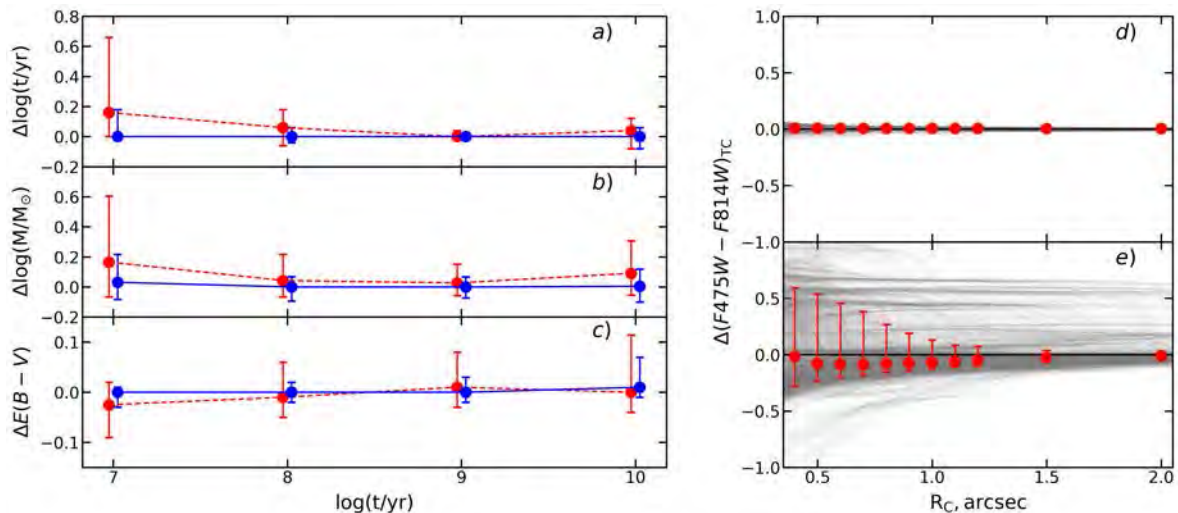


Fig. 1. Panels a-c) show cluster classification test results. Differences between the derived and input cluster parameters: a) age; b) mass; c) extinction $E(B-V)$. Markers - median differences, error bars - 16-84 percentile range. Dashed red line - results when photometry was performed using $R_{\text{ap}}=0.5$ arcsec; solid blue line - $R_{\text{ap}} \geq 1.0$ arcsec. Panels d-e) show differences of colour index $(F475W-F814W)_{\text{TC}}$ between measurements with apertures of $R_{\text{ap}}=3.0$ arcsec and $R_{\text{ap}}=R_C$. Red markers - median differences; error bars - 16-84 percentile range; grey lines - results for individual clusters. Panel d) shows models with post-main-sequence (post-MS) stars removed ($N=2700$); panel e) - models with all stars ($N=7300$).

- [1] P. de Meulenaer, R. Stonkutė, V. Vansevičius, *Astron. Astrophys.*, 602, A112 (2017)
- [2] J. J. Dalcanton, B. F. Williams, D. Lang et al., *Astrophys. J. Suppl. Ser.*, 200, 18 (2012)
- [3] R. Naujalis, R. Stonkutė, V. Vansevičius, *Astron. Astrophys.*, 654, A6 (2021)
- [4] E. Kriščiūnas, K. Daugevičius, R. Stonkutė, V. Vansevičius, *Astron. Astrophys.*, 677, A100 (2023)
- [5] T. M. Wainer, L. C. Johnson, A. C. Seth, *Astrophys. J.*, 928, 15 (2022)

STAR CLUSTERS AND SPIRAL ARMS OF THE M31 GALAXY

Eimantas Kriščiūnas¹, Karolis Daugevičius¹, Erikas Cicėnas¹, Rima Stonkutė¹, Vladas Vansevicius¹

¹Center for Physical Sciences and Technology, Saulėtekio av. 3, 10257 Vilnius, Lithuania
eimantas.krisciunas@ftmc.lt

Andromeda (M31) galaxy is the nearest (785 kpc; [1]) spiral galaxy making it one of the premier laboratories for understanding spiral galaxies like our own. Due to a high inclination (74° – 78°) of the M31 disk, it is difficult to determine the galaxy's large-scale structure. In particular, there is no clear consensus regarding the organization of spiral structure in M31. Therefore, star clusters can be excellent tracers in studies of galaxy formation, assembly and spiral structure, in the sense that significant star cluster numbers are typically produced during major star-forming (SF) episodes in galaxy disks. A substantial portion of the M31 disk was observed by the extensive Panchromatic Andromeda Treasury (PHAT) survey [2] performed with the *Hubble* Space Telescope (HST).

The aim of our study is to investigate the spiral structure of M31 galaxy based on the PHAT star clusters. Using aperture photometry data [3-5], we derived cluster parameters: age, mass, extinction, and metallicity. To investigate spiral structure face-on, we deprojected the M31 disk and star clusters assuming the position angle of the galaxy major axis of 37.7° and the inclination of disk of 77.5° .

In Fig. 1, we show the distribution of young star clusters (<50 Myr) with respect to the UV SF regions (grey contours) taken from [6]. Green logarithmic spirals are plotted to roughly follow the spiral structure, with a pitch angle of 3° and phase-shift of -40° . Some young star clusters and UV SF regions deviate from spiral arms, indicating inconsistency with the spiral pattern. Therefore, Fig. 1 clearly highlights the problems addressed in our study.

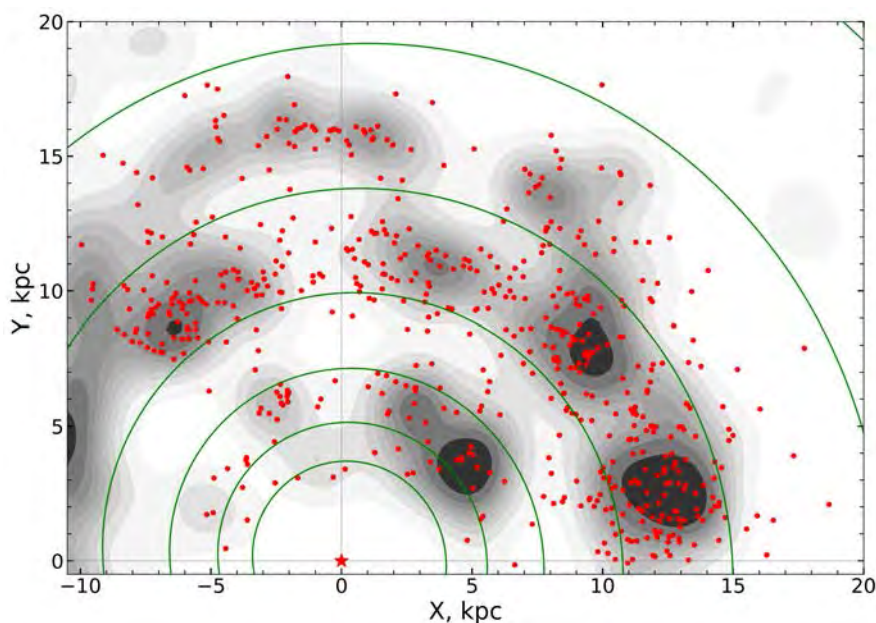


Fig. 1. Distributions of UV SF regions (grey contours) and young clusters (<50 Myr; red dots). Green lines show logarithmic spiral arms with a pitch angle of 3° .

[1] McConnachie, A. W., Irwin, M. J., Ferguson, A. M. N., et al. 2005, MNRAS, 356, 979

[2] Dalcanton, J. J., Williams, B. F., Lang, D., et al. 2012, ApJS, 200, 18

[3] Johnson, L. C., Seth, A. C., Dalcanton, J. J., et al. 2015, ApJ, 802, 127

[4] Naujalis, R., Stonkutė, R., and Vansevicius, V. 2021, Astron. Astrophys., 654, A6

[5] Kriščiūnas, E., Daugevičius, K., Stonkutė, R., and Vansevicius, V. 2023, Astron. Astrophys., 677, A100

[6] Kang, Y., Bianchi, L., and Rey, S. C. 2009, ApJ, 703, 614

LAMMPS AS A LIBRARY FOR THE THEORETICAL STUDY OF THE ROLE OF PHONONS IN ULTRAFAST DEMAGNETIZATION

Wojciech Marciniak^{1,2,3}, Joanna Marciniak³, Jan Rusz²

¹Institute of Physics, Faculty of Materials Engineering and Technical Physics, Poznań University of Technology, Piotrowo 3, 61-138 Poznań, Poland

²Department of Physics and Astronomy, Uppsala University, P.O. Box 516, 75120 Uppsala, Sweden

³Institute of Molecular Physics, Polish Academy of Sciences, M. Smoluchowskiego 17, 60-179 Poznań, Poland
wojciech.robe.marciniak@doctorate.put.poznan.pl

Ultrafast modification of the magnetism of materials by laser pulses has attracted significant attention since its discovery in 1996 [1] because of its potential applications in computing and data storage. The process involving the transfer of angular momentum between electrons, phonons, and magnons is a complex interaction of light and matter, and it is still only partly understood [2].

To allow us to investigate phonons evolution after a laser pulse, we implemented a simple approximation to modify molecular dynamics trajectory to enhance specific vibration modes. Using LAMMPS as a library feature [3], we created a framework that allows LAMMPS to handle data input, generate snapshots to be processed by our method and output the modified trajectory.

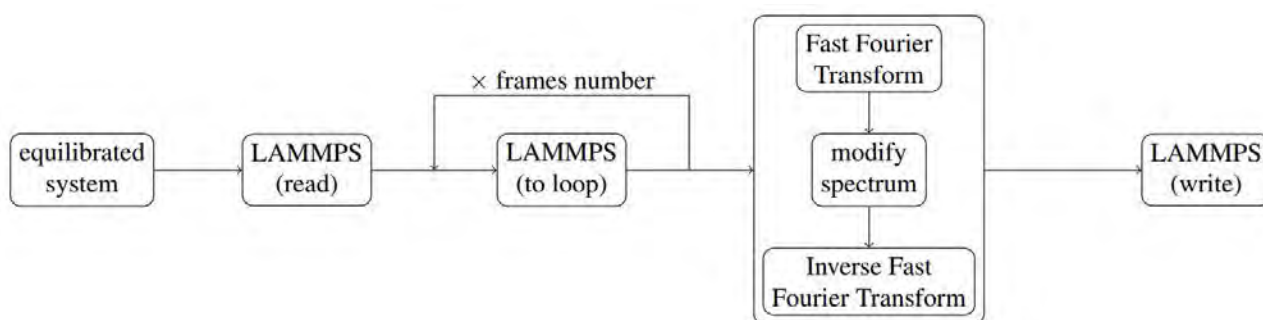


Fig. 1. A simplified schematic of the applied workflow.

Using the developed framework, we will study how phonons can contribute to re-establishing the equilibrium by carrying away the excess heat and angular momentum. We will evaluate the evolution of lattice vibrations from high temperatures of selected vibration modes towards an equilibrium using SNAP machine-learning interatomic potential (ML-IAP) [4]. Snapshots of the molecular dynamics trajectories will allow us to predict changes in the diffraction patterns and in electron energy loss spectra (EELS) in a time-resolved way [5,6].

W.M. wants to acknowledge the financial support of the Polish National Agency for Academic Exchange under the decision BPN/BEK/2022/1/00179/DEC/1. JR acknowledges the support of the Swedish Research Council, Olle Engkvist's Foundation, and Knut and Alice Wallenberg Foundation for financial support. The simulations were enabled by resources provided by the National Academic Infrastructure for Supercomputing in Sweden (NAISS) at NSC Centre, partially funded by the Swedish Research Council through grant agreement no. 2022-06725.

[1] Beaurepaire, E., et al. Ultrafast spin dynamics in ferromagnetic nickel. *Physical Review Letters*, 76(22), 4250.

[2] Fähnle, M., et al. (2018). Review of ultrafast demagnetization after femtosecond laser pulses: a complex interaction of light with quantum matter. *Am. J. Mod. Phys.*, 7(2), 68-74.

[3] Thompson, A. P., et al. (2022). LAMMPS -- a flexible simulation tool for particle-based materials modeling at the atomic, meso, and continuum scales. *Computer Physics Communications*, 271, 108171.

[4] Thompson, A. P., et al. Spectral neighbor analysis method for automated generation of quantum-accurate interatomic potentials. *Journal of Computational Physics*, 285, 316-330.

[5] Zeiger, P. M., and Rusz, J. (2020). Efficient and versatile model for vibrational STEM-EELS. *Physical Review Letters*, 124(2), 025501.

[6] Tauchert, S. R., et al. (2022). Polarized phonons carry angular momentum in ultrafast demagnetization. *Nature*, 602(7895), 73-77.

THEORETICAL INVESTIGATION OF ENERGY LEVELS FOR BA VI

Kotryna Šiškauskaitė¹, Gediminas Gaigalas¹, Pavel Rynkun¹, Laima Kitovienė¹

¹Institute of Theoretical Physics and Astronomy, Vilnius University
kotryna.siskauskaite@steam.vu.lt

This ion was selected for the investigation as it is of great importance to Astrophysics. It is evident that the lines can be observed in hot white dwarf stars [1]. In this work energy levels for Ba VI will be presented. The calculations for Ba VI are performed using general-purpose atomic structure package GRASP2018, based on multiconfiguration Dirac-Hartree-Fock and relativistic configuration interaction (RCI) methods.

As this ion is of Sb isoelectronic sequence, it was calculated using the same principle like in [2]. Active space (AS) method was used to compute radial wave functions layer by layer for four sets of virtual orbitals (AS₁₋₄). Single and double substitutions were done from multi reference set of orbitals up to 11s, 11p, 10d, 8f, 8g, 8h. Substitutions from [Kr]4d¹⁰ core shells were forbidden. After calculating AS₄, RCI method was used to further increase the accuracy of Ba VI energy level calculations. In total, 231 energy levels belonging to the configurations 5s²5p4f², 5s²5p²4f, 5s5p³4f, 5p⁵, 5s²5p²{5d,6p,6s}, 5s²5p³, 5s²5p5d², 5s5p³5d, 5s5p³6s and 5s5p⁴ were computed.

50 levels were selected based on the data availability at National Institute of Standards and Technology Atomic Spectra database (NIST) [3] for comparison. The relative difference to NIST data is displayed in Figure 1. The biggest disagreement is observed in 5s²5p²5d and 5s5p⁴ configuration levels, as the energies appear to be reversed in our calculations. The average relative difference compared to NIST [3] for AS₄ is 1.2%. In order to increase the accuracy of energy levels, core, core-valence, core-core correlations need to be investigated. During the conference further data from the calculations will be presented.

Conf.	^M L	J	E _{NIST} cm ⁻¹	AS ₃ %	AS ₄ %	Conf.	^M L	J	E _{NIST} cm ⁻¹	AS ₃ %	AS ₄ %
5s ² 5p ³	⁴ S	3/2	0.0	0.0	0.0	5s ² 5p ² (¹ D)5d	² G	7/2	212208.6	2.6	2.6
5s ² 5p ³	² D	3/2	17260.6	1.2	1.1	5s ² 5p ² (¹ D)5d	² G	9/2	222540	-0.3	-0.3
5s ² 5p ³	² D	5/2	23547.2	1.0	0.9	5s ² 5p ² (³ P)5d	⁴ P	5/2	214870.8	2.3	2.3
5s ² 5p ³	² P	1/2	36155.7	2.2	2.1	5s ² 5p ² (³ P)5d	⁴ P	3/2	217346.5	2.2	2.2
5s ² 5p ³	² P	3/2	49621	0.4	0.4	5s ² 5p ² (³ P)5d	⁴ P	1/2	218693.8	2.2	2.2
5s5p ⁴ (³ P)	⁴ P	5/2	128436.3	-2.2	-2.1	5s ² 5p ² (³ P)5d	² D	3/2	224093.2	0.9	0.8
5s5p ⁴ (³ P)	⁴ P	3/2	139920.1	-2.1	-2.1	5s ² 5p ² (³ P)5d	² D	5/2	228330.9	2.1	2.2
5s5p ⁴ (³ P)	⁴ P	1/2	142851.9	-2.0	-2.0	5s ² 5p ² (¹ D)5d	² P	1/2	234313.6	0.4	0.4
5s5p ⁴ (¹ D)	² D	3/2	158158.4	-0.7	-0.7	5s ² 5p ² (¹ D)5d	² P	3/2	246496.2	2.1	2.1
5s5p ⁴ (¹ D)	² D	5/2	163566.3	-0.8	-0.8	5s ² 5p ² (¹ D)5d	² D	3/2	235818.7	2.3	2.3
5s ² 5p ² (³ P)5d	² P	3/2	176498	-0.3	-0.3	5s ² 5p ² (¹ D)5d	² D	5/2	236640.5	3.1	3.0
5s ² 5p ² (³ P)5d	² P	1/2	229293.1	-0.6	0.6	5s ² 5p ² (³ P)5d	² F	7/2	242157.2	2.3	2.3
5s5p ⁴ (³ P)	² P	1/2	179076.6	4.8	4.8	5s ² 5p ² (³ P)5d	² F	5/2	257298.9	2.2	2.1
5s5p ⁴ (³ P)	² P	3/2	213042.9	3.4	3.4	5s ² 5p ² (¹ S)5d	² D	5/2	243103.4	-0.5	-0.5
5s ² 5p ² (³ P)5d	⁴ F	3/2	180293.1	-0.2	-0.2	5s ² 5p ² (¹ S)5d	² D	3/2	256774.8	1.8	1.8
5s ² 5p ² (³ P)5d	⁴ F	5/2	183552.2	-0.5	-0.5	5s ² 5p ² (³ P)6s	⁴ P	1/2	247725.6	-0.1	-0.1
5s ² 5p ² (³ P)5d	⁴ F	7/2	192561.2	-0.6	-0.6	5s ² 5p ² (³ P)6s	⁴ P	3/2	261563.8	-0.3	-0.3
5s ² 5p ² (³ P)5d	⁴ F	9/2	199080	-0.6	-0.6	5s ² 5p ² (³ P)6s	⁴ P	5/2	267649.7	-0.2	-0.2
5s ² 5p ² (¹ D)5d	² F	5/2	191382.2	-0.6	-0.6	5s ² 5p ² (¹ D)5d	² S	1/2	251008.8	2.6	2.6
5s ² 5p ² (³ P)5d	⁴ D	1/2	193882.1	-0.4	-0.4	5s ² 5p ² (³ P)6s	² P	1/2	265653.5	-0.2	-0.2
5s ² 5p ² (³ P)5d	⁴ D	7/2	196130.2	-0.5	-0.5	5s ² 5p ² (³ P)6s	² P	3/2	271083.2	-0.1	-0.1
5s ² 5p ² (³ P)5d	⁴ D	3/2	197255.4	-0.2	-0.2	5s ² 5p ² (¹ D)6s	² D	5/2	288565.1	-0.2	-0.2
5s ² 5p ² (³ P)5d	⁴ D	5/2	201857	-0.3	-0.3	5s ² 5p ² (¹ D)6s	² D	3/2	290903.6	-0.2	-0.2
5s5p ⁴ (¹ S)	² S	1/2	200937.6	0.0	0.0	5s ² 5p ² (¹ S)6s	² S	1/2	307387	0.1	0.1

Fig. 1. Comparison of energy levels computed in active spaces AS₃ and AS₄ with NIST [3] ASD recommended values for Ba VI.

[1] Rauch, T. Stellar laboratories III. New Ba V, Va VI, and Ba VII oscillator strengths and the barium abundance in the hot white dwarfs G191-B2B and RE 0503-289, *Astronomy and Astrophysics* 566, A10, 6 (2014)

[2] Radžiūtė, L., Gaigalas, G. Theoretical investigation of Sb-like sequence: Sb I, Te II, I III, Xe IV, and Cs V, *Atomic Data and Nuclear Data Tables*, Volume 152, 101585 (2023)

[3] A. Kramida, Yu. Ralchenko, J. Reader, and NIST ASD Team, NIST Atomic Spectra Database (ver. 5.10), [Online]. Available: <https://physics.nist.gov/asd> [2023, October 18]. National Institute of Standards and Technology, Gaithersburg, MD. (2022)

THE STUDY OF THE ATMOSPHERES AND MIXING PROCESSES OF MAGNETICALLY ACTIVE RS CVN GIANTS

Barkha Bale¹, Grazina Tautvaisiene¹, Renata Minkeviciute¹, Arnas Drazdauskas¹, Edita Stonkute¹, Sarunas Mikolaitis¹

¹Institute of Theoretical Physics and Astronomy (ITPA), Vilnius University
barkha.bale@ff.stud.vu.lt

Our primary focus is the examination of RS CVn stars, aiming to ascertain the carbon isotope $^{12}\text{C}/^{13}\text{C}$ and C/N ratios within these chromospherically active celestial bodies. Analyzing the abundances of carbon and nitrogen in their atmospheres offers valuable insights into chemical composition alterations induced by stellar evolution. The determinations of carbon and nitrogen abundances, along with the C/N ratios, serve as pivotal tools in the field of stellar evolution studies. To explore the influence of magnetic activity on mixing processes within the atmospheres of magnetically active stars, we are conducting an exhaustive investigation of CNO abundances and carbon isotope ratios in a selected group of RS CVn giant stars. High-resolution spectra, acquired from the 1.65 m telescope at the Moletai Astronomical Observatory of Vilnius University, were utilized for this study. The analysis focused on the C2 Swan (1,0) band head at 5135 Å and the C2 Swan (0,1) band head at 5635.5 Å to determine carbon abundance. Additionally, the interval 7990 – 8010 Å, encompassing the $^{12}\text{C}/^{14}\text{N}$ and $^{13}\text{C}/^{14}\text{N}$ bands, was employed for nitrogen abundance and carbon isotope ratio analysis. Oxygen abundance was derived from the forbidden [O I] line at 6300.31 Å. Our findings support earlier observations, indicating that in low-mass chromospherically active RS CVn stars, extra-mixing processes may commence below a luminosity function bump in red giants.

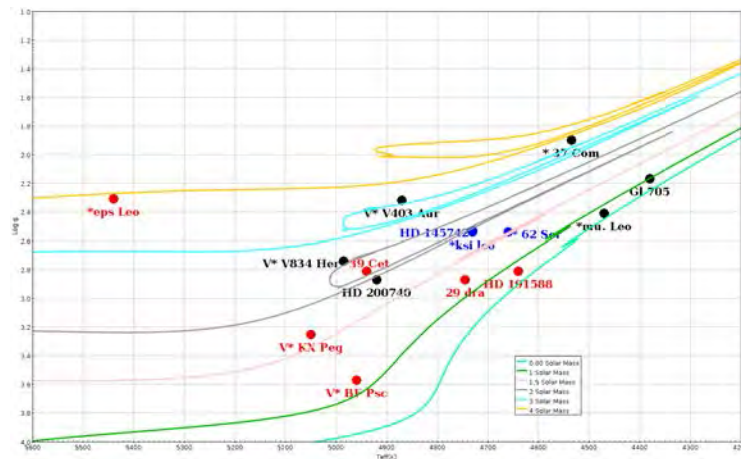


Fig. 1. The investigated stars in the log g versus T_{eff} diagram along with the PADOVA evolutionary tracks taken from Bressan et al. (2012). The red symbols indicate the stars which are below the red giant branch (RGB) luminosity bump, the blue colour indicates the stars which are at the RGB bump, and the black colour marks the stars that are above the RGB bump.

DEEP LEARNING FOR STAR CLUSTER DETECTION IN GALAXIES

Erikas Cicėnas^{1,2}, Karolis Daugevičius¹, Eimantas Kriščiūnas¹, Rima Stonkutė^{1,2}, Vladas Vansevicius¹

¹Center for Physical Sciences and Technology

²Vilnius University

erikas.cicenas@ftmc.lt

One of the most important objects when studying galaxies are stellar clusters. The stars in a cluster are of a similar age, composition, and distance, thereby making them exceptionally suitable to learn about a galaxy's star formation and dynamic history. As important as they are, locating them presents difficulties: so far, there are no adequate automated cluster detection methods and methods using experts or volunteers are employed. For this reason, we seek to employ modern machine learning algorithms, specifically a convolutional neural network (CNN), to automate the detection of clusters. Such a method would allow for repeated and fast detections of clusters in images. To train the model we use a large dataset of synthetic clusters covering a variety of ages, masses, and shapes. We project these clusters onto real observations from the Panchromatic Hubble Andromeda Treasury. We evaluate the performance of our model using various tests involving both synthetic and natural clusters. We compare these results to existing catalogues. We will also draw attention to the difference in performance by volunteers and our model. The presentation will detail the model, including training and validation, inferences and results from our tests and current challenges, unresolved issues, and the possibility of improvements.

EPR SPECTROSCOPY OF STRUCTURAL PHASE TRANSITION IN $\text{CH}_3\text{NH}_3\text{PbCl}_3$ HYBRID PEROVSKITE

Gediminas Usevičius¹, Michael A Hope², Justinas Turčak¹, Jūras Banys¹, Mantas Šimėnas¹

¹Faculty of Physics, Vilnius University, Sauletekio av. 9, 10222 Vilnius, Lithuania

²Institute of Chemical Sciences and Engineering, École Polytechnique Fédérale de Lausanne (EPFL), Lausanne, Switzerland

gediminas.usevicius@ff.vu.lt

Recently, hybrid organic-inorganic compounds have attracted immense attention of the scientific community due to their diverse physical and chemical properties. One of the most interesting and researched subgroups of hybrid perovskites is methylammonium (MA) lead halides MAPbX_3 (where $X = \text{I}, \text{Br}, \text{Cl}$), due to their potential applications in efficient and low-cost solar cells, LEDs, and photodetectors [1].

Here, we use electron paramagnetic resonance (EPR) spectroscopy to study the dynamics of methylammonium cations and structural phase transitions in methylammonium lead chloride $\text{CH}_3\text{NH}_3\text{PbCl}_3$. In this work, we employ temperature dependent multifrequency continuous-wave (CW) and pulsed EPR spectroscopy to characterize paramagnetic Mn^{2+} probe ions in MAPbX_3 . The temperature dependent CW spectra reveal a sudden increase in the zero-field splitting of the Mn^{2+} ions at about 175 K (Fig. 1). This indicates a first-order phase transition related to the deformation of the inorganic framework due to the tetragonal-orthorhombic symmetry lowering.

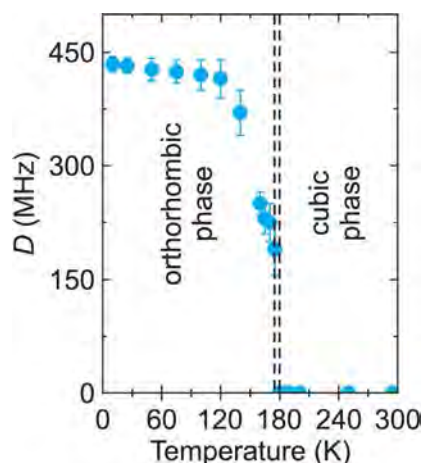


Fig. 1. Temperature dependence of the axial zero-field splitting parameter of $\text{MAPbX}_3:\text{Mn}$.

Using pulsed EPR spectroscopy, studying the temperature dependence of the T_1 relaxation time and the decoherence time T_2 of the Mn^{2+} centers in MAPbCl_3 , we found that T_1 is governed by the direct process and the Raman process due to optical phonons. We relate the obtained phonon energy of $59(4) \text{ cm}^{-1}$ to the dynamics of the inorganic framework.

This project has been funded by the Research Council of Lithuania (LMTLT) (agreement No. S-MIP-22-73).

[1] Kojima, A., et al., J. Am. Chem. Soc., 131, 6050-6051 (2009).

PHOTOPHYSICAL STUDY OF PURINE BASED METAL ION SENSORS

Kamile Tulaite¹, Justina Jovaisaite¹, Irina Novosjolova², Maris Turks², Gediminas Jonusauskas³, Saulius Jursenas¹

¹Institute of Photonics and Nanotechnology, Faculty of Physics, Vilnius University, Lithuania

²Institute of Technology of Organic Chemistry, Faculty of Materials Science and Applied Chemistry, Riga Technical University, Latvia

³Laboratoire Ondes et Matière d'Aquitaine, Bordeaux University, France
kamile.tulaite@ff.vu.lt

The purine heterocyclic system holds a significant role in biological and medicinal chemistry, primarily attributed to its intrinsic involvement in genetic information transcription and translation processes. These materials show potential applications as efficient chemical sensors, fluorescence imaging agents, photocatalysts, and sensitizers for photodynamic therapy (PDT) activated by light, including solar illumination.

The purine core proves highly advantageous for chemical modification due to well-established synthetic methods and its chemical structure, allowing to incorporate electron-donating functional groups at the C2, C6, or C8 positions of the purine core. Expanding the functionality of purine derivatives can be achieved by capitalizing on long-lived excited triplet and/or radical states. Additionally, there is the opportunity for a steady-state absorption shift towards the visible or even near-infrared range, aligning with the therapeutic window. Alternatively, derivatives featuring an external C8-complexing arm, working in conjunction with the purine N7, have been developed. Notably, there are only a limited number of recent examples showcasing purine-based metal ion sensors that leverage both the C6-substituent and the purine N7.

Here we present a detailed photophysical study of purine-based derivatives complexation processes in polar solvents and aqueous media in the field of chemical sensors. Several chemical sensor prototypes have been demonstrated for the detection of metal ions of different nature: alkali, alkaline earth, heavy and transition metals, which can be used in industry (acetonitrile as a solvent) as well as in biology and the environment (water). The synthesized compounds were able to detect traces of transition and heavy metal ions at ppb level. The new water-soluble compounds were found to exhibit high sensitivity to mercury (II) ions in water.

[1] J. Jovaisaite et al., Proof of principle of a purine D-A-D ligand based ratiometric chemical sensor harnessing complexation induced intermolecular PET, *Phys. Chem. Chem. Phys.*, 2020.

CMOS CAMERA SENSOR FOR DETECTION AND IMAGING OF PARTICLES OF IONIZING RADIATION

Jonas Jeffrey Haist¹, Anton Koroliov², Artūras Plukis²

¹Vilnius University

²Center for Physical Sciences and Technology
jonashaist@ff.stud.vu.lt

The ionizing radiation dosimeter was developed using a CMOS sensor from a 1MP camera, with an exposed silicon detector. The detector was placed in a 3D printed casing with an aperture in the lid to allow ionizing radiation to pass through. The module was shielded against optical photons and RF noise. For each measurement, 200 raw frames were captured, which were then processed in a Python program. The results obtained showed the number of high energy photons detected during the measurement period.

The calibration of the equipment was carried out using electrons from Sr-90 beta source emitters, comparing detected particle flux with declared parameters of the samples, achieving 5-8 percent uncertainty. A PHAROS (Light Conversion) femtosecond laser (wavelength - 1028 nm, pulse energy E_p - 1.5 mJ) was used to generate X-rays via inner-shell ionization. The laser beam was focused on a 30 μm diameter spot on the surface of a rotating copper disk. The flux of the X-ray source produced by the high-power laser radiation was examined while the optical power of the laser beam was incremented from 1 W to 6 W.

Results obtained were compared with a Si(Li) X-ray spectrometer (Amptek X-123), determining that the CMOS dosimeter successfully recorded a more intense X-ray flux compared to the X-ray spectrometer, which saturated at higher laser energies and was unable to detect a portion of the photons due to having a single sensor, opposed to the CMOS detector able to detect with 105 detection points. It was also found that the number of X-ray photons peaked when the optical power of the laser was set at 4 W and diminished afterwards with increasing power levels. Air ionization was also observed, but as expected, did not generate detectable X-rays.

FLUORESCENT VISCOSITY PROBES AS DIAGNOSTIC TOOLS FOR CANCER DETECTION

Artūras Polita¹

¹Vilnius University
arturas.polita@gmc.vu.lt

Viscosity is a key characteristic of biological membranes -- it governs the passive diffusion of solutes and affects the lipid raft formation and membrane fluidity. Moreover, viscosity measurements provide a convenient way to observe the compositional changes that take place in biological membranes and organelles, as the efficiency of lipid packaging and the order of lipids have a great influence on the viscosity values of lipid structures.¹ In this work, we explore the viscosity-sensitive dyes, called molecular rotors,^{2,3} as diagnostic tools for cancer detection. Through the use of fluorescence lifetime imaging microscopy (FLIM) in combination with organelle-specific BODIPY dyes, whose fluorescence lifetimes increase with increase in microviscosity, we investigate the order of lipids in lysosomes and lipid droplets of cancerous and non-cancerous live cells. Our results demonstrate that lipid droplets in cancerous cells have vastly different lipid packaging efficiencies between different cells in the same culture. In contrast, we show that lipid packaging efficiencies of lipid droplets are uniform in non-malignant cells. Finally, we demonstrate that both lysosomes and lipid droplets in malignant cells possess up to 3 times greater microviscosities compared to non-malignant cells.

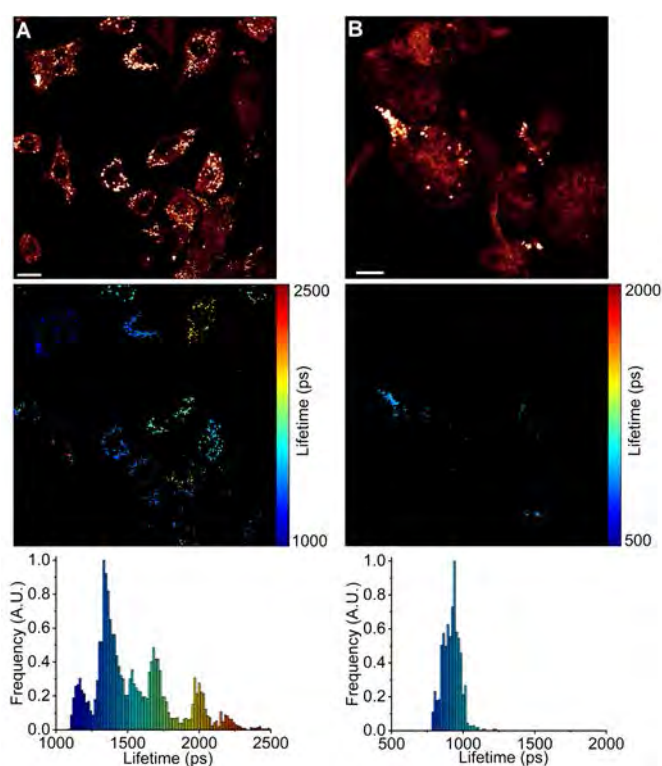


Fig. 1. FLIM of BODIPY-LD in lipid droplets of human lung cancer A549 cells (A) and human embryonic kidney HEK 293T cells (B). The top panel shows images of fluorescence intensity. FLIM images are shown in the middle panel. The corresponding lifetime histograms are shown in the bottom panel. Scale bars are 10 μm .

[1] A. Polita, M. Stancikaitė, R. Žvirblis, K. Maleckaitė, J. Dodonova-Vaitkūnienė, S. Tumkevičius, A. P. Shivabalan, G. Valinčius, RSC Adv., 2023, 13, 19257-19264.

[2] A. Polita, S. Toliautas, R. Žvirblis, A. Vyšniauskas, Phys. Chem. Chem. Phys., 2020, 22, 8296-8303.

[3] S. Toliautas, J. Dodonova, A. Žvirblis, I. Čiplies, A. Polita, A. Devišis, S. Tumkevičius, J. Šulskus, A. Vyšniauskas, Chem. - Eur. J., 2019, 25, 10342-10349.

SOLID STATE NMR STUDY OF HYBRID CALCIUM PHOSPHATES

Rokas Lemežis¹, Vytautas Klimavičius¹

¹Institute of Chemical Physics, Faculty of Physics, Vilnius University
rokas.lemezis@ff.stud.vu.lt

Calcium phosphates (CaPs) are a family of materials used for various applications such as bone regeneration, etc. Properties such as biocompatibility, bioactivity, and osteoconductivity are necessary for CaPs in bioapplications. Macroscopic properties and structures at the molecular level need to be investigated to determine newly synthesized CaPs applications.

In this study, solid state Nuclear Magnetic Resonance (NMR) was used to investigate 6 samples composed of calcium chlorapatite ($\text{Ca}_5(\text{PO}_4)_3\text{Cl}$) or goryainovite ($\text{Ca}_2(\text{PO}_4)\text{Cl}$). Samples were synthesized using different synthesis methods. ^{31}P and ^1H MAS BMR spectra were used to determine materials present in samples. Samples also were vacuumed to minimize the intensity of physisorbed/chemisorbed H_2O spectral line in ^1H MAS BMR spectra.

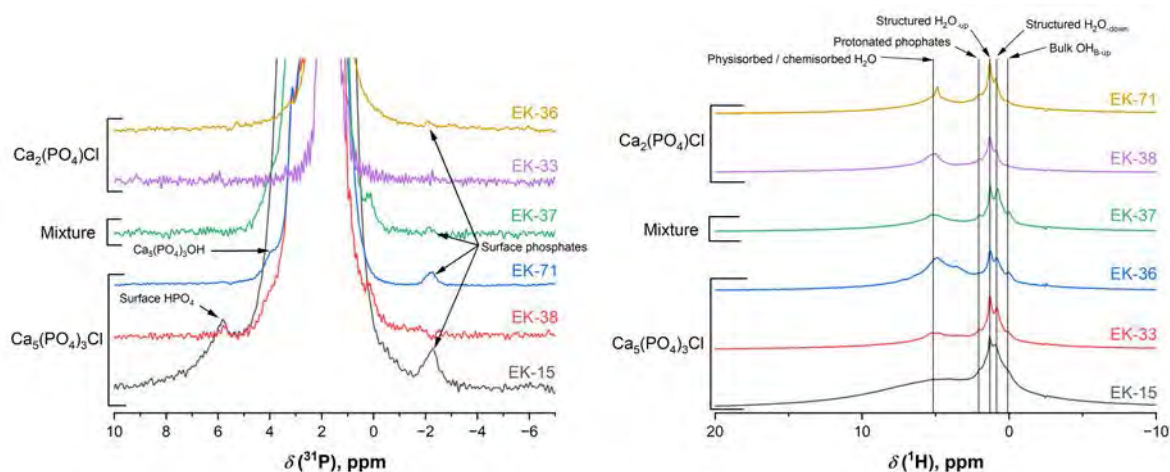


Fig. 1. ^{31}P (left) and ^1H (right) MAS BMR spectra with identified spectral lines.

It was found that surface phosphates, structured and physisorbed/chemisorbed H_2O and protonated phosphates were present in the samples.

BEYOND RARE EARTH: INVESTIGATING FECO ALLOYS UNDER STRAIN FOR PERMANENT MAGNETS

Wojciech Marciniak^{1,2,3}, Joanna Marciniak², José Ángel Castellanos-Reyes³, Mirosław Werwiński²

¹Institute of Physics, Faculty of Materials Engineering and Technical Physics, Poznań University of Technology, Piotrowo 3, 61-138 Poznań, Poland

²Department of Theory of Nanostructures and Quantum Materials, Institute of Molecular Physics, Polish Academy of Sciences, M. Smoluchowskiego 17, 60-179 Poznań, Poland

³Department of Physics and Astronomy, Uppsala University, Box 516, 75120 Uppsala, Sweden
joanna.marciniak@ifmpan.poznan.pl

In modern technology, permanent magnets play a crucial role. Today's strongest permanent magnets use rare earth elements, such as samarium and neodymium. However, these magnets have serious limitations, including a relatively low Curie temperature (T_C), restricting their application. Furthermore, the rare earth metals market experienced a significant price increase around 2011, prompting intensified research into alternative materials without these elements. Currently, rare earth element prices have risen again, so the quest for alternative permanent magnets remains relevant. FeCo alloys, particularly the $\text{Fe}_{0.4}\text{Co}_{0.6}$ body centered tetragonal alloy with lattice parameters c/a ratio close to 1.22, show promise, as indicated by Burkert *et al.*[1]. However, subsequent studies revealed structural relaxation in thin films with tetragonal deformation, leading to a body centered cubic structure for films thicker than about 15 monolayers.

Our research aims to broaden the understanding of magnetism in uniaxially deformed $\text{Fe}_{1-x}\text{Co}_x$ by investigating magnetic moments, magnetocrystalline anisotropy energy (MAE), and T_C of the alloys with Co content x in 0-1 range and c/a ratio ranging from 0.64 to 1.4. Density functional theory calculations using the full-potential local-orbital (FPLO)[2] and spin-polarized relativistic Korringa-Kohn-Rostoker (SPR-KKR)[3] codes provide magnetic moments and MAE. We approximate disordered alloys using two effective medium methods: the virtual crystal approximation (in FPLO) and the coherent potential approximation (in SPR-KKR). T_C is also determined with two methods: a qualitatively approximate disordered local moment method[4] and a quantitative method utilizing the intersection of Binder cumulants for two differently sized supercells to incorporate finite-size scaling in Monte Carlo calculations, which were conducted with UppASD code[5,6]. The approach reveals an additional high MAE region for squeezed structures with x higher than 0.7 and c/a lower than 0.85. Notably, the bct system with $c/a \approx 0.82$ lies along the fcc \rightarrow hcp transition; so, we also investigated bct(0.82) \rightarrow fcc and bct(0.82) \rightarrow hcp transitions.

W.M., J.M., and M.W. acknowledge the financial support of the National Science Centre Poland under the decision DEC-2018/30/E/ST3/00267. Part of the computations were performed on resources provided by the Poznan Supercomputing and Networking Center (PSNC).

J.Á.C-R acknowledges the support of Olle Engkvist

's Foundation and Knut and Alice Wallenberg Foundation for financial support. The UppASD simulations were enabled by resources provided by the National Academic Infrastructure for Supercomputing in Sweden (NAISS) at the NSC Centre, partially funded by the Swedish Research Council through grant agreement no. 2022-06725.

[1] T. Burkert *et al.*, Giant magnetic anisotropy in tetragonal FeCo alloys, *Phys. Rev. Lett.* 93, 027203 (2004)

[2] K. Koepf, H. Eschrig, Full-potential nonorthogonal local-orbital minimum-basis band-structure scheme, *Phys. Rev. B* 59, 1743 (1999)

[3] H. Ebert *et al.*, The Munich SPR-KKR Package, Version 7.7, 2017

[4] J. Staunton *et al.*, The disordered local moment picture of itinerant magnetism at finite temperatures, *J. Magn. Magn. Mater.* 45 (1) (1984) 15-22

[5] O. Eriksson *et al.*, *Atomistic Spin Dynamics: Foundations and Applications*. Oxford University Press, New York (2017)

[6] D. P. Landau, K. Binder, *A Guide to Monte Carlo Simulations in Statistical Physics*. Cambridge University Press, New York, NY (2005)

INVESTIGATION OF Z^0 BOSON USING CERN LHCb OPEN DATA

Nikolajus Elkana Eimutis¹, Marijus Ambrozas¹, Mindaugas Šarpis¹

¹Faculty of Physics, Vilnius University
nikolajus.elkana@gmail.com

Starting from the mid-20th century, the CERN laboratory has evolved into the foremost hub for fundamental physics, aiming not only to conduct groundbreaking research but also to inspire, educate, and unite nations. The primary focus of CERN lies on experiments conducted with the Large Hadron Collider (LHC), the world's largest and most powerful particle accelerator. Key experiments such as ATLAS and CMS explore a broad spectrum of physical phenomena, including the elusive Higgs boson, through high-energy particle collisions. Beyond accelerators and laboratories, the CERN Open Data project, initiated in 2014, enables enthusiasts worldwide to engage in data analysis with specific datasets.

This presentation provides an exploration of the intricate process through which data from the LHCb experiment reaches the CERN Open Data portal. The emphasis is on elucidating how this data, particularly regarding the Z^0 boson's decay into a muon pair, becomes accessible to a global audience.

Muons are subatomic particles that belong to the lepton family, sharing similarities with electrons but possessing greater mass. Due to their increased mass, muons play a crucial role in probing high-energy phenomena and are particularly significant in experiments involving particle accelerators like the LHC. Exploring the decay of the Z^0 boson into a muon pair through a Drell-Yan process, our research provides valuable insights into the fundamental interactions and properties of these particles, contributing as one of the initial analyses of LHCb data posted on the Open Data portal.

NIELSEN IDENTITIES IN THE STANDARD MODEL

Nojus Danyla¹, Simonas Draukšas²

¹Faculty of Physics, Vilnius University, Lithuania

²Institute of Theoretical Physics and Astronomy, Vilnius University, Lithuania
nojus.danyla@gmail.com

It is not always clear whether definitions of physical quantities is really physical, for example, it may be that the definition is gauge-dependent. One of investigating gauge-dependence is the use of Nielsen Identities [1] --- a generalised form of Slavnov-Taylor Identities [2], which come from BRST symmetry [3, 4]. These Identities enable us to express dependence on the gauge parameter in terms correlation functions containing BRST sources related to the gauge parameters.

This study focuses on understanding Nielsen Identities in the Standard Model, in which we investigate the gauge dependence of quark self-energies. We explore dependencies of quark self-energies on the gauge parameter in two distinct ways: 1) by calculating the Nielsen identities via a BRST Lagrangian; 2) by calculating quark self-energies and taking the derivative with respect to the gauge parameter. The goal is to check the consistency between the results obtained through both approaches.

In this presentation, we will introduce all the needed concepts as well as our progress.

[1] . Nielsen, On the gauge dependence of spontaneous symmetry breaking in gauge theories, Nuclear Physics B, Dec. 1975, 101, 173–188.

[2] . Gambino and P. A. Grassi, Nielsen identities of the SM and the definition of mass, Physical Review D, Aug. 2000, 62, 076002.

[3] . Becchi, A. Rouet, and R. Stora, Renormalization of gauge theories, Annals of Physics, June 1976, 98, 287–321.

[4] . V. Tyutin, Gauge Invariance in Field Theory and Statistical Physics in Operator Formalism, 2008.

EXTRACTING DIFFRACTIVE PROTONS AND BACKGROUND ANALYSIS FROM ATLAS FORWARD PROTON DETECTORS

Aneta Bien^{1,2}

¹Faculty of Electronics and Information Technology, Warsaw University of Technology, Poland

²Institute of Nuclear Physics, Polish Academy of Sciences, Poland
aneta.bien.stud@pw.edu.pl

The ATLAS experiment at CERN utilizes high-energy collisions between protons to investigate fundamental particles and forces. In certain processes, the so-called "diffractive interactions", the LHC protons may collide in a very unique manner and remain intact. They preserve their original state and scatter at extremely small angles (a few hundred microradians) before continuing their trajectory into the LHC beampipe [1]. To measure these protons, a set of ATLAS Forward Protons Detectors (Fig. 1, Left) are located around 210 meters away from the ATLAS. By studying the collisions with the forward proton scattering, scientists can gain insights into the underlying nature of diffraction, enhancing our comprehension of the sub-atomic scale, potentially unveiling new particles or forces beyond the Standard Model.

The signal recorded by the AFP detectors contains multiple components. Alongside the diffractive proton, there are additional contributions in the recorded data, including particles generated by the interaction of the diffractive proton with the beampipe and beam instrumentation along the ATLAS Interaction Point-detector path, the signal originating from the primary beam, and particle showers generated by the forward proton when it interacts with the AFP detector components (Fig. 1, Right). Extracting the proton signal involves extensive analysis of background sources in terms of their origin, multiplicity or spatial distribution and implementation of methods that will lead to the identification of the background in the data. An analysis was carried out both for Monte Carlo simulation and experimental data from AFP detectors collected during LHC run in 2022.

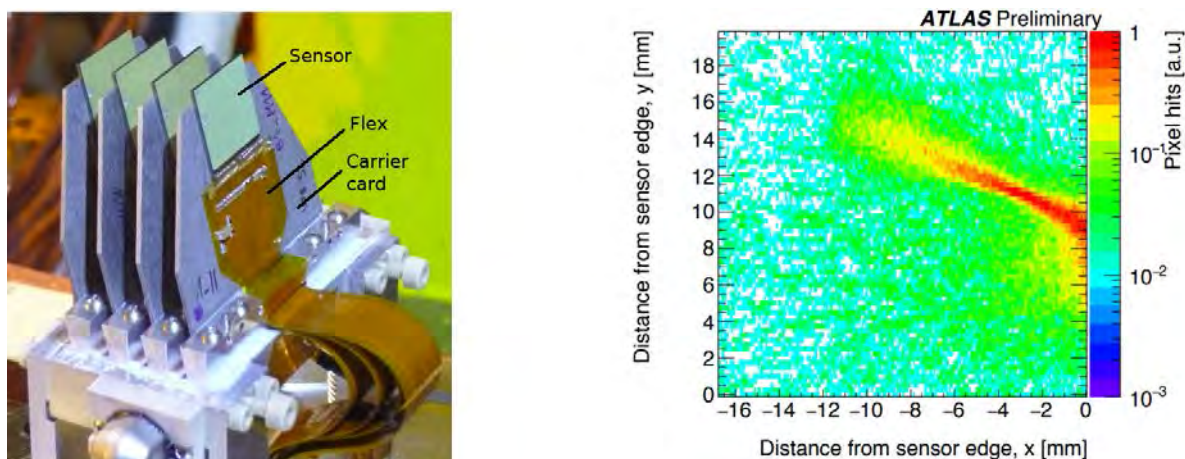


Fig. 1. Left: The AFP detector [2]. **Right:** Normalized pixel hit-maps in one of the AFP detector. The diagonal pattern corresponds to the detected diffractive proton [3].

[1] Maciej Lewicki, Overview of ATLAS Forward Proton detectors for LHC Run 3 and plans for the HL-LHC

[2] S. Grinstein et al., Module production of the one-arm AFP 3D pixel tracker. JINST, 12(01):C01086, 2017. Comments: PIXEL 2016 proceedings; Submitted to JINST

[3] Paula Agnieszka Erland. ATLAS Forward Proton detectors status and plans. Status of AFP. Technical report, CERN, Geneva, 2019.

NORMAL MODES OF SOLID-STATE PLASMA IN CONDITIONS OF BLOCH GAIN

Lukas Stakėla¹, Kirill N Alekseev¹

¹Center for Physical Sciences and Technology, Department of Optoelectronics, Vilnius, Lithuania
lukas.stakela@ftmc.lt

Theoretical predictions suggest that by using specially designed semiconductor structures, it is feasible to develop an inversionless Bloch laser, commonly known as a THz emitter [1]. This capability can be realized using semiconductor superlattices, which, in contrast to bulk semiconductors feature remarkably extended lattice periods. The high-frequency gain in superlattices is associated with negative differential conductivity [1,3], eliminating the need for population inversion and enabling the device to function at room temperature. However, comprehensive theoretical research is needed to fully grasp the underlying mechanisms facilitating the extension of emitted frequencies into the terahertz range.

To grasp the working mechanism behind such a system, we employ a model first suggested by Ignatov et al. [2]. Despite its age, this is still a poorly understood model that underlines the importance of plasma effects. The high-frequency conductivity of the superlattice can be calculated from a Boltzmann transport equation with Bhatnagar-Gross-Krook (BGK) operator and thus the eigenmodes of the emission can be found. If one considers the dielectric function of a superlattice in the limit of no spatial dispersion, when high-frequency conductivity is reduced to one calculated in the classical work [3], the description of the system is governed by a relatively simple cubic equation.

Our investigation of the cubic equation shows that there is good correspondence, at all frequencies except ones corresponding to the global extrema of the solutions, between the approximations found in [2] and full analytical solutions calculated in our work. Furthermore, we find interesting correlations between decay/amplification rates of different normal modes (low-frequency “relaxation mode” and high-frequency “hybrid Bloch-plasma mode”). These effects can potentially be applied to create plasmonic devices based on superlattices, such as THz amplifiers, detectors, and switchers.

[1] Esaki, L. and Tsu, R., IBM J. Res. Dev. 14, 61-65 (1970).

[2] Ignatov, A. A. and Shashkin, V. I., Sov. Phys. JETP 66, 526 (1987).

[3] Ktitorov, S. A., Simin, G. S. and Sindalovskii, V. Y., Fiz. Tverd. Tela 13, 2230-2233 (1971).

TOWARDS HIGHLY CONDUCTIVE NANOCRYSTALLISED VANADATE-PHOSPHATE GLASSES

K Gadomski¹, T K Pietrzak¹, Sz Starzonek², S J Rzoska³, J E Garbarczyk¹

¹Faculty of Physics, Warsaw University of Technology, Poland

²Laboratory of Physics, Faculty of Electrical Engineering, University of Ljubljana, Slovenia

³Institute of High Pressure Physics of the Polish Academy of Sciences, Poland

krzysztof.gadomski2.dokt@pw.edu.pl

In the last few decades, the growth of renewable power sources has been observed. Unfortunately, those power sources are heavily dependent on weather conditions. For this reason, battery systems are needed for power grid stabilization.

Vanadate-phosphate is a wide group of materials, and it has a long history of research and development. Crystalline VOPO₄ was investigated by e.g. M. S. Whittingham's team [1], Li₃V₂(PO₄)₃ was studied by e.g. L. F. Nazar's team [2]. However, corresponding glasses, including vanadate-phosphates, were at the edge of mainstream researches. E.g., 90 V₂O₅ · 10 P₂O₅ glasses and nanomaterials were studied by T. K. Pietrzak's team [3, 4]. Glassy material has conductivity around $\sigma = 7 \cdot 10^{-5}$ S/cm but after nanocrystallization the electronic conductivity dramatically increased to the level of $\sigma = 7 \cdot 10^{-2}$ S/cm at room temperature. Moreover, gravimetric capacity was also determined for this highly conductive material and it was at the level of 225 mAh/g in first cycle (C/20 current), but it dropped to 140 mAh/g in the third cycle.

The objective of this work is to synthesise a glassy analogue of 95 V₂O₅ · 5 P₂O₅ (i.e., with a higher content of vanadium) and optimize its electronic conductivity. For this purpose, many different measurement methods were used: XRD, SEM and EDX to confirm the glassy state, shape of the surface and to determine percentage of impurities, DSC to check glass thermal stability, and DC for electrical measurements. With this method, changes in material during heat treatment can be described, and correlations between changes in conductivity and other structural factors will be shown.

This work was supported by the National Science Centre (NCN, Poland) through OPUS-23 grant no. 2022/45/B/ST5/04005

[1] Z. Chen et al.: Electrochemical Behavior of Nanostructured e-VOPO₄ over Two Redox Plateaus. *J. Electrochem. Soc.* 160 (2013) A1777

[2] H. Huang et al.: Nanostructured Composites: A High Capacity, Fast Rate Li₃V₂(PO₄)₃ Carbon Cathode for Rechargeable Lithium Batteries. *Adv. Mater.*, 14: 1525-1528

[3] T.K. Pietrzak et al.: Electrical properties vs. microstructure of nanocrystallized V₂O₅-P₂O₅ glasses. *Journal of Power Sources* 194 (2009) 73-80

[4] T.K. Pietrzak et al.: Highly Conductive 90V₂O₅-10P₂O₅ Nanocrystalline Cathode Materials for Lithium-ion Batteries. *Procedia Engineering* 98 (2014) 28-35

CARRIER DYNAMICS IN Ga-POLAR AND N-POLAR InGaN QUANTUM WELL STRUCTURES

Lukas Šiaulyš^{1,2}, Monika Gudaitytė^{1,2}, Kazimieras Nomeika^{1,2}

¹Vilnius University

²Institute of Photonics and Nanotechnology

lukas.siaulyš@ff.stud.vu.lt

InGaN plays an important role in semiconductor devices including LEDs, laser diodes, solar cells, high-power electronics owing to its beneficial properties such as a direct and tunable bandgap, high internal quantum efficiency, high carrier mobility. However, nitride semiconductor devices suffer from efficiency droop issues at elevated free carrier densities. Moreover, by increasing In content in the InGaN devices, quantum efficiency significantly drops, which limits the production of efficient InGaN-based green light devices. Due to the crystalline symmetry of nitride semiconductors, different polarity structures can be achieved. While conventional growth is in the c-direction (Ga-polar), one can achieve N-polarity by changing the growth conditions. This could be promising in altering the electrical properties of transistor devices, enhancing In incorporation for longer wavelength devices. Thus, it is important to investigate free carrier recombination pathways in the structures of both polarities. In this study, we thoroughly investigate non-equilibrium carrier dynamics in Ga-polar and N-polar quantum well structures. We do this by employing light induced transient grating and time integrated photoluminescence techniques, which provide us carrier density dependent diffusivity, carrier lifetime, and internal quantum efficiency values. We then model carrier dynamics with a modified ABC model. While N-polarity InGaN samples have not been extensively studied within the science community, our study revealed relatively high radiative bimolecular recombination rates for these samples, which is a promising indication for further advancements in nitride-based devices.

THERMAL CONDUCTIVITY AND STRUCTURAL CHANGES IN ULTRA-HIGH PRESSURE TREATED SILICA GLASS -- A MOLECULAR DYNAMICS STUDY

Adam Puchalski¹, Anton Hul¹, Jihui Nie², Tomasz K Pietrzak¹, Paweł Kębliński²

¹Faculty of Physics, Warsaw University of Technology, Poland

²Department of Materials Science and Engineering, Rensselaer Polytechnic Institute, USA
adam.puchalski.stud@pw.edu.pl

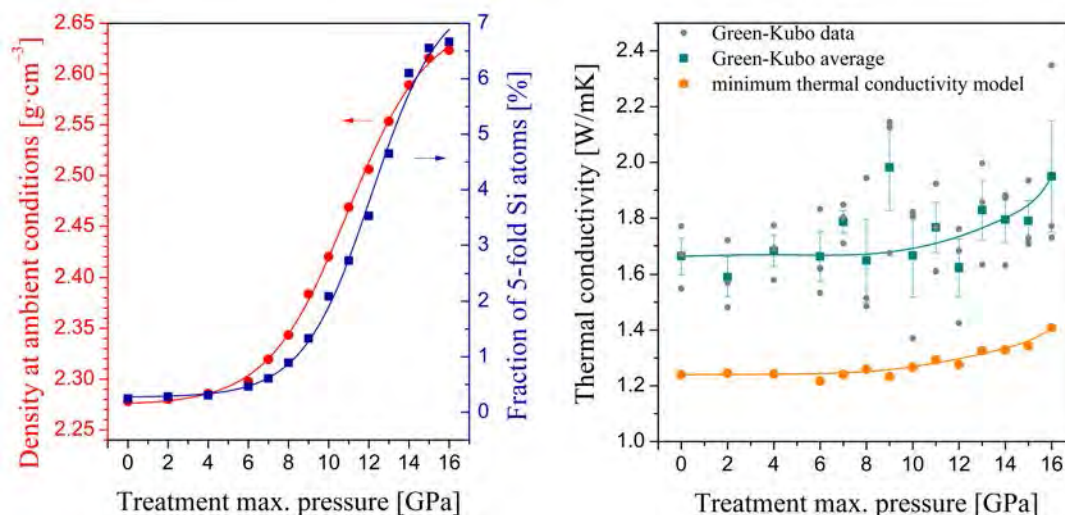


Fig. 1. The calculated density and 5-fold silicon fraction dependence on the maximal treatment pressure as well as the thermal conductivity change.

Silica is a common material with a wide range of commercial applications -- including the production of glass, concrete and semiconductors. Amorphous silica is considered an archetypal tetrahedral glass, and is a component of most glasses due to its abundance and exceptional glass-making properties [1]. The objective of this study [2] was to calculate the thermal conductivity of amorphous silicon oxide SiO₂ structures after they were treated under ultra-high pressure using molecular dynamics. Previous studies have concluded that silica glass undergoes permanent densification through the increase of silicon-oxygen coordination number when subjected to ultra-high pressure of the order of GPa [3,4], although to our knowledge no study of the influence of this process on thermal conductivity yet exists.

The amorphous silica structures were obtained by melt-quenching using the LAMMPS [5] molecular dynamics software and the SHIK-1 empirical potential [6]. Then, they were pressed to maximal pressures from 2 GPa to 16 GPa and subsequently relaxed. The thermal conductivity of these samples was determined using the equilibrium Green-Kubo method [7]. The results show an increase in thermal conductivity. They were compared with the minimum thermal conductivity model, which also predicts a rise in thermal conductivity, though not as sharp as the MD simulation suggests.

The increase in density was also investigated and compared with the literature. The local structure of the samples was investigated for high-pressure treatment induced changes. An increase in silicon-oxygen coordination was observed, caused by the increased fraction of 5-fold coordinated silicon. An interesting finding is the tendency of 5-fold silicon atoms to cluster.

This computational study gives a clue that high-pressure treatment of silica glass should lead to a noticeable and permanent increase in its thermal conductivity. Experimental confirmation of this phenomenon is still expected.

-
- [1] K. J. Rao, Structural chemistry of glasses. Amsterdam, Elsevier, 2002. chapter 12.
 [2] A. Puchalski, A. Hul, J. Nie, T. Pietrzak, and P. Kębliński, submitted to the Journal of Applied Physics, 2024.
 [3] P. W. Bridgman and I. Simon, Journal of Applied Physics, vol. 24, pp. 405-413, June 1953.
 [4] T. Deschamps et al. Journal of Physics: Condensed Matter, vol. 25, p. 025402, Nov. 2012.
 [5] A. P. Thompson et al. Computer Physics Communications, vol. 271, p. 108171, 2022.
 [6] S. Sundararaman et al. The Journal of Chemical Physics, vol. 148, no. 19, p. 194504, 2018.
 [7] R. Kubo et al. Journal of the Physical Society of Japan, vol. 12, no. 11, pp. 1203-1211, 1957.

PRINTABILITY OF MUCOADHESIVE SODIUM ALGinate/CHITOSAN GELS DELIVERING PHOTOSENSITIZER IN PHOTODYNAMIC THERAPY

Maria Skrodzka¹, Jerzy Detyna¹, Katarzyna Matczyszyn²

¹Department of Mechanics, Materials and Biomedical Engineering, Faculty of Mechanical Engineering, Wrocław University of Science and Technology

²Institute of Advanced Materials, Faculty of Chemistry, Wrocław University of Science and Technology
maria.skrodzka@pwr.edu.pl

Additive technologies have propelled the popularity of personalized medicine, expanding the adaptation of various biomaterials for incremental processing. Current research focuses on additive manufacturing of drug carriers and active substances for different therapies, e.g. photodynamic therapy (PDT), an increasingly common non-invasive approach for mucosa lesions. Sodium alginate (SA) and chitosan, natural-based, biocompatible polymers, exhibit the potential to deliver active substances [1-2]. The mucoadhesive properties of chitosan make it suitable for drug delivery through the mucosa, while the SA solution shows excellent printability [3].

This study aimed to determine how the addition of adhesion-enhancing chitosan and photosensitizer affects the printability of sodium alginate gels. Additionally, the influence of printing parameters - speed and pressure of the print head on printing accuracy - was examined. The study took into account the effect of printing speed (5, 7, 10 mm/sec), pressure (80-120 kPa), chitosan concentration (0%, 3%, 4%, 5%, added to SA in 1:2 mass ratio) and the presence of methylene blue on printing accuracy. To assess the quality of prints, the expansion coefficient (α) was used which determines the ability of the material to flow on the substrate on which it is deposited after printing.

Results indicate that chitosan enhances printing accuracy (Figure 1), but its excessive concentration causes nozzle clogging. MANOVA analysis shows that the spread of ink on the substrate is influenced by both the pressure and the head feed speed. The addition of a photosensitizer does not impact printing accuracy. Chitosan with mucoadhesive properties positively influences the printability of alginate ink with proper concentration adjustment. Research results show the possibility of the usage of sodium alginate/chitosan inks in applications where adhesion to the mucosa is required while at the same time ensuring high print quality. Moreover, the addition of methylene blue does not adversely affect printability, therefore this type of ink can be used as a photosensitizer carrier in PDT.

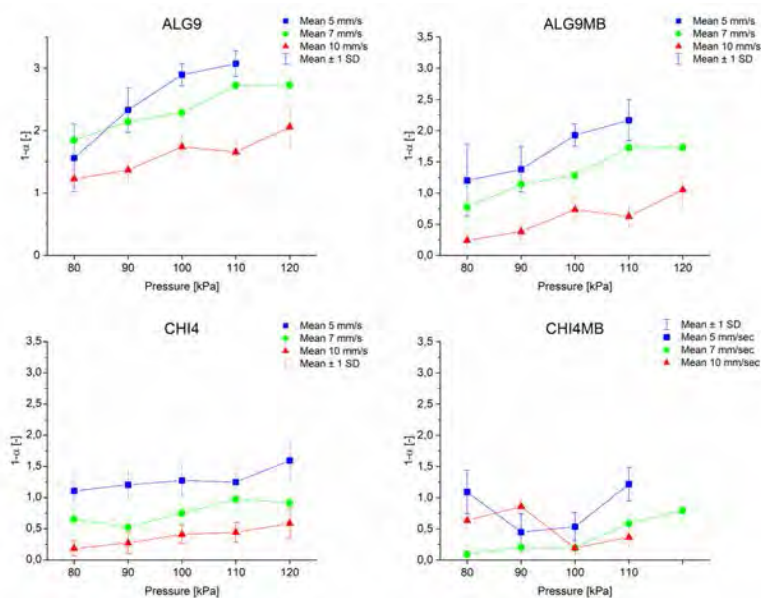


Fig. 1. Expansion ratio depending on pressure and printing speed for sample study groups

- [1] H. Liu et al., A functional chitosan-based hydrogel as a und dressing and drug delivery system in the treatment of wound healing. RSC Adv, vol. 8, no. 14, pp. 75337549, Feb. 2018.
 [2] D. S. Lima et al., pH-responsive alginate-based hydrogels for protein delivery. J Mol Liq, vol. 262, pp. 2936, Jul. 2018.
 [3] Á. Aguilar-De-leyva, V. Linares, M. Casas, and I. Caraballo, 3D printed drug delivery systems based on natural products. Pharmaceutics, vol. 12, no. 7, pp. 120, Jul. 2020.

A MECHANOCHEMICAL PROCESS FOR IMPROVING RESVERATROL PROPERTIES BY CO-CRYSTALLIZATION

Elena Mirabela Soare¹, Raul Augustin Mitran¹, Daniel Lincu¹, Irina Atkinson¹, Simona Ionitã¹, Adriana Rusu¹, Jeanina Pandele Cusu¹, Coca Iordache², Victor Fruth¹

¹Ilie Murgulescu Institute of Physical Chemistry, Romanian Academy

²TeraCrystal SRL, 67-103 Donat, 400293 Cluj Napoca, Romania

e.msoare96@gmail.com

Natural antioxidant compounds, such as trans-resveratrol, could be used as an alternative for the antibiotics used in meat production, without their disadvantages. The unique physical properties exhibited by novel solid forms of a drug, such as co-crystals, can impact key pharmaceutical parameters, including storage stability, compressibility, density as well as dissolution rates and solubility, which are essential factors in achieving suitable bioavailability.

Trans-Resveratrol is a promising bioactive compound with antibacterial activity, but low bioavailability due to its low aqueous solubility. Mechanochemical synthesis is an alternative route to solution-based co-crystal synthesis, offering higher energy efficiency, reduced solvent waste, high yields and improved recovery of the final product. The aim of this study is the mechanochemical synthesis of resveratrol (R)– piperazine (P) co-crystals, used as nutraceutical compounds. Different synthesis conditions (the nature and amount of added solvent, reaction time) were investigated and their influence on the co-crystal phase and purity were determined. A reaction time of up to 1 h is sufficient for the completion of the reaction. Non-toxic solvents (water, ethanol) can be used to obtain a desired co-crystal phase with high purity.

Acknowledgments:

This work was supported by a grant of the Romanian Ministry of Education and Research, CNCS-UEFISCDI, project number PN-III-P2-2.1-PTE-2021-0393, contract number PTE 98/2022.

SOLVENT-FREE MECHANOCHEMICAL SYNTHESIS OF CSPBBR₃ QUANTUM DOTS WITH SURFACE-PASSIVATING LIGANDS

Pijus Domantas Valentukevičius¹, Simas Šakirzanovas¹

¹Institute of Chemistry, Faculty of Chemistry and Geosciences, Vilnius University, Lithuania
pijus.valentukevicius@chgf.stud.vu.lt

Inorganic metal halide perovskites which have the general formula ABX₃ (where A = Cs⁺, Rb⁺, K⁺; B = Pb²⁺, Sn²⁺, Ge²⁺; X = I⁻, Br⁻, Cl⁻) are semiconducting materials with a high potential for optoelectronic applications. CsPbBr₃ nanoparticles (quantum dots) are promising for the development of LEDs [1], liquid crystal displays [2] and solar cells [3]. Metal lead halide perovskites are synthesized using various procedures such as hot-injection, microwave assisted synthesis, solvothermal, sonochemical and co-precipitation methods. In comparison, the mechanochemical synthesis method, which is also employed as ball-milling, is highly advantageous due to the ease of up-scaling for industrial production, no need of solvents and simplicity of procedure. Additionally, conventional methods often require the use of long-chain passivating-ligands which brings limitations for material post-processing and applicability [4]. In this work CsPbBr₃ quantum dots were successfully synthesized with the direct use of a short-chain ligand DDAB. Moreover, the influence of various solvent-free mechanochemical synthesis parameters were analyzed for the production of photoluminescent CsPbBr₃ quantum dots with two surface-passivating ligands (DDAB and an equimolar mixture of oleylamine and oleic acid). The resulting nano or microscopic-sized particle morphology was analyzed with SEM, phase purity – by XRD analysis and photoluminescence – by spectrofluorimetry. Our findings suggest that initial particle morphology of the CsPbBr₃ powder before the addition of surface-passivating ligands and subsequent ball-milling has a significant influence on the obtained nanoparticle morphology. Furthermore, the type of ligand being used for the synthesis influences the optimal material to ligand ratio, position of emission maxima (519 nm for the mixture of OLA with OA and 536 nm) and the resulting particle morphology.

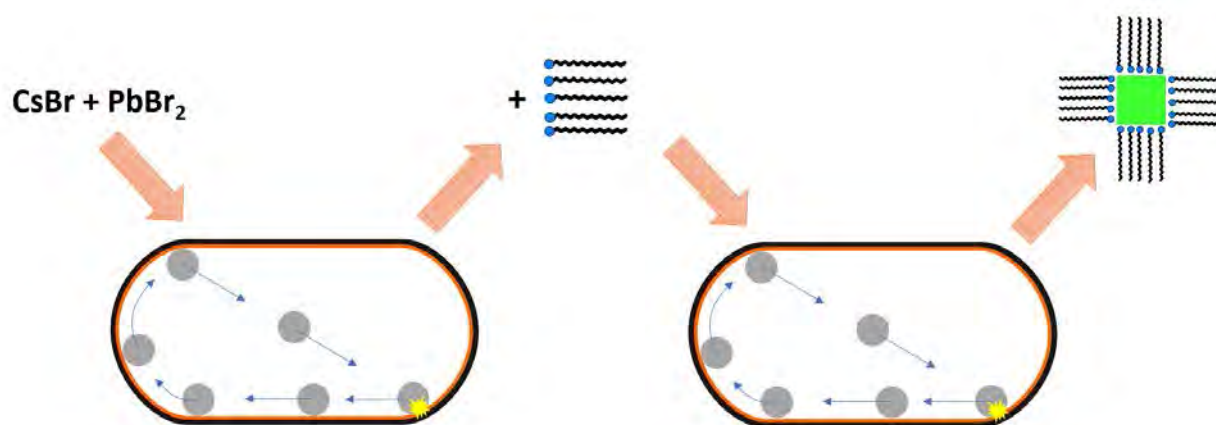


Fig. 1. Schematic diagram of the applied mechanochemical synthesis method with the use of surface-passivating ligands.

- [1] W. Cai et al., High-performance and stable CsPbBr₃ light-emitting diodes based on polymer additive treatment, *RSC Adv.*, 2019, 9, 27684.
 [2] L. Protesescu et al., Low-Cost Synthesis of Highly Luminescent Colloidal Lead Halide Perovskite Nanocrystals by Wet Ball Milling, *ACS Applied Nano Materials* 2018 1 3, 1300-1308.
 [3] S. Ullah et al., All-inorganic CsPbBr₃ perovskite: a promising choice for photovoltaics, *Mater. Adv.*, 2021, 2, 646-683.
 [4] S. Peng et al., Pure Bromide-Based Perovskite Nanoplatelets for Blue Light-Emitting Diodes, *Small Methods*, 3, 1900196.

SYNTHESIS OF 3-(2,4-DIHYDROXY-5-BENZYL)ALKYL CARBOXYLIC ACIDS AND THEIR DERIVATIVES

Vilius Petraška¹, Ieva Žutautė¹, Algirdas Brukštus¹

¹Vilnius University
vilius.petraska@chgf.vu.lt

HSP90 (Heat Shock Protein 90) is a chaperone protein that belongs to the heat shock protein class and has a mass roughly equal to 90 kDa. The protein is found in most animal kingdoms and accounts for 1-2% of all proteins located inside human cells. The chaperone is responsible for proper protein folding, their stabilization during heat stress conditions and assistance during degradation [1]. Cancer cells contain elevated levels of HSP90, which is vital to their migration, metastasis, proliferation and other processes occurring during tumor growth [2]. According to the data presented by the World Health Organization in 2022, cancer is a leading cause of deaths globally, responsible for around 10 million deaths annually [3]. Consequently, HSP90 has been subject to numerous studies over the last decade as a potential target for anti-cancer and anti-neurodegenerative medications [2].

The studies of radicicol (a natural product that binds competitively to HSP90) have shown that a resorcinol fragment with its hydroxy groups is crucial to the inhibition of the N-terminal domain, which contains the pre-eminent region of the protein — the ATP binding pocket [4]. Further studies revealed that for a drug molecule to bind effectively to the active site of the protein, it needs to contain an aromatic ring situated near the resorcinol moiety [5].

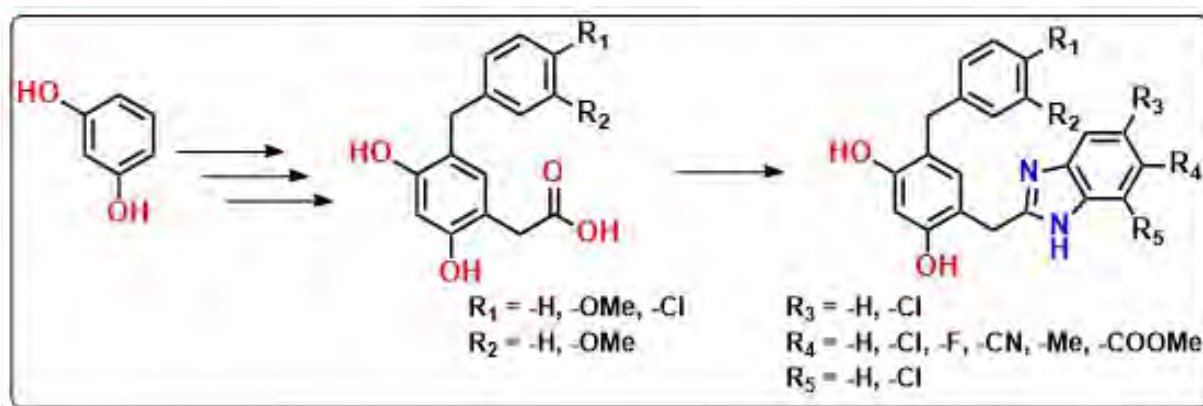


Fig. 1. Synthesis of benzimidazoles using resorcinol as a starting compound

The objective of this work is to synthesize various 3-(2,4-dihydroxy-5-benzyl)alkyl carboxylic acids and use them in the synthesis of potential resorcinol-based HSP90 inhibitors containing a benzimidazole moiety. The ten-step synthesis, its challenges and results as well as more details about HSP90 will be discussed during the presentation.

Acknowledgement: This research was funded by the Research Council of Lithuania (project no. P-ST-23-151).

- [1] Tsutsumi, S. et al. Charged linker sequence modulates eukaryotic heat shock protein 90 (Hsp90) chaperone activity. *PNAS*, 109(8), 2937 (2012).
 [2] Neckers, L., Neckers, K. Heat-shock protein 90 inhibitors as novel cancer chemotherapeutics an update. *Expert Opinion on Emerging Drugs*, 10(1), 137 (2005).
 [3] World Health Organization (2022, February 3). Cancer.
 [4] Schulte, T. W. et al. Interaction of radicicol with members of the heat shock protein 90 family of molecular chaperones. *Molecular Endocrinology* (Baltimore, Md.), 13(9), 1435 (1999).
 [5] Ardestani, M. et al. Heterocyclic Compounds as Hsp90 Inhibitors: A Perspective on Anticancer Applications. *Pharmaceutics*, 14(10) (2022).

CALCULATION OF HIGH-RESOLUTION UV SPECTRA OF DIATOMIC MOLECULES

Karolis Sarka^{1,2}

¹Center for Physical Sciences and Technology

²Sophia University

ksarka@eagle.sophia.ac.jp

Availability of accurate and high-resolution spectra for atmospheric and interstellar photochemistry modelling is a necessity when considering isotopic fractionation and shielding effects. There still are numerous diatomic compounds with missing UV absorption cross-sections that are very complicated to measure in laboratory setting. To provide some insight into sulfur photochemistry in Archean atmosphere, two key diatomic molecules should be highlighted: S₂ [1] and SO [2].

The *ab initio* potential energy curves were calculated for both compounds using Molpro2015 package at MRCI-F12+Q/aV(5+d)Z level of theory. The total absorption cross-sections for SO were calculated for A³Π ← X³Σ⁻ transition, and two nonadiabatically-coupled-potential ([C³Π - C³Π] ← X³Σ⁻, and [B³Σ⁻ - 3³Σ⁻] ← X³Σ⁻) transitions. For S₂ molecule, the photoabsorption spectra were calculated for the transitions between ground state, X³Σ_g⁻, and two excited states: B³Π_u and B³Σ_u⁻. The spectra were calculated using time-independent R-matrix theory for one-dimensional systems. With this approach we can obtain the numerical solutions for the energies and wavefunctions of all discrete vibrational states on all electronic potential energy curves. If required, we can also include the nonadiabatic coupling between electronic states.

As shown, the theory enables the calculation of highly accurate absorption cross-sections that can substitute, or extend, experimental spectra where the experiments are not feasible. Such spectra also provides a way towards studies of isotopic fractionation, self-shielding and photochemical modelling.

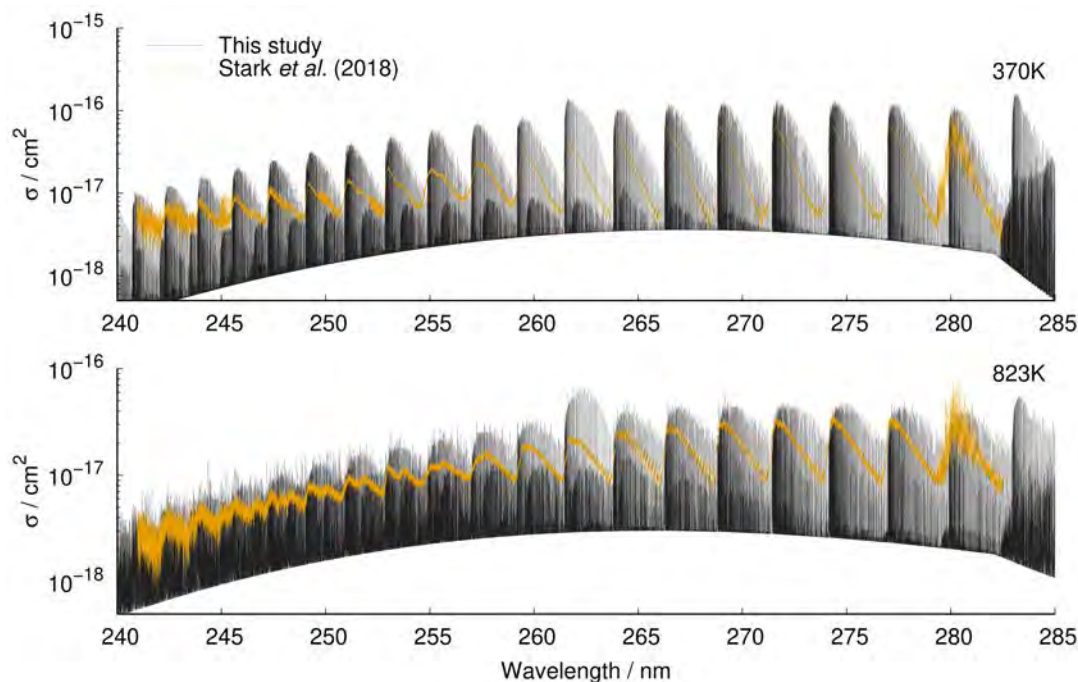


Fig. 1. Calculated absorption cross-sections and experimental spectra by Stark *et al.* [3] of sulfur dimer

[1] Sarka and Nanbu, ACS Earth Space Chem. 2023, 7, 12, 2374–2381

[2] Sarka and Nanbu, J. Phys. Chem. A 2019, 123, 17, 3697–3702

[3] Stark *et al.*, J. Chem. Phys. 2018, 148, 244302

DETECTING ATOMIC INTERACTIONS IN SMALL-MOLECULE CRYSTAL STRUCTURES

Andrius Merkys¹, Eglė Šidlauskaitė¹, Antanas Vaitkus¹

¹Sector of Crystallography and Chemical Informatics, Institute of Biotechnology, Life Sciences Center, Vilnius University, Lithuania
andrius.merkys@gmc.vu.lt

Crystallography provides researchers with exact positions of atoms composing crystal structures [1], but it is unable to capture chemical bonding. Therefore, distance-based heuristics are employed to detect chemical bonds. One such heuristic is based on the sum of per-element atomic radii for each pair of atoms in a structure. However, there are several different atomic radii tables with none of them accepted universally.

The most widely used atomic radii tables [2,3,4] were derived from data from the Cambridge Structural Database [5]. This database is distributed under a proprietary license, which imposes restrictions on the usage and spread of derivative works. Therefore, a completely independent workflow is needed to produce open atomic radii tables in an unsupervised manner. In this work, we have devised a workflow to derive atomic radii tables from data in the Crystallography Open Database [6].

Our workflow identifies the lowest density region in each pairwise interatomic distance distribution as the van der Waals gap [7]. This gap separates the observations coming from covalently interacting atom pairs from those originating chiefly from the van der Waals interactions. A Gaussian distribution mixture model is fitted on the distance distribution to find the lowest density region. Finally, atomic radii are calculated by solving an equation system constructed from pairwise radii sums.

Atomic radii table derived in this work follows the typical trend of other published tables. This observation confirms that it is possible to derive usable atomic radii tables from open small-molecule data in unsupervised manner. Review of the derived results, comparison between radii in published tables and visualization of covalent bond length determination for pair of chemical elements are available online [8], as well as a tool for structure validation using derived covalent radii [9].

-
- [1] Gražulis et al. Computing stoichiometric molecular composition from crystal structures. *Journal of Applied Crystallography*, 48(1):85–91, 2015
- [2] Meng et al. Determination of molecular topology and atomic hybridization states from heavy atom coordinates. *Journal of Computational Chemistry*, 12(7):891–898, sep 1991
- [3] Cordero et al. Covalent radii revisited. *Dalton Transactions*, 21:2832–2838, 2008
- [4] Pyykkö et al. Molecular Single-Bond Covalent Radii for Elements 1–118. *Chemistry—A European Journal*, 15(1):186–197, 2008
- [5] Groom et al. The Cambridge Structural Database. *Acta Cryst*, B72:171–179, 2016
- [6] Gražulis et al. Crystallography Open Database (COD): an open-access collection of crystal structures and platform for world-wide collaboration. *Nucleic Acids Research*, 40(D1):D420–D427, Jan 2012
- [7] Alvarez. A cartography of the van der Waals territories. *Dalton Transactions*, 42:8617–8636, 2015
- [8] Šidlauskaitė (2024). Covalent radii table. [online] Available at: http://databases.crystallography.lt:8080/contacts/website/cgi-bin/cov_radii_table.pl [Accessed 26 Jan. 2024]
- [9] Merkys (2024). Inter-atom contact checker. [online] Available at: http://databases.crystallography.lt:8080/contacts/website/cgi-bin/check_contacts.pl [Accessed 26 Jan. 2024]

SYNTHESIS OF 1-(2,4-DIFLUOROPHENYL)-5-OXOPYRROLIDINE-3-CARBOXYLIC ACID DERIVATIVES AND INVESTIGATION OF THEIR ANTICANCER ACTIVITY

Guoda Pranaitytė¹, Birutė Grybaitė¹, Vytautas Mickevičius¹, Vilma Petrikaitė², Ugnė Endriulaitytė²

¹Department of Organic Chemistry, Kaunas University of Technology, Lithuania

²Laboratory of Drug Targets Histopathology, Lithuanian University of Health Sciences, Lithuania
guoda.pranaityte@ktu.edu

One of the main causes of cancer is the multiplication of damaged cells and the formation of tumors [1]. New synthetic molecules are being synthesized and studied which could be characterized by antitumor activity and low toxicity. The list of drugs approved by U.S. FDA shows that fluorinated compounds are included in the composition of many medicinal molecules [2]. For this reason, molecules with a fluorine atom in the aromatic ring becoming an interesting object for research.

By reaction of 2,4-difluoroaniline (1) with itaconic acid, the starting compound 1-(2,4-difluorophenyl)-5-oxopyrrolidine-3-carboxylic acid (2) was prepared. Methyl 1-(2,4-difluorophenyl)pyrrolidin-2-one carboxylate (5) was obtained from the esterification reaction using catalytic amount of sulfuric acid. In order to synthesize a compound with functional group of hydrazide, methyl ester 5 was transformed into the hydrazide 6 by reaction with hydrazine monohydrate in refluxing isopropanol. The desired products 7a-b and 9a-h were obtained by stirring hydrazide 6 with corresponding aromatic aldehydes in isopropanol. Alkylation of compound 9 using iodoethane was carried out by dissolving the starting material in DMF, in strongly alkaline medium. (Fig. 1).

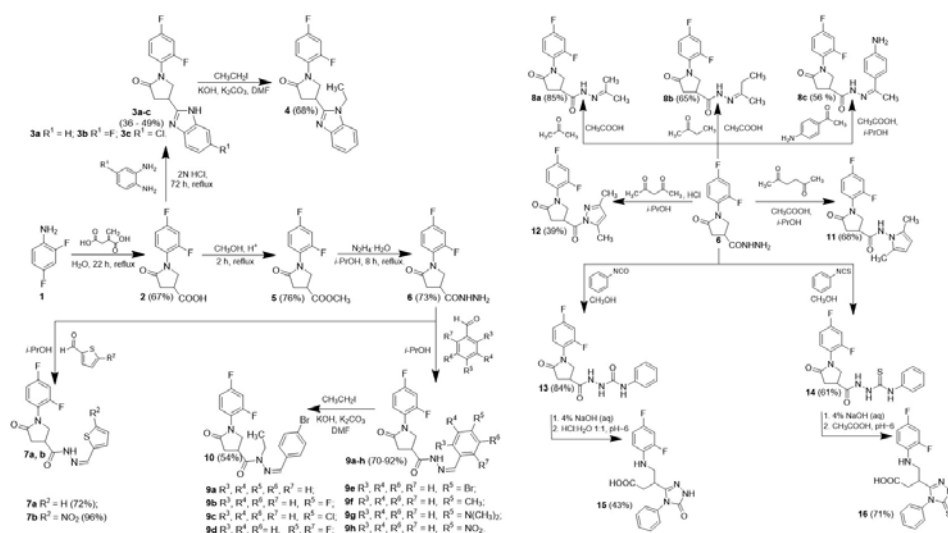


Fig. 1. Synthesis of 1-(2,4-difluorophenyl)-5-oxopyrrolidine-3-carboxylic acid derivatives

The activity of the synthesized compounds was studied against three types of cancer cells – breast cancer (MDA-MB-23), prostate cancer (PPC-1) and melanoma (A375). The cytotoxicity of pyrrolidinecarboxylic acid derivatives was investigated using MTT method. It was found that compounds 7b, 9a, 9c, 9e, 9f, 10 had the best anticancer activity against MDA-MB-231, PPC-1 and A375 cell lines (Fig. 2).

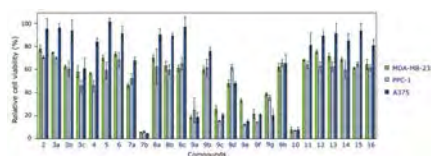


Fig. 2. Cytotoxicity of 1-(2,4-difluorophenyl)-5-oxopyrrolidine-3-carboxylic acid derivatives

[1] World Health Organization. Cancer. <<https://www.who.int/news-room/fact-sheets/detail/cancer>>

[2] YU, Y. et al. Fluorine-containing pharmaceuticals approved by the FDA in 2020: Synthesis and biological activity. Chinese Chemical Letters. t. 32 (2021), nr. 11, pp. 3342-3354. ISSN 1001-8417. ScienceDirect, <https://www.sciencedirect.com/science/article/pii/S1001841721003557>

FS-LASER MICROPROCESSING FOR SERS SUBSTRATES OF PERIODIC METALLIC STRUCTURES

Kernius Vilkevičius¹, Ilja Ignatjev², Evaldas Stankevičius¹

¹Department of Laser Technologies, Center for Physical Sciences and Technology, Lithuania

²Department of Organic Chemistry, Center for Physical Sciences and Technology, Lithuania
kernius.vilkevicius@ftmc.lt

Direct laser writing with single pulses of a tightly focused fs-laser beam enables fast fabrication of metallic nanostructures on thin films. The most common fabricated metal is gold, whose nanostructures' morphology depends on the pulse fluence. Wavelength-sized structures exhibit plasmonic properties, while the periodic arrangement of these makes it possible to achieve hybridized plasmons [1]. As plasmonic structures have an enhanced local electromagnetic field, they can be used in surface-enhanced Raman spectroscopy (SERS). The ordinary Raman scattering signal of the molecules is quite weak, thus the local enhancement leads to a significant amplification of the signal, making it suitable for single-molecule detection. The SERS signal intensity depends on the shape of the structure, as the strongest enhancement is observed at sharp corners called hot spots [2].

The periodic Au nanostructures on thin films of different thicknesses were fabricated using 343 nm wavelength pulses of varying fluences. This was done to investigate the effect of morphology and film thickness on the observed signal. The samples were covered with a monolayer of 4-mercaptobenzoic acid (4-MBA) for SERS detection. The variation in the fluence that leads to the distinct morphological states obtained results in different signal enhancement, with the round-shaped bumps having a weak response and needle-like jets providing a strong enhancement. The latter intensity depends on the needle tip size, as the hot spots are excited there. As the layer is thickened, the formation principle, as well as the jet shape itself, changes, leading to an additional tunability in the SERS signal. By varying these parameters and selecting the optimum conditions, it is possible to achieve a signal enhancement factor of 10^7 , suitable for precise detections of molecules.

The authors acknowledge the Research Council of Lithuania (LMT, Lithuania) for the received funding under project No. S-MIP-23-32.

[1] E. Stankevičius, et al., *Adv. Opt. Mater.* 9(12), 2100027 (2021)

[2] Z. Y. Li, *Adv. Opt. Mater.* 6, 1701097 (2018)

KCL CONCENTRATION EFFECTS ON THE FORMATION, STABILITY, AND SERS SIGNAL STRENGTH OF LASER-GENERATED GOLD, SILVER, AND HYBRID NANOPARTICLES

Vita Petrikaitė¹, Evaldas Stankevičius¹

¹Department of Laser Technologies, Center for Physical Sciences and Technology, Vilnius, Lithuania
vita.petrikaite@ftmc.lt

Nanoparticles of noble gold and silver metals have attracted major interest due to their optical, electronic, and catalytic properties, which are linked to the localized surface plasmon resonance (LSPR) phenomenon. Due to their unique properties [1], they are used in sensors, biological applications, Surface Enhanced Raman Scattering (SERS) [2], catalysts, nanotechnology, labeling, and electronics. The generation of noble metal nanoparticles has been extensively studied. Various techniques have been developed, including chemical reduction, electrochemical deposition, sol-gel processes, and laser ablation [2, 3]. Of these methods, laser ablation has gained momentum as a clean and environmentally friendly method of producing nanoparticles without the need for additional purification of toxic materials. However, one of the problems associated with laser ablation is the tendency of nanoparticles to aggregate, which limits further applications. To avoid particle aggregation, additional materials are added that contaminate otherwise clean method. Therefore, we tested a biocompatible material, potassium chloride (KCl). Salt is known to promote aggregation [4]. However, studies have shown that low salt concentrations can slow down the aggregation process [5]. These threshold concentrations were analyzed in this work.

In this study, the aggregation rate and extinction of gold, silver, and a mixture of nanoparticles formed in different concentrations of KCl solutions were studied over a period of 8 weeks. Gold and silver nanoparticles were generated from bulk targets immersed in 20 ml of different concentrations of KCl salt solutions: 0 mM to 20 mM. The targets were treated with a focused Nd:YAG laser ("Ekspla Baltic1064 HP", 1064 nm, 10 ns pulse duration). Extinction spectra and photographs of the resulting colloidal solutions were recorded weekly. Particle morphology, SERS signal strength, and zeta potential were also analyzed.

All particles formed by laser ablation in water and salt solution were characterized by a spherical shape and a negative zeta potential (-16 mV to 58,8 mV). During the study, we found optimal concentrations of KCl salt to maintain a stable solution without significant spectral deviations.

-
- [1] N. Li, et al., *Angew. Chem., Int. Ed. Engl.*, 53, 1756-1789 (2014).
 [2] E. Stankevičius, et al., *ACS Omega*, 6, 33889-33898 (2021).
 [3] V. Petrikaite, et al., *Opt. Mater.*, 137, 113535 (2023).
 [4] G. Wang, et al., *J. Phys. Chem. B*, 110, 20901-20905 (2006).
 [5] H. Kang, et al., *Chem. Rev.*, 119, 664-699 (2018).

IMPACT OF THE CRYSTAL STRUCTURE OF SILICA NANOPARTICLES ON RHODAMINE 6G ADSORPTION

Daniel Doveiko¹, Karina Kubiak-Ossowska², Yu Chen¹

¹Photophysics Group, Department of Physics, University of Strathclyde, Scottish Universities Physics Alliance, Glasgow, G4 0NG, U.K.

²Department of Physics, Archie-West HPC, University of Strathclyde, 107 Rottenrow, Glasgow G4 0NG, U.K.
daniel.doveiko.2018@uni.strath.ac.uk

Silicon is one of the most abundant elements on Earth with around 78% of Earth's crust consisting of various silicon and oxygen compounds [1]. Due to this, silica nanoparticles (SNPs) are widely used nanostructures for drug delivery, bonding and coating applications and others [2].

The properties of nanoparticles strongly correlate with their size hence it is critical to have an accurate way of measuring it. Commonly used techniques such as small angle x-ray scattering (SAXS), transmission electron microscopy (TEM) or dynamic light scattering (DLS) have drawbacks, such as being expensive and requiring complex sample preparation. Additionally, they might be inaccurate for particles under 10 nm size.

Potential methods that can be used to measure sizes of such constructs are time-resolved fluorescence anisotropy [3], and fluorescence recovery after photobleaching (FRAP) however, due to the size of the system it is impossible to determine experimentally how the dye is oriented on the SNP surface. As a result, its contribution to the measured complex size is unknown. Fortunately, the dye and SNP interaction mechanism can be studied using computational methods, such as molecular dynamics, which allow full insight into such processes on an atomistic scale.

In this work we used molecular dynamics simulations to get an insight into the rhodamine 6G (R6G) adsorption process to assess the most favourable conditions for successful adsorption and determine the impact of the dye to the measured complex size. Furthermore, we found that due to the geometric constraints and the requirement of correct dipole moment orientation, only one R6G molecule can adsorb on any sized SNP, and the R6G layer formation on the nanoparticle surface is not possible. Similar restrictions lead to the fact that the highest stable R6G oligomer is a dimer [4].

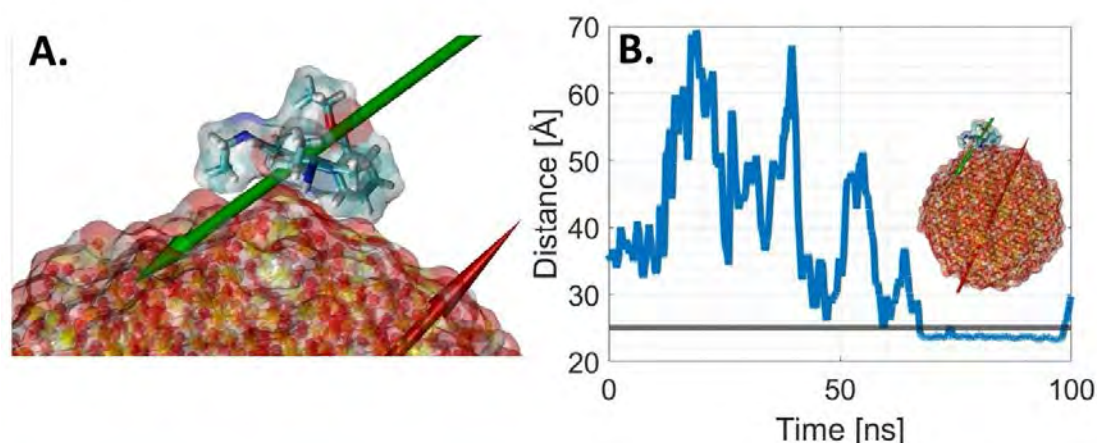


Fig. 1. Rhodamine 6G adsorption on the SNP surface **A.** R6G adsorbed on the surface of the SNP with visualized dipole moments; **B.** Distance plot between centre of masses (COM) of R6G and SNP.

[1] I.A. Ibrahim et al, Preparation of spherical silica nanoparticles: Stober silica. J. Am. Sci 2010

[2] C.S. Santos et al, Industrial applications of nanoparticles-a prospective overview. Materials Today Proceedings 2015

[3] C.D. Geddes et al, Fluorescence Anisotropy in Sol-Gels: Microviscosities or Growing Silica Nanoparticles Offering a New Approach to Sol-Gel Structure Elucidation. Journal of Fluorescence 2002

[4] Doveiko, D.; Kubiak-Ossowska, K.; Chen, Y., Impact of the Crystal Structure of Silica Nanoparticles on Rhodamine 6G: Adsorption A Molecular Dynamics Study. ACS Omega 2024

MXENE-BASED ELECTROCHEMICAL SENSOR FOR PRECISE AND SELECTIVE DETECTION OF LEAD IONS IN AQUEOUS SOLUTIONS

Ilya Navitski¹, Šarūnas Žukauskas¹, Alma Ručinskienė², Arūnas Ramanavičius^{1,3}

¹Department of Nanotechnology, State Research Institute Center for Physical Sciences and Technology (FTMC), Sauletekio Av. 3, LT-10257 Vilnius, Lith

²Department of Electrochemical Material Science, State Research Institute Center for Physical Sciences and Technology (FTMC), Sauletekio Av. 3, LT-10257 Vilnius, Lithuania

³Department of Physical Chemistry, Institute of Chemistry, Faculty of Chemistry and Geosciences, Vilnius University (VU), Naugarduko g. 24, LT-03225 Lithuania
ilya.nov42@gmail.com

While historically pervasive across various industries, the extensive use of lead has posed a significant threat to public well-being, particularly through the accumulation of large waste deposits contaminating groundwater. Consequently, this produces a pressing need for precise detection techniques capable of identifying lead ions, even at low concentration levels, and with high specificity. In our work, we explored an electrochemical sensor designed for the selective identification of dissociated lead ions in aqueous solutions, based on the specific interaction with pure MXenes.

The sensor was produced using the drop-casting method. The amalgamation of MXenes with Nafion was applied to a graphite electrode surface, repeated three times. The sensor's performance was assessed using differential pulse voltammetry (DPV), with focus on parameters such as the limit of detection (LOD) and sensitivity.

The proposed reaction mechanism involves a reversible conversion between lead ions and lead oxide (PbO) within the MXene layer. The resulting sensor exhibited exceptional selectivity, low LOD values, and the capability to directly detect lead ions in samples without the need for an extensive preparation process. This research establishes a foundation for advancing MXene-based electrochemical sensors, facilitating rapid, portable, and cost-effective testing across a diverse range of applications.

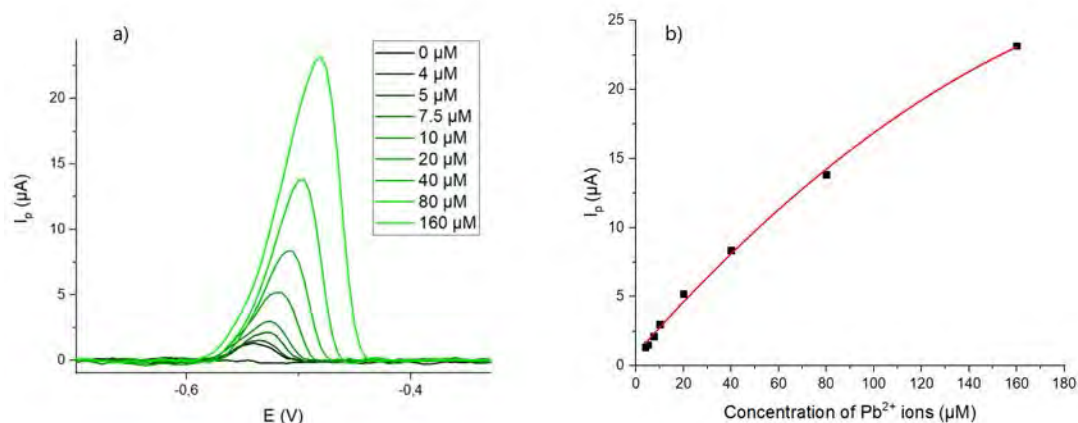


Fig. 1. Lead ion concentration curves determined by differential pulse voltammetry using a graphite/MXene+Nafion electrode within the range of 4 to 160 μM: a) illustrates the potential drift in response to the presence of lead ions in the sample and measured signal response; b) demonstrates the dependency of the signal on lead concentration

INVESTIGATION OF GRAPHENE/POLYPYRROLE COMPOSITES AND THEIR APPLICATION IN ELECTROCHEMICAL DOPAMINE SENSORS

Gintarė Rimkutė¹, Rasa Pauliukaitė², Gediminas Niaura², Jurgis Barkauskas¹, Justina Gaidukevič^{1,2}

¹Faculty of Chemistry and Geosciences, Vilnius University, Vilnius, Lithuania

²Center for Physical Sciences and Technology (FTMC), Vilnius, Lithuania
gintare.rimkute@chgf.vu.lt

The global sensor market is proliferating every year and is expected to reach \$345.77 billion by 2028 [1]. However, several issues still prevent the widespread impact and application of electrochemical sensors. It is mainly related to the materials used in these devices, which often lack the sensitivity and selectivity required for the detection of target analytes [2]. For this reason, current research is often focused on nanostructured carbon materials, which have many unique properties, including high electrical conductivity, biocompatibility, enzyme mimicking activity, and can be easily obtained using low-cost preparation methods [3].

The purpose of this work was to produce graphene-polypyrrole (GP) composites, characterize them, and investigate their sensitivity in the non-enzymatic detection of dopamine (DA). Three different graphite precursors with grain sizes of $<50 \mu\text{m}$, ≥ 150 , $\leq 830 \mu\text{m}$ and $\leq 2000 \mu\text{m}$ were intercalated with sulfuric acid and thermally treated to obtain exfoliated graphite (EG). EG samples were further modified with conductive polymer polypyrrole. The acquired samples were characterized using SEM, XPS, and Raman spectroscopy techniques. Electrochemical investigations were conducted using differential pulse voltammetry (DPV). Additionally, the potential application of the prepared GP nanocomposites for highly sensitive non-enzymatic DA sensors was explored.

Structural analysis showed that the sample obtained from the medium-size graphite grains (GP_2) had the lowest number of defects ($ID/IG = 0.483$) and the highest elemental nitrogen content (5.12 at.%) with 15.16 at.% as graphitic-N, known to improve electrocatalytic activity. Electrochemical investigations demonstrated that all GP samples were prospective for DA sensing. However, the electrode modified with the GP_2 showed the best performance. The sensitivity of this sensor was $2180 \mu\text{A}\cdot\text{mM}^{-1}\cdot\text{cm}^{-2}$ and the limit of detection was 78 nM.

[1] I. O'Connell, S. Chevella, G.M. Salgado, D. O'Hare, Precision Voltage Sensing in Deep Sub-micron and Its Challenges, in: Analog Circuits for Machine Learning, Current/Voltage/Temperature Sensors, and High-Speed Communication, Springer International Publishing, 137–163 (2022).

[2] C. Ferrag, K. Kerman, Grand Challenges in Nanomaterial-Based Electrochemical Sensors, *Frontiers in Sensors*, 1 (2020).

[3] Y. He, C. Hu, Z. Li, C. Wu, Y. Zeng, C. Peng, Multifunctional carbon nanomaterials for diagnostic applications in infectious diseases and tumors, *Mater Today Bio*, 14 (2022).

DOCKING SITE-MEDIATED PHOTOSTABILIZATION FOR SINGLE-MOLECULE AND SUPER-RESOLUTION IMAGING

Cindy Close¹, Michael Scheckenbach¹, Alan Szalai², Julian Bauer¹, Lennart Grabenhorst¹, Fiona Cole¹, Thorben Cordes³, Philip Tinnefeld¹, Viktorija Glembockyte¹

¹Department of Chemistry and Center for NanoScience Ludwig-Maximilians-University Munich

²CIBION-CONICET Buenos Aires, Argentina

³Department of Biology and Center for NanoScience Ludwig-Maximilians-University Munich
Cindy.Close@cup.lmu.de

DNA-PAINT is a single-molecule localization microscopy technique, relying on transient hybridization of fluorescently labeled single-stranded DNA imager strands to complementary docking strands on target molecules [1]. During acquisition, docking sites are imaged over the course of multiple binding, dissociation and photobleaching events. Through constant imager strand exchange, the limited photon budget of a single fluorophore is circumvented, making it possible to extract super-resolution images at high laser illumination intensities. Over long periods of continuous high-duty cycle excitation of fluorophores, DNA-PAINT binding sites can, however, be depleted [2]. Fluorophores in triplet excited states may generate singlet oxygen and downstream reactive oxygen species (ROS), damaging the docking sites and labeled target structures (**Figure 1a**). The use of triplet state quenchers (TSQ) and enzymatic scavenging systems is further limited to systems insensitive to pH change or high additive concentration. Inspired by fluorophore regeneration and self-repair mechanisms, we link the TSQ cyclooctatetraene to a DNA sequence [3], [4]. This photostabilizer strand binds directly next to the imager at the docking site, thereby allowing for self-regeneration and programmed exchange (**Figure 1b**). The presented contribution shows how this approach can increase the accessible photon budget. The method is characterized in a DNA origami model structure and applied to image microtubules in fixed cells. The improved longevity of DNA-PAINT docking sites is shown and the impact of photostabilizer strand regeneration is explored. The ability to mix and match optimal photostabilizer/dye pairs in this modular approach could be beneficial e.g., for multi-color measurements in structural biology, which often require multiple rounds of imaging, while preserving structural integrity of the sample. (**Figure 1c,d**)

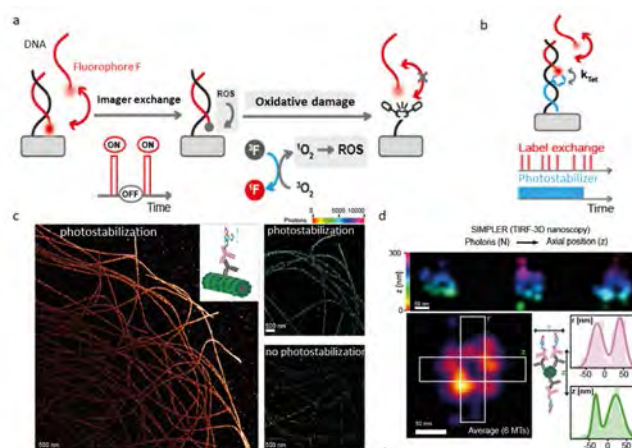


Fig. 1. a) Principle of DNA-PAINT and docking site damage via reactive oxygen species (ROS). b) Docking-site mediated photostabilization to prevent this damage. c) Impact of photostabilization on super-resolution measurements of cytoskeleton (microtubules) in cells. d) Demonstrating that, using the photostabilizer/fluorophore system, microtubules can be resolved in 3D.

- [1] R. Jungmann et al., Nano Letters 2010, 10, 4756.
 [2] P. Blumhardt et al., Molecules 2018, 12, 3165.
 [3] M. Scheckenbach et al., Angew. Chem. Int. Ed. 2020, 60, 4931.
 [4] L. Zhang et al., Angew. Chem. Int. Ed. 2022, 134 (19).

DEVELOPMENT OF A NEW SUPER-OXIDIZING PHOTOCATALYSTS AND THEIR APPLICATIONS IN C-H ACTIVATION REACTIONS VIA IDIOSYNCRATIC MECHANISTIC MODES

Jonas Žurauskas¹, Gustautas Snarskis¹, Barbara Chatinovska¹, Paulius Vaickūnas¹, Gediminas Kreiza¹, Kęstutis Zakarauskas², [Edvinas Orentas¹](mailto:Edvinas.Orentas@chf.vu.lt)

¹Vilnius University, Lithuania

²Lithuanian Energy Institute, Lithuania
edvinas.orentas@chf.vu.lt

Novel photocatalysts and their reactivity are reported as super-oxidants. Important leap towards a new understanding of green, oxidant and metal-free C-H functionalizations methodology is presented. Specifically crafted photoactive scaffolds demonstrates unique nature-mimicking reactivity. Novel mechanism opens new reactivities in the realm of photoredox catalysis is deciphered and outlined from the first-principles and experimentally. Multifunctional molecular instrument is devised which encompasses previously disembodied processes in a serially coupled interdependent events. The main emphasis was to push the boundaries of photoredox catalysis towards extremities (increasing excited state oxidation potentials to the record-breaking values), atom economy, easy accessible photocatalyst with low molecular weight, new mechanistic mode. Despite several decades of research directed towards photocatalysts design, such a simple and such a profound detail was overlooked. Not only this is fascinating from the perspective of pure mechanistic standpoint but is also highly sought after by the industrial chemistry branches because it greatly reduces the expenses and costs associated with the production line. By applying the principle of Occam's razor and reducing the system to the smallest set of elements it was in principle possible to achieve multifunctionality. Looking from the perspective of the atomic economy this is the most demanded of type of reaction in the chemists' toolbox.

NEAR-INFRARED SENSITIZED DEEP TISSUE PHOTOACTIVATION OF AZOBENZENE IN BIOMIMETIC CONDITIONS AT LOW PHOTON FLUENCES

Lukas Naimovicus^{1,2,3}, Ekin Opar⁴, Justas Lekavicius³, Edvinas Radiunas³, Helen Holzel⁵, Edvinas Orentas³, Karolis Kazlauskas³, Pau Gorostiza⁴, Pankaj Bharmoria², Kasper Moth-Poulsen^{5,6,7}

¹Department of Chemistry and Biochemistry, University of California - San Diego

²Institute of Materials Science of Barcelona (ICMAB-CSIC)

³Institute of Photonics and Nanotechnology, Vilnius University

⁴Institute for Bioengineering of Catalonia (IBEC)

⁵Department of Chemical Engineering, Universitat Politecnica de Catalunya (UPC)

⁶Catalan Institution for Research and Advanced Studies, ICREA

⁷Department of Chemistry and Chemical Engineering, Chalmers University of Technology

lnaimovicus@ucsd.edu

Near-infrared (NIR) triplet-sensitized *Z-E* photoswitching of azobenzene derivatives is a novel strategy of molecular isomerization with many promising applications including solar energy storage, photoactuation, and light-activated drug release. [1,2] The *Z-E* photoswitching of azobenzene derivatives is usually performed only *via* blue-green excitation, however, it implicates many possible implementations due to the low penetration depth of blue-green light. Therefore, a novel approach of direct triplet sensitization *via* NIR excitation shifting the action spectrum to the phototherapeutic region (650 nm to 850 nm) is regarded as a promising and viable alternative.

In this work, we generalize the approach for *Z-E* conversion of functionalized azobenzene chromophores (Azo-H, Azo-EH and Azo-MM) *via* NIR triplet sensitization by designing different photoswitch:sensitizer systems co-assembled within a liquid surfactant–protein in a bio-sustainable gelatin matrix. All azobenzene derivatives demonstrated *Z-E* photoisomerization upon excitation with 850 nm light *via* direct triplet sensitization despite a large endothermic triplet energy gap.

Herein, we also report the first example of triplet-sensitized *Z-E* photoisomerization of azobenzene derivatives with NIR light (850 nm) in aqueous biomimetic conditions at low photon fluence of 2.62 mW cm^{-2} by employing liquid and solid azobenzene derivatives in combination with palladium naphthalocyanine (PdNc), zinc phthalocyanine (ZnPc) and bacteriochlorin (BChl) sensitizers absorbing at 830 nm, 780 nm, and 730 nm, respectively. The biomimetic conditions are comprised of photoswitch:sensitizer ensembles trapped in a PF-127 artificial micellar membrane coated with a calcium-alginate hydrogel framework and placed below the 8 mm animal skin layer. Viable NIR triplet sensitized photoswitching is shown upon the 850 nm LED excitation as 10 consecutive cycles of conversion were observed with the action spectrum shift of 1.35 eV. Therefore, the developed approach provides a solid platform for *in vivo* photoactivation at 2-4 orders of magnitude lower photon fluences of NIR excitation compared to two photon absorption (2PA), excited state absorption (ESA), and triplet fusion upconversion (TF-UC).

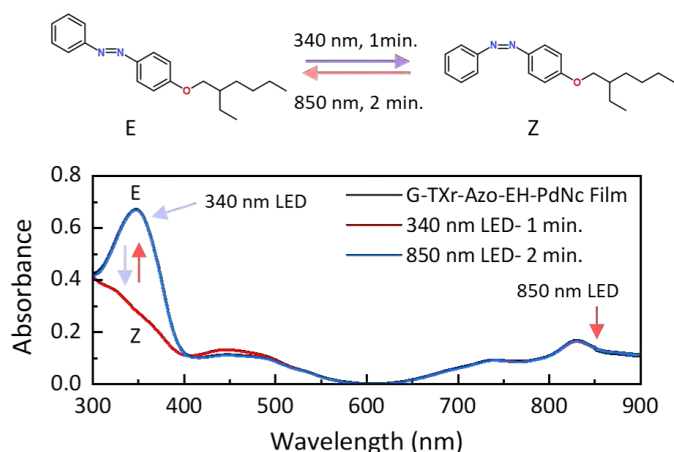


Fig. 1. E and Z form absorption spectra of triplet sensitized photoswitching film utilizing PdNc as a molecular sensitizer.

[1] Y. Wang et al., Nat. Rev. Mater. 2017, 2, 17020

[2] Y. Sasaki et al., Angew. Chem. Int. Ed., 2019, 58, 17827

STATISTICAL PROBABILITY OF SINGLET EXCITON GENERATION THROUGH TRIPLET-TRIPLET ANNIHILATION IN TES-ADT ANNIHILATOR

Justas Lekavičius¹, Edvinas Radiunas¹, Karolis Kazlauskas¹

¹Institute of Photonics and Nanotechnology, Faculty of Physics, Vilnius University, Lithuania
justas.lekavicius@ff.vu.lt

Triplet-triplet annihilation mediated photon upconversion (UC) is a process used to increase the energy of incoherent photons. This phenomenon could be applied in various fields, such as targeted drug delivery, bioimaging, photovoltaics and many others [1]. Each UC system is composed of at least two types of molecules: a sensitizer and an annihilator. The sensitizer is responsible for light absorption, triplet state generation through intersystem crossing (ISC) and triplet energy transfer (TET) to the annihilator. Meanwhile, the annihilator molecules undergo triplet-triplet annihilation (TTA), resulting in the formation of an emissive singlet state. The TTA process can produce quantum states with different multiplicities, however only the singlet ($M = 1$) is beneficial for photon upconversion. Hence, one of the most important parameters of an annihilator is a probability that TTA results in a singlet state, known as the statistical probability factor (f). f value directly impacts the UC quantum yield (Φ_{UC}) and is viewed as a limiting factor in many NIR-to-Vis UC systems. Recent studies show that the f values of many annihilators used in NIR-to-Vis upconversion (e.g., rubrene, diketopyrrolopyrrole derivatives) rarely exceed 20% [2,3]. Therefore, it is crucial to search for new annihilators with higher statistical factor values. The aim of this work is to thoroughly study the f factor of a 5,11-bis(triethylsilylethynyl)anthradithiophene (TES-ADT) annihilator, which could be used in various UC systems.

To evaluate statistical probability factor of the TES-ADT annihilator, it was paired with a metal-organic palladium phthalocyanine (PdPc) sensitizer. UC solutions in toluene with varying annihilator concentrations, as well as solid state samples, were prepared for this study. After determining the Φ_{UC} and other necessary parameters (TET, TTA and fluorescence quantum yields), the f factor values for each sample were calculated. The results indicate a notable trend: the f value tends to increase with the concentration of the annihilator in UC solutions, reaching up to 84% (Fig. 1 b). Moreover, the statistical factor value is also high in solid-state samples ($f \approx 60\%$). The increasing trend in the statistical probability factor could be attributed to the formation of dimers or larger aggregates, favouring the singlet state generation through TTA. In this work, aspects related to molecular geometry and energy levels are considered to explain the observed tendencies. The obtained results may be useful in the development of novel annihilators for photon upconversion.

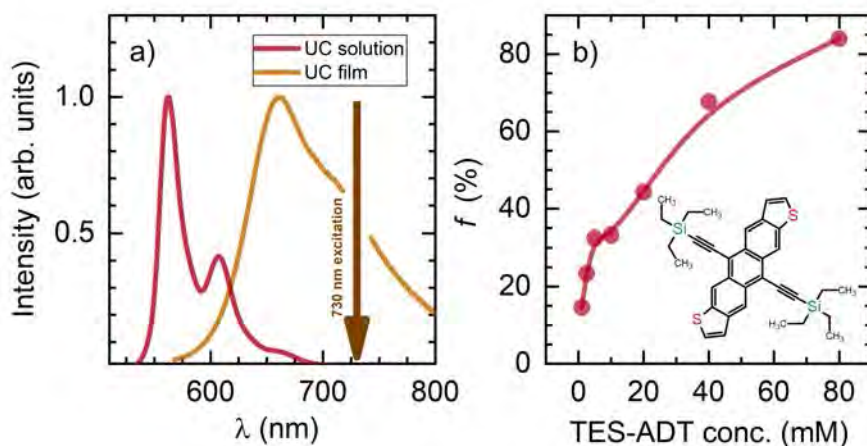


Fig. 1. a) Corrected emission spectra of the UC solution in toluene (1 mM TES-ADT, 15 μ M PdPc) and UC film. b) Statistical probability factor f of UC solutions with increasing TES-ADT concentration ($c_{PdPc} = 15 \mu$ M).

- [1] Bharmoria, P., et al., Triplet-triplet annihilation based near infrared to visible molecular photon upconversion. Chem. Soc. Rev., 2020, 49, 6529-6554 (2020)
- [2] Radiunas, E. et al., Impact of: t-butyl substitution in a rubrene emitter for solid state NIR-to-visible photon upconversion. Phys. Chem. Chem. Phys., 22, 7392 (2020)
- [3] Naimovičius, L. et al., Functionalized diketopyrrolopyrrole compounds for NIR-to-visible photon upconversion. J. Mater. Chem. C, 11, 698 (2022)

STUDY OF SARS-CoV2-S WILD-TYPE SPIKE PROTEIN INTERACTION WITH RANDOMLY AND ORIENTED ANTIBODIES BY QUARTZ CRYSTAL MICROBALANCE

Silvija Juciutė¹, Beatričė Urbaitė¹, Vincentas Mačiulis², Ieva Plikusienė^{1,2}

¹Faculty of Chemistry and Geosciences, Institute of Chemistry, Vilnius University

²State Research Institute Centre for Physical Sciences and Technology

silvija.juciute@gmail.com

In 2020, new SARS-CoV-2 virus emerged and spread around the world. Even though global pandemic was declared over, the SARS-CoV-2 virus was not eradicated. COVID-19 disease, which is caused by this virus, still causes health problems for people. There is high demand for diagnostic measures that can sensitively and rapidly detect virus molecules. Faster diagnosis leads to an earlier prescription of right medicine and more effective treatment of the patients.

In our study, we investigated how not mutated SARS-CoV-2 wild-type spike (SCoV2-S wild-type) protein interacts with monoclonal antibodies (mAbs-RBD) against SARS-CoV-2 spike proteins' receptor binding domain (RBD) when mAbs-RBD are immobilized in two different ways on the sensing gold surface. For random mAbs-RBD immobilization we used 11-mercaptoundecanoic acid (11-MUA) which forms self-assembling monolayer on the gold surface. Protein G was applied to form ordered mAbs-RBD layer on the sensing surface. After different immobilization procedures we investigated SCoV2-S wild-type interactions with mAbs-RBD.

Antigen-antibody interactions were investigated by quartz crystal microbalance with dissipation (QCM-D) method which allows to obtain the information about formed proteins layer viscoelastic properties. Further we used mathematical modelling for evaluation of rate and affinity constants for SCoV2-S wild-type and mAbs-RBD interactions. Moreover, we calculated mAbs-RBD and SCoV2-S wild-type proteins' layers thickness and surface mass densities.

MXENE BASED COLORIMETRIC SENSOR FOR SILVER ION DETECTION IN WATER

Raminta Bajarunaite¹, Simonas Ramanavicius², Martynas Talaikis², Anton Popov¹, Gediminas Niaura², Almira Ramanaviciene¹

¹NanoTechnas - Center of Nanotechnology and Materials Science, Institute of Chemistry, Faculty of Chemistry and Geosciences, Vilnius University, Naugar

²Department of Organic Chemistry, State Research Institute Center for Physical Sciences and Technology, Sauletekio ave. 3, 10257 Vilnius

raminta.bajarunaite@chgf.stud.vu.lt

These days, silver can be found in a variety of materials, such as jewellery, electronics, pharmaceuticals and many more. Unfortunately, a large amount of this element finds its way into the environment and gets exposed to living organisms. Although silver is known for its antibacterial properties, ionic silver has been shown to be mildly toxic to aquatic organisms and is known to have detrimental effects on the human body. That is why finding a reliable way to detect silver ions in drinkable water is important.

Lately, a novel two-dimensional (2D) transition metal carbide/nitride material group has garnered a large amount of attention for its excellent properties, such as high chemical stability, high electrical conductivity, and environment-friendly characteristics. Their hydrophilic nature and sizeable surface area render them potent adsorbents for many molecular or ionic systems. This work will show how a nanoplasmonic sensor composed of Ti_3C_2Tx MXenes could be used to detect a small amount of Ag^+ in the water supply.

For this investigation, intermediate Ti_3C_2Tx MXenes and different Ag^+ concentrations were mixed in buffer (pH = 3, 4, 5, 6), distilled water and tap water mediums. A spectrophotometer was used to measure the sensor's signals. This investigation shows that buffer solution interferes with Ag^+ reduction, causing a significant signal depression and a red shift from 450 nm to 650 nm compared to measurements done in distilled water. MXenes show a strong adsorption affinity and readily react with collateral ions found in the solution; consequently, better results are obtained when distilled water is used. However, this sensor shows a sufficient result when used in more natural conditions like tap water. A linear correlation between Ag^+ concentration and MXene absorption signal could be seen. Finally, we show that this sensor has the potential to be reiterative.

This project has received funding from the Research Council of Lithuania (LMTLT), agreement No S-PD-22-155.

DISSOLUTION ENHANCEMENT OF MEFENAMIC ACID USING SOLID DISPERSIONS OBTAINED BY WET GRANULATION TECHNIQUE

Volodymyr Yaremenko^{1,2,3}, Volodymyr Fedorenko^{1,3}, Svitlana Gureeva^{2,3}, Olena Ishchenko¹, Viktoriia Plavan¹, Volodymyr Bessarabov²

¹Department of chemical technology and resource saving, Kyiv National University of Technologies and Design, Ukraine

²Department of Industrial Pharmacy, Kyiv National University of Technologies and Design, Ukraine

³JSC Farmak, Ukraine

yaremenko.vv@knuud.edu.ua

A significant number of active pharmaceutical ingredients, including anti-inflammatory ones, have low solubility in water, which negatively affects their bioavailability and therapeutic effectiveness. Therefore, many anti-inflammatory drugs have large dosages. One of the most promising options for overcoming this problem is the use of solid dispersion systems (SDS), in which pharmaceutically acceptable polymers can capture molecules of the active substance, forming certain chemical bonds with them and forming a new, more amorphous structure. An amorphous solid dispersion of the active substance and a hydrophilic polymer demonstrates better wettability, water absorption capacity and porosity, which results in enhancement drug dissolution. Mefenamic acid (MA), a BCS class II drug, displays high permeability and low solubility, thereby exhibiting a poor dissolution profile. The purpose of this research was to obtain enhancement of the dissolution profile using solid dispersion obtained by wet granulation technique. To obtain SDS, such methods as the solvent evaporation method, spray drying, hot melt extrusion, co-milling, co-grinding, high-energy mixing (KinetiSol) are generally accepted and the most widespread. At the same time, along with the above-mentioned methods, it is promising to study the possibility of using wet granulation methods common in the pharmaceutical industry, such as fluid bed granulation and high shear granulation. SDS were produced by wet granulation using GPCG 2 Lab Systems Fluid Bed Dryer, Glatt, Germany and Vertical Lab Granulator VG 65/10, Glatt, Germany. The ratio of MA to polyvinylpyrrolidone (PVP K17) and to hydroxypropylmethylcellulose (HPMC) is 1:20. The dissolution of SDS was determined by spectrophotometry as the amount of MA that passed into the solution in 30 minutes with stirring, wavelength 282 nm, purified water was used as a reference solution. The dissolution medium is water, temperature (37±0.5) °C. Differential Scanning Calorimetry (DSC), Fourier Transform Infrared Spectroscopy (FTIR) were performed to characterize the obtained solid dispersions and to identify the physicochemical interaction between drug and polymer carrier, hence its effect on dissolution. Also optical microscopy was performed to study the morphology of the obtained particles, including because the pharmaco-technological characteristics of SDS very important for the prospect of their further use for finished dosage form (tablets, capsules, granules, sachet). Wet granulation methods make it possible to obtain SDS with MA and significantly improve its dissolution. SDS of MA and HPMC produced by wet granulation using high shear technology and fluidized bed technology show an enhancement in dissolution by 8.60 and 9.46 times, respectively. At the same time, SDS with PVP K17 do not demonstrate improved dissolution compared to pure MA. Such results are promising for further more detailed discussion and research.

[1] Bagade O.M., Kad D.R., Bhargude D.N., Bhosale D.R., Kahane S.K. Consequences and Impose of Solubility Enhancement of Poorly Water Soluble Drugs. *Research J. Pharm. and Tech.* 7(5), 598-607 (2014).

[2] Xingwang Z., Huijie X., Yue Z., Zhiguo M. Pharmaceutical Dispersion Techniques for Dissolution and Bioavailability Enhancement of Poorly Water-Soluble. *Pharmaceutics* 10(3), 74 (2018).

[3] Vasconcelos T., Marques S., das Neves J., Sarmento B. Amorphous solid dispersions: Rational selection of a manufacturing process. *Adv. Drug Deliv. Rev.* 100, 85 – 101 (2016).

STUDY OF DIFFERENT PARAMETERS IMPACT TO MICROPLASTIC REMOVAL FROM WATER USING LIGNIN-MAGNETITE NANOSORBENT

Austėja Burbulytė¹, Ieva Uogintė¹, Vaidas Pudžaitis²

¹Center for Physical Sciences and Technology, Department of Environmental Research, Saulėtekio av. 3, LT-10257 Vilnius

²Center for Physical Sciences and Technology, Department of Organic Chemistry, Saulėtekio av. 3, LT-10257 Vilnius
austejaburbulyte@gmail.com

Nowadays the world is facing the problem of plastic production. Every year tones of plastic products such as disposable dishes, bags and device packaging made for daily use. According to the latest data scientists counts that plastic production amounts are increasing every year. Figure 1 shows that in the 2022 plastic amount reached 400 Mt. per year. A major part of plastic is fossil based and only a relatively small part of plastic is recycled or made into bioplastic [1]. One type of plastic is microplastic whose particles size ranges from 5 mm to 1 μm . Microplastic particles dumped into freshwater systems: rivers, lakes, and oceans. In the environment these particles cause ecological and health protection problems. Various technologies are used for microplastic particles removal one of them is sorption. It is known that for sorbents synthesis can be used natural resources such as biomass wastes from industry. In this study from softwood sawdust was extracted lignin by alkali extraction method. Nanosorbent was synthesized from lignin and iron oxide magnetic nanoparticles. The sorption was evaluated by sorbing low-density polyethylene (LDPE) particles. After sorption microplastic particles was remove by external magnetic field. In this study the main step was investigate sorption process dependence by various parameters impact to LDPE removal efficiency. In this work it was showed, how solution pH, sorption time, sorbate concentration, sorbent dosage affects to removal efficiency.



Fig. 1. Plastic production rates [1]

Acknowledgement: The project is co-financed from the funds of the European Social Fund (project No. 09.3.3-LMT-K-712-23-263) under grant agreement with the Research Council of Lithuania (LMTLT).

[1] Plastics Europe, Plastics the fast facts, (2023-1)

DEVELOPMENT OF AN INNOVATIVE SCAFFOLD MADE FROM DECELLULARIZED HORSE BONE FOR BONE DEFECTS IN HORSES

Julia Niegowska¹, Łukasz Młynarski¹, Maciej Janeczek², Tomasz Gębarowski²

¹Students Scientific Society Department of Biostructure and Animal Physiology, Wrocław University of Environmental and Life Sciences, Poland

²Department of Biostructure and Animal Physiology, Wrocław University of Environmental and Life Sciences, Poland
121551@student.upwr.edu.pl

Veterinarians in their practice often encounter bone defects in horses. These are usually associated with past injuries or chronic inflammatory conditions, resulting in cystic changes. One of the most popular composites used in the therapy of bone defects is calcium hydroxyapatite, the main component of bones. Research indicates that granules and blocks of this compound, unfortunately exhibit poor manipulative properties and may have difficulty staying in the operative site. Empty spaces can form between hydroxyapatite and bone tissue, leading to mechanical instability of the bone. In response to this problem, allogeneic bones have become the gold standard in human medicine, but they are not yet available in the veterinary market. The aim of the research was to develop a method for bone decellularization to obtain an antigenically neutral bone filler. The experiments were conducted on horse bones. Initially, bone sections, containing mainly the spongy bone structure, were subjected to enzymatic digestion. Subsequently, they were rinsed to remove residual fats, and in the final step, they were sterilized radiographically. Samples were examined under a microscope. We have successfully developed an effective method of decellularization, ensuring the creation of a safe bone composite for transplantation in horses.

DESIGN AND INVESTIGATION OF 1,2,4-TRIAZOLE-3-YL THIOACETOHYDRAZIDES BEARING ALDIMINE MOIETY AS BIOLOGICALLY ACTIVE AGENTS

Aida Šermukšnytė¹, Vilma Petrikaitė², Kristina Kantminienė³, Ilona Jonuškienė¹, Ingrida Tumosienė¹

¹Department of Organic Chemistry, Kaunas University of Technology, Lithuania

²Laboratory of Drug Targets Histopathology, Institute of Cardiology, Lithuanian University of Health Sciences, Kaunas, Lithuania

³Department of Physical and Inorganic Chemistry, Kaunas University of Technology, Lithuania
aida.sermuksnyte@ktu.edu

Tumors are abnormal tissue masses resulting from uncontrolled cell growth, a characteristic of cancer. This widespread condition affects various organs, posing challenges for healthcare [1]. While cytotoxic drugs play a crucial role in cancer treatment, their limitations prompt the search for selective anticancer drugs. This study aims to enhance patient quality of life and revolutionize cancer therapy by developing substances targeting cancer cell vulnerabilities, such as immunotherapeutic strategies and specific drugs. Aldimine derivatives have shown promising efficacy against diverse tumor cells like those found in colon, leukemia, breast, and kidney cancers [2].

This work's objective is to synthesize variously substituted 1,2,4-triazole-3-yl thioacetohydrazides, and evaluate their anticancer properties.

1,2,4-Triazole-5-thione [3] reacted with ethyl chloroacetate in DMF, facilitated by triethylamine at ambient temperature, yielded ethyl 2-[[4-phenyl-5-[(phenylamino)ethyl]-4H-1,2,4-triazol-3-yl]thio]acetate in 80% yield. Subsequent reaction with hydrazine monohydrate in propane-2-ol at 60 °C produced 1,2,4-triazol-3-ylthioacetohydrazide in 94% yield. Further reaction of 1,2,4-triazol-3-ylthioacetohydrazide with corresponding aldehydes in methanol under reflux yielded target aldimines in the yield range of 29–98% [4, 5]. Structural confirmation of the novel compounds relied on ¹H and ¹³C NMR, IR, and MS spectroscopy.

Newly synthesized compounds were assessed for anticancer activity against melanoma IGR39, triple-negative breast cancer MDA-MB-231, and pancreatic carcinoma Panc-1 cell lines. Aldimines featuring 2-hydroxybenzene or 2-hydroxy-5-nitrobenzene moieties proved to be most effective against all tested cancer cells among the synthesized 1,2,4-triazole-3-thiol derivatives. Notably, derivatives with pyrrole and 4-(methylthio)benzene moieties, initially less active against IGR39, exhibited increased efficacy against triple-negative breast cancer cells. The substituents in these compounds may play a crucial role in achieving specificity against the typically more resistant MDA-MB-231 cell line. Testing on tumor spheroids simplified 3D cell models with hypoxia in their core, revealed that the most active compounds were 1,2,4-triazol-3-ylthioacetohydrazides containing pyrrole, 2-hydroxybenzene, and 2-hydroxy-5-nitrobenzene fragments.

Overall, from a range of 1,2,4-triazole-3-thiol derivatives, the chosen aldimines emerged as particularly promising anticancer agent-candidates, exhibiting significant cytotoxicity against the various tested cancer cell lines. Due to their encouraging initial results, these newly synthesized compounds have been earmarked for further studies and investigations.

[1] R.L. Siegel, K.D. Miller, H.E. Fuchs, A. Jemal, CAA Cancer J. Clin. 71, 2021, 7, 33.

[2] R.E. Ferraz de Paiva, E.G. Vieira, D. Rodrigues da Silva, C.A. Wegermann, A.M. Costa Ferreira, Front. Mol. Biosci. 7, 2021, 627272.

[3] I. Tumosiene, K. Kantminiene, A. Pavilonis, Z. Mazeliene, Z.J. Beresnevicius, Heterocycles 78, 2009, 59, 70.

[4] I. Tumosiene, I. Jonuskiene, K. Kantminiene, V. Mickevicius, V. Petrikaite, Int. J. Mol. Sci. 22, 2021, 7799.

[5] A. Sermuksnyte, K. Kantminiene, I. Jonuskiene, I. Tumosiene, V. Petrikaite, Pharmaceuticals. 15, 2022, 1026.

[6] M.A.G. Barbosa, C.P.R. Xavier, R.F. Pereira, V. Petrikaite, M.H. Vasconcelos, Cancers 14, 2021, 190.

INVESTIGATION OF A NOVEL TRICOMPONENT BACTERIAL ANTIPHAGE DEFENCE SYSTEM

Lukas Volodka¹, Inga Songailiene¹

¹Vilnius University, Life Sciences Center, Institute of Biotechnology, Department of Protein - DNA Interactions
lukas.volodka@chgf.stud.vu.lt

During the course of evolution bacterium have acquired numerous of antiviral defense systems which help them to evade bacteriophage infections. This research is focused on a newly identified tricomponent antiviral defense system TerY-P¹ organized in an operon. It has been demonstrated that that the system contributes to a significant immunity of bacteria against common *E. coli* phages T3, T7 and ϕ V-1². Cloning of the individual components fused with histidine affinity tags and cloning of full operon has been successfully performed, further followed by the expression of the defense system in uninfected *E. coli*. In the absence of phage infection, the heterologous expression so far has been observed only for one of the proteins TerY. We hypothesize that the system may work as an inducible toxic cascade, thus the other components may appear upon phage infection. Therefore, we checked if all components can be synthesized in cell-free expression system, which resulted in the expression of all the components. *In vivo* protein expression yielded 2 of the 3 components (TerY and TerP). Other information about the components comes from bioinformatical analysis which shed some light on their possible functional and structural aspects. In the ongoing experiments, we are planning to identify the target of phosphate modification, or the presence of the mRNA of the corresponding genes under different conditions.

-
- [1] Anantharaman, V., Iyer, L. M., & Aravind, L. (2012b). Ter-dependent stress response systems: Novel pathways related to metal sensing, production of a nucleoside-like metabolite, and DNA-processing. *Molecular BioSystems*, 8(12), 3142. <https://doi.org/10.1039/c2mb25239b>
- [2] Gao, L., Altae-Tran, H., Böhning, F., Makarova, K. S., Segel, M., Schmid-Burgk, J. L., Koob, J., Wolf, Y. I., Koonin, E. V., & Zhang, F. (2020). Diverse enzymatic activities mediate antiviral immunity in prokaryotes. *Science*, 369(6507), 1077–1084. <https://doi.org/10.1126/science.aba0372>

TOWARDS A NOVEL MODEL TO STUDY NUCLEAR AGING: BIOPHYSICAL CHARACTERIZATION OF AGE-TUNED MEMBRANES

Aivaras Vilutis^{1,2}, Nuno C Santos¹, Maria J Sarmento¹

¹Instituto de Medicina Molecular, Faculdade de Medicina, Universidade de Lisboa, Lisbon, Portugal

²NOVA Medical School, Faculdade de Ciências Médicas, NMS, FCM, Universidade NOVA de Lisboa, Lisbon, Portugal
aivaras.vilutis@medicina.ulisboa.pt

Aging is a major risk factor for various diseases, yet understanding of cellular aging is incomplete. Many aging-related changes emerge in the nucleus [1]. Recently, altered cell mechanical properties have become a hallmark of aging [2], with the nuclear envelope (NE) and lamins playing a pivotal role in maintaining nuclear integrity [3]. Although the interplay between NE and lamina during aging is not fully understood, we hypothesize that the lipidome of the NE influences lamin binding and organization. Our preliminary lipidomics findings indicate a decline in ether lipids with age progression. This might impact the biophysical properties of membranes and lead to differential lamin binding. Thus, we propose to create age-tuned synthetic models to investigate nuclear aging, NE-lamin interactions, and overall nuclear structural integrity.

Firstly, we designed membrane models mimicking the NE of both young and old healthy donors with distinct ether lipid content. To characterize the bulk membrane properties of our model vesicles, we performed DPH fluorescence anisotropy, Laurdan generalized polarization (GP), and time-dependent fluorescence shifts. We are using fluorescence correlation spectroscopy, confocal microscopy, and atomic force microscopy to quantify lamin-model interactions and characterize lamin polymerization. Our results indicate that a decrease in ether lipid content does not alter the hydrophobic core of the membrane but makes it more ordered closer to the surface. Such organization of the membrane can significantly impact how lamins interact with the models.

These findings serve as a foundation for upcoming experiments aimed at establishing a novel system to study nuclear aging. The incorporation of key lamina proteins into nucleus-sized models will provide new insights into protein-lipid interactions during healthy human aging. Furthermore, the highly tunable nature of these models will allow for modifications to study age-prone diseases.

[1] B. Schumacher and J. Vijg, "Age is in the nucleus," *Nature Metabolism*, vol. 1, no. 10, pp. 931–932, Oct. 2019

[2] T. Schmauck-Medina et al., "New hallmarks of ageing: a 2022 Copenhagen ageing meeting summary," *Aging*, vol. 14, no. 16, pp. 6829–6839, Aug. 2022

[3] R. de Leeuw, Y. Gruenbaum, and O. Medalia, "Nuclear Lamins: Thin Filaments with Major Functions," *Trends in Cell Biology*, vol. 28, no. 1, pp. 34–45, Jan. 2018

PHARMACOKINETIC EVALUATION OF CEFAZOLIN ANTIMICROBIAL PROPHYLAXIS IN SPINAL SURGERY

Justin Stivrins¹, Sigita Kazune²

¹University of Latvia
justins99@inbox.lv

Background Surgical site infections (SSI) following spine surgery significantly impact patient morbidity and mortality. Antibacterial prophylaxis (AP) using cefazolin is a key strategy for preventing SSI.

Aim. This observational study aimed to examine the pharmacokinetics of guideline-recommended cefazolin AP in spine surgery.

Methods. Nine patients (aged 50 ± 14 years, renal function 99 ± 30 mL/min/72kg) undergoing spine surgery received AP with 2 g cefazolin. Blood samples were collected at 5, 10, 30, 60 and 90 minutes intra-operatively for measuring total cefazolin concentrations by high performance liquid chromatography. Patients were monitored for SSI during and post-hospitalization. Total cefazolin concentrations at wound closure were compared to the target concentrations of ≥ 40 mg/L.

Results. The interval between cefazolin administration and wound closure ranged between 40 and 190 minutes. Total plasma cefazolin concentrations peaked at 214 ± 35 mg/L -1 within 15 minutes following cefazolin dose. Total plasma cefazolin concentrations at wound closure were 68 ± 30 mg/L -1 . 12.5 percent of cefazolin concentrations at wound closure were less than 40 mg/L. Longer surgery duration was associated with below-target concentrations. None of the patients in the study developed SSI.

Conclusion. The study demonstrates that current intraoperative AP with cefazolin achieves target plasma concentrations in the majority of patients. Duration of surgery is a critical factor in considering alternative dosing regimens.

THERAPEUTIC POTENTIAL OF T CELLS FOR PREMATURE OVARIAN INSUFFICIENCY TREATMENT IN MOUSE MODEL

Indrė Krastinaite¹, Greta Tamulaityte¹, Veronika Viktorija Borutinskaitė¹

¹Vilnius University, Life Sciences Center, Vilnius, Lithuania
indre.krastinaite@gmc.stud.vu.lt

Infertility is an increasingly widespread issue affecting around 12% of families worldwide [1]. Various syndromes, such as premature ovarian insufficiency (POI), cause female infertility and diminish the overall quality of patients' life. Current interventions, such as hormonal therapy and Assisted Reproductive Technology, are accompanied by various side effects and fail to treat the underlying causes of infertility [2]. In the preceding years, cell-based therapy became one of the new emerging potential treatments for a variety of conditions. The recently found associations between the pathogenesis of POI and the immune system [3] prompted us to choose T cells as the object of our study.

The aim of our study was to investigate peripheral blood cell and T cell potential for infertility treatment in POI mouse model (Fig. 1). During the research, we isolated peripheral blood mononuclear cells (PBMC) from the peripheral blood of the donor and CD4+/8+ positive T cell population using the Magnetic Activated Cell Sorting (MACS) method. Isolated T cells were positive for CD3 (98%), CD4 (72%), and CD8 (74%) cell surface markers and were expanded *in vitro* with IL-15, and IL-7 cytokines. PBMC or CD4+/8+ positive T cells were transplanted to chemotherapy-induced POI mouse ovaries. POI mice (untreated) and POI mice after PBMC treatment were mated with male mice. The pregnancy rate in both cases was 0%, meaning that mice were infertile. POI mice that received CD4+/8+ positive T cell treatment had restored fertility after mating (pregnancy rate 83%). Following cell treatments, we investigated Antimüllerian hormone (AMH) and TNF- α levels in the mouse serum and the expression of folliculogenesis-associated and fibrosis-associated genes in mouse ovaries and uterus and we found that results showed a positive therapeutic effects on reproductive function via molecular networks and hormonal system and restored fertility in POI mouse model.

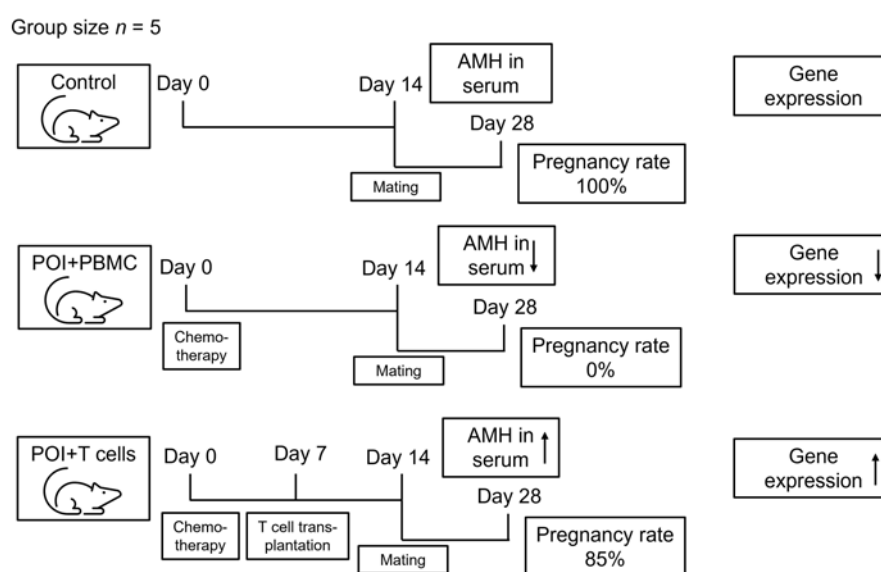


Fig. 1. Schematic representation of the study

The study was funded by the Research Council of Lithuania (project No. P-ST-23-76).

- [1] Szkodziak, F., Krzyzanowski, J., Szkodziak, P. (2020). Psychological aspects of infertility. A systematic review. *Journal of International Medical Research*, 48(6), 030006052093240.
- [2] Sunderam, S., Kissin, D. M., Zhang, Y., et al (2019). Assisted Reproductive Technology Surveillance-United States, 2016. *MMWR Surveillance Summaries*, 68(4), 1-23.
- [3] Huang, Y., Hu, C., Ye, H., et al (2019). Inflamm-Aging: A New Mechanism Affecting Premature Ovarian Insufficiency. *Journal of Immunology Research*, 2019, 8069898.

CONSEQUENCES OF LONG TERM EXPOSURE TO MICROPLASTICS AND EFFECTS ON CYTOGENETIC AND ANTIOXIDANT BIOMARKERS IN FISH

Agnė Bučaitė^{1,2}, Gintarė Sauliūtė¹, Milda Stankevičiūtė¹

¹Laboratory of Ecotoxicology, Nature Research Centre, Vilnius Lithuania

²Vilnius University Life Sciences Centre, Institute of Biosciences, Vilnius Lithuania
agne.bucaite@gamtc.lt

Microplastic (MP) pollution in aquatic ecosystems has become a serious environmental problem. However, the issue is slowly being recognized because the European Commission claims a 74% reduction in plastic pellet pollution by the end of the decade [1]. Polystyrene (PS) makes up only 5.2% of global plastic production [2] but it is not biodegradable due to its structural stability. This implies that it will continue to persist in aquatic environments for a long time even if the amount of mismanaged waste decreases in the future. To effectively manage and mitigate the consequences of anthropogenic pollution in aquatic ecosystems, the toxic potential of MP needs to be appropriately studied. The aim of this work is to evaluate changes in cytogenetic and antioxidant biomarkers after PS exposure in rainbow trout (*Oncorhynchus mykiss*). Fish were subjected to a diet containing PS for 3.7 months. Cytogenetic analysis was carried out using erythrocytic nuclear abnormalities assay [3]. The formation of micronuclei, nuclear buds, nuclear buds on filament, blebbed nuclei cells were assessed as genotoxicity endpoints, as well as 8-shaped, fragmented-apoptotic and bi-nucleated cells as cytotoxicity endpoints. In order to analyze changes in antioxidant system, catalase (CAT) activity in liver homogenate was evaluated. Samples were incubated with H₂O₂ and the absorbance of the ammonium molybdate-H₂O₂ complexes was measured [4]. Data analysis was performed using R software [5]. The frequency of all observed nuclear abnormalities did not differ significantly when compared to the control. Meanwhile, CAT activity decreased significantly compared to the control group. In conclusion, we observed that PS exposure had a significant impact on fish antioxidant capacity. Understanding the effects of MP exposure is crucial for assessing the potential risks associated with plastic pollution. Study was funded by the Research Council of Lithuania through the project S-MIP-22-51 (ARFA).

-
- [1] "Reducing microplastic pollution from plastic pellets," European Commission - European Commission. Accessed: Jan. 08, 2024. [Online]. Available: https://ec.europa.eu/commission/presscorner/detail/en/ip_23_4984
- [2] "Plastics – the fast Facts 2023" Plastics Europe. Accessed: Jan. 08, 2024. [Online]. Available: <https://plasticseurope.org/knowledge-hub/plastics-the-fast-facts-2023/>
- [3] M. Stankevičiūtė, T. Gomes, and J. A. C. González, "Nuclear abnormalities in mussel haemocytes and fish erythrocytes," ICES Techniques in Marine Environmental Science (TIMES), report, Oct. 2022. doi: 10.17895/ices.pub.21220031.v1.
- [4] M. H. Hadwan and H. N. Abed, "Data supporting the spectrophotometric method for the estimation of catalase activity," Data Brief, vol. 6, pp. 194–199, Mar. 2016, doi: 10.1016/j.dib.2015.12.012.
- [5] R Core Team, "R: A language and environment for statistical computing." R Foundation for Statistical Computing, Vienna, Austria. [Online]. Available: <https://www.R-project.org/>

BLOODSUCKING BITING MIDGES - NEGLECTED THREAT FOR WILD BIRDS

Margarita Kazak¹, Rasa Bernotienė¹

¹Laboratory of Entomology, Nature Research Centre, Lithuania
margarita.kazak@gamtc.lt

There are 1368 *Culicoides* biting midge species around the world [1] which can transmit more than 110 different arboviruses, bacteria, protozoa and helminths to humans and animals. However, because of their extremely small size, *Culicoides* remain the least studied of the major Dipteran vector groups [2]. *Haemoproteus* and *Trypanosoma* are just a small part of parasites, which can be transmitted by *Culicoides* biting midges to vertebrates. Wild animals, especially wild birds and their blood pathogens are studied less despite reports that parasites of some species can be pathogenic and affect the development and behavior of heavily infected individuals [3]. Avian trypanosomes have some interesting biological properties: they are cosmopolitan in distribution, extremely diverse and infect vertebrates with unique biology – the ones that can regularly migrate between different continents [4], so research on avian trypanosomes can help to explain the parasite distribution patterns. Nevertheless, the biology of avian trypanosomes (especially their life cycles in vectors – *Culicoides* biting midges) is still relatively little studied and vectors of only a few avian *Trypanosoma* species have been determined so far.

The purpose of this study was to determine *Culicoides* diversity and their infection with bird blood pathogens belonging to the family Trypanosomatidae. We collected parous biting midge females using UV light traps in four different study sites from May till September, 2022. Insects were identified to species level, molecular methods and microscopy were applied to estimate the natural trypanosomatid infections.

Both dixenous (*Trypanosoma*) and monoxenous (*Crithidia* sp. and *Herpetomonas zitiplika* – trypanosomatids infecting only insects) were found in nine different *Culicoides* species. The prevalence of trypanosomatid parasites in biting midges was 4.1 %. Detected trypanosomes – *Trypanosoma avium* and *T. bennetti* group – both are known to be bird blood parasites, mostly known from raptor birds. Interestingly, *T. avium* was found only in *C. segnis* biting midges; these insects are ornithophilic bloodsucking ectoparasites which might be potential avian trypanosome vectors in the wild. Other biting midge species – *C. punctatus*, *C. pictipennis*, *C. obsoletus* group, *C. kibunensis*, *C. impunctatus*, *C. festivipennis* – individuals were also found to be infected with trypanosomatid parasites.

-
- [1] Borkent, A., and Dominiak, P. (2020). Catalog of the biting midges of the world (Diptera: Ceratopogonidae). In Zootaxa (Vol. 4787);
 [2] Carpenter S., Groschup M. H., Garros C., Felipe-Bauer M. L., Purse B. V. (2013). *Culicoides* biting midges, arboviruses and public health in Europe. Antiviral Research (Vol. 100, Issue 1);
 [3] Molyneux, D.H., (1973). *Trypanosoma everetti* sp. nov. A trypanosome from the blackrumped waxbill *Estrilda t. troglodytes* Lichtenstein. Ann. Trop. Med. Parasitol. 67;
 [4] Valkiūnas, G. et al. (2011). Two New *Trypanosoma* Species from African Birds, with Notes on the Taxonomy of Avian Trypanosomes. Journal of Parasitology, Vol. 97.

ANALYSIS OF VIRULENCE FACTORS IN ISOLATES OF OPPORTUNISTIC PATHOGEN *STENOTROPHOMONAS MALTOPHILIA*

Radvilė Drevinskaitė¹, Laurita Klimkaitė¹, Jūratė Skerniškytė¹, Julija Armalytė¹

¹Institute of Biosciences, Life Sciences Center, Vilnius University, Vilnius, Lithuania
radvile.drevinskaite@gmc.stud.vu.lt

Stenotrophomonas maltophilia is an aerobic gram-negative bacterium that is widespread in the natural environment including soil, plants, and water sources. This bacterium of environmental origin is becoming an important opportunistic, nosocomial, multidrug-resistant pathogen associated with respiratory, bloodstream and urinary tract infections. Due to *S. maltophilia* innate resistance to various classes of antibiotics infections caused by this bacterium are difficult to treat and have high mortality rates of up to 69% [1]. Despite the wide range of clinical diseases associated with *S. maltophilia*, little information is available on the virulence factors of this bacterium. In addition to antibiotic resistance, the biofilm formation is considered a key virulence factor for *S. maltophilia* [2]. Secreted enzymes such as proteases, lipases and nucleases are thought to play an important role in *S. maltophilia* virulence, contributing to its ability to invade host tissues and degrade host components [3].

The aim of this study was to investigate the presence of genes encoding selected virulence determinants in 34 clinical and 43 natural isolates of *Stenotrophomonas maltophilia* from Lithuania. All clinical isolates were isolated from patients. Environmental isolates were isolated from various sources such as soil, water bodies and fish gut.

Genes encoding extracellular enzymes, toxins, components of secretion systems and iron uptake systems were selected for the detection of virulence factors. The analysis showed that the prevalence of most of the genes studied is similar in *S. maltophilia* isolates of natural and clinical origin. However, genes *stmPr1*, *afaD* and *zot*, encoding putative protease, adhesin and toxin respectively, were found to be exclusively present in isolates of clinical origin. The higher prevalence of virulence genes detected in clinical *S. maltophilia* isolates may be related to their importance in contributing to the ability of the bacterium to infect the host, to degrade various host components and to survive in clinical settings.

Acknowledgements: This research has received funding from the Research Council of Lithuania (LMTLT), project registration no. P-SV-23-156.

[1] Brooke JS. *Stenotrophomonas maltophilia*: an emerging global opportunistic pathogen. *Clin Microbiol Rev.* 2012 Jan;25(1):2-41.

[2] McCutcheon JG, Dennis JJ. The Potential of Phage Therapy against the Emerging Opportunistic Pathogen *Stenotrophomonas maltophilia*. *Viruses.* 2021 Jun 3;13(6):1057.

[3] Brooke JS. Advances in the microbiology of *Stenotrophomonas maltophilia*. *Clin Microbiol Rev.* 2021 May;34:e00030-19.

INVESTIGATION OF THE INTERACTIONS BETWEEN THE SOYBEAN PLANTS AND MICROORGANISMS USING STABLE ISOTOPES

Raminta Skipitytė^{1,2}, Rūta Barisevičiūtė¹, Monika Toleikienė²

¹Center for Physical Sciences and Technology, Lithuania

²Lithuanian Research Centre for Agriculture and Forestry, Lithuania
raminta.skipityte@ftmc.lt

The expanding body of research on the health benefits associated with pulse consumption has heightened interest in cultivating legumes, even in cooler climate regions like Lithuania. Although they are sensitive to climatic stresses, resulting in inferior-quality seeds. To solve this problem, there is a need for better management tools for nitrogen fixation in legumes. In turn, microorganisms and biostimulants can increase nitrogen fixation in legumes, and contribute to better seed quality formation. However, the relationship between plants and microorganisms in the rhizosphere exhibits complexity and diversity. Stable isotope probing presents a unique opportunity to observe subtle alterations in the nitrogen signature within plants, resulting from the utilization of diverse nitrogen sources. This technique allows for the precise tracking and analysis of even minor changes in the isotopic composition of nitrogen in plant tissues, enabling to discern variations arising from different nitrogen inputs or sources (in this case atmospheric N₂ or dissolved nitrogen in soil).

Our preliminary study of two varieties of soybeans (Laulema and Merlin) infected by two strains of microorganisms (Bactolife and Rhizofix 10) using the natural abundance of ¹⁵N (defined as delta¹⁵N) shows the effectiveness of these microorganisms in N₂ fixation, also related with higher nitrogen content (Fig. 1). The nitrogen isotopic ratio up to 2‰ shows the main sources of atmospheric nitrogen, meanwhile higher isotopic values reflect the input of nitrogen fertilizers. Thus, we demonstrated the potential of two strains of symbiotic microorganisms to better management practices for the cultivation of non-traditional legume species like soybean.

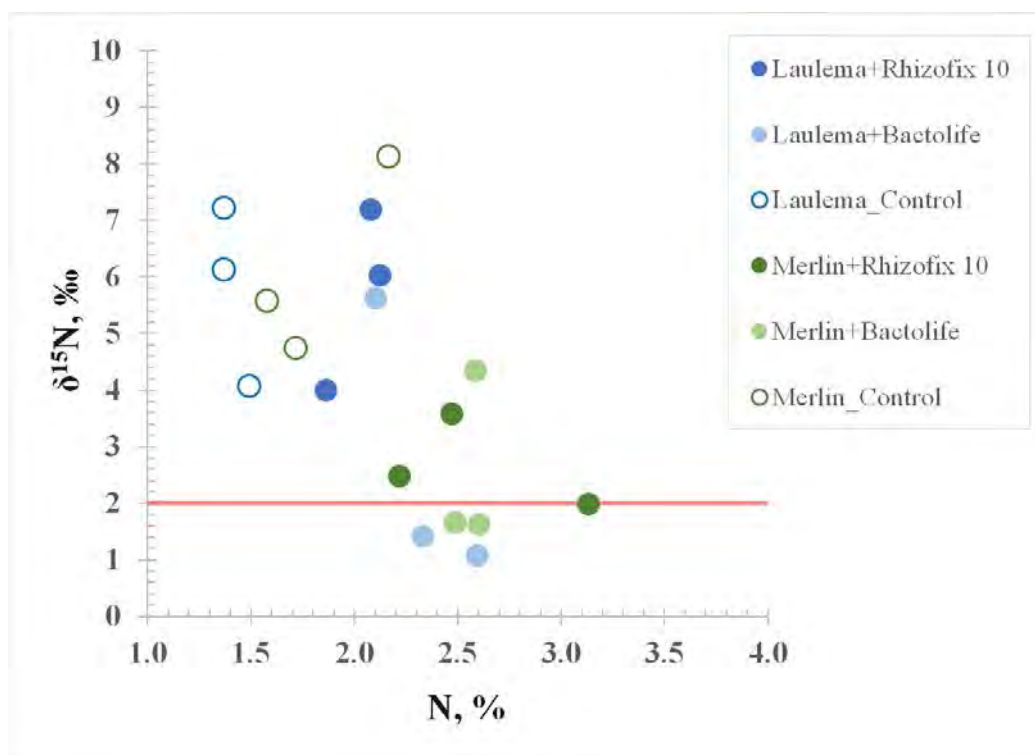


Fig. 1. Nitrogen stable isotope values (delta¹⁵N) and nitrogen content (N, %) in two varieties of soybeans (Laulema and Merlin) infected by two strains of microorganisms (Bactolife and Rhizofix 10).

Acknowledgments: we would like to acknowledge the Lithuanian Council of Sciences for funding the project NitroFixation under agreement Nr. S-MIP-22-56.

CARBON SUPPORTED METAL CATALYST FROM SEAWEED-DERIVED BIO-CHAR PREPARATION AND CHARACTERIZATION VIA CHEMISORPTION

Paulius Buidovas^{1,2}, Justas Eimontas¹, Raminta Skvorčinskienė¹

¹Lithuanian energy institute

²Kaunas university of technology
paulius.buidovas@lei.lt

Over the past two decades, an increase of nutrient levels in marine coastal waters has resulted in a surplus of primary production, which is defined by either massive phytoplankton blooms or opportunistic macroalgae. Seaweeds that become stranded can cause hypoxia, discharge harmful hydrogen sulfide into the water, cause animal mortality, and decrease biodiversity in marine and estuarine ecosystems. Seaweed is already harvested for food and hydrocolloid production; however it could also be used as a feedstock for the production of biochar – a carbon-rich “biological charcoal”. It is possible to get biochar with 1.15–1227 m²/g specific surface area measured by BET method, which is in line with many traditional catalysts. In this work, researchers aim to propose a method of producing iron and copper metal supported catalysts from seaweed found in the Baltic Sea processed via pyrolysis. The catalysts were characterized by temperature-programmed desorption (TPD), temperature-programmed reduction (TPR), H₂ and CO chemisorption.

STABLE ISOTOPES AS A TOOL TO TRACK C AND N PATHWAYS IN THE ROOT SYSTEMS

Agnė Veršulienė^{1,2}, Andrius Garbaras¹

¹Center for Physical Sciences and Technology

²Lithuanian Research Centre for Agriculture and Forestry

agne.versuliene@lammc.lt

Mycorrhizas (fungal roots) play vital roles in plant nutrient acquisition, performance and productivity in terrestrial ecosystems as soil nutrients, including NH_4^+ , NO_3 and phosphorus, are translocated from mycorrhizal fungi to plants. A stable isotope technique will be used to study mycorrhizal symbiosis as the mutually beneficial association between the roots of cereal plants and specific soil fungi.

The main aim of our project “The influence of mycorrhizal abundance on N transfer and C sequestration in the cereal/legume intercropping system by the ^{13}C and ^{15}N isotope method” will be to investigate the impact of mycorrhizal abundance on N_2 fixation, N transfer and C sequestration in cereal/legume intercropping system by the labelling ^{13}C and ^{15}N stable isotope method. To evaluate the role of mycorrhizal abundance on N transfer and C sequestration, it is important to investigate how its response to different cereal/legume intercropping system. The objectives of this project: (i) quantify the root mycorrhizal abundance of cereal/legume intercropping system; (ii) to study and compare the effect root mycorrhizal abundance on nutrient uptake, N_2 fixation and N transfer in cereal/legume intercropping system; (iii) to study the effect of mycorrhizal abundance on C sequestration in the soil in cereal/legume intercropping system; (iiii) to relate the physical cereal root parameters to plant productivity, yield quality and plant adaptation to climate change using intercropping systems.

The results obtained using the labeled stable isotope method to determine the C and N pathways in root systems with different mycorrhizal intensities will provide new insights into the importance of mycorrhizae and their impact on N cycling and C sequestration in soil under adverse environmental conditions. The established regularities would consider the assessment from the viewpoint of specific cropping systems i.e., cereals/legumes intercropping impact in terms of food quality, crop productivity, soil nutrient cycling and greenhouse gas emissions.

INVESTIGATING THE IMPACT OF ELAVL1 INHIBITION ON PANCREATIC CANCER CELL VIABILITY

Joris Dambrauskas¹, Darius Stukas²

¹Faculty of Chemistry and Geosciences, Vilnius University

²Surgical Gastroenterology Laboratory, Institute for Digestive Research, Lithuanian University of Health Sciences
joris.dambrauskas@chgf.stud.vu.lt

Introduction

An RNA binding protein, human antigen R (ELAVL1), is a key regulator of a molecular mechanism that is responsible for posttranscriptional gene regulation which is altered in pancreatic ductal adenocarcinoma (PDAC) cells. This, in turn, supports the pro-survival phenotype intrinsic to PDAC cells [1]. Thus, ELAVL1 inhibition could be considered a viable direction for cancer therapeutics [2], yet, it is still not clear how different inhibitors affect the cell.

Aim

This study aimed to investigate the effects of two known natural ELAVL1 inhibitors – 15,16-dihydrotanshinone-I (DHTS) [3] and pyrvinium pamoate (PP) [4] – on expression of ELAVL1 target mRNAs and proteins.

Methods

PDAC (BxPC-3) cells were treated with different concentrations of the two inhibitors for 24 hours. The IC50 doses of both inhibitors were determined through MTT assays. Then, doses that don't affect cell viability were used to evaluate the inhibition of ELAVL1 according to two of its targets – aryl hydrocarbon receptor (AHR) [5] and deoxycytidine kinase (dCK) [6]. Protein expression was assessed through western blot (WB) analysis and the quantities of respective mRNA transcripts – through quantitative real-time polymerase chain reaction (qRT-PCR).

Results

The results show that both DHTS and PP affect the cell metabolic activity in a similar manner with IC50 doses being comparable between inhibitors. Protein expression of AHR and DCK, was reduced in all cases, while there was an increase in mRNA being transcribed.

Conclusion

Inhibition of ELAVL1 may have a positive impact on the course of PC by decreasing expression of unfavourable proteins such as AHR. On the other hand, ELAVL1 also stabilizes DCK, which is required for gemcitabine to be effective. Thus, although ELAVL1 could potentially be used to contribute to the treatment of pancreatic cancer, it is important to consider the adjacent therapies used.

-
- [1] J. R. Brody and D. A. Dixon, "Complex HuR function in pancreatic cancer cells," *WIREs RNA*, vol. 9, no. 3, p. e1469, May 2018, doi: 10.1002/wrna.1469.
 [2] D. Goutas, A. Pergaris, C. Giaginis, and S. Theocharis, "HuR as Therapeutic Target in Cancer: What the Future Holds," *Curr. Med. Chem.*, vol. 29, no. 1, pp. 56–65, Jan. 2022, doi: 10.2174/0929867328666210628143430.
 [3] V. G. D'Agostino et al., "Dihydrotanshinone-I interferes with the RNA-binding activity of HuR affecting its post-transcriptional function," *Sci. Rep.*, vol. 5, no. 1, p. 16478, Nov. 2015, doi: 10.1038/srep16478.
 [4] J. Guo et al., "Inhibiting cytoplasmic accumulation of HuR synergizes genotoxic agents in urothelial carcinoma of the bladder," *Oncotarget*, vol. 7, no. 29, pp. 45249–45262, Jul. 2016, doi: 10.18632/oncotarget.9932.
 [5] D. Stukas et al., "Targeting AHR Increases Pancreatic Cancer Cell Sensitivity to Gemcitabine through the ELAVL1-DCK Pathway," *Int. J. Mol. Sci.*, vol. 24, no. 17, p. 13155, Aug. 2023, doi: 10.3390/ijms241713155.
 [6] C. L. Costantino et al., "The Role of HuR in Gemcitabine Efficacy in Pancreatic Cancer: HuR Up-regulates the Expression of the Gemcitabine Metabolizing Enzyme Deoxycytidine Kinase," *Cancer Res.*, vol. 69, no. 11, pp. 4567–4572, Jun. 2009, doi: 10.1158/0008-5472.CAN-09-0371.

INTRINSIC FIRING PROPERTIES OF THE MOUSE HIPPOCAMPAL PYRAMIDAL CA1 NEURONS DURING THE POSTNATAL DEVELOPMENT

Igor Nagula¹, Emilija Kavalnytė¹, Kornelija Vitkutė¹, Daiva Dabkevičienė², Urtė Neniškytė³, Aidas Alaburda¹

¹Institute of Biosciences, Life Sciences Center, Vilnius University, Vilnius, Lithuania

²National Cancer Institute, Vilnius, Lithuania

³VU-EMBL Partnership Institute, Life Sciences Center, Vilnius, Lithuania

igor.nagula@gmc.vu.lt

Postnatal development is a crucial period for hippocampus neuronal maturation and neural pathways organization, when neurons change morphologically and exhibit an increase in the number of ion channels in the membranes[1]. The maturation of neuronal pathways has primarily been investigated through anatomical and immunohistochemical studies, but, some features like an intrinsic firing properties and functional synaptic activity necessitates direct electrophysiological recordings. The majority of electrophysiological research on hippocampal development has primarily involved rats[2]. Combination of novel molecular and genetic tools developed for mice animal model[3] with electrophysiological profiles would provide an additional insight about mechanisms of hippocampus postnatal development. Moreover, sex also can potentially influence the developmental processes of the hippocampus[4]. The aim of this study was to evaluate the intrinsic firing properties during the postnatal development in hippocampal pyramidal CA1 neurons in different sex mice.

In this study we used wild-type mice of different ages (5 to 21 postnatal days), both males and females. We employed whole cell patch-clamp technique. The firing properties were evaluated as f-I (frequency-current) relation, indicating how neurons integrate inputs and encodes outputs in the frequency of action potentials. Spike frequency adaptation was also evaluated.

We have found that the f-I relation significantly decreases during the development both in males and females before and after the spike frequency adaptation. The spike frequency adaptation ratio did not significantly change during the development both in males and females. There are also no significant differences between sex groups.

[1] Moody, W.J, Bosma, M.M.: Ion Channel Development, Spontaneous Activity, and Activity-Dependent Development in Nerve and Muscle Cells. *Physiol. Rev.* 85, 883-941 (2005).

[2] Zhang, Z.: Maturation of Layer V Pyramidal Neurons in the Rat Prefrontal Cortex: Intrinsic Properties and Synaptic Function. *J. Neurophysiol.* 91, 1171-1182 (2004).

[3] Canales, C.P., Walz, K.: The Mouse, a Model Organism for Biomedical Research. In: *Cellular and Animal Models in Human Genomics Research*. Pp. 119-140. Elsevier (2019).

[4] Yagi, S., Galea, L.A.M.: Sex differences in hippocampal cognition and neurogenesis. *Neuropsychopharmacology.* 44, 200-213 (2019).

THE ESTABLISHMENT OF THREE NEW OVARIAN CANCER CELL LINES OPENS NEW AVENUE OF RESEARCH INTO TUMOR HETEROGENEITY AND CELL EVOLUTION

Eglė Žymantaitė^{1,2}, Agata Mlynska², Neringa Dobrovolskienė², Birutė Intaitė², Vita Pašukonienė²

¹Life Sciences Centre, Vilnius University, Lithuania

²National Cancer Institute, Vilnius, Lithuania

egle.zymantaite@gmc.stud.vu.lt

Ovarian cancer (OC) is one of the most fatal malignancies affecting women globally. The high level of heterogeneity of this cancer plays a big role in the lack of successful treatments. In the pursuit of studying cancer cell biology and testing new drugs, cell line models have emerged as the primary *in vitro* research model. However, recent data indicates that some of the frequently used OC cell lines in research no longer precisely represent their original tumor profile. Therefore, it is imperative to develop new cell lines that are well-characterized and closely resemble the various histological and molecular profiles of the tumor.

Our study has successfully established three distinct cell lines (CW1-NCI, CW2-NCI, SM-NCI) that were derived from different tumor pieces obtained from the same 62-year-old female patient diagnosed with high-grade serous ovarian carcinoma in the National Cancer Institute of Lithuania. To ensure accuracy, all newly established ovarian cell lines were observed and characterized at specific passages. The passaging process resulted in significant changes in the morphological characteristics of the cell lines, as well as differences in their ability to form 3D structures. Flow cytometry analysis was conducted on different cell line passages, revealing distinct marker expression profiles that proved the existence of cancer cell heterogeneity within the same tumor. The findings also demonstrated that the marker expression fluctuated across different cell passages, indicating the plasticity and evolution of cells in the culture until they reached a stable marker expression.

The findings of our study are significant in the comprehensive understanding of ovarian cancer heterogeneity, cell plasticity, and evolution during the culturing process. Moreover, the establishment of a new stable ovarian cancer cell line models will prove to be a valuable tool for future research.

DEVELOPMENT OF A DNA OLIGO-CAPTURE METHOD TO STUDY CANCER CELL METASTASIS IN ANIMAL MODELS

Roberta Pocevičiūtė¹, Šarūnas Tumas¹, Anna Malkova², Michael Sherman²

¹Cureline Baltic, Lithuania

²Faculty of Natural Sciences, Department of Molecular Biology, Ariel University, Israel
roberta.pocevicute@cureline.com

DNA barcoding is a method that allows to track and identify specimens over time using short, specific DNA sequences, which are integrated into the genome by lentiviral transduction. It is widely used to study organ development and cancer progression. Traditional cancer treatments are less effective against metastasis and there is a lack of effective cancer metastasis models for testing new cancer drugs on. Cell DNA barcoding is a valuable tool for evaluating potential cancer drugs on primary tumors and metastasis, allowing simultaneous tracking of differently barcoded cell lines, which allows to compare the drug effects across different cell populations in the same animal using next generation sequencing. Standard sequencing library preparation relies on 2 rounds of PCR amplification, which is time consuming and can lead to PCR artifacts.

This project aims to develop the protocol for DNA barcode capture by streptavidin-coated magnetic beads from mouse organs. Although PCR is mostly utilized for barcodes extraction, hybridization-based technique is more sensitive, less time consuming and cost-effective. This technique captures in hybridization formed complex made of targeted region (barcode) and biotinylated probe, which is later pulled with magnetic bead. Results of the capture were analyzed using gel electrophoresis and qPCR.

To validate this method, the capture system was optimized in vitro in the absence of any nonspecific DNA sequences and in the presence of nonspecific DNA. Optimal probe length, probe biotinylation, hybridization time and temperature were determined. A major improvement to the capture system was achieved when 5' biotinylated probe was changed to an internally biotinylated probe which captures barcodes 24 times more efficiently. Moreover, $1,31 \times 10^9$ of barcode copies were isolated, which is enough for capturing all unique barcodes in a mice organ, considering that cells were transfected with 5×10^6 of unique barcodes. Unspecific DNA had no impact on capture efficiency and barcodes fraction had no significant amount of unspecific DNA residues. Further steps are to optimize the extraction of barcodes from cell and organ lysates and compare the developed protocol with the PCR-based protocol.

METHYLATION PROFILING OF HOMEOTIC AND CHROMATIN REMODELING GENES IN CANCEROUS OVARIAN TISSUE

Rugilė Gineikaitė^{1,2}, Ieva Vaicekauskaitė^{1,2}, Rūta Čiurlienė¹, Rasa Sabaliauskaitė^{1,2}

¹Institute of Biosciences, Life Sciences Center, Vilnius University, Vilnius, Lithuania

²National Cancer Institute, Vilnius, Lithuania

rugile.gineikaite@gmc.stud.vu.lt

Ovarian cancer is the third most common gynecologic cancer in the world and has the highest mortality rate of all gynecologic cancers [1]. Due to asymptomatic progression, ovarian cancer is diagnosed in 4 out of 5 cases in advanced stages (III or IV), when cancer has spread and control of the disease is difficult [2]. Ovarian cancer is heterogenic disease, which complicates the diagnosis of the disease and the selection of the optimal treatment strategy, however, approximately 75% of ovarian cancer cases are high-grade serous carcinomas. Current diagnostic methods for ovarian cancer lack specificity and sensitivity, thus it is important to search for new modern diagnostic tools. In recent years, promoter hypermethylation of tumor suppressor genes has gained a lot of attention for its potential to be applied as a cancer biomarker. Methylation studies of homeotic and chromatin remodeling genes attracted clinicians because they are important for the development of various organs, including ovaries and are critical for maintaining normal functions and homeostasis. Therefore, dysfunctions of homeotic and chromatin remodeling genes are associated with various diseases, including the development and progression of ovarian cancer.

This study aimed to evaluate promoter methylation profiles of homeotic (*ALX4*, *CDX2* and *HOPX*) and chromatin remodeling (*ARID1A*) genes that act as tumor suppressor genes in cancerous ovarian tissues as potential ovarian cancer biomarkers for more accurate and specific diagnostics. In total methylation profile was evaluated in 51 tissue biopsy samples using methylation-specific PCR (MSP).

The results demonstrated that methylation profile of *HOPX* gene significantly differ between benign gynecological tumors and high-grade ovarian carcinoma patients, while methylation profiles of *ALX4* and *CDX2* genes showed tendency between benign gynecological tumors and high-grade ovarian carcinoma patients, and other less common types of gynecologic cancer patients. Methylation profile of *ARID1A* gene showed no significant differences.

Thus, we found out that homeotic genes have the potential to be used for the early detection of disease and prediction of response to therapeutic interventions and prognosis of outcome, improving the quality of patients lives. However, more extensive analysis must be performed to validate the studied biomarkers.

Acknowledgements: This study was funded by the National Cancer Institute.

-
- [1] Momenimovahed, Z., Tiznobaik, A., Taheri, S. and Salehiniya, H. (2019). Ovarian cancer in the world: Epidemiology and risk factors. *International Journal of Woman Health*, 11, 287-299.
- [2] Menon, U., Karpinskyj, C. and Gentry-Maharaj, A. (2018). Ovarian Cancer Prevention and Screening. *Obstetrics and Gynecology*, 131(5), 909-927.

NOTCH SIGNALING PATHWAY COMPONENTS AS POTENTIAL BIOMARKERS FOR THE DIAGNOSIS OF OVARIAN CANCER

Paulina Kazlauskaitė^{1,2}, Ieva Vaicekauskaitė^{1,2}, Rūta Čiurlienė¹, Rasa Sabaliauskaitė^{1,2}

¹National Cancer Institute, LT-08406 Vilnius, Lithuania

²Institute of Biosciences, Life Sciences Center, Vilnius University, LT-10257 Vilnius, Lithuania
paulina.kazlauskaite@gmc.stud.vu.lt

Ovarian cancer is one of the most common gynecologic cancers, exhibiting the highest mortality rate. In 2020, over 313,000 women worldwide were diagnosed with ovarian cancer, leading to more than 207,000 confirmed [1]. Typically, ovarian cancer is diagnosed at an advanced stage, known as high-grade serous ovarian cancer (HGSOC). The elevated mortality is linked to the absence of specific symptoms for ovarian cancer and the absence of well-established biomarkers. Currently utilized biomarkers in the clinic, CA-125 and HE4, have limitations. For instance, CA-125 is elevated in only 50% of early-stage tumors, and HE4 testing is not recommended in routine practice due to contradictory studies [2,3]. Addressing the critical need for improved diagnostic tools, the NOTCH signaling pathway emerges as a promising biomarker, showcasing a crucial oncogenic role in HGSOC and contributing to the development of ovarian cancer [4].

The aim of this research was to investigate gene expression changes of the NOTCH signaling pathway ligands *JAG2*, *DLL1*, and signaling pathway target *HES1*, to evaluate these genes as promising genetic biomarkers for the diagnosis of ovarian cancer.

During the study, mRNA expression changes were analyzed in 66 patients' tissues, suspected of ovarian cancer (including 42 HGSOC, 15 other gynecological cancers, and 9 benign gynecologic tumors). Genes expression was examined using reverse transcription quantitative PCR. Results were normalized to the reference gene *GAPHD*, and the $\log_2(2^{-\Delta CT})$ method was used to calculate genes relative expression.

The results showed that all studied genes were downregulated in HGSOC when compared to benign gynecologic tumors tissues, with significant downregulation of *DLL1* and *HES1* genes. The combined ROC curve panel of all three genes for distinguishing the class with HGSOC risk from benign cases showed an AUC of 0.99, $p < 0.0001$, sensitivity of 92.86%, and specificity of 100%. Furthermore, significant differences in relative expression of *DLL1* and *HES1* genes were found between HGSOC and other gynecological cancers groups. Finally, before treatment, patients with higher CA-125 value showed statistically significant differences ($p = 0.02$) in *HES1* gene relative expression compared to the norm of this biomarker.

In conclusion, our pilot study suggests that components of the NOTCH signaling pathway show promise as potential biomarkers for future ovarian cancer diagnostics. However, further comprehensive studies, including non-invasive samples, are essential to validate these genes as suitable biomarkers for the development of new cancer tests.

-
- [1] Sung, H., Ferlay, J., Siegel, R. L., Laversanne, M., Soerjomataram, I., Jemal, A., Bray, F. (2021). Global Cancer Statistics 2020: GLOBOCAN estimates of incidence and mortality worldwide for 36 cancers in 185 countries. *CA: A Cancer Journal for Clinicians*, 71(3), 209–249.
- [2] Charkhchi, P., Cybulski, C., Gronwald, J., Wong, F., Narod, S. A., Akbari, M. R. (2020). CA125 and ovarian Cancer: A Comprehensive review. *Cancers*, 12(12), 3730.
- [3] Colombo, N., Sessa, C., Du Bois, A., Ledermann, J. A., McCluggage, W. G., McNeish, I. A., Morice, P., Pignata, S., Ray-Coquard, I., Vergote, I., Baert, T., Belaroussi, I., Dashora, A., Olbrecht, S., Planchamp, F., Querleu, D., Baert, T., Banerjee, S., Belaroussi, I., Zeimet, A. G. (2019). ESMO–ESGO consensus conference recommendations on ovarian cancer: pathology and molecular biology, early and advanced stages, borderline tumours and recurrent disease. *Annals of Oncology*, 30(5), 672–705.
- [4] Zhou, B., Wanling, L., Long, Y., Yang, Y., Zhang, H., Wu, K., Chu, Q. (2022). Notch signaling pathway: architecture, disease, and therapeutics. *Signal Transduction and Targeted Therapy*, 7(1).

UPCONVERTING NANOCOMPLEX DELIVERY TO DISTINCT PHENOTYPES OF CANCER BY MESENCHYMAL STEM CELLS

Alėja Marija Daugėlaitė^{1,2}, Greta Butkienė¹, Simona Steponkienė¹, Vaidas Klimkevičius³, Vilius Poderys¹, Iлона Uzielienė⁴, Vitalijus Karabanovas^{1,5}, Ričardas Rotomskis^{1,6}

¹Biomedical Physics Laboratory of National Cancer Institute, Vilnius, Lithuania

²Faculty of Medicine, Vilnius University, Vilnius, Lithuania

³Institute of Chemistry, Faculty of Chemistry and Geosciences, Vilnius University, Vilnius, Lithuania

⁴Department of Regenerative Medicine, State Research Institute Centre for Innovative Medicine, Vilnius, Lithuania

⁵Department of Chemistry and Bioengineering, Vilnius Gediminas Technical University, Vilnius, Lithuania

⁶Biophotonics group of Laser Research Centre, Vilnius University, Vilnius, Lithuania

aleja.daugelaite@nvi.lt

Colorectal cancer is the third most common cancer diagnosed and the second leading cause of cancer-related deaths worldwide. It is often diagnosed at an advanced stage when treatment options are limited and usually non-specific [1]. Selective delivery of anticancer agents to the tumour is needed to avoid the side effects of cancer treatment. Mesenchymal stem cells (MSCs) can be used for this purpose. MSCs are found in specific niches in the body and can be isolated from a wide variety of tissues. The main sources of MSCs are bone marrow or adipose tissue, but much less is known about MSCs isolated from skin or menstrual blood, which is what our research focuses on. Nowadays, MSCs are being widely studied as a tool for the delivery of anticancer agents. Due to MSCs oncogenic properties it is hoped to use MSCs as a Trojan horse for the delivery of therapeutic nanoparticles directly to the tumour [2]. The dense extracellular matrix and high intracellular hypertension in tumours make diffusion and penetration of nanoparticles and other anticancer drugs inefficient. Therefore, MSCs can be employed as vehicles, so anticancer agents can be actively delivered to the interior of the tumour tissue. To fulfil the latter purpose, it is necessary to have a good understanding of MSCs ability to migrate towards the tumour, because the type of tumour and its microenvironment may affect the migration of MSCs.

The study aimed to investigate the migration of upconverting nanocomplexes (UCNP-Ce6) uploaded MSCs towards 3 different phenotypes of colorectal cancer cells.

To ensure that the UCNP-Ce6 complex is suitable for biological applications, we evaluated the accumulation and cytotoxicity of this complex in skin and menstrual blood MSCs, and colon cancer cell lines DLD-1, HCT116, LS1034. Results of confocal microscopy showed that UCNP-Ce6 accumulates inside cells and localizes in the perinuclear region. The cytotoxicity was assessed using the lactate dehydrogenase (LDH) cytotoxicity assay. Results showed that nanoparticles are biocompatible and have no dark toxicity after 24h. The efficiency of MSCs migration and the ability to transport nanoparticles was investigated using two sources of MSCs: skin and menstrual blood. The migration of MSCs was investigated using the Transwell migration assay in 2D and 3D environments. It was found that the migration efficiency of MSCs is different and depends on the phenotype of the colon cancer cells.

Overall, our results showed that active upconverting nanocomplex transportation using MSCs could increase the delivery of nanotherapeutics to cancer cells. The demonstrated potential of MSCs as nanoparticle carriers may lead to new opportunities for the development of targeted cancer therapy.

Acknowledgment This work is part of a project that was supported by the funds of Lithuania (Grant No. S-MIP-22-31).

[1] Xi Y, Xu P. Global colorectal cancer burden in 2020 and projections to 2040. *Translational Oncology*. 2021, 14(10):101174.

[2] Dapkute D, Pleckaitis M, Bulotiene D, Daunoravicius D, Rotomskis R, Karabanovas V. Hitchhiking Nanoparticles: Mesenchymal Stem Cell-Mediated Delivery of Theranostic Nanoparticles. *ACS Appl Mater Interfaces*. 2021, 22:13(37):43937–51.

PLANT-DERIVED NANOVESICLES DISPLAY WOUND HEALING PROPERTIES

Mėta Mackevičiūtė¹, Aistė Jekabsone^{1,2}, Zbigniew Balion²

¹Institute of Pharmaceutical Technologies, Faculty of Pharmacy, Lithuanian University of Health Sciences, Kaunas, Lithuania

²Preclinical Research Laboratory for Medicinal Products, Institute of Cardiology, Lithuanian University of Health Sciences, Kaunas, Lithuania
metamack@outlook.com

The process of wound healing is complex and often unresponsive to traditional treatment approaches, placing a considerable burden on patients [1]. Chronic nonhealing wounds are characterized by a reduction in the production of growth factors and chemokines, as well as impaired fibroblast proliferation, migration, and inflammatory responses [2]. Nanotechnology has emerged as a groundbreaking field, reshaping various aspects of medical science. Nanovesicles, which are present in various cell types, have bilayer membranes and possess unique compositions of nucleic acids, proteins, secondary metabolites, and lipids [3]. Such properties hold promise as therapeutic agents, and one of their versatile applications lies in the realm of wound healing. Plant-derived nanovesicles, known for their excellent compatibility with human body and penetration into skin cells, exhibit potential for enhancing wound healing [4]. Given the established efficacy of certain plant-derived nanovesicles in promoting wound closure, it becomes essential to identify specific sources of these vesicles and investigate their capacity for alleviating *in vitro* wound healing.

Commercial keratinocyte (HaCaT) and human skin fibroblast (BJ-5ta) cell lines were used in the study. Plant nanovesicles were isolated from lyophilized plant powder using polymeric precipitation method. The Bradford method was applied to characterize the obtained nanovesicles according to the total protein content, Trizol reagent was used to determine the amount of RNA, and nanoparticle analysis was performed (Nanosight S300). The effects of nanovesicles were evaluated by seeding keratinocytes and fibroblasts in 96-well plates, incubating these cells with nanovesicles for 48 hours and measuring proliferation with PrestoBlue™ reagent. *In vitro* wound studies were also performed using commercial skin cells to determine the effect of isolated nanovesicles on wound healing.

Following the extraction of nanovesicles derived from various plants (nettle, black currant berry, blueberry, rose, lion's mane mushroom, and lingonberry) and nanoparticle tracking analysis, it was observed that the size of these vesicles fell within the 50-250 nm range, consistent with existing literature descriptions. The isolated nanovesicles were found to contain substantial quantities of RNA and proteins. Cell viability was influenced by nanovesicle concentration, with higher concentrations leading to decreased viability, while lower concentrations had no negative impact on the cells. *In vitro* scratch test experiments revealed that nettle, blackcurrant, and blueberry nanovesicles at lower concentrations accelerated wound closure rates in both keratinocyte and fibroblast cell cultures. However, it is vital to be cautious regarding nanoparticle dosage, as higher concentrations may exert adverse effects on skin cells.

[1] Frykberg, R. G., Banks, J. Challenges in the Treatment of Chronic Wounds. *Advances in Wound Care*. 2015 Sep. 4(9):560-582.

[2] Schillreiff, P., Alexiev, U. Chronic Inflammation in Non-Healing Skin Wounds and Promising Natural Bioactive Compounds Treatment. *Int. J. Mol. Sci.* 2022. 23(9):4928.

[3] Zhou, C., Zhang, B., Yang, Y. et al. Stem cell-derived exosomes: emerging therapeutic opportunities for wound healing. *Stem Cell Res Ther.* 2023. 14(107).

[4] Prasai, A., Jay, J. W., Jupiter, D., Wolf, S. E., El Ayadi, A. Role of Exosomes in Dermal Wound Healing: A Systematic Review. *Journal of Investigative Dermatology*. 2022 Mar. 142(3): 662-678.

APPLICATION OF THE HIGH THROUGHPUT DARK-FIELD FULL-FIELD OPTICAL COHERENCE TOMOGRAPHY SYSTEM

Karolis Adomavičius¹, Austėja Trečiokaitė¹, Erikas Tarvydas¹, Danielis Rutkauskas¹, Egidijus Aukorius¹

¹Center for Physical Sciences and Technology, Department of Optoelectronics, Vilnius, Lithuania
Karolis.Adomavicius@ftmc.lt

Optical coherence tomography (OCT) is a non-invasive interferometric imaging technique. It can be applied in various situations, such as in-vivo retinal imaging for damage detection, diagnosing and monitoring retinal diseases, imaging deeper layers of human fingerprints, detecting sub-surface defects in optical glasses and etc. However, the spatial resolution, imaging speed and depth is still an issue in OCT. Recently, to speed up OCT imaging, Fourier-domain Full-Field OCT (FD-FF-OCT) has been introduced that uses a swept laser source and a super-fast camera to parallelize signal acquisition. In order to efficiently reduce coherence crosstalk noise in OCT images a multimode fiber can be implemented [1]. Such a system enabled us to visualize such hard-to-image retinal layers with $5\mu\text{m}$ spatial resolution.

The core of interferometer – beamsplitter is typically 50/50 and wastes almost 75% of light. Light going to the reference arm is practically all lost there because of the strong attenuation necessary when imaging biological tissue. Moreover, half of the light is sent back to the laser source instead of camera. However, by incorporating a small 45° pick-off mirror we were able to use 90/10 beamsplitter (Fig. 1). Such so called high-throughput dark-field (HTDF) [2] FD-FF-OCT configuration [2] allowed us to send more light on the sample and obtain most of the photons with the camera. With this HTDF implementation in our retinal FD-FF-OCT system we have demonstrated 3.5 times increase in signal on a USAF target sample mounted behind a scattering layer.

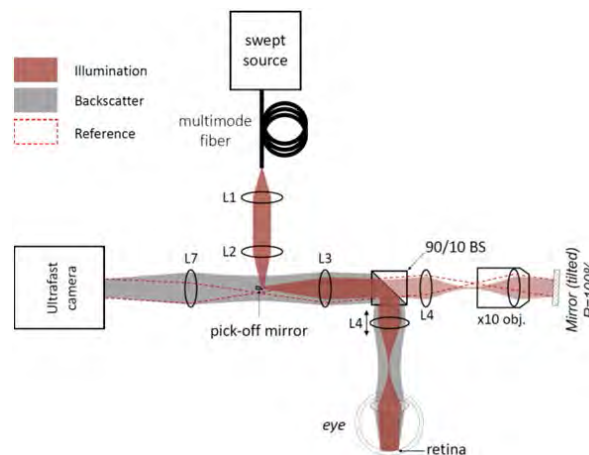


Fig. 1. Detailed scheme of high-throughput dark-field Fourier-domain FF-OCT system. System consists of swept-source laser, multimode fiber, from which light is collected and collimated via lenses L1-L2, redirected with pick-off mirror to the interferometer. Interferometer sends 90% of light to the eye and 10% to the reference. Reflected light is combined via same beamsplitter and directed to the camera. This time pick-off mirror acts as a dark-field mask for scattered light from the retina.

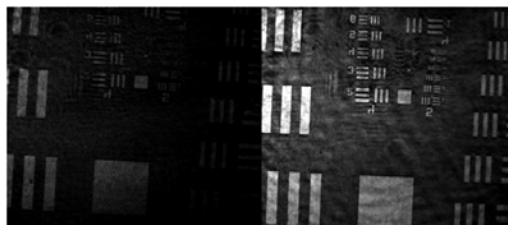


Fig. 2. SNR increase in the image of the USAF target mounted behind a scattering layer obtained with high-throughput FD-FF-OCT system (right) compared to a standard FD-FF-OCT system (left).

- [1] E. Aukorius, D. Borycki, and M. Wojtkowski, "Crosstalk-free volumetric in vivo imaging of a human retina with Fourier-domain full-field optical coherence tomography," *Biomed. Opt. Express*, vol. 10, no. 12, pp. 6390-6407, 2019.
- [2] E. Aukorius and A. Claude Boccara, "High-throughput dark-field full-field optical coherence tomography," *Opt. Lett.* 45, 455-458, 2020.

INVESTIGATION OF SUPERCONTINUUM GENERATION IN PHOTONIC CRYSTAL FIBERS WITH DIFFERENT CHARACTERISTICS USING FEMTOSECOND PUMP PULSES

Ieva Baltrukonytė¹, Jokūbas Pimpė¹, Julius Vengelis¹

¹Vilnius University, Faculty of Physics, Laser Research Center
 ievaltrukonyte@gmail.com

Phenomenon of supercontinuum generation is interesting and very useful in applications such like spectroscopy, telecommunications, and metrology [1]. Supercontinuum is a phenomenon when a sufficiently intense ultrafast pump pulse propagating through nonlinear media induces intensity-dependent refractive index, which results in nonlinear effects such like self-phase modulation (SPM), cross-phase modulation (XPM), four-wave mixing (FWM), stimulated Raman scattering (SRS) and soliton generation and fission [2]. A full information of such distorted pulse (temporal shape, phase, intensity, duration) can be retrieved by implementing cross-correlation frequency-resolved optical gating (XFROG) method, which requires two different pulses (well defined reference and unknown) [3]. Photonic crystal fibers are especially suitable for supercontinuum generation due to unique properties like tight light confinement, low effective mode area (increment of intensity of propagating light), flexibility to choose pump wavelength [1]. As nonlinear response is sufficiently increased by decreasing effective mode area, tapered photonic crystal fibers were invented and implemented to obtain higher spectral broadening [4].

The main objective of this work was to measure supercontinuum spectrum, characterize temporal profile of SC pulse in conventional or tapered PCFs and compare experimental results to determine quality of tapered fibers performed in FTMC, Department of Laser Technologies, Fiber Laser laboratory. SC was generated by directly pumping PCF by "FLINT" femtosecond laser oscillator with central wavelength of 1028 nm and repetition rate of 75.2 MHz.

After performing measurements of evolution of supercontinuum by increasing pump power and measurements of XFROG trace, spectral and temporal results of tapered or conventional PCFs were compared. To compare conventional PCFs, spectral and temporal characteristics differs remarkably due to different ZDW properties and fiber core size. Therefore, supercontinuum of respective tapered PCFs differs only quantitatively – spectral broadening was less efficient. Contrary to what was expected, tapered PCFs did not show any enhanced nonlinear response. Temporal characterization of tapered PCFs showed that light was probably leaking into other PCF core or cladding modes, resulting in intensity losses. Such results showed that manufacturing technique was insufficient in which tapering was conducted without applying air pressure to microstructure holes. This might have caused them to collapse and distort the geometry of microstructure region resulting in loss of intensity of propagating light.

-
- [1] K.P. Hansen, Introduction to nonlinear photonic crystal fibers, *Opt. Fiber Technol.* 2, (2005).
 [2] R. W. Boyd, Nonlinear optics, Third edition (Academic Press, Inc., USA, 2008).
 [3] R. Trebino, Frequency-Resolved Optical Gating: The Measurement of Ultrashort Laser Pulses (Springer, 2000).
 [4] S. Stark, P. St. J. Russel, Extreme Supercontinuum Generation to the Deep-UV, (2011)

PROCESSING OF THZ IMAGES USING DIFFERENT NEURAL NETWORK MODELS

Ugnė Šilingaitė^{1,2}, Ignas Grigelionis²

¹Vilnius University

²Center for Physical Sciences and Technology (FTMC)
ugne.silingaite@ff.stud.vu.lt

Terahertz (THz) images are often plagued with the problem of low spatial resolution due to the limited hardware capabilities and long imaging times. To address this challenge, various image processing methods are used. Recent advancements in machine learning models have yielded notable breakthroughs in addressing computer vision tasks, including their application in the domain of terahertz (THz) imaging. The goal of this work is to develop several neural network models aimed at enhancing resolution and bringing back the missing details in low-resolution terahertz (THz) images. To achieve this task, three convolutional neural network (CNN) generative adversarial (GAN) models – SRGAN, SRResNet and DeblurGan were trained on simulated data and reached PSNR values of 21,515 dB, 19,271 dB and 20,657 dB respectively. On real THz image data SRGAN and DeblurGan performed similarly and did manage to restore certain details from the test images, performing better than SRResNet model. In the analysis of actual terahertz (THz) image data, SRGAN and DeblurGan exhibited comparable performance, effectively restoring specific details from the test images, demonstrating better performance than SRResNet model. However, these models tend to over-restore details and introduce severe artifacts in the final image due to their extreme sensitive to noise, because of the strong mapping ability of the CNN type networks.

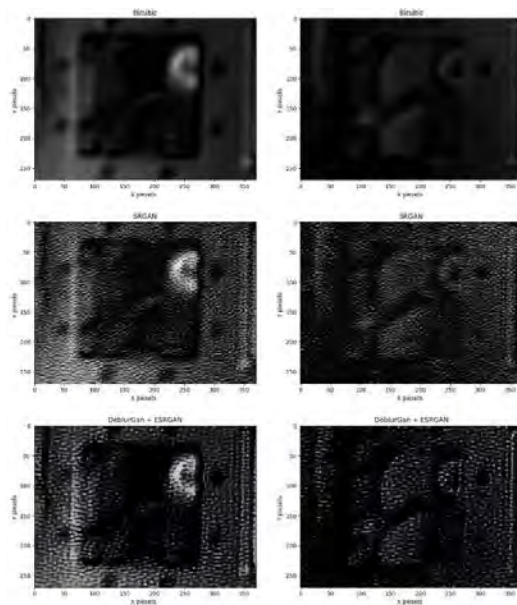


Fig. 1. Performance of different neural networks, using low resolution THz image as an input.

PICOSECOND LASER WELDING OF SODA-LIME GLASS WITH MHZ BURSTS

Neda Mažeikytė¹, Edgaras Markauskas¹

¹Department of Laser Technologies (LTS), Center for Physical Sciences and Technology (FTMC), Savanoriu Ave. 231, 02300 Vilnius, Lithuania
neda.mazeikyte@ftmc.lt

Laser-based glass welding offers great mechanical strength and increased longevity of the joint structures but, unlike traditional bonding techniques, does not suffer from creep, out-gassing, and aging [1]. Furthermore, it is a flexible and highly localized process that does not require an intermediate layer for the welding [1]. Ultrashort laser welding relies on nonlinear absorption, which prevents excessive heating of the surrounding material by confining the heat within a localized melt zone [1,2,3]. While welding of optical-contact glasses achieves the highest welding strength, it is difficult to meet the requirements for the optical contact, especially across a large area, even after polishing and cleaning [4,5]. For this reason, the development of laser welding of non-optical contact glasses attracted much attention.

In this work, multi-scan welding of two non-optical soda-lime glasses of 1 mm thickness with a pre-existing gap of 5-6 μm was performed with an ultrashort laser in single-shot pulses and MHz bursts. The laser radiation wavelength was 1064nm, pulse duration was 10 ps and 100kHz pulse repetition rate. Laser power, pulse repetition rate, focal position, marking speed, hatch distance, and number of pulses in a burst were optimized. After the welding, a longitudinal tensile test was performed to evaluate welding strength. Additionally, the quality of welds was evaluated via optical micrographs and light transmission measurements.

Results indicate (see figure 1) that the average weld strength increased with an increasing number of pulses in a burst. As a result, a maximum strength was achieved for 13 pulses in a burst. Analysis with an optical microscope revealed that the parameter window for a successful weld without cracks narrowed at a higher number of pulses in a burst.

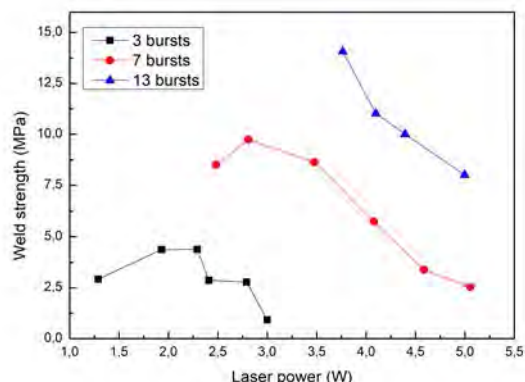


Fig. 1. Average weld strength dependence on the applied laser power with different number of pulses in the burst.

-
- [1] Zhang J, Chen S, Lu H, et al. The effect of gap on the quality of glass-to-glass welding using a picosecond laser. *Optics and Lasers in Engineering*. 2020.
 [2] Miyamoto I, Cvecek K, Okamoto Y, Schmidt M. Novel fusion welding technology of glass using ultrashort pulse lasers. *Physics Procedia*. 2010.
 [3] Miyamoto I. Local melting of glass material and its application to direct fusion welding by PS-laser pulses. *Journal of Laser Micro Nanoengineering*. 2007.
 [4] Jia X, Li K, Li Z, Wang C, Chen J, Cui S. Multi-scan picosecond laser welding of non-optical contact soda lime glass. *Optics and Laser Technology*. 2023.
 [5] Hang CC, Deng L, Duan J, Zeng X. Picosecond laser welding of glasses with a large gap by a rapid oscillating scan. *Optics Letters*. 2019.

DEBRIS REMOVAL TECHNIQUES FOR PICOSECOND LASER BOTTOM-UP MILLING OF FUSED SILICA

Aleksandras Kondratas¹, Miglė Mackevičiūtė¹, Juozas Dudutis¹, Paulius Gečys¹

¹Center for Physical Sciences and Technology, Savanoriu ave. 231, LT-02300, Vilnius, Lithuania
aleksandras.kondratas@ftmc.lt

Channels formed in glass have a variety of applications [1], for example in microelectrochemical systems, for the creation of nozzles, and others. Laser milling allows for the formation of small diameter and high-aspect-ratio channels [1]. Additionally, by focusing the laser beam to the bottom of the sample surface, parallel side walls are produced. Furthermore, scattering is reduced because debris does not go in the beam path, increasing the milled rate and depth [2]. Debris is often the limiting factor for the creation of high-aspect-ratio channels [3]. Therefore, additional debris removal methods need to be employed.

In this study, both continuous and pulsed airflow, no additional debris removal, and partial immersion of the sample in still distilled water (referred to as water-assisted) were employed, as illustrated in Fig. 1. Compressed airflow was blown at the laser interaction zone from a nozzle placed under the sample. Milling was done with a 1064 nm wavelength laser with a pulse duration of 13 ps (full-width-half-maxima) and the bottom-up technique. Firstly, the milling parameters were optimized to achieve the highest milling rate. After that, channels were milled through the entire 6.3 mm of fused silica, using various debris removal methods to find the smallest diameter. Lastly, tilted channels were formed by introducing an offset after each scanning loop to achieve the highest angle.

The smallest diameter was achieved when channels were formed using continuous airflow in 6.3 mm thickness fused silica which was further reduced when milling smaller 1 mm depth channels. However, water-assisted milling allowed the formation of a channel with a higher angle.

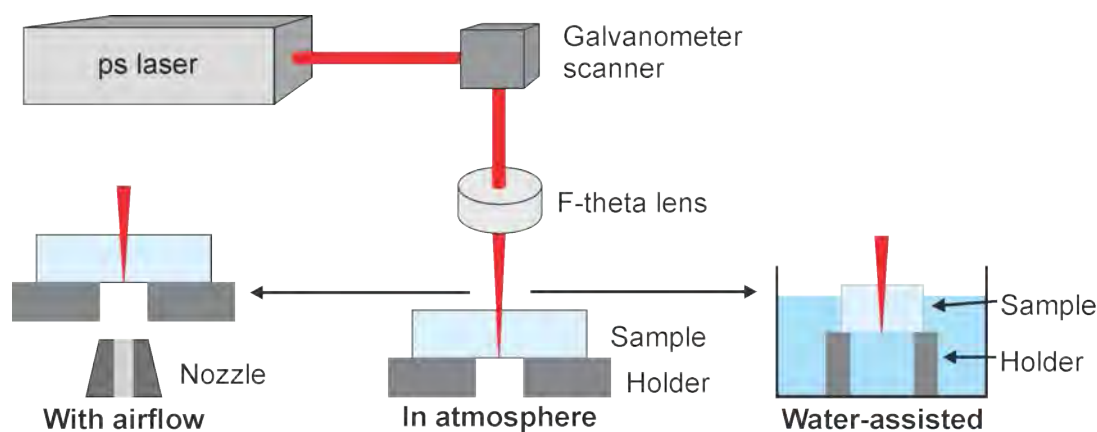


Fig. 1. Simplified experiment setup with different debris removal methods: compressed airflow, no additional removal, and partial immersion in water.

[1] L. A. Hof, J. A. Ziki, H. Jiang et al., Micro Hole Drilling on Glass Substrates-A Review, *Micromachines* (Basel), p. 53, Feb. 2017.

[2] X. Zhao and Y. C. Shin, Femtosecond laser drilling of high-aspect ratio microchannels in glass, *Appl Phys A Mater Sci Process*, pp. 713-719, Aug. 2011.

[3] J. Dudutis, G. Račiukaitis, E. Daknys et al., Quality and flexural strength of laser-cut glass: classical top-down ablation versus water-assisted and bottom-up machining, *Opt. Express*, Jan. 2022.

INVESTIGATION OF AN OPTICAL PARAMETRIC AMPLIFIER WITH SUBNANOSECOND PULSES BASED ON FAN-OUT GRATING DESIGN MgO:PPLN CRYSTAL USING CONTINUUM SEED

Simona Armalytė¹, Jonas Banys¹, Julius Vengelis¹

¹Laser Research Center, Faculty of Physics, Vilnius University, Saulėtekio av. 10, Vilnius, Lithuania
 simona.armalyte@ff.stud.vu.lt

Parametric light generators (OPGs) and amplifiers (OPAs) are convenient and simple devices to obtain a wide spectral tuning in the IR region. They are therefore widely used in applications such as spectroscopy, gas detectors, etc. [1, 2]. Some applications require laser radiation of subnanosecond (300 ps - 1 ns) durations at tunable frequencies, but such parametric frequency converters in particular are relatively poorly realized, due to the difficulties caused by the laser-induced damage threshold to the nonlinear medium (LIDT), which, for most materials, is lower than the threshold for parametric generation with subnanosecond pulses. Due to the high nonlinearity coefficient, OPG and OPA are often based on quasi-phase matching crystals, i.e. periodically poled crystals. The fan-out grating design used in this work is characterized by the fact that the grating periods change uniformly over the entire length of the crystal, which enables obtaining a uniform tuning of the wavelengths simply by translating the crystal. This tuning method is superior to temperature tuning because it is simpler, faster, and more reliable.

The aim of this study was to construct an optical parametric amplifier with a 25 mm in length fan-out grating design MgO:PPLN crystal, whose grating period changes continuously from 27,5 μm to 31,6 μm . The crystal was pumped by passively Q-switched Nd:YAG MOPA microlaser generating 1064 nm subnanosecond pulses with an average power of 1 W, a pulse duration of 520 ps, and a repetition rate of 1 kHz. As a seed, we used a continuum generated by photonic crystal fiber. The optimal pumping conditions were estimated and the energy and spectral characteristics of the device were investigated. A maximum conversion efficiency of 45% for OPG and 51% for OPA in the degeneracy region was achieved (Fig. 1). It was found that with such grating periods of the MgO:PPLN fan-out grating design crystal and in the cases of both OPG and OPA, we can obtain uniform wavelength tuning in the range of 1420 nm to 2128 nm (Fig. 2) at a crystal temperature of 200 $^{\circ}\text{C}$.

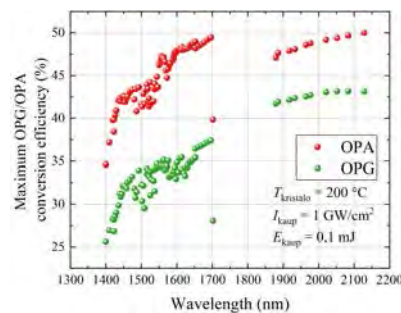


Fig. 1. The comparison of OPG and OPA conversion efficiencies

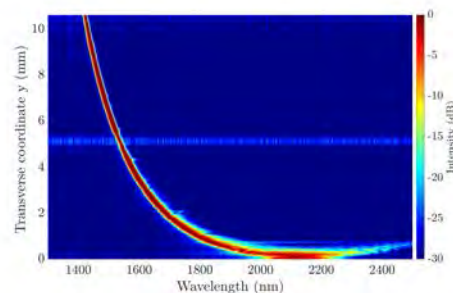


Fig. 2. OPG and OPA wavelength tuning range

- [1] G. Baxter, M. Payne, B. Austin, C. Holloway, J. Haub, Y. He, A. Milce, J. Nibler, B. Orr, Spectroscopic diagnostics of chemical processes: Applications of tunable optical parametric oscillators, *Appl. Phys. B* 71(5), 651-663 (2000).
 [2] S. Lambert-Girard, M. Allard, M. Piché ir F. Babin, Broadband and tunable optical parametric generator for remote detection of gas molecules in the short and mid-infrared, *Appl. Opt.* 54, 2594-2605 (2015).

NANO-PROCESSING BY FS-UV INTERFERENCE METHOD

Tadas Latvys¹, Darius Gailevičius¹, Dominyka Stonytė¹, Domas Paipulas¹, Vytautas Jukna¹

¹Laser Research Center, Faculty of Physics, Vilnius University, Vilnius LT-10223, Lithuania
tadas.latvys@ff.stud.vu.lt

Today material processing by ultrashort pulses in UV spectral domain allows us to achieve high precision and efficiency. However, in large-area surface patterning optical lithographic techniques [1] are still being used despite having limited selection of usable materials and requiring multiple processing steps, facilities and machines. Therefore, there is a demand for alternative methods such as fs-UV interference processing. This method can produce large areas of periodically arranged structures with a period close to the wavelength of the used fs-pulses. This ensures accurate and fast surface patterning without requiring additional preparation or post-processing.

Fs-UV interference method has a wide range of potential applications in photonics, nanotechnology, or biomedicine. Specifically, it can be utilized to produce functional surfaces that exhibit antireflective [2], antibacterial [3], or hydrophobic [4] properties.

In this presentation, we present our results for two-beam interference patterning using the third (343 nm) harmonic of an amplified Yb:KGW laser system, providing pulse durations of 240 fs. To achieve interference on the sample, a prototype machining head (Talbot interferometer) was constructed (Fig. 1a). This setup has many drawbacks when used with ultrashort pulses [5], thus a Kostenbauder matrix formalism [6] was employed to calculate optimal parameters for the alignment of the pulses. Consequently, homogeneous gratings with nanoscale feature sizes were fabricated on a silicon surface with periods of $\Lambda = 800$ nm (Fig. 1b). In addition, etching the gratings in a 1% KOH solution resulted in a 10-fold increase in structure height.

In summary, our study showcases the direct processing of centimeter-scale areas through an fs-UV interference method. The Talbot approach not only ensures ease of alignment and precise period control but also offers the advantage of having a compact configuration. Importantly, material removal can be controlled with nanoscale precision.

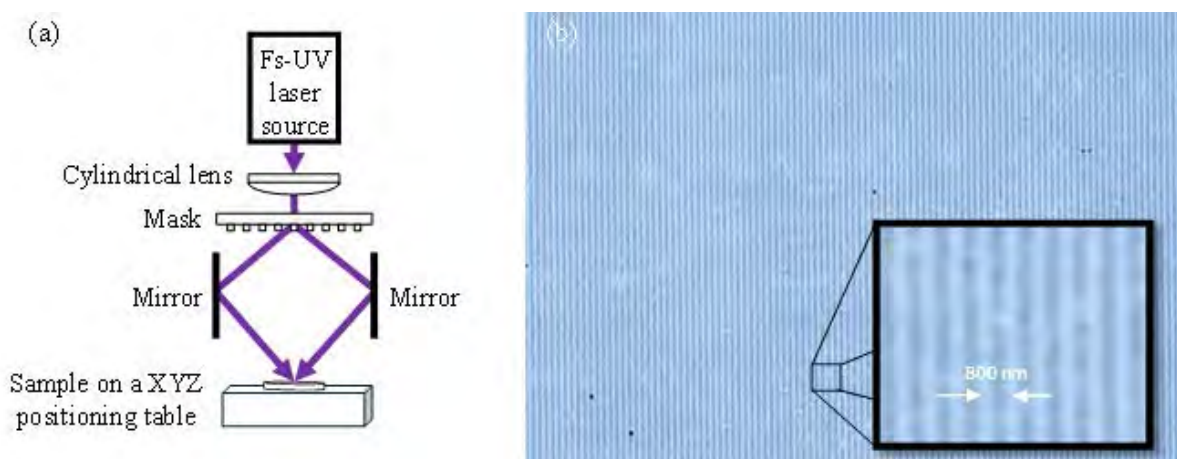


Fig. 1. (a) Talbot interferometer setup, (b) periodically patterned Si surface.

OPTIMIZING PHOTOVOLTAIC DEVICES THROUGH GALVANOMETRIC MIRROR-ASSISTED LASER ANNEALING

Gustas Mickevičius¹, Miglė Lenkauskaitė¹, Rokas Kondrotas¹, Marius Franckevičius¹

¹Center for Physical Sciences and Technology
gustas.mickevicius@ff.stud.vu.lt

Laser annealing is a promising method to boost photovoltaic device performance by affecting semiconductor material properties. The use of lasers provides precise control over energy delivery and spatial distribution, allowing modifying materials characteristics locally. Achieving uniform effects over the surface requires a nuanced approach, as there is no one-size-fits-all method. In this work, we used a nanosecond pulsed 532 nm wavelength laser. We explored two different strategies to anneal samples of antimony selenide. The first approach was to heat sample using a single laser beam and by changing filters, exposure time and frequency of the laser to simulate different annealing conditions. Another strategy was to focus laser beam and scan on the designated area on the sample. The scanning of the laser beam was realized using galvanometric mirrors. Various mirror control and laser parameters were tested to achieve uniformly annealed areas on the sample. To get the results, we went through several important steps. We started with using a single large laser beam, which posed challenges with non-uniform absorption within a 700-micrometer diameter for annealing our photovoltaic samples. Seeking improvement, we experimented with scanning and introduced a diaphragm and galvanometric mirrors. However, the scanning beams size led to uneven surface coverage. Recognizing the need for uniformly affected areas, we refined our approach by using a long focal length lens which contracted the beam's size to 160 micrometres and adjusting the parameters of the mirrors to achieve uniform coverage. This method allows for precise adjustments of the mirrors to accommodate variations in material or laser parameters, ensuring consistent and uniform impact on laser-irradiated surface areas. Importantly, the transition from a single beam to scanning resulted in an increase of affected area, expanding from 1 mm² to 25 mm². Nevertheless, our final setup encountered challenges, including uncovered areas caused by synchronized frequencies in laser and scanning settings, along with variations in thermal excitations that affected the scanning path width. However, through galvanometric mirror parameter adjustments, we effectively solved these problems, identifying optimal parameters for accurate scanning. The visual evidence from images (Fig. 1, a)) depicting uniform coverage solidifies the success of our approach. In conclusion, our laser annealing system achieves uniform coverage on samples, enhancing photovoltaic device performance. Moreover, it presents a potential alternative to moving-stage laser annealing systems. Its adaptability allows for the use of different lasers and samples, offering versatility and potential for optimizing material properties.

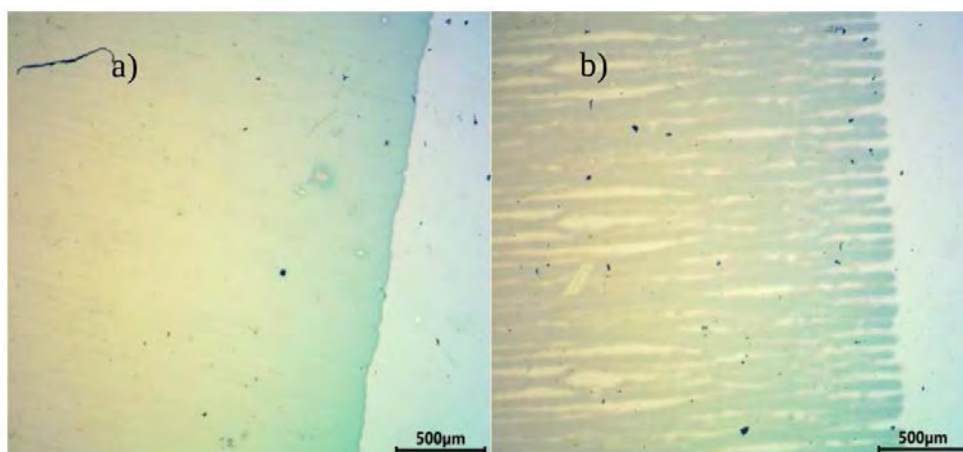


Fig. 1. Optical pictures of annealed samples. a) uniformly covered. b) inconsistently covered.

SUMMARY OF 2D PHOTONIC CRYSTALS

Andrius Zinkevičius¹, Ignas Lukošius²

¹Vilnius University

andrius.zinkevicius@ff.stud.vu.lt

Photonic crystals (PhCs) are periodic structures with lattice spacing which is big enough to diffract light. Under the right conditions light of certain wavelengths destructively interferes, forming a complete band gap. In this case any incident light of that wavelength completely reflects from the surface [1]. This property of PhCs makes it possible to control the propagation of light. Such photonic devices are used to make waveguides (WGs) with different characteristics - power beam and polarization splitters [2], polarization – maintaining WGs [3], to name a few. PhC logic gates are used to make optical processors [4], which consume exceptionally small amounts of energy. The characteristics of PhCs can be used for broader applications, such as sensing devices [5,6], as well as for more specific fields of interest (to improve the efficiency of thermophotovoltaic solar cells with PhC based absorbers [7]) which shows the potential for many undiscovered implementations. In this paper we summarize the characteristics of lattices in 2D spatial domain. 2D structures are especially common in scientific applications as the 1D lattices PhCs lack a spatial dispersion control and 3D PhCs are harder to fabricate [8]. Plane wave expansion method (PWEM) [9] is used to numerically calculate the band structures of those 2D lattices. In this work we use PWEM numerical algorithm to calculate dispersion properties of such structures. We also demonstrate the effects of spatial dispersion control near the photonic band edge, where light either propagates in such medium through means of self-collimation or negative refraction.

-
- [1] Cersonsky, R.K., Antonaglia, J., Dice, B.D. et al. The diversity of three-dimensional photonic crystals. *Nat Commun* 12, 2543 (2021).
- [2] Tao Liu, A. R. Zakharian, M. Fallahi, J. V. Moloney and M. Mansuripur, "Design of a compact photonic-crystal-based polarizing beam splitter," in *IEEE Photonics Technology Letters*, vol. 17, no. 7, pp. 1435-1437, July 2005.
- [3] Asmar Aming, Muhammad Uthman, Ratchapak Chitaree, Waleed Mohammed, and B. M. Azizur Rahman, "Design and Characterization of Porous Core Polarization Maintaining Photonic Crystal Fiber for THz Guidance," *J. Lightwave Technol.* 34, 5583-5590 (2016).
- [4] Kuramochi, E., Nozaki, K., Shinya, A. et al. Large-scale integration of wavelength-addressable all-optical memories on a photonic crystal chip. *Nature Photon* 8, 474-481 (2014).
- [5] Pacholski, C. Photonic Crystal Sensors Based on Porous Silicon. *Sensors* 2013, 13, 4694-4713.
- [6] Y. Liu and H. W. M. Salemink, "Photonic crystal-based all-optical on-chip sensor," *Opt. Express* 20, 19912-19920 (2012).
- [7] M. Grande et al., "Absorption and Losses in One-Dimensional Photonic-Crystal-Based Absorbers Incorporating Graphene," in *IEEE Photonics Journal*, vol. 6, no. 6, pp. 1-8, Dec. 2014.
- [8] A. Yadav, A. Kaushik, Y.K. Mishra, V. Agrawal, A. Ahmadivand, K. Maliutina, Y. Liu, Z. Ouyang, W. Dong, G.J. Cheng, Fabrication of 3D polymeric photonic arrays and related applications, *Materials Today Chemistry*, Volume 15, 2020.
- [9] Raymond C. Rumpf and Javier J. Pazos, "Optimization of planar self-collimating photonic crystals," *J. Opt. Soc. Am. A* 30, 1297-1304 (2013).

SPECTRAL BROADENING AND POST-COMPRESSION OF FEMTOSECOND YB:KGW OSCILLATOR PULSES

Titas Tamošauskas¹, Vaida Marčiulionytė¹, Jonas Banys¹, Gintaras Tamošauskas¹, Julius Vengelis¹, Audrius Dubietis¹

¹Laser Research Center, Faculty of Physics, Vilnius University, Saulėtekio av. 10, LT-10223 Vilnius, Lithuania
titas.tamosauskas@ff.stud.vu.lt

In the field of ultrafast optics, femtosecond pulsed lasers are pivotal due to their extensive applications in science and technology. The quest for shorter laser pulses is driven by the need for higher temporal resolution, greater peak power and precision in applications. Nonlinear phenomena such as: spectral broadening and post-compression are commonly used to achieve shorter pulses. Typically, multi-pass configurations are employed to achieve significant spectral broadening leading to losses and large delays with respect to the laser output [1]. Benefits of such complex systems are: high compression ratio and preserved beam quality. Commercial systems emerged recently as well [2].

We investigate prospects of compression with femtosecond Yb:KGW 76 MHz laser oscillator [3] low energy 210 nJ pulse with relatively low losses. Two setups for compression investigated, intermediate single-pass and double-pass through a nonlinear material – ZnS, possessing large nonlinearity when compared to most optical materials. First, self-phase modulation is achieved using a very high intensity laser beam and a nonlinear material so that the spectrum is broadened. Later post-compression is applied using Gires-Tournois mirrors with negative group velocity dispersion to achieve pulses that are shorter and have higher peak power than the original. The resulting and primary spectrum of the laser oscillator are shown in figure 1. This study shows that ZnS, low bandgap optical material, can be successfully used in the high average power multi-pass setup for spectrum broadening without damage.

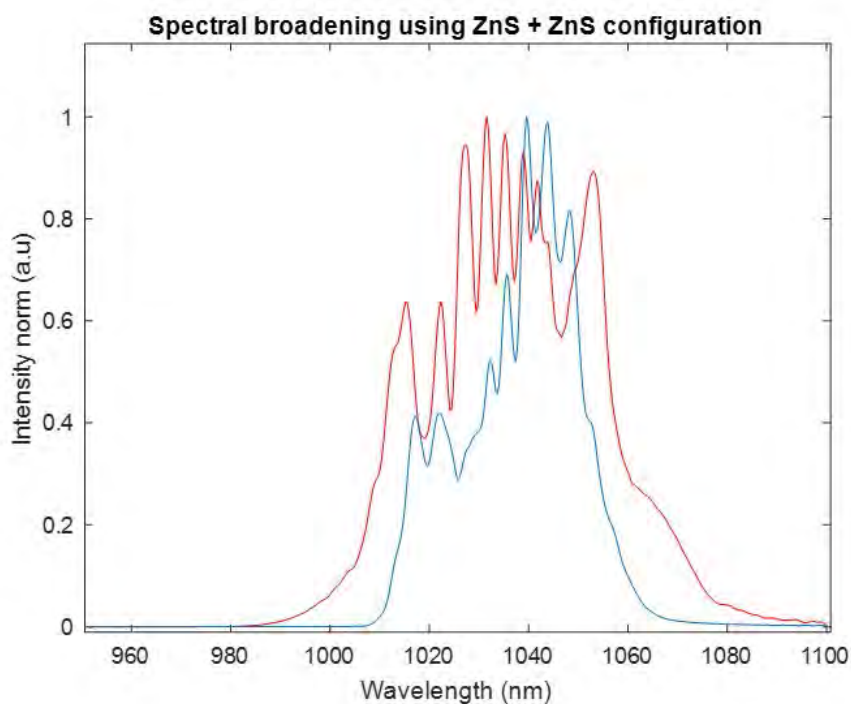


Fig. 1. The original spectrum of the femtosecond oscillator (blue) and the spectrum broadened in the ZnS + ZnS configuration (red).

[1] Victor Hariton, Kilian Fritsch, Kevin Schwarz, Nazar Kovalenko, Gonçalo Figueira, Gunnar Arisholm, and Oleg Pronin,

[2] n2-photonics GmbH, add-on modules (MIKSs) to spectrally broaden and temporally shorten pulses: <https://www.n2-photonics.de/products>

[3] Jonas Banys, Julius Vengelis, „Efficient single pass and double pass pre chirp managed Yb doped rod type fiber amplifiers using Gires Tournois interferometric mirrors“, *Optik International Journal for Light and Electron Optics*, (2022)

FEMTOSECOND ULTRAVIOLET LASER MODIFICATION OF GALLIUM NITRIDE THIN-FILM COATINGS

Paulius Zakarauskas¹, Dominyka Stonytė¹, Arūnas Kadys², Darius Gailevičius¹, Domas Paipulas¹

¹Laser Research Center, Faculty of Physics, Vilnius University, Sauletekio av. 10, LT-10223 Vilnius, Lithuania

²Center for Physical Sciences and Technology, Saulėtekio av. 3, LT-10257 Vilnius, Lithuania

paulius.zakarauskass@gmail.com

Gallium nitride has recently stood out as a material that has a lot of useful properties for electronic and optoelectronic appliances, such as wide band-gap (3,4 eV), high heat capacity, thermal conductivity, break-down voltage, electron mobility and high quantum efficiencies [1]. These properties make gallium nitride a valuable material in developing light emitting diodes (LEDs) [2], field effect transistors (FETs) [3], high-temperature devices [4] and many others. To manufacture these devices from gallium nitride a high-quality processing is needed.

Recent advancements in the development of ultrashort pulse lasers allow high-quality micro-processing of materials. It is well known that the use of ultrashort laser pulses, compared to longer ones, give more control in the ablation process and also increase the resolution of micro-processing, due to reduction of heat-affected zones (HAZ) because the temporal length of the pulse is lower than the length of thermal diffusion. Most approaches use femtosecond lasers with wavelengths longer than ultraviolet [5]. However, shorter wavelengths in UV spectral range could benefit in decreasing heat-affected zones due to linear (one photon) absorption and smaller focus point, because it is directionally proportional to the wavelength. This technique was tested with the use of longer nanosecond pulses of excimer UV lasers [6]. Nevertheless, laser processing using UV femtosecond laser pulses has seldom been studied.

In this study we directly ablate thin-film undoped gallium nitride using femtosecond ultraviolet laser pulses [257 nm, 100 kHz, 240 fs] with different pulse energy and pulse overlapping. The topographies of ablated regions were measured with a profilometer (repeatability $\sigma_{n-1} = 12$ nm). The ablated structures were characterized using three variables: ablation depth, ablation efficiency and average modified surface roughness S_a , calculated according to ISO 25178-3:2012. Our results indicate that the use of femtosecond UV laser pulses enable high resolution and high-quality ablation with minimal heat affected zones (HAZ) while processing wide band-gap materials such as gallium nitride. We demonstrate the efficient ablation with average surface roughness S_a values in the frame of [16 nm - 86 nm] without any post-processing.

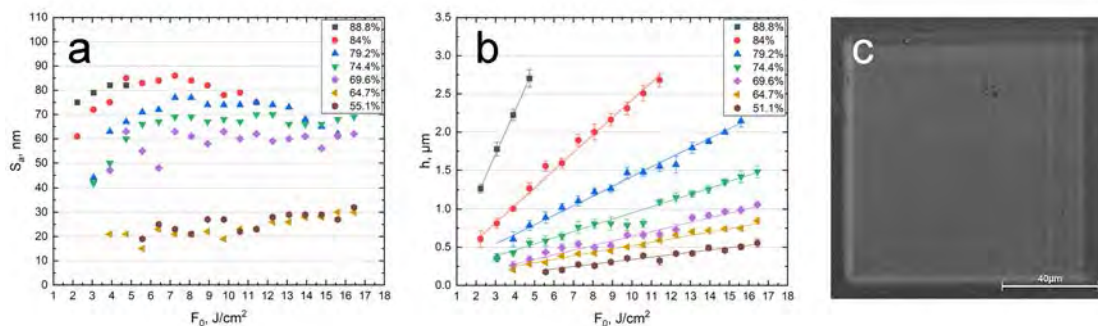


Fig. 1. Results of uGaN ablation using femtosecond UV pulses: (a) experimental data of average surface roughness of ablated areas as a function of pulse energy fluence, (b) experimental data of ablation depth as a function of pulse energy fluence, (c) SEM image of laser ablated area (PO = 79,2 %, $F_0 = 15,6 J/cm^2$, $S_a = 62$ nm).

- [1] L.K. Nolasco, G.F.B. Almeida, T. Voss, C.R. Mendonça, Femtosecond laser micromachining of GaN using different wavelengths from near-infrared to ultraviolet, *J. Alloys Compd.* 877, 160259 (2021).
- [2] S. Nakamura, T. Mukai, and M. Senoh, Candela-class high-brightness InGaN/AlGaN double-heterostructure blue-light-emitting diodes, *Appl. Phys. Lett.* 64 (13), 1687–1689 (1994).
- [3] H. W. Huang, C. C. Kao, J. T. Chu, H. C. Kuo, S. C. Wang and C. C. Yu, Improvement of InGaN-GaN light-emitting diode performance with a nano-roughened p-GaN surface, *IEEE Photon. Technol. Lett.* 17(5), 983-985 (2005).
- [4] J. Bonse, A. Rosenfeld, and J. Krüger, Implications of transient changes of optical and surface properties of solids during femtosecond laser pulse irradiation to the formation of laser-induced periodic surface structures, *Appl. Surf. Sci.* 257(12), 5420-5423 (2011).
- [5] T Kim, H.S Kim, M Hetterich, D Jones, J.M Girkin, E Bente, and M.D Dawson, Femtosecond laser machining of gallium nitride, *MSEB* 82(1–3), 262-264 (2001).
- [6] Yu-Tang Dai, Gang Xu, and Xin-Lin Tong, Deep UV laser etching of GaN epilayers grown on sapphire substrate, *J. Mater. Process. Technol.* 212(2), 492-496 (2012).

THZ METALENSES WITH DIFFERENT SPLIT RING RESONATOR GEOMETRIES

Karolis Redeckas^{1,2}, Kasparas Stanaitis^{1,2}, Vladislavas Čižas^{1,2}, Linas Minkevičius^{1,2}

¹Center for Physical Sciences and Technology

²Vilnius University

karolis.redeckas@ftmc.lt

Terahertz (THz) radiation, falling within the millimeter-micrometer wavelength range (0.1 THz - 10 THz) [1], represents a low-power, non-destructive form of electromagnetic waves. This unique region necessitates a combination of electronics and photonics methods for both radiation emission and detection [2]. THz radiation possesses a notable advantage in penetrating various dielectric objects like paper, rubber, and textiles. It has found applications in security, production quality control, imaging, and bio-fabric analysis [3]. Traditionally, these applications relied on costly and bulky lenses or mirrors for beam propagation control. However, metalenses, a combination of diffractive zoneplate lenses with metaatoms, offer a solution by utilizing smaller-than-wavelength geometrical shapes, specifically split ring resonators, for phase delay and polarization rotation [4].

In this research different sizes CSRR were used as phase delaying metaatoms for periodically changing subzones in Fresnel diffractive lens designs. Metaatoms shapes were precisely chosen to have delay difference equal to $\pi/2$ for lenses with 4 subzones. Traditional and Non-paraxial adjusted lens models created for 250 GHz frequency and simulations performed applying FDTD method.

Results show very similar focusing efficiency and performance regarding size and aberration adjustments, with the best performing ($R_{1min} = 140\mu m, R_{1max} = 196\mu m, R_{2min} = 110\mu m, R_{2max} = 154\mu m, \theta = 110^\circ$) lens. Non-paraxial design demonstrates higher electric field at focal point. The metalens also induces polarization rotation based on CSRR orientation.

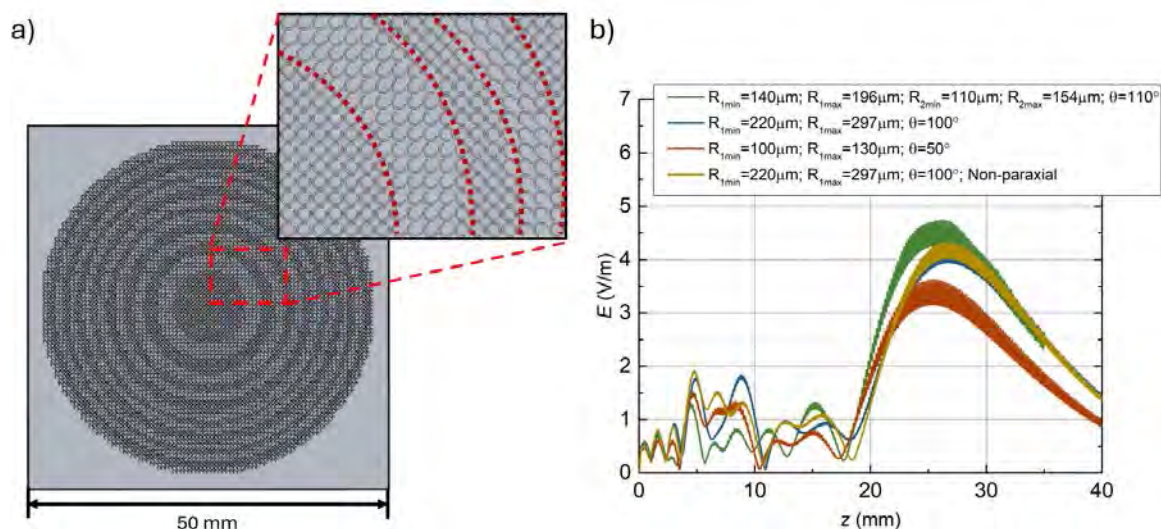


Fig. 1. Metalens model a) and electric field distribution along optical axis of metalenses with different metaatoms geometries b).

Research was funded by Lithuanian Science Council, project number: S-ST-23-190

[1] Nagatsuma, T. (2011). Terahertz technologies: present and future. IEICE Electronics Express, 8, 1127-1142.

[2] Leitenstorfer, A., et al. (2023). The 2023 terahertz science and technology roadmap. Journal of Physics D: Applied Physics, 56(22), 223001

[3] Mittleman, D. M. (2018). Twenty years of terahertz imaging. Optics Express, 26, 9417-9431.

[4] Ivaškevičiūtė-Povilauskienė, R., et al. (2023). Flexible terahertz optics: light beam profile engineering via C-shaped metallic metasurface, Front. Phys.

HOMODYNE IMAGING SET UP OPTIMIZATION: BEAM ENGINEERING OF ILLUMINATION AND COLLECTION USING HIPS BASED LENSES

Kasparas Stanaitis^{1,2}, Karolis Redekas^{1,2}, Augustė Bielevičiūtė¹, Linas Minkevičius^{1,2}

¹Center for Physical Sciences and Technology (FTMC)

²Vilnius University

kasparas.stanaitis@ftmc.lt

Optical imaging systems are convenient for commercial and scientific interests, finding applications in medicine, security, material analysis, and quality control[1]. While these systems are usually associated with using high-energy radiation (X-ray), leading to obvious disadvantages like ionizing effects and high costs. Terahertz imaging is a perfect solution for imaging system safety since it employs non destructive radiation, which can still penetrate most dielectrics. To achieve even better results interference based coherent imaging (homodyne detection) can be employed.

The objective of this study is to analyze optical component arrangement in THz homodyne imaging systems, with a focus on Gaussian and Bessel axicon lenses [Fig. 1]. These lenses were systematically altered in positions for the imaging system. Modulation transfer function (MTF) was evaluated along optical axis to obtain information about resolution of the imaging system. Contrast information was then utilized in order to obtain best possible conditions for highest resolution imaging on low absorption objects such as thin paper layers or even graphene.

The coherent imaging approach proved to be more effective, since little changes in absorption were depicted more accurately. Obtained results lead to conclusion, that lens types and positions matter in context of terahertz imaging. This research can be further expanded by using even more different types and compositions of lenses, employing non-paraxial optics and forming structured light[2].

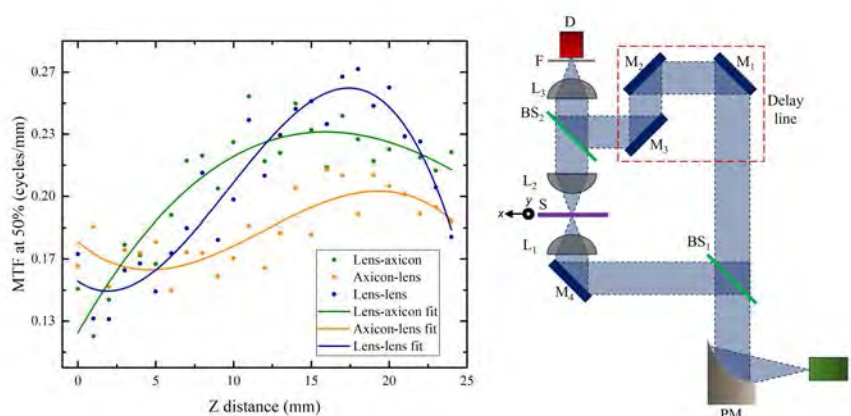


Fig. 1. Left - Obtained modulation transfer function values along optical axis with different compositions of Gaussian and Bessel lenses, Right - homodyne imaging setup (E - emitter, D - detector, PM, M - mirrors, L - lenses, BS - beam splitter, S - sample).

This research has received funding from the Research Council of Lithuania (LMTLT), project No [S-ST-23-205]

[1] Valušis, G., et al. (2021). Roadmap of terahertz imaging 2021. *Sensors*, 21(12), 4092.

[2] Ivaškevičiūtė-Povilauskienė, R., et al. (2022). Terahertz structured light: Nonparaxial Airy imaging using silicon diffractive optics. *Light: Science Applications*, 11(1), 326.

MICROSTRUCTURING OF HIGH BANDGAP MATERIALS USING FEMTOSECOND UV LASER PULSES FOR MULTI-LEVEL DIFFRACTIVE OPTICAL ELEMENTS

Vitalija Smirnovaitė¹, Dominyka Stonytė², Domas Paipulas³

¹Laser Research Center, Faculty of Physics, Vilnius University, Vilnius LT-10223, Lithuania
vitalija.smirnovaite@ff.stud.vu.lt

Micro-structuring of materials is one of the most widely applied fields in science and industry. The main objective of surface structuring is to tailor the properties of the outer layer of a material to meet specific functional, aesthetic, or performance requirements [1]. The complex interplay between laser characteristics and dielectric materials provides insight into how specific laser parameters shape the structural and functional properties of these materials. The diffraction limited focus point size is directly proportional to the wavelength, so a smaller spot size leads to the precision. Thanks to the short UV wavelength, it is possible to ablate materials with high precision and obtain a smooth surface morphology [2]. When the pulse is short, the laser energy is very intense on the target, resulting in a cleaner, more precise ablation process and ability for highly accurate control of the depth of the infringement [3].

The precision and smoothness is a must for the fabrication of DOE-phase micro structured elements. One of the most commonly used diffractive elements is the Fresnel zone plate, but due to the limited resolution and the size of the possible structure, researchers have developed a new diffractive element, the photon sieve [4]. It consists of a series of pinholes of different depths spread over the entire Fresnel zone plate. Photon sieves can be used to obtain a sharper focus, which is not dependent on the width of the zone area but on the dimensions of the pinholes [5].

This article describes the influence of laser parameters on the micro-structuring of fused quartz by single pulses of "PHAROS" femtosecond laser radiation. The results are analyzed, the dependences of depth, width and volume on the pulse energy are investigated and the most suitable parameters for fabricating photon sieves are selected. Five photon sieves of different periods ($T = 4, 5, 6, 8$ and $10\mu\text{m}$) have been created with a focal length of 9 mm .

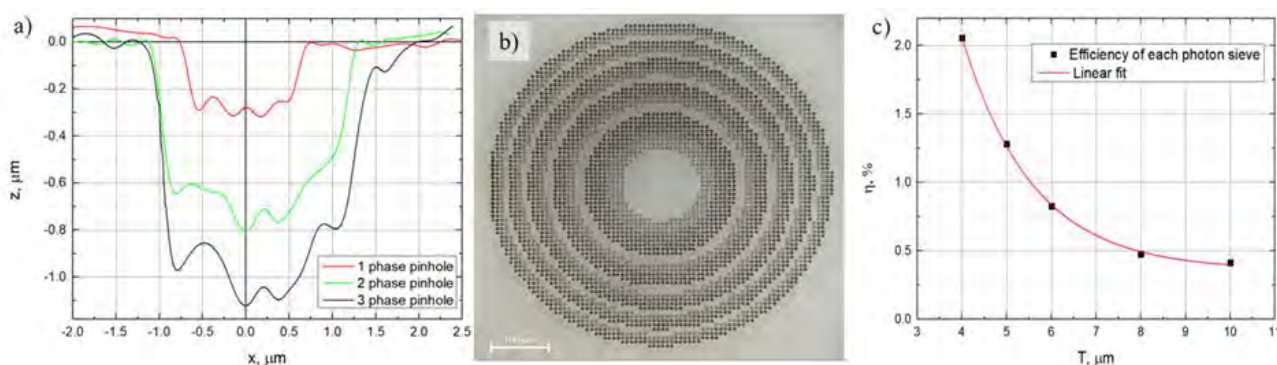


Fig. 1. a) the depth of pinholes illustrated by a graph, b) Photon sieve image by profilometer, c) Efficiency of different periods photon sieves.

The highest efficiency obtained was for a $T = 4\mu\text{m}$ period photon sieve, which was 2.06%. Compared to the studies using the same elemental design method, the efficiency value is 1.75 times higher ($\eta = 1,18\%$ [5]). Also, this efficiency is achieved with a focal length of 9 mm , that is 17 times smaller ($f = 150\text{mm}$ [5]).

- [1] Mangirdas Malinauskas, Albertas Žukauskas, Satoshi Hasegawa, Yoshio Hayasaki, Vyngantas Mizeikis, Ričardas Buividas, and Saulius Juodkzis. Ultrafast laser processing of materials: From science to industry, 8 2016.
- [2] J Zhang, K Sugioka, and K Midorikawa. Laser-induced plasma-assisted ablation of fused quartz using the fourth harmonic of a nd+:yag laser, 1998.
- [3] P. Balling and J. Schou. Femtosecond-laser ablation dynamics of dielectrics: Basics and applications for thin films. Reports on Progress in Physics, 76, 3 201
- [4] Wenbo Jiang, Song Hu, Lixin Zhao, Wei Yan, and Yong Yang. Design and application of phase photon sieve. Optik, 121:637–640, 4 2010.
- [5] Matthew N. Julian, David G. MacDonnell, and Mool C. Gupta. Fabrication of photon sieves by laser ablation and optical properties. Optics Express, 25:31528, 12 2017.

FOUR PASS DUAL CELL SBS-PCM AMPLIFIER

Domantas Klumbys¹, Paulius Mackonis¹, Augustė Černekytė¹, Augustinas Petrulėnas¹, Aleksei M Rodin¹

¹Solid State Laser Laboratory, Center for Physical Sciences and Technology, 231 Savanoriu Ave, 02300 Vilnius, Lithuania
domantas.klumbys@ftmc.lt

Efficient methods for generating high-energy picosecond pulses with high beam quality are still a challenge, as conventional picosecond pulse generation methods have certain limitations. Q-switching prevents pulses shorter than $\sim 0,3$ ns [1], while mode locking limits the pulse energy, to the order of μJ [2]. We have recently demonstrated energy-scalable an efficient self-seeded single-cell SBS configuration [3] to achieve the ultimate >10 times pulse compression of ~ 1.1 ns pulses from a commercially available Nd:YAG mini-laser. The shortest pulse width of ~ 93 ps at the output of the double-pass SBS-PCM Nd:YAG amplifier with an improved beam quality and reduced beam pointing fluctuations by a factor of 4 compared to a conventional MOPA was achieved [3]. The goal of this study was to further investigate and upgrade it to a four-pass self-seeded dual-cell SBS-PCM configuration (Fig. 1). Particular attention was also paid to ensuring a high-quality output beam, as well as the long and short-term stability of the laser.

In our experiment Nd:YAG passively Q-switched mini-laser operating at a repetition rate of 10 Hz was used as the source of initial pulses with a duration of 1.05 ns and an energy of ~ 2 mJ at a wavelength of 1064 nm. After four-pass Nd:YAG amplifier without SBS-PCM, ~ 20 mJ of pulse energy was achieved with a signal pulse energy of $270 \mu\text{J}$. However, taking into account the equations of Frantz-Novick maximum energy of ~ 45 mJ can be achieved with a maximum seed energy of 2 mJ.

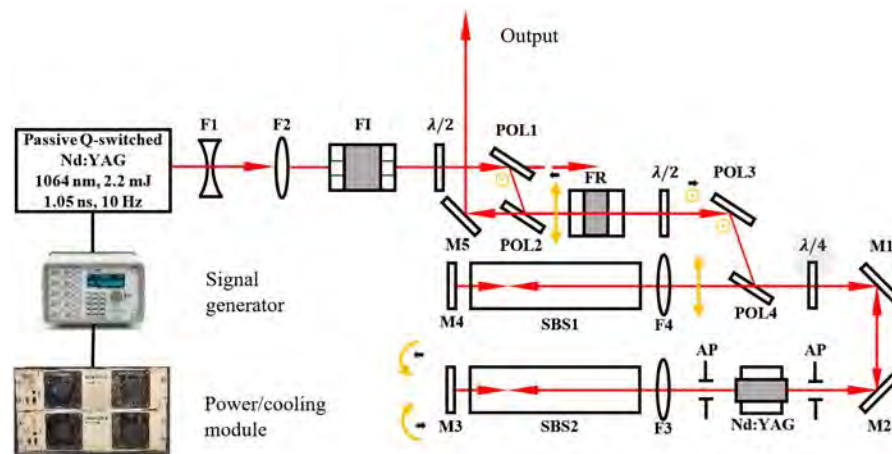


Fig. 1. SBS-PCM amplifier scheme: F1, F2 – beam expanding telescope; FI – Faraday isolator; FR – Faraday rotator; $\lambda/2$ – half-wave retardation plate; $\lambda/4$ – quarter-wave retardation plate; POL1, POL2, POL3, POL4 – thin-film polarizers; Nd:YAG – amplification module; M1, M2, M5 – 45° plane mirrors; M3, M4 – 0° plane mirrors; AP – aperture; SBS1, SBS2 –SBS cells.

Also, two SBS cells were implemented into this four-pass amplifier configuration to compress the pulse width and improve the beam quality. This self-seeded four-pass SBS-PCM amplifier layout lets us expand the laser beam diameter up to ~ 4 mm to avoid optical damage threshold and achieve up to ~ 40 mJ output pulse energy with Sub-90 ps pulse width.

To conclude high output pulse energy laser based on SBS-PCM in sub-90 ps scale with good beam quality was developed. It can be applied in dermatology as tattoo removal, as it has a good beam quality that prevents scar formation. Finally, this laser system also a good candidate for high-throughput interference patterning of a metal surface to impart water-repellent properties.

[1] B. Cole, L. Goldberg, A.D. Hays, High-efficiency $2 \mu\text{m}$ Tm:YAP Laser with a Compact Mechanical Q-Switch, *Opt. Lett.* 43, 170–173 (2018).

[2] U. Keller, K. J. Weingarten, F.X. Kartner, D. Kopf, B. Braun, I.D. Jung, R. Fluck, C. Honninger, N. Matuschek, J. A. der Au, Semiconductor saturable absorber mirrors (SESAM's) for femtosecond to nanosecond pulse generation in solid-state lasers. *IEEE J. Sel. Top. Quantum Electron* 2, 435–453 (1996).

[3] A.M. Rodin, A. Černekytė, P. Mackonis, A. Petrulėnas, Optimizing Self-Seeded Perfluorooctane SBS Compressor Configurations to Achieve 90 ps High-Energy Pulses, *Photonics* 10, 1060 (2023).

INVESTIGATION OF PUMP DEPLETION IN SUBNANOSECOND OPTICAL PARAMETRIC GENERATOR BASED ON PPLN CRYSTAL

Tomas Latvys¹, Viktorija Tamulienė¹

¹Laser Research Center, Faculty of Physics, Vilnius University, Lithuania
tomas.latvys@ff.stud.vu.lt

Optical parametric generators (OPGs) play important roles as tunable laser sources in the near- to mid-infrared region. Most commercially available OPGs operate within ultrashort (less than 100 ps) or long (more than 500 ps) pulse durations. The subnanosecond range between these values is largely unexploited due to the low optical damage threshold of the crystals. Several theoretical models have been proposed [1-3], however, none of them consider pump pulse being depleted as its energy is converted to signal and idler waves. The goal of this investigation was to create a model for optical parametric generation in periodically poled lithium niobate (PPLN) crystal, pumped by subnanosecond pulses when pump depletion is active.

Firstly, we utilised a quantum mechanical model [4,5] to define an effective length of quantum noise generation, then, we applied classical three wave interaction formulas and symmetrized split-step Fourier transform method to simulate the wave propagation in the PPLN crystal. This allowed us to compare the outputs of the parametric generation for different numbers of initial noise photons.

As seen in figure 1, the energy conversion curves match well if the propagation axis is moved by the effective length over which 1, 4 or 8 noise photons are generated. In each case, the curves saturate at $\sim 43\%$ for the signal and $\sim 19\%$ for the idler wave. The shapes of the temporal and spatial intensity profiles for different number of photons were also similar. In addition, by varying the crystal grating period Λ , we calculated the spectral widths (FWHM) for 6 gratings. Larger Λ values lead to spectral widths increase from 6.1 nm to 11.6 nm for the signal and 55.6 nm to 74.4 nm for the idler.

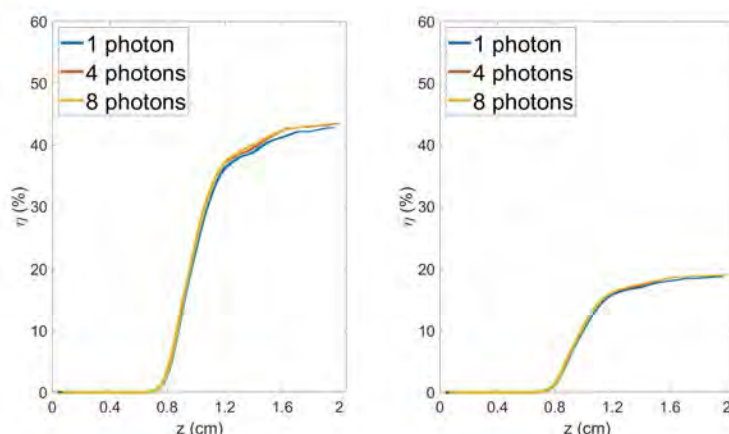


Fig. 1. Conversion efficiency η dependence on the position in the crystal z for signal (a) and idler (b) waves when z is moved by the effective length. Pump wavelength 1064 nm, pulse duration (FWHM) 100 ps, beam diameter ($1/e^2$) 40 μm , intensity $I_0 = 8.9 \text{ GW/cm}^2$, power $P = 27.6 \text{ mW}$.

To conclude, the developed model should provide a basis for understanding the optical parametric generation process in the subnanosecond regime and support the results of further research and development of more effective subnanosecond OPG systems under pump depletion.

-
- [1] L. Carrion and J. P. Girardeau-Montaut, Development of a simple model for optical parametric generation, *J. Opt. Soc. Am. B* 17, 78-83 (2000).
 [2] S. Acco, P. Blau, and A. Arie, Output power and spectrum of optical parametric generator in the superfluorescent regime, *Opt. Lett.* 33, 1264-1266 (2008).
 [3] B. Wang, X. Zou and F. Jing, Quantum analysis of optical parametric fluorescence in the optical parametric amplification process, *Journal of Optics* 17(5) (2015).
 [4] P. E. Powers, J. W. Haus, *Fundamentals of Nonlinear Optics* (2nd edition), Boca Raton: CRC press, 2017.
 [5] W. H. Louisell, A. Yariv, A. E. Siegman, Quantum Fluctuations and Noise in Parametric Processes. I., *Phys. Rev.* 124, 1646 (1961).

DEVELOPMENT OF INTEGRATION TECHNOLOGY OF DIFFRACTIVE STRUCTURES INTO PLASTIC SURFACE OF THE PRODUCTS

Erika Rajackaitė¹, Indrė Danisevičienė¹, Andrius Žutautas¹, Pranas Narmontas¹

¹Institute of Materials Science, Kaunas University of Technology, K. Baršausko St. 59, LT-51423 Kaunas, Lithuania
erika.rajackaite@ktu.lt

There are various applications where incorporating a hologram or a different light-diffracting surface relief pattern onto the exterior of a molded plastic component is advantageous to ensure the authentication of the product. It is important to develop techniques for widespread mass replicating plastic articles, with microstructures on their surfaces through injection or blow molding using a unitary mold piece in the shape of the object, with the hologram integrally formed on its inside surface. These microstructures can be formed through various techniques including attaching metal film replicas of holograms to the model, electrodeposition directly on a model with a surface relief pattern or forming the hologram directly on the model's surface using photosensitive materials [1-3].

In our research, diffractive elements were made from the creation of a unique graphic design to the final product – an original hologram with special security elements. The full hologram production cycle was used: mathematical modeling of diffractive structures, recording of the original hologram by dot-matrix technique, silver vacuum evaporation, electrochemical deposition of nickel master, and recombination. To achieve this, the design of the configuration of diffraction structures (arrangement of geometric figures, texts, symbols, selection of diffraction optical effects) and the investigation of the formed hologram were carried out, choosing the optimal constants of diffraction gratings, the parameters of the angular and spatial orientation of marks formed by diffraction means. Holograms have been thoroughly studied in terms of their morphology, structure, composition, mechanical and other properties. The overall goal is to improve the replication of surface relief holograms on molded plastic parts, offering authenticity and suitability of the production, which meets the global level, for its certified production.

[1] Dan Chen et al. *Advanced Materials* 2022, 34, 2200903.

[2] X. Wang et al. *Optics and Laser Technology* 2021, 135, 106687.

[3] Yangxi Fu et al. *Scientific Reports* 2020, 10, 22428.

DEVELOPMENT AND OPTIMIZATION OF A SUBNANOSECOND OPTICAL PARAMETRIC GENERATOR BASED ON COMBINED PPLN CRYSTAL STAGES

Augustė Stravinskaitė¹, Jonas Banys¹, Julius Vengelis¹

¹VU Laser Research Center, Saulėtekio al. 10, 10223 Vilnius
auguste.stravinskaite@ff.stud.vu.lt

Nowadays lasers have become necessary optical device capable of converting light from its natural incoherent state to coherent state. However, lasers have spectral limitations making wavelength extremely hard to change. In order to change the wavelength of laser radiation, parametric light generators are used which have a distinctive flexibility enabling them to provide radiation in an entire spectral range. Mostly optical parametric light generators are within ultrashort (less than 300 ps) and long (more than 1 ns) pulse durations, nevertheless due to certain physical limitations effective subnanosecond pulse (less than 1 ns and more than 300 ps) generators have not been constructed yet [1-3]. The aim of this work was to construct and investigate MgO:PPLN optical parametric generator pumped by second harmonic of subnanosecond Nd:YAG microlaser which will be used in the subsequent optical parametric amplifier system tuneable in the visible spectrum range. Additionally, investigate the latter crystal's properties. In this work the spectral and energy characteristics of the constructed OPG were measured. During optical parametric generation MgO:PPLN optical crystal gratings were from 6.85 μm to 8.65 μm and at 90°C difference frequency wave (idler wave) range was 1060 – 2160 nm, in near part of IR spectrum, and the signal was from 702 nm to 1060 nm, The maximum signal power at 1060 nm was 71 mW and the overall conversion efficiency at 1060 nm obtained 28.3%. The results of this work will be used for further development of an effective subnanosecond OPA system generating light in the visible spectrum range which as a seed source will use the investigated OPG system.

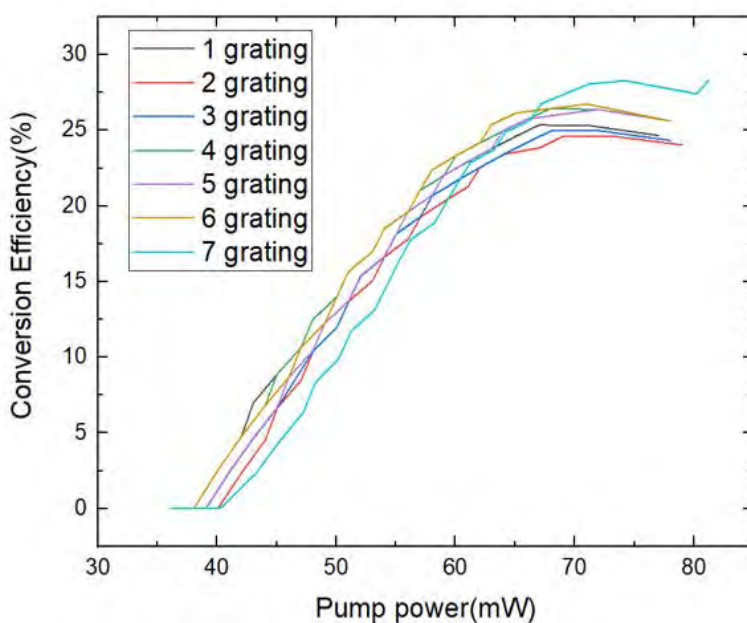


Fig. 1. Dependence of conversion efficiency on pump power for seven different wavelengths when the MgO:PPLN crystal temperature is 30 °C

- [1] M. H. Dunn and M. Ebrahimzadeh, Parametric Generation of Tunable Light from Continuous-Wave to Femtosecond Pulses, *Science* 286, 1513– 1518 (1999).
 [2] A. Dubietis, *Netiesinė optika*, (Publisher Vilnius University, Vilnius 2011).
 [3] R. W. Boyd, *Nonlinear Optics* ed. 3 (Academic press, New York 2008).

ACRYLIC RESINS FOR LASER 3D LITHOGRAPHY OF HIGHLY-POROUS MICROSTRUCTURES

Saulė Petrauskaitė¹, Ioanna Angeliki Petsi¹, Arūnas Čiburys¹, Antanas Butkus¹, Karolis Galvanauskas¹, Mangirdas Malinauskas¹

¹Laser Research Center, Faculty of Physics, Vilnius University, Lithuania
saule.petrauskaite@ff.stud.vu.lt

Inertial Confinement Fusion (ICF) is a potential way to produce energy by using high-power lasers to compress a fuel capsule. Low-density foams find common use as targets in experiments involving laser-plasma interactions because they can be converted into large-volume homogeneous plasmas. The major advantage of utilizing foam targets lies in their swift transition from a structured solid material to a nearly uniform plasma under intense radiation [1]. To produce such low-density foams lithography techniques are used. Particularly in this experiment, two photon polymerization that provides significant advantage in print resolution in creating three-dimensional microstructures [2].

In this research, our task is to create foams comprising exclusively of light elements for example hydrogen, carbon, and oxygen. For this purpose, we employ acrylic resins. Highly-porous microstructures play a crucial role in ICF, because they serve multiple functions, such as smooth the laser beam inhomogeneities, enhance the laser absorption as well as increase the ablation loading in a layered target configuration. However, a problem arises when using foams which contain only light elements as they tend to shrink during the two-photon polymerization process and structure development. Therefore extensive and varied research is necessary to identify the most suitable resin for low-density foams. This study focuses on investigating the optimal acrylic resin and photoinitiator for the development of low-density highly-porous microstructures, intended for application in ICF.

[1] Tikhonchuk, V. T., Gu, Y. J., Klimo, O., Limpouch, J., & Weber, S. Studies of laser-plasma interaction physics with low-density targets for direct-drive inertial confinement schemes. *Matter and Radiation at Extremes* 4.4 (2019): 1.5090965

[2] Wang, H., Zhang, W., Ladika, D., Yu, H., Gailevičius, D., Wang, H., Pan, C., Nair, P. N. S., Ke, Y., Mori, T., Chan, J. Y. E., Ruan, Q., Farsari, M., Malinauskas, M., Juodkasis, S., Gu, M., & Yang, J. K. W. Two-Photon Polymerization Lithography for optics and Photonics: Fundamentals, materials, technologies, and applications. *Advanced Functional Materials* 33.39 (2023): 202214211

LASER TWO-PHOTON PRINTING OF LOW-DENSITY 3D MICROSTRUCTURES OF ACRYLATE MATERIALS

Ioanna Angeliki Petsi^{1,2,3}, Saulė Petrauskaitė^{1,3}, Eulàlia Puig Vilardell^{3,4}, Antanas Butkus¹, Karolis Galvanauskas³, Darius Gailevičius³, Mangirdas Malinauskas³

¹Faculty of Physics, Vilnius University

²Faculty of Physics, University of Patras

³Laser research Center, Vilnius University, Vilnius LT-10223

⁴Erasmus Mundus joint Master Degree Europhotonics
aggpts@gmail.com

Inertial confinement fusion (ICF) is a nuclear fusion reaction that takes place by compressing and heating small pellets targets, that usually contain isotopes of hydrogen. Energy is disposed on the target's outer layer, which explodes and creates shock waves during the whole target. It is widely used for energy production. One of the main advantages of using foam targets for inertial confinement fusion reactions is that they can provide a low density with a high mechanical stiffness.[1] Additionally, parametric instabilities are sensitive to the plasma temperature and the density scale length, and those parameters are easily controlled using foams. Acrylate materials provide low density and it's the first time that woodpiles are fabricated with them using green light using two photon polymerization, which provides high precision in creating three-dimensional nanostructures, as foams.[2]

In this work, main goal is to investigate the fabrication parameters that provide high porosity woodpile foams with straight lines and the minimum possible shrink. These parameters are the writing speed, the average power and the development of the structures. The right material and geometry were investigated in order 3D woodpile foams of dimensions 1 mm in X and Y axis and 500 μm in Z axis to be fabricated using two photon lithography. The laser that was used for fabrication was Nanofactory with wavelength 517 nm and the objective was Mitutoyo 50x0.75 NA. The materials that were used are PETA (Pentaerythritol triacrylate), PETTA (Pentaerythritol tetraacrylate) and (PETA:PETTA)(60:40). Also, the suitable photoinitiator was also investigated. Irgacure 369 and Thioxanthen 9-one alfa were used in different concentrations.

This far, the best results came from structures of (PETA:PETTA)(60:40) and thioxanthen-9-one alfa 0.5%. The speed of the laser is 50 mm/s and the power 40 mW. The X and Y length is 1mm and the model's height 90 μm . In X and Y axis the porous size is 50 μm and in Z 30 μm . More experiments have to take place in order the height to reach the model's goal, which is 500 μm .

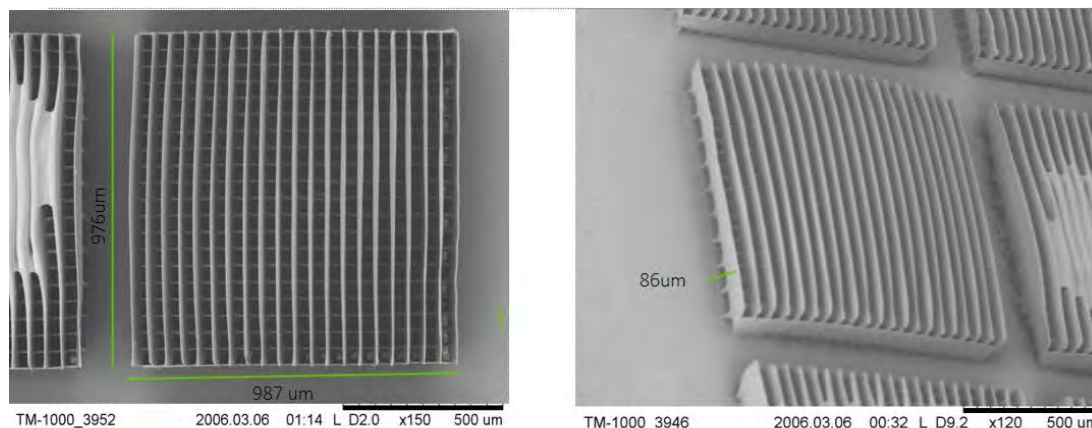


Fig. 1. Structures of (PETA:PETTA)(60:40) and thioxanthen-9-one alfa 0.5%. The speed of the laser is 50 mm/s and the power 40 mW. The X and Y length is 1 mm and the model's height 90 μm . In X and Y axis the porous size is 50 μm and in Z 30 μm .

- [1] V. Tikhonchuk, Y.J. Gu, O. Klimo, J. Limpouch, and S. Weber. Studies of laser plasma interaction physics with low-density targets for direct-drive inertial confinement schemes. *Matter and Radiation at Extremes*, 4(4):1–8, 2019.
- [2] A. Ostendorf and B.N. Chichkov. Two-photon polymerization: a new approach to micromachining. *Photonics spectra*, 40(10):72, 2006.

CREATING 3D MODELS OF NATURAL OBJECTS FROM 2D IMAGES USING MACHINE LEARNING

Andrius Jedik¹, Donatas Narbutis¹

¹Faculty of Physics, Vilnius University
andrius.jedik@ff.stud.vu.lt

This work explores approaches to the structure-from-motion problem [1] by employing well-established methods to reconstruct 3D objects from various selected yet limited 2D image sets. We utilize synthetically generated views (Fig. 1a) of textured meshes rendered with PyTorch3D [2] with variable image quality, as well as photographs of objects from the natural world (Fig. 1b).

Reconstructing 3D meshes from any given image set requires knowledge of the camera positions from which the shots were taken. Neither of the selected approaches to create datasets (synthetic or natural) did not involve a way of logging camera positions. To locate those positions, COLMAP package [3] was used to select intrinsic features of images, mark them as points within the pictures, cross-match them, and find a global solution (Fig. 1c). However, achieving a successful reconstruction of any given scene is not straightforward. Therefore, this work investigates the minimal quantity and quality of images required in various controlled synthetically generated datasets to ensure a robust reconstruction. Using the extracted camera view positions, we employ the Neural Radiance Field method (NeRF) to synthesize novel views and generate a point cloud much more detailed than that obtained by COLMAP.

The model used in this study is similar to the one presented in the original paper [4] introducing the concept of NeRFs. Such model utilizes a volumetric method to project rays out of the picture, interacting with pixel data, to reconstruct object

's density in 3D space. Synthetically generated models with recovered camera positions were employed to recreate 3D meshes (Fig. 1d) and explore the results achievable with limited quality and quantity image sets. Finally, natural world images were used to create acceptable quality meshes and 3D scene reconstructions.

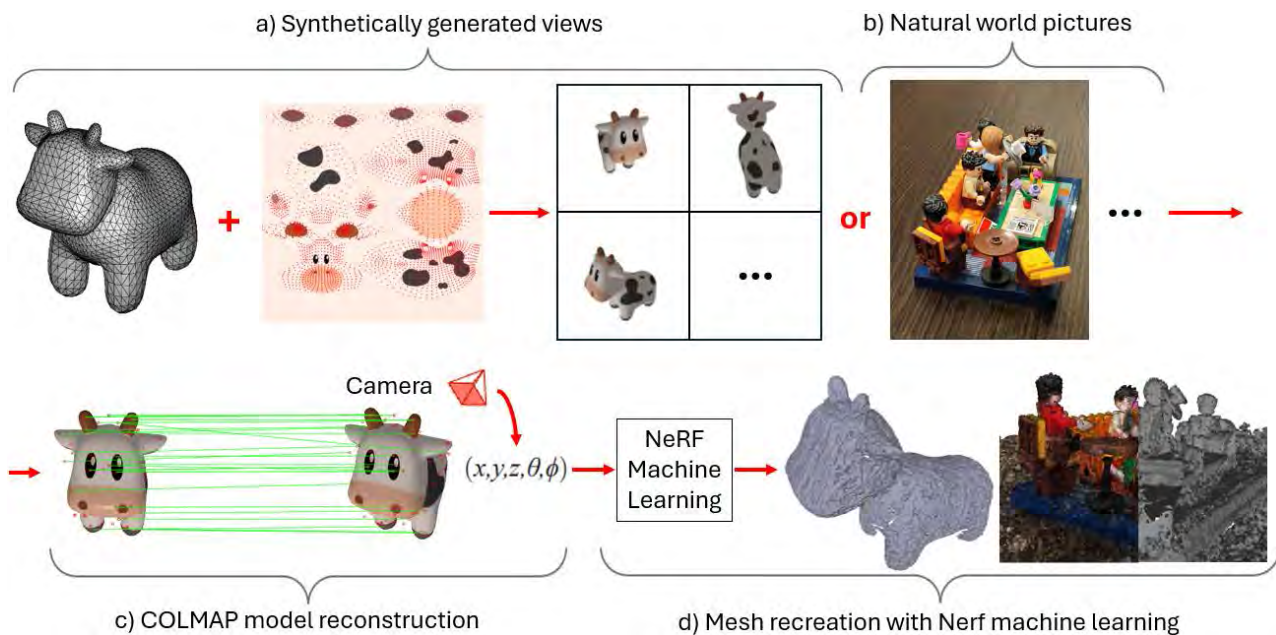


Fig. 1. Simplified workflow of 3D mesh reconstruction. a) Using Pytorch3D selected picture texture is transformed around mesh vertice map to create 3D object mesh and a set of views. b) Selected natural world object is photographed. c) Using COLMAP before mentioned sets of images are reconstructed and their camera view positions are extracted. d) Using NeRF machine learning and given coordinates of a picture set camera views, 3D meshes are generated.

[1] Hartley, R. I., Zisserman, A. (2004). A Brief Overview of Structure from Motion. International Journal of Computer Vision.

[2] Ravi, N. et al. (2020). Accelerating 3D Deep Learning with PyTorch3D. arXiv:2007.08501.

[3] Schönberger, J. L., Frahm, J.-M. (2016). Structure-from-Motion Revisited. In Conference on Computer Vision and Pattern Recognition (CVPR).

[4] Mildenhall, B. et al. (2020). NeRF: Representing Scenes as Neural Radiance Fields for View Synthesis. In ECCV.

EPR OF NEUTRON-RADIATION-INDUCED DEFECTS IN GGG

Jekabs Cirulis¹, Uldis Rogulis¹, Andris Antuzevics¹

¹Institute of Solid State Physics, University of Latvia, 8 Kengaraga Street, Riga, LV-1063, Latvia
Jekabs.Cirulis@cfi.lu.lv

Gallium gadolinium garnet (GGG) is one of the most studied garnet materials utilised for its optical and scintillator properties when doped with rare earth (RE) ions [1]. These properties enable the use of the material in solid state lasers and scintillator detectors. GGG belongs to the garnet crystal family and is similar in properties to many frequently studied materials. These materials have excellent optical properties as they are transparent and can be doped with RE ions. GGG in comparison to alternative materials has improved mechanical properties, it is more chemically inert and thermally stable.

It is important to study permanent defects induced by ionising radiation in scintillator materials, because they have inhibiting effects on the functionality of the material. Scintillator operation is enabled by the fading of defects that eventually emit electromagnetic radiation close to the visible light spectrum [2].

Multiple paramagnetic defects, which can be detected using electron paramagnetic resonance (EPR) methods, have been reported in GGG [3]. Broad lines with g-factor of ~ 2 have been measured, which were related to Gd clusters.

Radiation-induced centres have been previously reported [4], but mechanisms behind their formation could not be explained.

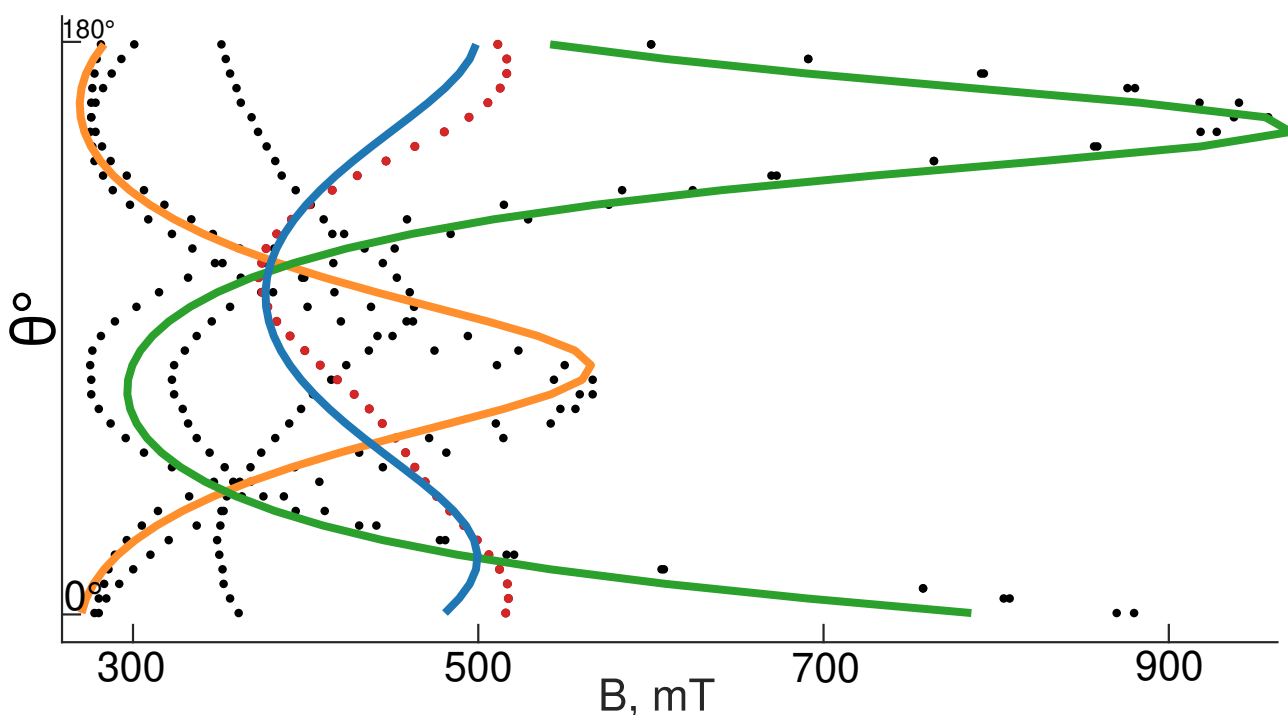


Fig. 1. EPR resonance angular dependence rotating GGG around one of the principal crystal axes. Dots are experimental points and lines represent simulations.

In this study, EPR spectra of neutron radiation-induced defects in GGG have been analysed. The defects possess highly anisotropic g-factors, which are not characteristic for these types of materials. Two distinct types of radiation induced defects in GGG have been observed and mechanisms of their formation are discussed.

-
- [1] A. Kaminska et al., Merging of the 4 F 3/2 level states of Nd 3+ ions in the photoluminescence spectra of gadolinium-gallium garnets under high pressure, *Physical Review B* 84.7, 075483, (2011)
 [2] I. I. Syvorotka et al., Optical properties of pure and Ce3+ doped gadolinium gallium garnet crystals and epitaxial layers, *Journal of Luminescence* 164, 31-37, (2015)
 [3] V. Singh et al., EPR and optical investigation of ultraviolet-emitting Gd3Ga5O12 garnet. *Journal of Materials Science: Materials in Electronics* 29, 944-951, (2018)
 [4] N. Mironova-Ulmane et al., EPR and optical spectroscopy of neutron-irradiated Gd3Ga5O12 single crystals, *Nuclear Instruments and Methods in Physics Research Section B: Beam Interactions with Materials and Atoms* 480, 22-26, (2020)

DISCRIMINATION OF PATHOGENIC YEAST AND BACTERIA BY MEANS OF ATR IR SPECTROSCOPY

Gerda Anužienė¹, Irmantas Arūnas Čiužas², Eglė Lastauskienė², Justinas Čeponkus¹

¹Institute of Chemical Physics, Faculty of Physics, Vilnius University, Saulėtekio Av. 3, LT-10257 Vilnius, Lithuania

²Institute of Biosciences, Life Sciences Center, Vilnius University, Saulėtekio Av. 7, LT-10257 Vilnius, Lithuania
gerda.anuziene@ff.vu.lt

Pathogenic microorganisms such as bacteria and fungi can cause infectious diseases. Antibiotics are used for the treatment of bacterial infections and antifungals for yeast caused infections. Discrimination between bacterial and fungal infection is important because of the different treatment strategies which can be applied while treating patients. For example, the prescription of antibiotics to patients with fungal infection can complicate the course of the disease by eliminating the bacterial members of the skin microbiota. Methods which are used nowadays for pathogenic microorganisms' identification require sample preparation and/or cultivation and takes a long time until the identification results are obtained, especially in the case of eukaryotic microorganisms. ATR IR spectroscopy is a non-destructive method and often does not require sample preparation. The collection of the ATR IR absorption spectrum takes several minutes therefore the identification of pathogenic microorganisms can be accomplished faster [1-3].

In this work, the method of an attenuated total reflection of infrared radiation (ATR IR) spectroscopy was applied for the analysis. A total of 177 ATR IR absorption spectra were collected which includes two types of yeast (*Candida guilliermondii*, *Candida parapsilosis*), three types of bacteria (*Staphylococcus aureus*, *Streptococcus pyogenes*, *Escherichia coli*) and mixtures between pathogenic yeast and bacteria.

ATR IR absorption spectra of mixtures of *C. guilliermondii*-*S. aureus*, *C. parapsilosis*-*E. coli* and *C. parapsilosis*-*S. Pyogenes* at the ratios 1:1, 1:2, 1:3, 2:1, 3:1, 2:3, 3:2 were measured to test the ATR IR suitability to discriminate microorganisms in mixtures. The main spectral difference was observed in 1360 cm^{-1} – 1280 cm^{-1} region. As the ratio of the mixture changes, the position of the polysaccharides δ (CH), Amide III spectral bands changes (Fig. 1. (a)). In order to assess the applicability of the FTIR ATR spectral method in clinical diagnostics, k-means statistical analysis was performed. In Fig. 1. (b) most of ATR IR absorption spectra of pure bacteria are located in the part of the diagram marked with red ellipse, while most the pure yeast spectra are located in the part of the diagram marked with blue ellipse. The spectra of the mixtures are located between the mentioned parts of the diagram, depending on the dominant microorganism in the sample.

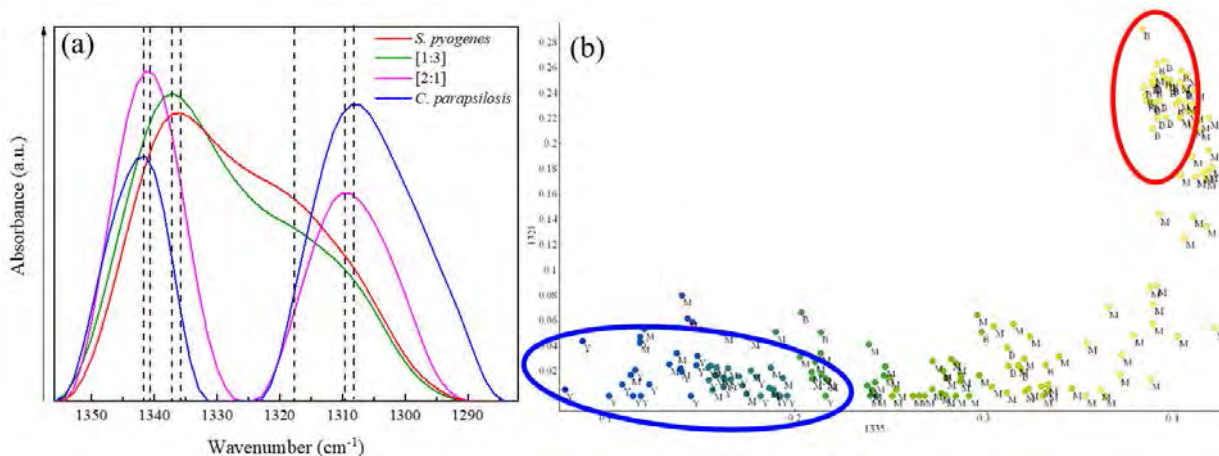


Fig. 1. (a) ATR IR absorption spectra of pure yeast, pure bacteria, and mixture, (b) k-means plot of ATR IR absorption spectra of bacteria, yeast, and their mixtures.

[1] M. Pigłowski, Int. J. Environ. Res. Public Health 16, 477 (2019)

[2] M. Harz, P. Rösch, J. Popp, Cytometry 75A, 104-113 (2009)

[3] B. Buszewski, A. Rogowska, P. Pomastowski, M. Zloch, V. Railean-Plugaru, J. AOAC Int 100, 1607-1623 (2017)

WATER VAPOR INTERACTION WITH LIQUID ETHANOL WAS INVESTIGATED USING THE TERAHERTZ TIME-DOMAIN SPECTROSCOPY TECHNIQUE.

Ihor Krapivin¹, dr Ramūnas Adomavičius¹

¹Center For Physical Sciences And Technology
 ihor.krapivin@ftmc.lt

This study develops a novel ethanol purity monitoring method based on the terahertz time-domain spectroscopy system. Historically, ethanol was used as a general anesthetic and has modern medical applications as an antiseptic, disinfectant, and solvent for some medications. It is used as a chemical solvent in the synthesis of organic compounds and as a fuel source. Some applications require the use of ultra-pure ethanol. For example, in the pharmaceutical industry, even a small amount of water in the solvent may cause problems in chemical reactions during research for purposes such as drug discovery. In this case, a real-time monitoring method is a promising analytical technology to guarantee the quality of the manufactured products. Our method is a promising solution for the real-time measurements of chemical reactions for quality control in pharmaceutical manufacturing.

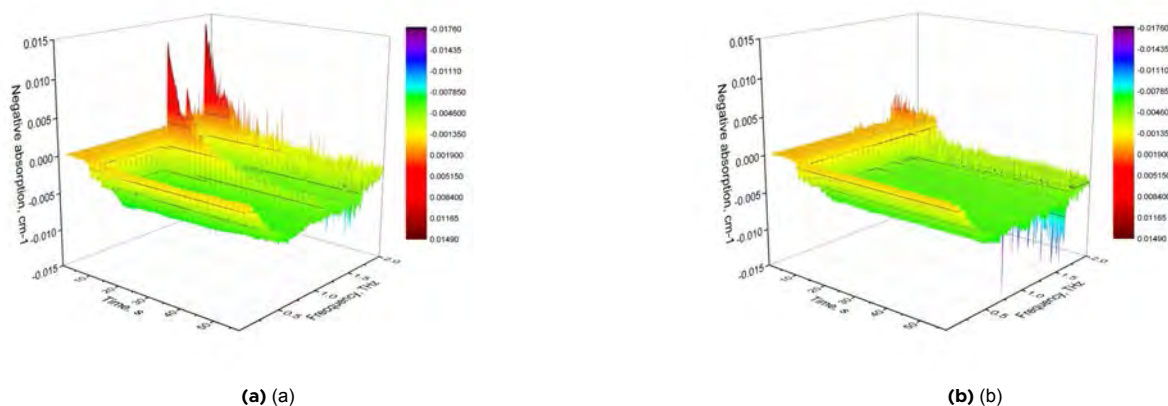


Fig. 1. Temporal development of transmittance spectra of 34 cm tube after injection of 10 ml ethanol. (a) 99.8% rectified ethanol and (b) 96% medicinal ethanol

The experiments were carried out by injecting small amounts of liquid alcohol into a closed tube filled with atmospheric air. The transmittance spectra of such a tube depended on the terahertz absorption of water and alcohol vapor and the interaction of water vapor with the liquid alcohol surface. In the vapor state, the absorption intensity of the alcohol molecule is similar to that of the water molecule, but the terahertz absorption spectra of both materials are significantly different. Moreover, a strong interaction between liquid alcohol and water molecules in the vapor state was observed (Fig. 1). Vapor spectroscopic testing has been shown to prove a more sensitive detection of low concentrations of water in ethanol than liquid phase [1] testing.

[1] K. Horita, K. Akiyama, H. Satozono, T. Sakamoto, K. Takahashi, Terahertz Time-Domain Attenuated Total Reflection Spectroscopy by a Flow-Through Method for the Continuous Analysis of Hydrated Ethanol

STRUCTURE OF VALERIC ACID MONOMERS AND DIMERS. MATRIX ISOLATION INFRARED SPECTROSCOPY STUDY

Jogile Macyte¹, Rasa Platakyte¹, Joanna Stocka¹, Valdas Sablinskas¹

¹Institute of Chemical Physics, Vilnius University, Saulėtekio av. 3, 10257 Vilnius, Lithuania
jogile.macyte@ff.vu.lt

Carboxylic acids are often studied using vibrational spectroscopy because they serve as excellent model systems for understanding processes involved in more complex molecular structures [1]. While the hydrogen bonding properties of saturated carboxylic acids have been studied for decades, there are still unanswered questions about the structure of such systems and the hydrogen bonds formed between these molecules. Research has shown that the first three carboxylic acids of the homologous series can form at least two types of dimers [2]. Valeric acid, also known as pentanoic acid ($C_5H_{10}O_2$), is described as a straight, saturated chain alkyl carboxylic acid [3]. Recent calculations predict another stable conformers of valeric acid monomer with non-linear alkyl chain. The main objective of this work is to identify experimentally observable structures of valeric acid (refer to Figure 1) using matrix isolation infrared spectroscopy in conjunction with theoretical calculations. The second goal is to determine structure of valeric acid dimers. The questions of possibility to observe open type dimers similar as in the lighter acids of valeric acid will be addressed.

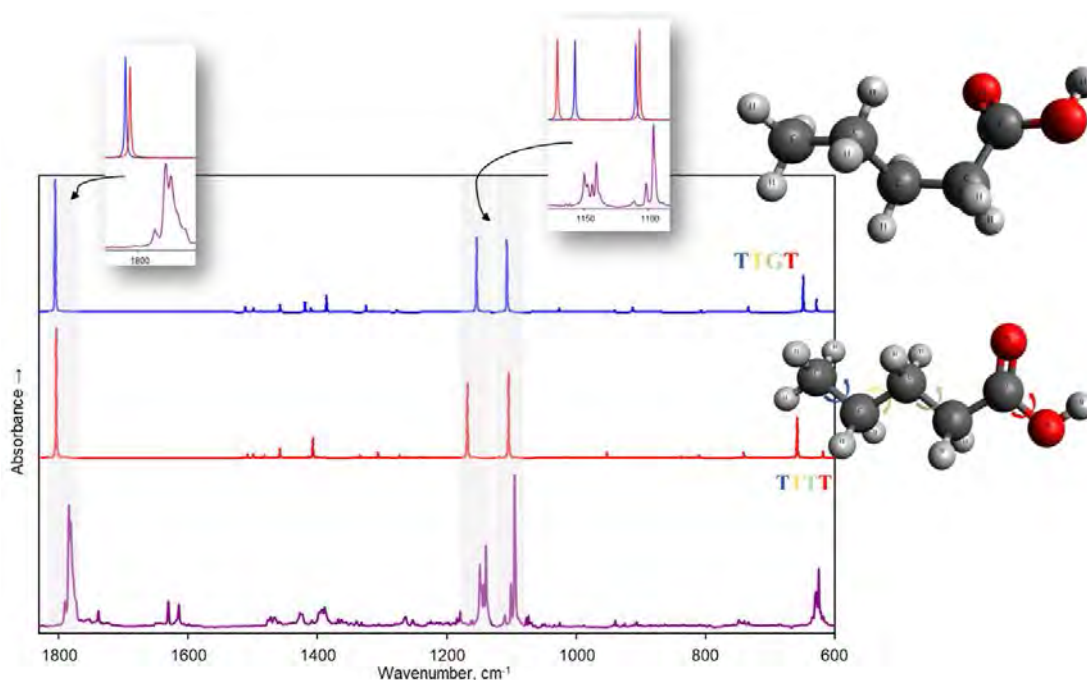


Fig. 1. FTIR absorption spectrum (lower curve) of valeric acid, isolated in neon 3 K matrix. The figure also shows the theoretically predicted spectra of conformers TTGT (upper curve) and TTTT (middle curve). The calculations were performed using MP2/cc-pVTZ theory level.

The theoretical calculations were carried out using the MP2 - Møller-Plesset expansion extension which contains truncated second orders, supplemented with the Dunning correlation matched basis set (triple zeta). The MP2 calculations show that the TTGT conformation has the lowest energy, which is $\Delta E = -0.3$ k J/mol. The experimental FTIR absorption spectra of valeric acid isolated in a neon matrix, together with the theoretical spectra of the two most stable conformers, are shown in Figure 1. Comparison of the experimental spectra with calculated ones of the two lowest energy conformers (see fig. 1) allowed us to identify bands belonging to the both conformers. The band corresponding to C=O stretching vibration at 1802 cm^{-1} for TTTT and 1803 cm^{-1} for TTGT conformer. These results demonstrate that in low-temperature matrices there are two valeric acid monomer conformers at different concentrations. The results on dimer structure and stability will be demonstrated from matrix isolation infrared spectroscopy results.

[1] J. Ceponkus et al. Lithuanian Journal of Physics, Vol. 49, No. 1, pp. 53–62 (2009)

[2] V. Sablinskas et al. Journal of Molecular Structure 976 (2010) 263–269

[3] Schaechter M. Encyclopedia of Microbiology. 3rd ed. Amsterdam: Elsevier/Academic Press; (2009)

APPLICATION OF TERAHERTZ TIME-DOMAIN SPECTROSCOPY TO STUDY THE CURING PROCESSES OF EPOXY RESINS

Mykolas Šikas¹, Ramūnas Adomavičius¹

¹Center for Physical Sciences and Technology, LT-10257, Saulėtekio av. 3, Vilnius, Lithuania
mykolas.sikas@ftmc.lt

Epoxy resins are polymers which display unique resistances and mechanical properties: heat and chemical resistance, water resistance, dielectric properties. Due to their properties, epoxy resins are often used in the aviation, automotive, shipbuilding and electronics industries. The two components are mixed to start a chemical reaction which causes the resin to harden. In our work we show that the terahertz time-domain spectroscopy (THz-TDS) technique can be an excellent tool for monitoring the polymerization of the resin, since the curing process clearly changes its optical properties in the THz wavelength range.

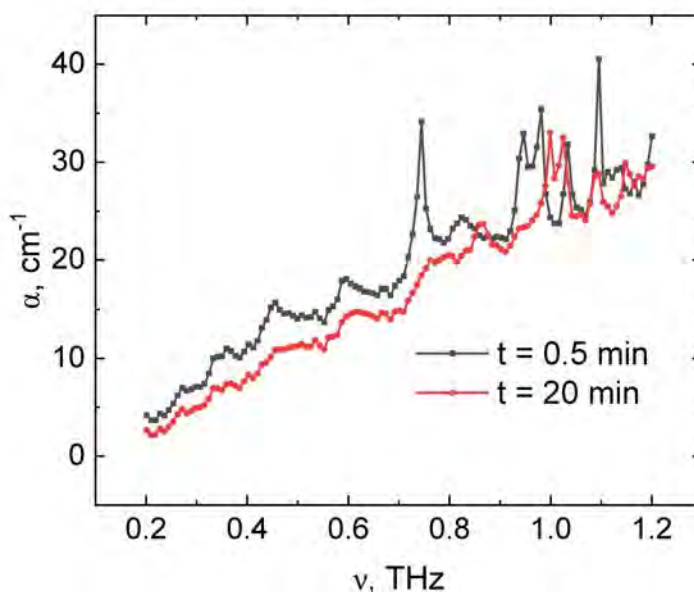


Fig. 1. Absorption spectra of liquid (black line) and solid (red line) epoxy resin.

As seen in Fig. 1, the absorption spectra of liquid epoxy resins are characterized by several absorption lines. As the resins cure, the center frequencies of some lines change, and some lines disappear. It was also found that the transparency of epoxy resins to terahertz radiation depend on their state: liquid, colloidal or solid. The least transparent epoxy resin is in a colloidal state; the most transparent - fully cured epoxy resin. The proposed measurement technique can be applied when creating various modifications of epoxy resin and monitoring the nuances of its drying. In a broader sense, our results indicate that THz-TDS methodology can be a useful tool for monitoring of chemical reactions.

RAMAN ASSISTED STUDY OF THE IMPACT OF ANNEALING TEMPERATURE FOR THE FORMATION AND STRUCTURE CHANGES FOR TIN SULFIDE FILMS

Boldizsár Zsiros¹, Ieva Barauskiene², Attila Farkas¹, Ingrida Ancutiene², Asta Bronusiene²

¹Budapest University of Technology and Economics

²Kaunas University of Technology
assta09@gmail.com

In recent years, nanostructured semiconductors have gained significant interest due to their high potential application in electronic, optical, and semiconductor devices. The fundamental properties of these nanostructured materials depend on their architectures, including geometry, morphology, and hierarchical structures [1,2]. Metal sulfides are one of the most important semiconductor materials that can be made using many different synthesis routes. Solution based synthesis has many advantages, such as being inexpensive, having short duration. Moreover, the application of abundant non-toxic components allows to reduce energy consumption indirectly through a simpler waste treatment or more efficient processing of raw materials with less CO₂. A successive ionic layer adsorption and reaction (SILAR) method is one of the chemical methods for making uniform films. The obtained thin films were characterized using Raman, X-Ray diffraction, scanning electron microscopy (SEM), and ultraviolet-visible (UV-Vis) spectroscopy. The effect of annealing temperature on the morphology and phase of tin sulfide has been investigated. In this work, ascorbate stabilized tin sulfide on the fluorine doped tin oxide (FTO) glass slides was synthesized by an eco-friendly and low-waste SILAR process. The main aim of the process is to immerse the substrate into two separately placed precursor solutions, then wash with distilled water in order to wash loosely bounded ions. To improve the solubility of tin(II) chloride in distilled water, environmentally-safe and biodegradable L-ascorbic acid was used as a reducing and capping agent [3]. X-Ray diffraction results showed change in the phasic composition of the deposited films. Non-annealed films consist of SnS and Sn₂S₃, where SnS (mineral Herzenbergite) is the dominant [3]. Moreover, Raman chemical imaging, together with X-Ray diffraction patterns, confirms phasic changes for non-annealed and annealed samples. Annealing increases the oxidation number of Sn atoms. According to Raman maps, sample annealed at 200 °C has very similar chemical properties compared to the non-annealed sample, so annealing effects are significant only at higher temperatures. Samples annealed at 300 °C are neither dominantly SnS or SnS₂ containing, the proportion of the two is close to equal. Sample film annealed at 400 °C consist mostly of SnS₂, higher temperature annealing cause oxidation of tin atoms. Ultraviolet-visible spectroscopy was done to calculate bandgap values of the films obtained. In this current work, a facile, eco-friendly technique to synthesize L-ascorbate acid stabilized tin sulfide thin films is described. This material is fairly cheap, environmentally clean and has interesting properties.

-
- [1] M Salavati Niasari et al Shape selective hydrothermal synthesis of tin sulfide nanoflowers based on nanosheets in the presence of thioglycolic acid *J Alloys Compd*
 [2] MS Fuhrer et al Crossed Nanotube Junctions *Science*
 [3] A Bronusiene et al Effect of ascorbic acid on the properties of tin sulfide films for supercapacitor application *Surfaces and Interfaces*

MICROWAVE COUPLING OF A NOVEL SUPERCONDUCTING EPR MICRORESONATOR

Ignas Pocius¹, Gediminas Usevičius¹, Paulina Vertbaitytė¹, Jūras Banys¹, Mantas Šimėnas¹

¹Faculty of Physics, Vilnius University, Lithuania
ignas.pocius@ff.stud.vu.lt

Electron paramagnetic resonance (EPR) is a powerful technique used to study and manipulate electron spins in various compounds ranging from functional materials to proteins. Recently, major advances in EPR sensitivity were achieved using planar superconducting microresonators^{1,2}. However, microresonators fabricated from low-temperature superconductors have severe limitations for conventional EPR due to their low temperature of operation and susceptibility to the external magnetic field. For this reason, microresonators fabricated from high- T_C superconductors are gaining attention.

Here, we use CST Microwave Studio computational electromagnetics tool to simulate microwave coupling characteristics of a planar EPR spiral microresonator coupled to an antenna via a Bruker MD-5 dielectric ring resonator (Fig. 1). First, we investigate the effect of the microwave antenna on the coupling strength to Bruker MD-5 resonator. After finding the overcoupled position, we explore the characteristics of a planar EPR microresonator on its position and rotation in the dielectric resonator. We also explore the dependence of the frequency of a spiral resonator on its length, while coupled to a co-planar waveguide and the Bruker MD-5 dielectric ring resonator. We compare our simulation results with the experimental observations and further discuss the best coupling geometry.

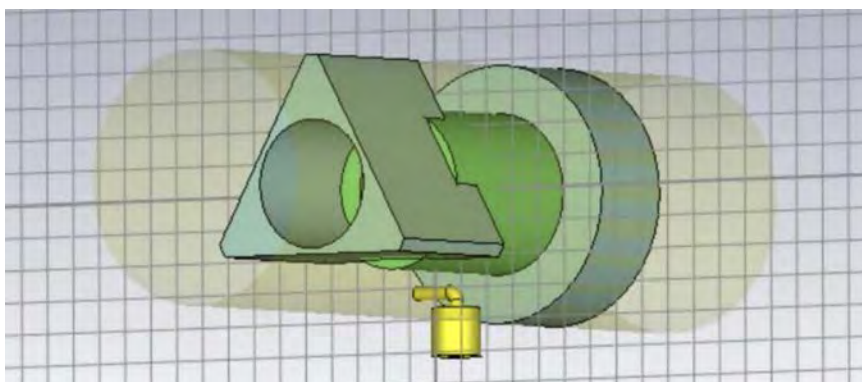


Fig. 1. Model of a Bruker MD-5 dielectric resonator.

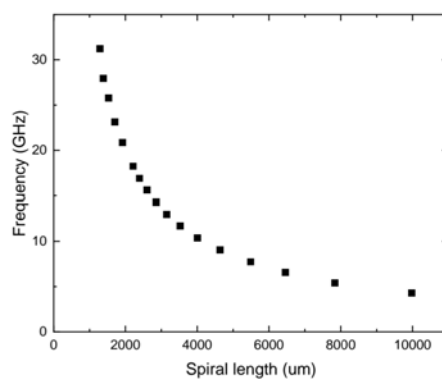


Fig. 2. The frequency dependence of the S_{11} parameter of a spiral EPR microresonator placed inside the dielectric resonator.

-
- [1] A. Bienfait, et al., Reaching the quantum limit of sensitivity in electron spin resonance, *Nat. Nanotechnol.* 11, 253-257 (2016).
 [2] J.J.L. Morton, P. Bertet, Storing quantum information in spins and high-sensitivity ESR, *J. Magn. Reson.* 287, 128-139 (2018).
 [3] Ghirri, A. et al. YBa2Cu3O7 microwave resonators for strong collective coupling with spin ensembles, *Appl. Phys. Lett.* 106, 184101 (2015).

CATHODOLUMINESCENCE IN NEW GENERATION NITRIDE COMPOUNDS

Gabija Soltanaite¹, Žydrūnas Podlipskas¹, Viktorija Mickūnaite¹

¹Vilnius university
gabija.soltanaite@ff.stud.vu.lt

The possibility to modify AlN and AlScN properties such as piezoelectricity and mechanical stability to meet the needs of contemporary devices encourages the investigation of new generation nitride derivatives and the optimization of their composition. This scientific work is dedicated to studying cathodoluminescence of new generation nitride compounds -- a series of AlScN samples containing scandium concentrations from 14% up to 41%, including a sample of AlN.

As the amount of scandium atoms in the material increases, so does the likelihood of internal structure disruption -- the formation of defects that affect the mechanical and electrical properties of the material. Defect levels of vacancies and oxygen complexes within the material's bandgap determine radiative and non-radiative recombination processes. Radiative recombination, observed between donor and acceptor levels as evidenced in cathodoluminescence, dominates spectral features of the material.

It is measured that as the concentration of Sc atoms in AlScN increases, the position of the dominant spectral peak shifts to the longer wavelength spectrum and is determined by radiative recombination from complex oxygen defects in the crystal lattice. Additionally, at higher excitation power densities, a significant increase in the cathodoluminescence intensity of defect levels is observed, indicating an increasing density of radiative recombination channels -- thermally activated complex oxygen defects in the material. When performing cathodoluminescence measurements at increasing modification densities, an increase in intensity is observed in compounds where the Sc concentration predominates up to 23%. Irreversible thermal modification, potentially occurring at a critical modification density, is observed when the Sc concentration in the compound reaches 41%.

[1] Deng, R., Evans, S. R., & Gall, D. (2013). Bandgap in Al_{1-x}Sc_xN. *Applied Physics Letters*, 102(11).

[2] Chen, D., Wang, J., Xu, D., & Zhang, Y. (2009). The influence of defects and impurities in polycrystalline AlN films on the violet and blue photoluminescence. *Vacuum*, 83(5), 865–868.

TERAHERTZ IMAGING USING PHASE CONTRAST METHOD

Adrianna Nieradka¹, Mateusz Kakuża¹, Mateusz Surma¹, Paweł Komorowski², Agnieszka Siemion¹

¹Faculty of Physics, Warsaw University of Technology, Poland

²Institute of Optoelectronics, Military University of Technology, Poland
adrianna.nieradka.dokt@pw.edu.pl

Over the past few years, research and technology in the field of terahertz (THz) radiation has developed significantly. This is due to the non-ionising properties of this radiation, characterised by a much longer wavelength than that of the visible range. Applications of this radiation are increasingly being found in fields such as medicine, biology or safety. It is therefore a motivation to continue research into spatial filtering, with suitable personalised optical elements to enable imaging of transparent elements in this frequency range.

Spatial filtering method is a promising technique, that can be used to visualize transparent objects with the use of a 4f optical setup (Fig.1) with much larger apertures than in the previous research [1].

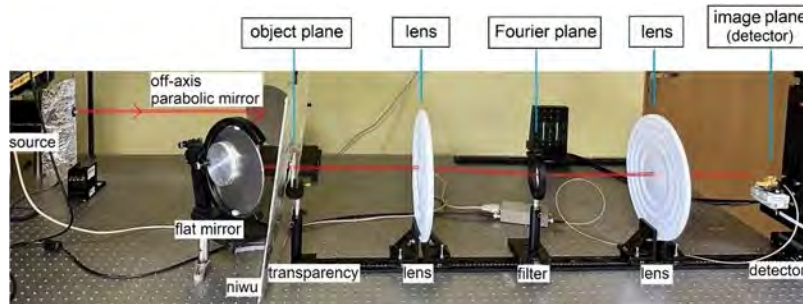


Fig. 1. A 4f optical setup consisting of: source and detector - based on Schottky diodes, reflective interference neutraliser, collimating mirror, flat mirror, transparency, two double-sided focusing HDPE lenses (focal lengths $f = 300$ mm) and phase filter.

It was decided to focus on two of the main spatial filtering methods. The first is the Positive Phase Contrast (PPC) method, which allows imaging after the insertion of a phase filter introducing a phase delay of $\pi/2$ into the setup in the focal plane. The second method used is the Negative Phase Contrast (NPC) method, which uses phase filters introducing a phase delay of $3/2 \pi$, thus obtaining an image opposite to that obtained using the PPC method. The choice of these methods is due to the linear relationship between the received irradiance in the image plane and the phase shift introduced by the object in the input [1].

After performing relevant simulations to find proper sizes of filters, it was proceeded with analysis of suitable materials from which optical object could be made. It was important to find materials with a relatively low refractive index and a low absorption coefficient, so that obtained objects were transparent at the chosen frequency [2] and possible to manufacture by FDM method in 3D printing [3].

The experiment confirmed the performance as well as proved the suitability of this method in the THz range, the effects of which can be seen in Fig. 2. It also showed some unexpected effects associated with very long wavelengths, which inspired further research.

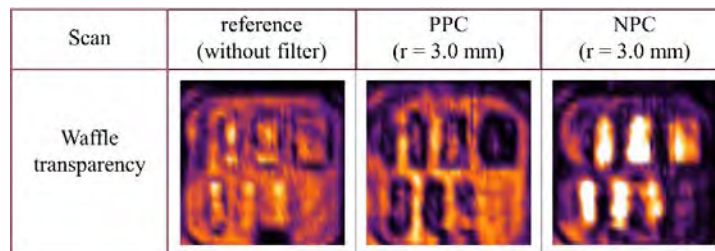


Fig. 2. Normalised scans in the imaging plane for transparency: without filter, using the positive phase contrast method and a filter with radius $r = 3$ mm, using the negative phase contrast method and a filter with radius $r = 3$ mm, (scan size: $100 \times 100 \text{ mm}^2$).

[1] SIEMION, Agnieszka, et al. Spatial filtering based terahertz imaging of low absorbing objects. *Optics and Lasers in Engineering*, 2021, 139: 106476.

[2] ZHANG, Xi-Cheng; XU, Jingzhou. *Introduction to THz wave photonics*. New York: Springer, 2010, DOI: <https://doi.org/10.1007/978-1-4419-0978-7>.

[3] KALUZA, Mateusz, et al. THz optical properties of different 3D printing polymer materials in relation to FTIR, Raman, and XPS evaluation techniques. In: 2022 47th International Conference on Infrared, Millimeter and Terahertz Waves (IRMMW-THz). IEEE, 2022. p. 1-2.

INVESTIGATING THE OPTICAL ATTRIBUTES OF SELAGIBENZOPHENONES AND THEIR COMPLEXES WITH GRAPHENE QUANTUM DOTS

Vilius Čirgelis^{1,2}, Ringailė Lapinskaitė², Andrej Dementjev², Karolina Maleckaitė², Linas Labanauskas², Renata Karpicz²

¹Vilnius University

²Center of physical sciences and technology

vilius.cirgelis@ftmc.lt

Selagibenzophenones (SelB) constitute a group of substances derived from plants of the Selaginella genus. These plants are traditionally used in Chinese and Indian medicine to treat conditions such as asthma or local injuries. Research has indicated that these substances possess various biological properties, including antibiotic, antibacterial, or anticancer effects.

Graphene quantum dots (GQD) are nanoparticles with unique and beneficial characteristics, such as chemical stability, low toxicity, small size enabling good penetration, and the ability to fluoresce with quantum yield of 50 percent. GQDs can be utilized as drug nanocarriers, necessary for delivering the active substance to the target cell, thereby protecting other cells.

The aim of the study was to examine the changes over time in the fluorescence spectra of SelB molecules and to assess the formation of complexes with GQD in solvents such as dimethyl sulfoxide (DMSO) and tetrahydrofuran (THF). The optical properties of SelB, GQD, and their mutual complexes were investigated using optical methods. During the study, the absorption, fluorescence, fluorescence excitation, Coherent Anti-Stokes Raman Scattering (CARS) spectra, and fluorescence quenching kinetics of SelB, GQD, and a mixture of GQD+SelB in a 1:15 ratio were measured. The size of the formed complexes was measured utilizing CARS microscopy.

In tetrahydrofuran (THF) solvent, the spectra of the substances do not yield meaningful results because the absorption, fluorescence and fluorescence excitation spectra overlap with the material spectra. However, the measured fluorescence quenching kinetics in this solvent reveal the formation of complexes. When measuring the fluorescence quenching kinetics at 445nm (GQD maximum), the decay of GQD is monoexponential, with an average relaxation time of ≈ 9 ns. In contrast, the relaxation times for the mixtures are approximately two times shorter (ranging from 4.8ns to 5.3ns) with a three-exponential approximation.

In the DMSO solvent, the spectras also show formation of complexes. The absorption spectra show the disappearance of one of the GQD absorption bands, the one peaking at 250nm. The fluorescence spectra provide evidence of complex formation, when excited with 350nm light, the spectras of the mixtures are similar to GQD fluorescence spectra, but with a slightly different spectral shape. Excitation of the complex with UV light (250-290nm) results in fluorescence spectra that is similar to the corresponding SelB materials. The fluorescence excitation spectra of the mixtures, regardless of the chosen emission wavelength, closely match the excitation spectra of individual SelB molecules. The fluorescence quenching kinetics also suggest molecular interaction. For the complexes, the relaxation durations are approximately four times shorter than GQD relaxations (ranging from 1.5 to 2.2ns) with two-exponential approximation.

EPR SPECTROMETER WITH ARBITRARY WAVEFORM GENERATION

Justinas Turčak¹, Jūras Banys¹, Vidmantas Kalendra¹, Mantas Šimėnas¹

¹Vilnius University
justinas.turcak@ff.stud.vu.lt

In present day, there are several different realisations of quantum technologies, such as superconducting qubits, ion traps, photonic and electron spins. Some of the most promising platforms are electron spin qubits in solid state systems [1,2], offering both long coherence time and accessibility by micro-electronic devices, such as micro-resonators [3], that manipulate spin qubits based on electron paramagnetic resonance (EPR). For full controllability of such qubits, sensitive EPR spectrometers that could produce long variable frequency pulse sequences with arbitrary waveform are necessary. These types of commercial spectrometers already exist, but they have limited functionality and are very expensive.

Here, we present a home-built pulsed EPR spectrometer (Fig. 1) operating at 2.5 – 12 GHz frequency range. Microwave excitation is generated using a vector signal generator (R&S SGS100A) with envelope of pulses established by an arbitrary waveform generator (Keysight P9336A) with maximum sample rate of 1.28 GSa/s. The generated pulse sequence is amplified by 25 W solid-state power amplifier. Operation of all devices is controlled using python code. We benchmark the performance of the constructed spectrometer against a standard Bruker E580 EPR spectrometer.

This research was supported by funding from European Union HORIZON-MSCA-2021-PF-01 Marie Skłodowska Curie Fellowship (Project ID: 101064200, SPECTR).

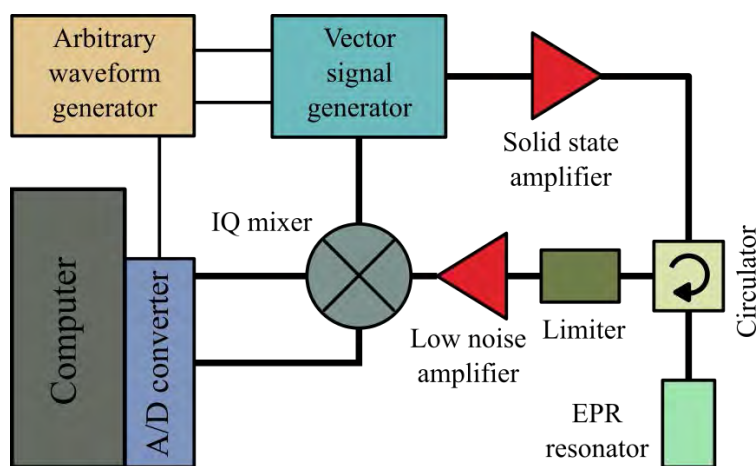


Fig. 1. Block diagram of an AWG-based pulsed EPR spectrometer.

[1] A. M. Tyryshkin et al., Electron spin coherence exceeding seconds in high-purity silicon, *New Materials*, 12, 143-147 (2012).

[2] G. Wolfowicz et al., Atomic clock transitions in silicon-based spin qubits, *Nature technology*, 8, 561-564 (2013).

[3] J. O Sullivan et al., Spin-Resonance Linewidths of Bismuth Donors in Silicon Coupled to Planar Microresonators, 14, 064050 (2020).

INFLUENCE OF SHORT- AND LONG-RANGE ORDER ON STRUCTURAL AND MAGNETIC PROPERTIES OF Fe-Co-C ALLOYS WITH A TETRAGONAL DEFORMATION: A FIRST-PRINCIPLES STUDY

Wojciech Marciniak^{1,2,3}, Mirosław Werwiński²

¹Institute of Physics, Faculty of Materials Engineering and Technical Physics, Poznań University of Technology, Piotrowo 3, 61-138 Poznań, Poland

²Institute of Molecular Physics, Polish Academy of Sciences, M. Smoluchowskiego 17, 60-179 Poznań, Poland

³Department of Physics and Astronomy, Uppsala University, P.O. Box 516, 75120 Uppsala, Sweden

wojciech.robe.marciniak@doctorate.put.poznan.pl

Fe-Co alloys with induced tetragonal strain are promising materials for rare-earth-free permanent magnets [1]. However, as ultrathin-film studies have shown, tetragonal Fe-Co structures tend to rapidly relax toward a cubic structure as the thickness of the deposited film increases [2].

We will present a full configuration-space analysis in the density functional theory approach for $(\text{Fe}_{1-x}\text{Co}_x)_{16}\text{C}$ supercells with a single C impurity in one of the octahedral interstitial positions and for the full range of Co concentrations x . Interstitial doping with small atoms, like B, C, or N, is one of the main methods of inducing the stable strain in the bulk Fe-Co alloy. We will discuss all assumptions and considerations leading to calculated lattice parameters, mixing enthalpies, magnetic moments, and averaged magnetocrystalline anisotropy energies (MAE). We will present a comprehensive qualitative analysis of the structural and magnetic properties' dependence on short- and long-range ordering parameters described in Ref. 3.

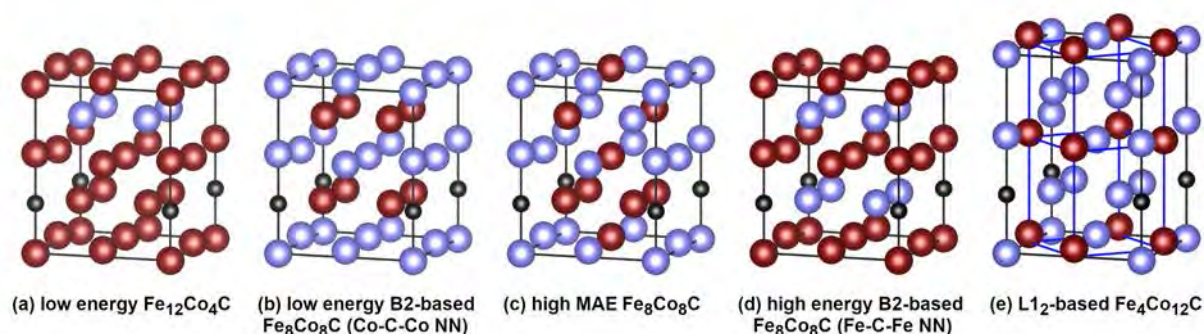


Fig. 1. Exemplary structures evaluated in our research [3].

The work relies on the thermodynamic averaging method and large sample count to obtain accurate MAE values from approximate density functional theory calculations with full-potential local-orbital (FPLO) code [4]. We place the utilized method in the context of several chemical disorder approximation methods, including effective medium methods (virtual crystal approximation and coherent potential approximation) and special quasirandom structures method applied to Fe-Co-based alloys. We observe a structural phase transition from the body-centered-tetragonal structure above 70% Co concentration and confirm the structural stability of Fe-Co-C alloys in the tetragonal range. We show the presence of a broad MAE maximum around about 50% Co concentration and notably high MAE values for Co content x as low as 25%. In addition, we show the presence of a positive correlation between MAE and mixing enthalpy.

Apart from the qualitative results contained in Ref. 3, we will present magnetic moments, magnetocrystalline anisotropy energies, and Curie temperatures (calculated according to disorders local moment approximation [5]) for selected high-symmetry structures, reevaluated with higher computational accuracy.

[1] Burkert, T., et al., (2004). Giant magnetic anisotropy in tetragonal FeCo alloys. *Physical Review Letters*, 93(2), 027203.

[2] Reichel, L., et al., (2014). Increased magnetocrystalline anisotropy in epitaxial Fe-Co-C thin films with spontaneous strain. *Journal of Applied Physics*, 116(21).

[3] Marciniak, W., and Werwiński, M., (2023). Structural and magnetic properties of Fe-Co-C alloys with tetragonal deformation: A first-principles study. *Physical Review B*, 108(21), 214433.

[4] Koepf, K., and Eschrig, H., (1999). Full-potential nonorthogonal local-orbital minimum-basis band-structure scheme. *Physical Review B*, 59(3), 1743.

[5] Staunton, J., et al., (1984). The "disordered local moment" picture of itinerant magnetism at finite temperatures. *Journal of Magnetism and Magnetic Materials*, 45(1), 15-22.

COMPETING DYNAMICS IN COMPARTMENTAL VOTER MODEL

Justas Kvedaravičius¹, Aleksejus Kononovičius²

¹Vilnius University, Faculty of Physics

²Vilnius University, Institute of Theoretical Physics and Astronomy
justas.kvedaravicius@ff.stud.vu.lt

Modelling opinion dynamics requires making assumptions that would be simple enough mathematically yet sufficient to recreate real populations statistical characteristics. Coming up with new sorts of agent interactions and states proved fruitful but difficult to compare against empirical data [1]. A way to overcome this was proposed in [2] through the inclusion of agent migration in spatial domain. The idea was generalized in [3] by proposing a compartmental voter model (CVM) - its dynamics described by agent migration to and from compartments. In this research we investigate an extension of CVM by including state changes leading to competing dynamics.

The CVM proposes entry and exit transition rates which follow the form of noisy voter model. Thus indicating that the model belongs to the group of voter models and that number of k type agents in compartment i ($X_i^{(k)}$) are Beta distributed. The CVM entry and exit rates read:

$$+\lambda_i^{(k)} = [N^{(k)} - X_i^{(k)}] (\varepsilon^{(k)} + X_i^{(k)}), \quad (1)$$

$$-\lambda_i^{(k)} = X_i^{(k)} \left((M-1)\varepsilon^{(k)} + [N^{(k)} - X_i^{(k)}] \right), \quad (2)$$

Competing dynamics are introduced by assuming additional state change rate of the same form as migration rate in CVM. Inclusion of these rates changes total entry/exit rates. We mark them v and note that they define transitions to and from compartment as well as transition within the compartment via type change:

$$+v_i^{(k)} = [N^{(k)} - X_i^{(k)}] (\varepsilon^{(m)} + X_i^{(k)}) + [N_i - X_i^{(k)}] (\mu^{(k)} + X_i^{(k)}), \quad (3)$$

$$-v_i^{(k)} = X_i^{(k)} \left((M-1)\varepsilon^{(k)} + [N^{(k)} - X_i^{(k)}] \right) + X_i^{(k)} \left(\sum_{m \neq k}^T \mu^{(m)} + [N_i - X_i^{(k)}] \right). \quad (4)$$

Here T is a total number of agent types, $\pm v_i^{(k)}$ marks entry and exit rates for agent type k in compartment i . The rates of competing dynamics cannot be simplified to noisy voter model rates due to two different sorts of factors $N^{(k)} - X_i^{(k)}$ and $N_i - X_i^{(k)}$. $N^{(k)}$ corresponds to the total number of k type agents and N_i equals total number of any type agents in compartment i . The model can be viewed as two coupled voter models with varying total number of agents N .

In the research we further explore $X_i^{(k)}/N_i$ and $X_i^{(k)}/N^{(k)}$ distributions dependency on model parameters M , T , $\mu^{(k)}$, $\varepsilon^{(k)}$. Further, calculations of Kramers-Moyal coefficients allow to approximate the model to Fokker-Planck equation. A finite form of the equation can suggest coefficient values for a simplified form.

[1] A. Peralta, J. Kertesz, G. Iniguez, Opinion dynamics in social networks: From models to data. arXiv preprint arXiv:2201.01322 (2022).

[2] J. Fernandez-Gracia, K. Suchecki, J. J. Ramasco, M. Miguel, V. Eguiluz, Is the voter model a model for voters, Physical Review Letters 112, 158701 (2014).

[3] A. Kononovicius, Compartmental voter model, Journal of Statistical Mechanics: Theory and Experiment 2019, 103402 (2019).

CHALLENGES IN NEURAL QUANTUM STATE PERFORMANCE: INSIGHTS FROM THE BOSE-HUBBARD MODEL WITH MAGNETIC FIELD

Eimantas Ledinauskas^{1,2}, Egidijus Anisimovas¹

¹Vilnius University

²Baltic Institute of Advanced Technology

eimantas.ledinauskas@ff.stud.vu.lt

In the field of ground state search and simulation of evolution for many-particle quantum systems, Neural Quantum States (NQS) are emerging as one of the leading methods [1]. Their expressive power and the diversity of possible architectures enable the efficient modeling of systems that are infeasible with other existing approaches [2]. However, NQS methods typically experience a significant drop in performance when applied to frustrated systems [3]. Currently, it remains unclear whether this issue can be completely addressed through modifications to the methods, or if it represents a fundamental limitation of NQS. In this work, we study the performance of NQS in the case of the Bose-Hubbard model under an external magnetic field. This model can exhibit frustration phenomena due to the presence of two length scales: one associated with the lattice period and the other with the magnetic length. We apply our previously developed method for ground state search [4] and systematically test various hypotheses regarding the reasons for the decrease in NQS accuracy with increasing magnetic field strength. Based on our findings, we propose and assess adjustments aimed at enhancing performance.

-
- [1] Dawid, A., Arnold, J., Requena, B., Gresch, A., Płodzień, M., Donatella, K., ... Dauphin, A. (2022). Modern applications of machine learning in quantum sciences. arXiv preprint arXiv:2204.04198.
- [2] Sharir, O., Shashua, A., Carleo, G. (2022). Neural tensor contractions and the expressive power of deep neural quantum states. *Physical Review B*, 106(20), 205136.
- [3] Bukov, M., Schmitt, M., Dupont, M. (2021). Learning the ground state of a non-stoquastic quantum Hamiltonian in a rugged neural network landscape. *SciPost Physics*, 10(6), 147.
- [4] Ledinauskas, E., Anisimovas, E. (2023). Scalable imaginary time evolution with neural network quantum states. *SciPost Physics*, 15(6), 229.

NON--PHOTOCHEMICAL QUENCHING IN PHOTOSYNTHETIC ANTENNA

Dominykas Borodinas^{1,2}, Jevgenij Chmeliov^{1,2}

¹Institute of Chemical Physics, Faculty of Physics, Vilnius University, Lithuania

²Department of Molecular Compound Physics, Centre for Physical Sciences and Technology, Vilnius, Lithuania

dominykas.borodinas@ff.stud.vu.lt

Over billions of years of evolution, various photosynthetic organisms have developed different photosynthetic apparatus. Despite their vast diversity, all these apparatus are designed in a very similar way: the so-called light-harvesting antenna is composed of pigment molecules usually bound to a protein scaffold. The mutual arrangement of these pigment-protein complexes, as well as their spectroscopic properties, ensures optimal absorption of the incoming photons and can lead to extremely efficient (up to $\sim 99\%$) delivery of the generated electronic excitations to a reaction center [1]. Despite the ever-growing knowledge about the structural organization of these complexes and excitation energy transfer dynamics in photosystem II, specific molecular mechanisms responsible for such high efficiency of excitation energy transfer are still not fully understood. To explain fluorescence measurements, fluctuating light-harvesting antenna model was formulated, which takes into account the continuous spatial rearrangement of the pigment-protein complexes within the photosynthetic membrane [2].

This work aims to expand the previously suggested fluctuating light-harvesting antenna model, introducing constant excitation generation and dissipation parameters depicting constant illumination conditions and molecular relaxation. The time evolution of the excitation in such a system can be described by a diffusion equation

$$\frac{\partial}{\partial t} p(\mathbf{r}, t|R) = D \nabla_d^2 p(\mathbf{r}, t|R) + G - k_{\text{dis}} p(\mathbf{r}, t|R), \quad (1)$$

with the initial condition $p(\mathbf{r}, t=0|R) = \delta(\mathbf{r})$ and boundary condition given by $p(\mathbf{r}, t|R)|_{|\mathbf{r}|=R} = 0$. Here $p(\mathbf{r}, t|R)$ is the density of the survived excitation at the time moment t , parametrically depending on R , the distance to the reaction center; D is the diffusion constant; ∇_d^2 is the Laplacian in a d -dimensional system; d represents the effective dimensionality of the antenna during the transfer of excitation energy. An average steady fluorescence quantum yield $\langle F_{st}(Dc^2/d) \rangle_x$ was obtained by taking into account the average concentration of excitation traps, c . Numerical solutions demonstrated that with the same number of excitation traps, the intensity of the steady fluorescence decreases faster in systems with higher dimensionality (Fig. 1).

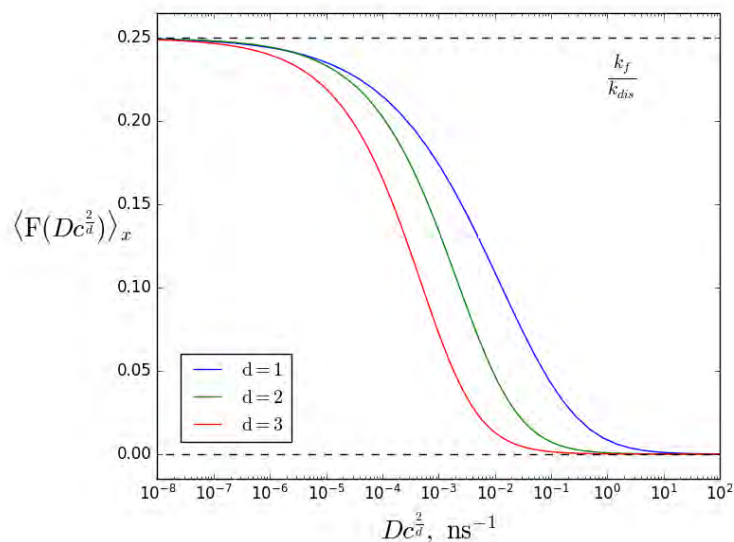


Fig. 1. Steady fluorescence quantum yield in various dimensions.

[1] Blankenship, R. E. *Molecular Mechanisms of Photosynthesis*; Blackwell Science: Oxford, 2002.

[2] J. Chmeliov, G. Trinkunas, H. van Amerongen, and L. Valkunas, Light harvesting in a fluctuating antenna, *Journal of the American Chemical Society*, 2014, 136, 8963–8972.

HIGH-FREQUENCY APPROXIMATION FOR PERIODICALLY DRIVEN QUANTUM SYSTEMS IN THE VICINITY OF RESONANCES

Yakov Braver¹, Egidijus Anisimovas¹

¹Vilnius University
jakov.braver@ff.vu.lt

Intriguing dynamical quantum many-body effects such as prethermalisation, ergodicity breaking, and localisation observed in driven systems [1,2] are usually studied theoretically under the assumption that the external drive, $\hat{V}(t)$, is time-periodic. This allows one to employ the Floquet theory [3,4] and construct an effective time-independent Hamiltonian \hat{H}_{eff} that fully characterises dynamics of the system [5]. Although guaranteed to exist, effective Hamiltonians can be derived analytically in a few simple cases only. Otherwise, a high-frequency expansion proves useful, whereby \hat{H}_{eff} is constructed as an expansion in powers of $\hat{V}(t)/\omega$, where ω is the driving frequency [6]. This procedure becomes particularly transparent when formulated in the Floquet–Hilbert space, wherein the time-dependent Hamiltonian is mapped onto a time-independent one (called the Floquet Hamiltonian or the quasienergy operator), represented by an infinite matrix possessing block structure [3,4,7]. However, the high-frequency expansions currently described in the literature are inapplicable when the driving is resonant with transitions between states of the undriven system.

In this work, we derive a high-frequency expansion that treats the case of resonant driving. The derivation amounts to formulating a degenerate perturbation theory in the Floquet–Hilbert space and block-diagonalising the quasienergy operator to construct an approximation of \hat{H}_{eff} . To demonstrate the validity of the derived expressions, we apply them to the driven Bose–Hubbard model [8] and calculate the quasienergy spectrum (eigenvalues of \hat{H}_{eff}), which are physically significant. We perform calculations for different resonant conditions $nU = m\omega$ (U is the interaction strength of the Bose–Hubbard model; n and m are integers) and compare the results with numerically exact ones, which can only be obtained for small systems. The developed theory is seen to approximate the exact results in great detail.

-
- [1] D. A. Abanin, E. Altman, I. Bloch, and M. Serbyn, Colloquium: Many-body localization, thermalization, and entanglement, *Rev. Mod. Phys.* **91**, 021001 (2019).
- [2] W. W. Ho, T. Mori, D. A. Abanin, and E. G. Dalla Torre, Quantum and classical Floquet prethermalization, *Ann. Phys-New York* **454**, 169297 (2023).
- [3] J. H. Shirley, Solution of the Schrödinger equation with a Hamiltonian periodic in time, *Phys. Rev.* **138**, B979–B987 (1965).
- [4] H. Sambe, Steady states and quasienergies of a quantum-mechanical system in an oscillating field, *Phys. Rev. A* **7**, 2203–2213 (1973).
- [5] N. Goldman and J. Dalibard, Periodically driven quantum systems: Effective Hamiltonians and engineered gauge fields, *Phys. Rev. X* **4**, 031027 (2014).
- [6] M. Bukov, L. D'Alessio, and A. Polkovnikov, Universal high-frequency behavior of periodically driven systems: from dynamical stabilization to Floquet engineering, *Adv. Phys.* **64**, 139–226 (2015).
- [7] A. Eckardt and E. Anisimovas, High-frequency approximation for periodically driven quantum systems from a Floquet-space perspective, *New J. Phys.* **17**, 093039 (2015).
- [8] A. Eckardt, Colloquium: Atomic quantum gases in periodically driven optical lattices, *Rev. Mod. Phys.* **89**, 011004 (2017).

STRONG LONG-RANGE INTERACTIONS AND GEOMETRICAL FRUSTRATION IN SUBWAVELENGTH RAMAN LATTICES

Domantas Burba¹, Gediminas Juzeliūnas¹, Ian B Spielman², Luca Barbiero³

¹Institute of Theoretical Physics and Astronomy, Vilnius University, Lithuania

²Joint Quantum Institute, University of Maryland, USA

³Institute for Condensed Matter Physics and Complex Systems, Politecnico di Torino, Italy
domantas.burba@ff.vu.lt

Non-local interactions are the key building block to allow for a spontaneous breaking of the translational symmetry. The latter represents one of the most fundamental symmetries in physics as it reflects the formation of periodic structures of mass and electric charge. Quantum matter with such a feature falls in the class of spontaneously symmetry broken (SSB) many-body phases with broken translational invariance. Although this peculiar symmetry breaking fixes the most energetically favourable distance between elementary constituents, examples of these SSB phases occur in physical systems with characteristic length scale. These range from electronic systems and liquid of ^4He to neutron stars. This recurrence has made the investigation and creation of such states of matter of central importance. In this respect, quantum simulators made of ultracold magnetic atoms with large magnetic dipolar momentum (e.g., erbium) represent a promising and powerful resource. However, current setups only explore frustrated regimes with weak local interactions or regimes where quantum fluctuations are suppressed. To the best of our knowledge, there are no experimental schemes able to simultaneously realize long-range interactions and geometrical frustration.

Here we consider a possible alternative to current setups - a recently realized [1] subwavelength lattice formed by a pair of counter-propagating [2]. It was shown that one may precisely control the tunneling amplitude, range, and phase by tuning the detunings. One also achieves significantly stronger interactions in the proposed scheme due to its subwavelength nature. Thus, one may realize intriguing phases of matter, such as density waves and chiral superfluids. Our results show three possible scenarios may occur, depending on the lattice depth and detunings. For deep optical lattices, we find quasi long-range order of the single particle Green's function, thus signalling the presence of a normal superfluid. For lower lattice depths, a regime characterized by long-range order takes place. This phase is characterized by spontaneously generated chiral currents and therefore, is an example of a chiral superfluid. Finally, density waves of period two or three were observed for a large range of detuning values.

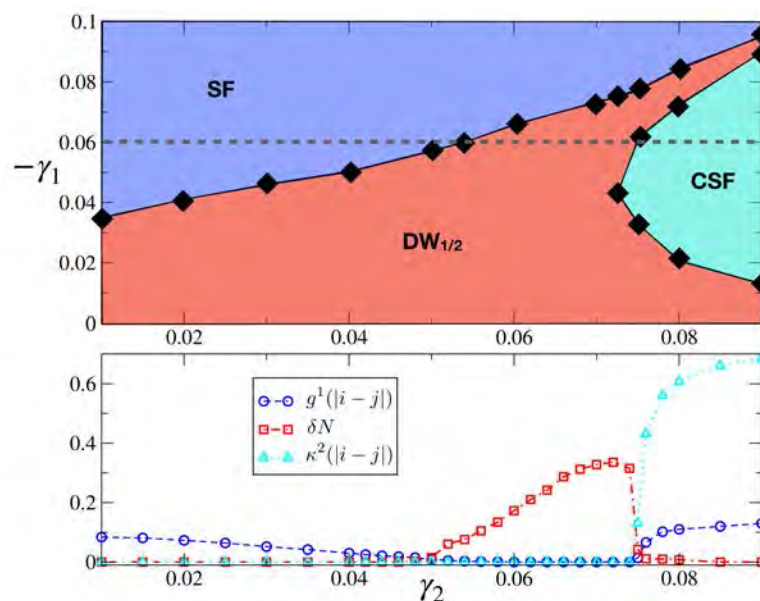


Fig. 1. Upper panel: Phase diagram of the extended Bose-Hubbard model for the case when $N = 5$ internal states are considered as function of γ_1 and γ_2 . Lower panel: Various order parameters as function of γ_2 for fixed $\gamma_1 = -0.6$, see the dashed grey line in the upper panel. These results have been obtained by considering a particle density $\bar{n} = 1/2$, $\Omega/E_R = 3.5$, a system size of $L = 180$ sites.

[1] R. P. Anderson, D. Trypogeorgos, A. Valdés-Curiel, Q.-Y. Liang, J. Tao, M. Zhao, T. Andrijauskas, G. Juzeliūnas, and I. B. Spielman, Phys. Rev. Research **2**, 013149 (2020).

[2] D. Burba, M. Račiūnas, I. B. Spielman, and G. Juzeliūnas, Phys. Rev. A **107**, 023309 (2023).

EVALUATING METHODS FOR ESTIMATING THE HURST EXPONENT IN TIME SERIES A COMPARATIVE ANALYSIS OF ACCURACY AND APPLICATION

Danielius Kundrotas¹, Rytis Kazakevičius²

¹Faculty of Physics, Vilnius University, Saulėtekio av. 9, Vilnius LT-10222, Lithuania

²Institute of Theoretical Physics and Astronomy, Vilnius University, Saulėtekio av. 3, Vilnius LT-10257, Lithuania
danielius.kundrotas@ff.stud.vu.lt

The Hurst exponent (H) is a statistical measure used to understand the long-term memory of time series, characterized by persistence and anti-persistence phenomena. Accurate estimation of H is crucial in diverse fields, such as finance, geophysics, and telecommunications, due to its ability to indicate the future tendency of a system based on its historical behavior. Numerous methods have been developed for estimating H , each with varying degrees of complexity and accuracy. This research reviews these methods, focusing on popular ones like box-counting, Katz, detrended fluctuation analysis, mean squared displacement (MSD), and Higuchi. To evaluate the reliability of these methods, fractional Brownian motion was used as a benchmark due to its well-defined Hurst parameter. Our analysis revealed that the Higuchi method and MSD provided the most accurate estimations of H . Additionally, these methods were applied to other long-memory processes to further validate their effectiveness. This work contributes to the field by identifying the most reliable numerical methods for estimating the Hurst exponent, providing a foundation for future studies and practical applications in analyzing time series with long-range dependencies.

NANO ZEOLITES AS ELECTROCATALYSTS FOR OER IN ALKALINE MEDIA

Jadranka Milikić¹, Sara Knežević², Kristina Radinović¹, Ana Nastasić¹, Aleksandar Jović³, Aldona Balčiūnaitė⁴, Radmila Hercigonja¹, Biljana Šljukić^{1,5}

¹University of Belgrade, Faculty of Physical Chemistry, Studentski trg 12-16, 11158 Belgrade, Serbia

²University of Belgrade, Faculty of Chemistry, Studentski trg 12-16, 11158, Belgrade, Serbia

³Državni univerzitet u Novom Pazaru, Departman prirodno-matematičkih nauka, Vuka Karadžića bb, Novi Pazar

⁴Center for Physical Sciences and Technology, Saulėtekio Ave. 3, Vilnius LT-10257, Lithuania

⁵CeFEMA, Instituto Superior Técnico, Universidade de Lisboa, 1049-001 Lisbon, Portugal
jadrankamilikic87@gmail.com

Term nanozeolites refers to a group of zeolites with particle size smaller than 200 nm and a narrow particle size distributions [1]. They are typically composed of single particles that are not agglomerated. Possibility of inserting different cations as well as high surface area and porosity of nanozeolites makes them attractive for applications in electrocatalysis. Herein, NiY and CuY zeolites were prepared by ion-exchange starting from parent NaY zeolite and subsequently ball-milled to prepare nanozeolite counterparts as evidenced by scanning electron microscopy. These were evaluated for oxygen evolution reaction (OER) as the anodic reaction in water electrolyzers. It is known that OER is a multi-step process that limits the efficiency of the water splitting process used for production of green hydrogen [2]. Both nanozeolites demonstrated moderate activity for the OER with CuY demonstrating somewhat better performance in terms of lower overpotential, higher current densities recorded and lower Tafel slope. Future studies aiming to enhance the nanozeolites' performance for OER will include coupling nanozeolites with highly conductive materials such as carbon nanostructures as well as more detailed study of their stability under OER polarisation conditions.

[1] C. Chen, B. Hou, T. Cheng et al., The integration of both advantages of cobalt-incorporated cancrinite-structure nanozeolite and carbon nanotubes for achieving excellent electrochemical oxygen evolution efficiency, *Catalysis Communications* 180, 106708 (2023).

[2] J. Milikić, S. Stojanović, Lj. Damjanović-Vasilić et al., Porous cerium-zeolite bifunctional ORR/OER electrocatalysts in alkaline media, *Journal of Electroanalytical Chemistry* 944, 117668, (2023).

AB INITIO STUDY OF VIBRATIONAL PROPERTIES OF DIVACANCY DEFECTS IN 4H-SiC

Vytautas Žalandauskas¹, Rokas Silkinis¹, Lasse Vines², Lukas Razinkovas^{1,2}, Marianne Etzelmüller Bathen²

¹Center for Physical Sciences and Technology (FTMC), Vilnius, Lithuania

²Department of Physics Centre for Materials Science and Nanotechnology, University of Oslo, Norway
vytautas.zalandauskas@ftmc.lt

Silicon carbide (SiC) is a wide bandgap material with great potential for high-power and high frequency electronic devices. Furthermore, certain deep-level semiconductor defects have potential applications as qubits and single photon emitters for quantum technologies (QT). SiC hosts a wide variety of defects with QT-compatible properties. In multi-component semiconductors, such as SiC, these defects can often inhabit several configurations with different characteristics. Therefore, a detailed characterization of different defect configurations and their electro-optical properties is essential.

Our study employed first-principles calculations to study four neutral divacancy configurations (hh , kk , hk , and kh) and their vibrational properties in the 4H-SiC polytype. The labels h and k refer to the distinct hexagonal and pseudo-cubic lattice sites in 4H-SiC, respectively. Using the r^2 SCAN density functional [1], we have determined the zero-phonon line (ZPL) energies and zero-field splitting (ZFS) values, which are in close agreement with experimental data [2]. Furthermore, we calculated the spectral functions of electron-phonon coupling using a novel embedding methodology [3]. The calculated luminescence lineshapes provide excellent agreement with the experimental data. Additionally, the obtained absorption cross-sections give a comprehensive picture of the contributions of each neutral divacancy defect configuration to the observed photoluminescence spectra.

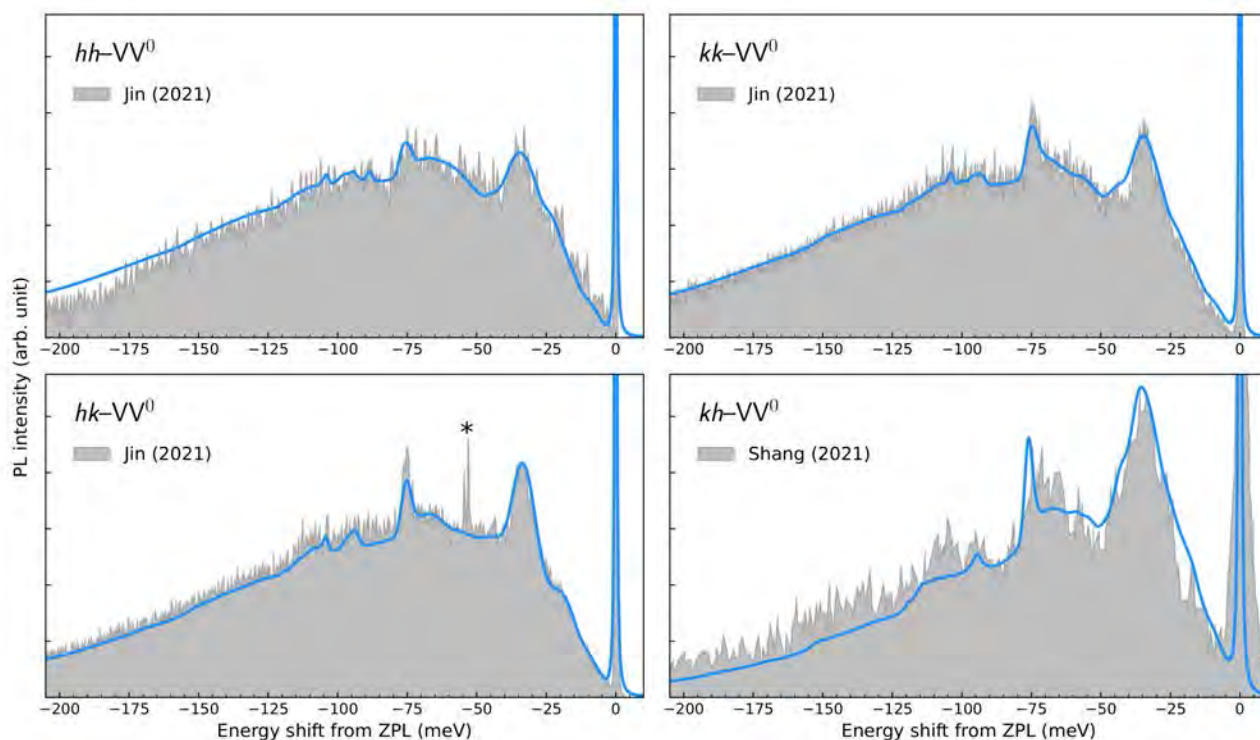


Fig. 1. Optical spectra of emission. Blue lines are calculated photoluminescence (PL) line shapes while the gray area represents experimental data [4, 5].

- [1] J. W. Furness et al. The journal of physical chemistry letters 11(19) p. 8208-8215 (2020).
- [2] A. L. Falk et al. Nature communications 4(1) p. 1819 (2013).
- [3] L. Razinkovas et al. Physical Review B 104(4) p. 045303 (2021).
- [4] Y. Jin et al. Physical Review Materials 5 p. 084603 (2021).
- [5] Z. Shang et al. Physical Review Applied 15 p. 034059 (2021)

ANALYSIS OF GNSS LOCALIZATION ACCURACY IN URBAN AREA USING RAY TRACING

Karolis Stankevičius¹, Rimvydas Aleksiejūnas¹

¹Institute of Applied Electrodynamics and Telecommunications, Faculty of Physics, Vilnius University
karolis.stankevicius@ff.vu.lt

Rising number of GNSS (Global Navigation Satellite System) enabled devices also comes with an increasing need for higher accuracy positioning. This was addressed to an extent by modernizing navigation systems and introducing new civilian L5 signals. However, higher overall number of available signals does not guarantee better position determination especially in urban environments, where GNSS positioning accuracy suffers from diffraction, multipath and reflections from surrounding buildings¹. Due to these effects the total sum of GNSS signals at the receiver is comprised from line-of-sight (LOS) direct reception and non-line-of-sight (NLOS) diffracted and reflected signals. This introduces a significant error in position determination, because GNSS receivers operate under the assumption that all received signals are LOS signals². Therefore, it is important to perform environment specific GNSS analysis.

GNSS raw-signal measurements have been conducted in city environment (Fig. 1 right) giving detailed information about carrier to noise ratio (Fig. 1 left), pseudorange, code-phase and carrier-phase. Measurements were performed using automotive grade Quectel LG69T AA GNSS receiver with survey grade Beitian BT-300S GNSS antenna. Measured localization accuracy has been compared against ray tracing simulations using 3D vector building data obtained from OpenStreetMap dataset³. The simulation environment is built using Open source ray tracing package Opal: open-source C++ ray tracing library based on NVIDIA OptiX framework which uses 3D ray-launching algorithm⁴, and NVIDIA RTX 3060 graphics card.

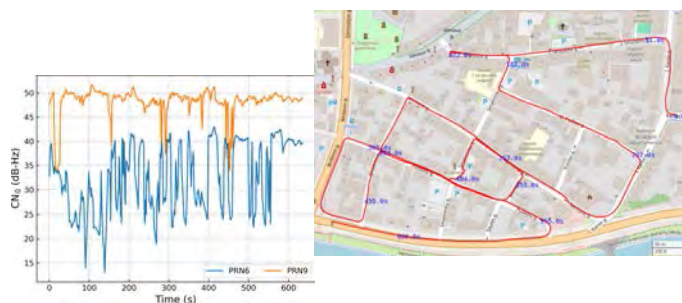


Fig. 1. Carrier to noise ratio of different GPS satellites over time (left) and path taken during raw GNSS measurements (right).

Carrier-phase and code-phase estimations of localization errors have been extracted from ray tracing results. From the results, close correlation between error statistics and NLOS diffracted rays can be observed. This suggests possibility of using ray tracing simulation data to identify areas with high diffraction and multipath probabilities. Based on such spatial information, the correction filters can be applied to GNSS signal prior to using it for location estimation. The results of ray tracing depend on the spatial resolution of building data. Therefore, for future applications, we plan to use LIDAR derived buildings data with decimeter-scale accuracy. For that ray tracing algorithms should be updated to account for more complex mesh-type data structures.

[1] T. Suzuki, Mobile robot localization with gnss multipath detection using pseudorange residuals, *Advanced Robotics*, vol. 33, no. 12, pp. 602–613, 2019.

[2] B. Friebel, M. Schweins, N. Dreyer, and T. Kürner, Simulation of GPS localisation based on ray tracing, *Advances in Radio Science*, vol. 19, pp. 85–92, 2021.

[3] OpenStreetMap contributors, Planet dump retrieved from www.planet.osm.org, www.openstreetmap.org, 2017.

[4] E. Egea-Lopez, J. M. Molina-Garcia-Pardo, M. Lienard, and P. Degauque, Opal: An open source ray-tracing propagation simulator for electromagnetic characterization, *PLOS ONE*, vol. 16, p. e0260060, Nov. 2021.

OPTICAL PROPERTIES OF CERIUM DOPED MULTICOMPONENT GARNET TYPE SCINTILLATORS GROWN BY LIQUID PHASE EPITAXY

Mikas Iršėnas¹, Augustas Vaitkevičius¹, Saulius Nargelas¹, Arnoldas Solovjovas¹, Vitaliy Gorbenko², Yuriy Zorenko², Gintautas Tamulaitis¹

¹Vilniaus University, Institute of Photonics and Nanotechnology, Saulėtekio al. 3 Vilnius

²Department of Physics of Kazimierz Wielki University in Bydgoszcz, Powstanców Wielkopolskich str., 2, 85-090 Bydgoszcz, Poland
mikas.irsenas@ff.stud.vu.lt

The applicability of scintillators in the detection of ionizing radiation depends predominantly upon several key parameters, including their light yield, scintillation decay time, afterglow characteristics, radiation tolerance, and energy resolution. Scintillators with a cerium-doped multi-component garnet structure have demonstrated a high light yield and a strong resistance to ionizing radiation. These attributes make them particularly suitable for application in high-energy physics experiments and medical imaging. Nonetheless, a significant limitation of these crystals is their susceptibility to the formation of substitution-type defects, which degrade their scintillation response time—a critical parameter for their effectiveness. One proposed solution for this issue involves the fabrication of scintillators by the liquid-phase epitaxy (LPE) method. This process is conducted at lower temperatures, which is hypothesized to result in a reduced probability of defect formation. The aim of this study is to investigate the impact of compositional variations on the optical properties of scintillators grown by the LPE method.

Four samples of cerium-doped multicomponent garnet structure scintillators grown on an undoped YAG substrate were investigated: $\text{Lu}_3\text{Al}_5\text{O}_{12}:\text{Ce}$, $\text{Y}_3\text{Al}_5\text{O}_{12}:\text{Ce}$, $\text{Tb}_3\text{Al}_5\text{O}_{12}:\text{Ce}$, and $\text{Gd}_{2.5}\text{Lu}_{0.5}\text{AG}:\text{Ce}$.

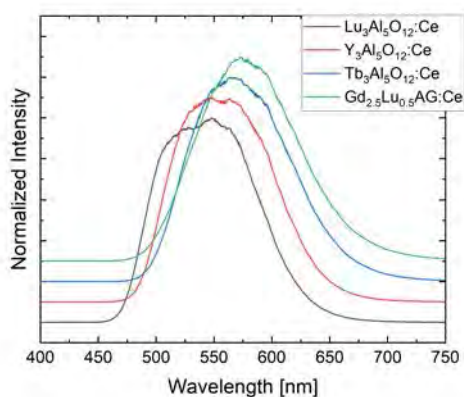


Fig. 1. Photoluminescence spectra of scintillating layers with different compositions (indicated), shifted for clarity.

The investigation of macroscopic emission characteristics, including emission kinetics and their temperature dependency, was conducted using a system composed of a pulsed laser integrated with an optical parameter amplifier for adjusting the laser wavelength, along with a cryosystem to control the sample temperatures. Microscopic emission properties, specifically the uniformity of photoluminescence intensity and the mean wavelength, were investigated utilizing a laser scanning confocal microscope connected to a spectrophotometer.

The experiments showed that the photoluminescence spectrum exhibits the greatest redshift in $\text{Gd}_{2.5}\text{Lu}_{0.5}\text{AG}:\text{Ce}$ relative to the $\text{Lu}_3\text{Al}_5\text{O}_{12}:\text{Ce}$ garnet, as illustrated in Figure 1. There is a decline in average intensity corresponding with the increase of ionic radius, following the order $\text{Lu}^{3+} < \text{Y}^{3+} < \text{Tb}^{3+} < \text{Gd}^{3+}$. The $\text{Tb}_3\text{Al}_5\text{O}_{12}:\text{Ce}$ sample demonstrated the highest variability in intensity, wavelength distribution, and the temperature-dependence of scintillation decay. These results are interpreted by the difference in ionic radius of Lu^{3+} , Y^{3+} , Tb^{3+} and Gd^{3+} ions in the scintillator matrix and the interaction of the lattice-building atoms with activator ions Ce^{3+} , as well as by the structural inhomogeneities in the scintillator layers occurring in the growth process.

CONTACT CHARACTERISTICS OF P-TYPE GaN GROWN USING INDIUM SURFACTANT

K German¹, M Vaičiulis¹, M Biveinytė¹, V Rumbauskas¹, K Nomeika¹, Y Talochka¹, A Kadys¹

¹Institute of Photonics and Nanotechnology, Faculty of Physics, Vilnius University, Saulėtekio av. 3, 10257, Vilnius
karolina.german@ff.stud.vu.lt

The first discovery of p-type gallium nitride (p-GaN) grown by metalorganic vapor phase epitaxy (MOVPE) and doped with magnesium (Mg) was made by Japanese researchers by exposing the crystal to a low-energy electron beam [1]. The primary advancement in p-type GaN technology has been achieved through thermal annealing in a nitrogen atmosphere, which effectively activates the Mg acceptors by removing hydrogen. Hydrogen is known to passivate Mg by forming complexes that prevent Mg from effectively accepting electrons, thus hindering its p-type doping capabilities. However, defects such as nitrogen vacancies can compensate for the p-type GaN during growth. Despite this, the commercial significance of p-type GaN is considerable, although some challenges remain in understanding and optimizing the growth process.

In the technology for growing III-group nitride crystals, indium (In) can be part of the InGaN alloy and surfactant component. It has been demonstrated that In enhances the surface morphology of GaN, reduces deep-level trap concentrations, increases luminescence efficiency, extends free exciton recombination time, and improves hole conductivity [2]. This study will demonstrate that using In as a surfactant also alters the contact resistance.

We grew p-type GaN samples in an MOVPE reactor and varied parameters such as temperature and the flow rates of Mg and In metalorganics. We adjusted the In flow rate to assess the contact resistance while keeping other parameters stable. Initially, we used MICROTTECH LaserWriter photolithography to pattern a photoresist layer with the geometric design of the photomask. We deposited Ni/Au contacts onto the patterned areas in an electron beam evaporation (EBE) chamber. Finally, we calculated the contact resistance by measuring the IV characteristics and using the transmission-line matrix (TLM) method.

To summarize the experimental findings, we observed that the In surfactant influences the contact resistance. We found that as the In concentration increases, the contact resistance decreases (Fig. 1). Furthermore, the In surfactant increases the carrier diffusion length.

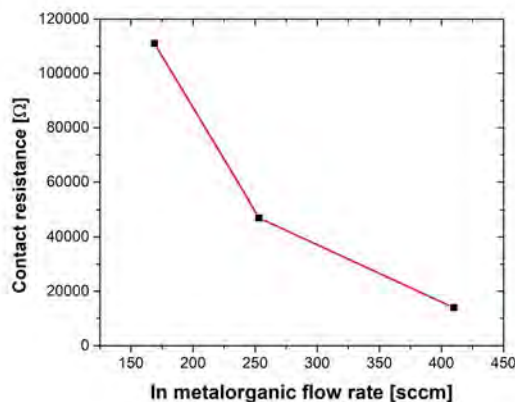


Fig. 1. Contact resistance dependency from In concentration.

Keywords: MOVPE, GaN, p-type, contact, resistance.

[1] H. Amano, M. Kito, K. Hiramatsu, and I. Akasaki, Jpn. J. Appl. Phys. 28, L2112 (1989).

[2] E. Kyle, S. Kaun, et al, USA, J. Appl. Phys. 106, L222103 (2015).

THE EFFECT OF MONOATOMIC OXYGEN ON CARBON-SPUTTERED QUARTZ CRYSTALS

Eivydas Trioška¹, Mindaugas Viliūnas², Greta Merkininkaitė¹, Simas Šakirzanovas¹

¹Institute of Chemistry, Vilnius University, Naugarduko 24, LT-03225, Vilnius, Lithuania

²Institute of Chemical Physics, Vilnius University, Saulėtekio 9, LT-10222 Vilnius, Lithuania
eivydas.trioska@chgf.stud.vu.lt

Atomic oxygen (AO), a predominant form of oxygen in outer space, offers an effective and minimally invasive way to remove carbon-based contaminants from various surfaces without health and environmental concerns. The efficiency of AO cleaning was estimated using a Quartz Crystal Microbalance (QCM) sensor, carbon-sputtered 6 MHz quartz crystals and a K-type thermocouple, while AO was introduced with a plasma generator.

The experimental procedure is depicted in Figure 1. Step 1: initial mass and ambient temperature measurements

($m_1 = -0.032 \mu\text{g}/\text{cm}^2$, $t_1 = 22.3 \text{ }^\circ\text{C}$) over a 4-minute period. Step 2: mass change and temperature measurements

($m_2 = 0.226 \mu\text{g}/\text{cm}^2$, $t_2 = 20.0 \text{ }^\circ\text{C}$) during an 8-minute period with gas flow (without plasma). Step 3: highest instantaneous mass change and temperature measurements ($m_3 = -50.663 \mu\text{g}/\text{cm}^2$, $t_3 = 70.5 \text{ }^\circ\text{C}$) with plasma for a 4-minute period.

Step 5: mass change and temperature measurements ($m_4 = -5.985 \mu\text{g}/\text{cm}^2$, $t_4 = 24.4 \text{ }^\circ\text{C}$) after a 13-minute cooldown. Results are promising for upcoming measurements, because both instantaneous and long-lasting mass changes are present ($m_3 = -50.663 \mu\text{g}/\text{cm}^2$ and $m_4 = -5.985 \mu\text{g}/\text{cm}^2$ respectively).

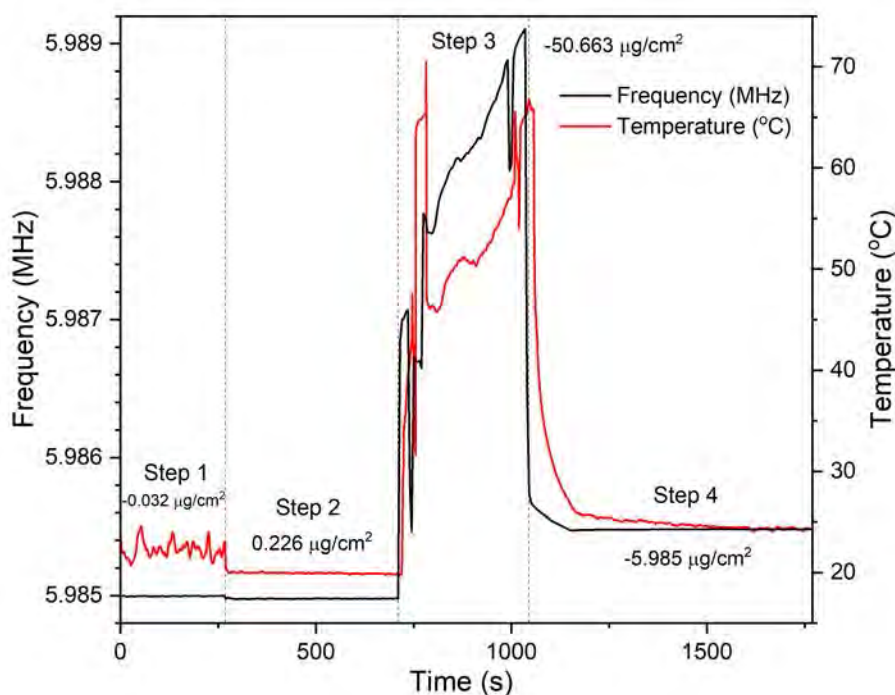


Fig. 1. QCM frequency and temperature relation.

Acknowledgment

The authors acknowledge financial support from the European Research Executive Agency (REA) (Grant Number: 101061336)

INVESTIGATION OF SCINTILLATING CHARACTERISTICS IN MOCVD GaN STRUCTURES WITH CHEMICALLY MODIFIED SURFACES

Giedrius Juškevičius¹, Tomas Čeponis¹, Jevgenij Pavlov¹

¹Institute of Photonics and Nanotechnology, Vilnius University, Saulėtekio av. 3, LT-10257, Vilnius, Lithuania
giedrius.juskevicius@ff.stud.vu.lt

The search for new materials and the formation of radiation-tolerant sensors devoted for the space industry, the medical diagnostics instruments and the high-energy physics applications is necessary. Binary direct-gap compounds such as gallium nitride (GaN) are effective in producing dual-response (i.e., capable of detecting electrical and optical signals) devices [1]. But due to imperfect MOCVD growing technologies, the formation of various technological defects, which are usually inhomogeneously distributed throughout the crystal wafer [2], is inevitable. These defects determine the optical and electrical characteristics of devices. Therefore, it is important to investigate the distribution of defect species within the MOCVD grown GaN wafer area in order to improve the growth regimes as well as to identify the areas of best quality. Light extraction efficiency (LEE) is another parameter which should be enhanced for efficient device operation. This can be achieved by modifying the surface of the material by using the chemical (wet) etching method [3]. It has been shown that the chemical etching procedures significantly modify the structure of dislocations and their occupied areas and might be the reason of the increase of intensity of scintillation signals in MOCVD GaN based sensors [4].

The aim of this work was the modification of MOCVD grown GaN surfaces by potassium hydroxide (KOH) and phosphoric acid (H_3PO_4) and comparative analysis of variations of optical characteristics in respect to etching regimes. The research methodologies like time-integrated photoluminescence (TI-PL), microwave-probed photoconductivity (MW-PC) transient techniques were applied for the investigation. While surface control was realized by optical microscopy imaging.

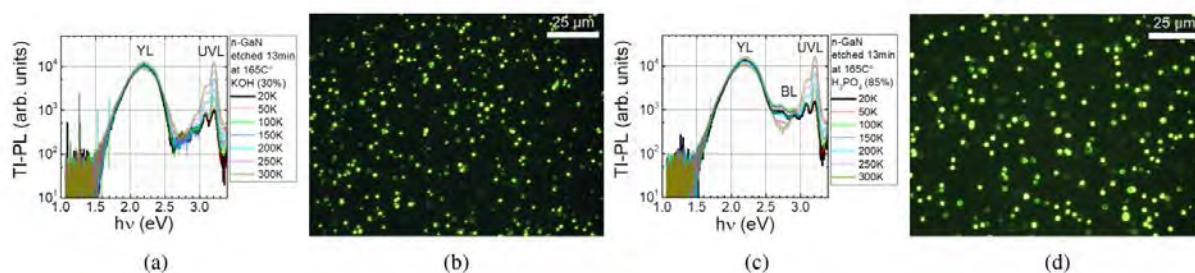


Fig. 1. The TI-PL spectra measured in chemically etched MOCVD GaN (a – KOH, c – H_3PO_4). The optical microscopy images taken in chemically etched MOCVD GaN layers (b – KOH, d – H_3PO_4) under UV illumination.

It was deduced by the analysis of PL spectra that the defect distribution in the MOCVD GaN wafer is inhomogeneous, with more carbon and oxygen impurities accumulating at the edges of wafer. It was shown that carrier surface recombination lifetime can be increased by modifying the MOCVD GaN surface using chemical etching. The dislocations act as centers of attraction for point defects, resulting variations in bulk carrier lifetime. The blue luminescence band was observed in H_3PO_4 etched layers, however this band was absent in KOH modified MOCVD GaN. The variations of intensity of PL bands might be related to modification of space charge region, surrounding the dislocation cores and acting as non-radiative recombination centers. The variations of PL and MW-PC characteristics in chemically etched MOCVD GaN will be presented and discussed.

- [1] E. Gaubas, I. Brytavskiy, T. Ceponis, A. Jasiunas, V. Kalesinskas, V. Kovalevskij, D. Meskauskaitė, J. Pavlov, V. Remeikis, G. Tamulaitis and A. Tekorius, In situ variations of carrier decay and proton induced luminescence characteristics in polycrystalline CdS, 2014, J. Appl. Phys. 115, 243507.
- [2] J. Su, E. A. Armour, B. Krishnan, S. M. Lee, G. D. Papasouliotis, Stress engineering with AlN/GaN superlattices for epitaxial GaN on 200 mm silicon substrates using a single wafer rotating disk MOCVD reactor, 2015, Journal of Materials Research 30, 2846–2858.
- [3] H. Fang, X.N. Kang, C.Y. Hu, T. Dai, Z.Z. Chen, Z.X. Qin, B. Zhang, G.Y. Zhang, Studies of improving light extraction efficiency of high power blue light-emitting diode by photo-enhanced chemical etching, 2007, Journal of Crystal Growth, 298, 703-705.
- [4] Y. Yao, Y. Ishikawa, Y. Sugawara, Revelation of dislocations in HVPE GaN single crystal by KOH etching with Na_2O_2 additive and cathodoluminescence mapping, 2016, Superlattice Microst., 99, 83-87.

COMPARISON OF SPECTRAL PROPERTIES OF SEMICONDUCTOR STRUCTURES EQUIPPED WITH METALLIC (Ti/Au) OR N-TYPE GaAs METASURFACES

Barbora Škėlaitė^{1,2}, Vladislovas Čižas¹, Kęstutis Ikamas³, Vytautas Jakštas⁴, Domas Jokubauskis¹, Andrius Bičiūnas¹, Andrzej Urbanowicz¹, Marius Treideris⁴, Renata Butkutė¹, Linas Minkevičius¹, Ignas Grigelionis¹

¹Center for Physical Sciences and Technology, Department of Optoelectronics, Vilnius, Lithuania

²Vilnius University, Institute of Photonics and Nanotechnology, Vilnius, Lithuania

³Vilnius University, Institute of Applied Electrodynamics and Telecommunications, Vilnius, Lithuania

⁴Center for Physical Sciences and Technology, Department of Physical Technologies, Vilnius, Lithuania
barbora.skelaite@ff.stud.vu.lt

Ever-growing field of terahertz (THz) technology require compact and easy to operate solid state thermal emitters. Currently most popular solutions comprise a considerably complicated structure and can operate only in cryogenic temperatures [1]. Thermal emitters equipped with metasurfaces could be an attractive alternative. They can provide spectrally narrow resonant emission, operate at elevated temperatures [2] and do not require additional bulky and expensive external equipment. In this work two types of n-GaAs/GaAs semiconductor structures were investigated and compared. The first one consisted of 0.2 μm -thick Ti/Au metasurface, while the second was equipped with 5 μm -thick *n*-type GaAs metasurface. The metasurface structures were made up from periodic square shaped metacells to form a top layer of the thermal emitters.

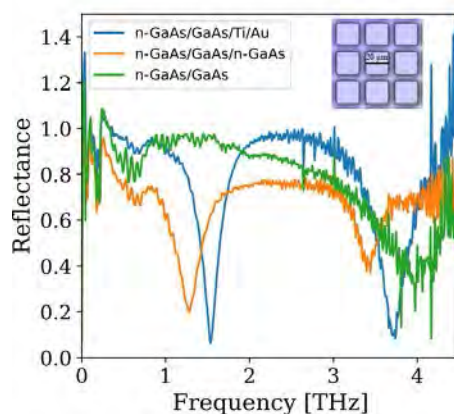


Fig. 1. Experimental reflection spectra of plain semiconductor (green) and semiconductor structures with n-GaAs metasurface (orange) and Ti/Au metasurface (blue). Insert shows metasurface of n-GaAs/GaAs/n-GaAs structure.

Thermal emitter structures equipped with metasurfaces were investigated both theoretically and experimentally to measure emittance, absorbance and reflectance spectra of the samples. From the obtained results it is seen, that by equipping semiconductor structures with metasurfaces the distinct spectral features appear if compared to bare *n*-GaAs/GaAs structures (Fig. 1). Both of the samples equipped with metasurfaces showed clear dependence of resonant frequency on the size of the metacell, where resonant frequency dropped with increasing metacell size. Moreover, thermal emitters equipped with metallic (Ti/Au) metasurfaces provided up to 30 % broader emission bandwidth compared to *n*-type GaAs metasurfaces.

Research was funded by Research Council of Lithuania (LMTLT), Project No. P-ST-23-213

[1] A. Leitenstorfer, et al., J. Phys. D: Appl. Phys. 56, 223001 (2023).

[2] F. Alves, et al., Opt. Express 20, 21025-21032 (2012).

COMPOSITE ALLOY FORMATION BY LASER METAL 3D PRINTING

Karolis Stravinskas¹

¹Center for Physical Sciences and Technology
karolis.stravinskas@ftmc.lt

17-4 PH stainless steel is one of the most commonly used materials in the SLM process Fig. 1 due to its mechanical properties and corrosion resistance. Despite these advantages, the alloy has a rough surface and is known for its brittleness. Ceramic materials are not suitable for direct laser sintering, but are increasingly being used as a fastening material for a metal matrix. The search for metal-ceramic composite mixtures with thermal conductivity, low expansion coefficient and strength is becoming one of the most important research directions in the field of high technology.

17-4 PH metal material and metal-ceramic composite mixture of which 94% of the mass consists of 17-4 PH powder and the remaining 6% - SiC ceramic particles are used for the study Fig.2. During the experiment, an EOS M280 laser printing machine is used to form 3D objects. During all printing processes, the powder layer thickness of 40 μm is maintained, as well as the hatching distance of 100 μm and the laser power, which reaches 164 W. The laser scanning speed is changed, obtaining different energy densities, which are selected as 61, 67 and 73 J/mm^3 . The obtained samples were analysed by using SEM EDS, optical profilometer, as well as performing density, strength and hardness measurements.

It was found that the surface of the composite alloy has a more uniform surface, the roughness is reduced by 30% and ranges from 8 to 16 μm , and of the 17-4 PH material from 12 to 26 μm depending on the energy density. The mechanical property measurement results showed that the strength limit of the composite material dropped by 20% and reached 766 MPa, while for the 17-4 PH material it was 988 MPa. The hardness of the 17-4 PH + 6% SiC mixture decreased by 8% to 92 HRB, while for the metal alloy it reached 98 HRB. However, the results of the relative elongation showed that value of relative elongation for the composite mixture is 8.5% higher than 17-4 PH.

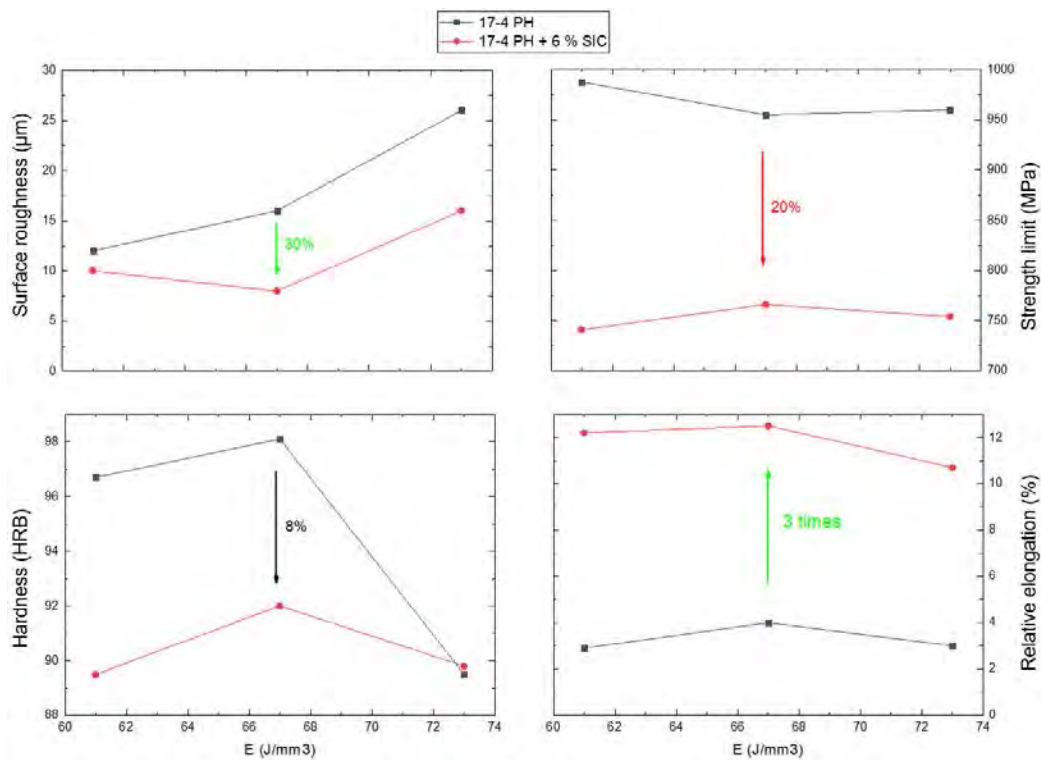


Fig. 1. Comparison of properties of SLS printed samples from 17-4 PH and 17-4 PH + % SiC mixture

ADDITIVE MANUFACTURING OF LAB-ON-CHIP PLATFORMS SUPPORTED BY HYDROGEL MATRIX FOR IN VITRO STUDIES

Adrianna Cieślak¹, Agnieszka Krakos², Julita Kulbacka^{3,4}, Jerzy Detyna¹

¹Department of Mechanics, Materials and Biomedical Engineering, Faculty of Mechanical Engineering, Wrocław University of Science and Technology, Wrocław

²Department of Microsystems, Faculty of Electronics, Photonics and Microsystems, Wrocław University of Science and Technology, Wrocław, Poland

³Department of Molecular and Cellular Biology, Faculty of Pharmacy, Wrocław Medical University, Wrocław, Poland

⁴Department of Immunology, State Research Institute Centre for Innovative Medicine, Vilnius, Lithuania
adrianna.cieslak@pwr.edu.pl

Due to the rapidly developing epidemiological situation of cancers, the scientific world is focusing on developing more innovative cancer research methods. Combining knowledge and skills in biomedicine and engineering is key to achieving this development. Therefore, research focusing on providing new instruments, fabricated in the form of microfluidic lab-on-chips (LOC) utilizing additive manufacturing (AM) supported by hydrogel matrix (HM) was provided towards innovative cancer cell studies, especially with a view to photodynamic therapy (PDT).

In this work, 3D printing of a biocompatible HM (technology: extrusion) on glass and polymer substrates was used to fabricate a LOC platform (Fig. 1). The polymer substrates were additively manufactured using photo-resins, such as VisiJet M3 Crystal (technology: MultiJet) and KeyGuide (technology: Digital Light Processing). Next, the key structural part of the platforms – HM – was prepared utilizing the following compositions of natural polymer powders such as sodium alginate, gelatin, chitosan, agar, and methylcellulose. Thus, various biocompatible inks could be obtained.

The AM process of hydrogels is presented in Fig. 1. The cross-linking process of the biopolymers was conducted using a calcium chloride solution (0.1M). The AM procedure involved e.g. the printing pattern, syringe speed, ink temperature, dosing speed, extrusion pressure, and nozzle diameter. The goal of AM of the HM was to include microchannels and microchambers in the matrix to provide spatial cell culture and transport of nutrients and oxygen. Nevertheless, the following difficulties were encountered during this process, e.g.: lack of repeatability, clogging of the printing nozzle, and geometry instability. However, most of these problems were solved; ultimately, the deposited layers had defined geometries, allowing for the implantation of cancer cells.

As part of the 3D printing experiments, the geometrical reproduction of the designed 3D model was evaluated. Additionally, the control ink was a commercial ink dedicated to the BIO X 3D printer used. The H69AR lung cancer cells, highly resistant to therapeutics, were used for *in vitro* studies. The culture was carried out to check the cytotoxicity of the LOC materials. For this purpose, cell viability and proliferation assays ensuring qualitative (Trypan Blue staining) and quantitative (Presto Blue reagent) evaluation were done. The reference was the control sample (cells in culture medium), in which viability was assumed to be 100%.

The primary research showed the high applicability of the device, however further investigation has to be done. The next step will be the optimization of the LOC platform – AM of LOC with microchannels, e.g., for cell perfusion. Furthermore, the research will focus on developing and applying anticancer PDT directly on the chip.

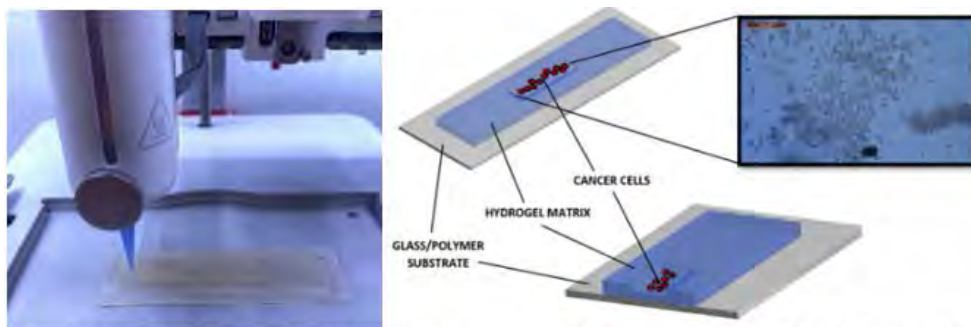


Fig. 1. Example of ink extrusion. Graphic representation of the prototype of the LOC platform and the culture of the H69AR cancer cells in a hydrogel matrix.

THE IMPACT OF A MIXED-HOST EMISSIVE LAYER FOR HIGH-EFFICIENCY BLUE TADF OLED STABILITY

Goda Grybauskaitė¹, Kristupas Bagdonas¹, Gediminas Kreiza¹, Edvinas Orentas², Saulius Juršėnas¹, Karolis Kazlauskas¹, Dovydas Banevičius¹

¹Vilnius University, Institute of Photonics and Nanotechnology, Saulėtekio ave. 3, Vilnius, Lithuania

²Vilnius University, Department of Organic Chemistry, Naugarduko g. 24, Vilnius, Lithuania
goda.grybauskaite@ff.stud.vu.lt

In the last decade organic light emitting diodes (OLEDs) that employ thermally activated delayed fluorescence (TADF) emitters have been extensively investigated due to the ability to achieve nearly 100% internal quantum efficiency [1]. Unlike red and green, blue OLEDs still lag in long-term stability [2]. Recently, a method of using a mixed-host system in the emissive layer has been proposed, resulting in higher device efficiency, slower roll-off and better stability than its single host equivalent [3].

This work aims to show an increase in blue DMeCzIPN emitter-based OLEDs' efficiency and lifetime when using a mixed-host emissive layer. Devices were fabricated through vacuum deposition in five batches utilizing widely used OLED host materials mCBP and mCBP-CN. Each emissive layer comprised a different ratio of the host materials doped with 7% DMeCzIPN emitter. The optimal host ratio was determined to be 3:1 for mCBP to mCBP-CN, resulting in up to 18.8% external quantum efficiency (EQE), whereas neat mCBP host devices only exhibited EQE of 9.8%. In terms of stability, the LT_{50} time (the loss of initial brightness L_0 by half) at $L_0 \sim 1000 \text{ cd/m}^2$ was determined to be around 10h for the optimal mixed-host ratio device and around 2h for the neat mCBP host device (see Fig. 1). The substantial increase in efficiency and prolonged stability suggests that selecting appropriate host materials and choosing the optimal ratio for the emissive layer can advance the research of blue TADF OLEDs, unlocking their full potential for commercial application.

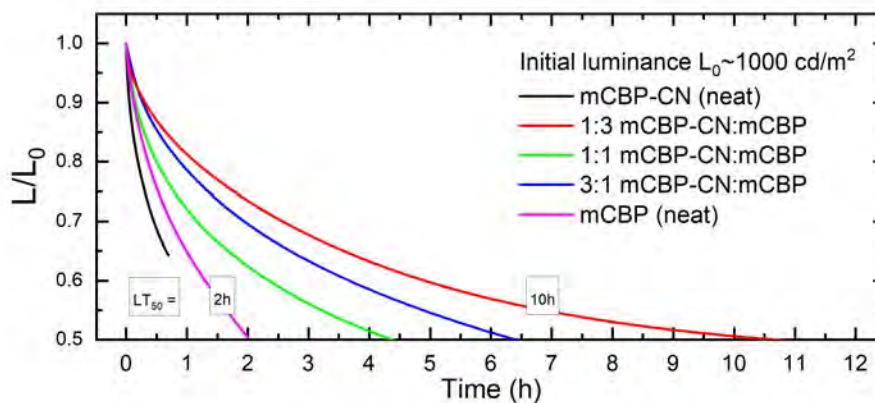


Fig. 1. DMeCzIPN emitter-based OLED luminance vs. time at $L_0 \sim 1000 \text{ cd/m}^2$ initial luminance.

- [1] H. Uoyama, K. Goushi, C. Adachi et al., Highly efficient organic light-emitting diodes from delayed fluorescence, *Nature*, 492, 234–238 (2012).
 [2] D. Banevičius, G. Puidokas, G. Kreiza et al., Prolonging blue TADF-OLED lifetime through ytterbium doping of electron transport layer, *J. Ind. Eng. Chem.*, 128, 515-520 (2023).
 [3] W. Li, J. Tang, Y. Zheng et al., Improved stability of blue TADF organic electroluminescent diodes via OXD-7 based mixed host, *Front. Optoelectron.*, 14, 491–498 (2021).

NATURAL GRAPHITE AND IRON SULFIDE USED AS NEGATIVE ELECTRODE MATERIALS FOR SODIUM-ION BATTERIES

Eglė Ūsovienė¹, Egidijus Griškonis¹

¹Kaunas University of Technology
egle.usoviene@ktu.edu

To transition from fossil fuels to more sustainable energy systems there should be more energy-storing solutions offered in the current market [1]. The most prominent and widely used are Lithium-ion batteries (LIB's) which in recent years have become costly and deficient. To combat this problem new electrical energy storage solutions must be introduced into the current market. Sodium-ion batteries (SIB's) are a good solution because of sodium's abundance and low cost but to be offered in the current market their properties must match or be better than LIB predecessors [2]. For this to happen new research of SIB electrode materials must be conducted. The most prominent and widely used negative electrode materials is graphite but in order to offer better quality new negative electrode materials, the addition of various other compounds to graphite are being explored [3]. Iron sulfides could be an excellent addition to natural graphite because of its high theoretical capacity and low cost [4].

In this research work 4 methods of SIB negative electrode preparation with iron sulfides and natural graphite have been explored and compared. These electrodes were prepared using a hydrothermal method with different reagents used for iron sulfide synthesis and added natural graphite at 180°C temperature for 2 hours. The reagents used in the hydrothermal vessel for the sample preparation were:

- $\text{FeSO}_4 \cdot 7\text{H}_2\text{O}$, Na_2SO_3 , Graphite (Sample C/FeS1);
- $\text{FeSO}_4 \cdot 7\text{H}_2\text{O}$, $\text{Na}_2\text{S}_2\text{O}_3$, S, Graphite (Sample C/FeS2);
- $\text{FeCl}_3 \cdot 6\text{H}_2\text{O}$, EtOAc, Thiourea, Graphite (Sample C/FeS3);
- $\text{FeSO}_4 \cdot 7\text{H}_2\text{O}$, Thiourea, Sulfur, Graphite (Sample C/FeS4).

After carrying out obtained sample scanning electron microscopy (SEM) imaging samples indicated different properties when using different reagents for iron sulfide preparation. When comparing SEM results with natural graphite, samples C/FeS1 and C/FeS2 show clear changes on the surface and growth of FeS nanoparticles, which differ from those of natural graphite. Samples C/FeS3 and C/FeS4 SEM images don't show clear growth of FeS nanoparticles, which could mean their form could resemble those of natural graphite.

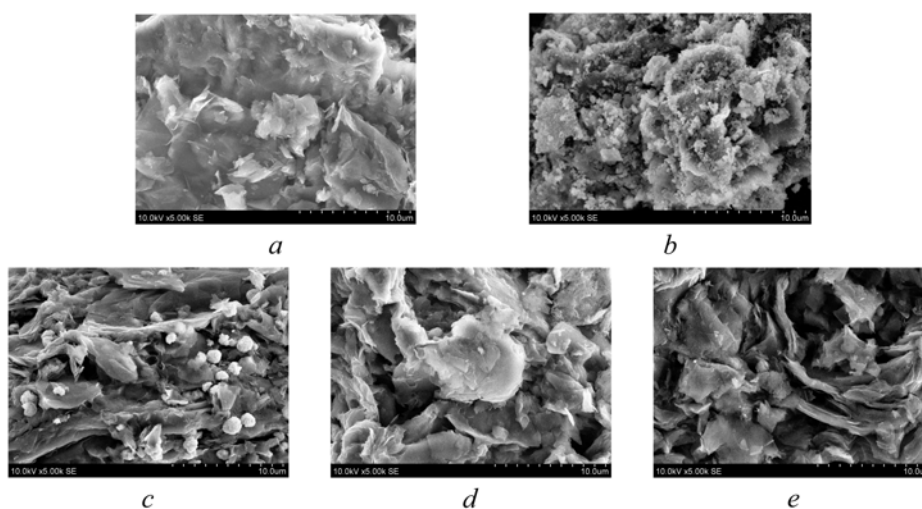


Fig. 1. Sample SEM analysis results: a – natural graphite; b – C/FeS1; c – C/FeS2; d – C/FeS3; e – C/FeS4.

[1] Olabi A. G., et al., Critical review of energy storage systems, Energy, Vol. 214, 2021

[2] Nayak P. K., et al., From Lithium Ion to Sodium Ion Batteries: Advantages, Challenges, and Surprises, Angewandte Chemie, Vol. 57, p. 102-120, 2018

[3] Xu Q., et al., Binary iron sulfides as anode materials for rechargeable batteries: Crystal structures, syntheses, and electrochemical performance, Journal of Power Sources, Vol. 379, p. 41-52, 2018

[4] Tang Q., et al., Binary Iron Sulfide as a Low-Cost and High-Performance Anode for Lithium-Sodium-Ion Batteries, ACS Applied Materials and Interfaces, Vol. 12, p. 52888-52898, 2020

2,5-DIPHENILOXAZOLE (PPO) APPLICATION FOR PHOTON UPCONVERSION FROM VISIBLE TO UV REGION

Naglis Vasarevičius¹, Manvydas Dapkevičius², Justas Lekavičius³, Džiugas Krencius⁴, Steponas Raišys⁵, Karolis Kazlauskas⁶

¹Institute of Photonics and Nanotechnology

²Vilnius University

naglis.vasarevicius@ff.stud.vu.lt

In recent years, the greatest success has been made in achieving high-efficiency triplet-triplet annihilation-based upconversion (TTA-UC) within the visible region. The potential applications are spread over a wide range of fields, including photocatalysis, UV light-induced photosynthesis, and even enhanced security features for documents. Despite these advancements in the visible spectrum, the pursuit of systems demonstrating high efficiency in converting visible (VIS) to ultraviolet (UV) light poses an ongoing challenge.

In TTA-UC two triplet excitons energies are combined to create one, higher energy singlet exciton state. TTA-UC systems consist of two molecules. Sensitizer molecule, which absorbs light strongly in the VIS region and generates triplets through intersystem crossing. Annihilator molecule, which fuses triplet energies together and generates singlet excitons. Here, Ir-C molecule and CBDAC are used as sensitizers while PPO is used as the annihilator.

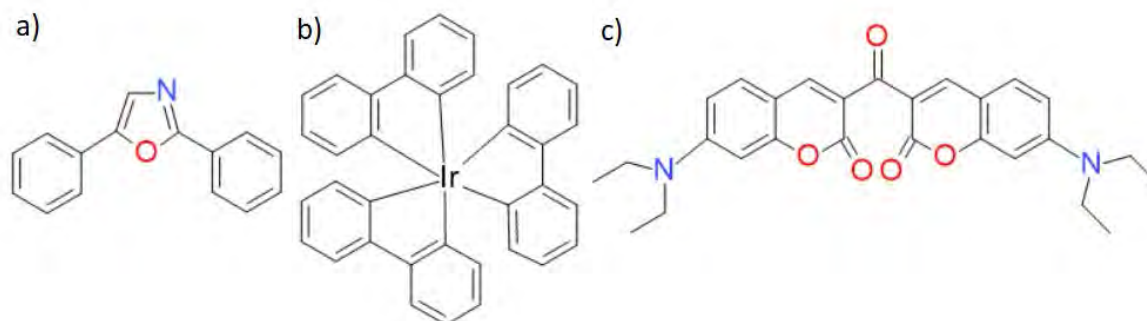


Fig. 1. a) 2,5-diphenyloxazole (PPO), b) iridium complex (Ir-C), c) 3,3'-Carboxylbis(7-diethylaminocoumarin)(CBDAC).

This work aimed to characterize the photophysical properties of PPO&Ir-C and PPO&CBDAC systems. Parameters like upconversion lifetime, fluorescence efficiency, upconversion efficiency and upconversion excitation threshold were measured to determine the statistical probability of PPO. Utilizing PPO as an emitter and Ir-C as a sensitizer in a photon upconverting solution, a concentration of PPO of 10 mM and Ir-C of 0.1 mM was identified as the optimal system, yielding the highest upconversion efficiency. The obtained results reveal a notably high threshold level (182.7 W/cm²) while an upconversion quantum efficiency (UCQY) of 2.4 % shows that Ir-C is not a suitable sensitizer as the UCQY is way lower compared to other systems employing PPO with different sensitizers. One of the reasons for the poor performance of this system could be the short lifetime of 1.5 us in Ir-C. CBDAC, however, shows a triplet lifetime of 21.8 us [1] which enhances the efficiency of the system.

[1] Uji, M., Harada, N., Kimizuka, N., Saigo, M., Miyata, K., Onda, K., & Yanai, N. (2022). Heavy metal-free visible-to-UV photon upconversion with over 20% efficiency sensitized by a ketocoumarin derivative. *Journal of Materials Chemistry C*, 10(12), 4558-4562. <https://doi.org/10.1039/d1tc05526g>

EXPLORING PHENOTHIAZINE AND ITS DERIVATIVES: HTMS FOR EFFICIENT DOPING FREE FLUORESCENT AND MULTIPLE-RESONANCE TADF OLEDs

Melika Ghasemi², Ramakant Gavale¹, Faizal Khan¹, Dmytro Volyniuk², Juozas Vidas Grazulevicius², Rajneesh Misra¹

¹Department of Chemistry, Indian Institute of Technology Indore

²Department of Polymer Chemistry and Technology, Kaunas University of Technology
melika.ghasemi@ktu.edu

According to spin statistics, by electronic excitation singlet and triplet excitons are theoretically generated in a 1:3 ratio, where triplet excitons are lost as heat and only singlet excitons are converted into photons, utilizing 25% of the exciton generation factor, leading to an external quantum efficiency (EQE) of about 5%-7.5% in devices. In organic light-emitting diodes (OLEDs), obtaining an efficient and stable fluorescent with high quantum efficiency is very desirable [1–3].

A series of novel metal-free organic compounds featuring phenothiazine and Tetraphenylethylene moieties were meticulously designed, synthesized, and characterized for their potential as blue/green emitters and hole transporting layers (HTLs) for OLEDs. The impact of donor moiety presence and absence on the device efficiencies were investigated. The photophysical studies revealed that all the compounds exhibit fluorescence, photoluminescence quantum yield of up to 39.64%, good thermal stability and hole transporting capabilities ($1.56 \times 10^{-4} \text{ cm}^2/\text{Vs}$ and $1.27 \times 10^{-4} \text{ cm}^2/\text{Vs}$ at $5 \times 10^5 \text{ V/cm}$ electric field) (Fig. 1b), all suitable for OLED applications. The compounds were tested as the emissive layer in doping free fluorescent devices obtaining EQE of 4.33% with a turn on voltage of 3.60V (Fig. 1a). The compounds were also used as HTL in multiple-resonance thermally activated OLEDs, resulting in EQE up to 7.45% and low turn on voltage of 4.60V (Fig. 1c).

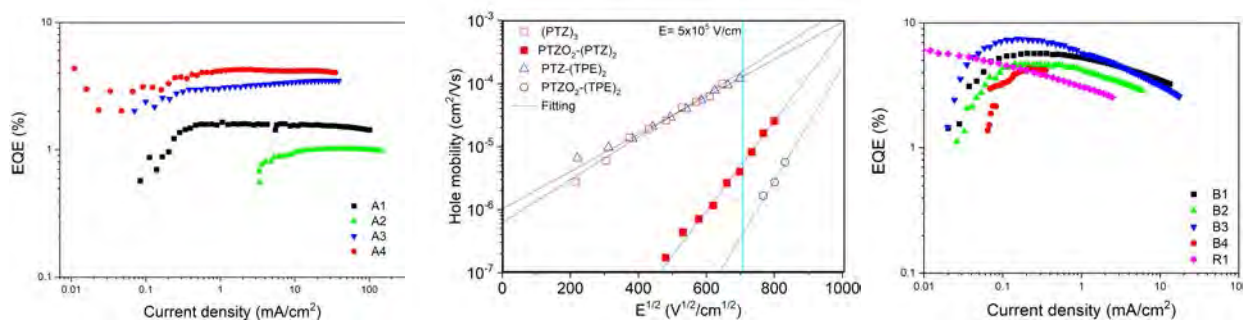


Fig. 1. (a) EQE versus current density as EML, (b) hole mobility versus electric field, and (c) EQE versus current density as HTL.

Acknowledgment

This project has received funding from the Research Council of Lithuania (Project “ELOS” No S-MIP-21-7).

- [1] H. Kaji, H. Suzuki, T. Fukushima, K. Shizu, K. Suzuki, S. Kubo, T. Komino, H. Oiwa, F. Suzuki, A. Wakamiya, Y. Murata, C. Adachi, Purely organic electroluminescent material realizing 100% conversion from electricity to light, *Nat Commun* 6 (2015) 1–8.
- [2] M. Pope, H.P. Kallmann, P. Magnante, Electroluminescence in organic crystals [16], *J Chem Phys* 38 (1963) 2042–2043.
- [3] H. Nie, Z. Zhao, Tang Ben Zhong, Aggregation-induced Emission Luminogens for Non-doped Organic Light-emitting Diodes, (2016).

3D LASER STRUCTURIZATION OF LUMINESCENT MATERIALS

Artūr Harnik¹, Ugnė Usaitė², Simas Šakirzanovas², Greta Merkininkaitė², Mangirdas Malinauskas¹

¹Laser Research Center, Faculty of Physics, Vilnius University, Vilnius LT-10223, Lithuania

²Institute of Chemistry, Faculty of Chemistry and Geosciences, Vilnius University, Vilnius LT-03225, Lithuania
artur30912@gmail.com

Luminescent materials have a wide array of different applications: from extensive use in lightings, displays and in medicine as markers to more niche uses as high temperature and pressure sensors. Furthermore, studies of luminescent materials have also been gaining more traction due to new innovative methods of their manufacturing as well as new quite promising applications. In this study a wide array of luminescent materials, as well as some initial results of synthesis and experimentation on luminescent materials will be provided and reviewed.

Luminescent materials used in laser structurization can be divided into two categories: organic and hybrid materials. Some good examples of a polymer doped with organic dyes were presented by A. Žukauskas et al. [1], and C.R. Mendonca et al. [2]. The main drawbacks of pure-organic phosphors as dopants seem to be low concentration and photostability of the dye in polymer matrix. A different example of a polymer doped using inorganic dopant was shown by J. Winczewski et al. [3]. In the aforementioned source, the only mentioned drawback is nonradiative relaxation. It should also be noted that while purely organic phosphors have a characteristic wider emission spectre, inorganic phosphors have a narrow emission spectre. Some promising results were also obtained in this study on the subject of YAG ($Y_3Al_5O_{12}$) synthesis inside a structurized polymer by utilising a femtosecond laser system. Figure 1 shows SEM images of microstructures obtained by laser irradiation:

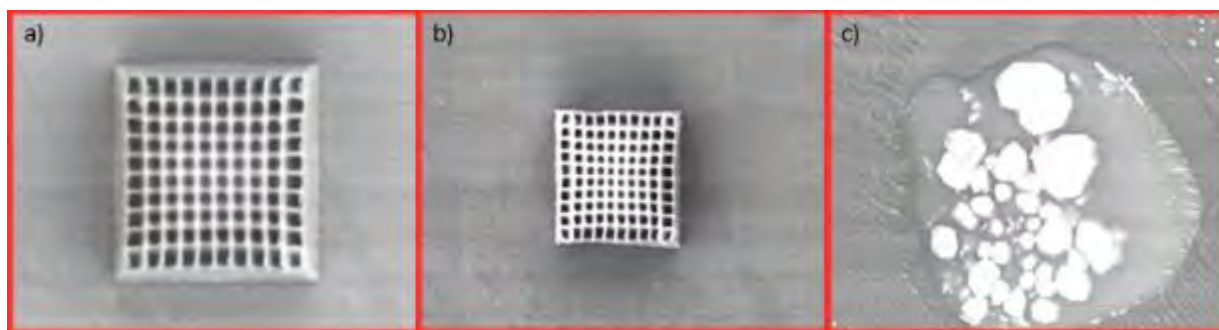


Fig. 1. 2500 times enlarged SEM image of a) microstructures obtained post-laser irradiation b) microstructures obtained after heating the sample in 600°C temperature c) microstructures obtained after further heating the sample in 1600°C temperature.

Initial results of the study show that polymer microstructures shrink when heated at 600°C. At 1600°C calcination removes the organic matter while leaving behind crystalline inorganic YAG. Unfortunately, synthesized YAG hasn't

retained the structures obtained during laser irradiation, so it's still a work in progress and the method has yet to be perfected.

This study shows that both types of luminescent materials still seem to have their characteristic drawbacks and as such can still be improved.

[1] A. Žukauskas, M. Malinauskas and the others. Organic dye doped microstructures for optically active functional devices fabricated via two-photon polymerization technique. *Lith. J. Phys.* 2010. 50. 55-61.

[2] C.R. Mendonca, D.S. Correa and the others. Three-dimensional fabrication of optically active microstructures containing an electroluminescent polymer. *Appl. Phys. Lett.* 2009. 95. 113309.

[3] J. Winczewski, M. Herrera and the others. Additive Manufacturing of 3D Luminescent $ZrO_2:Eu^{3+}$ Architectures. *Adv. Opt. Mater.* 2022. 10. 2102758.

TRI/TETRAPHENYLETHENYL COUPLED PHENOXAZINE AND PHENOTHIAZINE BASED HIGHLY FLUORESCENT MATERIALS SHOWING AIEE FOR OLEDs

Ehsan Ullah Rashid¹, Monika Cekaviciute¹, Jurate Simokaitiene¹, Juozas Vidas Grazulevicius¹, Dmytro Volyniuk¹, Khrystyna Ivanyuk², Pavlo Stakhira²

¹Department of Polymer Chemistry and Technology, Kaunas University of Technology, K. Barsausko st. 59, 51423, Kaunas, Lithuania

²Lviv Polytechnic National University, S. Bandera 12, 79013 Lviv, Ukraine
ehsan.rashid@ktu.edu

In order to develop effective blue emitters for organic light-emitting diodes (OLEDs), this work intends to synthesise three compounds based on phenoxazine and phenothiazine that are coupled with phenylethenyl using a single-step Buchwald-Hartwig approach. Results from photophysical studies suggest that, with increasing water percentage, compound dispersions in water-THF mixes exhibit strong aggregation-induced enhanced emission (AIEE). Cyan fluorescence is the most intense emission. Toluene solutions of the compounds have photoluminescence quantum yields ranging from 3-26%, and solid films have values ranging from 13.5-53%. The AIEE phenomenon is thought to be responsible for this finding. Computational simulations grounded on density functional theory were used to quantify intramolecular charge transfer, dihedral angles, border molecular orbitals, excitation energies, and wavelengths. Analyses of compounds' internal reorganisation energies, grounded on Marcus theory, reveal high levels of hole mobility. Cyclic voltammetry estimates the ionisation potentials and electron affinities of the compounds to be between 5.15 and 3.31 eV and 2.08 and 2.24 eV, correspondingly. Blue-cyan emission with an electroluminescence maximum of around 500 nm is shown by OLEDs built employing synthetic compounds as the host. External quantum efficiencies of 2.5–6% and brightness levels exceeding 1000 cd/m² are characteristics of the manufactured devices.

STUDY OF TIMING RESOLUTION OF PROTON IRRADIATED SILICON LOW GAIN AVALANCHE DETECTORS

Margarita Biveinytė¹, Tomas Čeponis¹, Laimonas Deveikis¹

¹Vilnius University, Institute of Photonics and Nanotechnology
margarita.biveinyte@ff.stud.vu.lt

Silicon is the most widely used semiconductor in micro- and nano-electronics applications. Silicon-based particle sensors are widely employed in high-energy and nuclear physics experiments for radiation registering. One of the most prominent examples is the Large Hadron Collider (LHC) based at the European Organization for Nuclear Research (CERN) where silicon-based sensors are employed for particle tracking applications. Silicon-based Low Gain Avalanche Detectors (LGAD) with additional p⁺ gain layer are characterised by their high time resolution and radiation hardness. Due to these properties LGADs are a promising alternative for p-i-n structure particle sensors in the future LHC upgrades [1]. The improvement of timing resolution on tracking sensors allows collecting only the data of time-compatible events and rejecting those events that cannot be associated to a track due to an excessive time difference [2].

However, high-energy radiation creates electrically active defects within the bandgap of the material, which determine the deterioration of sensors functional characteristics, e.g., increase of leakage current, decrease of charge collection efficiency, etc. [3], which also influence sensors temporal response. Therefore, it is important to characterise the devices before and after irradiation in order to evaluate the influence of radiation on the timing resolution of the sensor and predict its variations.

In this work, two sets of LGADs produced by Hamamatsu Photonics (HPK) [4] and Centro Nacional de Microelectronica (CNM) [5] with an active area of 1.3×1.3 mm² were investigated in a collaboration with CERN. The samples were irradiated with high energy protons (24 GeV) with fluences in the range of 10¹³ - 10¹⁵ p/cm². The timing resolution of the samples were examined and the correlations between its variations and proton fluences will be presented.

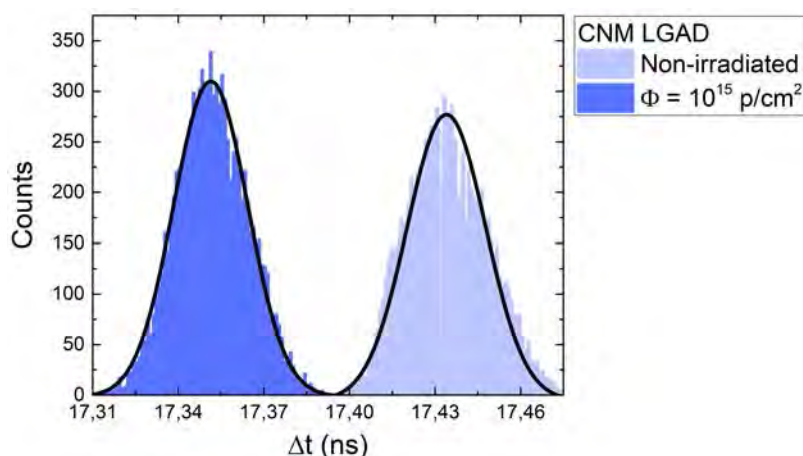


Fig. 1. Comparison of the distributions of time delay between laser pulse and detector signal between non-irradiated and irradiated with protons of fluence 10¹⁵ p/cm² samples.

-
- [1] B. Schmidt, J. Phys. Conf. Ser. Vol. 706 (2), 2016, p. 022002.
 [2] M. Carulla et al., Nucl. Instrum. Methods Phys. Res., Vol. 924, 2019, p. 373-379.
 [3] H. Spieler, Semiconductor Detector Systems, Oxford University Press, New York, 2005.
 [4] www.hamamatsu.com (last checked 25 January 2024).
 [5] www.imb-cnm.csic.es (last checked 25 January 2024).

LASER-ANNEALING FOR ANTIMONY SELENIDE (Sb₂Se₃) DEFECT PASSIVATION AND IMPROVEMENT OF Sb₂Se₃ THIN-FILM SOLAR CELL PARAMETERS

Rokas Kondrotas¹, Miglė Lenkauskaitė¹, Gustas Mickevičius¹, Marius Franckevičius¹, Vidas Pakštas¹

¹Center for Physical Sciences and Technology (FTMC)
migle.lenkauskaite@ff.stud.vu.lt

Antimony selenide (Sb₂Se₃) is a promising absorber material for photovoltaic application that has been widely researched for the past ten years. However, the main parameters of Sb₂Se₃ thin-film solar cells (such as efficiency, open-circuit voltage, short-circuit current and fill factor) still remain limited due to the presence of complex defects in the material [1]. In this study, we present an approach for minimizing defects at the interface of Sb₂Se₃ using laser-annealing strategy. The latter allowing the energy induced upon exposure to be precisely localized in time and space enables changes in crystallinity of the material [2]. During our experiments Sb₂Se₃ was deposited on FTO-coated glass substrates using the vapor transport deposition method. Sb₂Se₃ solar cell had Au contacts deposited on areas annealed with a laser as pictured in Figure 1.



Fig. 1. Sb₂Se₃ solar cell with Au contacts.

We show that laser annealing done with a 532 nm pulsed laser with varying values in power density slightly improved the main parameters characterising the performance of Sb₂Se₃ thin-film solar cells. Open-circuit voltage reached 310 mV compared to 300 mV in a reference cell. The efficiency value increased from 3,06 % to 3,37 %.

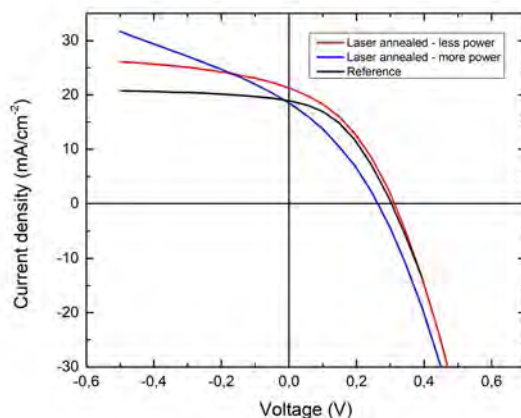


Fig. 2. Current-voltage (J-V) curves measured for a reference cell (black line), for a laser-annealed area with the most improved (red line) and decreased (blue line) parameters.

These results are considered to be related to an improved quality of the pn junction of the cell. Observed enhancement indicates the possibility that further experiments using different wavelength pulsed lasers could provide us with a better insight into correlation between the choice of a laser for the annealing process and the parameters of Sb₂Se₃ thin-film solar cells. In conclusion, this laser-annealing strategy has the potential for passivating various defects in the material and enhancing the performance of Sb₂Se₃ thin-film solar cells.

[1] C. Chen, K. Li, J. Tang, Ten Years of Sb₂Se₃ Thin-Film Solar Cells, Solar RRL, 2022.

[2] R. Nielsen, T. Hemmingsen, T. Bonczyk, et al., Laser Annealing and Solid-Phase Epitaxy of Selenium Thin-Film Solar Cells, ACS Applied Energy Materials, 2023.

CHARGE CARRIER MOBILITY IN Si IRRADIATED WITH FAST ELECTRONS

Paula Baltaševičiūtė¹, Algirdas Mekys¹, Leonid Makarenko², Šarūnas Vaitekoniš¹, Juozas Vidmantis Vaitkus¹

¹Vilnius University

²Belarusian State University

paula.baltaseviciute@ff.stud.vu.lt

Silicon material is widely used in semiconductor electronic devices, including irradiation detectors. Its demand is increased with grand applications for large facilities like CERN and many scientists are involved in the research to make Silicon detectors more irradiation resistant by exploiting defect engineering. To make it efficient, the research focuses on techniques like CV, IV, DLTS, TSC, photo absorption and more [1-4], capable to identify the impurities and their impact on the material parameters required for the device performance.

One of the popular techniques is charge carrier transport investigation exploiting Hall and magnetoresistance (MR) effects simultaneously. It is widely used to investigate electrical properties of semiconductors, including n-type Si, but much less information is available for boron doped p-type irradiated Si, where interstitial type defects are essential. So, this work is dedicated to applying Hall and MR effects to evaluate charge carrier transport peculiarities in p-type boron doped Si irradiated with fast electrons.

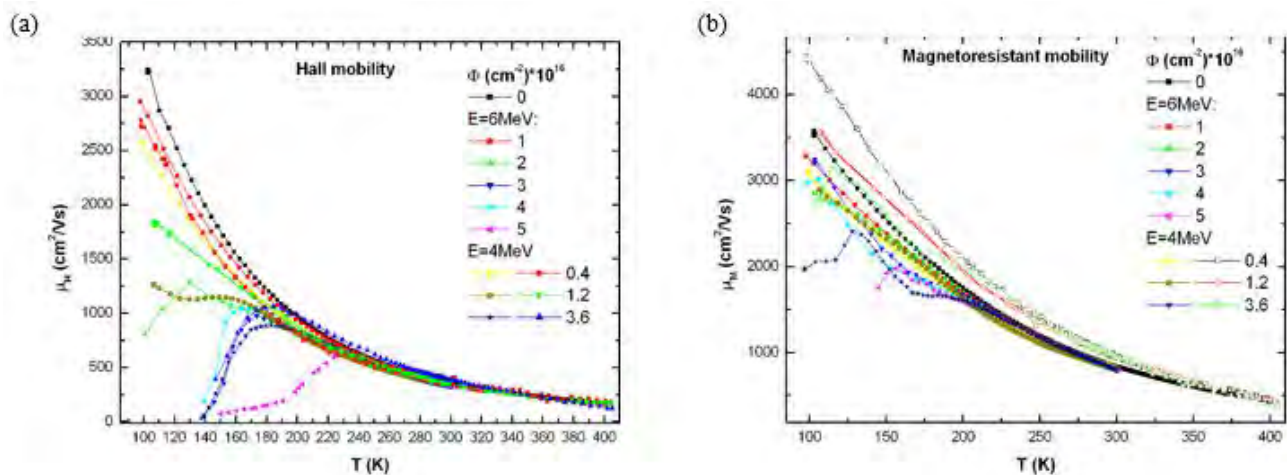


Fig. 1. Hall (a) and MR (b) mobility temperature dependencies for various irradiation fluencies

The measurements show a significant drop of Hall signal at lower temperatures, simultaneously with MR remaining high (Fig. 1). Charge carrier dependence on temperature reveals thermal activation energy (0.35-0.39eV), which was attributed to known point defect CiOi.

-
- [1] L. F. Makarenko et al, Phys. Status Solidi A 216 (2019) 1900354
 [2] C. Liao et al, Nucl. Ins. Phys. Res. A 1061 (2024) 169103
 [3] C. Besleaga et al, Nucl. Ins. Phys. Res. A 1017 (2021) 165809
 [4] V. P. Markevich et al, J Appl. Phys. 115 (2014) 012004

TRIPHENYLAMINE-BASED MONOLAYERS FOR OPTOELECTRONIC DEVICES

Aida Drevilkaukaitė¹, Artiom Magomedov¹, Vytautas Getautis¹

¹Kaunas University of Technology
aida.drevilkaukaite@ktu.edu

As energy consumption continues to grow, the need for more energy increases. Renewable energy has gained significant interest from both scientists and the industry over the past decade, with solar energy remaining the most popular source. To enhance absorption and efficiency, new technologies need to be developed as well as new materials need to be used.

Even though there is no perfect material for all, self-assembled monolayers (SAMs) are becoming the reference for hole-transporting materials in inverted perovskite solar cells (iPSCs) due to low material cost and simple layer formation. One of the most well-known SAMs is phosphonic acid with a carbazole moiety and different functional groups [1]. Although SAMs have shown promising results, there is still a lack of information on how the molecular structure of the SAMs is related to the electrical properties of the iPSC. Understanding how structural changes in SAM molecules are linked to performance in photovoltaic devices is crucial for modeling molecules with optimal performance and efficiency in different devices.

Phosphonic acid is known to make a strong bond with oxide surfaces [2] Yet, some authors shows that boronic acids might be better option because they are less acidic and potentially more stable in the device [3]. However, boronic acid compounds are known as materials that has lower stability and weaker bond with the surface compared to phosphonic acid. This research aims to determine whether triphenylamine-based phosphonic acid monolayers with different functional groups are a better choice than boronic acids for making efficient and stable solar cells. We used DFT calculations to predict dipole moments. Moreover, materials synthesis was performed using Hirao-Coupling reaction mechanism. The structural characterization was performed using NMR ¹H and ¹³C spectra and mass spectrometry. Additionally, devices with the mentioned materials will be constructed and characterized using a solar simulator.

[1] Al-Ashouri, A. et al., *Science* 2020, 370, 1300–1309 DOI: 10.1126/science.abd40

[2] Paniagua, S.A. et al., *Chemical Reviews* 2016, 116, 7117–7158 DOI: 10.1021/acs.chemrev.6b00061

[3] H. Guo et al, *National Science Review* 2023, DOI: 10.1093/nsr/nwad057

BROMOQUINOXALINE DERIVATIVES AS ORGANIC ROOM TEMPERATURE PHOSPHORESCENCE; SYNTHESIS AND INVESTIGATION

Mohamed Hassan Saad Abdella¹, [Jurate Simokaitiene](mailto:jurate.simokaitiene@ktu.lt)¹, Juozas Vidas Grazulevicius¹

¹Kaunas University of Technology
jurate.simokaitiene@ktu.lt

Organic luminophores with room temperature phosphorescence (RTP) or thermally induced delayed fluorescence are attractive alternatives to organic metal complexes due to their low cost, abundance, environmental friendliness, flexibility in synthesis, and high stability. [1]. sluggish intersystem crossover (ISC) can be a result of poor spin-orbit coupling [2]. As a result, achieving long-lived emission from triplet states is a difficulty. To enable efficient long-term emission, molecular design techniques that enhance ISC should be used. Organic compounds may be chemically changed by introducing heavy halogen atoms, and have significant spin-orbit coupling characteristics, which accelerate both the rate from T1 to S0 and the rate of ISC from S1 to Tn [3]. In this study, we developed a variety of simple brominated quinoxaline derivatives that were tested as RTP luminogens. By using a one-step imidization reaction [4], bromine substituted quinoxaline derivatives were synthesized from benzil or 4,4'-dibromobenzil and 3,6-dibromobenzene-1,2-diamine or benzene-1,2-diamine, respectively. The synthesised compounds showed RTP properties. Compounds with bromo atoms at the C-5 and C-8 quinoxaline positions exhibited the highest oxygen sensitivity.

-
- [1] Z. Xu et al. *Mater. Adv.*, 2 p. 5777-5784 (2021).
[2] Z. Wang et al. *Chem. Eur. J.*, 26(5) p. 1091-1102 (2020).
[3] Kenry et al. *Nat. Comm.* 10(2111) p. 1-15 (2019).
[4] M. Tingoli et al. *European J. Org. Chem.*, 2 p. 399-404 (2011).

3-(N,N-DIPHENYLAMINO)CARBAZOLE DONOR CONTAINING BIPOLAR DERIVATIVES WITH VERY HIGH GLASS TRANSITION TEMPERATURES AS POTENTIAL TADF EMITTERS FOR OLEDs

Daiva Tavgeniene¹, Raminta Beresneviciute¹, Gintare Krucaite¹, Sujith Sudheendran Swayamprabha², Jwo-Huei Jou², Saulius Grigalevicius¹

¹Department of Polymer Chemistry and Technology, Kaunas University of Technology, Radvilenu plentas 19, LT 50254, Kaunas, Lithuania

²Department of Materials Science and Engineering, National Tsing-Hua University, No.101, Kaungfu Rd. Hsin-Chu 30013 Taiwan, ROC
daiva.tavgeniene@ktu.lt

Blue light emitting derivatives, particularly the pure organic materials with suitable light colour and high morphological stability are very relevant in the OLEDs industry [1]. Achieving of a suitable light colour and suitable morphological stability in pure organic emitters is a hot investigations field in last years. At this time very actively studied TADF (thermally activated delayed fluorescent) emitters have also solved a disadvantage that only singlet excitons are used for traditional OLEDs [2].

We present well defined electroactive bipolar derivatives containing 3-(N,N-diphenylamino)-9H-carbazole as donor and (bis)phenylsulfone or benzophenone as acceptor fragments. Such structures are interesting as potential TADF emitting materials and we tested the derivatives in this field. 3-(N,N-Diphenylamino)carbazole fragment is useful for emitting properties of the materials and the bipolar nature is responsible for suitable transfer of charges in the emitting layer. Variation of the rigid aromatic structures also enabled us to synthesize the group of amorphous materials having very high values of glass transition temperature and also emitting derivatives for OLEDs. Novel electro-active bipolar derivatives have been prepared using 3-(N,N-diphenylamino)carbazole as electron donor fragment connected with various electron acceptors. The derivatives can form homogeneous solid amorphous layers with very high glass transition temperatures of 111–173 °C. The materials, which were well soluble in common organic solvents, were tested as emitting materials dispersed in 4,4'-bis(N-carbazolyl)-1,1'-biphenyl (CBP) host. The OLED with the emitter bis[4-(3-(N,N-diphenylamino)carbazol-9-yl)phenyl] sulfone exhibited the best overall performance. The OLED using the emitter demonstrated low turn-on voltage of 3.0 V, maximum brightness exceeding 2630 cd/m², current efficiency of 3.2 cd/A, power efficiency of 2.2 lm/W and EQE exceeding 1.7 % at 100 cd/m². For the technically important brightness of 1000 cd/m² efficiencies above 2.5 cd/A were obtained. The results demonstrate that some of the materials could be further investigated as potential TADF emitters.

Acknowledgements: This research was conducted in the frame of the project with support from the Research Council of Lithuania (grant No. S-LU-24-7).z

[1] Wang, S.; Zhang, H.; Zhang, B.; Xie, Z.; Wong, W.Y. Towards high-power-efficiency solution-processed OLEDs: Material and device perspectives. *Mater. Sci. Eng., R* 2020, 140, 100547.

[2] Teng, J.M.; Wang, Y.F.; Chen, C.F. Recent progress of narrowband TADF emitters and their applications in OLEDs. *J. Mater. Chem. C* 2020, 8, 11340-11353.

AMBIPOLAR HOSTS FOR BLUE TADF OLEDs: ASSESSMENT OF THE DEVICE PERFORMANCE AND LIFETIME

Kristupas Bagdonas¹, Goda Grybauskaitė¹, Gediminas Kreiza¹, Edvinas Orentas², Saulius Juršėnas¹, Karolis Kazlauskas¹, Dovydas Banevičius¹

¹Vilnius University, Institute of Photonics and Nanotechnology, Saulėtekio al. 3, Vilnius

²Vilnius University, Department of Organic Chemistry, Naugarduko g. 24, Vilnius
kristupas.bagdonas@ff.stud.vu.lt

In the past few years materials using thermally activated delayed fluorescence have experienced enormous attention thus allowing organic light emitting diodes (OLED) to reach internal quantum efficiency of 100%¹. However commercially viable devices must possess a high external quantum efficiency, which can be achieved by optimizing the OLED's architecture. Structural refinement is only achievable when the exciton distribution in emitting layer (EML) is known². It has been shown that by inserting a small amount of emitter that emits in another part of the spectrum it is possible to map exciton location in EML³.

The aim of the research was to show how exciton positions in EML depends on mixed host concentration. Using a well understood green **4CzIPN** emitter as pre, a portion of EML would be doped with it. By comparing the green shift of OLED's spectrum peak to the position of the probe in a mixed host, the exciton distribution will be determined.

Vacuum-deposited devices had an EML consisting of a mixed host **mCBP-CN:mCBP** doped with 7% **DMeCzIPN** emitter and probed with 2% **4CzIPN**. The device structure (see Fig. 1) is based on the past work of the scientific group⁴. OLEDs exhibited EQE up to 19% and the highest brightness up to 130000 cd/m² at a current density of 2500 mA/cm². The obtained results (see Fig. 1) show that the spectrum peak characteristics depend on the probe's position. At OLED turn-on, all devices exhibited spectrum peaks around 502 nm wavelength, meaning that the recombination zone is uniformly distributed in the EML. By increasing the voltage, devices with a probe further from the HTL showed a smaller peak shift, indicating that the recombination zone shifted towards the ETL.

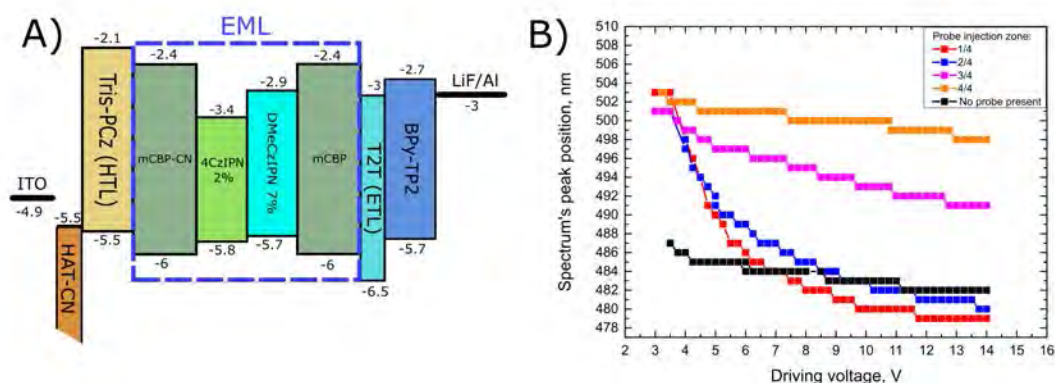


Fig. 1. A) Energy level diagram of mixed host OLED; B) Emission spectrum peak position vs driving voltage and its dependency on probe position

[1] Liang, X., Tu, Z.-L. and Zheng, Y.-X. Thermally Activated Delayed Fluorescence Materials: Towards Realization of High Efficiency through Strategic Small Molecular Design. *Chem. – Eur. J.* 25, 5623–5642 (2019).

[2] Mac Ciarnáin, R. et al. A Thermally Activated Delayed Fluorescence Green OLED with 4500 h Lifetime and 20

[3] Xu, M. et al. Analyzing exciton distribution in organic light-emitting devices using near-infrared probes. *Appl. Phys. Lett.* 122, 261107 (2023).

[4] Kreiza, G. et al. Ambipolar hosts for blue TADF OLEDs: Assessment of the device performance and lifetime. *Org. Electron.* 120, 106849 (2023).

PLASMON-ENHANCED VISIBLE LIGHT ABSORPTION FOR PHOTOCATALYTIC WATER SPLITTING

Klaudijus Midveris¹, Tomas Klinavičius¹, Andrius Vasiliauskas¹, Šarūnas Meškiniš¹, Muhammad Haris¹, Asta Tamulevičienė^{1,2}, Tomas Tamulevičius^{1,2}

¹Institute of Materials Science, Kaunas University of Technology, Lithuania

²Department of Physics, Kaunas University of Technology, Lithuania

klamid@ktu.lt

One of the most studied methods for producing hydrogen is photoelectrochemical (PEC) water splitting, which uses solar energy and semiconductors that are readily available on Earth [1]. The efficiency of the H₂ evolution process under solar light has been greatly enhanced using heterostructure photocatalysts made of semiconductor materials, coupled with plasmonic noble metal nanoparticles (NPs). This is enabled through the excitations of the conduction band electrons at the metal-dielectric interface. Light may be focused and “folded” onto a thin semiconductor film utilizing fabricated heterojunction structures, enhancing absorption characteristics by generating surface plasmon polaritons (SPPs) propagating at the metal/semiconductor interface as well as localized surface plasmons (LSPs) produced in noble metal nanoparticles [2]. This work investigates the effects of characteristic LSPs in quasi-random distributions of plasmonic metal nanoparticles on the visible light absorption and photocatalytic efficiencies of semiconducting TiO₂ as a vital comparative prerequisite for the utilization of plasmonic NPs organized into ultrathin periodic arrays with photonic spacings, able to support surface lattice resonances (SLRs), that show orders of magnitude stronger localized electromagnetic fields [3].

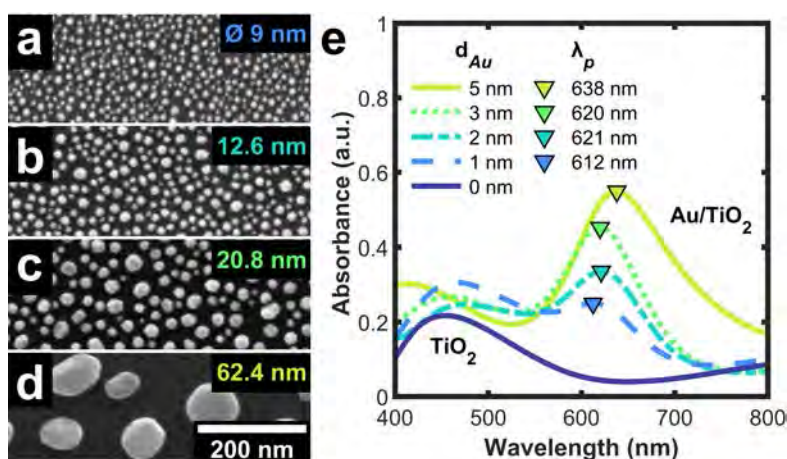


Fig. 1. SEM micrographs of Au nanoparticles (a-d) formed on 160 nm thickness TiO₂ thin film surface (numbers in the top-right corner indicate mean particle diameter) by dewetting different thickness d_{Au} Au films and characteristic LSPR enhanced absorption spectra peaks λ_p of 600 °C annealed Au-TiO₂ thin films (e).

The work was supported by the Research Council of Lithuania (LMT) project No. S-MIP-23-93.

[1] ZHOU, Peng, NAVID, Ishtiaque Ahmed, MA, Yongjin XIAO, Yixin, WANG, Ping, YE, Zhengwei, ZHOU, Baowen, SUN, Kai and MI, Zetian. Solar-to-hydrogen efficiency of more than 9 percent in photocatalytic water splitting. Nature 2023.

[2] ATWATER, HA, MATERIALS, A Polman. Plasmonics for improved photovoltaic devices. Nature 2010.

[3] JUODĖNAS, Mindaugas, TAMULEVIČIUS, Tomas, HENZIE, Joel, ERTS, Donats and TAMULEVIČIUS, Sigitas. Surface Lattice Resonances in Self-Assembled Arrays of Monodisperse Ag Cuboctahedra. ACS Nano 2019.

NEW BIPOLAR DERIVATIVES WITH DIPHENYLSULFONE OR DIPHENYLPHENONE AS TADF BASED EMITTERS OLEDs

Gintare Krucaite¹, Daiva Tavgeniene¹, Saulius Grigalevicius¹, Yi-Ting Chen², Yu-Hsuan Chen², Chih-Hao Chang², Raminta Beresneviute¹

¹Department of Polymer Chemistry and Technology, Kaunas University of Technology, Radvilenu plentas 19, Kaunas, Lithuania

²Department of Electrical Engineering, Yuan Ze University, Chungli, Taoyuan, Taiwan
gintare.krucaite@ktu.lt

To resolve the energy crisis, there has been huge interest in the development of lighting technologies that are energy-efficient, cleaner and more affordable. Organic light-emitting diodes (OLEDs), which are mainly formed of thin films of organic molecules, have been regarded as the sustainable and very attractive strategy to achieve the goal [1, 2, 3].

The TADF based emitters EM1–EM2 were prepared in reactions of the 3-(N,N-diphenylamino)-9H-carbazole with 9-(4-(4-fluorophenylsulfonyl)phenyl)carbazole or 4-(carbazol-9-yl)-4'-fluorobenzophenone, correspondingly.

Bipolar derivatives having thermally activated delayed fluorescence (TADF) functions were synthesized by multistep synthetic procedure by using 3-(N,N-diphenylamino)-9H-carbazole and 9-(4-(4-fluorophenylsulfonyl)phenyl)carbazole or 4-(carbazol-9-yl)-4'-fluorobenzophenone in the final step. The materials have high thermal stabilities and form molecular glasses with very high glass transition temperatures of 140 °C - 143 °C.

The compounds were tested in multilayer TADF based organic light emitting diodes (OLEDs). The most efficient green device demonstrated low turn-on voltage of 2.2 V, maximum luminance of 60155 cd/m² and high peak efficiency values of 12.1% (35.4 cd/A and 46.3 lm/W). At higher practical luminance of 100 cd/m² or 1000 cd/m², the device remained also highly efficient with 12.1% and 11.1%, correspondingly.

Acknowledgements. This research was also conducted in the frame of the project with support from the Research Council of Lithuania (Grant No. S-LU-24-7).

-
- [1] 1. S. W. Park, D. Kim, Y. M. Rhee, Overcoming the Limitation of Spin Statistics in Organic Light Emitting Diodes (OLEDs): Hot Exciton Mechanism and Its Characterization, *Int. J. Mol. Sci.* 24 (2023) 12362-12383.
 [2] 2. I. Siddiqui, S. Kumar, Y. F. Tsai, P. Gautam, Shahnawaz, K. Kesavan, J. T. Lin, L. Khai, K. H. Chou, A. Choudhury, S. Grigalevicius, J. H. Jou, Status and Challenges of Blue OLEDs: A Review, *Nanomaterials*. 13 (2023) 2521-2588.
 [3] 3. Z. Zhou, X. Xie, Z. Sun, X. Wang, Z. An, W. Huang, Recent advances in metal-free phosphorescent materials for organic light-emitting diodes, *J. Mater. Chem. C*. 11 (2023) 3143-3162.

SYNTHESIS AND CHARACTERIZATION OF NITROGEN MODIFIED REDUCED GRAPHENE OXIDE

Rūta Aukštakojytė¹, Rasa Pauliukaitė², Justina Gaidukevičė^{1,2}

¹Institute of Chemistry, Faculty of Chemistry and Geosciences, Vilnius University, Naugarduko Str. 24, LT-03225, Vilnius, Lithuania

²Department of Nanoengineering, Center for Physical Sciences and Technology, Savanorių Ave. 231, LT-02300
ruta.aukstakojyte@chgf.vu.lt

The successful application of reduced graphene oxide (rGO) in supercapacitors, (bio)sensors, fuel or solar cells strongly depends on its physicochemical properties. Recent research suggests that introducing heteroatoms (B, N, P, S) into rGO can significantly modify its electrochemical, electronic, and structural characteristics [1,2]. It is well known that nitrogen-rich sites in rGO can notably improve electrochemical activity, especially, in the presence of pyrrolic-N and pyridinic-N bonding configurations. N-doping also increases the electrical conductivity of graphene-based materials due to the formation of N-graphitic atoms in the lattice and enhances the specific surface area by larger defect sizes and a more porous structure [2]. In the case of B-doping, incorporating boron can create additional sites on the carbon surface, enhancing both hydrophilicity and material durability [3]. Consequently, the B- and N-codoped rGO (BN-rGO) samples synthesized with improved structural and electrochemical properties show promise as cost-effective and metal-free electrode materials for supercapacitors or (bio)sensors. This study focuses on the synthesis process and characterization of BN-rGO nanostructures. BN-rGO samples are prepared by a two-stage synthesis method: initially, a hydrothermal treatment of a graphene oxide/NH₄BF₄ mixture at 180 °C temperature for 20 hours, followed by thermal annealing in a tube furnace at 850 °C temperature for 30 min under Ar atmosphere. Various techniques, including scanning electron microscopy, transmission electron microscopy, energy dispersive X-ray spectroscopy, Raman spectroscopy, and nitrogen adsorption-desorption isotherms at 77 K, are used to analyze the impact of B- and N-incorporating on morphology and structure of rGO.

[1] Kaushal, S.; Kaur, M.; Kaur, N.; Kumari, V.; Singh, P. P. Heteroatom-doped graphene as sensing materials: a mini re-view. *RSC Adv* 2020, 10, 28608–28629.

[2] Li, D.; Duan, X.; Sun, H.; Kang, J.; Zhang, H.; Tade, M.O.; Wang, S. Facile synthesis of nitrogen-doped graphene via low-temperature pyrolysis: The effects of precursors and annealing ambience on metal-free catalytic oxidation. *Carbon* 2017, 115, 649–658.

[3] Gul, I.; Yar, M.; Ahmed, A.; Hashmi, M.A.; Ayub, K. Permeability of boron- and nitrogen-doped graphene nanoflakes for protium/deuterium ion. *RSC Adv* 2022, 12(7), 3883–3891.

DEPOSITION OF NICKEL-ION COATINGS USING MORPHOLINE BORANE AS A REDUCING AGENT

Dmytro Shyshkin^{1,2}, Zita Sukackienė¹, Jūratė Vaičiūnienė¹, Loreta Tamašauskaitė-Tamašiūnaitė¹, Eugenijus Norkus¹

¹Center for Physical Sciences and Technology (FTMC)

²Vilnius University

dmytro.shyshkin@ftmc.lt

In this study we investigate the deposition conditions of nickel-iron (NiFe) binary alloy coatings using low-cost and straightforward electroless metal deposition with morpholine borane (MB) as a reducing agent. The effect of Fe^{2+} concentration on the morphology, structure, and composition of the NiFe binary alloy coatings has been investigated. The plating solution consisted of 0.14 M nickel sulfate, 0.05 M ethylenediaminetetraacetic acid, 0.1 M sodium malonate, 0.2 M glycine, 0.2 M morpholine borane, and different concentrations of iron sulfate (0.5 mM, 1 mM, 5 mM, and 10 mM). The plating bath operated at a temperature of 60 °C. The morphology, structure and composition of the obtained NiFe binary alloys have been characterized by Scanning Electron Microscopy, Energy Dispersive X-ray Analysis, X-ray diffraction, and Inductively Coupled Plasma Optical Emission Spectroscopy. It was found that $\text{Ni}_{90}\text{Fe}_{10}$, $\text{Ni}_{80}\text{Fe}_{20}$, $\text{Ni}_{60}\text{Fe}_{40}$, and $\text{Ni}_{30}\text{Fe}_{70}$ coatings were deposited on copper surface than the concentration of Fe^{2+} in the plating solution was 0.5 mM, 1 mM, 5 mM, and 10 mM, respectively. The deposition rate for the $\text{Ni}_{90}\text{Fe}_{10}$, $\text{Ni}_{80}\text{Fe}_{20}$, $\text{Ni}_{60}\text{Fe}_{40}$, and $\text{Ni}_{30}\text{Fe}_{70}$ coatings was approximately 2.6, 3.6, 1.1, and 1.4 $\text{mg cm}^{-2} \text{h}^{-1}$, respectively.

Acknowledgment This research was funded by a grant (No. P-MIP-23-467) from the Research Council of Lithuania.

AN ENHANCED HYDROGEN EVOLUTION REACTION PERFORMANCE BY NICKEL-MANGANESE BIMETALLIC ELECTROCATALYSTS TOWARDS ALKALINE NATURAL SEAWATER AND SIMULATED SEAWATER SPLITTING

Sukomol Barua¹, Aldona Balčiūnaitė¹, Jūratė Vaičiūnienė¹, Loreta Tamašauskaitė-Tamašiūnaitė¹, Eugenijus Norkus¹

¹Department of Catalysis, Center for Physical Sciences and Technology (FTMC), Vilnius, Lithuania
sukomol.barua@ftmc.lt

In this work, 3D nickel-manganese (NiMn) bimetallic coatings have been studied as efficient and stable electrocatalysts towards the hydrogen evolution reaction (HER) in simulated seawater (1 M KOH + 0.5 M NaCl, @SSW) and alkaline natural seawater (1 M KOH + natural seawater, @ASW). These binary coatings have been electrodeposited on a titanium substrate using a facile electrochemical deposition method through a dynamic hydrogen bubble template technique. The as-deposited NiMn/Ti coatings with variable Mn concentrations produce typical globular and unique porous architecture with abundant pores of different sizes. The HER activity of these fabricated catalysts was investigated by using Linear Sweep Voltammetry (LSV) in alkaline seawater and simulated seawater at different temperatures, whereas, the morphology and composition were characterized by scanning electron microscopy (SEM) and inductively coupled plasma optical emission spectroscopy (ICP-OES). The NiMn/Ti-3, NiMn/Ti-4, and NiMn/Ti-5 were prepared using different chemical bath compositions, where Ni:Mn molar ratios were 1:3, 1:4 and 1:5, respectively.

The as-prepared NiMn/Ti-5 electrocatalyst exhibits excellent HER activity in simulated seawater with an ultra-low overpotential of 64.2 mV to reach the benchmark current density of 10 mA cm⁻². Notably, a current density of 10 mA cm⁻² is also attained by the NiMn/Ti-5 electrocatalyst with a comparably low overpotential of 76.5 mV in alkaline natural seawater. The current densities increase ca. 1.75–2.35 times with an increase in temperature from 25 °C to 75 °C for HER in both electrolytes. This bimetallic catalyst has exhibited excellent long-term stability at a constant potential of -0.232 V (vs. RHE) and a constant current density of 10 mA cm⁻² for 10 hours that convincingly pledged its higher durability and robust nature for real-life seawater splitting technology.

TERNARY NICKEL-IRON-PHOSPHOROUS ELECTROCATALYSTS FOR ALKALINE HYDROGEN EVOLUTION REACTION

Raminta Šakickaitė^{1,2}, Zita Sukackienė², Aldona Balčiūnaitė², Loreta Tamašauskaitė Tamašiūnaitė², Eugenijus Norkus²

¹Vilnius University, Faculty of Physics, Salėtekio ave. 9, LT10222 Vilnius, Lithuania

²Center for Physical Sciences and Technology (FTMC), Saulėtekio ave. 3, LT10257 Vilnius, Lithuania
raminta.sakickaite@ff.stud.vu.lt

In 2020, the European Union provided a Hydrogen strategy [COM/2020/301] for fostering sustainable economic growth, reducing carbon emissions, and advancing energy security by promoting the development and integration of clean hydrogen technologies. The efficiency of the hydrogen evolution reaction (HER) remains a challenge for low-cost hydrogen production via water splitting. In this study, ternary nickel-iron-phosphorous (NiFeP) coatings with different Fe amounts of 4, 8, and 12 at.% were synthesized using the electroless metal plating method. The morphology and composition of the NiFeP coatings were characterized using scanning electron microscopy (SEM) and energy-dispersive X-ray spectroscopy (EDX), whereas the electrocatalytic activity towards HER was examined by linear sweep voltammetry (LSV) in 1 M KOH solution at a scan rate of 2 mV s⁻¹.

It has been found that Ni₈₅Fe₄P₁₂, Ni₈₀Fe₈P₁₂, and Ni₇₅Fe₁₂P₁₂ coatings with crack-free and globular morphology were successfully prepared using the electroless metal plating and sodium hypophosphite as a reducing agent. HER investigation results in Fig. 1 show that, among the investigated catalysts, the lowest onset potential of -250 mV at -1 mA cm⁻², overpotential of -325 mV at -10 mA cm⁻² and Tafel slope of 71.5 mV dec⁻¹ gives the Ni₈₅Fe₄P₁₂ coating with a lowest amount of Fe (4 at.%), indicating the highest activity of this catalyst for HER. The calculated Tafel slopes were 71.5, 72.3, and 77.5 mV dec⁻¹ for Ni₈₅Fe₄P₁₂, Ni₈₀Fe₈P₁₂, and Ni₇₅Fe₁₂P₁₂ coatings, respectively, indicating that HER might occur through the Volmer–Heyrovsky mechanism - which is for water molecules or H₂ to adsorb onto an electrode to generate MH_{ads} species. The obtained catalysts showed perspective as good candidates as cathode materials for hydrogen production in alkaline media.

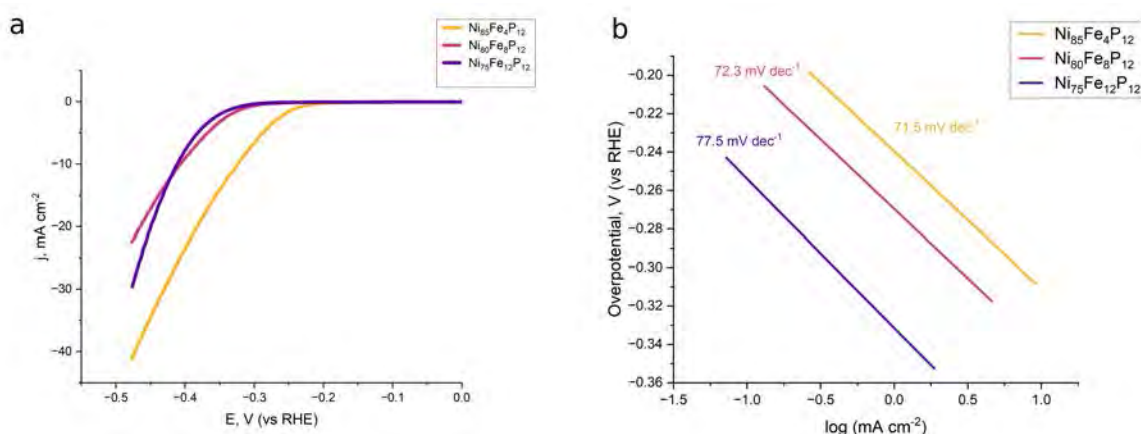


Fig. 1. LSV curves recorded for Ni₈₅Fe₄P₁₂, Ni₈₀Fe₈P₁₂, and Ni₇₅Fe₁₂P₁₂ coatings in 1 M KOH at 2 mV s⁻¹ (a) and Tafel slopes for corresponding curves (b)

Subscript besides Ni, Fe and P indicates at%, total of 100% (due to mathematical rule of rounding not all subscripts might add up to 100%)

TIPS-NPH AND IRIIDIUM COMPLEX SYSTEM FOR PHOTON UPCONVERSION FROM VISIBLE LIGHT TO UV

Džiugas Krencius¹, Naglis Vasarevičius¹, Manvydas Dapkevičius¹, Justas Lekavičius¹, Steponas Raišys¹,
Karolis Kazlauskas¹

¹Vilnius University
dziugas.krencius@ff.stud.vu.lt

Certain photocatalytic reactions, such as those involved in wastewater treatment and water splitting, demand the use of high-energy UV photons. Nevertheless, the deficiency of natural sunlight intensity in the UV region and the suboptimal efficiency and limited lifespan of artificial light sources pose significant challenges. Moreover, photochemical catalysis applications like laser 3D printing necessitate the concentration of energy at a specific point, circumventing any material between that point and the light source. A potential resolution to these issues is the implementation of Vis-to-UV photon upconversion (UC).

In our investigation, we explored a UC system comprising the annihilation properties of 1,4-Bis((triisopropyl silyl)ethynyl)naphthalene (TIPS-Nph) and the sensitizing capabilities of an iridium complex (Ir-C). Initially, the fluorescence quantum yields (QY) of TIPS-Nph solutions were measured. These measurements yielded promising results, with a QY reaching 53.5%. While solutions are impractical for real-world applications, subsequent measurements of drop-casted TIPS-Nph films proved encouraging. Emitter concentration optimization in films with a polystyrene matrix demonstrated a fluorescence QY as high as 44%.

Encouraged by these standalone emitter results, we prepared solutions incorporating the Ir-C sensitizer. Two solutions with a 0.1mM sensitizer to 1mM emitter and then a 10mM concentration ratio achieved UC-QY of 2.8% and 3.2%, respectively. However, drop-casted films with 0.5% (weight) sensitizer and varying emitter concentrations for optimization in polystyrene matrix showed no photon upconversion. Presence of impurities was determined in the emitter which was likely to cause lack of upconversion in the films.

IRON AND CERIUM ION EXCHANGE ON ZEOLITE AS BIFUNCTIONAL ELECTROCATALYST FOR OER AND ORR IN ALKALINE MEDIA

Ana Nastasić¹, Jadranka Milikić¹, Kristina Radinović¹, Aldona Balčiūnaitė², Vladislav Rac³, Biljana Šljukić^{1,4}

¹University of Belgrade, Faculty of Physical Chemistry, Studentski trg 12-16, 11158 Belgrade, Serbia

²Center for Physical Sciences and Technology, Sauletekio Ave. 3, Vilnius LT-10257, Lithuania

³Faculty of Agriculture, Department of Chemistry, University of Belgrade, Nemanjina 6, 11080 Zemun, Serbia

⁴CeFEMA, Instituto Superior Tecnico, Universidade de Lisboa, 1049-001 Lisbon, Portugal

ana.nastasic8@gmail.com

Metal-air batteries (MABs) and unitized regenerative fuel cells (URFCs) are one of the most promising electrochemical devices for energy conversion and storage that could support the energy transition from fossil fuels to clean and sustainable energy sources [1]. The oxygen reduction reaction (ORR) and the oxygen evolution reaction (OER) are key reactions for rechargeable MABs and URFCs. Therefore, their performance is highly dependent on the design and activity of the ORR/OER bifunctional electrocatalyst [2].

Zeolites are recognized as promising electrode materials due to their unique structure, large surface area, as well as exceptional ion-exchange capacity and adsorption [2,3]. Herein, the electrocatalytic activity of the material obtained by ion exchange of iron and cerium on zeolite (FeCeZM) was examined towards ORR and OER in alkaline media (**Fig. 1**).

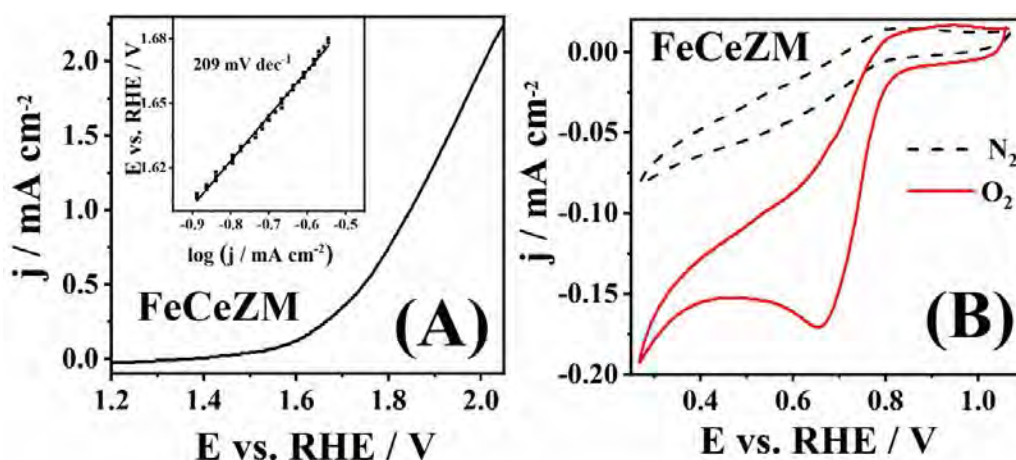


Fig. 1. OER polarization curve (iR-corrected) of FeCeZM with the corresponding Tafel plots in inset (A), and CVs of FeCeZM in N₂- and O₂- saturated 1 M KOH (aq) at 5 mV s⁻¹ (B).

The OER polarization curve (**Fig. 1A**) shows an onset potential of 1.69 V and Tafel slope of 209 mV dec⁻¹. The aforementioned OER kinetic parameters of FeCeZM are comparable to those reported for other modified zeolite materials in literature [2]. FeCeZM was examined in N₂- and O₂- saturated 1 M KOH solution (**Fig. 1B**) by cyclic voltammetry (CV). A characteristic well-defined peak was observed in the O₂- saturated solution at 0.66 V showing a current density of -0.17 mA cm⁻², in contrast to the N₂-saturated solution in which no peak was observed. This peak corresponds to the reduction of O₂ and indicates that the FeCeZM material is active for the ORR. FeCeZM showed catalytic activity for both OER and ORR, making it a potentially good bifunctional ORR/OER electrocatalyst.

[1] Y. Arafat et al., *Adv. Energy Mater.* 11, 2100514 (2021)

[2] J. Milikić et al., *J. Electroanal. Chem.* 944, 117668 (2023)

[3] J. Milikić et al., *Synth. Met.* 292, 117231 (2023)

INTEGRATION OF SILVER NANOPARTICLE POLYMER NANOCOMPOSITES AND 3D PRINTING TECHNOLOGIES FOR DURABLE ANTIMICROBIAL COVERS

Mindaugas Illickas¹, Asta Guobienė¹, Karolis Gedvilas^{2,3}, Mantvydas Merkis⁴, Brigita Abakevičienė^{1,4}

¹Kaunas University of Technology, Institute of Materials Science, Lithuania

²Faculty of Natural Sciences, Vytautas Magnus University, Lithuania

³Research Institute of Natural and Technological Sciences, Lithuania

⁴Department of Physics, Kaunas University of Technology, Lithuania
mindaugas.ilickas@ktu.edu

Efforts to combat microorganisms focus on surface modification and antimicrobial coatings, emphasizing the direct application of biocidal substances without affecting bulk properties. Advances in antimicrobial materials involve polymer-solvent-active material composites [1], resulting in varied antimicrobial effects. 3D scanning and printing enable the creation of intricate, flexible coatings [2], suitable for frequently touched surfaces to reduce the spread of microorganisms and pathogens. In this work, AgNP synthesized through photochemical methods [3] are combined with a PVB polymer matrix to create a silver nanoparticles - polymer nanocomposite (AgNP-PVB). This nanocomposite is applied as a thin-film coating on customized protective covers produced using 3D scanning and printing. An algorithm developed in Matlab reconstructs the 3D model. To assess the antiviral effect, 10-well substrates are 3D printed, with 8 wells filled with the test solution for 24 hours. The 9th and 10th wells were maintained as controls, and after 24 hours, the same test solution was added to them before PCR analysis. At 500 ppm AgNP concentration, the antiviral assay showed a test well cycle threshold (Ct) value of 30.78 ± 2.00 , while the control well had a Ct value of 25.92 ± 0.04 . At 200 ppm, the test well Ct value was 28.22 ± 0.88 , and the control well had a Ct value of 24.65 ± 0.40 . The coating's Ct values were akin to the 200 ppm control wells, with a test value of 25.27 ± 1.41 and a control value of 24.61 ± 0.11 , indicating that even the Flexible 80A polymer itself possesses antiviral properties. The work conducted pilot 3D printing to apply tested coatings on various objects, choosing a door handle cover as a frequently touched item. Using a 3D model obtained through scanning, the cover was reconstructed with a developed algorithm. This research contributes to durable antiviral coatings, addressing the prevention of infectious disease transmission in various environments.

[1] G. Isopencu, et al., Recent Advances in Antibacterial Composite Coatings, *Coatings* 12 (2022).

[2] J. Wang, et al., Stereolithographic (SLA) 3D printing of oral modified-release dosage forms, *International Journal of Pharmaceutics*, 503(1–2), 207–212 (2016).

[3] M. Schmallegger, et al., Bis(acyl)phosphine Oxides as Stoichiometric Photo-Reductants for Copper Nanoparticle Synthesis: Efficiency and Kinetics, *ChemPhotoChem*, 6(12) (2022).

IMPROVING THE STABILITY OF PEROVSKITE FILMS IN AMBIENT CONDITIONS

Illia Filipas¹, Mantas Marčinkas¹, Artiom Magomedov¹, Matas Steponaitis¹

¹Department of Organic Chemistry, Kaunas University of Technology, Lithuania
illia.filipas@ktu.edu

Perovskite solar cells have recently emerged as an attractive renewable energy alternative due to their low production cost and superior efficiency. However, improving the stability of perovskite films remains a major challenge. In particular, one of the factors, accelerating the degradation of the perovskite is its sensitivity to ambient moisture. It makes it difficult to fabricate devices without the nitrogen gloveboxes, because of the increased spread of the results.

In our work, we are testing the strategy of the post-treatment of the perovskite film by spin-coating the carbazole-based phosphonic acid, containing hydrophobic fluorine atoms on top of it. The phosphonic acid fragment is expected to strongly bind to the surface of the perovskite, while the carbazole unit with fluorine serves as protection against moisture. In addition, the presence of a semiconducting unit could potentially have a beneficial effect on the performance of the devices.

The stability of the films was inspected visually, by storing samples at the 20-30 % humidity environment. For the control samples, already after 1 week, complete discoloration happened. On the other hand, for the samples treated with hydrophobic material, the dark brown color remained even after one month of storage. In the continuation of the work the proposed method will be tested in the devices, expecting to see improvements in processability of the perovskite solar cell devices. In addition, more materials will be tested, to elucidate the impact of various substituents on the resilience of the films.

INVESTIGATION OF THE SMARTPHONE CAMERA WITH SOLID-STATE ILLUMINATION FOR HYPERSPECTRAL IMAGING

Agnė Urbonaitė¹, Pranciškus Vitta¹

¹Institute of Photonics and Nanotechnology, Faculty of Physics, Vilnius University, Lithuania
agne.urbonaite@ff.stud.vu.lt

Every camera including those in smartphones can be called quasi-hyperspectral imaging devices due to the typical three- or four-color channel imaging. In particular Red (R), Green (G), Blue (B) and sometimes IR colors are captured separately resulting in a stack of monochromatic pictures. Such an approach is sufficient for taking the best memories of your life but usually is not sufficient for the analytical and scientific analysis of the objects under investigation. Therefore, a choice of sophisticated and expensive imaging instruments in the market is available and expanding each year. In particular, multicolor imaging devices and even imaging spectrophotometers (hyper spectral cameras) are available and applied for scientific purposes. Unfortunately, such devices are sophisticated, bulky, expensive and very difficult to operate.

In this work we present a slightly different approach of hyperspectral imaging where standard smartphone camera in combination with multicolor illumination system is applied. Such a system could be applied in variety of fields ranging from artwork investigation to medical examination or sophisticated laparoscopy surgery. The aim of the work is to develop the principles of the smart solid-state lamp with direct control from the smartphone to take pictures at different illumination regimes (different colors). To accomplish this task the camera properties of the brand-new smartphone (Google Pixel 7 pro) were investigated and tested at different regimes. In particular, dynamic linearity, flat field pixel mapping, sensitivity spectra, etc. were measured. Furthermore, the proof of concept was demonstrated by taking pictures at different illumination regimes, and color discrimination ability calculated.

To conclude we have demonstrated that even consumer-market-grade smartphone camera might be operated as multispectral imaging device for a specific task. On the other hand the applicability limitation of such an approach has to be taken into account.

STUDY OF CARRAGEENAN FERRIC OXIDE TENSION SENSORS

Elena Deneb Casas Borregón¹, Jūratė Jolanta Petronienė², Vytautas Bučinskas²

¹Universidad Politécnica de Madrid

²Vilnius Gediminas Technical University

elena-deneb.casas-borregon@stud.vilniustech.lt

This research presents a comprehensive exploration of the development and experimental study of piezoresistive sensor prototypes based on carrageenan and ferric oxide (Fe_2O_3), while also highlighting their key features and properties. These materials, abundant and accessible, showcase promising potential for the spread of green technologies in sensing applications.

Carrageenan, recognized for its favorable structure and compatibility with biomedical applications, takes centre stage as the foundational element of the sensor. Its selection is strategic, capitalizing on its properties to optimize sensor performance. Simultaneously, the inclusion of Fe_2O_3 in the sensor design exploits its semiconductor properties, facilitating the exploration of current variations induced by strain and establishing a reliable range of effective sensing.

Incorporating glycerol becomes essential to improve elasticity and shield the material from environmental impact. This addition ensures flexibility, preserving the sensor's integrity across diverse conditions. The research not only contributes to sustainable sensing technologies but also highlights the affordability, accessibility, and eco-friendly attributes of carrageenan and Fe_2O_3 based sensors, showcasing their potential applications in various fields.

[1] U. Žaimis, J. J. Petronienė, A. Dzedzickis, and V. Bučinskas. Biodegradable Carrageenan-Based Force Sensor: An Experimental Approach. *Sensors*, vol. 23, no. 23, p. 9423, Nov. 2023. doi: 10.3390/s23239423.

SYNTHESIS AND INVESTIGATION OF VANILLIN-BASED VITRIMERS

Brigita Kazlauskaitė¹, Sigita Grauzėlienė¹, Jolita Ostrauskaitė¹

¹Department of Polymer Chemistry and Technology, Kaunas University of Technology, Lithuania
b.kazlauskaite@ktu.edu

Vitrimeres are a class of materials that exhibit a dynamic covalent behavior similar to that of traditional polymers, but with the ability to undergo reversible chemical transformations without losing their material properties [1]. This dynamic nature allows to be reshaped, reprocessed, and recycled multiple times without losing their mechanical properties [2]. The ability to undergo reversible reactions makes vitrimers attractive for applications in self-healing, recyclable and shape-memory polymers.

The aim of this research was to synthesize sustainable materials using functionalized vanillin due to its antibacterial and antifungal properties which are relevant nowadays. Functionalized vanillin can be a good alternative to the most widely used cross-linker with the bisphenol A fragment, as it has a vanillin-based backbone with high rigidity and thermal stability. Studies have suggested that bisphenol A can mimic the action of the hormone estrogen in the body. There is ongoing research and debate regarding the potential health effects of bisphenol A exposure, with concerns raised about its possible links to reproductive, developmental, and endocrine-related issues [3]. Consequently, functionalized vanillin (Fig. 1) together with other monomers in different ratios was chosen for the preparation of UV-curable resins. Functionalized bisphenol A was chosen to compare the properties of the resulting polymers. The synthesized vitrimers showed reprocessability, shape memory, and self-healing properties due to a sufficient amount of hydroxyl and ester groups that are beneficial for transesterification reactions. The properties of vanillin-based vitrimers were similar to those of bisphenol A-based vitrimers.

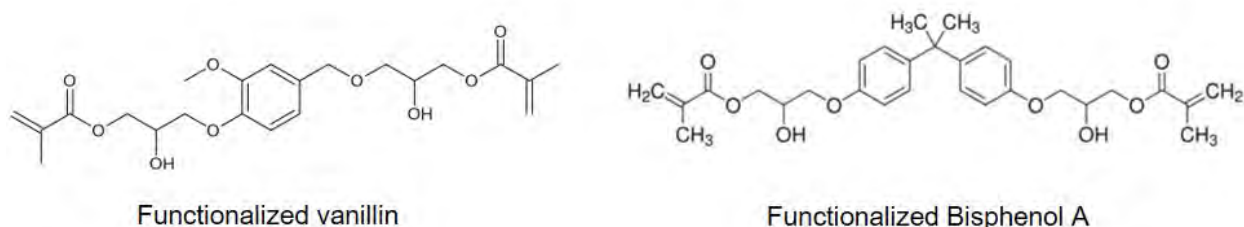


Fig. 1. Chemical structures of functionalized vanillin and Bisphenol A.

Acknowledgement. This research was funded by the Research Council of Lithuania (project No. S-MIP-23-52).

-
- [1] W. Post, A. Susa, R. Blaauw et al., A Review on the Potential and Limitations of Recyclable Thermosets for Structural Applications, *Polymer Reviews* 60, 359-388 (2020).
 [2] B. Zhang, K. Kowsari, A. Serjouei et al., Reprocessable thermosets for sustainable three-dimensional printing, *Nature Communications* 9, 1831, (2018).
 [3] H. E. Costa, E. Cairrao, E. Effect of bisphenol A on the neurological system: A review update. *Archives of Toxicology*, 98, 1-73 (2024).

SYNTHESIS, CHARACTERIZATION, AND APPLICATION OF POLYVINYLPIRROLIDONE (PVP)/MnFe COMPOSITE FOR WATER SPLITTING

Karina Vjūnova^{1,2}, Huma Amber¹, Jūratė Vaičiūnienė¹, Loretta Tamašauskaitė-Tamašiūnaitė¹

¹Center for Physical Sciences and Technology

²Vilnius University

karina.vjunova@chfg.stud.vu.lt

Electrochemical water splitting is one of the best methods for producing hydrogen and oxygen on an industrial scale, but the high cost and unavailability of noble metals on a commercial level limit its application for hydrogen and oxygen evolution reactions (HER and OER). Developing cost-effective and efficient non-noble metal-based electrocatalysts for HER and OER is challenging. In this work, the hydrothermal synthesis method has been employed for the preparation of the PVP/MnFe composite. The surface morphology, structure, and composition of the PVP/MnFe composite have been characterized using scanning electron microscopy (SEM), X-ray diffraction (XRD), and inductively coupled plasma optical emission spectroscopy (ICP-OES). The activity of PVP/MnFe nanocomposite has been investigated for HER and OER in 1 M KOH solution by recording linear sweep voltammograms (LSVs) at a scan rate of 2 mV s⁻¹. It was found that the synthesized PVP/MnFe composite contained 14 wt.% of Mn and 86 wt.% of Fe and exhibited an onset potential of -0.14 V for HER and 1.53 V for OER, indicating a good activity for both reactions.

SPECTROSCOPIC ANALYSIS OF FIVE RV TAURI TYPE STARS WITH NO IR EXCESS

Karina Korenika¹, Kārlis Puķītis¹

¹Laser Centre, Faculty of Physics, Mathematics and Optometry, University of Latvia, Latvia
karina.korenika.cl@gmail.com

The main characteristic of RV Tauri type variable stars is the presence of pulsation caused alternating deep and shallow minima in their light curves. Many of these stars possess a peculiar photospheric abundance pattern called depletion – those chemical elements that have high dust condensation temperature are systematically underabundant. The peculiarity is generally thought to be caused by re-accretion of gas from a dusty disc [1]. This surrounding structure causes IR excess in spectral energy distribution of RV Tauri type objects. Indeed, depletion has been observed mainly for those stars that have IR excess; however, there are a few depleted ones that show no excess [2]. Probably for these latter objects the disc, that caused the depletion, has dissipated. Evolution of discs surrounding RV Tauri type stars and other related objects is very poorly understood.

We have observed spectra of 11 RV Tauri type stars that have no IR excess with the main goal of searching for depletion patterns. The observations were carried out with the high-resolution Fiber-fed Echelle Spectrograph (FIES) at the Nordic Optical Telescope and Vilnius University Echelle Spectrograph (VUES) at the 1.65-metre telescope in the Molėtai Astronomical Observatory. Here we present first results of spectroscopic analysis for five of the observed stars: V399 Cyg, V894 Per, AA Ari, HD 172810, and V457 Cyg.

We identify absorption lines of multiple chemical elements in the spectra and measure their equivalent widths. These are used to derive photospheric parameters and chemical element abundances. The calculations are done by using the code SPECTRUM [3] and ATLAS model atmospheres [4]. Photospheric parameters are determined by employing the method of excitation and ionization balance for iron lines. Derived effective temperatures are in range of 4000 to 8000 K, surface gravities are no higher than $\log g = 2.5$ and iron abundances range from $[\text{Fe}/\text{H}] = -1.5$ to $+0.3$. Only in the case of V457 Cyg, the abundance pattern indicates depletion (Figure 1).

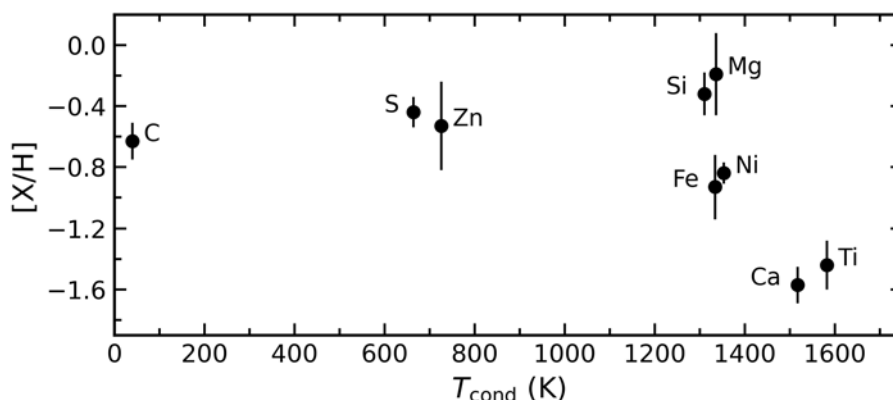


Fig. 1. Photospheric abundances of V457 Cyg as a function of dust condensation temperature, for which values from the study [5] are used. Vertical lines show the standard deviation of the calculated abundances.

We acknowledge the support from the Latvian Council of Science, project “Advanced spectroscopic methods and tools for the study of evolved stars”, project No. lzp-flpp-2020/1-0088.

-
- [1] G.-M. Oomen, H. Van Winckel, O. Pols, and G. Nelemans, Modelling depletion by re-accretion of gas from a dusty disc in post-AGB stars, *Astronomy & Astrophysics*, 629, A49 (2019).
 [2] I. Gezer, H. Van Winckel, Z. Bozkurt, et al., The WISE view of RV Tauri stars, *Monthly Notices of the Royal Astronomical Society*, 453, 133 (2015).
 [3] R. O. Gray and C. J. Corbally, The Calibration of MK Spectral Classes Using Spectral Synthesis. I. The Effective Temperature Calibration of Dwarf Stars, *The Astronomical Journal*, 107, 742 (1994).
 [4] R. L. Kurucz, ATLAS12, SYNTH, ATLAS9, WIDTH9, et cetera, *Memorie della Societa Astronomica Italiana Supplementi*, 8, 14 (2005).
 [5] K. Lodders, Solar System Abundances and Condensation Temperatures of the Elements, *The Astrophysical Journal*, 591, 1220 (2003).

CHEMICAL ANALYSIS OF SOLAR TWIN AND ANALOGUE STARS

Ugnė Jonauskaitė¹, Edita Stonkutė²

¹Institute of Theoretical Physics and Astronomy, Faculty of Physics, Vilnius University
ugne.jonauskaite@ff.stud.vu.lt

The existence of planets near other stars has been assumed since ancient times, but only in 1995 was a planet near a sun-like star - Pegasus 51 - discovered and confirmed. The study of exoplanets is a new and rapidly developing field of astrophysics and the discovery of this exoplanet was awarded the Nobel Prize in Physics in 2019.

Our Sun has planets orbiting around it and it is the best analysed star in the whole universe. Solar twin and analogue stars are important to exoplanet research as they have similar atmospheric characteristics to the Sun. Because of this, it is safe to assume that their evolution history should be similar as well. These stars are useful when researching the differences between stars with confirmed different planets and stars without confirmed planets.

But the success of these observations heavily depends on ground-based telescopes, whose data analysis will help to characterize the stars and, simultaneously, the planets orbiting them.

Therefore in order to better understand the planetary hosts and their planets from Moletai astronomical observatory data I determined the abundances of magnesium and silicon for 30 solar twin and analogue stars with confirmed exoplanets. In this poster, I will present my findings.

Part of this project has received funding from the Research Council of Lithuania (LMTLT), agreement No S-ST-23-108.

INVESTIGATING THE CONNECTION BETWEEN GALACTIC OUTFLOW AND GALAXY PROPERTIES

Milda Valytė¹, Kastytis Zubovas^{1,2}

¹Institute of Theoretical Physics and Astronomy, Vilnius University, Lithuania

²Department of Fundamental Research, Center for Physical Sciences and Technology, Lithuania
 milda.valyte@ff.stud.vu.lt

Understanding the impact of active galactic nuclei (AGN) on the formation and evolution of galactic outflows is crucial for gaining insights into galaxy evolution. These outflows can influence the interstellar medium, which affects star formation. To deepen our understanding of the mechanisms driving outflows and galaxy evolution it is important to comprehend how parameters of AGN (such as AGN luminosity L_{AGN} and the black hole mass M_{BH}) and the host galaxy (such as the virial mass and bulge gas fraction) relate to the characteristics of galactic outflows, such as mass transfer rate, outflow radius, velocity, energy and momentum rates.

In this study we employed the MAGNOFIT (Massive AGN OutFlow Investigation Tool) software package [1] to model 50,000 AGN wind-driven outflows. For each of the main outflow properties, we checked which of the AGN and galaxy parameters are primarily controlling it with the use of the residual method [2]. We also investigated how outflow properties depend on various galaxy parameters in narrow ranges of L_{AGN} and M_{BH} to determine which other properties of the modelled systems are important in determining outflow evolution.

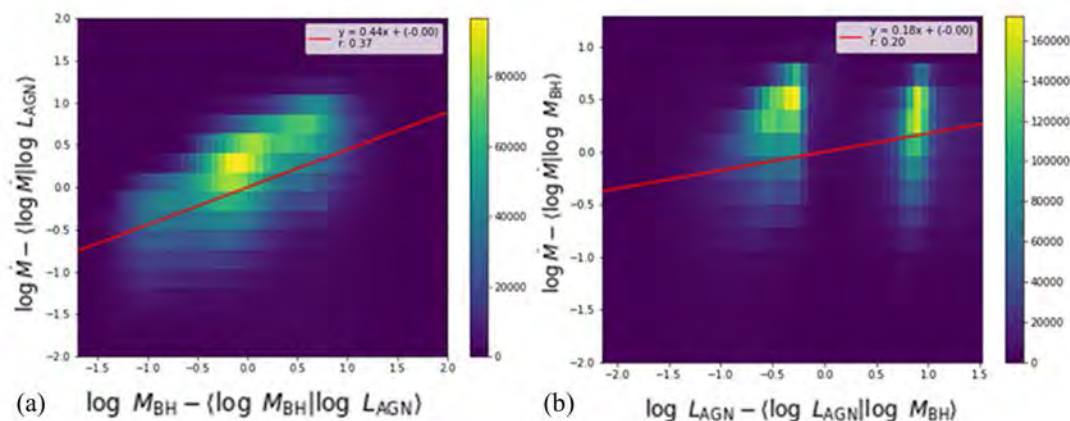


Fig. 1. Correlation between residuals of mass outflow rate and particular galaxy parameters. (a) Correlation between $\log \dot{M} - \langle \log \dot{M} | \log L_{\text{AGN}} \rangle$ and $\log M_{\text{BH}} - \langle \log M_{\text{BH}} | \log L_{\text{AGN}} \rangle$. (b) Correlation between $\log \dot{M} - \langle \log \dot{M} | \log M_{\text{BH}} \rangle$ and $\log L_{\text{AGN}} - \langle \log L_{\text{AGN}} | \log M_{\text{BH}} \rangle$.

Overall, the simulated outflow properties and their correlations with galaxy parameters agree with observational data. We find that both AGN luminosity and black hole mass play a critical role in shaping galactic outflows. In particular, Figure 1 presents results from our residual study, suggesting that the black hole mass is a more influential parameter in regulating the mass outflow rate than AGN luminosity. This finding is supported by the fact that removing the influence of M_{BH} weakens the correlations between mass outflow rate and all other system parameters. In this study we will present an analysis of correlations between outflow and galaxy properties for both simulated and real systems, showcasing how both the AGN and the host galaxy combine to produce the diversity of outflows.

[1] Zubovas, K.; Bialopetravičius, J.; Kazlauskaitė, M. *Monthly Notices of the Royal Astronomical Society* 2022, 515, 1705-1722.

[2] Shankar, F.; Bernardi, M.; Sheth, R. K.; Ferrarese, L.; Graham, A. W.; Savorgnan, G.; Allevato, V.; Marconi, A.; Läsker, R.; Lapi, A. *Monthly Notices of the Royal Astronomical Society* 2016, 460, 3119-3142.

ANALYSIS OF SPECTRAL LINES FOR STARS VIA SYNTHETIC SPECTRA

Dzmitry Viarbitski¹, Markus Ambrosch¹

¹Institute of Theoretical Physics and Astronomy, Vilnius University
dzmitry.viarbitski@ff.stud.vu.lt

Atmospheric parameters of stars are among the most important data received from a star. Processing the spectrum and knowing the class of the star allows you to find out such information as the temperature of the photosphere (T_{eff}), the acceleration of free fall on the surface ($\log(g)$), the metallicity ($[Fe/H]$) and the turbulent velocity (V_t). Thus, it becomes possible to obtain basic information about the state of the star and assume its further evolution [1- 4].

After the spectrum is obtained it is possible to process regions of the spectrum of a star at specific wavelengths that correspond to the lengths of the absorption bands of any element, it can be oxygen, nitrogen, or the most important element for studying, iron. To do this, the Python programming language software, as well as the Splat-VO program, were used.

By means of data selection, it is also possible to generate a synthetic spectrum using Moog and/or Turbospectrum softwares, if the entered data is correct, the resulting spectrum will coincide with the spectrum from the stars obtained by the observations and by using fitting algorithm. After the processing of the required number of wavelengths and the graph of the growth curve is satisfactory, the work is completed by overlaying the data in a spectrum and comparing it with the original one.

Using synthetic spectra is one way to analyze stellar spectra. Generating the spectra is slow, so trying out all possible combinations of the input parameters can take a very long time. The main advantage of this method is that it can also measure the abundances of molecules in stellar atmospheres, for example, CN and TiO. This is not possible with other methods and is why we use synthetic spectra

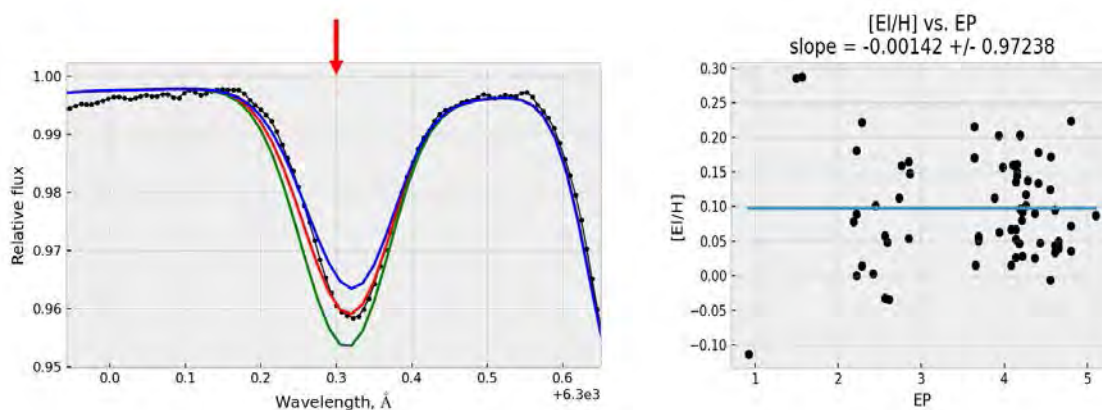


Fig. 1. *Spectrum analysis procedure with substitution of specific numerical parameters (free-fall acceleration, turbulent velocity, temperature, metallicity) with the presented result of superimposing the synthetic one on the real spectrum*

-
- [1] R. Brahm, A. Jordán, J. Hartman, G. Bakos, Monthly Notices of the Royal Astronomical Society, 467 (1), 971–984 (2017)
 [2] P. de Laverny, A. Recio-Blanco, C. C. Worley, B. Plez, A&A, 544 A126 (2012)
 [3] R. T. Coelho, Monthly Notices of the Royal Astronomical Society, 440 (2) 1027 (2014)
 [4] M. Bergemann, R.-P. Kudritzki, B. Davies, GeoPlanet: Earth and Planetary Sciences, Determination of Atmospheric Parameters of B-, A-, F- and G-Type Stars, 217 (2014)

ACHIEVING LONG-LASTING ROOM TEMPERATURE PHOSPHORESCENCE IN PHENOTHIAZINE CRYSTALS

Vilius Stankevičius¹, Jonas Žurauskas², Paulius Vaickūnas², Steponas Raišys¹, Edvinas Orentas², Karolis Kazlauskas¹

¹Institute of Photonics and Nanotechnology, Vilnius University, Vilnius, Lithuania

²Department of Organic Chemistry, Vilnius University, Vilnius, Lithuania
vilius.stankevicius@ff.stud.vu.lt

Room temperature phosphorescence (RTP) has a great potential to be used for various applications in sensing, data encryption, anti-counterfeiting, bioimaging and microcrack detection owing to their unique photophysical properties [1]. Typically, RTP emission is achieved in inorganic material-based systems, including rare earth metals, which are associated with high processing costs, poor biocompatibility, etc. Recently, the focus has shifted to organic RTP systems due to their tunability of emission wavelength, low cost and ease of processing.

For practical applications, RTPs must be efficient and have a long phosphorescence lifetime, which is in principle a challenging task, since promoting intersystem crossing for high-yield triplet generation usually accelerates their lifetime [2, 3]. It is therefore necessary to understand the mechanisms that determine long and efficient RTP and to identify the limiting factors of the processes involved in RTP, so that new RTP systems with improved RTP properties can be achieved.

In this work, new phenothiazine 5,5-dioxide RTP emitters have been synthesized and their RTP properties have been studied. All three phenothiazine 5,5-dioxide based compounds adopted crystal structure which ensured rigid environment for reduced non-radiative triplet deactivation allowing to achieve RTP in the green spectral region with phosphorescence lifetime up to 0.85 s. In addition, it has been shown that rigid crystal structure hampered permeability of atmospheric oxygen therefore retained triplet lifetime even working under ambient conditions.

-
- [1] Y. Wang, J. Yang, M. Fang, Y. Gong, J. Ren, L. Tu, B. Z. Tang, Z. Li, New Phenothiazine Derivatives That Exhibit Photoinduced Room-Temperature Phosphorescence. *Adv. Funct. Mater.* 2021, 31, 2101719. DOI: 10.1002/adfm.202101719
- [2] H. Ma, Q. Peng, Z. An, W. Huang, Z. Shuai, Efficient and Long-Lived Room-Temperature Organic Phosphorescence: Theoretical Descriptors for Molecular Designs, *J. Am. Chem. Soc.*, 2019 141 (2), 1010-1015. DOI: 10.1021/jacs.8b11224
- [3] J. Jovaišaitė, S. Kirschner, S. Raišys, G. Kreiza, P. Baronas, S. Juršėnas, M. Wagner, Diboraanthracene-Doped Polymer Systems for Colour-Tuneable Room-Temperature Organic Afterglow, *Angew. Chem. Int. Ed.* 2023, 62, e202215071. DOI: 10.1002/anie.202215071

Functionalization and Properties Investigations of Benzothiophene Derivatives

Arnas Kovševič¹, Indrė Jaglinskaitė¹, Vilija Kederienė¹

¹Department of Organic Chemistry, Faculty of Chemical Technology, Kaunas University of Technology
arnas.kovsevici@ktu.edu

Due to their diverse biological properties, benzo[b]thiophenes are heterocyclic compounds widely used in pharmaceuticals. Benzo[b]thiophene derivatives have anti-allergic, antibacterial, and anti-inflammatory effects. They are receptor modulators and antioxidants. [1]

It has been established that benzo[b]thiophene derivatives can be potential drugs in cancer treatment, as the inhibition of protein tubulin polymerization and cell proliferation characterizes them. [2] The drugs Raloxifene, intended for the treatment of osteoporosis during postmenopause, and Zileuton, an antiasthmatic drug, are based on them. [1] In addition, benzo[b]thiophene compounds are used in solar cells and thin-film devices due to their fluorescent properties. [3]

N-substituted benzo[b]thiophene derivatives are also used in the pharmaceutical industry because of their biological properties, such as antifungal, antibacterial and anti-inflammatory properties. [4] In addition, the drug Encenicline was discovered, which is active against schizophrenia and Alzheimer's disease. [1]

Also, these compounds are not only biologically active substances but also have luminescent properties so that they can act as efficient emitters. [5]

For further synthesis, benzo[b]thiophene derivatives were chosen due to their wide application. After choosing the optimal conditions at the beginning of the study, the initial derivative of 3-aminobenzo[b]thiophene was synthesized. Various reaction methodologies were employed to investigate the reactivity of 3-aminobenzo[b]thiophene-2-methylcarboxylate with different substituents. A detailed analysis was conducted on the structure of the 3-aminobenzo[b]thiophene derivatives obtained.



- [1] Kesharwani, T. et al. Green synthesis of benzo[b]thiophenes via iron(III) mediated 5-endo-dig iodocyclization of 2-alkynylthioanisoles. *Tetrahedron Letters*, 2016, 57, 411-414.
- [2] Romagnoli, R. et al. Synthesis and Biological Evaluation of 2- and 3-Aminobenzo[b]thiophene Derivatives as Antimitotic Agents and Inhibitors of Tubulin Polymerization. *Journal of Medicinal Chemistry*, 2007, 50(9), 2273-2277.
- [3] Choi H. et al. Novel organic dyes containing bis-dimethylfluorenyl amino benzo[b]thiophene for highly efficient dye-sensitized solar cell. *Tetrahedron*, 2007, 63(15), 3115-3121.
- [4] Isloor, A. M., B. Kalluraya, K. S. Pai. Synthesis, characterization and biological activities of some new benzo[b]thiophene derivatives. *European Journal of Medicinal Chemistry*, 2010, 45(2), 825-830.
- [5] Fukuzumi, K., et al. Synthesis of Benzo[c]thiophenes by Rhodium(III)-Catalyzed Dehydrogenative Annulation. *The Journal of Organic Chemistry*, 2016, 81(6), 2474-2481.

HYDROGELS WITH THE ADDITION OF MODIFIED STARCH AND CLAY OF THE MONTMORILLONITE TYPE

Anastasiia Godunko¹, Irina Liashok¹, Viktoriia Plavan¹, Olena Ishchenko¹, Viacheslav Shvets¹

¹ Kyiv National University of Technology and Design
lyashok.io@knuutd.com.ua

Hydrogels are polymeric materials capable of absorbing and holding a large amount of water without dissolving in it, have increased sorption properties, biocompatibility, and biodegradability, which makes them attractive for use in the biomedical field, agriculture, and other industries [1]. The addition of montmorillonite-type clay increases mechanical strength of hydrogels, forms a network of connections, which improves structural properties and makes them more resistant to deformations [2]. This is important for the use of such materials in technologies where high strength is required [3]. The purpose of this work is to develop the technology for obtaining hybrid hydrogel materials based on the polymer composition of polyvinyl alcohol (PVA) with the addition of carboxymethylated starch (CMS) and montmorillonite-type clay and to study their sorption properties.

The paper proves the possibility of obtaining hybrid hydrogels by the cryostructuring method based on a mixture of PVA:CMS polymers in a 1:1 ratio with the addition of montmorillonite type clay (M-5). It was established that compositions with the clay component content below 8 parts by volume form a stable structure of the hydrogel material. In the work, the swelling of samples of the filled hydrogel matrix in distilled water was investigated and the sorption properties were determined by the gravimetric method.

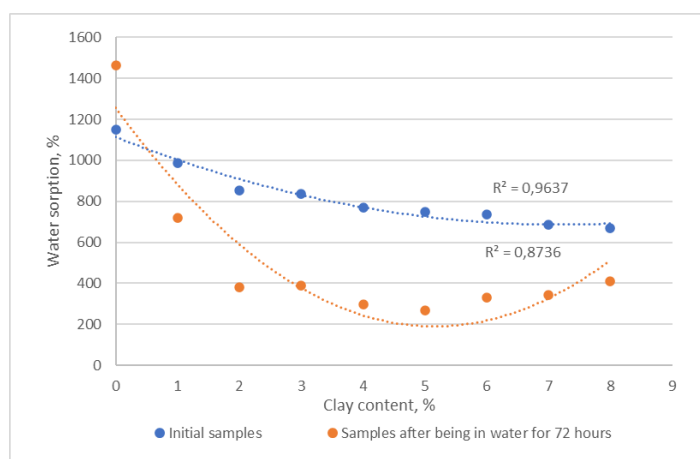


Fig. 1. Moisture content of samples of hydrogels based on polyvinyl alcohol and carboxymethylated starch depending on the amount of clayn

It was established that the clay-filled hydrogel systems collapse, reaching the equilibrium value of sorption within 72 hours. For samples containing 1 volume part of clay, sorption decreases by 270 % and is 720 % in the equilibrium state. The maximum decrease in sorption by 480 % is observed for samples that contain 5 volume parts of clay and is 300 % in the equilibrium state. When studying the desorption of hybrid hydrogel materials, it was established that the addition of montmorillonite-type clay slows down the process of hydrogel desorption. At the same time, the maximum desorption rate is observed during the first 5-7 hours of the experiment for all samples, and is on average 60 % / h for the sample that does not contain clay, and 30 % / h for samples containing montmorillonite clay.

Thus, polymer compositions based on PVA:CMS in a 1:1 ratio with the addition of montmorillonite-type clay in the amount of 1-2 parts by volume can be recommended for obtaining cryohydrogels with increased sorption properties and slower drying speed.

- [1] C. Vasile, New developments in medical applications of hybrid hydrogels containing natural polymers, *Molecules*, 25.7, 1539 (2020).
 [2] M. Peiying, W. Zhou, J. Yibei, H. Zongwang, X. Lu, J. Jinlong, Yu. Fulai, Xia Hui, Zhang Yi, Clay-based nanocomposite hydrogels with microstructures and sustained ozone release for antibacterial activity, *Colloids and Surfaces A: Physicochemical and Engineering Aspects*, 641, 128497 (2022).
 [3] Y. Budash, V. Plavan, N. Tarasenko, O. Ishchenko, M. Koliada. Effect of Acid Modification on Porous Structure and Adsorption Properties of Different Type Ukrainian Clays for Water Purification Technologies. *Journal of Ecological Engineering*, 24(5), 210-221 (2023).

PROPELLANT SELECTION FOR ENHANCED DRUG DELIVERY IN WOUND-HEALING TOPICAL AEROSOLS

Mariia Popova¹, Olena Saliy¹

¹Department of Chemical and Biopharmaceutical Technologies, Kyiv National University of Technologies and Design, Kyiv, Ukraine

popova.me@knutd.edu.ua

Over the past few years pressurized pharmaceutical technology has been rapidly advancing. Pressurized dosage forms offer advantages over other forms such as convenience and hygiene of application, high efficient at relatively low drug substance costs. From literary sources it is known that depending on amount of propellant in container consumer properties such as spot size, case of application and percentage of concentrate released front aerosol container depend on amount of propellant. Our research focused on justifying concentration of chosen propellant - a combination of saturated hydrocarbons (propane, butane, isobutane). The aerosol cans with a capacity of 200 ml were filled with a pre-made concentrate solution of 93 g sealed with continuous-action valves, and a mixture of propane, butane and isobutane (45:50:5) was added to aerosol can. The amount of mixture ranged from 15% (29.75 g) to 20% (40.25 g) of aerosol can. The concentration increase step was 5%. To choose optimal concentration of propellant, we investigated its impact on technological indicators of aerosol: dispensing type, appearance, thickness, drying time, spot size, and percentage of content released from can. The results are presented in Table 1.

N	Propellant content, % in the container	Concentration (g), propellant	Aerosol characteristics			
			Spraying	Consumer properties	Drying time, min.	Percentage of expel, %.
1	14.88	29.75	Cylinder pressure is low, contents of the canister are not completely discharged	Colorless spot, small spray area, the spot spreads, spray area 2 cm	8-10 m	94,23±5
2	15.75	31.5	Cylinder pressure is low, contents of the canister are not completely discharged	Colorless spot, small spray area, the spot spreads, spray area 2 cm	7-10 m	94,67±5
3	16.63	33.25	Smooth	Colorless spot, spray area 4 cm	5-8 m	93,27±5
4	17.50	35.0	Smooth	Colorless spot, spray area 5 cm	5-6 m	97,83±5
5	18.38	36.75	Smooth	Colorless spot, spray area 5 cm	4-6 m	93,42±5
6	19.25	38.50	Harsh, noisy, uneven expel of liquid	Low release of solution from the canister, spray area 7 cm	2-3 m	83,12±5
7	20.13	40.25	Harsh, noisy, uneven expel of liquid	Low release of solution from the canister, spray area 7 cm	1-3 m	75,13±5

Fig. 1. Consumer characteristics of aerosol depending on propellant concentration

Based on the conducted research, it can be asserted that type and quantity of propellant significantly influence atomization process. Regarding the dispensing type and external appearance of the spray formed from samples containing a mixture of propane, butane, and isobutane (17.5%), it was observed to be colorless with a smooth shiny surface and a smooth dispensing type. It was found that an increase in concentration of propellant from 15 to 20% results in an increase in amount of sprayed solution. This, in our opinion, is associated with type of aerosol dispensing, an increase in percentage of gaseous phase, and a decrease in solution's density. However, as thickness of spray spot increases, drying time also increases. The latter, in turn, is related to indicator of percentage of content released from the aerosol container. It has been proven that an increase in amount of propellant from 19 to 20% leads to a decrease in percentage of content released from cans to 83.12±5%. Further increase in propellant results in a gradual reduction of this indicator.

Therefore through comparative analysis was established that optimal choice is use of a propellant mixture of propane, butane and isobutane (45:50:5) at a concentration of 17.5%.

[1] Saliy, O. O., Popova, M. E., Tarasenko, H. V., & Yarovenko, V. S. (2022). Аналіз основних тенденцій розвитку ринку лікарських засобів, що знаходяться під тиском, у фармацевтичній та ветеринарній практиці. *Social Pharmacy in Health Care*, 8(3), 60-70.

[2] Tarasenko V., Tachtaulova N., Shmatenko O., Goncharenko N. et al. (2020). The Influence of Propellant on the Technological Qualities of a Floating Aerosol. *Asian Journal of Pharmaceutics* (Apr-Jun 2020). 14(2) : 297-300. (Web of Science)

OPTIMIZATION OF THE COMPOSITION OF A SOLID DISPERSED SYSTEM OF NIMESULIDE OBTAINED BY CENTRIFUGAL FIBER FORMATION

Viktoriia Lyzhniuk¹, Viktor Kostyuk¹, Vadym Lisovyi^{1,2}, Andriy Goy¹, Galina Kuzmina¹, Volodymyr Bessarabov¹

¹Department of Industrial Pharmacy, Kyiv National University of Technologies and Design, Ukraine

²Department of Chemical Technology and Resource Saving, Kyiv National University of Technologies and Design, Ukraine
v.lyzhniuk@kyivpharma.eu

For many years, nimesulide-based nonsteroidal anti-inflammatory drugs have been among the most well-known drugs for relieving acute toothache and many different inflammatory diseases. However, the widespread use of these drugs is limited by the low solubility of the active pharmaceutical ingredient (API) in water (0.01 g/l) [1]. This leads to the use of high doses of nimesulide and the occurrence of undesirable side effects. Therefore, research aimed at increasing the solubility of nimesulide is very important.

The analysis of literature sources shows that in recent years the technology of solid disperse systems (SDS) has shown promising results in increasing the solubility of a significant number of water-insoluble anti-inflammatory drugs.

In this study, we used an innovative centrifugal fiber forming technology to produce solid dispersed nimesulide systems. SDS of nimesulide were prepared by fusing API, polymer, and excipient in the working area of the centrifugal fiber forming machine. The resulting melt was then moved through the filter by centrifugal force and solidified into fibers in the air flow. Polyvinylpyrrolidone K-17 (PVP K-17), a pharmaceutically acceptable polymer carrier, was selected. To increase the yield of the fibers formed, sucrose was used, the addition of which to the composition allows the melting point of the mixture to be reduced.

It was found that the design of a solid dispersed system based on nimesulide and PVP K-17 in a percentage ratio of 5:95 can improve the solubility of APIs by 2.85 times. On the other hand, when 5 % of PVP K-17 was replaced by sucrose, the degree of solubility increase was increased to 3.12 times. With a further increase in sucrose in the composition of SDS to 10 % and 20 %, it was possible to increase the degree of increase in the solubility of nimesulide by 3.63 times and 4.88 times, respectively. Subsequently, an increase in the sucrose concentration in the composition had the opposite effect, which led to a decrease in the solubility of nimesulide. It is worth noting that sucrose affects not only the solubility of nimesulide but also the yield of the resulting SDS fibers. It was found that the solid dispersion of nimesulide, which was formed only from K-17 without the addition of sucrose, has a yield of 55.72 %. At the same time, when 5 % sucrose is added to the system, the fiber yield increases to 69.64 %, and when 20 % sucrose is added, the yield of SDS was increased to 71.40 %. For the first time, a new method for increasing the solubility of nimesulide was developed based on the centrifugal formation of SDS fibers. It has been established that the optimal content of components for preparing polymeric SDS of nimesulide by the method of centrifugal fiber formation is a ratio of PVP K-17, sucrose, and nimesulide in a proportion of 75:20:5. This composition increases the solubility of the API by 4.88 times and has a high yield of fibers at 71.40 %.

[1] K. D. Rainsford, Consensus Report Group on Nimesulide. Nimesulide—a multifactorial approach to inflammation and pain: scientific and clinical consensus, *Current medical research and opinion*, 22(6), 1161-1170 (2006). <https://doi.org/10.1185/030079906X104849>

UV TO NIR EMITTING UPCONVERTING NANOPARTICLES FOR APPLICATIONS IN THERANOSTICS

Egle Ezerskyte^{1,2}, Greta Butkiene², Arturas Katelnikovas¹, Vaidas Klimkevicius^{1,2}

¹Faculty of Chemistry and Geosciences, Institute of Chemistry, Vilnius University, Lithuania

²Biomedical Physics Laboratory, National Cancer Institute, Lithuania

egle.ezerskyte@chgf.vu.lt

Theranostics is a field in medicine that combines diagnostic and therapeutic tools, either simultaneously or sequentially, to achieve more accurate detection and efficient treatment of cancer which stands as one of the leading causes of death worldwide [1-3]. Recently, inorganic lanthanide-doped nanoparticles (NPs) that exhibit upconversion luminescence (low energy photons absorbed are combined and emitted as the ones of higher energy) are gaining ground in theranostics [4]. Firstly, NPs are small enough to enter cancerous cells providing localized effects [5]. Secondly, upconverting NPs are excited using NIR radiation which pass deeper through tissues if compared to UV or visible radiation [6]. Furthermore, the luminescence of such particles has high signal to noise ratio that provides high contrast imaging [6]. However, for upconverting NPs to be applicable in theranostics, they must emit light at specific regions, determined by utilization envisioned. For instance, emission in red spectral region is necessary for photodynamic therapy, emission in UV or blue spectral region enables the release of drugs attached to the surface of the NPs, and emission in NIR region provides bioimaging using NIR camera [4,7,8]. It means that NPs emitting in multiple spectral regions would offer both diagnostic and therapeutic properties contained within a single type of NPs. All in all, upconverting NPs possessing the characteristics described above show great prospects towards a more precise diagnosis and treatment of cancer.

This presentation will describe synthesis and post-synthesis treatment of upconverting core-shell-shell structured $\text{NaGdF}_4:15\%\text{Eu}^{3+}@\text{NaGdF}_4:49\%\text{Yb}^{3+},1\%\text{Tm}^{3+}@\text{NaGdF}_4:5\%\text{Yb}^{3+},40\%\text{Nd}^{3+}$ NPs that emit light in the range from UV to NIR (see Fig. 1). Furthermore, the presentation will include detailed analysis of structural and optical properties of NPs produced along with evaluation of their colloidal stability (aqueous, biological media) and biocompatibility.

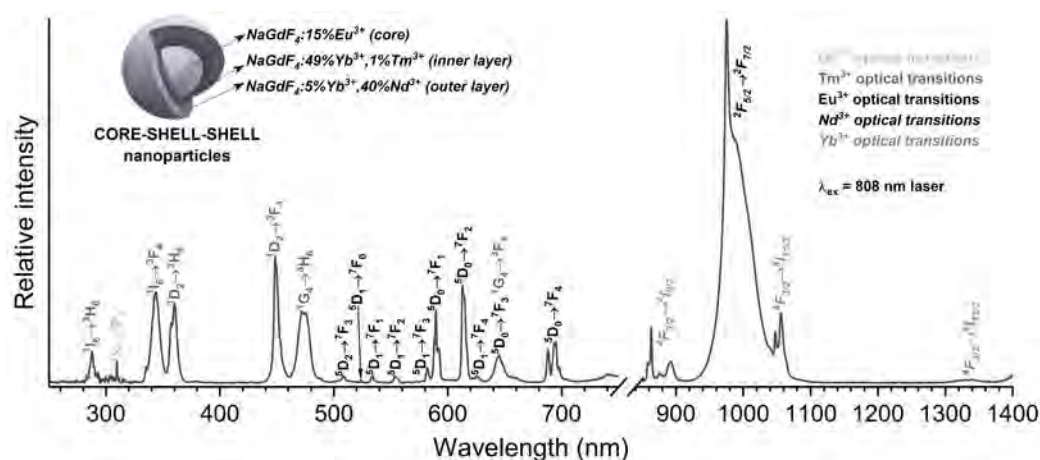


Fig. 1. Emission spectra of core-shell-shell NPs investigated under 808 nm laser radiation.

- [1] W. A. Weber et al., "The Future of Nuclear Medicine, Molecular Imaging, and Theranostics," *Journal of Nuclear Medicine*, vol. 61, no. Supplement 2, pp. 263S-272S, 2020.
- [2] R. L. Siegel, K. D. Miller, N. S. Wagle, and A. Jemal, "Cancer Statistics, 2023," *CA: A Cancer Journal for Clinicians*, vol. 73, no. 1, pp. 17-48, 2023.
- [3] B. S. Chhikara and K. Parang, "Global Cancer Statistics 2022: the Trends Projection Analysis," *Chemical Biology Letters*, vol. 10, no. 1, p. 451, 2023.
- [4] G. Chen, H. Qiu, P. N. Prasad, and X. Chen, "Upconversion Nanoparticles: Design, Nanochemistry, and Applications in Theranostics," *Chemical Reviews*, vol. 114, no. 10, pp. 5161-5214, 2014.
- [5] C. M. Beddoes, C. P. Case, and W. H. Briscoe, "Understanding Nanoparticle Cellular Entry: a Physicochemical Perspective," *Advances in Colloid and Interface Science*, vol. 218, pp. 48-68, 2015.
- [6] D. Jaque, C. Richard, B. Viana, K. Soga, X. Liu, and J. García Solé, "Inorganic Nanoparticles for Optical Bioimaging," *Advances in Optics and Photonics*, vol. 8, no. 1, pp. 1-103, 2016.
- [7] C. Wang, L. Cheng, and Z. Liu, "Upconversion Nanoparticles for Photodynamic Therapy and Other Cancer Therapeutics," *Theranostics*, vol. 3, no. 5, pp. 317-30, 2013.
- [8] L. L. Fedoryshin, A. J. Tavares, E. Petryayeva, S. Doughan, and U. J. Krull, "Near-Infrared-Triggered Anticancer Drug Release from Upconverting Nanoparticles," *ACS Applied Materials & Interfaces*, vol. 6, no. 16, pp. 13600-13606, 2014.

RESISTIVITY AND LOW FREQUENCY NOISE OF HYBRID COMPOSITES WITH CARBON NANOTUBES AND IRON NANOINCLUSIONS

Frydrichas Mireckas¹

¹Vilnius University

frydrichas.mireckas@ff.vu.lt

Polymer composites with carbon and metal nanoinclusions are a prospective class of materials, merging polymer processing technologies with the features of nanoparticles, such as excellent electric and thermal conductivity [1]. Hybrid composites containing two or more different types of fillers are particularly promising, as desired material properties can be achieved by using a lower concentration of fillers [2]. In carbon and metal reinforced composites, conductive filler particles form a percolative network in the dielectric polymer matrix, where charge transfer occurs via carrier hopping or tunnelling, and in the case of hybrid composites, the emergence of synergistic effects may result in different mechanisms of carrier transfer occurring simultaneously through multiple percolation networks [3].

Low frequency noise spectroscopy is an effective method for investigating charge carrier transport mechanisms in such materials, as filler-dependent charge carrier number fluctuations reflect in the observable electric noise spectra [4]. Of notable significance is $1/f$ noise, a superposition of many Lorentzian noise components in the material that exhibits a spectral density inversely proportional to the frequency, as the level of $1/f$ noise determines the limit of sensitivity for sensors [3].

The resistivity and low frequency (10 Hz – 20 kHz) noise characteristics of hybrid composites with single-walled carbon nanotubes (CNTs) and iron nanoinclusions (Fe, 800 nm) were investigated in a temperature range of (75–365) K to identify dominant charge transfer mechanisms. Composites were prepared via melt processing of polydimethylsiloxane (PDMS) and different concentrations of CNTs (0.5 wt.%) and Fe (65 wt.%, 75 wt.%, 82 wt.%).

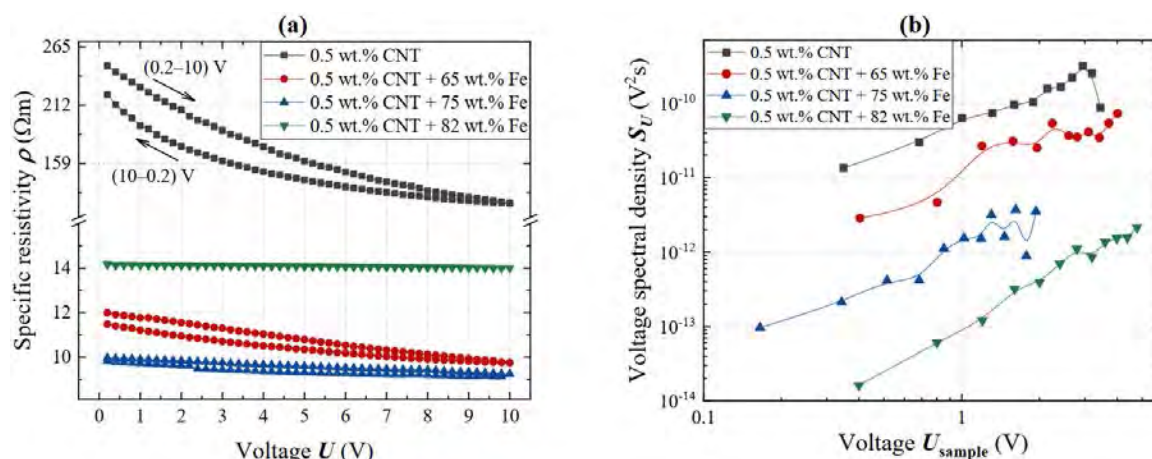


Fig. 1. (a) Specific resistivity dependency on increasing and decreasing voltage; (b) voltage noise spectral density dependency on voltage (room temperature, 86 Hz).

Specific resistivity is found to be less variable with voltage and less anisotropic for composites with greater Fe content (Fig. 1a). The inclusion of Fe in the hybrid composites lowers the resistivity by approximately one order of magnitude. Increasing the Fe concentration in the hybrid composites initially results in a small decrease in resistivity, but a slight increase is observed at 82 wt.% Fe, possibly due to agglomeration.

Low frequency voltage noise spectra consist of $1/f^\alpha$ noise and Lorentzian type components. For the proportionality of low frequency voltage noise spectral density to the voltage $S_U \sim U^b$, the exponent b is lower than 2 (Fig. 1b). This indicates an increased contribution of tunneling processes [3]. The intensity of noise relates to the concentration of Fe in the composite, with composites with more Fe exhibiting lower levels of noise.

- [1] Z. Spitalsky et. al. Carbon nanotube-polymer composites: Chemistry, processing, mechanical and electrical properties. Progress in Polymer Science 2010, 35(3), 357-401.
- [2] A. Kumar et. al. Carbon nanotube- and graphene-reinforced multiphase polymeric composites: review on their properties and applications. Journal of Materials Science 2019.
- [3] M. Tretjak et. al. Low Frequency Noise and Resistivity Characteristics of Hybrid Composites with Onion-Like Carbon and Multi-Walled Carbon Nanotubes. Fluctuation and Noise Letters 2019, 18.
- [4] M. Tretjak et. al. Noise and Electrical Characteristics of Composites Filled with Onion-Like Carbon Nanoparticles. Polymers 2021, 13(7), 997.

STRUCTURE OF CAPROIC ACID MONOMERS AND HYDROGEN BOND COMPLEXES. MATRIX ISOLATION IR SPECTROSCOPY STUDY

Simona Bučinskaitė¹, Redas Kazlauskas¹, Jogilė Mačytė¹

¹Vilnius University
redas.kazlauskas@ff.stud.vu.lt

Hydrogen bonds have a significant effect on the properties of small molecules and macromolecules. In trying to understand complex systems quite often model studies of small molecule systems are used. The properties of hydrogen bonds have been an object of study for many decades but there are still many unanswered questions regarding the structure of such systems and the hydrogen bonds that form between these molecules. Findings show that the first three homologous series of carboxylic acids can form at least two types of dimers [1]. Most of the research regarding higher series of carboxylic acids suggests that only cyclical dimers can form in these acids.

The method of low temperature matrix isolation allows for the isolation of molecules from interacting with their surroundings by placing them in crystals made up of inert gas molecules. The infrared spectra of these types of samples have very narrow spectrum lines which allow for identification of different molecule structures.

In the picture we can see an infrared absorption spectrum in the region of C=O stretching and O-H deformational vibrations of caproic acid (hexanoic acid $\text{CH}_3(\text{CH}_2)_4\text{COOH}$) isolated in an argon matrix. When the sample is at a temperature of 3K in the region between $1800\text{--}1750\text{ cm}^{-1}$ of the spectre a wide, structured line is visible which is attributed to C=O group stretching vibrations of the caproic acid monomers. Based on the shape of this line and how it evolves with temperature an assumption can be made that during the experiment we are observing more than one type of monomer in the sample. The quantum chemistry calculations also confirm the possibility that at least two conformers of similar energy levels can exist.

Additional spectral lines that are observed at 1749 cm^{-1} and 1724 cm^{-1} cannot be explained by cyclical dimers or water and acid complexes so it can be assumed that in a low temperature inert argon environment low amounts of non cyclical caproic acid dimers also form. While performing annealing experiments the spectral line component which was allocated to higher frequency monomers was shrinking faster than the lower frequency component. Based on the calculation results the higher frequency monomer spectral line part is linked with the molecular structure of the caproic acid in which the carboxylic group is not in one plane with the aliphatic chains plane.

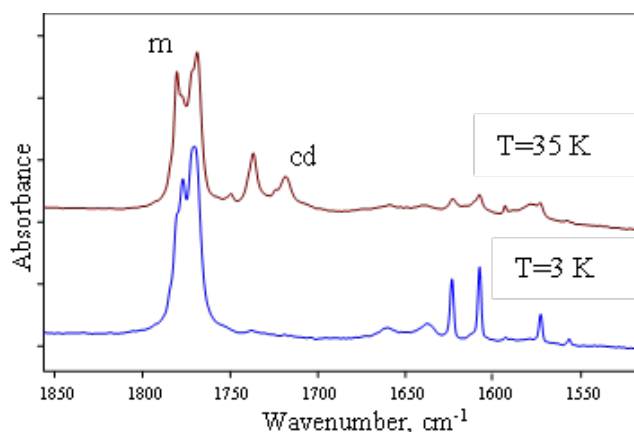


Fig. 1. Infrared absorption spectra of caproic acid isolated in Argon at 3K (bottom) and warmed to 35 K (top). (m - monomer, cd – cyclic dimer)

Keywords: Matrix isolation, carboxylic acid, IR spectroscopy.

[1] [1] V. Sablinskas et al. Journal of Molecular Structure 976 (2010) 263–269.

INVESTIGATION OF SARS-COV-2 OMIKRON SPIKE PROTEIN REAL-TIME INTERACTIONS WITH SPECIFIC MONOCLONAL ANTIBODIES

Justina Liesyte¹, Silvija Juciute^{1,2}, Vincentas Maciulis^{1,2}, Ieva Plikusiene^{1,2}

¹Nanotechnas, Nanotechnology and Materials Sciences Center, Faculty of Chemistry and Geosciences, Vilnius University, Naugarduko 24, Vilnius, Lithuania

²State Research Institute Centre for Physical Sciences and Technology, Department of Nanotechnology, Sauletekio Avenue 3, Vilnius, Lithuania
justina.liesyte@chgf.stud.vu.lt

Since the beginning of 2020, people's lives have been profoundly changed by the rapid spread of the SARS-CoV-2 virus, which can cause COVID-19 – a disease associated with pneumonia and multiorgan failure [1]. Due to the rapid spread of the disease, it has become important to understand how the structural proteins of the virus bind to specific antibodies. The huge number of infections and deaths made such studies essential. A particularly important area in this context is the development and application of immunosensors. All immunosensors are based on the specificity of molecular recognition of antigens or antibodies. Immunosensors can be subdivided according to the detection principle used. The main sensors developed are electrochemical, optical, and acoustic immunosensors [2].

SARS-CoV-2 Spike protein is composed of two functional subunits. One of those subunits has a receptor binding domain (RBD), which is responsible for binding the virus to the host cell receptor. This study aimed to use a combined method of spectroscopic ellipsometry (SE) and quartz crystal microbalance with dissipation (QCM-D) to investigate the interaction between SARS-CoV-2 spike protein and specific antibodies and to assess the formed immune complex thermodynamic properties. The results obtained from SE allowed to assess the thickness of monolayers and to calculate the surface mass density of dry proteins and the data acquired from QCM-D allowed to calculate the surface mass density of wet proteins and the amount of PBS in the monolayers and to assess the viscoelastic properties of the formed monolayers. The results present that the monolayer of immobilized monoclonal antibodies was found to be rigid, while the monolayer of antigens formed during their interaction with antibodies presented viscoelastic properties.

Acknowledgment: This project has received funding from the Research Council of Lithuania (LMTLT), agreement No [S-LZ-23-1]

[1] I. Pagani, S. Ghezzi, S. Alberti, G. Poli, E. Vicenzi, Origin and evolution of SARS-CoV-2, *The European Physical Journal Plus*, 138(2) (2023)
[2] P. B. Lippa, L. J. Sokoll, D. W. Chan, Immunosensors: principles and applications to clinical chemistry, *Clinica Chimica Acta*, 314(1,2) (2001)

INVESTIGATION OF MXENES ADSORPTION POTENTIAL FOR AZURE A AND METHYLENE BLUE DYES pH-RESPONSIVE BEHAVIOR AND ADSORPTION KINETICS

Anton Popov³, Martynas Talaikis², Germantė Paulikaitė¹, Simonas Ramanavicius², Gediminas Niaura²

¹Vilnius University

²Center for Physical Sciences and Technology

³NanoTechnas - Center of Nanotechnology and Materials Science

germante.paulikaite@chgf.stud.vu.lt

Water pollution poses a significant threat to ecosystems, human health, and the overall well-being of our planet. The presence of contamination has reached alarming levels, demanding innovative, sustainable, and fast solutions [1]. This study aims to explore the potential of MXenes as a novel class of two-dimensional materials, effectively removing organic contaminants. MXenes exhibit high surface area, excellent conductivity, and strong adsorption capabilities. Synthesis consists of selective Al layer etching from MAX phase precursor, resulting in a layered structure that can be adapted for specific applications such as surface-enhanced Raman spectroscopy [2], biofuel cells [3], etc. The study includes experimental assessments of MXenes performance in removing organic pollutants such as Methylene Blue and Azure A from aqueous samples in a pH range from 4 to 6. Preliminary results demonstrate the promising potential of MXenes' effectiveness to adsorb and remove organic dyes due to the large active surface area. The adsorption efficiency and adsorption coefficients of MXenes were calculated for both dyes in all pH solutions. Moreover, reaction kinetics indicate superior fast adsorption performance. In conclusion, research signifies the importance of exploring innovative materials to combat water pollution, and MXenes may be the solution to it. The promising results suggest that MXenes could offer a sustainable and efficient adsorbent for the removal of organic pollutants.

This project has received funding from the Research Council of Lithuania (LMTLT), agreement No S-PD-22-155.

-
- [1] B. Senthil Rathi, P. Senthil Kumar, Dai-Viet N. Vo. Critical review on hazardous pollutants in the environment: Occurrence, monitoring, fate, removal technologies and risk assessment 2021. <https://www.sciencedirect.com/science/article/abs/pii/S0048969721042078>
- [2] Adomavičiūtė-Grabusová S, Ramanavičius S, Popov A, Šablinskas V, Gogotsi O, Ramanavičius A. Selective enhancement of SERS spectral bands of salicylic acid adsorbate on 2D Ti₃C₂T_x-based MXene film. *Chemosensors* 2021;9:223. <https://doi.org/10.3390/ijms21239224>
- [3] Ramanavicius S, Ramanavicius A. Progress and Insights in the Application of MXenes as New 2D Nano-Materials Suitable for Biosensors and Biofuel Cell Design. *Int J Mol Sci* 2020;21. <https://doi.org/10.3390/ijms21239224>.

OPTICAL SECOND HARMONIC GENERATION IN GaN WAVEGUIDE STRUCTURE

Ignas Dailidėnas¹, Roland Tomašiūnas¹

¹Institute of Photonics and Nanotechnology, Vilnius University
ignas.dailidenas@ff.vu.lt

To create modal phase matching, most common approach is to use periodic poling structure, which can be troubling to manufacture. Our research investigates attractive all *GaN* based structure with modal phase matching second harmonic generation abilities. Our goal was to grow second-harmonic generator (SHG) *N*-polar *GaN*/*Al*₂*O*₃/*Ga*-polar *GaN*/*AlGa**N*/*AlN*/*Sapphire* using metal-organic chemical vapor deposition (MOCVD) technique for *Nd* : *YAG* lasers. For our theoretical model main variable was width of *GaN* layers. The waveguide structure of 507nm *Ga*-polar and 91nm *N*-polar *GaN* sandwich, separated by 20nm atomic layer deposition (ALD) of an *Al*₂*O*₃ layer was grown on sapphire and 420nm *AlGa**N* epilayer. Structure was tested using endfire method with femtosecond laser and peak conversion was observed around 1080nm. In conclusion by changing widths of *GaN* layers, this structure SHG can be used for tunable spectrum second-harmonic generation, but more research and fine tuning is required

SYNTHESIS OF LaMnO₃ NANOPARTICLES AND INVESTIGATION OF THEIR STRUCTURAL, MORPHOLOGICAL AND MAGNETIC PROPERTIES

Evaldas Lugauskas¹, Dovydas Karoblis¹, Gediminas Niaura^{2,3}, Dominika Zakutna⁴, Aivaras Kareiva¹

¹Institute of Chemistry, Vilnius University, Naugarduko 24, LT-03225 Vilnius, Lithuania

²Department of Organic Chemistry, Center for Physical Sciences and Technology, Sauletekio Ave. 3, 10257, Vilnius, Lithuania

³Institute of Chemical Physics, Faculty of Physics, Vilnius University, Sauletekio Ave. 3, 10257, Vilnius, Lithuania

⁴Department of Inorganic Chemistry, Faculty of Science, Charles University in Prague, Hlavova 2030-8, 128 000 Prague 2, Czech Republic

evaldas.lugauskas@chgf.vu.lt

Main objective - to synthesize LaMnO₃ nanoparticles via sol-gel polyacrylamide route, find out the phase purity, particle size and morphology dependance on reaction parameters and to analyze the magnetic properties of the obtained samples.

Lanthanum manganite (LaMnO₃) is a perovskite type material, which can be described with the general formula of ABX₃ (A and B cations, X - oxygen or halogens). The ideal perovskite structure is cubic, although it can occupy almost any structures due to defects in the crystal structure (orthorhombic, tetragonal, hexagonal...). LaMnO₃ that was obtained via this method has the rhombohedral R-3c structure.

This compound has various useful properties, such as colossal magnetoresistance, chemical stability in various mediums and in a vast temperature range, electrical conductivity, antiferromagnetic properties in bulk and superparamagnetic properties as nanoparticles [1], [2]. It can also be utilized for photocatalytic reactions, such as the degradation of various dyes in contaminated wastewater [3].

The sol-gel polyacrylamide synthesis route was used for the preparation of LaMnO₃. Although this material can be made via various methods, but most often they require complicated instruments, costly reagents and the final product has a large particle size distribution. The polyacrylamide route is optimal for the synthesis of nanoparticles, due to it being both cost and time effective, it does not produce any toxic byproducts and it provides the ability to reliably obtain nano-sized particles due to the creation of a polymeric scaffold with a large surface area [4].

During our research, the purity and structure of the samples was ascertained via X-ray diffraction, FT-IR and Raman spectroscopies, the size and morphology were investigated by utilizing Scanning Electron Microscopy (SEM) and Brunauer-Emmett-Teller (BET) analysis. The magnetic susceptibility studies were performed in order to evaluate the magnetic behavior.

[1] M.N. Iliev et al, Raman monitoring of the dynamical Jahn-Teller distortions in rhombohedral antiferromagnetic LaMnO₃ and ferromagnetic magnetoresistive La_{0.98}Mn_{0.96}O₃, 2000, 341, 2257-2258.

[2] S.A. Hosseini et al, Selective catalytic reduction of NO_x by CO over LaMnO₃ nano perovskites prepared by microwave and ultrasound assisted sol-gel method, 2018, 85, 3, 647-656

[3] P. Sfirloaga et al, Investigation of Catalytic and Photocatalytic Degradation of Methyl Orange Using Doped LaMnO₃ Compounds, Processes 2022, 10(12), 2688

[4] Shi-Fa Wang et al, Magnetic Nanocomposites Through Polyacrylamide Gel Route, Nanoscience and Nanotechnology Letters 6(9), 758-771

OPTIMIZATION OF SYNTHESIS PARAMETERS FOR WELL-DEFINED UPCONVERTING NANOPARTICLES

Viktorija Vrubliauskaitė¹, Eglė Ežerskytė¹, Vaidas Klimkevičius¹

¹Institute of Chemistry, Faculty of Chemistry and Geosciences, Naugarduko 24, LT-03225, Vilnius, Lithuania
viktorija.vrubliauskaite@chgf.stud.vu.lt

Lanthanide-doped upconverting nanoparticles (UCNPs) exhibit a unique capability to convert near-infrared (NIR) radiation into higher energy light (visible or UV), making them promising candidates for applications in bio-related fields. NIR irradiations can penetrate through the skin into deeper tissues without causing extensive heating, making NIR-excited UCNPs extensively researched for potential utilization in theranostics, bioanalytics, and bioimaging. Additionally, these UCNPs show promise for applications such as super-resolution imaging, NIR-II imaging, encoded barcodes, fingerprinting, NIR vision, optogenetics, UCNP-assisted photochemical manipulations, optical tweezers, 3D printing, lasing, UCNP-molecule nano hybrids, etc [1]. However, the effective application of UCNPs in various fields necessitates well-defined morphological and optical properties, and the variation of synthesis conditions are the main parameter which can be adapted to engineer these qualities.

This work focuses on optimizing synthesis parameters of UCNPs with general formula $\text{NaGdF}_4:18\%\text{Yb}^{3+},2\%\text{Er}^{3+}$. The impact of synthesis temperature, as well as the molar ratio of lanthanide salt to NH_4F , on the changes in morphology and optical properties of UCNPs were assessed. Particle size, shape and uniformity were analyzed by SEM imaging, crystal phase, and purity by X-Ray diffraction. Additionally, emission intensity and lifetime were determined using photoluminescence (PL) spectroscopy.

The empirical data obtained in this study provides further insights into the influence of synthesis conditions on the properties of $\text{NaGdF}_4:18\%\text{Yb}^{3+},2\%\text{Er}^{3+}$ UCNPs. This knowledge is essential in tailoring the particles for specific applications and further modification.

[1] K. Malhotra, D. Hrovat, B. Kumar, G. Qu, J. Van Houten, R. Ahmed, P.I.A. E. Piunno, P. T. Gunning, and U. J. Krull. Lanthanide-Doped Upconversion Nanoparticles: Exploring A Treasure Trove of NIR-Mediated Emerging Applications. *ACS Applied Materials Interfaces* 2023 15 (2), 2499-2528.

THE DEVELOPMENT OF GLUCOSE BIOSENSOR BASED ON DENDRITIC GOLD NANOSTRUCTURES MODIFIED BY CONDUCTING POLYMERS

Natalija German¹, Anton Popov¹, Arunas Ramanavicius², Almira Ramanaviciene¹

¹State Research Institute Centre for Innovative Medicine, Department of Immunology and Bioelectrochemistry, Vilnius, Lithuania

²Vilnius University, Department of Physical Chemistry, Faculty of Chemistry and Geosciences, Vilnius, Lithuania
natalija.german@imcentras.lt

The emergence of nanotechnology has opened up new horizons for the development of electrochemical biosensors [1]. Some notable properties of nanomaterials, such as high surface area and the ability to facilitate charge transfer between the redox center of the enzyme and the electrode, are exploited in the design of biosensors to improve sensitivity and selectivity and reduce response time [2]. Dendritic gold nanostructures (DGNs) are novel nanomaterials that show great promise in various biomedical applications [3]. Various conducting polymers such as polyaniline (PANI) [4] and polypyrrole (Ppy) [5] are widely used in electrocatalysis and for the immobilization of biological molecules.

The main aim of the investigations was to evaluate the efficiency of PANI and Ppy layers formed by enzymatic polymerization on the surface of the graphite rod (GR) electrode initially premodified by electrochemically synthesized DGNs and drop-casted glucose oxidase (GOx). The principle of DGNs electrochemical formation, enzymatic polymerization on GR electrode and electrochemical investigation in the presence of phenazine methosulfate (PMS), are represented in Fig. 1. Analytical characteristics of biosensors based on PANI/GOx/DGNs/GR and Ppy/GOx/DGNs/GR electrodes were evaluated and compared. It was investigated that glucose biosensor based on Ppy/GOx/DGNs/GR electrode was characterized by 0.0594 mA/mM cm² of sensitivity, 0.070 mM of the limit of detection, until 19.9 mM linear glucose determination range, 7.39 proc. of the repeatability and 33 days of the storage stability. Improved glucose biosensor based on the Ppy/GOx/DGNs/GR electrode was successful applicable in real samples (human serum and saliva, milk, juice and wine). Developed glucose biosensor could be used for biomedical purposes, for food and beverage control and biofuel cells.

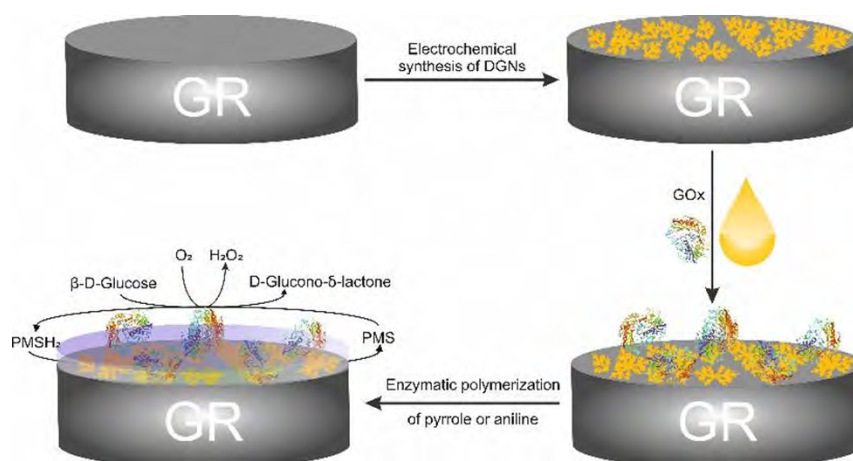


Fig. 1. Schematic representation of developed glucose biosensor

Acknowledgments. This research was funded by a grant (No. S-MIP-20-18) from the Research Council of Lithuania.

- [1] J. Wang, Nanomaterial-based electrochemical biosensors, *Analyst* 130, 421–426 (2005).
- [2] H. Heli, O. Amirzadeh, Non-enzymatic glucose biosensor based on hyperbranched pine-like gold nanostructure, *Materials Science and Engineering C* 63, 150–154 (2016).
- [3] A. Ramanaviciene, N. German, A. Kausaite-Minkstimiene, A. Ramanavicius, Glucose biosensor based on dendritic gold nanostructures electrodeposited on graphite electrode by different electrochemical methods, *Chemosensors* 9 (2021).
- [4] K. Crowley, M.R. Smyth, A.J. Killard, A. Morrin, Printing polyaniline for sensor applications, *Chemical Papers* 67, 771–780 (2013).
- [5] N. German, A. Ramanavicius, J. Voronovic, A. Ramanaviciene, Glucose biosensor based on glucose oxidase and gold nanoparticles of different sizes covered by polypyrrole layer, *Colloids and Surfaces A: Physicochemical and Engineering Aspects* 413, 224–230 (2012).

INTERNAL QUANTUM EFFICIENCY OF GaAsBi/GaAs QUANTUM WELLS

Aistė Butkutė¹, Aivaras Špokas¹, Andrea Zelioli¹, Bronislovas Čechavičius¹, Sandra Stanionytė², Augustas Vaitkevičius^{1,3}, Evelina Dudutienė¹, Renata Butkutė¹

¹Department of Optoelectronics, Center for Physical Sciences and Technology, Lithuania

²Department of Characterisation of Materials Structure, Center for Physical Sciences and Technology, Lithuania

³Institute of Photonics and Nanotechnology, Faculty of Physics, Vilnius University, Lithuania
aiste.butkute@ftmc.lt

One category of materials currently under investigation as potential near-infrared emitters are GaAsBi quantum well (QW) structures [1]. With an increase in Bi content, the bandgap of GaAsBi significantly shifts to longer wavelengths and exhibits reduced sensitivity to the temperature, which makes GaAsBi QW structures a promising active medium for tunable optoelectronic devices, which do not require additional cooling [2]. However, the growth of GaAsBi quantum structures requires low growth temperatures, which leads to a high point defect density, resulting in a significant reduction in GaAsBi photoluminescence (PL) intensity.

To optimize the growth of GaAsBi structures it is necessary to investigate optical properties and quantitatively assess emission efficiency of it. Although there are several groups around the world growing GaAsBi structures and investigating optical properties of it, no group has yet attempted to quantitatively evaluate the internal quantum efficiency (IQE) of GaAsBi QW.

Therefore, in this work, temperature and excitation dependent PL is used to investigate optical properties of GaAsBi structures and quantitatively evaluate the IQE of GaAsBi. Emission efficiency of GaAsBi QWs was investigated using relative excitation-dependent PL measurements and applying ABC method (Fig. 1), which determines IQE as ratio of radiative recombination and total recombination rate [3]. Obtained IQE values were compared with GaAsBi IQE values acquired using other methods. Moreover, a contribution from trap-assisted Auger non-radiative recombination to IQE value was also considered.

Quantitatively assessed emission efficiency allows not only to compare structures grown and characterized in different laboratories, but also to evaluate the amount of non-radiative recombination.

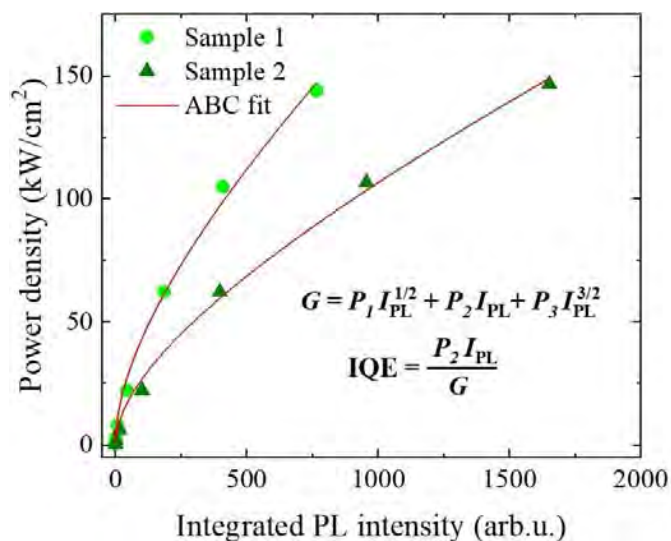


Fig. 1. IQE evaluation using excitation-dependent PL measurement.

[1] R. D. Richards et al. Phys. Stat. Sol. (B) 259(2), 2100330 (2022).

[2] K. Alberi et al. Appl. Phys. Lett. 91, 051909 (2007).

[3] Y. S. Yoo et al. Appl. Phys. Lett. 102, 211107 (2013).

INFLUENCE OF SI ADDITIVES ON THE STRUCTURE OF NANOCRYSTALLISED Na₂VFe₂(PO₄)₃ ALLUAUDITE-LIKE GLASSES

Martyna Jankowska¹, Krzysztof Gadomski¹, Maciej Nowagiel¹, Tomasz K Pietrzak¹, Linda F Nazar²

¹Faculty of Physics, Warsaw University of Technology, Poland

²Department of Chemistry and the Waterloo Institute for Nanotechnology, University of Waterloo, Ontario, ON, Canada
martyna.jankowska.stud@pw.edu.pl

Last few decades, intensive development of batteries has been observed. Right now, they are used almost everywhere: in electric cars, smartphones, and even to stabilize power output from renewable power sources. In the last case, sodium-ion batteries (NIBs) are expected to be a sustainable and cheap alternative to lithium ones [1]. Alluaudites, first described by Fisher in 1955 [2], are among the prospective cathode materials for NIBs, with a theoretical gravimetric capacity close to 170 mAh/g [3]. However, poor electrical conductivity is one of the main obstacles to their implementation.

Previous studies on amorphous analogs of cathode materials for Li-ion batteries show a significant increase in electrical conductivity as a result of their thermal nanocrystallization due to the occurrence of the preferable conditions for the polaron hopping mechanism of conduction [5]. A similar procedure can be successfully applied to sodium compounds as well.

In our previous research, we studied materials with a nominal composition of Na₂Fe₃(PO₄)₃, Na₂Fe₂V(PO₄)₃, and Na₂FeMnV(PO₄)₃. Thermal treatment of glassy samples led to nanocrystallisation of the alluaudite phase [4]. We observed a significant (5 orders of magnitude) and irreversible conductivity increase, resulting in nanomaterials with $\sigma(25^\circ\text{C}) \approx 1$ mS/cm. We also elaborated optimal synthesis conditions to obtain alluaudite-like nanomaterials with maximum possible phase purity [6]. We performed electrochemical characterisation of the most prospective samples in prototype sodium cells. Their average performance, however, did not reflect the superior electrical conductivity of the active material.

Therefore, in this work, we decided to synthesise Na₂Fe₂V(PO₄)₃ alluaudite-like glass with an addition of silicon oxide. It is expected that SiO₄ tetrahedra might change the ion transport in nanocrystalline materials from 1D to 2D and, consequently, improve electrochemical performance. In this work, we present thermal (DSC), structural (XRD), and electrical (IS) properties of our materials.

[1] V. Palomares et al., *Energy & Environmental Science* 5 (2012), 5884–5901

[2] D.J. Fisher, *American Mineralogist* 40 (1955), 1100–1109.

[3] K. Trad et al., *Chemistry of Materials* 22 (2010), 5554–5562.

[4] A.E. Chamryga et al., *Journal of Non-Crystalline Solids* 526 (2019), 119721.

[5] T.K. Pietrzak et al., *Materials Science and Engineering B* 213 (2016), 140–147.

[6] M. Nowagiel et al., *Materials* 14(17) (2021), 4997.

INVESTIGATION OF THE USE OF AlGaAs/InGaAs QUANTUM WELL FOR NIR EMITTERS

Andrea Zelioli¹, Aivaras Špokas¹, Gustas Petruševičius¹, Bronislovas Čechavičius¹, Evelina Dudutienė¹, Renata Butkutė^{1,2}

¹Department of Optoelectronics, Center for Physical Sciences and Technology, Sauletekio 3, 10257 Vilnius, Lithuania

²Institute of Photonics and Nanotechnology, Vilnius University, Sauletekio av. 3, LT-10257 Vilnius
andrea.zelioli@ftmc.lt

Near infrared emitters (NIR) lasers are used in many different applications from material processing, communication, consumer electronics, atmospheric monitoring to the medical.

One particular type of laser structure that is suitable for many of these applications due to its flexibility is the vertical external cavity laser (VECSEL). This structure is comprised of a mirror and an active area that consist of quantum wells. The composition and design of these quantum wells allows to modify the emission energy of the laser.

In our work we are focused on the fabrication and optimization of a source that emits at 976nm. This wavelength finds different application one of which is the generation of 488nm light via frequency doubling.

To due to the power lost during the conversion of light it is particularly important to improve the output power of the device.

To achieve this we studied how a different QW design in which InGaAs/GaAs QW are substituted by InGaAs/AlGaAs/GaAs structure can allow to increase the photoluminescence (PL) intensity. During the work structures were grown on semi-insulating GaAs substrate using molecular beam epitaxy technique.

Different series of samples were analysed, in the first series samples with one quantum well were grown. The Al content in the barriers was varied from 0% up to 30%, the thickness of the barriers was changed from 5nm up to 25nm. The In content in the quantum well was 21%.

The PL spectra of all the structures was measured. Matching computational simulations and the spectra of the grown structures we were able to compare the effect of different barriers design, and growth conditions.

The second series of samples was grown to study the effect of Al in a full VECSEL chip geometry were 12 QWs are used.

MOCVD GaN SENSORS WITH CHEMICALLY ETCHED SURFACES

Gertrūda Pociūtė¹, Tomas Čeponis¹, Jevgenij Pavlov¹

¹Institute of Photonics and Nanotechnology, Vilnius University
gertruda.pociute@ff.stud.vu.lt

Gallium nitride (GaN) is a wide band gap III-V semiconductor which is perspective for fabrication of the modern solar-blind photo-sensors and particle detectors applied in radiation monitoring, medical diagnostics and high energy physics experiments [1]. Metalorganic Chemical Vapor Deposition (MOCVD) is a commonly used method for growing crystalline layers of GaN, where the density of dislocations in such layers can reach 10^{10} cm^{-2} [2]. These dislocations, being charged and surrounded by space charge region, act as non-radiative recombination centers and also affect the mobility of carriers [3]. The dislocations in GaN crystals often degrades the performance of GaN-based devices (a screw and mixed components generally cause leakage current in GaN crystals). The strain field of the dislocations and decoration with background impurities influence the electrical and optical characteristics of GaN-based devices [4]. An important role plays an open or closed dislocation core in determination of the leakage current [5]. It has also been shown that the chemical etching of GaN surface significantly modifies the structure of dislocations and their occupied areas and impacts the intensity of scintillation signals (Fig. 1) in MOCVD GaN layers.

In this work the modifications of MOCVD GaN surfaces were performed by using a potassium hydroxide (KOH 30%) and phosphoric acid (H_3PO_4 85%) solutions to evaluate the impact of chemical etching on the changes of the electrical and optical properties of MOCVD GaN layers. The electrodes were formed on these structures using indium (In) eutectic deposition followed by sintering procedures. Several contact and contactless methods were used for the study of electrical and optical properties of chemically etched MOCVD GaN structures.

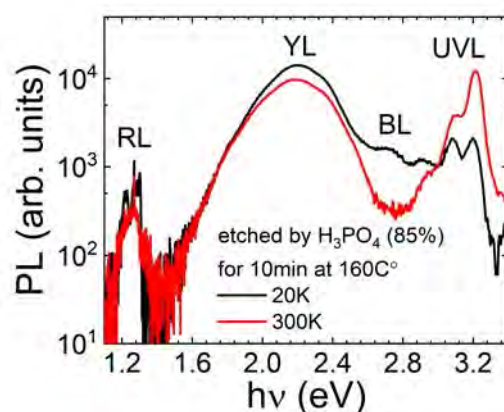


Fig. 1. The TI-PL spectra measured in chemically etched MOCVD GaN at 20K and 300K.

Measurements of electrical and optical properties of chemically etched MOCVD GaN sensors were carried out in the 20-300 K temperature range. The comparative analysis of variations of these characteristics in chemically etched MOCVD GaN will be presented and discussed.

CATHODOLUMINESCENCE AT THE VICINITY OF DEFECTS IN III-NITRIDES

Viktorija Mickūnaitė¹, Mantas Migauskas¹, Žydrūnas Podlipskas¹

¹Vilnius University
viktorija.mickunaite@ff.stud.vu.lt

Unique properties of III-nitrides such as high dielectric breakdown voltage, chemical and thermal stability, tunable bandgap allowing spectral coverage from IR to UV make them attractive materials for applications in the fields of microelectronics and optoelectronics. Quantum efficiency and spectral characteristics of semiconductors are highly influenced by defects introduced during growth.

The aim of this work was to investigate defect influence on spectral properties and to find correlation between peak wavelength and integrated intensity of various III-nitride materials using hybrid technique of scanning electron microscopy and cathodoluminescence spectroscopy. The Attolight Chronos SEM-CL microscope was used for analysis, and Python code correlated cathodoluminescence intensity with peak wavelength which was evaluated by Pearson's coefficient.

It was found that in InGaN and AlGaN samples, defects like dislocations and stacking faults induce morphology changes, influencing alloy or quantum well fluctuations resulting in peak wavelength shifts at the vicinity of these sites. It was observed that optical properties and correlation between peak wavelength and CL intensity in GaN samples are highly influenced by density of point defects. It was also shown that energy shifts in all samples can occur due to tensile and compressive strain region formation around dislocations and atom segregation phenomenon.

This study emphasizes the complex interplay between defects and material properties which provides valuable insights for optimizing III-nitride devices.

ELECTROCHEMICAL IMMUNOSENSOR BASED ON GOLD NANOSTRUCTURES FOR THE DETECTION OF ANTIBODIES AGAINST SARS-COV-2 SPIKE PROTEIN

Kristina Sobol¹, Katarzyna Blazevic¹, Benediktas Brasiunas¹, Almira Ramanaviciene¹

¹NanoTechnas - Center of Nanotechnology and Materials Science, Institute of Chemistry, Faculty of Chemistry and Geosciences, Vilnius University
kristina.sobol@chgf.stud.vu.lt

Electrochemical immunosensors have become fundamental tools in various fields, including biomedical diagnostics, disease progression monitoring, environmental surveillance, food quality control, forensic analysis, and biomedical research. These highly specific analytical systems demonstrate exceptional sensitivity and efficiency, enabling precise identification of analyte presence and its concentration in a sample [1].

The principle operation of an electrochemical immunosensor is based on the electrochemical signal recording after the specific interaction between immobilized antigen and antibodies present in the solution. Essential requirements for immunosensors are their selectivity, sensitivity, repeatability, accuracy, and reproducibility. To enhance the sensitivity of the immunosensor, the surface of the electrode is frequently modified with nanomaterials, known for their unique physical, chemical, and optical properties. Compared to traditional immunosensors, nanomaterial-based immunosensors are more specific and sensitive, allowing the detection of lower analyte concentration [2].

In this study, an electrochemical immunosensor was developed for investigation of the interaction between immobilized SARS-CoV-2 virus S protein and specific monoclonal antibodies. The impact of various gold nanostructures formed on the electrode on the performance of the immunosensor was evaluated. Additionally, the influence of non-specific interactions on the analytical signal was investigated, along with methods used to reduce such effect. This research contributes valuable insights into the optimization and application of electrochemical immunosensors for biomedical diagnostics.

Acknowledgement

This research was funded by a grant (No. S-MIP-22-46) from the Research Council of Lithuania.

[1] M. Zembala, Z. Adamczyk, Measurements of streaming potential for mica covered by colloid particles, *Langmuir* 2000, 16, 1593-1602 (1999).
[2] T. Luxbacher, *The ZETA Guide: Principles of the streaming potential technique*. 27-30. (Anton Paar GmbH, 2014).

CONSIDERATION OF THE STABILITY OF A MOLECULARLY IMPRINTED POLYMER LAYER CONCERNING ITS THICKNESS

Greta Pilvenytė¹, Raimonda Bogužaitė¹, Vilma Ratautaitė¹, Arūnas Ramanavičius^{1,2}

¹Bioanalysis laboratory, Department of Nanotechnology, State Research Institute Center for Physical Sciences and Technology

²Department of Physical Chemistry, Institute of Chemistry, Faculty of Chemistry and Geosciences, Vilnius University
greta.pilvenyte@ftmc.lt

Molecularly imprinted polymers (MIP) are developed through the polymerisation of functional monomers in the presence of template molecules. However, a key step in the preparation of MIPs is template extraction after polymerisation. Polypyrrole has gained significant attention in sensor development due to its electrical conductivity, straightforward synthesis, and good mechanical properties. This makes it a promising option for the cost-effective fabrication of sensitive biosensors[1].

Achieving optimal stability and adhesion is crucial for reliable sensing. One prominent solution is the optimisation of the deposited layer thickness. Challenges such as detachment and reduced sensitivity can be addressed through precise layer thickness control, allowing for enhanced binding interactions with target molecules.

This presentation considers the stability of polypyrrole-based MIP layers with methylene blue molecule imprints, polymerised on an indium tin oxide-modified glass electrode. The polymer layer thickness is adjusted by varying the number of electropolymerisation cycles (5, 7, and 10) using cyclic voltammetry. Monitoring changes in absorbance were used for the evaluation of layer thickness[2]. This analytical approach provides valuable insights into optimising the design of molecularly imprinted polypyrrole electrodes for stable sensors.

-
- [1] G. Pilvenyte et al., Molecularly imprinted polymers for the recognition of biomarkers of certain neurodegenerative diseases. *J. Pharm. Biomed. Anal.*, 2023, 228, 115343.
[2] R. Boguzaitė et al., Towards Molecularly Imprinted Polypyrrole-Based Sensor for the Detection of Methylene Blue. *Chemosensors* 2023, 11, 549.

APPLICATION OF GOLD NANORODS TOWARDS THE DEVELOPMENT OF ELECTROCHEMICAL BIOSENSORS

Marina Šapauskienė¹, Viktorija Lisytė¹, Almira Ramanavičienė¹, Anton Popov¹

¹Vilnius University
marina.sidorova@chgf.stud.vu.lt

Gold nanoparticles (AuNPs) are attracting great research interest due to their unique physical and chemical properties. This makes them multifunctional materials suitable for applications in various fields such as medicine, environment, and engineering [1].

Among AuNPs, gold nanorods (AuNRs) are in high demand due to the tunability and sensitivity of their longitudinal surface plasmon resonance [2, 3]. The anisotropic structure of AuNRs exhibits two surface plasmon bands corresponding to surface electron oscillation on the transverse and longitudinal sides [4]. The size, shape, and surface functionality of AuNPs are dependent on the synthesis method [5-6].

The main objective of this research was to synthesize AuNRs of different lengths using different synthesis methods and to determine their electrochemical properties. The obtained AuNRs were characterized using SEM and UV-VIS techniques. These techniques allowed a detailed description of the structural and optical properties of the AuNRs and provided valuable insights into the synthesis. The cyclic voltammetry was used to evaluate the electroactive surface area of the electrodes modified with AuNRs. The results of the electrochemical characterization of electrodes were crucial to a more profound understanding of the potential applications of AuNRs.

-
- [1] Yao L, et al., Applications and safety of gold nanoparticles as therapeutic devices in clinical trials. *J Pharm Anal.* 2023;13(9):960–7.
[2] Amendola V, et al., Surface plasmon resonance in gold nanoparticles: a review. *J Phys Condens Matter.* 2017, 29(20), 203002.
[3] Cao, J. et al. Gold nanorod-based localized surface plasmon resonance biosensors: A review. *Sens. Actuators B Chem.* 2014, 195: 332-351.
[4] Wu, H.Y. et al. Seed-mediated synthesis of high aspect ratio gold nanorods with nitric acid. *Chem. Mater.* 2005, 17(25), 6447-6451.
[5] Yeh Y-C, et al. Gold nanoparticles: Preparation, properties, and applications in Bionanotechnology. *Nanoscale.* 2012;4(6):1871–80.
[6] Brasiunas B, et al. The effect of gold nanostructure morphology on label-free electrochemical Immunosensor Design. *Bioelectrochemistry.* 2024 Apr;156:108638.

LUMINESCENT POLYMER COATINGS: ENCAPSULATING PEROVSKITE QUANTUM DOTS ON GLASS SURFACE

Živilė Stanionytė¹, Vaidas Klimkevičius¹

¹Institute of Chemistry, Faculty of Chemistry and Geosciences, Vilnius University, Naugarduko str. 24, LT-03225, Vilnius, Lithuania
zivile.stanionyte@chgf.stud.vu.lt

The increasing popularity of renewable sources has led to a heightened focus on the development and research of technologies aimed at enhancing the efficiency of energy conversion. Halide perovskite quantum dots (PQDs) have garnered significant scientific attention as promising luminescent materials with the potential to increase the efficiency of solar cells. This is attributed to their exceptional optical and electronic properties, including a high absorption coefficient and a tunable bandgap [1]. However, the broader application of these materials is limited due to their poor optical stability under exposure to environmental conditions like moisture, oxygen, light and heat [2]. Addressing this issue includes the approach to establish a physical barrier between the PQDs and their surroundings through embedding them within a polymer matrix [3].

In this study, all-inorganic metal halide CsPbBr₃ PQDs were synthesized via an ultrasound-induced hot-injection route and later immobilized in polymethylmetacrylate (PMMA) matrix on a glass surface using the spin-coating technique. The optimal conditions for the coating formation have been determined by evaluating the effect of rotation speed, number of layers and waiting time between layers. By employing post-synthesis ion exchange modification to adjust the bandgap of PQDs, coatings emitting diverse wavelengths across the visible spectrum were achieved. The structural properties of the synthesized PQDs have been investigated via X-ray diffraction analysis and the quality of formed PQDs-polymeric coatings was evaluated with electronic microscopy. The photoluminescence properties (absorption and emission spectra, quantum yield and temperature dependence of emission intensity) have been also evaluated.

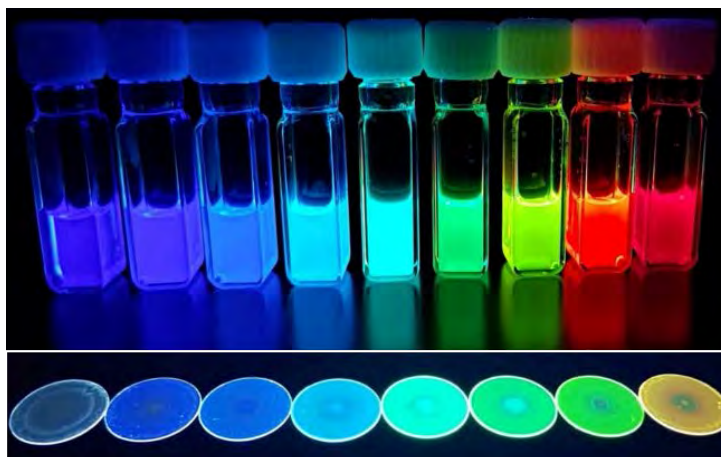


Fig. 1. Color gamut of obtained multicolor PQDs in toluene (top) and immobilized in polymer matrix (bottom) under UV excitation (λ_{ex} 365 nm).

-
- [1] J. Chen, D. Jia, E. M. J. Johansson, A. Hagfeldt, X. Zhang, Emerging perovskite quantum dot solar cells: feasible approaches to boost performance, *Energy Environ. Sci.*, 14 (2021) 224-261.
 [2] Y. Wei, Z. Cheng, J. Lin, An overview on enhancing the stability of lead halide perovskite quantum dots and their applications in phosphor-converted LEDs, *Chem. Soc. Rev.*, 48 (2019) 310-350.
 [3] L-C. Chen, C-H. Tien, Z-L. Tseng, Y-S. Dong, S. Yang, Influence of all-inorganic halide perovskite CsPbBr₃ quantum dots combined with polymer matrix, *Materials*, 12(6) (2019) 985.

EXTENDED REALITY IN NANOTECHNOLOGY

Šarūnas Ščefanavičius¹, Raman Levoshka², Ilse-Christine Gebeshuber²

¹Vilnius University

²Technical University of Vienna
sarunas.scefanavicius@ff.stud.vu.lt

Currently, nanotechnology faces a big problem that it is difficult to teach and learn because of the small size of the nanomaterials. Extended Reality offers a way to solve this problem. In my research during Erasmus studies at Technical University of Vienna, Austria me and my colleague Raman Levoshka developed three-dimensional models of nanomaterials and nanostructures using Augmented Reality (AR) to visualize the concepts better. The nanomaterials were chosen to be graphene, carbon nanotube, carbon buckyball and lastly to showcase the full potential of AR – Space Elevator. The models were created using Rhino and Grasshopper software, and visualized using Abode Aero software. This project aimed to implement Extended Reality into Nanotechnology to give more access to the study of nanomaterials. Additionally, it makes communication between researchers and consumers, professors and students, manufacturers and investors more accessible in terms of nanotechnology.

ANALYSIS OF SILVER NANOPARTICLE LAYER FORMATION ON LASER-INDUCED PERIODIC SURFACE STRUCTURES

Mantas Mikalkevičius¹, Nadzeya Khinevich¹, Tomas Tamulevičius^{1,2}, Asta Tamulevičienė^{1,2}

¹Institute of Materials Science of Kaunas University of Technology, K. Baršausko Str. 59, LT-51423, Kaunas, Lithuania

²Department of Physics of Kaunas University of Technology, Studentų Str. 50, LT-51368, Kaunas, Lithuania
mantas.mikalkevicius@ktu.edu

Generation of laser-induced periodic surface structuring (LIPSS) is a fast and low-cost method for nanostructure formation. Nano-ripples can act as a template for metal nanoparticle deposition, which exhibits plasmonic properties. Layer of nanoparticles deposited on a template shows enhancement of Raman scattering signal and could be used to detect low-concentration analyte molecule.

In this study, surface of crystalline silicon was structured with femtosecond laser pulses (Pharos) to induce LIPSS on the surface that alters wetting properties of the surface. Later on chemically synthesized silver nanoparticles of 100 nm diameter were deposited on the Si LIPSS by drop evaporation and monolayer formation methods. In the drop evaporation method, a drop of colloidal solution was dispersed on periodic structures and dried at 3 different temperatures: 35 °C, 21 °C, and 4 °C. Furthermore, a monolayer of nanoparticles was created in the water-hexane interface and later on transferred onto the structures by capillary flow. SEM surface analysis showed that deposition of nanoparticles strongly depends on the temperature during the process. At 35 °C nanoparticles were deposited randomly all over the surface, at 21 °C nanoparticles started to follow the pattern but grooves were not filled completely, and at 4 °C all the grooves were filled with nanoparticles. A deposition from a water-hexane interface was most effective as nanoparticles covered a surface of periodic structures as a closely packed layer (see Fig. 1).

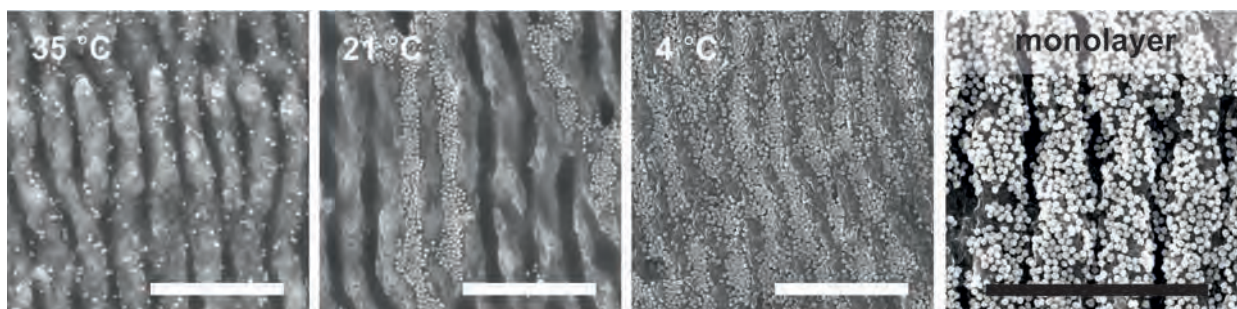


Fig. 1. SEM surface image of deposited nanoparticles on periodic structures. Scale bar is 3 μm

SIZE-DEPENDENT PROPERTIES OF YTTERBIUM DOPED CESIUM LEAD HALIDE PEROVSKITE PARTICLES

Daniel Rodz¹, Simona Streckaitė¹, Vidmantas Gulbinas¹

¹Department of Molecular Compound Physics, Center for Physical Sciences and Technology, Vilnius, Lithuania
rodz.daniel@yahoo.com

Perovskites have shown to be promising materials in the field of photovoltaics, where an efficiency of 25.5% for perovskite solar cells [1]. Perovskites are also promising materials in some other applications, for example 23% for light emitting diodes [2] was reached. Ytterbium doped lead halide perovskites, show an interesting quantum-cutting phenomenon where one high energy photon absorbed by the perovskite is down-converted into two low energy photons emitted by Yb³⁺ ions. Such materials have been shown to be efficient in luminescent solar concentrators which applied on top of conventional Si solar cells they may enhance their efficiency [3].

Although ytterbium doped perovskites are already being tested in various applications [3,4], many methods for their fabrication are still not easy or environmentally friendly. This is mainly due to the complicated nature of preparation methods [5] and the use of volatile and/or dangerous solvents [5]. In this work we apply facile mechanosynthesis method for the synthesis of CsPbCl₃ doped with Yb³⁺ [6]. This method requires only simple grinding and heating to produce samples with high photoluminescence quantum yield (PLQY) of ytterbium in near infrared (NIR) region. We investigate structural and optical properties of the powders, most importantly NIR PLQY and how efficiently ytterbium is incorporated in the fabricated samples, depending on the grain size by applying steady-state and time-resolved absorption and other techniques.

After grinding and annealing of precursor materials, the prepared Yb³⁺-doped CsPbCl₃ perovskite powders (with 5% of Pb²⁺ ions exchanged by Yb³⁺ ions) were sieved into 3 grain size groups: smallest <25 μm, medium 75-100 μm and largest >200 μm particles. For biggest particles of >200 μm size, we observe fastest excitonic decay which should indicate efficient energy transfer to Yb³⁺ ions (Fig. 1b). However, QY of ytterbium emission explored with relation to the particle size show that smaller particles of less than 100 μm exhibit higher NIR PLQY than the largest particles (Fig. 1b). The processes which limit the energy conversion efficiency are yet to be defined with additional structural and spectroscopic studies.

We are also exploring ways of synthesising ytterbium doped perovskite quantum dots (QDs). For now synthesis of non-doped perovskites were achieved using simple grinding method, opposed to the standard hot injection method [5]. New experiments are under way, which may help develop a methodology for easy synthesis of high NIR PLQY perovskite QDs.

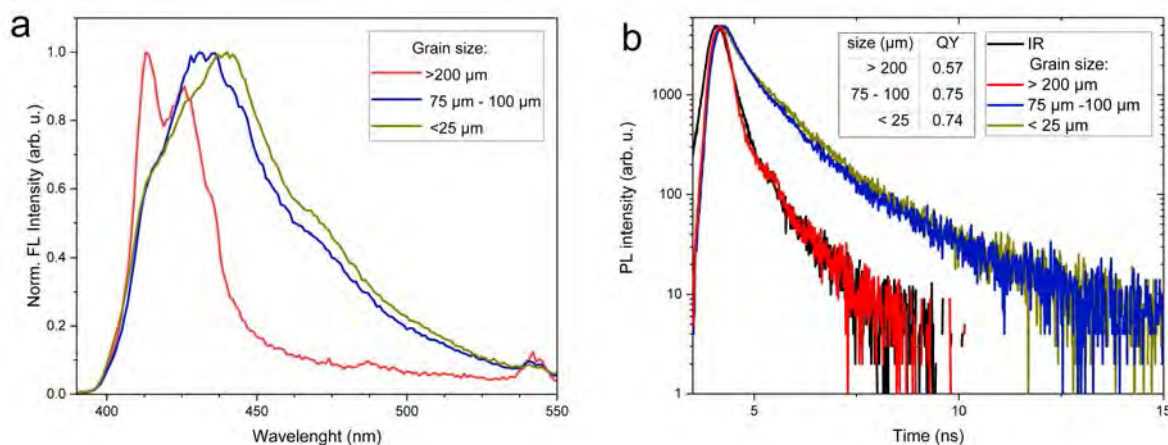


Fig. 1. Fluorescence (FL) spectra (a) and kinetics at emission (b) of CsPb_{0.925}Yb_{0.05}Cl₃ powder depending on the grain size. Inset in (b) shows QY of the samples.

- [1] Min, H., Lee, D.Y., Kim, J. et al. Nature, 2021 598, 444–450
- [2] Fakhruddin, A., Gangishetty, M.K., Abdi-Jalebi, M. et al. Nat Electron 5, 203–216 (2022)
- [3] Xiao Luo, Tao Ding, Xue Liu et al. Nano Letters 2019 19 (1), 338–341
- [4] Huang, H.; Li, R.; Jin, S. et al, ACS Appl. Mater. Interfaces 2021, 13 (29), 34561– 34571
- [5] Huang, H.; Li, R.; Jin, S. et al, ACS Appl. Mater. Interfaces 2021, 13 (29), 34561– 34571
- [6] Streckaitė Simona, Mikiušis Lukas, Maleckaitė Karolina et al. Journal of Materials Chemistry (2023) C. 11. 10.1039/D3TC02631K

STABILIZATION OF DELTA-Bi₂O₃ PHASE AT ROOM TEMPERATURE BY THERMAL NANOCRYSTALLIZATION OF BISMUTH OXIDE GLASSES

Maciej Nowagiel¹, Julien Trébosc², Olivier Lafon², Tomasz Płociński³, Marek Wasiucionek¹, Jerzy E Garbarczyk¹, Tomasz K Pietrzak¹

¹Faculty of Physics, Warsaw University of Technology, Poland

²Unité de Catalyse et de Chimie du Solide, Université de Lille, France

³Faculty of Materials Science and Engineering, Warsaw University of Technology, Poland
maciej.nowagiel.dokt@pw.edu.pl

Crystalline δ -Bi₂O₃ is the best-known O²⁻ ion conductor, but it is stable in a relatively narrow temperature range 729–825°C only. Its very high ionic conductivity (1 S/cm at 750°C) has motivated many researchers to look for a method to stabilize this fluorite-type structure to much lower temperatures. So far, the successful strategies to achieve the stabilization of the δ phase have included doping (e.g. by rare-earth elements [1]) or synthesis in form of thin layers [2].

In this research, however, we first obtained Bi₂O₃ glasses at various synthesis conditions. Al and Si additives, originating from the crucibles used in melting, facilitated the glass formation upon quenching. Then we subjected them to appropriate thermal treatment [3]. As a result, materials with various crystalline Bi₂O₃ phases were obtained: δ , β and γ – depending on the synthesis conditions. The phases (including δ) were found to be stable down to room temperature. The microstructure of samples was investigated by electron microscopy techniques (both SEM and HRTEM). The grains of δ -Bi₂O₃ phase were observed usually as < 100 nm nanocrystallites, confined in a residual glassy matrix. In the case of grains of β and γ phases their sizes were much larger – of the order of micrometers.

MAS NMR and TEM studies were applied to determine the local order around Al and Si dopants, and to investigate their role in the stabilization of the Bi₂O₃ phases. From this experiment, one can conclude that Al and Si additives are rather unlikely to stabilize directly the δ -like phase, because they seem to remain in the residual amorphous matrix. On the contrary, they are believed to participate in the formation of glass and induce the confinement effect of pure δ -Bi₂O₃ nanocrystallites.

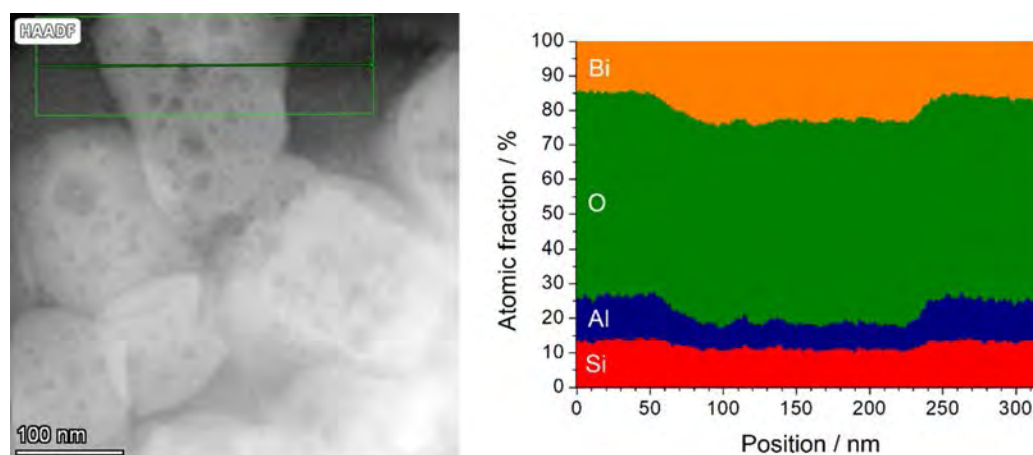


Fig. 1. Transmission electron microscopy (TEM) image of δ -Bi₂O₃ crystalline grains confined in amorphous matrix (left) with atomic composition across the line going through selected grain obtained by EDX method (right).

Acknowledgments

This research was funded by POB TechMat of WUT within the IDUB program, and by National Science Centre (NCN), Poland, in frames of a grant Preludium BIS 2 no. 2020/39/O/ST5/00897. NMR experiments were funded from the European Union's Horizon 2020 program, grant agreement No 731019 (EUSMI).

[1] M. Leszczynska et al., J. Mater. Chem. A 2 (2014) 18624–18634.

[2] H.T. Fan et al., Thin Solid Films 513 (2006) 142–147.

[3] T.K. Pietrzak et al., Scientific Reports 11 (2021) 19145.

DESIGN AND SYNTHESIS OF MOLECULAR BUILDING BLOCKS FOR MODULAR SUPRAMOLECULAR CAVITANDS

Nojus Radzevičius¹, Edvinas Orentas¹

¹Institute of Chemistry, Faculty of Chemistry and Geosciences, Vilnius University, Naugarduko str. 24, Vilnius, Lithuania
nojus.radzevicius@chgf.stud.vu.lt

Cavitands are macrocyclic molecules containing a permanent intramolecular cavity for non-covalent binding of guest molecules. The most commonly encountered types of cavitands are cyclodextrins and cyclic phenol-formaldehyde oligomers. Such compounds have many potential applications as synthetic enzymes¹, drug delivery systems², or filters for removing polyaromatic contaminants from aqueous systems³. However, existing cavitand designs suffer from high symmetry and poor capabilities of functionalization and cavity size modification, which severely limits their potential.

Our current research is based around a system that enables the modular synthesis of various different-sized cavitands from a small selection of molecular building blocks through cyclocondensation reactions. The system is centered around derivatives of bicyclic V-shaped compound **1**. Methods for the synthesis and resolution of enantiomerically pure (+)-**1**⁴ and both enantiomers of the heterocyclic variant (+)-**2** and (-)-**2**⁵ have been developed. Bifunctionalized symmetric synthons **5** and **6** for Friedlander and Fischer cyclocondensations have also been successfully synthesized and tested in the corresponding condensation reactions. However, synthesis of cavitands has been unsuccessful due to solubility problems and self-condensation side reactions emerging after functionalization with bulky solubilizing groups. Future plans include alternative routes of functionalization and synthesis of model cavitands.

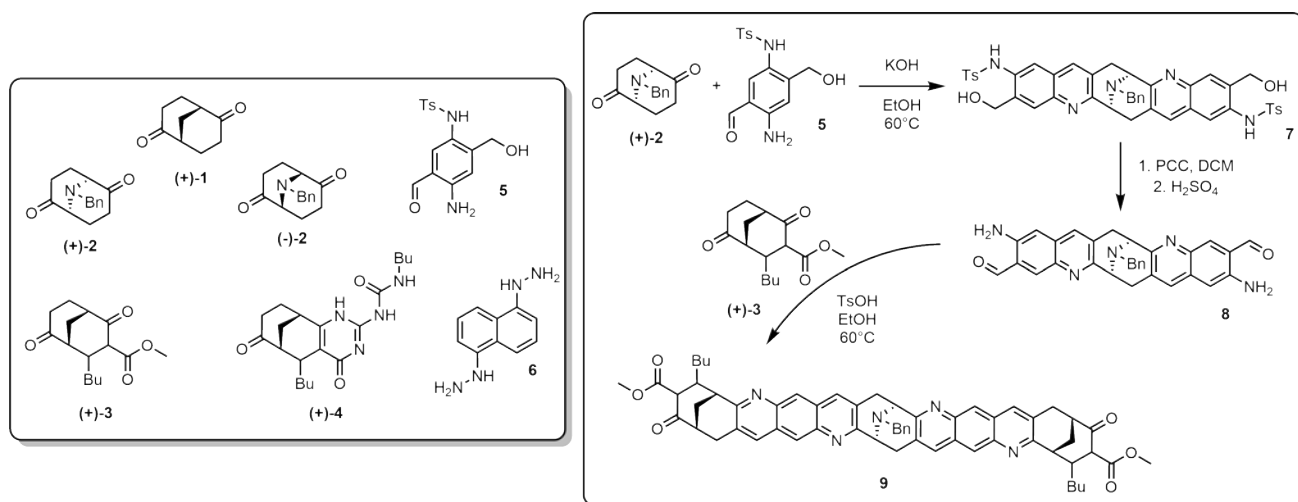


Fig. 1. Prepared molecular building blocks (left) and model cavitand synthesis (right).

- [1] B.W. Purse, P. Ballester and J. Rebek, Reactivity and molecular recognition: amine methylation by an introverted ester, *J Am Chem Soc*, 125, 14682 (2003)
- [2] R. Challa, A. Ahuja, J. Ali and R.K. Khar, Cyclodextrins in drug delivery: An updated review, *AAPS PharmSciTech*, 6, E329 (2005)
- [3] APedrini et al., Reusable Cavitand Based Electrospun Membranes for the Removal of Polycyclic Aromatic Hydrocarbons from Water, *Small*, 18, 2104946 (2022)
- [4] C.J. Wallentin et al., Bakers Yeast for Sweet Dough Enables Large Scale Synthesis of Enantiomerically Pure Bicyclo(3.3.1)nonane 2,6 dione, *Synthesis (Stuttg)*, 2009, 864 (2009)
- [5] V. Bieliūnas, D. Račkauskaitė, E. Orentas and S. Stončius, Synthesis, enantiomer separation, and absolute configuration of 2,6 oxygenated 9 azabicyclo(3.3.1)nonanes, *J Org Chem*, 78, 5339 (2013)

ELECTROCHEMICAL SENSOR DEVELOPMENT FOR MELAMINE DETECTION

Ernestas Brazys¹, Vilma Ratautaitė², Arūnas Ramanavičius^{1,2}

¹Department of Physical Chemistry, Institute of Chemistry, Faculty of Chemistry and Geosciences, Vilnius University, Lithuania

²Department of Nanotechnology, State Research Institute Center for Physical Sciences and Technology (FTMC), Lithuania
ernestas.brazys@chgf.stud.vu.lt

Melamine is a compound usually used in the plastics industry to produce melamine–formaldehyde resins. It contains a large amount of nitrogen (66 % by mass). The worldwide outbreaks of misuse by unethical manufacturers of this property and adding melamine to dairy products to inflate measured protein levels are described in the literature. One of them was in 2008 when melamine-containing milk caused urinary stones in children under the age of 3 in China [1]. It was established that melamine is nephrotoxic to humans and the consumption of it can cause renal diseases. Therefore, melamine was limited to 2.5 ppm in dairy products by the responsible authorities, including the European Community and the US Foods and Drug Administration. To enforce these regulations, a wide variety of methods have been developed to detect melamine. In this presentation, melamine detection by employing molecularly imprinted polypyrrole is demonstrated [2].

The typical molecular imprinting procedure consists of a few steps: 1) self-assembly of monomer, cross-linker, and template molecules to form pre-polymerization complexes; 2) chemical or electrochemical polymerization; 3) the polymerization step is then followed by the removal of the template, which generates the binding sites in the structure of the polymer, which are specific or complementary to the template molecules [3]. This characteristic can be used in the development of sensors for specific detection [4].

In this study, the melamine-imprinted polypyrrole-based (MIP) sensor was developed [2]. The pre-polymeric mixture contained 50 mM of pyrrole as a monomer and 5 mM of melamine as a template in a 10 mM PBS solution, pH 7.4. The polymeric layer was deposited electrochemically directly on the surface of a graphite electrode by a sequence of potential pulses. The template molecules were extracted by washing the polymer in 1 M H₂SO₄ solution for 60 min. In comparison, an electrode was modified with a non-imprinted polypyrrole layer (NIP). Further, both MIP and NIP layers were modified with 3.5 nm, 6 nm, and 13 nm diameter gold nanoparticles (AuNPs), and gold (I) complexes during the polymer preparation step.

The properties of all polypyrrole films were evaluated by differential pulse voltammetry (DPV) using a 10 mM PBS solution (pH 7.4) with 5 mM K₃[Fe(CN)₆]/K₄[Fe(CN)₆] redox probe. The interaction between melamine and polymer layers was assessed by the comparison of oxidation peak currents of the aforementioned system and calculating the apparent imprinting factor. The most optimum results were achieved by MIP modified with 0.05 nM AuNPs with a diameter of 3.5 nm.

[1] A. K. C. Hau et al. Melamine toxicity and the kidney. *JASN*, 20 (2009).

[2] E. Brazys et al. Molecularly imprinted polypyrrole-based electrochemical melamine sensors. *Microchem. J.*, 199 (2024).

[3] V. Ratautaitė et al. Electrochemical sensors based on L-tryptophan molecularly imprinted polypyrrole and polyaniline. *J. Electroanal. Chem.*, 917 (2022).

[4] V. Ratautaitė et al. Evaluation of the interaction between SARS-CoV-2 spike glycoproteins and the molecularly imprinted polypyrrole. *Talanta*, 253 (2023).

ANTIOXIDANT CONTENT OF FOOD PACKAGES MADE FROM POLYETHYLENE

Toma Petrulioniene¹, Tomas Murauskas²

¹Center for Physical Sciences and Technology (FTMC)

²Vilnius university

toma.petrulioniene@ftmc.lt

Polyethylene is used in many fields due to its uncomplicated modification, especially in food packaging. It exhibits outstanding chemical resistance, high tensile strength, and low density. Unfortunately, to manufacture the desired packages, all kinds of additives must be added. All these additives can migrate to food through the functional barrier and contaminate it, causing human health problems. Though antioxidants as a group of potential migrants, is only one of many groups of additives. Determining antioxidant levels in food packages helps to clarify the migration levels of these compounds, and assess potential health risks.

An objective of this study was to determine levels of Irganox 1010 and Irgafos 168 in food packages made from polyethylene. Composition of selected food packages was identified by attenuated total reflectance Fourier-transform infrared spectrometry, and the analysis of antioxidant levels were carried out using liquid chromatography tandem mass spectrometry.

DISSOLUTION-PRECIPIATION SYNTHESIS OF MAGNESIUM WHITLOCKITE FROM AMORPHOUS CALCIUM PHOSPHATE

Gabrielė Eglė Budžytė¹, Rūta Raišeliėnė¹, Inga Grigoravičiūtė¹, Aivaras Kareiva¹, Aleksej Žarkov¹

¹Institute of Chemistry, Vilnius University, Naugarduko 24, LT-03225 Vilnius, Lithuania
gabregle@gmail.com

Calcium phosphates (CPs) represent the most widespread class of ceramic biomaterials used for bone regeneration purposes due to their excellent biological performance and similarity in chemical composition to natural bone. Magnesium whitlockite (Mg-WH, $\text{Ca}_{18}\text{Mg}_2(\text{HPO}_4)_2(\text{PO}_4)_{12}$) can be considered as a Mg-substituted CP, which naturally occurs in humans. This compound is known to be the second most abundant biomineral in human body. Despite the presence of high content of Mg-WH in the human body, it is not so widely used in clinics, basically due to the challenges in the preparation of this material. Nevertheless, in recent years, Mg WH attracted significantly more attention as a number of studies reported various synthetic approaches and characterization of Mg-WH. It was demonstrated that Mg-WH possesses some superior properties compared to those of frequently used biomaterials such as calcium hydroxyapatite (HAp, $\text{Ca}_{10}(\text{PO}_4)_6(\text{OH})_2$) or tricalcium phosphate (TCP, $\text{Ca}_3(\text{PO}_4)_2$). Remarkable member of the CPs family is amorphous CP (ACP), which is metastable and highly reactive due to its non-crystalline nature. Consequently, ACP can be used as a precursor for the synthesis of other phosphate-based materials. In the present work, we report the synthesis of Mg-WH using ACP as starting material. Phase conversion of ACP to Mg-WH occurs in an aqueous medium in the presence of Mg ions. The influence of synthesis parameters such as temperature, duration and concentration of Mg ions was investigated in detail. The phase crystallinity and purity was analyzed using powder X-ray diffraction and FTIR spectroscopy. The morphological features and chemical composition of the synthesized products were studied by SEM/EDX analysis.

ANALYSIS OF WATER SORPTION OF FILMS BASED ON MODIFIED STARCH

Olena Ishchenko¹, Daria Kuchynska¹, Irina Liashok¹, Maria Kuchynska¹

¹Kyiv National University of Technology and Design

e.ishchenko5@gmail.com

The material based on PVA with the addition of natural polymers and medical preparations will have a prolonged effect, it is easy to adjust their elastic properties; active substances are well released and eliminated from them. This opens up prospects for obtaining biocompatible films with antiseptic and fungicidal properties. The influence of citric acid concentration (1 mol/l and 0,5 mol/l) and treatment time (1,5; 2,0; 2,5 hours) on the process of starch modification was studied. Samples of corn starch were treated with acid and kept in a drying cabinet at a temperature of 60 °C. Six samples were prepared - 3 samples with a concentration of 1 mol/l and 3 samples with a concentration of 0,5 mol/l. The solutions were prepared according to the following composition – 30 g of starch, 165 ml of distilled water, and citric acid with a concentration of 1 or 0,5 mol/l. Study of physical and mechanical properties depending on the moisture content of the samples, water vapor sorption and fungal resistance of the films was carried out.

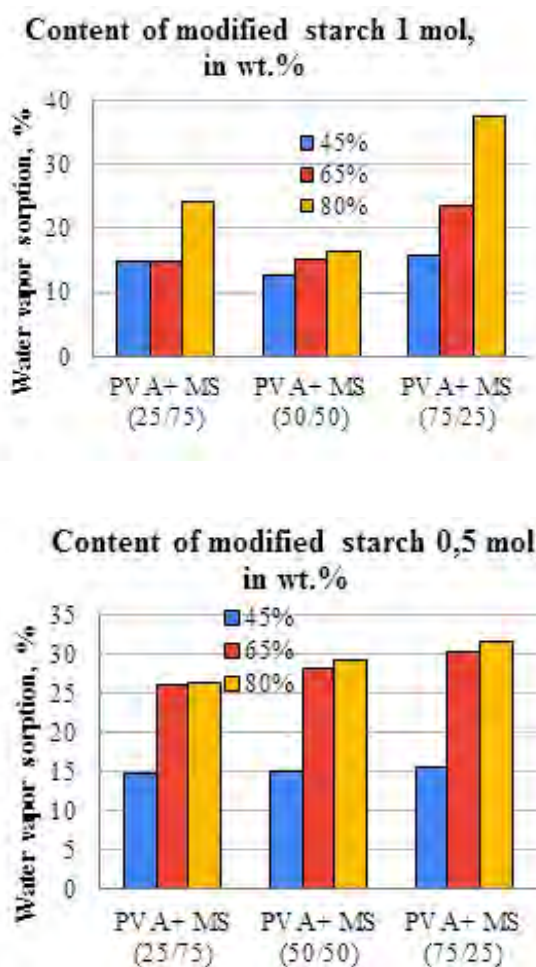


Fig. 1. Influence of starch modification conditions on sorption properties of films based on starch

It was observed that at 45% and 60% moisture for films based on starch, the sorption of water vapor increases to 5%. As the starch content increases at a humidity of 80%, sorption decreases. It can be assumed that the change in physical and mechanical properties occurs as a result of the formation of a structural network between carboxyl groups in modified starch and PVA macromolecules. Films based on modified starch are more homogeneous and transparent.

[1] BeMiller, J. N., Whistler, R. L. (2009). Starch: chemistry and technology. Dxford: Academic Press

[2] Almasi H, Ghanbarzadeh B, Entezami AA (2010) Physicochemical properties of starch-CMC— nanoclay biodegradable films. Int J Biol Macromol 46(1):1-5.

[3] Omojola, M. O., Orishadipe, A. T., Afolayan, M. O., Adebiji and Adedayo, B. 2012. "Preparation and Physicochemical Characterization of Icacina Starch Citrate – A Potential Pharmaceutical/Industrial Starch." Agriculture and Biology Journal of North America 3 (1):11-6.

AN ATTEMPT TO SYNTHESIZE MESOPOROUS SILICA BY A DIFFERENT SILICA PRECURSORS AND POROGENS

Gerardas Laurinavičius¹, Vilius Poškus¹

¹Vilnius University, The Faculty of Chemistry and Geosciences
gerardas.laurinavicius@chgf.stud.vu.lt

Mesoporous materials play an important role in material science, especially in sample preparation techniques like solid phase extraction and solid phase microextraction. Solid phase extraction and microextraction relies on interaction between two different phases – a solid sorbent and a liquid or a gas so it is important that the solid sorbent has a high surface area. This can be achieved by making materials with porous structures. These materials are classified into three categories: microporous, mesoporous, and macroporous materials. Mesoporous materials, compared with other two types of porous materials, comes with a big advantages: narrow pore size distribution and high surface area, can be made with different materials such as silica or various metal oxides, have biocompatibility and low toxicity.

Silica is a perfect candidate for mesoporous sorbents – it can be easily modified and has a rather good chemical stability against organic solvents. Usually, the synthesis of mesoporous silica sorbent starts with a silica source (typically TMOS or TEOS orthosilicates) porogen and a catalyst. After the reaction, organic porogen is removed by heating or using a solvent extraction method. The latter steps involve surface modification via variable reactions which can give a desired functionality and selectivity.

In this study we tried to make mesoporous silica via different synthesis methods that involved: three different silica sources (TMOS, TEOS and APTES), different reaction catalysts (acid, urea and self-catalysis) and two different porogens P123 and CTAB. The synthesis methods were selected and modified according to the porogens used in the original scientific publications.

HYDROGEN GENERATION ON CoFe CoFeMn AND CoFeMo COATINGS DEPOSITED ON Ni FOAM VIA ELCTEROLESS METAL PLATING

Huma Amber¹, Karina Vjunova^{1,2}, Zita Sukackiene¹, Dijana Šimkūnaitė¹, Jurate Vaiciuniene¹, Loreta Tamasauskaite-Tamasiunaite¹, Eugenijus Norkus¹

¹Department of Catalysis, Center for Physical Sciences and Technology (FTMC), Vilnius, Lithuania

²Faculty of Chemistry and Geosciences, Vilnius University, Vilnius, Lithuania

huma.amber@ftmc.lt

Hydrogen has emerged as one of the most promising future energy carriers in recent years, owing to concerns over the depletion of fossil fuel supplies, environmental pollution, and global warming attributable to the greenhouse effect caused by a steep increase in carbon dioxide and other gases. However, highly efficient hydrogen production is a critical issue. Borohydrides have received much attention as potential hydrogen storage materials due to their high hydrogen capacities. Among borohydrides, sodium borohydride (NaBH₄) is recognized as an ideal candidate for hydrogen storage and generation due to its multi-advantages, such as its non-flammability, high stability in alkaline solution, low-cost, non-toxic nature, easy handling, availability and a large H₂ storage capacity (10.9 wt%).

In this study, the catalytic hydrogen generation was evaluated on the cobalt-iron (CoFe), cobalt-iron-manganese (CoFeMn), and cobalt-iron-molybdenum (CoFeMo) coatings deposited on the Ni foam substrate using the electroless metal plating method and morpholine borane as the reducing agent. The characterization of the surface morphology, structure, and composition of resulted coatings was done using scanning electron microscopy (SEM) and inductively coupled plasma optical emission spectroscopy (ICP-OES). The catalytic activity of the prepared CoFe/Ni, CoFeMn/Ni, and CoFeMo/Ni catalysts was investigated for hydrogen generation from an alkaline NaBH₄ solution at different temperatures. It was found that the hydrogen generation rate of ca. 5.2, 7.8, and 11.7 L min⁻¹ g⁻¹ was achieved by using the CoFe/Ni, CoFeMo/Ni, and CoFeMn/Ni coatings, respectively, at 343 K. Among the investigated catalysts, CoFeMn/Ni exhibits the lowest activation energy of 62.4 kJ mol⁻¹ and the highest hydrogen generation rate of 11.7 L min⁻¹ g⁻¹ at 343 K.

ELECTRON-POOR ACRIDONES AND ACRIDIINIUMS AS SUPER PHOTOOXIDANTS INMOLECULARPHOTOELECTROCHEMISTRY BY UNUSUAL MECHANISMS

Jonas Žurauskas^{1,2}, Edvinas Orentas¹, Paulius Vaickūnas¹, Soňa Boháčová³, Shangze Wu², Valeria Butera⁴, Simon Schmid², Michał Domański², Tomáš Slanina³, Joshua P Barham²

¹Vilnius University, Lithuania

²University of Regensburg, Germany

³Institute of Organic Chemistry and Biochemistry, Czech Republic

⁴Central European Institute of Technology, Czech Republic

jonas.zurauskas@chemie.uni-regensburg.de

Electron-deficient acridones and in situ generated acridinium salts are reported as potent, closed-shell photooxidants that undergo surprising mechanisms. When bridging acyclic triarylamine catalysts with a carbonyl group (acridones), this completely diverts their behavior away from open-shell, radical cationic, 'beyond diffusion' photocatalysis to closed-shell, neutral, diffusion-controlled photocatalysis. Bronsted acid activation of acridones dramatically increases excited state oxidation power (by +0.8 V). Upon reduction of protonated acridones, they transform to electron-deficient acridinium salts as even more potent photooxidants ($E_{1/2}^* = +2.56\text{--}3.05\text{ V vs SCE}$). These oxidize even electron deficient arenes where conventional acridinium salt photooxidants have thus far been limited to electron-rich arenes. Surprisingly, upon photoexcitation these electron-deficient acridinium salts appear to undergo two electron reductive quenching to form acridinide anions, spectroscopically-detected as their protonated forms. This new behaviour is partly enabled by a catalyst preassembly with the arene, and contrasts to conventional SET reductive quenching of acridinium salts. Critically, this study illustrates how redox active chromophoric molecules initially considered photocatalysts can transform during the reaction to catalytically active species with completely different redox and spectroscopic properties.[1]

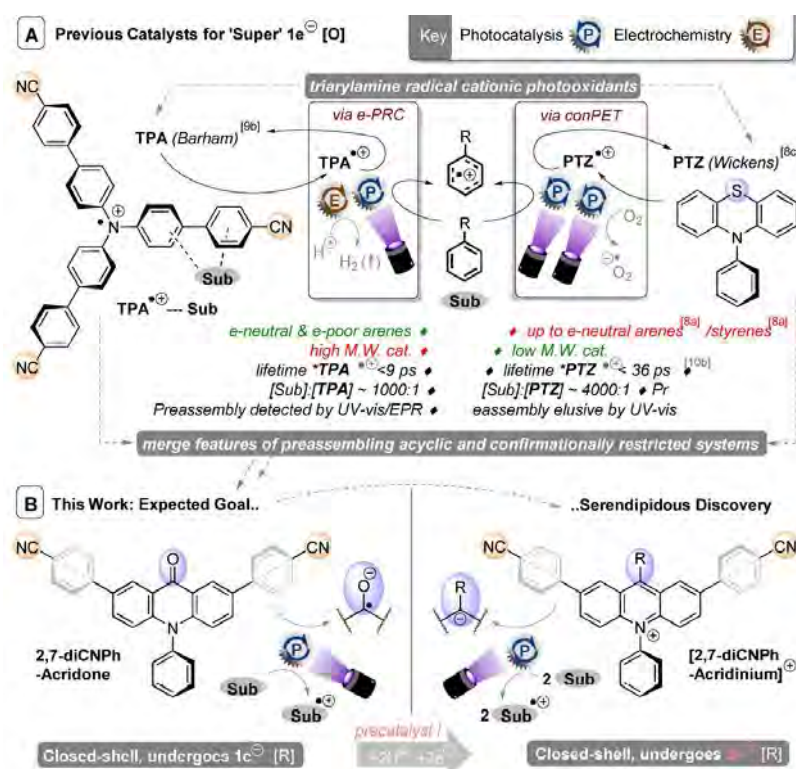


Fig. 1. Expectations versus Reality.

[1] J. Žurauskas, S. Boháčová, S. Wu, V. Butera, S. Schmid, M. Domański, T. Slanina and J. P. Barham, *Angew. Chem., Int. Ed.*, 2023, 62

ASSEMBLY AND RESEARCH OF ARTIFICIAL ROOT SYSTEM

Ernestas Svirbutavičius¹, Šarūnas Žukauskas², Arūnas Ramanavičius^{1,2}

¹Department of Physical Chemistry, Institute of Chemistry, Faculty of Chemistry and Geosciences, Vilnius University (VU), Naugarduko Str. 24, LT-03225

²Department of Nanotechnology, State Research Institute Center for Physical Sciences and Technology (FTMC), Sauletekio Av. 3, LT-10257 Vilnius, Lithuania
ernestas.svirbutavicius@chgf.stud.vu.lt

The escalating pace of urbanization has increased the demand for clean and sustainable energy resources. Within this context, the plant microbial fuel cell (PMFC) emerges as a promising approach for power generation from plants. In a PMFC configuration, living plants are intricately integrated into the anode of the microbial fuel cell, where bioenergy is generated through microbial activity acting upon plant root exudates [1].

To obtain possibility to observe and analyze biological processes, we can use artificial root nodule. Similar to natural root nodules, artificial root nodule structure creates a localized hypoxic environment and supports N₂-fixing symbiotic bacteria, facilitating the biological fixation of atmospheric nitrogen [2]. This artificial organic system can effectively generate solid biomass as a natural fertilizer in the presence of additional renewable energy [3].

In this study, we aim to fabricate synthetic root structures (Fig. 1) combined with microbial cultures, subsequently cultivating these constructs in a manner akin to microbial fuel cells (MFCs). This approach requires the incorporation of artificial roots designed to mimic the biological interface of plant roots with microbial communities. The microbial culture introduced to these synthetic root systems serves as a surrogate for the natural rhizosphere, establishing a controlled experimental setup conducive to investigating electrochemical processes analogous to those observed in MFCs. By adopting this artificial root-based framework, we hope to mimic how real plant roots interact with microbes in the soil and understand the electrochemical dynamics involved in bioenergy generation.

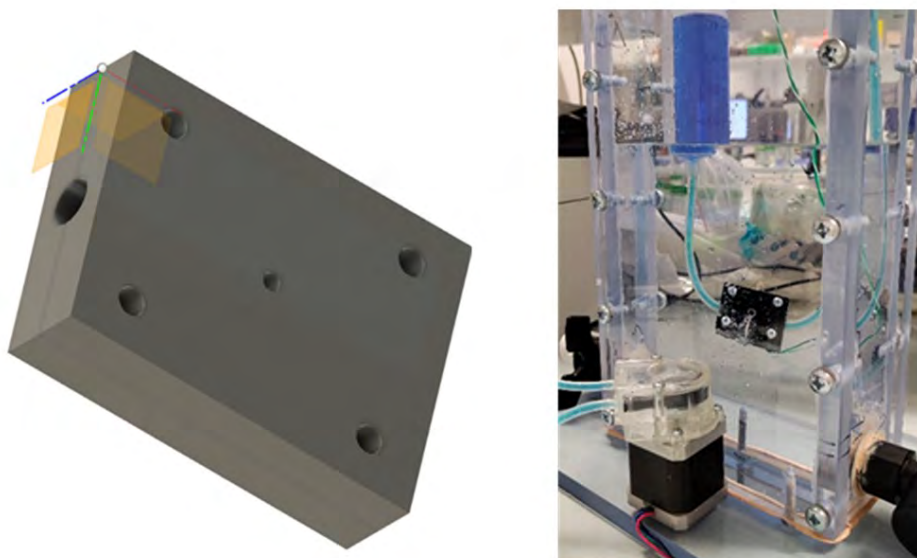


Fig. 1. Design of the 3D-printed PMFC vessel.

- [1] Strik, D.P.B.T.B., et al., Microbial solar cells: applying photosynthetic and electrochemically active organisms. *Trends in Biotechnology*, 29(1): p. 41-49 (2011)
- [2] Lu, S., X. Guan, and C. Liu, Electricity-powered artificial root nodule. *Nature Communications* 11(1): p. 1505 (2020)
- [3] Liu, C., et al., Ambient nitrogen reduction cycle using a hybrid inorganic–biological system. *Proceedings of the National Academy of Sciences*, 114(25): p. 6450-6455 (2017)

SYNTHESIS OF NEW 3-(2-OXOBENZO[D]OXAZOL-3(2H)-YL)PROPANOIC ACID DERIVATIVES

Birutė Grybaitė¹, Birutė Sapijanskaitė-Banevič¹, Rita Vaickelionienė¹, Kazimieras Anusevičius¹, Vytautas Mickevičius¹

¹Kaunas University of Technology, Department of Organic Chemistry, Radvilėnų pl. 19, 50254 Kaunas, Lithuania
birute.grybaite@ktu.lt

The novel research and many scientific publications demonstrate the 2-oxobenzo[d]oxazole fragment to be versatile for drug discovery. Nowadays a large number of pharmaceuticals are developed for medicinal use but the increasing resistance of pathogens to available pharmaceuticals has created an essential demand for new efficient classes of antimicrobial agents. A unique small-ring heterocycle – oxazole containing nitrogen and oxygen atoms, play an important role in medicinal chemistry and is widely used in the development of bioactive compounds, drugs, as well as industrial products [1, 2]. Pharmaceuticals based on oxazole and its derivatives are used in medical practice for the treatment of hypertension, Alzheimer's disease, diabetes, schizophrenia, allergies and act as anti-cancer, antimicrobial, antifungal agents [3].

In this study, the prepared compound 1 was used as a precursor for the preparation of hydrazide 3 by the hydrozonolysis reaction by combining methyl 3-(2-oxobenzo[d]oxazol-3(2H)-yl)propanoate 2 with the hydrazine monohydrate (Scheme 1). 3-(2-(1H-benzo[d]imidazol-2-yl)ethyl)benzo[d]oxazol-2(3H)-one 4 was synthesized in the Phillips reaction by reacting compound 1 with 1,2-phenylenediamine in a mixture of hydrochloric acid and water (1:2). Acid 1 was esterified with methanol at reflux for 2 hours in the presence of a catalytic amount of sulfuric acid in the reaction mixture. The obtained methyl ester 2 was transformed into hydrazide 3 using hydrazine monohydrate in 2-propanol. Condensation of compound 3 with aromatic or heterocyclic aldehydes in propan-2-ol and using a catalytic amount of glacial acetic acid led to the formation of N'-benzylidene hydrazides 5–9. The structures of the obtained compounds were confirmed by the data of the ¹H, ¹³C NMR and FT-IR spectroscopy and elemental analysis.

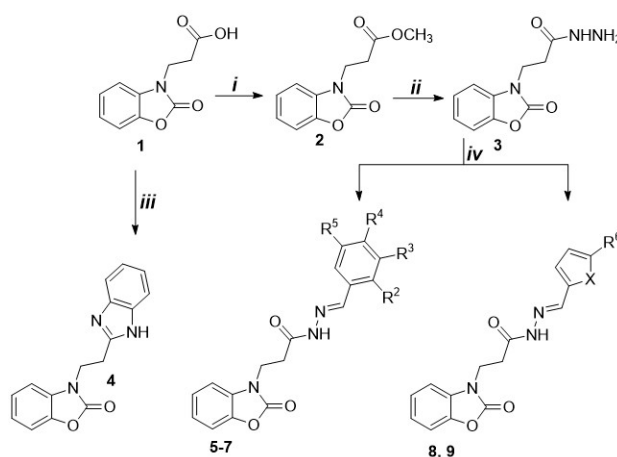


Fig. 1. Synthesis of new 3-(2-oxobenzo[d]oxazol-3(2H)-yl)propanoic acid derivatives 2-9. **5** R²,R³,R⁴,R⁵=H; **6** R²,R³,R⁵=H, R⁴=F; **7** R³,R⁵=H, R²,R⁴=F; **8** X=S; R⁶=H; **9** X=S; R⁶=NO₂; Reagents and conditions: *i*) MeOH, H₂SO₄, D, *ii*) i-PrOH, N₂H₄ · H₂O, D, *iii*) o-phenylenediamine, HCl:H₂O mixture, reflux, NH₃ · H₂O, *iv*) i-PrOH, aromatic or heterocyclic aldehyde, glacial AcOH.

[1] M. V. J. Nora de Souza, Synthesis and biological activity of natural thiazoles: An important class of heterocyclic compounds. *J. Sulphur Chem.* 2005, 26, 429-449.

[2] P. K. Sasmal, S. Sridhar, J. Idhal, Facile synthesis of thiazoles via an intramolecular thia-Michael strategy. *Tetrahedron Lett.* 2006, 47, 8661-8665.

[3] H. Arslan, O. Algül, T. Önkol, Vibrational spectroscopy investigation using ab initio and density functional theory analysis on the structure of 3-(6-benzoyl-2-oxobenzo[d]oxazol-3(2H)-yl)propanoic acid. *Spectrochimica Acta Part A.* 2008, 70, 606-614.

DEVELOPMENT OF ORALLY DISINTEGRATING FILMS BASED ON BIOPOLYMERS AND PLANT EXTRACTS

Emilija Galkauskaite¹, Ramune Rutkaite¹, Vaida Kitryte-Syrpa², Dovile Liudvinaviciute¹, Michail Syrpas²

¹Department of Polymer Chemistry and Technology, Kaunas University of Technology, Lithuania

²Department of Food Science and Technology, Kaunas University of Technology, Lithuania
emilija.galkauskaite@ktu.edu

One of the most progressive pathologies in the world are various oral cavity infections. Developing the new ways to treat these diseases are very important. Orally disintegrating films (ODFs) are thin, flexible films made of hydrophilic polymers, pharmacologically active substances, plasticizers, flavorings, dyes and sweeteners. There are many reports on films that quickly disintegrate in the oral mucosa and immediately release biologically active components into the systemic circulation. However, self-disintegrating films with prolonged activity are still underexplored and could be effective method for the local treatment of periodontal diseases, caries, stomatitis, and other infections in the oral cavity.

The main goal of this research work was the formation of multi-layered ODFs from various biopolymers and natural plant extracts and investigation of their properties. Polymeric films of various composition were formed by solvent casting method using chitosan, hydroxyethyl cellulose, hydroxypropyl cellulose, methylcellulose, cellulose acetate, polyvinyl alcohol, emulsifier Tween80, plasticizer glycerin and cross-linking agent citric acid. The hop extract both in pure and encapsulated forms was immobilized in the polymer films. The mechanical, thermal and hydrophobic properties of the various films were evaluated. Moreover, the solubility and swelling in artificial saliva solution was determined. The release of bioactive components from polymer films into saliva model solution was investigated by using spectroscopic method. More than 85.7 percent of hop extract were released from the polymeric films into the saliva simulant within 168 hours.

Acknowledgement. This project has received funding from the Research Council of Lithuania (LMTLT), agreement No S-ST-23-46.

SILVER-TIN OXIDE NANOPARTICLES FOR SHELL ISOLATED NANOPARTICLE ENHANCED RAMAN SPECTROSCOPY

Vytautas Taurelé¹, Tatjana Charkova²

¹Vilnius University

²Center for Physical Sciences and Technology

vytautas.taurele@chgf.stud.vu.lt

Silver nanoparticles (Ag NPs) are suitable for constructing devices of optic, electronic, solar, etc. systems. The anti-pathogenic properties also make them attractive as diagnostic tools in medical sciences and environmental protection [1]. Any successful application requires modification of the silver surface. Different coatings (polymers, graphene, transition metals, etc.) prevent aggregation and degradation of Ag NPs and also solve potential biocompatibility issues. Ag core-shell systems are widely used in shell-isolated nanoparticle-enhanced Raman spectroscopy (SHINERS) [2]. Such nanoparticles scattered on the analyzed surface act as small amplifiers of the Raman signal. As a result, informative spectra of the analyte can be recorded (see in fig.).

Tin oxide is a promising protective coating as it is stable over a wide pH range, making Ag core-SnO₂ shell nanoparticles (Ag/SnO₂ NPs) convenient to use. This work reports the synthesis of up to 80 nm Ag/SnO₂ NPs coated with up to 10 nm of SnO₂. The Ag/SnO₂ NPs are appropriate for SHINERS experiments, and the SnO₂ shell is thick enough to prevent nanoparticle aggregation and preserve Raman signal intensity.

-
- [1] W. J. Stark, P. R. Stoessel, W. Wohleben, A. Hafner, Industrial applications of nanoparticles, *Chem. Soc. Rev.* 44 (2015) 5793–5805. <https://doi.org/10.1039/c4cs00362d>
- [2] J. F. Li, Y. J. Zhang, S. Y. Ding, R. Panneerselvam, Z. Q. Tian, Core-shell nanoparticle-enhanced Raman spectroscopy, *Chem. Rev.* 117(7) (2017) 5002–5069. <https://doi.org/10.1021/acs.chemrev.6b00596>

APPLICATION OF COMPUTATIONAL METHODS IN THE DESIGN OF MOLECULARLY IMPRINTED POLYMERS

Enayat Mohsenzadeh¹, Vilma Ratautaite¹, Arunas Ramanavicius^{1,2}

¹Department of Nanotechnology, State Research Institute Center for Physical Sciences and Technology (FTMC), Sauletekio Ave. 3, Vilnius LT-10257, Lithuania

²Department of Physical Chemistry, Institute of Chemistry, Faculty of Chemistry and Geosciences, Vilnius University (VU), Naugarduko str. 24, LT-03225 Vilnius
enayat.mohsenzadeh@ftmc.lt

Molecularly imprinted polymers (MIPs) are synthetic receptors capable of selectively recognising a specific target. MIPs are made by polymerisation of functional monomers in the presence of the analyte that forms a polymer film decorated with tailor-made cavities for the target (template) molecules [1]. The process of MIP synthesis has the challenging steps as follows: a) Selection of best monomer(s), crosslinking agent(s), and solvent; b) Polymerisation; c) Template removal to make complementary binding sites; d) Sensitivity and selectivity studies through rebinding step. On one hand, extensive and costly procedures, and on the other hand, methods such as molecular mechanics, molecular dynamics, Monte Carlo, quantum mechanics, and statistical simulations have made these leveraging computational methods widely used in the stepwise process of MIP preparation [2].

Calculations are performed for the selection of the best reagents in the pre-polymerisation mixture such as monomer(s), crosslinking agent, and solvent system, and their relevant optimal ratios. It is found that the simulation of polymerisation facilitates optimisation of this step and models the polymeric structure of MIPs making it plausible to analyse the resulting binding sites. The selectivity and sensitivity of MIPs are evaluated by computations showing the mechanism of recognition of specific targets and the binding affinities. The reviewed papers proved the significance of computational methods for a greener approach and their widespread applicability in the MIP design.

[1] Pilvenyte, G. et al. Molecularly imprinted polymers for the recognition of biomarkers of certain neurodegenerative diseases. *Journal of Pharmaceutical and Biomedical Analysis* 228, 115343 (2023).

[2] Mohsenzadeh, E. et al. Application of computational methods in the design of molecularly imprinted polymers (review). *TrAC Trends in Analytical Chemistry* 171, 117480 (2024).

PHOTOCATALYTIC DEGRADATION OF LOW-DENSITY POLYETHYLENE IN AQUEOUS SOLUTION USING TiO₂ NANOPARTICLES DEPOSITED ON CLAY KAOLINITE

Sonata Pleskytė¹, Ieva Uogintė¹, Steigvilė Byčenkienė¹

¹Department of Environmental Research, Center for Physical Sciences and Technology
sonata.pleskyte@ftmc.lt

Over the years, an increasing number of microplastics with particles diameter ranging from 0.1 μm to 5 mm have been observed in various environmental systems such as water, soil, and air. These small particles are difficult to recycle, easily absorb toxic substances and can enter animal and human bodies through food chain [1]. Hence, there is an urgent need for remediation of the microplastic pollution.

Among different microplastic remediation methods (chemical degradation, biodegradation) photocatalytic degradation has shown the highest degradation efficiency. This microplastic degradation method can be performed under milder conditions than biological or chemical degradation and is suitable for a wide range of plastic polymer [2]. Modified TiO₂ photocatalysts have been used for the degradation of various plastic polymers under different degradation conditions and have shown a degradation efficiency ranging from 6.4% for high-density polyethylene (HDPE) to 81% for polyvinyl chloride (PVC) films [3]. Incorporation of TiO₂ within the clay layers increases the specific surface area of TiO₂ nanoparticles. This results in a mesoporous structure that enhances adsorption properties and decreases the band gap energy which indicates better absorption of light in a wider wavelength range [4].

In this work, TiO₂ nanoparticles and TiO₂/kaolinite nanocomposites were synthesized by sol-gel method. We chose naturally occurring kaolinite which has easy preparation without requiring the use of strong acids or other solvents. These materials were used for a small-sized (300 μm) low-density polyethylene (LDPE) microplastic photodegradation under UV light irradiation in aqueous solution. This study presents TiO₂/kaolinite nanocomposite application for the removal of microplastics.

-
- [1] R. Li et al., "Investigating the effects of biodegradable microplastics and copper ions on probiotic (*Bacillus amyloliquefaciens*): Toxicity and application," *J Hazard Mater*, vol. 443, Feb. 2023, doi: 10.1016/j.jhazmat.2022.130081.
- [2] Y. He, A. U. Rehman, M. Xu, C. A. Not, A. M. C. Ng, and A. B. Djurišić, "Photocatalytic degradation of different types of microplastics by TiO_x/ZnO tetrapod photocatalysts," *Heliyon*, vol. 9, no. 11, Nov. 2023, doi: 10.1016/j.heliyon.2023.e22562.
- [3] R. Xu, L. Cui, and S. Kang, "Countering microplastics pollution with photocatalysis: Challenge and prospects," *Progress in Natural Science: Materials International*, vol. 33, no. 3, Chinese Materials Research Society, pp. 251–266, Jun. 01, 2023, doi: 10.1016/j.pnsc.2023.08.006.
- [4] S. Sharma, A. Devi, and K. G. Bhattacharyya, "Photocatalytic Degradation of Methylene Blue in Aqueous Solution with Silver-Kaolinite-Titania Nanocomposite under Visible Light Irradiation," *Journal of Nanostructures*, vol. 12, no. 2, pp. 426–445, Mar. 2022, doi: 10.22052/JNS.2022.02.018.

PREPARATION AND INVESTIGATION OF MULTI-LAYERED ORALLY DISINTEGRATING FILMS

Dovilė Liudvinavičiūtė¹, Emilija Galkauskaitė¹, Vesta Navikaitė-Šnipaitienė¹, Vaida Kitrytė-Syrpa², Michail Syrpas², Ramunė Rutkaitė¹

¹Department of Polymer Chemistry and Technology, Kaunas University of Technology

²Department of Food Science and Technology, Kaunas University of Technology
dovile.liudvinaviciute@ktu.lt

Oral administration of pharmaceuticals is the most preferred drug delivery method amongst patients due to its ease of administration, non-invasiveness and acceptability [1]. Orally disintegrating films (ODFs) are polymer-based, thin, flexible and pharmacologically active films, which applied to the oral mucosa begin to disintegrate/dissolve and release active components [2]. Oral diseases often require local and prolonged treatment and ODF could be considered as the best drug delivery system. ODFs can be formulated as a single- or multi-layered films, allowing controlled release of active substances. ODFs are typically obtained by solvent casting method, where casting liquid contains film forming material, solvent, plasticizer, anti-adherent, sweetener, color and flavor additives. Bio-based polymers or biodegradable polymers are gaining interest as good film forming materials for ODFs formation, due to their hydrophilic nature and non-toxicity.

The aim of present study was to obtain two- and three-layer films using bio-based or biodegradable polymers as film formers for possible application for ODFs and to evaluate their mechanical and physicochemical properties.

Three two-layer films and one three-layer film were obtained using poly(vinyl alcohol), 2-hydroxyethyl cellulose, methyl cellulose, chitosan, cellulose diacetate, hydroxypropyl cellulose as film forming materials by solvent casting method. Each layer of the multi-layer film contained 83.34 wt.% of polymer, 8.33 wt.% of glycerol as plasticizer and 8.33 wt.% of citric acid as cross-linker. Main characteristics of multi-layered films, such as solubility and swelling in a simulated salivary fluid, contact angle, mechanical properties were evaluated.

Acknowledgement. This project has received funding from the Research Council of Lithuania (LMTLT), agreement No S-MIP-23-78.

[1] M. Irfan, S. Rabel, Q. Bukhtar, M.I. Qadir, F. Jabeen, A. Khan. Orally disintegrating films: A modern expansion in drug delivery system. *Saudi Pharmaceutical Journal* 24, 537–546, (2016).

[2] S. Mazumder, et al. Quality by Design approach for studying the impact of formulation and process variables on product quality of oral disintegrating films, *International Journal of Pharmaceutics* 527, 151-160 (2017)

BLACK CURRANT SEEDS A SOURCE OF BIOACTIVE COMPOUNDS WITH PROFOUND HEALTH BENEFITS

Indrė Pocevičienė¹, Laura Jūrienė¹, Audrius Pukalskas¹, Renata Baranauskienė¹, Petras Rimantas Venskutonis¹

¹Kaunas University of Technology
indcer1@ktu.lt

Blackcurrant seeds emerge as residual by-products following berry processing. Typically disregarded in the industry and discarded alongside other berry waste, recent research over the last decade has compelled scientists to reevaluate these seeds as a potential source of valuable bioactive compounds. Following the chemical composition research conducted using standard methodology, it was revealed that the seeds consist of 18.29 % fats, 16.77 % proteins, and 58.68 % carbohydrates. The remaining percentages account for moisture and mineral substances. In particular, a substantial portion of the carbohydrates is attributed to dietary fiber, averaging 51.84 g per 100 g of seeds, with total fermentable sugars determined at 4.9 g per 100 g of seeds. The supercritical CO₂ extraction process yielded a lipophilic extract with a 15.66 % yield. The major predominant triacylglycerols (TAG) in the seeds extract were identified as unsaturated LLLn (21.23 ± 0.46 %) and OLnL (20.77 ± 0.28 %). Additionally, the extract was found to be a rich source of α-tocopherol (537.95 ± 19.79 μg/g) and β-sitosterol (5176.05 ± 189.22 μg/g), both important bioactive compounds. While Gas chromatography coupled with time-of-flight mass spectrometry (GC×GC-TOF/MS) analysis of aroma compounds revealed the presence of various compounds, including hexanal, furfural, and terpenes, the concentrations of these aroma compounds were relatively lower compared to those of blackcurrant peel. The findings collectively demonstrate the high potential of blackcurrant seeds as a valuable source of bioactive compounds for incorporation into sustainable superfood blends or functional food products.

ISOTOPIC COMPOSITION OF CARBONACEOUS AEROSOLS FOR SEASONAL OBSERVATION

Durre Nayab Habib¹, Andrius Garbaras², Inga Garbarienė³, Agne Mašalaitė⁴

¹Vilnius University
durre.nayab@ftmc.lt

An aerosol is an ensemble of solid, liquid, or mixed-phase particles suspended in air. Carbonaceous aerosols mainly contain carbon compounds. The isotopic composition can provide unique information about source emissions as well as physical and chemical processes in the atmosphere. The seasonal variation of carbon isotopic composition will be presented in two distinct environments urban and coastal sites. Year-round samples were collected from 1 January 2014 to 30 December 2014 every single day. There were 72 filter samples from urban background site (Vilnius) and 103 aerosol samples from the coastal site (Preila). The findings of this study reveal seasonal variations in PM1 total carbon (TC) concentrations at both the urban and coastal sites. These observations align with studies conducted in different regions, stressing the influence of primary regional sources on TC levels. The monthly averaged $\delta^{13}\text{C}_{\text{TC}}$ values of aerosol particles from both sites demonstrated a prominent seasonal cycle, reflecting variations in the isotopic composition of carbon in these particles. The monthly averages exhibited a wide range, from $-28.4 \pm 0.8 \text{‰}$ to $-25.3 \pm 0.1 \text{‰}$ at both sites, with standard deviations varying from 0.1 ‰ to 0.9 ‰. Notably, distinct seasonal variations in $\delta^{13}\text{C}_{\text{TC}}$ were observed, with enrichment in winter and depletion in spring at the urban site, indicating shifts among emission sources. In contrast, the coastal site exhibited relatively stable isotopic composition throughout most of the year, with minimal variations between the monthly averaged values. The highest values occurred during the winter months, while the remaining months displayed nearly constant isotopic composition. These findings provide insights into sources and seasonal dynamics of aerosol particles isotopic composition at these sites. Overall, these findings contribute to our understanding of air quality dynamics in the studied areas and provide valuable insights for future environmental monitoring and policy decisions.

DI-TERT-ALKYLPHOSPHINE SYNTHESIS AND INVESTIGATION OF CHEMOENZYMATIC SYNTHESIS OF THEIR PRECURSORS - TERTIARYACETATES

Jonas Paukštys^{1,2,3}, Tomas Paškevičius¹, Ringailė Lapinskaitė¹, Nina Urbelienė², Linas Labanauskas¹, Rolandas Meškys²

¹Department of Organic Chemistry, Center for Physical Sciences and Technology, Akademijos st. 7 LT-08412 Vilnius

²Department of Molecular Microbiology and Biotechnology, Institute of Biochemistry, Life Sciences Centre, Vilnius University, Sauletekio Ave 7, LT-10257 Vilnius

³Faculty of Chemistry and Geosciences, Vilnius University, Naugarduko st. 24, LT-03225 Vilnius
jonas.paukstys@gmc.stud.vu.lt

Bulky di-*tert*-alkylbiaryl phosphines are used in palladium catalysed cross-coupling reactions (Buchwald amination, Suzuki-Miyaura cross coupling, Heck reaction, etc) [1]. More efficient catalysts may be developed by modifying steric and electronic properties of these ligands. However, synthesis of di-alkyl phosphines involves multiple steps [2] and toxic, highly reactive reagents [3]. Our newly developed method eliminates some of these challenges using easier to handle tris(trimethylsilyl)phosphine (P(TMS)₃) (Fig.1). Phosphine nucleophile generated *in situ* from P(TMS)₃ and triflic acid reacts with an electrophilic tertiary carbocation. The final product of this umpolung (P⁻/C⁺) reaction is an easily isolatable air-stable phosphine triflate salt.



Fig. 1. Synthesis of di-*tert*-alkyl phosphine salts using P(TMS)₃

Currently tertiary acetates are synthesised chemically, however chemoenzymatic reactions present a greener, more energy-efficient, and in some cases, less labour-intensive means to synthesize organic molecules in comparison to traditional methods [4]. In our study a wide variety of esterases were tested for acetylation and hydrolysis of tertiary alcohols and esters (Fig. 2). Most efficient enzymes were selected for further investigations.

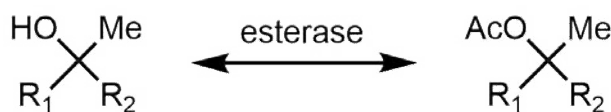


Fig. 2. Chemoenzymatic synthesis of tertiary acetates

[1] Surry, D.S.; Buchwald, S.L. Biaryl phosphane ligands in palladium-catalyzed amination. *Angew. Chem. Int. Ed.* 2008, 47 (34), 6338-6361

[2] Kendall, A.J.; Tyler, D.R. The synthesis of heteroleptic phosphines. *Dalton Trans.* 2015, 44 (28), 12473-12483

[3] Barber, T.; Argent, S.P.; Ball, T.L. Expanding Ligand Space: Preparation, Characterization, and Synthetic Applications of Air Stable, Odorless Di-*tert*-alkylphosphine Surrogates. *ACS Catalysis*, 2020, 10 (10), 5454-5461

[4] Roddan, R.; Carter, E.M., Thair, B.; Hailes, H.C. Chemoenzymatic approaches to plant natural product inspired compounds. *Nat. Prod. Rep.* 2022, 39 (7), 1375-1382

FABRICATION OF 3D BORON CARBIDE BY COMBINING STEREOLITHOGRAPHY AND PYROLYSIS

Robertas Virkėtis¹, Greta Merkininkaitė¹, Vaidas Klimkevičius¹, Simas Šakirzanovas¹

¹Institute of Chemistry, Faculty of Chemistry and Geosciences, Vilnius University, Vilnius LT-03225, Lithuania
 robertas.virketis@chgf.stud.vu.lt

Additive manufacturing-based 3D printing is a groundbreaking technology that is rapidly gaining traction in the industrial sector. It opens up exciting opportunities for creating diverse structures or complete devices in a significantly shorter timeframe, reducing the duration from conceptualization to the production of the final physical object. The use of homogenous photoactive materials in 3D printing is favored for achieving enhanced properties, ensuring a consistent composition and uniform characteristics in the printed objects. This uniformity contributes to enhanced structural integrity, increased mechanical strength, and the attainment of a smoother surface for the structures. In contrast, the inclusion of particles in a monomer mixture may introduce variability, potentially compromising the quality of the print and the structural uniformity.

Boron carbide stands out as a promising material for numerous technical applications owing to its exceptional properties. This material boasts desirable characteristics such as low density, high strength, excellent wear resistance, exceptional hardness, and chemical inertness [1]. As a result, the focus here is on synthesizing organoboron compounds and subsequently forming them by combining stereolithography with pyrolysis to create intricate and precisely shaped 3D objects of boron carbide.

Initially, a boron-containing organic monomer, namely 2-(5,5-dimethyl-1,3,2-dioxaborinan-2-yloxy)ethylmethacrylate (referred to as boron methacrylate monomer), was synthesized through an esterification reaction detailed in article [2]. Verification of successful synthesis was confirmed through proton nuclear magnetic resonance analysis (see fig. 1. a)), showcasing a product yield of approximately 60%. Subsequently, utilizing ultraviolet three-dimensional printing, structures of boron acrylate polymer were crafted (see fig. 1. b)), followed by pyrolysis at 1300°C in an N₂ atmosphere, resulting in a measured shrinkage of 60%. Furthermore, X-ray diffraction analysis (XRD) of the final product will be presented to confirm the formation of the crystalline.

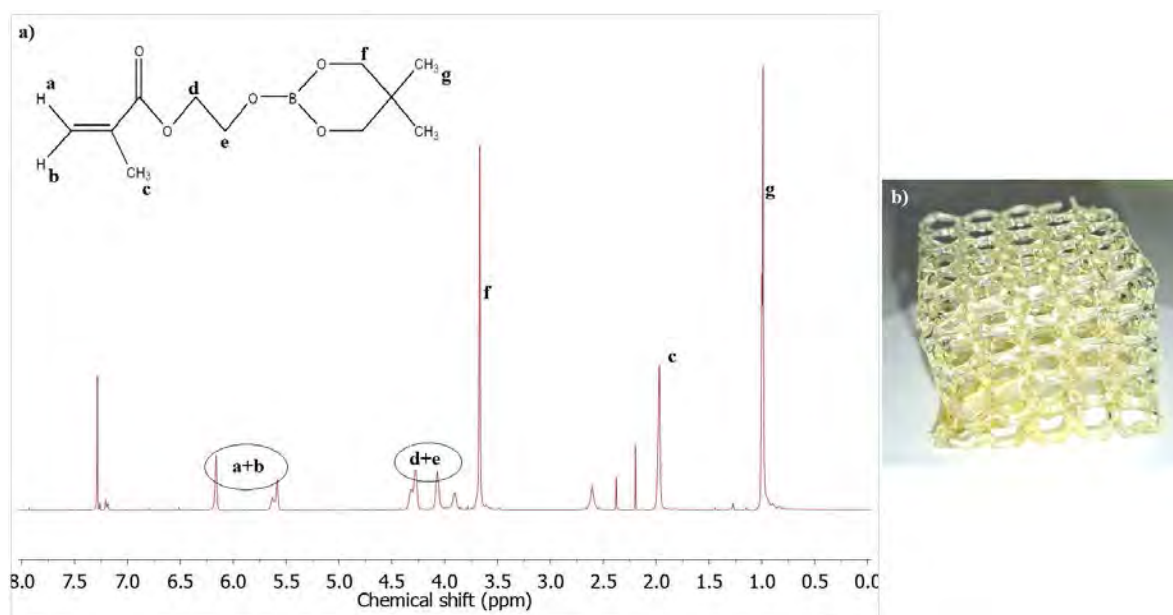


Fig. 1. a) ¹H-NMR spectra of boron methacrylate monomer in CDCl₃, b) Image of boron methacrylate polymer.

The integration of organoboron acrylate synthesis, 3D stereolithography, and pyrolysis has been emerged as a promising method for creating small, intricately detailed structures made of boron carbide. The suggested viable solution for crystalline boron carbide 3D printing at the microscale has the potential to significantly enhance the range of tools available in the printing industry.

[1] W. Zhang. (2021). A review of tribological properties for boron carbide ceramics. *Progress in Materials Science*, Volume 116. Online ISSN 0079-6425, <https://doi.org/10.1016/j.pmatsci.2020.100718>

[2] T. Ç. Çanak, K. Kaya, I. E. Serhatlı. (2014). Boron containing UV-curable epoxy acrylate coatings. *Progress in Organic Coatings*, Volume 77, Issue 11, Pages 1911-1918. Online ISSN 0300-9440, <https://doi.org/10.1016/j.pogcoat.2014.06.021>

MANGANESE DOPING EFFECT ON CRYSTAL STRUCTURE AND MAGNETIC PROPERTIES OF LUTETIUM FERRITE

Andrius Pakalniškis¹, Gediminas Niaura², Ramūnas Skaudžius¹, Aivaras Kareiva¹

¹Institute of Chemistry, Vilnius University, Naugarduko 24, LT-03225 Vilnius, Lithuania

²Department of Organic Chemistry, FTMC, Sauletekio Ave. 3, LT-10257, Vilnius, Lithuania
andrius.pakalniskis@chgf.vu.lt

The combination of both magnetic and electrical properties requires significant challenges to be overcome in order to be possible. Firstly, the classically known magnetic and electric properties arise from opposite phenomena. Ferroelectric properties arise from the hybridization of empty 3d orbitals and magnetic ones require them to be partially filled. To avoid this problem other mechanisms driving ferroelectricity were discovered. They include lone pair, spin driven, geometric, and charge ordering [1]. Also, the coupling between the two is often weak. Lastly, at least one of the properties occurs at temperatures lower than room temperature. The solution to the problems is not simple or clear and in most cases is different for every material. As such the search for new multiferroic materials is still ongoing.

One potential compound is hexagonal LuFeO₃. Hexagonal LuFeO₃ is a polar compound where ferroelectricity is caused by geometric factors, mainly the displacement of Lu ions in the crystal structure [2]. The metastable structure can be stabilized by either strain during thin film preparation or by doping. Dopant effects on magnetic and electrical properties are still not clear. Even the phase formation is complicated and the stability regions of the hexagonal phase are difficult to describe as they differ for each of the dopants while also being sensitive to the preparation method and even the calcination temperature [3].

In this work we provide insights into the stabilization of hexagonal LuFeO₃ by Mn doping prepared by the sol-gel method. The concentration stability regions for the hexagonal phase at different calcination temperatures were described using X-ray diffraction analysis. Particle morphology was determined using SEM analysis. Lastly, we also provide additional information on the behavior of magnetic properties not only caused by the crystal structure changes but also on the effect of doping.

[1] M. Kumar, et al., Advances and future challenges in multifunctional nanostructures for their role in fast, energy efficient memory devices, *Mater. Lett.* 277 (2020) 128369

[2] S.M. Disseler, et al., Multiferroicity in doped hexagonal LuFeO₃, *Phys. Rev. B.* 92 (2015) 054435

[3] A. Pakalniškis, et al., Crystal Structure and Concentration Driven Phase Transitions in Lu(1-x)ScxFeO₃ Prepared by the Sol Gel Method, *Materials (Basel)*. 15 (2022) 1048

SYNTHESIS OF 6-(5-ARYL-1,2,3-THIADIAZOL-4-YL)-(4-BENZYL)BENZENE-1,3-DIOLS AS POTENTIAL HSP 90 INHIBITORS

Gabija Griškonytė¹, Algirdas Brukštus¹, Ieva Žutautė¹

¹Vilnius University

gabija.griskonyte@chgf.stud.vu.lt

Inhibitors of the Hsp90 chaperone protein hold significant potential in the quest for anticancer drugs. Hsp90 client proteins play a crucial role in regulating various functions of human cells, including signal transduction, protein trafficking and cell proliferation. However, these proteins are prone to mutation and are overexpressed in cancer cells. Therefore, inhibiting them holds substantial promise for combating cancer [1]. Results from clinical and preclinical studies indicate that Hsp90 inhibitors may enhance the effectiveness of other cancer treatments, such as chemotherapy or immunotherapy [2]. 4,5-diaryl-1,2,3-thiadiazoles are promising anticancer agents, and many similar compounds have yet to be thoroughly investigated [3]. This research aims to synthesize 6-(5-aryl-1,2,3-thiadiazol-4-yl)-(4-benzyl)benzene-1,3-diols **3** as potential Hsp90 inhibitors.

The synthesis is carried out in five steps to obtain the target compounds. The first and third steps of the synthesis are the same and involve Friedel-Crafts acylation. After the first reaction, the obtained ketones are reduced with Pd-C, in H₂ gas atmosphere and gives 4-(benzyl)benzen-1,3-diols **1**. The final stage of the synthesis is the Hurd-Mori cyclization reaction. Ethyl carbazate is attached to the successfully isolated compounds **2**, the five-membered ring is cyclized with thionyl chloride and final products **3** are obtained.

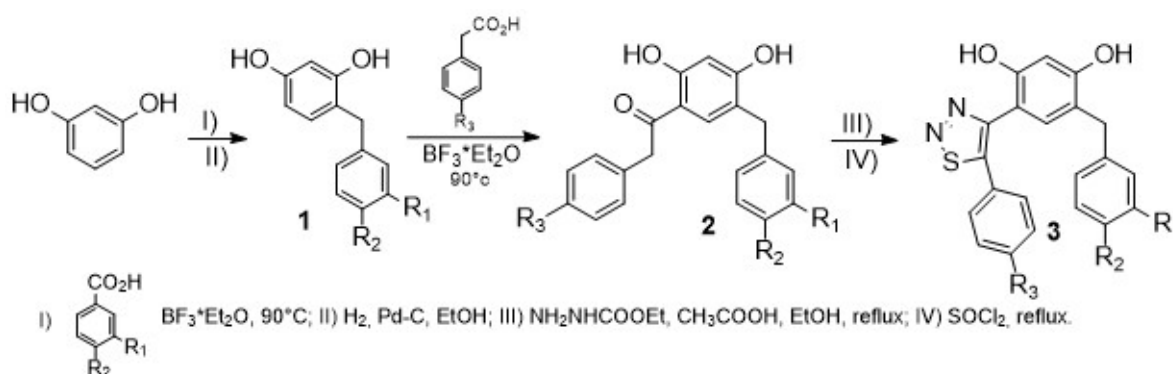


Fig. 1. General scheme of reactions.

[1] G. Garg, et al., *Adv Cancer Res.* 2016, 129.

[2] Z. Li, Y. Luo, *Oncology Reports*, 2023, 6.

[3] A. Irfan, et al., *Appl. Sci.* 2021, 11, 5742.

NMR STUDY OF BIOACTIVE IONIC LIQUIDS

Lukas Mikalauskas¹, Vytautas Klimavičius¹

¹Institute of Chemical Physics, Faculty of Physics, Vilnius University
lukas.mikalauskas@ff.stud.vu.lt

Bioactive Room Temperature Ionic Liquid (b-RTIL) is a class of RTIL that is made of biomolecules and thus b-RTIL is compatible with living organisms. Due to composition b-RTILs are widely applied in the medical field in drug delivery systems and can increase non-soluble drug solubility in water.

In this study high-resolution Nuclear Magnetic Resonance (NMR) was used to investigate choline lysinate [Ch][Lys] and choline tryptophanate [Ch][Try] in a water mixture. [Ch] is involved in the metabolism process while [Try] and [Lys] are involved in protein biosynthesis. Diluted [Ch][Try] water solution was investigated by ¹H, ¹³C, ¹⁵N 1D and 2D NMR. The solutions were measured in b-RTIL concentration from 10⁻⁶ to 1 molar fraction. Additionally, glibenclamide (Gli) solubility was examined in [Ch][Lys] and [Ch][Try] water mixtures. Glibenclamide is used to treat type II diabetes.

It was found that the [Ch]⁺ ¹H chemical shifts reach the plateau at around $\chi_{\text{RTIL}} = 2.5 \times 10^{-4}$ molar freq. in [Ch][Try] water mixture and at $\chi_{\text{RTIL}} = 1.4 \times 10^{-4}$ molar freq. in [Ch][Lys] water mixture. [Try]⁻ protons' chemical shift stabilizes at $\chi_{\text{RTIL}} = 5 \times 10^{-5}$ molar freq. [Lys]⁻ ¹H chemical shift never reaches the plateau. Chemical shift minima were registered at $\chi_{\text{RTIL}} = 0.1$ molar freq. for almost all protons in the cation and both anions.

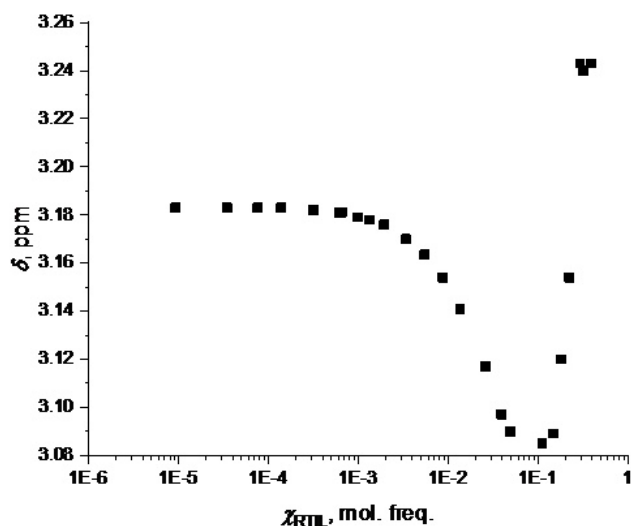


Fig. 1. [Ch]⁺ ¹H of (CH₃)₃-X chemical shift dependency of b-RTIL concentration in [Ch][Lys] and water solution.

Finally, both [Ch][Lys] and [Ch][Try] increase glibenclamide's solubility in water.

NICKEL CATALYSTS FOR HYDROGEN GENERATION

Gitana Valeckytė¹, Zita Sukackienė¹, Virginija Kepenienė¹, Irena Stalnionienė¹, Vitalija Jasulaitienė¹, Jūratė Vaičiūnienė¹, Loreta Tamašauskaitė Tamašiūnaitė¹, Giedrius Stalnionis¹, Eugenijus Norkus¹

¹Center for Physical Sciences and Technology
gitana.valeckyte@ftmc.lt

During this work, Ni/Cu, NiCo/Cu, NiMn/Cu, NiCoMn/Cu catalysts were formed using the chemical method of metal deposition. The surface morphology, internal structure and chemical composition of the obtained catalysts were analyzed using field emission scanning electron microscopy, X-ray photoelectron spectroscopy and induced plasma optical emission spectroscopy. It was determined that the prepared coating particles consist of oval-shaped agglomerates with a size of 40 nm to 1.6 μm. The studies of the composition of the catalysts showed that the Ni loading ranges from 59.75 to 475.15 μg/cm², Co – 549.5 to 614 μg/cm², Mn – 0.06 to 0.745 μg/cm². The catalytic properties of the formed catalysts for sodium borohydride hydrolysis reaction were investigated. The two-component NiCo coating was characterized by the highest catalytic activity. It was determined of this catalyst an activation energy of 56.4 kJ/mol and an H₂ evolution rate of 1.24 ml/min at 30 °C and 14.59 ml/min at 70 °C.

SYNTHESIS AND LUMINESCENT PROPERTIES OF EU-DOPED $\text{Ca}_2\text{PO}_4\text{Cl}$

Paulina Pažerauskaitė¹, Artūras Katelnikovas¹, Aleksej Žarkov¹

¹Institute of Chemistry, Vilnius University, Naugarduko 24, LT-03225 Vilnius, Lithuania
paulina.pazerauskaite@chgf.stud.vu.lt

Functional materials with adjustable luminescence have become a research hotspot for their broad application prospects. As one of the most common and highly efficient activators, an Eu^{2+} ion possesses broadband absorption in the UV to blue regions, as well as multicolor emission. Calcium phosphates are the family of materials, widely used in different areas including the development of optical materials. Calcium chlorapatite (ClAp, $\text{Ca}_5(\text{PO}_4)_3\text{Cl}$) and goryainovite ($\text{Ca}_2\text{PO}_4\text{Cl}$) are calcium halophosphate minerals occurring in nature. Synthetic ClAp found its practical application in purification of water and sediments from heavy metals, lanthanide-doped ClAp was investigated in terms of optical properties. $\text{Ca}_2\text{PO}_4\text{Cl}$ is a less studied material, most of the papers being focused on the preparation and investigation of optical properties in lanthanide-doped $\text{Ca}_2\text{PO}_4\text{Cl}$. In the present work, Eu-doped $\text{Ca}_2\text{PO}_4\text{Cl}$ powders with various Eu content were synthesized and comprehensively characterized. Phase purity and crystal structure of the synthesized samples were studied by X-ray diffraction (XRD) and infrared spectroscopy (FTIR). Morphological features of synthesized powders were investigated by scanning electron microscopy (SEM). Luminescent properties were investigated by means of photoluminescence measurements. Excitation spectra, emission spectra and decay curves of the samples were studied. Temperature-dependent photoluminescence measurements were performed as well.

Acknowledgements. This project has received funding from the Research Council of Lithuania (LMTLT), agreement No S-MIP-23-85.

TUNABLE THERMO-RESPONSIVE COPOLYMERS VIA RAFT POLYMERIZATION: EFFECTS OF COMPOSITION ON PHASE TRANSITION IN AQUEOUS SOLUTIONS

Kristina Bolgova¹, Vaidas Klimkevicius¹

¹Faculty of Chemistry and Geosciences, Institute of Chemistry, Vilnius University
kristina.bolgova@chgf.stud.vu.lt

Stimuli-responsive polymers, particularly amphiphilic macromolecules with distinct affinities for polar and nonpolar solvents, have recently garnered significant scientific interest [1]. The intricate self-organization of hydrophilic and hydrophobic units within these macromolecules, influenced by external stimuli (temperature, ionic strength, and solvent quality) opens up avenues for applications in diverse fields, including medicine, biochemistry, and microelectronics [2].

The advancement of RAFT methods has enabled the synthesis of a wide range of amphiphilic copolymers with unique architectures, including brush polymers. This study focuses on the synthesis and investigation of statistical copolymers, specifically p(DEGMA-co-OEG_xMA) ($x = 5, 9$), synthesized through RAFT polymerization.

Various analytical techniques, including ¹H NMR, FT-IR, molecular sieve chromatography (MSC), and dynamic light scattering (DLS), were employed to characterize the copolymers.

From the NMR data, the structure of the copolymers was determined, and the exact composition, which is very close to the original monomer composition, was calculated. Using DLS method lower critical dissolution temperatures (LCST) of synthesized polymers were measured. It was found that the LCST values of the copolymers increased with increasing number of OEG_xMA ($x = 5, 9$) monomeric units in the copolymer composition.

The copolymers p(DEGMA-co-OEG₅MA) and p(DEGMA-co-OEG₉MA) with relatively high amount of DEGMA monomeric units in composition (80 and 90 mol%, respectively), exhibited LCST values close to human body temperature. This indicates their potential applications in medicine, pharmacy, and biotechnology.

[1] Kavaliauskaite, M. et. al. *Polymers* 2022, 14, 229.

[2] Korde, J. M. et.al. *Ind. Eng. Chem. Res.* 2019 58 (23), 9709-9757.

PM₁ CHARACTERIZATION FOR CONNECTED-FLOW EVENTS OVER THE BALTIC SEA BETWEEN HYLTEMOSSA AND PREILA

Agnė Minderytė¹, Axel Eriksson², Erik Ahlberg², Steigvilė Byčenkienė¹, Adam Kristensson², Julija Pauraitė¹

¹Center for Physical Sciences and Technology

²Lund University

agne.minderyte@ftmc.lt

Aerosol particle chemical composition and mass concentrations undergo significant changes due to long-range air mass transport, and yet the role of sea and oceans in aerosol chemical composition remains poorly understood. While previous studies have explored shipping-related aerosol properties or aerosol size distributions during connected flow events across the Baltic Sea, few studies have comprehensively investigated the impact of PM₁ removal over the sea, leaving a gap in our understanding of aerosol dynamics.

In this study, we examined 4 months of data (December 2017 to March 2018) of PM₁ chemical composition in two observation stations: Hyltemossa in Sweden and Preila in Lithuania. Simultaneous measurements of aerosol chemical composition were performed with ToF-ACSM (Aerodyne Research, Inc) in Hyltemossa and Q-ACSM in Preila. Equivalent black carbon (eBC) mass concentrations were measured using Aethalometers AE33 and AE31 (Magee Scientific) in Hyltemossa and Preila, respectively.

The influence of PM₁ removal over the sea on submicron particle composition was studied during the 14 connected flow events (in total 100 hourly trajectories) between Hyltemossa and Preila. The backward air mass transport trajectories were modelled using the Hybrid Single-Particle Lagrangian Integrated Trajectory (HYSPLIT) model with the Global Data Assimilation System (GDAS) meteorological databases at the NOAA Air Resources Laboratory's web server. The investigation focused solely on trajectories that passed upwind of Hyltemossa, extending 500 km over the Baltic Sea downwind and arriving at Preila.

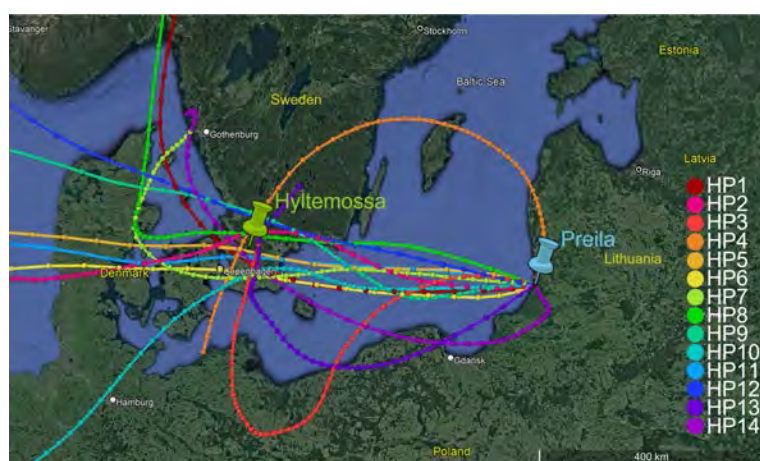


Fig. 1. 48-hour backward air mass trajectories for the connected flow events

Meteorological impact was taken into consideration and events with precipitation were evaluated separately. The results provide a better understanding of aerosol characterisation in the south-eastern Baltic Sea background environments and aerosol mass removal over the sea.

BISMUTH DOPED LASER-INDUCED (Bi-LIG) GRAPHENE ELECTROCHEMICAL SENSOR FOR THE DETECTION OF HEAVY METALS

Pamela Rivera¹, Aivaras Sartanavičius¹, Romualdas Trusovas¹, Rasa Pauliukaite¹

¹Center for Physical Sciences and Technologies
pamela.rivera@ftmc.lt

Heavy metals (HM) are among the main environmental pollutants affecting human health [1]. They bioaccumulate in the body, inducing cell membrane and DNA damage and disrupting protein function and enzymatic activity; leading to illnesses such as cancer, immune system deficiencies, mental growth retardation, and malnutrition [2].

Produce consumption is one major route of exposure to HMs for humans. Therefore, HM monitoring in the agricultural context is critical to prevent and mitigate the risk of poisoning in the food chain. Electrochemical sensors are suitable for HM monitoring since they are accurate, portable, and robust sensing devices. However, the intricate fabrication process of sensing materials hinders their scalability and reproducibility thus preventing their adoption as the staple for routine HM monitoring.

In this work, we investigate bismuth-doped laser-induced graphene (Bi-LIG) as a candidate electrode material for the simultaneous detection of Zn, Pb, and Cd at trace level using square wave anodic stripping voltammetry (SWASV). Bi-LIG electrodes result from an easily scalable single-step fabrication process and promise enhanced electroanalytical performance due to the synergy between the properties of LIG; flexibility, chemical resistance and porosity, and the electrocatalytic properties of the bismuth nanoparticle [3].

Bi-LIG is synthesized from polyimide film coated with a bismuth and chitosan ink before the laser induction process. The obtained Bi-LIG will be studied using Raman spectroscopy to determine the quality of the graphene, and XRD will be applied to study the composition of the bismuth nanoparticles synthesized by laser induction. Additionally, the electrochemical properties of synthesized sensing material will be investigated utilizing cyclic voltammetry (CV) and electrochemical impedance spectroscopy (EIS). Finally, the sensing material will be applied for the simultaneous detection of Zn, Pb, and Cd using SWASV, and its analytical performance will be compared to that of bismuth film on the glassy carbon electrode.

-
- [1] A. Alengebawy, S. T. Abdelkhalek, S. R. Qureshi, and M. Q. Wang, "Heavy metals and pesticides toxicity in agricultural soil and plants: Ecological risks and human health implications," *Toxics*, vol. 9, no. 3, 2021, doi: 10.3390/toxics9030042.
- [2] D. Witkowska, J. Słowik, and K. Chilicka, "Heavy Metals and Human Health: Possible Exposure Pathways and the Competition for Protein Binding Sites," *Molecules*, vol. 26, no. 19, p. 6060, Oct. 2021, doi: 10.3390/molecules26196060.[2] D. Witkowska, J. Słowik, and K. Chilicka, "Heavy Metals and Human Health: Possible Exposure Pathways and the Competition for Protein Binding Sites," *Molecules*, vol. 26, no. 19, p. 6060, Oct. 2021, doi: 10.3390/molecules26196060.
- [3] G. Zhao, X. Wang, G. Liu, and N. Thi Dieu Thuy, "A disposable and flexible electrochemical sensor for the sensitive detection of heavy metals based on a one-step laser-induced surface modification: A new strategy for the batch fabrication of sensors," *Sens Actuators B Chem*, vol. 350, p. 130834, Jan. 2022, doi: 10.1016/j.snb.2021.130834.

REDOX CONTROLLED BREATHING OF SUPRAMOLECULAR CAPSULE

Gabija Sergejevaitė¹, Domantas Valčekas¹, Edvinas Orentas¹

¹Department of Organic Chemistry, Vilnius University, Naugarduko g. 24, LT-03225, Vilnius, Lithuania
gabija.sergejevaite@chgf.stud.vu.lt

The molecular recognition utilizing well-defined molecular constructs is the key subject of supramolecular chemistry. Metal coordination or hydrogen bonds (H-bonds) are usually employed in formation of molecular capsules that are well suited to observe the complexation phenomena and inquire into the nature of non-covalent interactions [1]. Highly flexible building blocks despite their simpler synthesis are rarely used, compared to rigid, preorganized scaffolds, due to absence of entropic penalty reduction when forming molecular aggregates. Modulation of the host-guest chemistry by extending beyond simple covalent adjustment of the cavity size represents a highly sought-after strategy to construct dynamic supramolecular receptors that are reminiscent of enzymes [2]. In nature, induced fit, conformational selection and allosteric control, operating by conformational changes of the host in response to stimuli present, are the principles governing the substrate binding and activation. In our report, we present a redox control approach over cavity size of a simple molecular capsule from tripodal monomer, containing three ureidopyrimidinone (UPy) 4H-bonding units, trimesic acid core and linkers with disulfide moiety (Fig. 1A). We have shown that such monomers are capable of forming well-defined dimeric capsules. Furthermore, these capsules are capable of undergoing reversible conformational shifts and changing size and shape of their cavity by applying redox conditions that dissociate and reform disulfide links (Fig 1B).

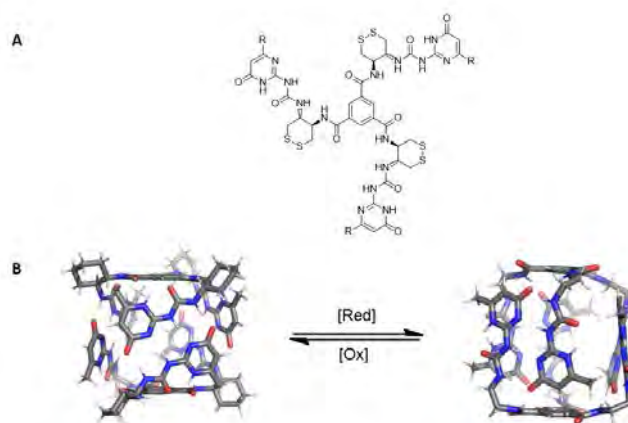


Fig. 1. A. Chemical structure of the supramolecular monomer. B. Redox induced change of capsular cavity.

[1] A. Morgan Conn and J. Rebek, Self-assembling Capsules. *Chem. Rev.*, 97, 1647-1668 (1997).
 [2] Jozeliunaite, A., et al., *J. Am. Chem. Soc.*, 145 (1), 455- 464, (2023).

MULTILAYER CAPACITOR AS AN ELECTROCHEMICAL SENSOR FOR MEASURING HYDROGEN PEROXIDE

Alvydas Radžius¹, Šarūnas Žukauskas², Arūnas Ramanavičius^{1,2}

¹Department of Physical Chemistry, Institute of Chemistry, Faculty of Chemistry and Geosciences, Vilnius University (VU), Naugarduko g. 24, LT-03225 Lt

²Department of Nanotechnology, State Research Institute Center for Physical Sciences and Technology (FTMC), Sauletekio Av. 3, LT-10257 Vilnius, Lithuania
alvydas.radzius@chgf.stud.vu.lt

Hydrogen peroxide (H_2O_2) is a widely utilized compound in laboratories, serving various purposes such as: an oxidizing agent, a reagent, or a cleaning/disinfecting agent. Unfortunately, the compound exhibits degradation, particularly in highly concentrated solutions, even at low temperatures. Traditional methods for assessing its concentration, such as titration, are time-consuming and require additional reagents.

To address this issue, an electrochemical sensor can be used to measure the concentration of H_2O_2 in solutions. In this study, a multilayer capacitor was employed as the sensing element due to its low cost of manufacturing, small physical size and compatibility with electronic systems.

Chronoamperometric measurements were performed using a three-electrode system, applying a potential of +0.3 V and introducing H_2O_2 concentrations ranging from 0.5 mmol to 5.7 mmol. The acquired chronoamperogram demonstrated distinct changes in the amperometric signal with each addition of H_2O_2 .

Using a multilayer capacitor, electrochemical measurements were successfully conducted in the solution. The resulting amperometric signal exhibited a linear dependence on the concentration of H_2O_2 , with a determined sensitivity of $3.46\text{E-}7$ A/mM. This electrochemical sensing approach offers a rapid and efficient means of quantifying H_2O_2 concentrations, presenting a valuable alternative to traditional titration methods.

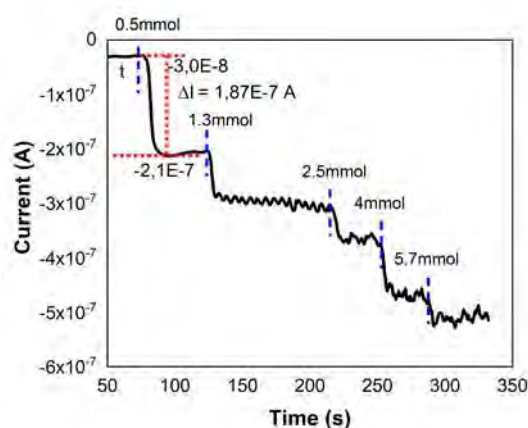


Fig. 1. Chronoamperogram obtained via a multilayer capacitor, +0.3 V in a three-electrode system, signal response from increasing the concentration of H_2O_2 in the electrolyte solution.

SACCHAROMYCES CEREVISIAE CELL MODIFICATION WITH NICKEL AND FERRIC HEXACYANOFERRATES FOR THE APPLICATION IN BIO-FUEL CELL CONSTRUCTION

Gabija Adomaitė¹, Aušra Valiūnienė¹

¹Vilnius university
kav.gabija@gmail.com

Although *Saccharomyces cerevisiae* cells are popular in the formation of bio-fuel cells due to their low cost and availability, the conductivity of yeast cell walls limits charge transfer. This research aims to enhance the yeast cell wall conductivity by modifying *Saccharomyces cerevisiae* cells with iron (III) hexacyanoferrate (II) and nickel hexacyanoferrate (II). The conductivities of modified yeast cells were measured using cyclic voltammetry. Additionally, bio-fuel cells were constructed, and their power was measured under different resistances. Changes in bio-fuel cell power over time were also recorded.

HYBRID NASICON TYPE BATTERIES MATERIALS SOLID-STATE NMR RESEARCH

Matas Manionis¹, Vytautas Klimavicius¹

¹Vilnius University

matas.manionis@ff.stud.vu.lt

Widely used lithium ion batteries face problems such as the reduction of effectiveness after a long time usage, dendrite and toxic salt formation, complicated disposal. A NASICON type material $\text{NaTi}_2(\text{PO}_4)_3$, made from naturally abundant sodium, is a potential candidate for anode synthesis, of next generation batteries, because of its thermal and structural stability and good ionic conductivity. To analyze how batteries work and why they fail, a reliable spectroscopy method called Nuclear Magnetic Resonance (NMR) is used, to measure and investigate structures of crystalline and amorphous compounds on a molecular scale. By using NMR relaxation filter methods it is possible to create a library of ^{23}Na , ^{31}P and ^1H nuclei spectra and use it to investigate potential batteries alternatives.

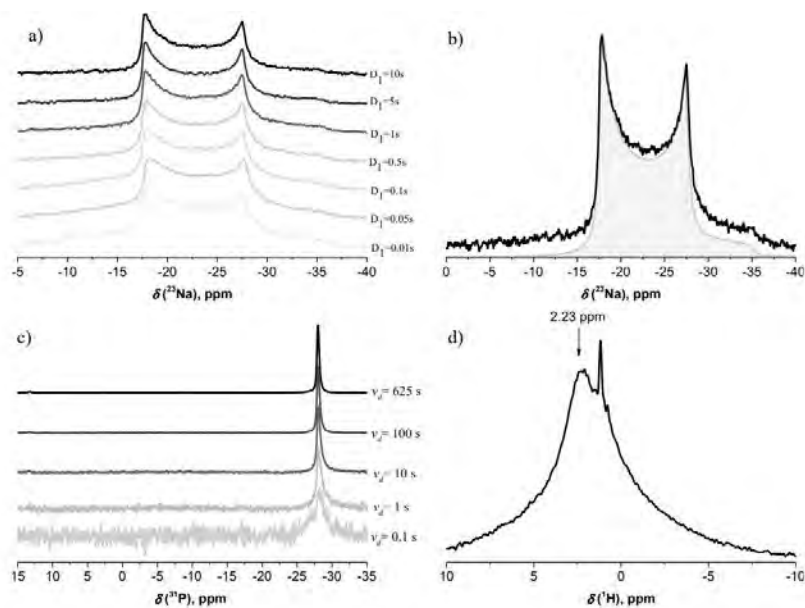


Fig. 1. a) ^{23}Na spectrum with different impulse delay times, b) ^{23}Na spectrum approximated with theoretical curves c) ^{31}P spectrum with different impulse delay times d) ^1H spectrum .

[1] Wu, M., Ni, W., Hu, J., & Ma, J. (2019). NASICON-Structured $\text{NaTi}_2(\text{PO}_4)_3$ for sustainable energy storage. *Nano-Micro Letters*, 11(1).

SYNTHESIS AND OPTICAL PROPERTIES OF CR-SUBSTITUTED BETA-TRICALCIUM PHOSPHAITE

Jonas Stadulis¹, Sapargali Pazylbek¹, Arturas Katelnikovas¹, Aleksej Zarkov¹

¹Institute of Chemistry, Vilnius University, Naugarduko 24, LT-03225 Vilnius, Lithuania
jonas.stadulis@chgf.stud.vu.lt

Calcium phosphates (CPs) are the family of materials, widely used in different areas such as medicine and bone regeneration, catalysis, sensors, removal of heavy metals from water, as host matrices for the development of optical materials etc. One of the CPs most frequently used for the fabrication of bioceramics is beta-tricalcium phosphate (β -TCP, $\text{Ca}_3(\text{PO}_4)_2$); moreover, this host material can be used for the development of luminescent materials employing the substitution of Ca by other optically active ions. In the present work, Cr^{3+} -doped β -TCP powders with various Cr content were synthesized by wet precipitation method using $\text{Ca}(\text{NO}_3)_2 \cdot 4\text{H}_2\text{O}$, $\text{Cr}(\text{NO}_3)_3 \cdot 9\text{H}_2\text{O}$ and $(\text{NH}_4)_2\text{HPO}_4$ as starting materials. As prepared precipitates were filtered, washed with water and ethanol and dried in an oven at 50 °C overnight. For the synthesis of β -TCP dried precipitates were annealed at 1000 °C for 5 hours. Phase purity and crystal structure of synthesized samples were studied by X-ray diffraction (XRD), electron paramagnetic resonance (EPR) and infrared spectroscopy (FTIR). Chemical composition of the samples was determined by inductively coupled plasma optical emission spectrometry (ICP OES). Morphological features of synthesized powders were investigated by scanning electron microscopy (SEM). Optical properties were investigated by means of photoluminescence measurements. Excitation spectra, emission spectra and decay curves of the samples were studied. Temperature-dependent photoluminescence measurements were performed as well.

Acknowledgements

This project has received funding from the Research Council of Lithuania (LMTLT), agreement No S-MIP-23-85.

SYNTHESIS OF FUNCTIONALISED *m*-TERPHENYLS AND CHEMOENZYMATIC SEPARATION OF ATROPISOMER

Kristupas Volbikas^{1,2,3}, Tomas Paškevičius¹, Ringailė Lapinskaitė¹, Nina Urbelienė², Linas Labanauskas¹, Rolandas Meškys²

¹Department of Organic Chemistry, Center for Physical Sciences and Technology, Akademijos st. 7 LT-08412 Vilnius

²Department of Molecular Microbiology and Biotechnology, Institute of Biochemistry, Life Sciences Centre, Vilnius University, Saulėtekio Ave 7, LT-10257 Vilnius

³Faculty of Chemistry and Geosciences, Vilnius University, Naugarduko st. 24, LT-03225 Vilnius
kristupas.volbikas@chgf.stud.vu.lt

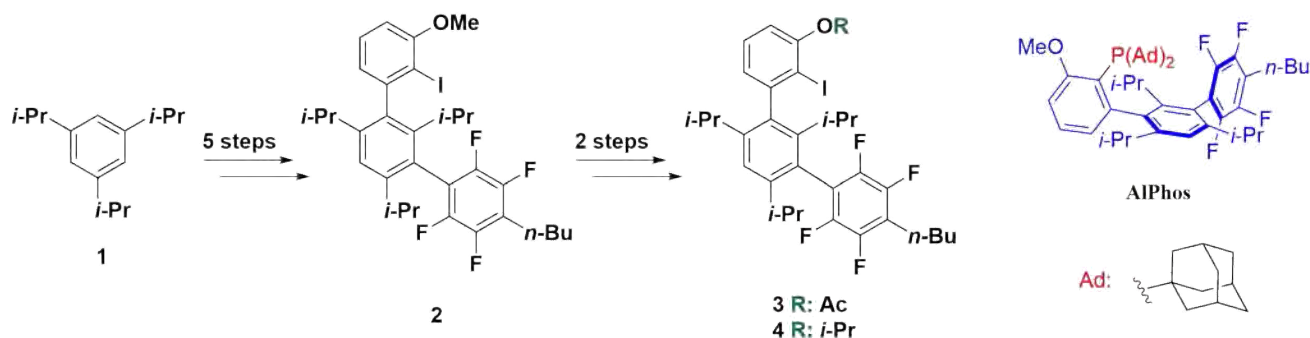


Fig. 1. General scheme for *m*-terphenyl synthesis. Structure of phosphine ligand **AIPhos**

Fluorinated aromatic substances are widely used in medicine¹ and agriculture². However, their synthesis remains complicated with commonly used methods being non-selective, requiring harsh conditions and resulting in modest product yields for sensitive substrates. A possible solution to these problems is the use of transition-metal catalysis. Its application in C-F bond formation remained elusive until relatively recently and is still requiring more research to be done.³ Thus, our team is developing new ligands, based on the structure of **AIPhos**⁴ (Fig. 1. right side), for palladium (0/II) catalysed C-F cross-coupling reactions, with the aim of expanding the (hetero)aromatic substrate range of these reactions. These ligands consist of a di-*tert*-alkylphosphine (Fig. 1. colored red) coupled with a *m*-terphenyl backbone (Fig. 1. colored blue). My work covers the synthesis and modification of the *m*-terphenyl backbone.

Furthermore, these *m*-terphenyl backbones possess axial chirality. Synthetic methods for atropisomer separation are usually difficult, require specialised equipment and reagents.⁵ Different esterases have been successfully used to separate (hetero)biaryl atropisomers with high enantioselectivity and good yields, although *m*-terphenyl compounds have yet to be studied.⁶ This work will bring a better understanding on how different esterases interact with highly hydrophobic atropisomeric substrates such as acetate **3**.

[1] Gillis, E. P.; Eastman, K. J.; Hill, M. D.; Donnelly, D. J.; Meanwell, N. A.; J. Med. Chem. 2015, 58, 8315-8359

[2] Jeschke, P.; ChemBioChem 2004, 5, 570-589

[3] Campbell, M. G.; Ritter, T.; Chem. Rev. 2015, 115, 612-633

[4] Sather, A. C.; Lee, H. G.; Valentina, R.; Yang, Y.; Müller, P.; Buchwald, S. L.; J. Am. Chem. Soc. 2015, 137, 13433-13438

[5] Carlsson, A.; Karlsson, S.; Munday, R. H.; Tatton, M. R.; Acc. Chem. Res. 2022, 55 (20), 2938-2948

[6] Olivia; Berreur, J.; Beatrice; Clayden, J.; Acc. Chem. Res. 2022, 55 (23), 3362-3375

CHARACTERIZATION OF TRANS-STILBENE NANOCRYSTALS IN POLYESTERENE FILMS BY CARS AND AFM MICROSCOPY AND OPTICAL SPECTROSCOPY

Ivan Halimski¹, Renata Karpicz¹, Andrej Dementjev¹, Marija Jankunec², Jevgenij Chmeliov^{1,3}, Mindaugas Macernis³, Darius Abramavicius³, Leonas Valkunas^{1,3}

¹Department of Molecular Compound Physics, Center for Physical Sciences and Technology, Lithuania

²Institute of Biochemistry, Life Sciences Center, Vilnius University, Lithuania

³Institute of Chemical Physics, Faculty of Physics, Vilnius University, Lithuania
ivan.halimski@ftmc.lt

The most well-known feature of stilbene molecules is *trans-cis* isomerization, which makes them perspective for molecular switches [1]. Moreover, isomers themselves found their own applications. For example, *trans*-stilbene (Tstilbene) could be used as neutron detector for radiation detection [2]. The knowledge about properties of Tstilbene in different conditions (temperature, concentration, etc.) is critically important for applications and, probably, to expand the scope of application.

In the previous studies, unusual Tstilbene fluorescence dependence on temperature [3], as well as aggregation-related spectroscopic optical properties dependent on concentration, were investigated [4]. The thickness of the stilbene-containing film is another important parameter that could affect the sample's properties. Combination of steady-state and time-resolved optical spectroscopy with Coherent Anti-Stokes Raman Scattering (CARS) and Atomic Force Microscopy (AFM) provides an opportunity to understand, how changes in structure (aggregation, dimerization) affect spectroscopic behavior.

In this work, we investigate Tstilbene aggregation and crystallization in polystyrene (PS) matrix in thin films. The effect of both film thickness (by varying PS concentration in chloroform) and Tstilbene concentration (by varying Tstilbene mass-ratio in PS matrix) are studied.

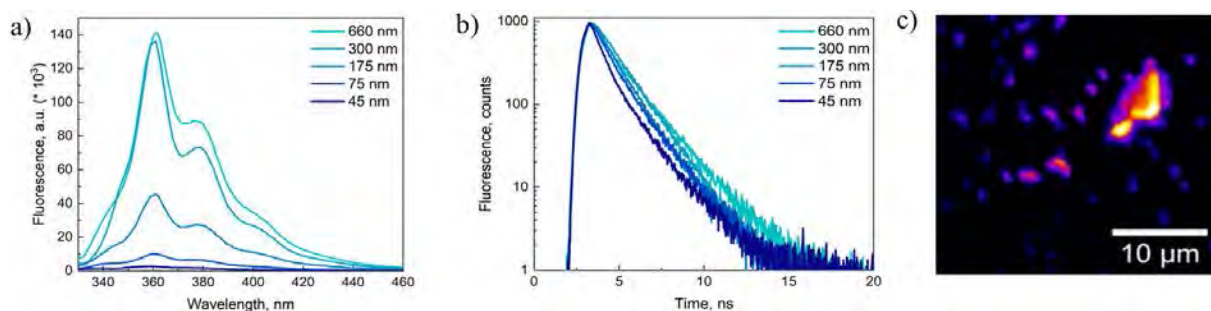


Fig. 1. Fluorescence spectra of 80% Tstilbene dependent on film thickness b) Corresponding time-resolved fluorescence spectra (kinetics) at $\lambda_{em} = 360$ nm. c) CARS image of 80% Tstilbene 175 nm PS film (scan $30\mu\text{m} \times 30\mu\text{m}$).

Such data analysis techniques, as kinetics fitting with sample-decay and stretched-exponential [5,6] decay models, spectra and kinetics decomposition, combined with microscopy analysis provide information about formation of aggregates of different sizes, their influence on optical properties. Moreover, here we show dependence on properties (concentration and thickness) being changed simultaneously. That means, it is possible to *control* structure via changing parameters.

- [1] V. Nagarajan et al., *Condens. Matter Phys.* 21, 43010 – 43012, 2018.
 [2] L. Carman et al., *Journal of Crystal Growth.* 368, 56 – 61, 2013.
 [3] R. Karpicz, et al., *Phys. Chem. Chem. Phys.* 23, 3447 – 3454, 2021.
 [4] R. Karpicz, et al., *Phys. Chem. Chem. Phys.* 25, 21183 – 21190, 2023.
 [5] J.R. Lakowicz, *Principles of fluorescence spectroscopy*, 2010.
 [6] J. Tamosiunaite, et al., *Chemical Physics.* 572, 111949 – 111960, 2023.

EVALUATING THE ROLE OF GREEN INFRASTRUCTURE IN REDUCING TRANSPORT-RELATED MICROPLASTICS FOR STRENGTHENING URBAN ENVIRONMENTAL HEALTH

Abdullah Khan¹, Valda Araminienė², Ieva Uogintė¹, Lina Davulienė¹, Iveta Varnagirytė-Kabašinskiė², Valda Gudynaitė-Franckevičienė², Algis Džiugys³, Edgaras Misiulis³, Steigvilė Byčėnkiė¹

¹Centre for physical sciences and technology (FTMC), Saulėtekio Ave. 3, Vilnius, Lithuania

²Lithuanian Research Centre for Agriculture and Forestry, Instituto al. 1, Akademija, LT-58344 Kėdainiai distr., Lithuania

³Lithuanian Energy Institute, Breslaujos st. 3, LT-44403 Kaunas, Lithuania

abdullah.khan@ftmc.lt

Tire and road wear microplastics (TRWMPs) are among the most significant non-exhaust pollutants emitted by motor vehicles, leading to serious environmental and health problems [1]. Among the many sources of microplastics (MPs), the contribution of traffic-related MPs has become a significant problem due to their widespread dispersion by atmospheric circulation. Each year, approximately 6.1 million tons of TRWMPs are emitted into the environment [2]. Consequently, the inhalation of these particles is a significant exposure route to humans, resulting in some serious health issues. The health risk of atmospheric MPs depends upon their abundance and other physiochemical properties such as size, shape, and chemical composition [3].

The study aimed to assess the potential of green space proximity to high-traffic streets in mitigating the presence of MPs and associated human health risks. In Kaunas City, Lithuania (54°51'00.7"N 24°01'46.5"E), a hedge of *Thuja occidentalis* (0.6 m in width, 1.5 m in height, and a length of 19 m), situated between street and residential houses, was selected to imitate green space. Airborne MPs samples were collected using passive deposition onto Petri dishes with 8 cm diameter glass fiber filters at varying distances (0, +1, +2 meters) from the street over a 24-hour period. The MP samples were collected every month from June to October 2023. Microscopic techniques were employed to quantify the abundance, morphology, and colour of the MPs particles. The chemical composition of MP particles was measured by the LUMOS II spectroscope.

The results indicate a variation in MPs levels, ranging from 2.8 to 0.25 MP/cm², based on the proximity to streets. The predominant forms observed in the samples are fragments and black-coloured particles, constituting 90-100% of the total. Analysis reveals that the MPs particles primarily consist of polypropylene and polyurethane (40.9%), both of which are commonly present in vehicle tires.

[1] Liu, Meixuan et al. Chemical composition and potential health risks of tire and road wear microplastics from light-duty vehicles in an urban tunnel in China. *Environmental Pollution* 330 (2023) 121835.

[2] Ly, Alfonse, and Zeinab El-Sayegh. Tire wear and pollutants: An overview of research. *Archives of Advanced Engineering Science* 1.1 (2023): 2-10.

[3] Bakand, Shahnaz, Amanda Hayes, and Finance Dechsakulthorn. Nanoparticles: a review of particle toxicology following inhalation exposure. *Inhalation toxicology* 24.2 (2012): 125-135.

SYNTHESIS AND LUMINESCENT CHARACTERIZATION OF DOPED

$\text{Na}_{1-x}\text{AlGe}_{1-0.5x}\text{O}_4\text{:X}$ PHOSPHORS

Gabija Janauskaite¹, Martynas Misevicius¹

¹Institute of Chemistry, Faculty of Chemistry and Geosciences, Vilnius University, Lithuania
gabija.janusauskaite@chgf.stud.vu.lt

The demand for energy-efficient lighting has spurred research into luminescent materials, crucial for the development of next-generation technologies. As white light-emitting diodes (LEDs) gain prominence for their efficiency, long life, and minimal energy consumption, there's a growing need to explore novel luminescent materials. Recently, increasing attention has been paid to germanate compounds, which are suitable for the development of phosphors due to their low synthesis temperature and excellent physicochemical properties.

Sodium aluminum germanate NaAlGeO_4 has a monoclinic structure with the symmetry space group $P2_1/n$. The lattice parameters of NaAlGeO_4 are $a = 8.783 \text{ \AA}$, $b = 15.432 \text{ \AA}$, $c = 8.252 \text{ \AA}$, and the lattice angles $\alpha = 90.00^\circ$, $\beta = 90.00^\circ$, $\gamma = 90.09^\circ$. NaAlGeO_4 is characterized by unique optical and electronic properties, including high thermal stability, strong photoluminescence, and high transparency in the visible and near-infrared range. Furthermore, its composition and crystal structure render it well-suited for diverse applications, including serving as a host material for rare earth ions in solid-state lighting and functioning as a dielectric material for capacitors.

During this study, a sequence of $\text{Na}_{1-x}\text{AlGe}_{1-0.5x}\text{O}_4\text{:X}$ samples doped with varying concentrations of Bi^{3+} , Ce^{3+} , Dy^{3+} , Eu^{3+} , Pr^{3+} , Sm^{3+} and Tb^{3+} ions were synthesized using the solid-state synthesis method. The obtained samples underwent characterization through the powder X-ray diffraction (XRD) technique and photoluminescence (PL) measurements, including excitation and emission spectra, luminescence decay times, and quantum efficiencies. The XRD analysis demonstrated that all samples exclusively consisted of the pure NaAlGeO_4 phase. Insights from the PL measurements revealed specific emission characteristics for each ion: red emission in Eu^{3+} -doped samples, yellow emission in Dy^{3+} -doped samples, blue emission in Bi^{3+} and Ce^{3+} -doped samples, orange-red emission from Pr^{3+} , orange emission from Sm^{3+} , and green emission from Tb^{3+} .

Acknowledgment: This research has been funded by Lithuanian Science Council (LMT)s Studentsresearch practice project No. S-ST-23-193

MODELLING OF PORPHINE NANOTUBE ABSORPTION SPECTRA

Eimantas Urniežius¹, Darius Abramavičius¹

¹Vilnius University, Faculty of Physics, Institute of Chemical Physics, Saulėtekio al. 3, LT-10257 Vilnius
 eimantas.urniezius@ff.stud.vu.lt

Zwitterionic meso-tetra(4-sulfonatophenyl) porphyrin and a number of its derivatives self-assemble into tubular aggregates. These aggregates are both found occurring in nature, such as most prominently in the chlorosomes of green bacteria, but can also be synthesized in a laboratory setting. These aggregates have already found use in areas such as photodynamic therapy (PDT) and optoelectronics.[1]

Porphine aggregates have unique optical properties, which can be seen in their absorption and circular dichroism spectra in the range of visible light. It is important to understand the optical responses of these aggregates to better know how to apply them. To achieve this an idealised mathematical model was used, where each molecule in the aggregate was associated with a single point, and arranging them in a helical structure with each point having four optical transition dipole vectors assigned to it. The spectra themselves were calculated by finding the exciton states of the aggregate. These states were found by solving the stationary Schroedinger equation with a hamiltonian constructed with the interactions between each molecule's respective dipole vectors as its off-diagonal elements. These were then used to calculate both the absorption and circular dichroism spectra of the idealised tube.

Using this relatively simple model we were able to calculate spectra that closely aligns with experiment in its shape and peak positions in both the B and Q bands. To achieve this, many different configurations of dipole vectors and molecules of the aggregate were tested in order to find which closest resembled the experiment. Moreover, taking into account that even a relatively short tube contained thousands of molecules, computational resource use was also taken into account. To that end, the length of the aggregate, adequate to get the highest possible accuracy while also taking up the minimal amount of computation time, was determined.

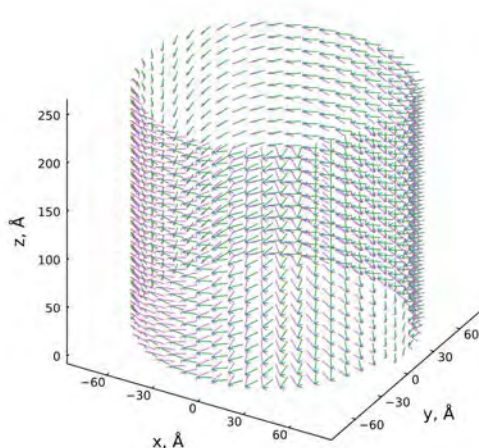


Fig. 1. Model of tubular aggregate with dipole vectors

[1] M. C. A. Stuart J. Knoester S. M. Vlaming, R. Augulis and P. H. M. van Loosdrecht. Excitonspectra and the microscopic structure of self-assembled porphyrin nanotubes. J. Phys. Chem. B,2009.

SYNTHESIS OF CARBAZOLE-BASED MATERIAL WITH ACCEPTOR MOIETIES FOR PEROVSKITE SOLAR CELL TECHNOLOGY

Guostė Kaleininkaitė¹, Aida Drevilkauskaitė¹, Vytautas Getautis¹, Artiom Magomedov¹

¹Department of Organic Chemistry, Kaunas University of Technology, Lithuania
guoste.kaleininkaite@ktu.edu

Pollution free sources of renewable energy have become gradually more relevant in the last decade. Inexhaustible solar energy has been one of the prime areas of research and it has been established as a cost effective and reliable source of energy. In the last decade of research, significant progress has been made in the development of new materials for 3rd generation solar cell technology, specifically perovskite solar cells. One of the specific problems is related to the use of C₆₀ as an electron transporting material [1]. However, the available electron-transporting chromophores have failed to substitute it, mostly due to the problems related with solubility. Therefore, it is important to find new structural concepts, that would avoid such limitations.

The aim of our work is to synthesize new electron transporting materials-candidates by introducing an indanedione acceptoring unit in the third and sixth position of 9-ethyl-9H-carbazole via two-step synthesis. First, by synthesizing 9-ethyl-9H-carbazole-3,6-dicarbaldehyde from N,N-dimethylformamide and 9-ethyl-9H-carbazole with the use of POCl₃ in 1,2-dichloroethane, and later substituting the two formyl groups with indanedione in ethanol.

The first round of synthesis resulted in a target compound, as was confirmed by the NMR spectroscopy method. However, high yields have not been achieved. The main reason lies in reduced reactivity of the monoaldehyde, and the complicated purification process of the intermediate compound. Further optimization of reaction conditions and ratio of reactants for the first step is required. After optimization, the photoelectrical properties of the materials will be evaluated.

[1] M. Stolterfoht et al., Visualization and suppression of interfacial recombination for high-efficiency large-area pin perovskite solar cells. *Nat Energy*, **3**, 847–854 (2018).

INVESTIGATION OF HOLE TRANSPORT IN SMALLMOLECULE - POLYMER BLENDS

Danielius Sakavicius¹

¹Institute of Chemical Physics, Faculty of Physics, Vilnius University
danielius.sakavicius@ff.stud.vu.lt

Research on hole transport in organic layers is an important and complex scientific field that has emerged due to the rapid development of modern materials science and engineering. The main disadvantages of organic electronic devices are the low mobility of charge carriers in them and poor resistance to environmental influences. In small-molecule organic compounds, higher charge carrier mobilities are achieved than in polymers. However, effective control over layer morphology remains a challenge [1]. On the other hand, polymer layers offer superior controllability in terms of structure. Consequently, combining small molecule materials with polymers holds great promise for the development of novel charge transport layers in organic electronic devices. In such compounds, polymers may simultaneously act as charge transporting components and supporting structural matrices. While the addition of polymers should enhance layer integrity, it's crucial to optimize the composition as it could potentially impact charge carriers transport.

For some of newly synthesized carbazole-based hole transporting materials [2], obtaining high-quality layers without cracks in sufficiently large areas is challenging, if not impossible, task. Therefore, these materials were blended in various ratios with well-known hole-transporting polymer PEPC (Poly(9-(2,3-epoxypropyl) carbazole)). Surface of casted layers was controlled by microscopy and AFM, while the charge transport in the layers was investigated by well-known methods such as ToF and photo-CELIV [3]. Obtained results show that a good layer structure without compromising hole transport can be achieved at the optimized composition. These results will facilitate investigation of novel hole transport materials.

[1] Hamilton, R., et al, High-Performance Polymer-Small Molecule Blend Organic Transistors. *Adv. Mater.*, 21: 1166-1171. (2009)

[2] Jegorovė, A., et al, Starburst Carbazole Derivatives as Efficient Hole Transporting Materials for Perovskite Solar Cells. *Sol. RRL*, 6: 2100877, (2022)

[3] N. Nekrašas, et al, Features of current transients of photogenerated charge carriers, extracted by linearly increased voltage, *Chemical Physics*, Volume 404, Pages 56-59, (2012)

LARGE AMOUNT SYNTHESIS OF MAGNESIUM WHITLOCKITE NANOPOWDERS FROM AN ENVIRONMENTALLY FRIENDLY INITIAL REACTANT

Rūta Raišeliene¹, Greta Linkaitė¹, Aleksej Žarkov¹, Aivaras Kareiva¹, Monika Skruodienė², Inga Grigoravičiūtė¹

¹Institute of Chemistry, Vilnius University, Naugarduko 24, LT-03225 Vilnius, Lithuania

²Center for Physical Sciences and Technology, Sauletekio av. 3, 10257 Vilnius, Lithuania
ruta.raiseliene@chgf.vu.lt

Thousands of people annually have health problems related to bone fractures caused by osteoporosis, trauma, cancer, and various diseases, that frequently require surgical treatment for bone regeneration [1]. Calcium phosphate (CaP) compounds are widely studied and used as bone substitutes due to their similar composition to the inorganic part of bone, their biocompatibility, and ease of fabrication [2]. The most popular and investigated substitutes are hydroxyapatite (HA), tricalcium phosphate (TCP), octacalcium phosphate (OCP), and biphasic calcium phosphate (BCP). Magnesium whitlockite (Mg-WH, $\text{Ca}_{18}\text{Mg}_2(\text{HPO}_4)_2(\text{PO}_4)_{12}$) occupies a significant place in the mineral part of human bone, induces osteogenic differentiation, rapid bone formation, and undoubtedly has outstanding substitute properties [3]. Due to the mentioned properties, Mg-WH is relevant in medicine: in bone reconstruction and treatment procedures.

The main idea of our investigation was to synthesize a large amount of Mg-WH nanopowders via a simple, inexpensive, low-temperature dissolution-precipitation (DP) method from an environmentally friendly gypsum ($\text{CaSO}_4 \cdot 2\text{H}_2\text{O}$) powder as a starting material. DP synthesis is appropriate for the fabrication of CaP material as well as Mg-WH compound [4]. The obtained product was investigated by powder X-ray diffraction (XRD) analysis, scanning electron microscopy (SEM), Fourier-transform infrared spectroscopy (FTIR), Brunauer–Emmett–Teller (BET) measurements, and Energy-dispersive X-ray (EDX) analysis.

Acknowledgments. This project has received funding from the Research Council of Lithuania (LMTLT), agreement No. P-SV-202.

[1] I. Lodoso-Torrecilla et. al., Calcium phosphate cements: Optimization toward biodegradability, *Acta Biomaterialia* 119, 1-12 (2021)

[2] H.-J. Kang et. al., Comparative study on biodegradation and biocompatibility of multichannel calcium phosphate based bone substitutes, *Mat. Sc. and Eng.: C* 110, 110694 (2020)

[3] J. Jeong et. al., Synergistic Effect of Whitlockite Scaffolds Combined with Alendronate to Promote Bone Regeneration *J. Tissue Eng. Reg. Med.* 19, 83-92 (2022)

[4] K. Ishikawa, Bone Substitute Fabrication Based on Dissolution-Precipitation Reactions, *Materials* 3, 1138-1155 (2010)

BENZOPHENONE-BASED TWISTED DONOR-ACCEPTOR-DONOR DERIVATIVES AS BLUE EMITTERS FOR HIGHLY EFFICIENT FLUORESCENT OLEDs

Dovydas Blazevicius¹, Iram Siddiqui², Prakalp Gautam², Gintare Krucaite¹, Daiva Tavgeniene¹, Mangey Ram Nagar², Krishan Kumar³, Subrata Banik⁴, Jwo-Huei Jou², Saulius Grigalevicius¹

¹Department of Polymer Chemistry and Technology, Kaunas University of Technology, Lithuania

²Department of Materials Science and Engineering, National Tsing Hua University, Taiwan

³School of Chemical Sciences, Indian Institute Of Technology-Mandi, Kamand 175005, Himachal Pradesh, India

⁴Department of Chemistry, School of Chemical and Biotechnology, SASTRA Deemed University, Thanjavur 613401, Tamil Nadu, India

dovydas.blazevicius@ktu.lt

Organic light-emitting diodes (OLEDs) technology has outperformed other technologies in recent decades [1]. OLEDs are the ultimate technology for display and are stepping rapidly into lighting. At present, there is an intensive need for high-performance deep-blue emitters in full-color display and solid-state lighting. However, as the emission peaks shift towards the deep-blue region, the nonradiative transition rate of metal d-orbitals tends to increase, making it difficult to achieve a high efficiency altogether [2]. To solve the problem, small-molecules fluorescent materials have re-gained attention due to their high color purity and low cost. The synthesis of bicarbazole-based host materials was carried out by the three-step synthetic route as shown in Figure 1. Herein, we introduce a series of donor-acceptor-donor (D-A-D) twisted derivatives based on carbazole-benzophenone moieties.

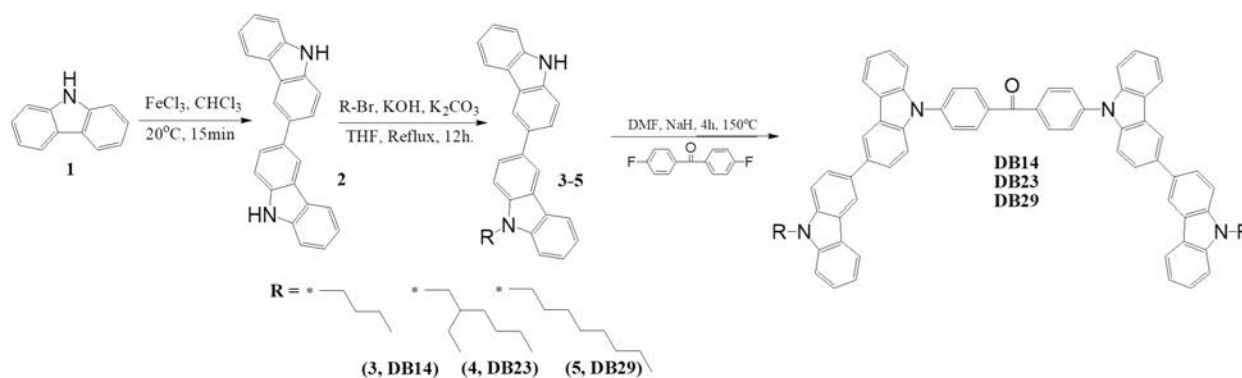


Fig. 1. Synthetic pathway of bicarbazole-based materials.

This work was dedicated to development of a group of twisted donor-acceptor-donor (D-A-D) derivatives incorporating bicarbazole as electron donor and benzophenone as electron acceptor for potential use as blue emitters in OLEDs. The derivatives were synthesized in a reaction of 4,4'-difluorobenzophenone with various 9-alkyl-9'H-3,3'-bicarbazoles. The materials, namely, DB14, DB23, and DB29, were designed with different alkyl side chains to enhance their solubility and film-forming properties of layers formed using the spin-coating from solution method. The new materials demonstrate high thermal stabilities with decomposition temperatures >383 °C, glass transition temperatures in the range of 95–145 °C, high blue photoluminescence quantum yields of over 52%, and short decay times, which range in nanoseconds. Due to their characteristics, the derivatives were used as blue emitters in OLED devices. Some of the OLEDs incorporating the DB23 emitter demonstrated a high external quantum efficiency (EQEmax) of 5.3%, which is very similar to the theoretical limit of the first-generation devices.

Acknowledgements

We acknowledge support from the Research Council of Lithuania (grant No. S-MIP-22-84).

[1] C.-Y. Chan, L.-S. Cui, J. Kim, H. Nakanotani, C. Adachi, C. Chan, L. Cui, J.U. Kim. Rational Molecular Design for Deep-Blue Thermally Activated Delayed Fluorescence Emitters, *Advanced Functional Materials* 28, 1706023 (2018).

[2] J.H. Lee, C.H. Chen, P.H. Lee, H.Y. Lin, M.K. Leung, T.L. Chiu, C.F. Lin. Blue Organic Light-Emitting Diodes: Current Status, Challenges, and Future Outlook. *Journal of Materials Chemistry C* 7, 5874–5888 (2019)

NEW 4H-BONDING MOTIF

Vladyslava Romadina¹, Nojus Radzevičius¹, Edvinas Orentas¹

¹Vilnius University, Department of Organic Chemistry
edvinas.orentas@chf.vu.lt

Hydrogen bonding is a highly adaptable non-covalent molecular interaction that is extensively employed by nature to fulfill crucial life functions such as maintaining structural integrity, facilitating catalytic processes, and enabling replication. The term "hydrogen bonding motifs" pertains to particular configurations of hydrogen bonds inside molecular structures, serving as fundamental units for the construction of modular assemblies of hydrogen-bonded dynamic structures. The association strength of an array is determined by the overall number and arrangement of individual hydrogen bonds. In order to form supramolecular polymers, it is necessary to have quadruply bonding motifs to ensure adequate aggregation. In this study, we introduce a novel molecular structure, present its synthesis, and aggregation properties.

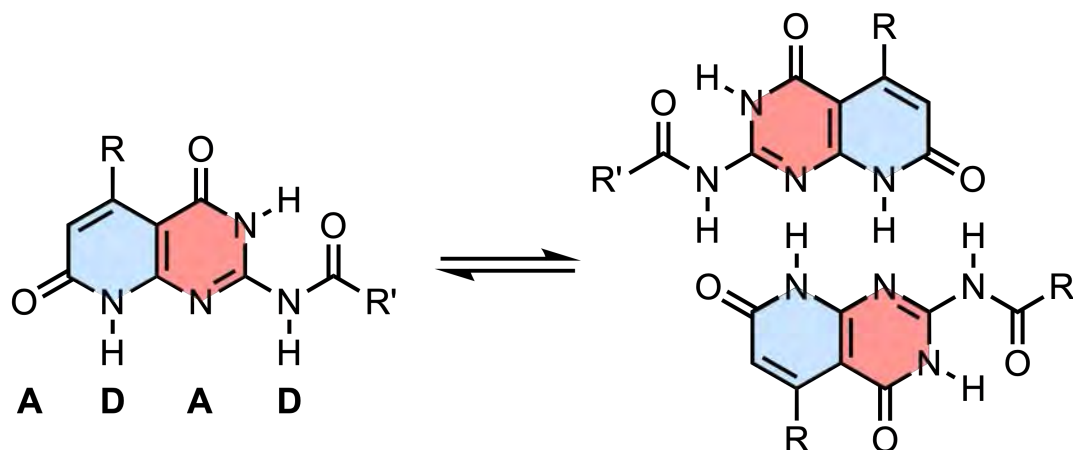


Fig. 1. Chemical structure and dimerization of the 4H-bonding motif

RESPONSIVE BEHAVIOR OF GRAFT COPOLYMERS BASED ON CHITOSAN

Migle Savicke¹, Ramune Rutkaite¹

¹Kaunas University of Technology, Department of Polymer Chemistry and Technology
migle.babelyte@ktu.edu

Poly(*N*-isopropylacrylamide) (PNIPAAm) is synthetic polymer which shows solubility changes in water around a specific temperature, which is well known as the lower critical solution temperature (LCST). This polymer is one of the most commonly used thermo-responsive polymers, because its phase transition temperature is close to the temperature of the human body. Recently, copolymers with grafted PNIPAAm side chains are highly researched, taking into account their great opportunities in biomedical field including drug delivery systems. One of the most perspective biopolymers which could be used as the backbone of these graft copolymers is chitosan. The importance of this polymer for biomedical application is due to its biodegradability, biocompatibility, low toxicity and pH-sensitivity. Therefore, the combination of synthetic PNIPAAm and chitosan in the macromolecular structures could be promising as dual-responsive (pH- and thermoresponsive) graft copolymers can be obtained.

The aim of the present work was to investigate thermal and pH-responsive behavior of chitosan-*graft*-poly(*N*-isopropylacrylamide) copolymers in aqueous solutions. Herein, seven chitosan-*graft*-poly(*N*-isopropylacrylamide) (CS-*g*-PNIPAAm) copolymers were synthesized by free-radical polymerization of CS and NIPAAm in aqueous solution using potassium persulfate (PPS) as an initiator. By changing molar ratio of CS:NIPAAm from 1:0.25 to 1:10 the copolymers with different composition were prepared. The obtained copolymers were characterized by X-ray, ¹H-NMR, FT-IR spectroscopy and other techniques. The thermo- and pH-responsive behavior of synthesized copolymers was assessed by cloud point, particle size and zeta potential measurements.

THIANTHRENE-BASED COMPOUNDS FOR OXYGEN SENSING APPLICATIONS

Lukas Dvylys¹, Rasa Keruckienė¹, Matas Gužauskas¹, Melika Ghasemi¹, Juozas Vidas Gražulevičius¹

¹Department of Polymer Chemistry and Technology, Kaunas University of Technology, Lithuania
lukas.dvylys@ktu.edu

Room temperature phosphorescence (RTP) is a phenomenon where certain materials emit light at ambient temperatures, with a delay after the removal of the excitation source [1]. Unlike fluorescence, which has rapid nanosecond lifetimes, RTP involves the transition of excited molecules to long-lived triplet states lasting milliseconds to seconds [2]. RTP exhibits intensity differences between air and oxygen-free environments, indicating the involvement of oxygen-sensitive triplets [1]. Organic compounds used in oxygen sensing have crucial roles in analytical chemistry and sensor technology, showcasing unique optical or electrochemical properties that modulate in the presence of oxygen. These compounds are utilized for their sensitivity to oxygen concentration changes, leading to alterations in emission characteristics [3]. The implementation of these sophisticated organic materials in sensing platforms contributes to advancements in fields such as environmental monitoring, biotechnology, and medical diagnostics, facilitating precise and real-time detection of oxygen levels in diverse applications [4].

Thianthrene and its derivatives have garnered significant attention in recent years for their promising potential as effective materials in oxygen sensing applications [5]. Thianthrene derivatives possess a conjugated molecular structure that facilitates efficient intersystem crossing, a crucial process for phosphorescence. The presence of sulfur atoms in the thianthrene molecule contributes to enhanced spin-orbit coupling, which promotes efficient triplet state formation. The rigidity of the molecular structure and the extended conjugation in thianthrene derivatives further stabilize the triplet state, allowing for extended phosphorescence lifetimes at room temperature [5].

In this work, two thianthrene-based compounds with different electron acceptors were synthesized. Their thermal, electrochemical, and photophysical properties will be presented.

-
- [1] J. Yang, et al., Stimulus-Responsive Room Temperature Phosphorescence Materials: Internal Mechanism, Design Strategy, and Potential Application, *Acc Mater Res* 2 (2021) 644-654.
- [2] M. Gmelch, et al., High-Speed and Continuous-Wave Programmable Luminescent Tags Based on Exclusive Room Temperature Phosphorescence (RTP), *Advanced Science* 8 (2021) 2102104.
- [3] E. Armagan, et al., Reversible and Broad-Range Oxygen Sensing Based on Purely Organic Long-Lived Photoemitters, *ACS Appl Polym Mater* 3 (2021) 2480-2488.
- [4] Y. Wang, et al., A high-performance optical trace oxygen sensor based on the room-temperature phosphorescence from palladium (II) octaethylporphyrin, *Measurement* 206 (2023) 112275.
- [5] A. Tomkeviciene, et al., Bipolar thianthrene derivatives exhibiting room temperature phosphorescence for oxygen sensing, *Dyes and Pigments* 170 (2019) 107605.

NAPHTHALIMIDE-BASED DERIVATIVES ENABLING HIGH-EFFICIENCY OLEDs

Raminta Beresneviute¹, Prakalp Gautam², Mangey Ram Nagar², Gintare Krucaite¹, Daiva Tavgeniene¹, Jwo-Huei Jou², Saulius Grigalavicius¹

¹Department of Polymer Chemistry and Technology, Kaunas University of Technology, Radvilenu Plentas 19, LT50254 Kaunas, Lithuania

²Department of Materials Science and Engineering, National Tsing Hua University, No. 101, Section 2, Guangfu Rd., East District, Hsinchu, Taiwan, 30013
raminta.beresneviute@gmail.com

Organic light-emitting diodes (OLEDs) transcend the capabilities of conventional diodes, excelling in performance, durability, and manufacturing processes [1]. Notably, OLEDs offer self-illumination, wide viewing angles, rapid response times, high color contrast, low operating temperatures, exceptional color rendering index (CRI), soft and diffused emission, full-spectrum color reproduction, color tunability, planar design, spectrum tailoring, unbreakable construction, lightweight and thin form factor, flexibility, transparency, ease of molecular design, utilization of sustainable materials, energy-saving characteristics, human and eco-friendliness, and low driving voltages [2]. Organic electroactive materials are extensively synthesized and studied as components of the mentioned devices. Bipolar organic derivatives can be used as materials of emitting layer of OLEDs.

In this study, we present new potential emitters containing naphthalimide core as electron acceptor and carbazole or arylcarbazole fragments as electron donors. Some of the new materials demonstrated promising electroluminescent characteristics as emitters in the OLED devices. The structures of compounds are shown in Figure 1.

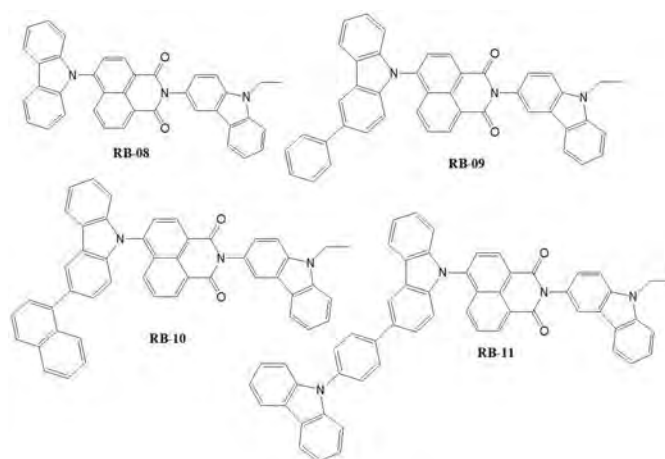


Fig. 1. Structures of compounds

These compounds exhibit desirable characteristics such as a wide bandgap, high decomposition temperatures (306–366 °C) and very high glass transition temperatures (133–179 °C). The experimental results showed that one incorporating 5 wt% RB-11 emitter demonstrated superior performance, achieving maximum power efficacy of 7.7 lm/W, maximum current efficacy of 7.9 cd/A and maximum external quantum efficiency of 3.3%. The CIE coordinates of (0.29, 0.52) of RB11 emitter based device indicated an efficient and stable green OLED with peak emission at 520 nm. Finally, the synthesized naphthalimide-based compounds show promising potential as efficient green emitters for OLED applications. These cost-effective materials exhibit suitable photophysical, electrochemical, and thermal properties, making them suitable for a range of display and solid-state lighting applications.

[1] Jou, J.-H. Introduction to OLED; Gau Lih Book 10, Ltd.: Taiwan, 2015; ISBN 978-986-378-031-1.

[2] Jou, J.-H.; Singh, M.; Su, Y.T.; Liu, S.H.; He, Z.K. Blue-Hazard-Free Candlelight OLED. *J Vis Exp* 2017

IMPACT OF TERTIARY AMINO LINKAGES ON THE PROPERTIES OF ELECTROACTIVE PHENOTHIAZINYL-BASED COMPOUNDS

Domantas Lekavičius¹, Rasa Keruckienė¹, Matas Gužauskas¹, Juozas V Gražulevičius¹

¹Department of Polymer Chemistry and Technology, Kaunas University of Technology, Lithuania
domantas.lekavicius@ktu.edu

Organic light-emitting diode (OLED) technology has made significant advances in performance and becoming widely used in smartphone displays [1]. Self-emitting ability, transparency, true dark tone, and capability of being made flexible are some of the features of OLED displays, leading to a superior performance compared with liquid crystal displays. In addition to displays, OLEDs are also a strong candidate for lighting applications [2].

In this work, the effects of introducing tertiary amino linkages to phenothiazine derivatives, which act as delayed emission fluorophores, will be presented. The said compounds consist of either a pyridine- or benzonitrile moiety as an acceptor and phenothiazine as a donor. The compounds were synthesized by Buchwald-Hartwig cross-coupling reaction. The resulting electroactive compounds are thermally stable with 10 percent weight loss temperatures of 270 and 308 °C. Repeated scans of cyclic voltammetry showed that both compounds exhibit reversible oxidation. The emission type of the pyridine-containing phenothiazine derivative was found to be triplet-triplet annihilation, and the benzonitrile-containing derivative exhibited room-temperature phosphorescence. Further investigation in the benzonitrile-containing species showed perfect reversible oxygen sensing and fast oxygen response. This suggests that the compound shows promise as an analyte for oxygen sensing.

Acknowledgment. This research has received funding from the Research Council of Lithuania (LMTLT), agreement No. S-MIP-23-50.

[1] Shihao Liu, Wenfa Xie, Chun-Sing Lee, Organic light-emitting diodes, what's next, *Next Nanotechnology*. (2023).

[2] A. Salehi et al. Recent advances in OLED optical design. *Adv. Funct. Mater.* (2019)

MODIFICATION OF METAL OXIDE SURFACES WITH REGENERABLE PHOSPHOLIPID BILAYERS FOR THE DEVELOPMENT OF REUSABLE BIOSENSORS

Anastasija Aleksandrovič¹, Inga Gabriūnaitė¹, Aušra Valiūnienė¹

¹Vilnius University, Faculty of Chemistry and Geosciences, Institute of Chemistry
anastasija.aleksandrovic@chgf.stud.vu.lt

Recently, studies related to tethered phospholipid membranes (tBLM's) formed on electrically conductive surfaces modified with self-assembled monolayers (SAM's), have attracted increasing interest. The main application of such systems is the development of biosensors. Typically, biosensors are developed on gold surfaces, although they have poor membrane regeneration properties and are expensive. As a cheaper alternative to gold substrates, metal oxide surfaces might be used because of the possibility of membrane regeneration.

In this work we formed tBLM's of various compositions on a fluorine doped tin oxide (FTO) surface chemically modified with several silane group compounds and investigated the interaction between membranes and proteins, and conditions for regeneration after the protein incorporation into a membrane. As phospholipids are readily soluble in many kinds of alcoholic solvents, while proteins are not, the main goal of this work was to specify the optimal conditions for the removal of the phospholipid membrane and the protein from the surface. After properly removing the protein-affected phospholipid bilayer, the FTO surface should stay modified with SAM and could be used for the repeatable membrane formation. The work investigates how the efficiency of membrane regeneration depends on the composition of the SAM and the phospholipid membrane.

SYNTHESIS OF BIPHASIC CALCIUM PHOSPHATE GRANULES UNDER STATIC AND ROTATING CONDITIONS FROM ENVIRONMENTALLY BENIGN PRECURSOR - GYPSUM

Greta Linkaitė¹, Rūta Raišeliene¹, Aivaras Kareiva¹, Monika Skruodienė², Inga Grigoravičiūtė¹

¹Institute of Chemistry, Vilnius University, Naugarduko 24, LT-03225 Vilnius, Lithuania

²Center for Physical Sciences and Technology, Sauletekio av. 3, 10257 Vilnius, Lithuania

greta.linkaite@chgf.vu.lt

Synthetic calcium phosphates (CaPs) are effective biomaterials for bone regeneration due to their similarity to the inorganic component of bone and specific biological properties such as osteoinductivity, osteoconductivity, and biodegradability. An ideal synthetic substitute for implantation should serve as a temporary scaffold, gradually degrading as part of the osseous tissue remodeling process. This degradation involves the release of calcium and phosphate ions, facilitating the replacement of the scaffold by newly formed bone. Achieving appropriate degradation kinetics is crucial for bone regeneration, aligning with the rate of new bone formation to enhance healing and minimize complications. Biphasic calcium phosphate, a widely used CaP-based biomaterial, offers flexibility in adjusting biodegradability by incorporating two distinct CaP phases in varying concentrations [1].

In the present work, biphasic calcium phosphate granules, consisting of various amounts of magnesium whitlockite and carbonated hydroxyapatite phases, were synthesized via a low-temperature dissolution-precipitation process under static and rotating conditions using gypsum as a starting material. Powder XRD patterns, FTIR spectra, N₂ adsorption-desorption isotherms, and SEM images were obtained for the samples.

[1] A. Guliani et. al., Integrated 3D Information for Custom-Made Bone Grafts: Focus on Biphasic Calcium Phosphate Bone Substitute Biomaterials, International Journal of Environmental Research and Public Health 17(14), 4931 (2021)

SOLID PHASE EXTRACTION BASED ON CATION EXCHANGE SORBENTS FOLLOWED BY FAST GAS CHROMATOGRAPHY TECHNIQUE TO DETERMINE PSYCHOACTIVE SUBSTANCES

Nerijus Karlonas¹

¹The State Forensic Medicine Service, Toxicology Laboratory, Didlaukio 86E, LT-08303 Vilnius, Lithuania
nerijus.karlonas@vtmt.lt

The main aim of my study was to develop a new sensitive and specific method based on a fast gas chromatography with negative-ion chemical ionization mass spectrometry using solid-phase extraction (SPE) for the quantification of zaleplon and zopiclone at trace level in low-volume blood and urine samples. To the best of my knowledge, this method has been used for the first time for the optimization of sample preparation at different pH values (pH 1.0 - 10.0). A comparison of two SPE sorbents for the determination of both analytes was investigated. The analytes were well retained on Oasis MCX and Oasis HLB sorbents, also sufficient extraction efficiency was achieved at pH 9.0. For further study, a hydrophilic-lipophilic (polymeric) sorbent Oasis HLB was selected due to the polarity of the sorbent surface and its large surface area (830 m² g⁻¹) in order to achieve efficient extraction of the analytes in a single step. The surface area is one of the most important factors for extracting the analytes from blood or urine samples by SPE. Special attention was paid to the selection of washing and eluting solvent in the SPE procedure, resulting in a very pure and free-from-moisture extract, which can successfully be applied for gas chromatography-mass spectrometry. Different solvents or mixtures of solvents for elution of the adsorbed analytes, and washing step-eliminating interferences in the sorbent were tested. Finally, the results have shown that the developed method is accurate, selective, precise, very fast with excellent recovery, low limits of detection and quantification, and it was demonstrated that this method is applicable for the determination of trace concentrations of zaleplon and zopiclone in whole blood and urine samples. The developed method can be applied in routine toxicological analysis during the investigation of both clinical and forensic cases.

EVALUATION OF AEGOPODIUM PODAGRARIA ANTIOXIDANT AND ANTIMICROBIAL ACTIVITY USING DIFFERENT EXTRACTION SOLVENTS

Ugnė Gabrytė¹, Rūta Mickienė¹, Audrius Sigitas Maruška¹

¹Faculty of Natural Sciences, Instrumental Analysis Open Access Centre, Vytautas Magnus University, Kaunas, Lithuania
ugne.gabryte@stud.vdu.lt

The problems of the modern world, such as increasing threats to human health or bacterial resistance to antibiotics show an increasing urgency to research natural substances with potential solutions or mitigating effects. A widely distributed plant in Lithuania ground elder (*Aegopodium podagraria*) is a well-known medicinal plant, that accumulates a wide variety of biologically active phytochemicals, such as polyacetylenes falcariol and falcariindiol, essential oils, vitamins, coumarins, phenolic acids and flavonoids in its various parts [1]. Because of these phytochemicals, the plant exhibits antibacterial and antioxidant properties that have been identified in plant extracts [2].

This research aims to determine the total phenolic content, flavonoid concentration, antioxidant and antimicrobial activity of the plant using different extraction solvents. Leaves, stems and roots were used for the experiment and the extraction was carried out using 3 different solvents – water, 50 % ethanol, and olive oil. Extraction of the herb was performed by incubation shaking maceration method. The amount of biologically active compounds and antioxidant activity were determined by spectrophotometric methods. Antimicrobial effect against 5 different bacteria was determined by well diffusion method.

The results showed that the concentration of biologically active compounds in the extracts depended on the extraction solvent – the highest number of phenolic compounds (9,57 mg RE/g in leaves and 5,73 mg RE/g in stems) was determined in ethanol extracts, the highest number of flavonoids (3,87 mg RE/g in leaves and 3,25 mg RE/g in stems) – in oil extracts. Root extracts demonstrated different results – the highest concentration of phenolic compounds (5,99 mg RE/g), flavonoids (0,36 mg RE/g) and antiradical activity (2,16 mg RE/g) were all obtained using water as an extraction solvent. A correlation between the concentration of phenolic compounds and antioxidant activity was established. The ethanolic root extract showed inhibitory effects on *Micrococcus luteus*, *Staphylococcus aureus*, *Pseudomonas aeruginosa* and *Leuconostoc mesenteroides*, while leaf extracts were also effective on *E. coli*. The established antimicrobial and antioxidant properties of *Aegopodium podagraria* indicate the plant's potential applicability in food, pharmaceutical, cosmetic and other industries.

[1] Kyrbassova, E. A., Dyuskaljeva, G., Baitasheva, G. U., & Imanova, E. M. (2019). Biological and phytochemical features of underground organs of medicinal plants of the genus *aegopodium* L. *Experimental Biology*, 78(1), 28-35.

[2] Jakubczyk, K., Janda, K., Styburski, D., & Łukomska, A. (2020). Goutweed (*Aegopodium podagraria* L.)—botanical characteristics and prohealthy properties. *Advances in Hygiene and Experimental Medicine*, 74, 28-35.

PHYSICAL AND CHEMICAL CHARACTERISTICS OF MICROPLASTIC PARTICLES IN LITHUANIAN RIVERS

Tomas Stonkus¹

¹Vilnius University
tomas.stonku@gmail.com

Plastic has become one of the most widespread materials since its beginnings as a phenol-formaldehyde resin. At its core, plastic was designed to improve human living conditions, but today it has become a real danger to the environment and the safety of the planet [1]. In recent decades, the increase in usage of various synthetic polymers in various industries has led to a climb in microplastic presence in aquatic environments. These micro particles, often measuring less than 5 millimeters. Both primary microplastics (such as microbeads in various skincare products) and secondary microplastics (those arising from the degradation of large plastic particles) find their way into the marine and terrestrial ecosystem where they unleash numerous detrimental ecological damages [2]. The numerous physical and chemical properties of microplastics further complicate their impact on aquatic organisms and ecosystems. Lithuania, with its rich tapestry of rivers, lakes, and wetlands, provides a unique context for studying the complexities of microplastic pollution. As plastic dumping activities continue to escalate, understanding the specific physical and chemical attributes of microplastics in Lithuanian freshwaters becomes imperative for devising targeted strategies. This research aims to contribute to the wider understanding of microplastic contamination by investigating the distinctive characteristics (such as size, color, form and chemical composition) of pollutants within Lithuanian river systems. Using integration of environmental science, chemistry, this study aims to provide more knowledge of microplastic contamination in Lithuanian freshwater environments.

Acknowledgment: We would like to thank the schools, teachers, and students who participated in the Plastic Pirates project and helped collect data on litter pollution along the Lithuanian riverbanks. Also, we would like to thank the Lithuanian non-formal education agency for the opportunity to join the Plastic Pirates Lietuva project.

[1] Khaled Ziani, Corina-Bianca Ioniță-Mîndrican, Magdalena Mititelu, Sorinel Marius Neacșu, Carolina Negrei, Elena Moroșan, Doina Drăgănescu, Olivia-Teodora Preda. Microplastics: A Real Global Threat for Environment and Food Safety: A State of the Art Review

[2] Charles Obinwanne Okoye, Charles Izuma Addey, Olayinka Oderinde, Joseph Onyekwere Okoro, Jean Yves Uwamungu, Chukwudozie Kingsley Ikechukwu, Emmanuel Sunday Okeke, Onome Ejeromedoghene, Elijah Chibueze Odii. Toxic Chemicals and Persistent Organic Pollutants Associated with Micro-and Nanoplastics Pollution

ENVIRONMENT-DEPENDENT CHLOROPHYLL-CHLOROPHYLL CHARGE TRANSFER STATES IN Lhca4 PIGMENT-PROTEIN COMPLEX

Gabrielė Rankelytė^{1,2}, Jevgenij Chmeliov^{1,2}, Andrius Gelzinis^{1,2}, Leonas Valkunas^{1,2}

¹Institute of Chemical Physics, Faculty of Physics, Vilnius University, Lithuania

²Department of Molecular Compound Physics, Centre for Physical Sciences and Technology, Vilnius, Lithuania
gabriele.rankelyte@gmail.com

Photosynthesis is one of the most important processes on Earth. The most efficient organisms that carry out photosynthesis are land plants. In the thylakoid membrane of chloroplasts there are two systems that carry out photosynthesis – Photosystem I (PSI) and Photosystem II (PSII), both with their own light harvesting complexes - LHCI and LHCII. PSI is the most efficient light-to-energy conversion apparatus with quantum yield almost equal to 1 [1]. One of the conditions needed for high efficiency is very fast energy transfer between the molecules in light harvesting complex. Light-harvesting complex of PSI absorbs and emits light at the longest wavelengths compared to other pigment-protein complexes. In plants light harvesting antenna of PSI is composed of four species of LHCI complexes. They all have very similar structure, however, their spectral properties are different. The most red-shifted peak (at around 733 nm) is observed in the fluorescence spectrum of Lhca4 light harvesting sub-complex [2].

The excitation dynamics in LHCI is highly affected by the charge-transfer (CT) states that occur between two or more pigments (chlorophylls or carotenoids). Some sites in which CT states occur in LHCI are known, however, they do not completely explain the spectral properties of this antenna, such as the red-shifted peak in fluorescence spectrum. The energy of the excited states of pigments (including the CT states) are highly affected by the surrounding environment, consisting of other pigments and the protein chain. Therefore, it is necessary to account for the environment in order to model light-harvesting complexes properly.

The structure of Lhca4 was obtained as the 4th chain of PSI supercomplex structure, freely accessible on Protein Data Bank (PDB) [3]. We performed quantum chemical calculations to obtain energies of chlorophyll dimer CT states in vacuo. We then included the environment (single chlorophylls, carotenoids and the protein chain molecules in their ground state) in our calculations by obtaining atomic partial charges of both environmental blocks and dimers of interest and evaluating the electrostatic interaction between these charges (see Figure [fig:Energy-level-diagram]). In case of the protein chain, we estimated the most probable protonation pattern in neutral solution and also looked into other possible protonation patterns. The energy shifts caused by the environment were calculated considering 9 different possible protonation patterns of the protein and were compared to those obtained when the protein chain was considered to be in its most probable (estimated) protonation state.

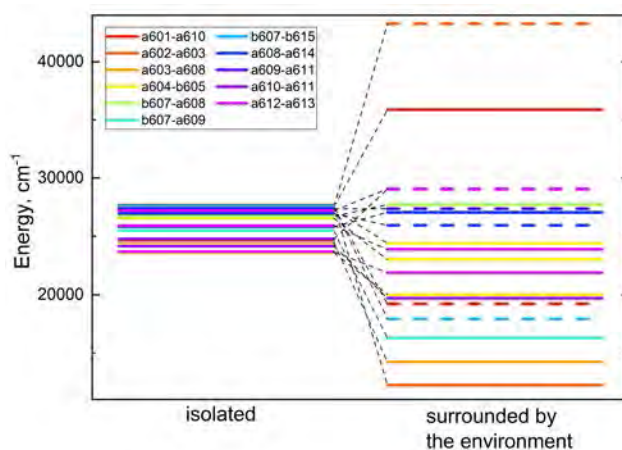


Fig. 1. Energy level diagram of dimer CT state energies.

[1] R. Croce and H. van Amerongen, Light-harvesting in Photosystem I, *Photosynthesis Research* 116, 153-166 (2013).

[2] T. Morosinotto et al., Pigment-pigment interactions in Lhca4 antenna complex of higher plants Photosystem I, *Journal of Biological Chemistry* 280, 20612-20619 (2005).

[3] X. Qin et al., Structural basis for energy transfer pathways in the plant PSI-LHCI supercomplex, *Science* 348, 989-995 (2015).

ELECTRONIC EXCITED STATES OF PHTHALOCYANINES

Darius Likandrovas¹, Andrius Gelzinis^{1,2}, Jevgenij Chmeliov^{1,2}, Leonas Valkunas^{1,2}

¹Faculty of Physics, Vilnius University, Vilnius, Lithuania

²Department of Molecular Compound Physics, Centre for Physical Sciences and Technology, Vilnius, Lithuania

darius.likandrovas@ff.stud.vu.lt

Phthalocyanines are widely used for applications in electronics, solar cells, optical storage devices, etc., due to their photophysical characteristics. To understand phthalocyanines properties, it is beneficial to analyze their electronic structure, using quantum chemistry calculations. These calculations can provide useful insights into electronic excited states, which are particularly significant as they govern processes such as absorption of light, fluorescence, chemical reactions [1].

In the present work, quantum chemical calculations and analysis of Zinc 2,9,16,23-tetra-tert-butyl-29H,31H-phthalocyanine (ZnTTBPc) and 2,9,16,23-tetra-tert-butyl-29H,31H-phthalocyanine (TTBPc) monomers were completed. At first, geometry of ZnTTBPc and TTBPc molecules was optimized in a vacuum using density functional theory (DFT) with three functionals: B3LYP, wB97X-D, LC-BLYP. Then the excited states values for each molecule were calculated using time-dependent density functional theory (TD-DFT). These calculations have shown that ZnTTBPc possess doublet degeneracy for the two lowest excited states [2] - such degeneracy arises from D4h point symmetry and in TTBPc case this degeneracy vanishes – the energy gap between the two lowest excited states is 15-150 nm, depending on the functional employed. The obtained results correlate with the experimental data [3]. After the initial set of calculations with monomers the next step was to examine the collective states of dimers using the same procedure. In this work it is also considered whether the results with monomers and dimers change when considering the environment – which is described with the polarizable continuum model (PCM). Chloroform was used as the solvent.

State	Symmetry	Energy (nm)	Intensity	State	Symmetry	Energy (nm)	Intensity
1	A	633.77	0.5274	1	A	619.35	0.5586
2	A	616.72	0.5853	2	A	619.34	0.5586
3	A	340.86	0.2465	3	A	353.45	0.0000
4	A	335.37	0.0000	4	A	353.45	0.0000
5	A	305.26	0.0000	5	A	322.42	0.0000
6	A	303.28	0.4882	6	A	320.78	0.0000
7	A	295.84	0.0000	7	A	315.25	0.0451
8	A	293.09	0.0000	8	A	315.25	0.0451
9	A	292.83	0.0000	9	A	310.30	0.0000
10	A	285.70	0.0000	10	A	304.94	0.0000

Fig. 1. Calculated TTBPc and ZnTTBPc electronic excited states respectively, using wB97X-D functional.

[1] Martin, R. M. (2020). Electronic structure. <https://doi.org/10.1017/9781108555586>

[2] Feng, S., Wang, Y., Ke, Y., Liang, W., & Zhao, Y. (2020). Effect of charge-transfer states on the vibrationally resolved absorption spectra and exciton dynamics in ZnPc aggregates: Simulations from a non-Markovian stochastic Schrödinger equation. *The Journal of Chemical Physics*, 153(3). <https://doi.org/10.1063/5.0013935>

[3] Martynov, A. G., Mack, J., May, A. K., Nyokong, T., Gorbunova, Y. G., & Tsivadze, A. Y. (2019). Methodological survey of simplified TD-DFT methods for fast and accurate interpretation of UV–VIS–NIR spectra of phthalocyanines. *ACS Omega*, 4(4), 7265–7284. <https://doi.org/10.1021/acsomega.8b03500>

THERMOPLASTIC CELLULOSE ACETATE COMPOSITES WITH INORGANIC FILLERS

Rokas Jakubauskas¹, Ramunė Rutkaitė¹, Dovilė Liudvinavičiūtė¹, Laura Pečiulytė¹, Joana Bendoraitienė¹, Kęstutis Baltakys², Andrius Gineika²

¹Department of Polymer Chemistry and Technology, Kaunas University of Technology, Lithuania

²Department of Silicate Technology, Kaunas University of Technology, Lithuania
rokas.jakubauskas@ktu.edu

With the increasingly growing production of synthetic polymers, waste management is becoming a global issue. This leads to massive waste disposal in landfills, where eventually discarded polymers end up in the natural ecosystem, disrupting the normal habitat of living organisms, and plastic waste incineration increasing greenhouse gas emissions. Biodegradable cellulose acetate (CA), a modified natural polymer, is an excellent alternative to synthetic plastics, given that it could reach similar mechanical properties to its counterparts. CA cannot withstand heat treatment without decomposition. However, by using plasticizers, thermally processable CA mixtures can be formed. Moreover, inorganic minerals can be used as fillers in polymer composites to increase the melt fluidity and enhance mechanical, thermal and/or dielectric properties of the products.

In this study, the thermoplastic CA composites were formed from CA, various plasticizers, namely, polyethylene glycol, triacetin, triethyl citrate, and two types of inorganic filler particles: waste silica gel particles from aluminum fluoride production and opoka rock particles, which were hydrothermally treated and calcinated beforehand. By varying the amounts of CA, plasticizers and filler particles, a set of thermoplastic mixtures was prepared and thermally processed using twin-screw extrusion, by assessing the extrusion parameters. Additionally, the samples were formed by injection molding, and their thermal, mechanical and hydrophobicity properties were evaluated for the purpose of appraising these bioplastic composites in potential applications.

Acknowledgement. This project has received funding from the Research Council of Lithuania (LMTLT), agreement No S-ST-23-52.

SYNTHESIS AND INVESTIGATION OF NATURAL OIL-BASED SHAPE-MEMORY PHOTOPOLYMERS

Viltė Šereikaitė¹, Auksė Navaruckienė¹, Jolita Ostrauskaitė¹

¹Department of Polymer Chemistry and Technology, Kaunas University of Technology, Radvilenu Rd. 19, LT-50254
Kaunas, Lithuania
vilte.sereikaite@ktu.edu

The increasing recognition of pollution and environmental challenges stemming from the utilization of petroleum-derived materials is propelling scientific investigations aimed at substituting frequently employed harmful products with bio-based alternatives [1]. Shape memory polymers are smart materials that can be deformed and fixed into a temporary shape and can recover their permanent shape after the release of the external stimulus. Due to their appealing qualities like structural flexibility, lightweight nature, affordability, ease of processing, high elastic strain, biocompatibility, and biodegradability, they are gaining significant interest in industrial, aerospace, textile, and medical applications [2].

In this study, photopolymers were synthesized by photocuring of resins containing natural oil-based monomers and other biobased comonomers, using ethyl-(2,4,6-trimethylbenzoyl)-phenylphosphinate as photoinitiator. Real-time photorheometry was used to monitor the evolution of photocuring process. The chemical structure of the photopolymers was confirmed by Fourier transform infrared spectroscopy, Soxhlet extraction and swelling test. The thermal properties of the photopolymers were investigated by dynamic mechanical thermal analysis and thermogravimetric analysis. It was determined that photocuring rate, rheological, and thermal properties of the resulting photopolymers depended on the initial composition of the resins. Samples of all synthesized photopolymers were able to obtain a new shape while heated above their glass transition temperature, maintain it after cooling below their glass transition temperature, and return to their primary shape after heating again above their glass transition temperature. These behaviors have determined these photopolymers as shape memory polymers.

Acknowledgement. This research was funded by the Research Council of Lithuania (project No. S-MIP-23-52).

-
- [1] Pezzana, L., Malmström, E., Johansson, M., Sangermano, M. UV-Curable Bio-Based Polymers Derived from Industrial Pulp and Paper Processes. *Polymers* 2021, 13, 1530.
[2] Dayyoub, T., Maksimkin, A.V., Filippova, O.V., Tcherdyntsev, V.V., Telyshev, D.V. Shape Memory Polymers as Smart Materials: A Review. *Polymers* 2022, 14, 3511.

MAGICAL MANDRAGORA OFFICINARUM L.: UNLOCKING THE SECRETS OF PHYTOCHEMISTRY AND BIOACTIVITIES

Goda Jašinskaitė¹, Petras Rimantas Venskutonis¹, Ona Ragažinskienė²

¹Kaunas University of Technology

²Vytautas Magnus University
goda.jasinskaite@ktu.edu

Mandragora Officinarum L. (mandrake) is a perennial herbaceous plant from the nightshade (*Solanaceae*) family, native to the Mediterranean region. The plant has a rich history of uses from the ancient times for its healing and psychotropic properties. However, its wider use has declined due to the presence of tropane alkaloids, which can lead to poisoning, if used improperly.

In general, the number of publications on *M. Officinarum* chemical composition and bioactivities is rather scarce. The majority of the previously performed studies were focusing on its alkaloids. The aim of this study was to fractionate oven and freeze-dried *M. Officinarum* fruits (berries), roots and leaves in to the lipophilic and higher polarity fractions by using consecutive extraction with supercritical CO₂ and pressurized liquids using the increasing polarity solvents and to evaluate the phytochemical composition and antioxidant potential of the fractions obtained. First of all, proximate composition of *M. Officinarum* berries and roots was evaluated by using standard methods. After measuring the quantities of proteins, fats, insoluble fibers, minerals and moisture content, extraction with supercritical CO₂ was carried out.

The content of lipophilic fractions isolated at 350MPa pressure and 50°C temperatures was approximately 0,5% for the roots and 8% for fruits. Additionally, the total amount of phenolic compounds and ABTS radical scavenging activity were also determined in the roots, fruits and leaves of this plant. The same assays were also carried out not only with dry raw material but also with various extracts: CO₂, ethanol, acetone and water.

SYNTHESIS AND CHARACTERIZATION OF ALKALINE EARTH METALS SUBSTITUTED LANTHANUM MOLYBDATE

Giedrė Gaidamavičienė¹, Artūras Žalga¹

¹Faculty of Chemistry and Geosciences, Institute of Chemistry, Vilnius University, Naugarduko str. 24, LT-03225 Vilnius, Lithuania
giedre.prievelyte@chf.vu.lt

In recent decades, solid oxide fuel cells (SOFCs) have garnered attention for their clean and efficient energy production. Currently, one of the most widely used electrolytes is yttria-stabilized zirconia, but its excellent ionic conductivity is only noticeable at high temperatures (1000 °C), thereby limiting its practical use [1].

One of the most promising electrolytes operating at low temperatures is La₂Mo₂O₉ (LAMOX). This compound crystallizes into two different crystallographic modifications: the low-temperature monoclinic α -phase and the high-temperature cubic β -phase. Above 580 °C, a phase transition to the β -phase occurs, significantly enhancing oxygen-ion conductivity by almost two orders of magnitude. To stabilize the high-temperature phase at room temperature, various ions can be used to dope lanthanum and molybdenum sites. Substituting alkaline earth metals into lanthanum sites not only suppresses the phase transition but also increases the concentration of oxygen vacancies, leading to higher ionic conductivity [2].

This study is focused on the synthesis of La_{2-x}M_xMo₂O_{9x/2} (M=Ca²⁺, Sr²⁺, Ba²⁺; x=0.01–0.2) ceramic using a tartaric acid-assisted aqueous sol-gel synthesis technique. X-ray diffraction analysis was used to identify the crystal structure and detect impurity phases of the heat-treated ceramics. It was estimated that by the increase in the alkaline earth metal radius, the substitution limit of the corresponding element in the LAMOX system also increases. Moreover, DSC analysis revealed that with the increase of the substitution degree in the multicomponent oxide, the intensity of the phase transition tends to decrease. However, after further substitution by alkaline earth metal in the final ceramic material, the intensity of the phase transition starts to increase again due to the formation of impurity phases in the as-formed crystalline mixture.

[1] A. Das, Lakhanlal, I. Shajahan, et al., Dilatometer studies on LAMOX based electrolyte materials for solid oxide fuel cells, *Materials Chemistry and Physics* 258, 123958 (2021)

[2] D. Zhang, Z. Zhuang, et al., Electrical properties and microstructure of nanocrystalline La_{2-x}AxMo₂O₉-Y (A Ca, Sr, Ba, K) films, *Solid State Ionics* 181, 1510-1515 (2010)

DICYANOISOPHORONE BASED SOLID STATE EMITTERS FOR ORGANIC LIGHT EMITTING DIODES

Khushdeep Kaur¹, Asta Dabuliene¹, Juozas Vidas Grazulevicius¹

¹Kaunas University
khushdeep.kaur@ktu.edu

Donor-Acceptor based solid state emitters are promising candidates for organic light emitting diodes (OLED's), solid-state lasers, sensors etc., owing to their ease of fabrication and tunable structures.^{1,2} In this regard, dicyanoisophorone can act as a strong acceptor unit in combination with a series of donor units of varying strength for the design of efficient materials because non-linear optical activity (NLO) and charge transporting properties of semiconducting devices are highly influenced by nature of donor, π -bridge and acceptor fragments.^{2,3} In a recent report, NLO susceptibility of (E)-2-(3-(4-bromostyryl)-5,5-dimethylcyclohex-2-en-1-ylidene)malononitrile is found to be higher than that of the previously reported compounds.⁴ In continuation to our interest to develop novel bipolar materials for semiconducting devices, a series of novel D-A compounds were designed and synthesized based on (E)-2-(3-styryl-5,5-dimethylcyclohex-2-en-1-ylidene)malononitrile as an acceptor unit and thianthrene, phenoxathiine, carbazole, and fluorene fragments as donors. Photophysical, thermal, electrochemical, and electroluminescent properties of the materials were studied to establish the structure-property relationship. Conclusively, the newly synthesized D-A materials can also be suitable for photonic and optical devices particularly for organic photodetectors.

-
- [1] Zheng, Zheng; Yu, Zhipeng; Yang, Mingdi; Jin, Feng; Zhang, Qiong; Zhou, Hongping; Wu, Jieying; Tian, Yupeng (2013). Substituent Group Variations Directing the Molecular Packing, Electronic Structure, and Aggregation-Induced Emission Property of Isophorone Derivatives. *J. Org. Chem.* 78(7), 3222–3234.
- [2] Shivani; Mishra, Akriti; Kaur, Paramjit; Singh Kamaljit (2023). Perpetual Extension of Conjugation of Fluorene-Based Donor–Acceptor Dyads Yield Diminished Nonlinear Optical Response. *J. Phys. Chem. C.*, 127, 2, 1260–1272.
- [3] Lin, Tao; Liu, Xiaojun; Lou, Zhidong; Hou, Yanbing; Teng, Feng (2014). Theoretical study on charge injection and transport properties of six emitters with push–pull structure. *Chem Phys*, 440, 47–52.
- [4] Bharath, D.; Kalainathan, S. (2014). Studies on optically induced nonlinear absorption and refractive index of Br1 crystal for near IR optical switching application. *Opt. Laser Technol.*, 59, 24–31.

SYNTHESIS AND CHARACTERIZATION OF ELECTROCONDUCTIVE POLYMERS FOR THE PRODUCTION OF A SARSCOV2 ANTIBODY SENSOR

Felix Lücke¹, Šarūnas Žukauskas², Arūnas Ramanavičius^{1,2}

¹Department of Physical Chemistry, Institute of Chemistry, Faculty of Chemistry and Geosciences, Vilnius University (VU), Naugarduko Str. 24, LT-03225 Lithuania

²Department of Nanotechnology, State Research Institute Center for Physical Sciences and Technology (FTMC), Sauletekio Av. 3, LT-10257 Vilnius, Lithuania
felix.lucke@chgf.stud.vu.lt

The aim of the research was to prepare, synthesize and characterize electroconductive polymers for sensing of SARS-Cov-2 antibodies. The first step in achieving this goal was to find the best method to synthesize the polymer polyaniline from aniline, which will be the basis for the rest of the sensor. On this basis different surface modifications and protein immobilization methods were explored and the resulting sensing capabilities compared. A proof of concept was built in the form of a Glucose sensor. For that, the protein was absorbed onto the surface via physical adsorption. The absorbed protein was crosslinked with Glutaraldehyde through protein-aldehyde interactions [1]. Two different approaches were tested for the COVID-antibody sensor, the first based on the same mechanism as the glucose sensor, the second utilizes an EDC/NHS linker to directly attach the covid spike protein to the working electrode via a chemical bond [2].

For all electrochemical experiments a three-electrode-set-up was used. The working electrode (WE) was a graphite rod with polyaniline on the tip surface, the counter electrode (CE) was platinum wire that formed a cage like structure around the WE and the reference electrode (RE) was a 3M Ag/AgCl electrode. The polymerization and deposition of Aniline was performed using Cyclic Voltammetry (CV). The sensor abilities were tested with Differential Pulse Voltammetry (DPV) in a redox mediator with increasing concentrations of the analyte. As Fig. 1 indicates we were able to construct a Highly sensitive covid antibody sensor based on Polyaniline.

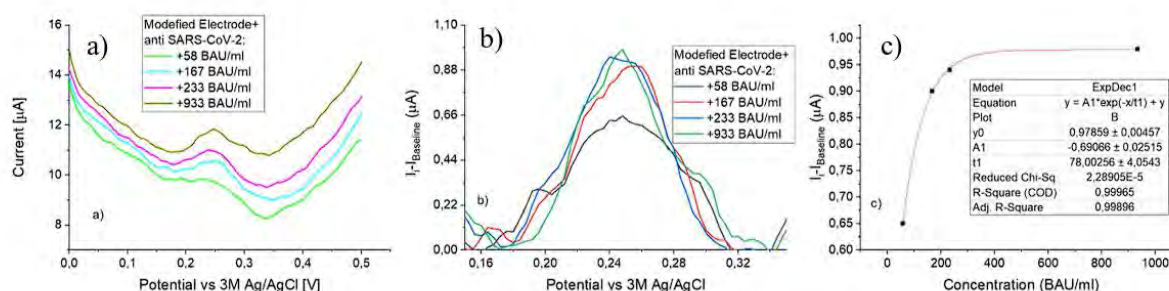


Fig. 1. DPV data of the COVID-antibody sensor built using the EDC/NHS system. a) Raw data, b) Baseline corrected data, c) Concentration curve made using the baseline corrected data and Exponential decay fit.

- [1] M. Le Salem, Y. Mauguen, T. Prangé, Structural Biology and Crystallization Communications Revisiting glutaraldehyde cross-linking: the case of the Arg-Lys intermolecular doublet, Structural Communications Acta Cryst. 66 (2010) 225–228. <https://doi.org/10.1107/S1744309109054037>
- [2] Bart, J., Tiggelaar, R., Yang, M., Schlautmann, S., Zuilhof, H., Gardieniers, H. (2009). Room-temperature intermediate layer bonding for microfluidic devices. Lab on a Chip, 9(24), 3481–3488. <https://doi.org/10.1039/B914270C>

SYNTHESIS OF NEW COMPOSITION PRASEODYMIUM DOPED LUTETIUM AND GADOLINIUM ALUMINUM GARNETS MODIFIED BY SCANDIUM AND BORON ELEMENTS TO IMPROVE LUMINESCENCE PROPERTIES

Greta Inkrataite¹, Jan-Niklas Keil², Thomas Jüstel², Agne Kizalaite¹, Ramunas Skaudzius¹

¹Institute of Chemistry, Faculty of Chemistry and Geosciences, Vilnius University, Naugardukas st. 24, LT-03225 Vilnius, Lithuania

²Department of Chemical Engineering, Münster University of Applied Sciences, Stegerwaldstraße 39, 48565 Steinfurt, Germany
greta.inkrataite@chgf.vu.lt

In order to convert high energy radiation, such as gamma or X-rays, into visible light scintillators are needed. Praseodymium doped lutetium aluminum garnets have high density, thermal stability, rather efficient luminescence processes which are needed for a good scintillator. However, further optimization of short decay time is needed. Luminescence decay is important because if it is very short then more signals can be measured within a defined timeframe, resulting in a better resolved and higher quality image in CT devices. One way to improve materials' properties is to doping compounds with different elements. One of these elements is boron. Boron can be used as a flux, also B³⁺ has a suitable neutron capture cross section and can help absorb gamma radiation [1-3]. Lutetium aluminum scandium garnets doped with Pr³⁺ and/or B³⁺ were obtained as a result. These garnets are synthesized and studied for the first time. In this work, the phase purity and morphology of the samples were analyzed with X-ray diffraction, SEM. Photoluminescence properties such as emission, excitation spectra, decay curves, quantum efficiency and temperature dependency spectra have been investigated. Radioluminescence was also measured. The positive impact of boron addition into the garnet structure on the luminescence properties will be discussed in detail.

-
- [1] C. Foster, Y. Wu, M. Koschan, et. al., Boron Codoping of Czochralski Grown Lutetium Aluminum Garnet and the Effect on Scintillation Properties, *Journal of Crystal Growth* 486, 126 – 129 (2018).
 [2] D. S. McGregor, Materials for Gamma-Ray Spectrometers: Inorganic Scintillators, *Annual Review of Materials Research* 48, 254-277 (2018).
 [3] G. Inkrataite, M. Kemere, A. Sarakovskis, R. Skaudzius, Influence of boron on the essential properties for new generation scintillators, *Journal of Alloys and Compounds* 875, 160002 (2021).

SEARCH AND CHARACTERISATION OF BINDERS FOR AQUEOUS SODIUM ION BATTERIES

Adolfas Žukauskas^{1,2}, Nadežda Traškina², Jurgis Pilipavičius^{1,2}, Linas Vilčiauskas^{1,2}

¹Vilnius university

²Center for physical technologies and sciences
adolfas.zukauskas@gmail.com

Binders play a crucial role in rechargeable batteries by preserving the structure of electrodes. Binders are usually used in small amounts, because they do not participate in electrodes electrochemical reactions, but despite the small amount in the overall electrode composition binders have a significant impact on battery performance. In order to ensure a reliable electrode performance customization of binders is crucial. The most commonly used binder is poly(vinylidene) difluoride due to its chemical and electrochemical stability, mechanical strength. However, it displays poor adhesion to electrode components, especially when it comes to emerging high-capacity active materials, PVDF is an electrical insulator, meaning, that electrodes need additional additives to function properly. Also in order to use PVDF a toxic and rather expensive solvent N-Methyl-2-pyrrolidone is needed, which has a high boiling point, which leads to more energy wasted during the evaporation of solvent. This research focuses on finding greener and cheaper alternatives for PVDF in aqueous sodium ion batteries. The aim of this study was to create anodes, using commercially available cheap polymers and sodium titanium phosphate in order to study the polymer stability and behavior in aqueous sodium ion batteries. Properties of the anodes were investigated by cyclic voltammetry and galvanostatic cycling. The selected commercial polymers were Polyvinyl Butyral 30, Laropal A 81, Paraloid B67, Plexigum PQ611, Paraloid B48N, Paraloid B82, Paraloid B44 and Regalite R1125. The selected materials were tested in order to see if they could be applicable as binders for anodes. Out of the 8 polymers PVBA showed the best results due to its high viscosity, high initial capacity and capacity fade comparable to PVDF. Also the methacrylate based binders showed good electrochemical stability and electrodes made with them were comparable to PVDF containing ones. The main shortcoming of these electrodes is minor cracking, which could be mitigated by using different solvents and polymer concentrations. The worst performing binders were aldehyde and hydrocarbon based. They were difficult to work with, showed bad electrochemical activity and no mechanical suture they will not be further investigated.

[1] Chen, H.; Ling, M.; Hencz, L.; Ling, H.Y.; Li, G.; Lin, Z.; Liu, G.; Zhang, S. Exploring Chemical, Mechanical, and Electrical Functionalities of Binders for Advanced Energy-Storage Devices. *Chem. Rev.* 2018, 118, 8936–8982, doi:10.1021/acs.chemrev.8b00241.

[2] Cholewinski, A.; Si, P.; Uceda, M.; Pope, M.; Zhao, B. (2021). Polymer Binders: Characterization and Development Toward Aqueous Electrode Fabrication for Sustainability. *Polymers*. 13. 631. 10.3390/polym13040631.

MOLECULAR DYNAMICS SIMULATIONS OF 1-BUTYL-3-METHYLIMIDAZOLIUM TETRAFLUOROBORATE IONIC LIQUID

Gvidas Ropė¹, Kęstutis Aidas²

¹Institute of Chemical Physics, Vilnius University, Lithuania
gvidas.lope@ff.stud.vu.lt

Ionic liquids are compounds that are made entirely of ions and have a melting point below 100°C. In the last two decades, ionic liquids became a major scientific area on account of applications in organic chemistry, solar energy, and pharmaceutical manufacturing where it is used in many chemical reactions as solvents, catalysts, reagents, or combinations of these [1].

Experimental, theoretical, and molecular modeling research methods must be applied to describe the application of ionic liquids for specific applications. One of the most common nanostructure analysis mechanisms used in this research is molecular dynamics simulations.

In this work, MD simulations were applied to simulate 1-butyl-3-methylimidazolium tetrafluoroborate [C4mim][BF₄] ionic liquid and to analyze its intermolecular structure.

The parameters of the force field potential, which were taken from B. Doherty's research article, were determined, and 1-butyl-3-methylimidazolium tetrafluoroborate was modeled using "GaussView" software before running the simulations [2,3]. Thereafter, the MD simulations were carried out in an NPT ensemble where the density of the simulated ionic liquid was registered until its fluctuation became negligible with a value of 1,15 g/ml. Afterwards, the simulations were run in an NVT ensemble where the trajectories of molecules were noted.

Here we focus on radial distribution functions, which were calculated between cations' C10 atoms as well as between cations' imidazolium rings' H2, H4, H5, and anions' B atoms. The coordination numbers were also calculated between the pairs mentioned. In both RDFs clear peak points are visible therefore the formation of polar and nonpolar regions takes place. The calculated values of coordination numbers show us that the strongest interaction between cations' imidazolium rings and anions appears in the H2-B atom pair.

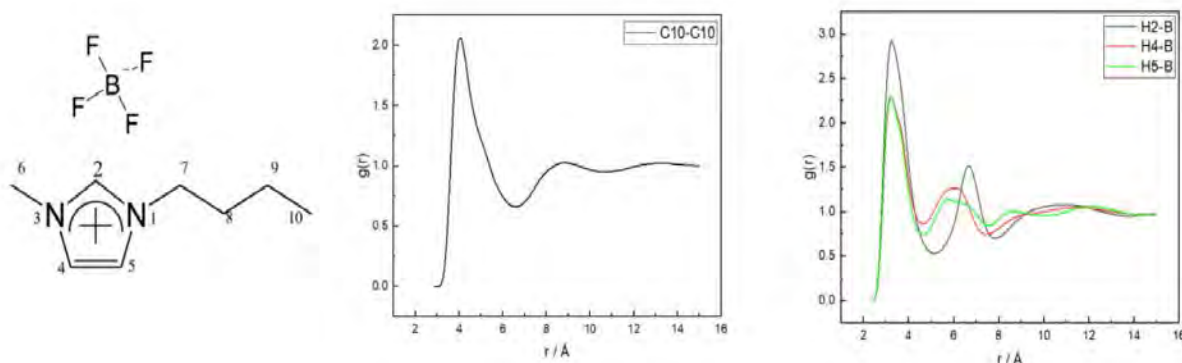


Fig. 1. [C4mim][BF₄] structure with main atom numbers [4] and calculated RDFs between cations' C10 atoms as well as between cations' imidazolium rings' H2, H4, H5 and anions' B atoms.

Acknowledgements: Computations were performed on resources provided by the High Performance Computing Center "HPC Saulėtekis" at Vilnius University, Lithuania.

- [1] Z. Lei, B. Chen, Y. Koo and D. R. Macfarlane, Chem. Rev. 117, 6633–6635 (2017).
 [2] F. Jensen, ISBN 978-0470011874 (2007).
 [3] B. Doherty, X. Zhong, S. Gathiaka, B. Li and O. Acevedo, J. Chem. Theory Comput. 13, 6131-6145 (2017).
 [4] Y. Jeon, J. Sung, D. Kim, C. Seo, H. Cheong et al., J. Phys. Chem. B, Vol. 112, No. 3 (2008).

FORMATION AND INVESTIGATION OF BIPOLAR AQUEOUS SODIUM ION BATTERIES

Dovilė Škarnulytė¹, Milda Petrulevičienė², Jurga Juodkazytė², Linas Vilčiauskas^{1,2}

¹Institute of Chemistry, Vilnius University, Naugarduko 24, LT-03225 Vilnius, Lithuania

²Centre for Physical Sciences and Technology, Sauletekio av. 3, LT-10257, Vilnius, Lithuania
dovile.skarnulyte@chgf.stud.vu.lt

Renewable energy is being developed to replace conventional energy sources, contribute to the climate change mitigation programme, and achieve energy independence. Energy storage systems are an integral part of sustainable energy systems. Currently, energy storage systems mostly rely on Li-ion batteries, which are expensive, not environmentally friendly and flammable. Therefore, safer, cheaper and more environmentally friendly batteries are being developed. Aqueous Na-ion batteries are a promising alternative to Li-ion batteries, however, their energy densities are lower due to narrow electrochemical stability window of water [1]. Therefore, bipolar Na-ion batteries are designed, leading to increased voltage of batteries and energy density as well [2]. In this work, sodium vanadium titanium phosphate (NVTP) was used as anode and cathode for the formation of symmetric bipolar NVTP|NVTP coin type cells. Bipolar batteries were assembled using two and three stacked layers, to reach voltage up to 3.6 V. Moreover, electrolytes of two different composition were applied and investigated. In the Fig. 1. results of galvanostatic charge discharge cycling of NVTP|NVTP coin type cells containing 2 and 3 stacked layers are presented. Fast capacity fade can be observed, which is mostly due to disbalancing and parasitic reactions issues. Coulombic efficiency, capacity retention and self-discharge time of bipolar NVTP|NVTP batteries were compared.

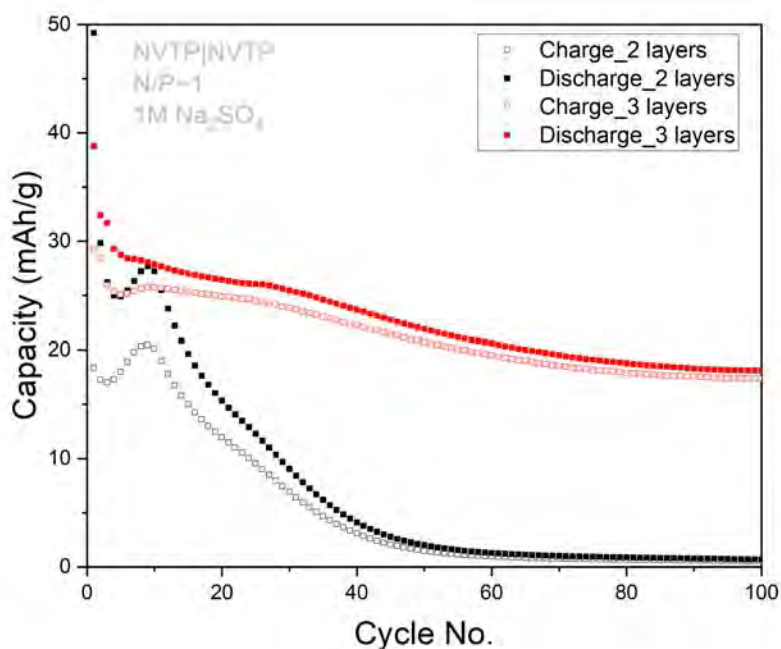


Fig. 1. GCD cycling performance of symmetric NVTP batteries containing 2 and 3 stacked layers in 1M Na₂SO₄ electrolyte at 1C rate

[1] Gintarė Plečkaitytė et al. J. Mater. Chem. A, 2021, 9, 12670-12683

[2] P. Mohana Sundaram, Chhail Bihari Soni, Sungjemmenla, S.K. Vineeth, C. Sanjaykumar, Vipin Kumar, Journal of Energy Storage, 2023, 63, 107139

SYNTHESIS AND LUMINESCENT PROPERTIES OF EU-DOPED STRONTIUM CHLORAPATITE

Simona Bendziute¹, Inga Grigoraviciute¹, Arturas Katelnikovas¹, Aleksej Zarkov¹

¹Vilnius University
simona.bendziute@chgf.stud.vu.lt

Optical materials with adjustable luminescence attract a lot of attention due to their broad application possibilities. Most commonly Eu^{2+} -doped materials are synthesized in reducing atmosphere; nevertheless, some specific inorganic matrices allow for the stabilization of Eu^{2+} oxidation state in air atmosphere. Self-reduction phenomenon is known for the materials such as borates, silicates and phosphates. Overall, phosphate matrices are widely employed for the preparation of lanthanide-activated phosphors. One of the promising hosts is strontium chlorapatite ($\text{Sr}_5(\text{PO}_4)_3\text{Cl}$). This matrix is able to adopt a variety of isovalent and aliovalent ions including lanthanides.

In this work, Eu-doped $\text{Sr}_5(\text{PO}_4)_3\text{Cl}$ powders with various Eu content were synthesized and analyzed. The optimization of synthesis conditions in terms of temperature, time, precursor-to-flux ratio and Eu concentration was performed. Phase purity and crystal structure of synthesized products were studied by powder X-ray diffraction (XRD) and Fourier-transform infrared spectroscopy (FTIR). Morphological properties were investigated using scanning electron microscopy (SEM). Luminescent properties were investigated by means of photoluminescence measurements. Excitation and emission spectra of the samples were studied. Temperature-dependent photoluminescence measurements were performed as well.

STRUCTURAL AND NMR PROPERTIES OF SUPRAMOLECULAR COMPLEXES OF DRUG MOLECULES

Benjaminas Malmiga¹, Kęstutis Aidas²

¹Faculty of Chemistry and Geosciences, Vilnius University

²Institute of Chemical Physics, Faculty of Physics, Vilnius University
benjaminas.malmiga@chgf.stud.vu.lt

Cavitands are molecules found within the field of supramolecular chemistry that are capable of forming host-guest complexes acting as containers for smaller molecules. The formation of such complexes is determined by non-covalent interactions, bearing a resemblance to biological structures such as enzymes. The similarity between enzymes and cavitands is also apparent for their ability to confine and orient molecules for unusual reactions [1]. The container-like structures of cavitands allow for the separation of solvent and guest molecule - resorcinarene cavitands form such structures and the resulting non-polar cavity may prove useful in the solvation of water-insoluble reagents [2, 3]. The aforementioned qualities of cavitands make them relevant in drug delivery systems, chemical synthesis, etc.

The cavitand introduced by de Mendoza is a cup-shaped molecule that contains four 2-benzimidazolone (cyclic carbamide) bridges, enabling the cavitand to form dimers via hydrogen bonds (Fig. 1) [4]. The base portion of the molecule is a resorcinarene ring, which has four groups of pyridine "feet" attached to it [5]. This particular cavitand containing pyridine groups demonstrates good solubility in water making it useful for manipulating hydrophobic compounds in water solutions. NMR spectra measured by Zhang et. al., indicate the formation of cavitand-ibuprofen and cavitand-albendazole complexes in aqueous solutions (Fig. 2 & 3). The nonsteroidal anti-inflammatory ibuprofen and anti-parasitic albendazole are drugs that are poorly soluble in water, making them useful for evaluating the cavitand complex.

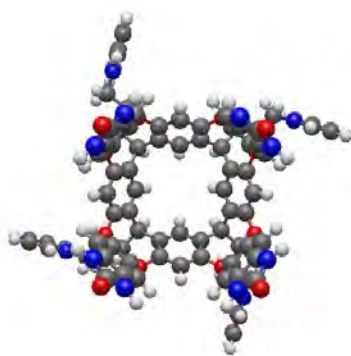


Fig. 1. Resorcinarene Cavitand

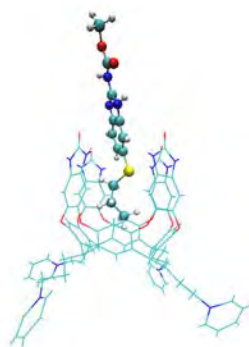


Fig. 2. Cavitand-albendazole complex

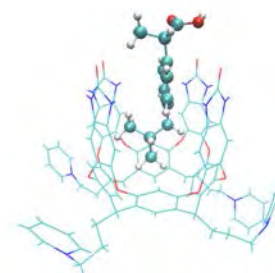


Fig. 3. Cavitand-ibuprofen complex

In this work, classical MD simulations and QM/MM calculations of the ibuprofen and albendazole molecules confined within the supramolecular cavitand were performed aiming to evaluate the intermolecular structure of the complex in aqueous solution. The initial geometries were constructed using Gaussian, utilizing the HF/6-31+G* basis set. MD simulations were performed using AMBER. Our MD simulations show the formation of a stable complex between the drug molecules and the cavitand. The registered trajectories provide insight into the formation and stability of the complex. Furthermore, QM/MM calculations of NMR spectra provide further insights into the structural properties of the complex.

Acknowledgement. Computations have been performed on the resources provided by the high-performance computing center "HPC Saulėtekis" of Vilnius University.

-
- [1] Moran et. al., Cavitands: Synthetic Molecular Vessels, *Journal of the American Chemical Society* 104 (21), 5826-5828 (1982)
 [2] Ajami et. al., Social Isomers of Picolines in a Small Space, *Chemistry* vol. 19,50 (2013).
 [3] Tzeli et. al., Theoretical Study of Hydrogen Bonding in Homodimers and Heterodimers of Amide, Boronic Acid, and Carboxylic Acid, Free and in Encapsulation Complexes, *Journal of the American Chemical Society* vol. 133, no 42, pp. 16977-16985 (2011).
 [4] Ebbing et. al., Resorcinarenes with 2-Benzimidazolone Bridges: Self-aggregation, Self-Assembled Dimeric Capsules, and Guest Encapsulation, *Proceedings of the National Academy of Sciences*, vol. 99, no. 8, pp. 4962-4966 (2002).
 [5] Zhang et al., Complexation of Alkyl Groups and Ghrelin in a Deep, Water-Soluble Cavitand, *Chem. Commun...*, vol. 50, no. 38, pp. 4895-4897 (2014)

SYNTHESIS OF TARGETED CONDENSED THIOIMIDAZOLES

Martyna Paulauskaitė¹, Gintarė Sapežinskaitė², Indrė Misiūnaitė¹, Ieva Žutautė¹

¹Faculty of Chemistry and Geosciences, Vilnius University, Lithuania

²Faculty of Medicine, Vilnius University, Lithuania

martyna.paulauskaite@chgf.stud.vu.lt

There is an increasing interest in the research of protein aggregation and the formation of amyloid structures in various scientific fields. This heightened interest is driven by the connection between amyloid deposition and numerous serious medical conditions, including Alzheimer and Parkinson diseases, type II diabetes, and many systemic amyloidoses. In today's world, these disorders pose a major threat to human health and well-being, so more detailed research is needed [1]. A growing number of studies have described a variety of inhibitors targeting self-assembled amyloidogenic proteins, and some of these are presently undergoing clinical trials. These inhibitors can be categorized into small molecules, short peptides, and antibodies [2].

Recent preliminary studies of imidazothiazines synthesized in our laboratory have shown potential inhibition of amyloid aggregation. Consequently, targeted synthesis of imidazothiazoles, imidazothiazines and imidazothiazepines from aryl propargylic bromides and the corresponding imidazoles for inhibition of amyloid aggregation is in progress. A more detailed analysis of the synthesis will be discussed during the presentation. Studies are being carried out on insulin, a commonly used protein to study the formation of amyloid fibrils [3], and on alpha-synuclein, a Parkinson's disease-related protein [4].

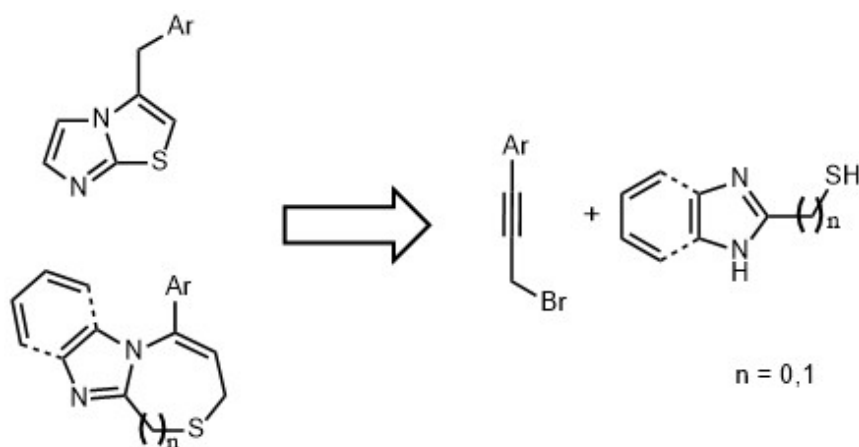


Fig. 1. Retrosynthetic scheme for the targeted synthesis of imidazothiazoles, imidazothiazines and imidazothiazepines

- [1] F. Chiti, C. M. Bobson, Protein Misfolding, Amyloid Formation, and Human Disease: A Summary of Progress Over the Last Decade. *Annu. Rev. Biochem.* 2017, 86, 27-68.
 [2] B. Cheng, et. al., Inhibiting toxic aggregation of amyloidogenic proteins: A therapeutic strategy for protein misfolding diseases. *Biochim. Biophys. Acta.* 2013, 1830 (10), 4860-4871.
 [3] A. Sakalauskas, et. al., Concentration-dependent polymorphism of insulin amyloid fibrils, *PeerJ.* 2019, 7 1-13.
 [4] M. Ziaunys, et. al., Polymorphism of Alpha-Synuclein Amyloid Fibrils Depends on Ionic Strength and Protein Concentration. *Int. J. Mol. Sci.* 2021, 22, 12382.

CAPDROP: A NOVEL METHOD FOR PERIPHERAL BLOOD scRNA-seq

Emilė Pranauskaitė¹, Linas Mažutis¹

¹Department of Single Cell Analytics, Institute of Biotechnology, Life Sciences Center, Vilnius University, Vilnius, Lithuania
emilepra@gmail.com

Droplet microfluidics is a high-throughput technology for analyzing individual cells isolated in nanoliter-volume droplets. This approach addresses cell heterogeneity challenges, enabling the comparison of cell states and types in complex samples [1]. However, conventional droplet-based systems encounter limitations when it comes to executing multi-step operations which can be challenging to implement.

Our research group developed a microfluidics-based technique for single-cell isolation in semi-permeable capsules [2,3], that selectively retains large molecules, such as genomic material or mRNA, while allowing small molecules, such as enzymes or other reaction components, to passively diffuse throughout the shell. As a result of this selective permeability, it becomes possible to perform multi-step reactions on millions of individual cells. When compared to other systems with similar properties, the semi-permeable capsules exhibit improved retention of encapsulated cells and yield higher quantities of whole-genome amplification [2].

Here, we adapted capsules to create a novel single-cell RNA sequencing (scRNA-seq) platform to profile fragile and hard-to-capture cells. Traditional droplet-based scRNA-seq faces challenges in sequencing cells that are sensitive to environmental factors. One of these cell types is neutrophils which are characterized by a high concentration of internal RNases, which, upon stimulation, can degrade the transcriptome of both the neutrophils and the surrounding cells. Taking advantage of capsules, we demonstrated that it is possible to effectively neutralize RNases effect and subsequently recover diverse cell types. The capsules carrying purified cellular RNA are used as microreactors for barcoding and subsequent library preparation. We term this new technique ČapDrop and show that CapDrop recovers the peripheral blood cell composition close to theoretical values, therefore addressing a significant limitation of droplet-based scRNA-seq technology. Our findings underscore the potential of the CapDrop platform as a promising method for sequencing sensitive biological samples. The flexibility and efficiency offered by CapDrop open new avenues for exploring cellular heterogeneity and advancing single-cell RNA sequencing methodologies.

[1] Zilionis, R., Nainys, J., Veres, A., Savova, V., Zemmour, D., Klein, A. M., and Mazutis, L. (2016). Single-cell barcoding and sequencing using droplet microfluidics. Nature Publishing Group.

[2] Leonaviciene, G., Leonavicius, K., Meskys, R., and Mazutis, L. (2020). Multi-step processing of single cells using semi-permeable capsules. *Lab on a Chip*, 20(21), 4052–4062.

[3] Leonaviciene, G., and Mazutis, L. (2022). RNA cytometry of single-cells using semi-permeable microcapsules. *BioRxiv*, 2022.09.24.509327.

COMPARATIVE STUDIES OF THE ANTIOXIDANT PROPERTIES OF DIOSMIN AND QUERCETIN IN THE MODEL SYSTEM OF DOPAMINE OXIDATION

Iryna Povshedna¹, Vladyslav Udovytskyi¹, Iryna Pashchenko¹, Viktoriia Lyzhniuk¹, Vadym Lisovyi^{1,2},
Volodymyr Bessarabov¹, Andriy Goy¹

¹Department of Industrial Pharmacy, Kyiv National University of Technologies and Design, Ukraine

²Department of Chemical Technology and Resource Saving, Kyiv National University of Technologies and Design, Ukraine
povshedna.io@knuud.edu.ua

Parkinson's disease (PD) is a common neurodegenerative disorder. It is associated with the degeneration of dopaminergic neurons and is characterized by tremor, postural instability, rigidity, and hypokinesia. The treatment of PD primarily involves symptomatic therapy, which includes administering levodopa, which is converted to dopamine in the brain [1]. However, treating PD with levodopa is problematic because both levodopa and its metabolite dopamine can be oxidised, usually by oxidative stress. Therefore, additional administration of antioxidants is needed to prevent oxidation of levodopa and dopamine.

Flavonoids are a well-known group of antioxidants, which are biologically active phenolic substances found in various plants. Recent studies have shown that some flavonoids can protect dopaminergic neurons by inhibiting dopamine oxidation and modulating antioxidant signaling pathways [2-3].

The study examined the effect of two well-known bioflavonoids, diosmin and quercetin, on the rate of dopamine oxidation and compared their antioxidant activity in this system. Kinetic studies were conducted using the spectrophotometric method, which recorded the increase in the optical absorption of the reaction mixture over time at a wavelength of 500 nm. The rate of dopamine oxidation was determined by calculating the first-order reaction rate constant.

Analyzing the dependence of the first-order reaction rate constant of dopamine oxidation on the concentration of diosmin in the system, it can be argued that a dose-dependent effect of oxidation inhibition is observed. When diosmin was added to the system at a concentration of 25 μM , the rate of dopamine oxidation significantly decreased by 3.07 times: $K_{H(0)}^1 = (3.90 \pm 0.03) \times 10^{-3}$ 1/s and $K_{H(25)}^1 = (1.27 \pm 0.04) \times 10^{-3}$ 1/s ($p \leq 0,05$); with an increase in concentration to 50 μM the rate of dopamine oxidation decreased by 4.02 times: $K_{H(50)}^1 = (0.97 \pm 0.08) \times 10^{-3}$ 1/s, and at a concentration of 100 μM – 5.57 times: $K_{H(100)}^1 = (0.70 \pm 0.05) \times 10^{-3}$ 1/s.

Instead, when quercetin was added to the system at a concentration of 25 μM the rate of dopamine oxidation decreased significantly by only 1.35 times: $K_{H(0)}^1 = (3.90 \pm 0.03) \times 10^{-3}$ 1/s and $K_{H(25)}^1 = (2.88 \pm 0.04) \times 10^{-3}$ 1/s ($p \leq 0,05$). When the quercetin concentration is increased to 50 and 100 μM the oxidation rate decreases by 1.65 and 3.02 times, respectively: $K_{H(50)}^1 = (2.36 \pm 0.06) \times 10^{-3}$ 1/s and $K_{H(100)}^1 = (1.29 \pm 0.03) \times 10^{-3}$ 1/s.

It has been established that the bioflavonoids diosmin and quercetin exhibit antioxidant properties in relation to dopamine oxidation. However, diosmin is a more effective inhibitor of dopamine oxidation. Therefore, it is advisable to prefer diosmin when modelling a pharmaceutical composition for use in combination therapy with levodopa drugs for the treatment of Parkinson's disease.

[1] E. K. J. Pauwels, G. J. Boer. Parkinson's Disease: A Tale of Many Players. Medical principles and practice : international journal of the Kuwait University, Health Science Centre, 32(3), 155–165 (2023). <https://doi.org/10.1159/000531422>

[2] S. L. Hor, S. L. Teoh, W. L. Lim. Plant Polyphenols as Neuroprotective Agents in Parkinson's Disease Targeting Oxidative Stress. Current drug targets, 21(5), 458–476 (2020). <https://doi.org/10.2174/1389450120666191017120505>

[3] Z. D. Zhou; S. P. Xie, W. T. Saw, P.G.H. Ho, H.Y. Wang, L. Zhou, Y. Zhao, E.K. Tan. The Therapeutic Implications of Tea Polyphenols against Dopamine (DA) Neuron Degeneration in Parkinson's Disease (PD). Cells, 8, 911 (2019). <https://doi.org/10.3390/cells8080911>

INHIBITION OF PERIODONTAL DISEASES SPECIFIC MIRNAS: NEW THERAPEUTIC APPROACH

Gabrielė Židonytė¹, Benita Buragaitė-Staponkienė¹, Kristina Šnipaitienė¹, Adomas Rovas², Alina Purienė², Raminta Vaičiulevičiūtė³, Eiva Bernotienė³, Sonata Jarmalaitė¹

¹Human Genome Research Group, Institute of Biosciences, Life Sciences Center, Vilnius University, Vilnius Lithuania

²Institute of Odontology, Faculty of Medicine, Vilnius University, Vilnius, Lithuania

³Department of Regenerative Medicine, State Research Institute Centre for Innovative Medicine, Vilnius, Lithuania
gabriele.zidonyte@gmc.stud.vu.lt

Periodontal diseases comprise a wide range of inflammatory conditions affecting the supporting structures with a serious form called periodontitis (PD) that affects up to 50 % of people worldwide [1]. When left untreated, PD is one of the main causes of tooth loss. The first choice of rehabilitation for tooth loss is dental implants, but even up to 23 % of them do not adhere properly, and that results in peri-implantitis (PI), causing irreversible damage [2]. Multiple PD pathogenesis mechanisms are epigenetically regulated, and microRNAs (miRNAs) are considered as one of the key modulators that influences periodontal homeostasis [3]. This study aimed to identify PD-associated miRNAs in gingival tissue and evaluate the therapeutic potential of miRNA inhibition technology in managing PD and PI.

Microarray analysis of gingival tissue samples (N=16) revealed 140 upregulated miRNAs in inflamed gingival tissues compared to periodontally healthy tissues. Fifteen selected miRNAs were further analyzed by performing quantitative reverse transcription PCR in an extended cohort of gingival tissue samples (N=80). Analysis revealed that the levels of miR-146a-5p were significantly lower in PD-affected individuals compared to periodontally healthy participants. Severe forms of PD were associated with increased levels of miR-140-3p and -145-5p and decreased levels of miR-125a-3p. Moreover, the correlation between periodontal outcome parameters indicating the worse clinical status of PD and increased levels of miR-140-3p, -145-5p, and decreased levels of miR-125a-3p, was observed. MiRNAs abundantly expressed in gingival tissues, namely, miR-140-3p, -145-5p, -146a-5p, and -195-5p, were selected for further functional analysis.

Functional analysis of PD-specific miRNAs was performed in human bone marrow mesenchymal stem cells (hBM-MSCs). These cells were cultivated on cell culture plastic and medical titanium surface by transfection with inhibitors of selected miRNAs (antagomiRs). The efficacy of antagomiR treatment was evaluated under various transfection conditions by analyzing the expression levels of the targeted miRNAs. Analysis revealed that inhibitors of miR-140-3p significantly decrease the expression levels of miR-140-3p by 1.7-fold in cells cultured on plastic 2 days after transfection. While in cells cultured on medical titanium expression of miR-140-3p and -145-5p was most decreased 3 and 2 days after antagomiR transfection, respectively, although the expression differences were statistically non-significant ($P > 0.050$).

The current study revealed that miRNAs play an important role in the pathogenesis of periodontal diseases. However, further studies are essential to evaluate the potential of miRNA inhibition technology in treating periodontal diseases.

[1] Nazir MA., Prevalence of periodontal disease, its association with systemic diseases and prevention (2017)

[2] Sun Z., Ma L. et al., The overview of antimicrobial peptide-coated implants against oral bacterial infections (2023)

[3] Luan X., Zhou X. et al., MicroRNAs and Periodontal Homeostasis. Journal of Dental Research (2017)

INVESTIGATION OF ANXA4 FUNCTION IN CELL PLASMA MEMBRANE PERMEABILIZATION, RESEALING AND CELL VIABILITY POST-ELECTROPORATION

Dominykas Makarovas¹, Baltramiejus Jakštys², Saulius Šatkauskas³

¹Biochemistry Cathedral, Faculty of Natural Sciences, Vytautas Magnus University, Kaunas, Lithuania

²Research Institute of Natural and Technological Sciences, Vytautas Magnus University, Kaunas, Lithuania

³Cell and Tissue Biotechnology Research Group, Vytautas Magnus University, Kaunas, Lithuania
dominykas.makarovas@stud.vdu.lt

Electroporation (EP) is a technique where the application of brief, high-voltage electric pulses leads to the permeabilization of the cellular plasma membrane, potentially through the formation of electro pores. However, the precise mechanism of electroporation remains unexplained.[1] Critical parameters influencing the efficacy of EP include the intensity, duration, and number of electric pulses, with excessive levels of any parameter potentially compromising cell viability.[2] Post-EP, the recovery of plasma membrane integrity is essential for cell survival, highlighting the role of annexin family proteins, particularly annexin A4 that is known to be involved in membrane repair processes after activation by Ca^{2+} ions. Despite ongoing research spanning over four decades, information about the impact of proteins on the restoration of cell plasma membrane post-EP is missing, despite numerous publications on calcium influence on cell plasma membrane recovery after EP. This study aimed to investigate the influence of Ca^{2+} ions on the recovery of the cells membrane following EP. Response of wild-type MCF7 cells, with an intact annexin A4 gene, in contrast to MCF7-ANXA4⁻ knockout (KO) cells, where annexin A4 gene's expression was disrupted were investigated.

Cell viability was assessed using the MTS assay, while the dynamics of plasma membrane repair and electroporation were evaluated via flow cytometry, specifically through the quantification of propidium iodide permeable cells. Electroporation was conducted using a single 100 μs electric pulse at various intensities, with a CaCl_2 concentration set at 2 mM. Interestingly, we determined that MCF7-WT cells are less sensitive to the adverse effects of electroporation compared to MCF7-ANXA4⁻ (KO) cells. Furthermore, results showed that calcium had a negative impact on the viability of both cell lines, despite having a positive impact on reducing electroporation level. In contrast, cell plasma membrane recovery after pulsing in calcium medium had a significant negative impact on cell plasma membrane recovery by increasing amounts of permeable cells in both cell lines 35 mins after EP. These observations suggest that annexin A4 may play a critical role in the plasma membrane repair and cell viability after electroporation when calcium ions are involved, challenging the presumed importance of this protein in the cellular recovery process.

[1] E. Neumann, et al. "Gene transfer into mouse lymphoma cells by electroporation in high electric fields," *EMBO*, 1(7): 841-845, 1982.

[2] B. Jakštys, et al. "Correlation between the loss of intracellular molecules and cell viability after cell electroporation," *Bioelectrochemistry*, 135: 107550, 2020.

CREATION OF MUTANT VARIANT K102R OF YEAST SACCHAROMYCES CEREVISIAE GENE SUP35

Ieva Jankauskaitė¹, Justina Versockienė¹, Eglė Lastauskienė¹

¹Institute of Biosciences, Life Sciences Center, Vilnius University, Saulėtekio Av. 7, LT-10257, Vilnius, Lithuania
ieva.jankauskaite@gmc.stud.vu.lt

Prions are altered, infectious forms of native proteins that can acquire new functions/lose old ones, aggregate, self-proliferate, spread and cause neurodegenerative diseases in humans and other mammals. In yeast prions are inherited through the cytoplasm, while in mammals — transmitted extracellularly. *Saccharomyces cerevisiae* is an excellent model organism because of its cellular machinery similarity to higher eukaryotes, universal DNA transformation system, and at least 10 different prion domains identified in them. Prion [PSI⁺] of Sup35 protein is one of the best-studied yeast prions.

The fact that prions are resistant to various elimination factors encourages the search for reasons of this and possible solutions. It was found that *in vivo* Sup35 protein is accessible to proteases, but the resistance to degradation is determined by the arrangement of amino acids and their properties. Usually lysines in the N-domain of the protein must be ubiquitinated in order for a protein to be directed for proteosomal degradation. Therefore, this work attempts to change the only lysine in 102 position in the N-domain of Sup35 protein to arginine.

In order to create mutant variant K102R of yeast *SUP35* gene primers were created and site-directed mutagenesis was used to change one nucleotide in the sequence through three independent PCR reactions. Later — Sup35K102RGFP was inserted into pJET1.2/blunt cloning vector and successfully multiplied in *Escherichia coli* DH5 α cells.

For the first time mutant variant of *SUP35* gene K102R was created. Sup35K102RGFP from pJET1.2/blunt vector can be used to ligate to yeast shuttle vector pRSCup. Then using fluorescent microscopy method native protein and mutated protein prionization can be compared. It is expected that mutant Sup35 protein variant K102R is more prone to prionization and therefore more resistant to degradation in proteasome but to affirm that more experiments has to be done.

MINIMIZING CHEMOTHERAPY SIDE EFFECTS: CALCIUM SONOPORATION

Reda Rulinskaitė¹, Rūta Palepšienė¹, Saulius Šatkauskas¹, Renaldas Raišutis², Martynas Maciulevičius^{1,2}

¹Biophysical Research Group, Vytautas Magnus University, Lithuania

²Ultrasound Research Institute, Kaunas University of Technology, Lithuania

reda.rulinskaite@vdu.lt

In chemotherapy, the main goal is to eliminate cancerous cells by inhibiting their proliferation and metastasis to other organs. Chemotherapy can lead to adverse short-term and long-term side effects such as infertility, alopecia [1]. **Calcium (Ca^{2+}) ions** are significant for signal transduction pathways, due to being one of the most common intracellular signal transmitters between various signal compartments of the cell [2]. The disruption of intracellular Ca^{2+} homeostasis in a cell could play a crucial role in the destruction of cancer cells. It has been shown that Ca^{2+} serves an essential role in electroporation and demonstrates a potential for anti-cancer treatment [3]. In attaining spatio-temporally controlled delivery of anticancer drugs, sonoporation (SP) employs non-invasive application of medical ultrasound (US) in conjunction with microbubbles (MBs). SP might prove more efficacious than electroporation, however, Ca^{2+} delivery and application for sonotherapy has not been sufficiently studied. The utilization of Ca^{2+} in cancer treatment presents a promising avenue for the substantial mitigation of adverse side effects associated with conventional cytotoxic agents.

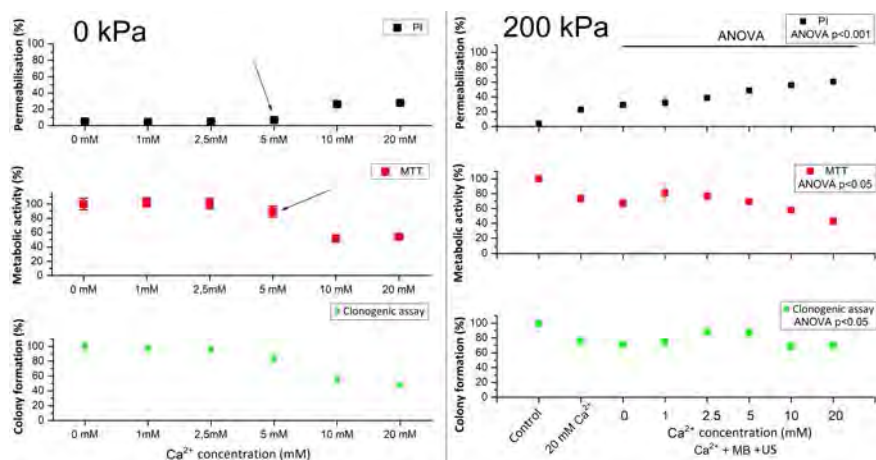


Fig. 1. Membrane permeabilization (propidium iodide (PI) assay, 20 min), metabolic activity (MTT test, 48h) and cell viability (clonogenic assay, 6 days) evaluated in different groups without US (left panel) and after Ca^{2+} delivery via US (right panel).

During the experiment, by using of PI, MTT and clonogenic assays, it was determined that the mortality of mouse breast cancer (4T1) cells increased from 5mM Ca^{2+} concentration, which was a turning point for the metabolic activity of cells and their viability. Our preliminary data indicate that Ca^{2+} transport, induced by MB cavitation, for 4T1 cells is not lethal in the presence of 200 kPa US, as the results of the clonogenic assay indicate the recovery of cell viability after 6 days (Fig. 1). The ANOVA test showed that increasing the Ca^{2+} concentration at 200 kPa US has a tendency to increase cell death. Moreover, the differences between the control (0 mM Ca^{2+}) and the therapeutic (Ca^{2+} +SP) group are up to 30% (according to PI and MTT tests), which indicates the permeabilization of the cell plasma membrane and the disturbance of metabolic activity.

This work was supported by the grant: “The development of controlled cancer treatment modality based on Ca^{2+} delivery via ultrasound (S-PD-22-51)” from the Research Council of Lithuania.

[1] Brianna, S. H. Lee, Chemotherapy: how to reduce its adverse effects while maintaining the potency, *Medical Oncology* 40, 3 (2023).

[2] L. Conrard, D. Tytca, Regulation of Membrane Calcium Transport Proteins by the Surrounding Lipid Environment, *Biomolecules* 9, 513 (2019).

[3] S. K. Frandsen, M. Vissing, J. Gehl, A Comprehensive Review of Calcium Electroporation - A Novel Cancer Treatment Modality, *Cancers* 12, 290 (2020).

EXPLORING THE IS200/IS605 FAMILY TRANSPOSABLE ELEMENTS FOR NOVEL GENOME EDITING TOOLS

Gytis Druteika¹, Tautvydas Karvelis¹

¹Vilnius University, Life Sciences Center
gytis.druteika@gmc.vu.lt

Mobile genetic elements (MGE), such as transposons, bacteriophages, plasmids, and insertion sequences (IS), were historically called 'junk DNA' of the prokaryotic and eukaryotic genomes. Nowadays, the significance of MGEs is well understood since they are the driving force of evolution, allowing organisms to rapidly adapt to changing environmental conditions [1]. One of the most widely distributed groups of insertion sequences belongs to the IS200/IS605 family. Structurally, these transposons are not very complex, as the IS200/IS605 family sequences only encode proteins required for transposition: TnpA and TnpB. TnpA is a transposase responsible for the mobility of IS, while TnpB turned out to be an evolutionary ancestor of CRISPR-Cas effector nucleases, which are widely used in gene editing experiments [2, 3]. However, the large size of commonly used Cas9 and Cas12 effectors complicates their delivery to the target cells. Recently, the transposon-encoded TnpB was applied as a programmable tool for gene editing in human cell cultures. Considering its miniature size, compared to Cas9 or Cas12 nucleases, TnpB has promising properties for broad application in various gene editing assays [4, 5]. Nevertheless, due to the high expectations for efficiency, specificity, and the requirement for nucleases to target a wide range of genes, there is a great need for discovering novel programmable DNA-targeting proteins. Since TnpB-encoding insertion sequences are extremely widespread, this study aimed to characterize a set of TnpB homologs. Bioinformatic analysis and sequence alignments enabled us to select diverse representatives from several groups of TnpB homologs. By using biochemical assays, we determined the requirements for the TAM sequence, which is recognized by the TnpB protein, and for the guide RNA. This study contributes to current knowledge about diverse TnpB proteins and will be valuable for further characterization of these potential gene editing tools.

-
- [1] Krupovic, M., Shmakov, S., Makarova, K. S., Forterre, P. & Koonin, E. V. Recent Mobility of Casposons, Self-Synthesizing Transposons at the Origin of the CRISPR-Cas Immunity. *Genome Biol Evol* 8, 375–386 (2016).
- [2] Sadler, M., R. Mormile, M. & L. Frank, R. Characterization of the IS200/IS605 Insertion Sequence Family in Halanaerobium Hydrogeniformans. *Genes (Basel)* 11, (2020).
- [3] Kapitonov, V. V., Makarova, K. S. & Koonin, E. V. ISC, a Novel Group of Bacterial and Archaeal DNA Transposons That Encode Cas9 Homologs. *J. Bacteriol.* 198, 797–807 (2016).
- [4] Karvelis, T. et al. Transposon-associated TnpB is a programmable RNA-guided DNA endonuclease. *Nature* 599, 692–696 (2021).
- [5] Altae-Tran, H. et al. The widespread IS200/IS605 transposon family encodes diverse programmable RNA-guided endonucleases. *Science* 374, 57–65 (2021).

STRUCTURAL VARIABILITY OF PRION PROTEIN AMYLOID FIBRILS DEPENDS ON AGITATION INTENSITY

Kamile Mikalauskaite¹, Mantas Ziaunys¹, Vytautas Smirnovas¹

¹Institute of Biotechnology Life Sciences Center Vilnius University
kamile.mikalauskaite@gmc.vu.lt

Aggregation of amyloid proteins to form amyloid fibrils is associated with certain neurodegenerative diseases such as Alzheimer's or prion diseases. Despite the great efforts of scientists to understand all the features of the occurrence mechanism of these diseases, many questions in this field remain unanswered. The amyloid protein aggregation process is often influenced by various environmental factors, including solution pH, ionic strength, or protein concentration. Different secondary structures of fibrils are frequently formed under varying aggregation conditions, but polymorphism of resulting fibrils can also be observed under identical conditions. In this study, we investigate whether the agitation intensity of samples can influence the formation of different fibril strains.

Prion protein aggregation was conducted under identical conditions (60°C, 2 M guanidine hydrochloride, 50 mM phosphate buffer pH 6.0, with 3 mm glass bead), with only the agitation intensity of the samples changed (100-600 rpm). To assess the variability in the secondary structure of the resulting fibrils, 24 samples were analyzed for each condition. Fourier transform infrared spectroscopy was employed to investigate the secondary structure of the fibrils after aggregation, and atomic force microscopy was used to determine the morphology of fibrils with different secondary structures.

The research results indicate that the agitation intensity of the samples affects the variability of the formed amyloid fibrils. Analysis of the Fourier transform infrared spectra revealed that the lowest variability in the sample structures occurred at 400 rpm, resulting in the formation of only one fibril strain. These fibrils also exhibited different binding modes of the fluorescent dye thioflavin-T and displayed stability under denaturing conditions.

CRISPR-CAS9 GENOME ENGINEERING IN *KLUYVEROMYCES MARXIANUS* FOR ENHANCED SECRETION OF RECOMBINANT ANTIBODIES

Justina Žičkutė¹, Danguolė Žiogienė¹, Alma Gedvilaitė¹

¹Department of Eukaryote Gene Engineering, Institute of Biotechnology, Life Sciences Center, Vilnius University, Lithuania
zickutejustina@gmail.com

Recombinant antibodies (RABs) are important in diagnostics, research, biotechnology, and therapeutics due to their high specificity, stability, and ease of modification [1]. Yeasts, which are easily genetically modified and cultivated, are often preferred as a cost-effective system for RABs production. The species *Kluyveromyces marxianus* is known for its efficient production and secretion of properly folded and active native and recombinant proteins, including RABs [2]. To improve RABs production technologies, yeasts can be genetically modified to create mutant strains with enhanced protein secretion properties.

Protein glycosylation, a crucial post-translational modification, involves attaching a glycan to a protein, ensuring its proper folding, activity, and stability. Dolichol kinase (DK), encoded by the essential *SEC59* gene, plays a role in glycosylation processes within the endoplasmic reticulum [3]. The reduced activity of DK, along with changes in glycosylation levels and the activity of other proteins in the secretory pathway, may lead to enhanced recombinant protein secretion [4]. Enhanced RABs secretion can also be achieved by reducing the activity of intracellular peptidases, as RABs are highly prone to proteolysis and often undergo degradation [5].

The aim of this study was to apply efficient CRISPR-Cas9 genome editing technology to construct a *K. marxianus* strain that displays improved secretion of RABs. In this investigation, a *K. marxianus* yeast WSS- $\Delta pep4$ strain was created by introducing mutations encoding G418S and I432S changes in the DK amino acids, and by disrupting the gene encoding vacuolar peptidase (*PEP4*). The introduction of mutations in the DK-encoding gene led to changes in DK activity, as indicated by reduced glycosylation efficiency of carboxypeptidase Y in the WSS strain. Additionally, the disruption of the *PEP4* gene in yeast resulted in a decrease in the proteolytic degradation of RABs. A secretion assay of the single-chain antibody fragment (scFv) linked to an antibody fragment crystallizable Fc (scFv-Fc) against *Gardnerella vaginalis* vaginolysin was performed and detected in yeast growth medium by Western blot. The results indicated that the constructed *K. marxianus* WSS- $\Delta pep4$ strain secreted recombinant scFv-Fc protein more efficiently compared to the wild-type *K. marxianus* strain. However, the secretion of RABs in yeast also depends on the specific properties of the recombinant protein, and further studies are necessary. The newly constructed *K. marxianus* WSS- $\Delta pep4$ mutant strain could be beneficial for future research aimed at enhancing RABs production technologies.

[1] Ma, H., & O'Kennedy, R. (2017). Recombinant antibody fragment production. *Methods*, 116, 23–33.

[2] Nambu-Nishida, Y., Nishida, K., Hasunuma, T., & Kondo, A. (2018). Genetic and physiological basis for antibody production by *Kluyveromyces marxianus*. *AMB Express*, 8(1), 56.

[3] Kale, D., Kikul, F., Phapale, P., Beedgen, L., Thiel, C., & Brügger, B. (2023). Quantification of dolichyl phosphates using phosphate methylation and reverse-phase liquid chromatography–high resolution mass spectrometry. *Analytical Chemistry*, 95(6), 3210–3217.

[4] Žiogienė, D., Valavičiūtė, M., Norkienė, M., Timinskas, A., & Gedvilaitė, A. (2019). Mutations of *Kluyveromyces lactis* dolichol kinase enhances secretion of recombinant proteins. *FEMS Yeast Research*, 19(3), foz024.

[5] Gast, V., Sandegren, A., Dunås, F., Ekblad, S., Güler, R., Thorén, S., Tous Mohamedano, M., Molin, M., Engqvist, M. K. M., & Siewers, V. (2022). Engineering *Saccharomyces cerevisiae* for the production and secretion of Affibody molecules. *Microbial Cell Factories*, 21(1), 36.

THERMODYNAMIC AND DIELECTRIC PROPERTIES OF THE IMMUNE COMPLEXES BETWEEN SPECIFIC ANTIBODY AND SARS-CoV-2 B.1.1.529 SPIKE PROTEIN

Beatričė Urbaitė¹, Silvija Juciūtė^{1,2}, Ieva Plikusienė^{1,2}

¹Faculty of Chemistry and Geosciences, Institute of Chemistry, Vilnius University, Naugarduko 24, Vilnius, Lithuania

²State Research Institute Centre for Physical Sciences and Technology, Sauletekio Avenue 3, Vilnius, Lithuania
beatrice.urbaite@chgf.stud.vu.lt

Investigating thermodynamical properties of antibody-antigen immune complex formation is crucial for a deeper understanding of molecular mechanisms involved in immune responses. The ability of SARS-CoV-2 virus to spread is related to the mutation in the structural proteins of the virus. The mutations in the Spike protein are linked to the virus's survival capability, rate of spread, and disease severity [1].

That's why it is very important to understand how immune complex between specific antibodies and mutated Spike protein is formed and what are the thermodynamic properties of such process. In this study we investigated how immune complex of recombinant specific monoclonal antibodies and SARS-CoV-2 Spike protein B.1.1.529 is formed in real time. Hence, the affinity interaction between immobilized specific monoclonal antibodies and SARS-CoV-2 B.1.1.529 (omicron variant) Spike protein was conducted by combining two methods: Spectroscopic ellipsometry (SE) and quartz crystal microbalance with dissipation (QCM-D) simultaneously. These highly-precise, real-time and label-free methods provided real-time kinetics.

In this work the kinetics study was used to calculate thermodynamic parameters of the formation of immune complex, such as association and dissociation rate constants (k_a and k_d), the stable antigen-antibody complex rate constant (k_r), the equilibrium association and dissociation constants (K_A and K_D) and to assess the surface mass density of immune complexes.

[1] Magazine N. et al., *Viruses*. 2022 Mar; 14(3): 640

PURIFICATION AND ACTIVITY OF THE CHIMERIC SEPTU ANTI-VIRAL DEFENSE SYSTEM

Marija Duchovskytė¹, Dalia Smalakyte¹, Gintautas Tamulaitis¹

¹Institute of Biotechnology, Life Sciences Center, Vilnius University, Lithuania
marija.duchovskyte@chgf.stud.vu.lt

In order to withstand frequent bacteriophages' attacks, prokaryotes have developed multiple sophisticated defense mechanisms. For instance, CRISPR-Cas provides immunity to bacteria and archaea by recalling past phage infections, and restriction-modification (RM) systems target specific viral genomic sequences [1]. Given the enormous diversity of viruses, it is likely that more different bacterial defense systems exist than previously described [2]. Over the past few years, systematic analyses of prokaryotic genomes followed by experimental validation have uncovered numerous previously unknown anti-phage defense systems [3]. Here, we focus on a recently discovered anti-viral defense system called Septu.

The Septu defense system operates using two proteins: putative ATPase PtuA and HNH nuclease PtuB [3]. In previous experiments, we were unable to purify both the ATPase and the nuclease belonging to the same Septu system from *B. thuringiensis* or *B. weihenstephanensis*. Thus, in this study we present the chimeric Septu system composed of *B. thuringiensis* PtuA and *B. weihenstephanensis* PtuB. We evaluated its activity against *E. coli* phages and tested various nucleic acids as substrates *in vitro*.

[1] H. G. Hampton, et al. The arms race between bacteria and their phage foes. *Nature* 577, 327-336 (2020)

[2] L. Gao, et al. Diverse enzymatic activities mediate antiviral immunity in prokaryotes. *Science* 369(6507), 1077-1084 (2020)

[3] S. Doron, et al. Systematic discovery of antiphage defense systems in the microbial pangenome. *Science* 359(6379) (2018)

ANALYSIS OF PROBIOTIC BACTERIA *LACTICASEIBACILLUS PARACASEI* SMALL RNAs INVOLVED IN STRESS RESPONSE

Odilija Safinaite¹, Milda Mickute¹, Renatas Krasauskas¹, Giedrius Vilkaitis¹

¹Department of Biological DNA Modification, Institute of Biotechnology, Life Sciences Center, Vilnius University
odilija.safinaite@gmail.com

One of lactic acid bacteria that can be found in human body is *Lacticaseibacillus paracasei*, which is also present in fermented foods such as cheese or pickles. It is a probiotic bacterium that balances the microbial flora to improve digestion and fortify the immune system. Notably, *L. paracasei* is resistant to a variety of stressors, including acidic conditions and bile salts, which is essential for survival in the gastrointestinal tract [1]. These bacteria adapt to various unfavourable situations by using elaborated mechanisms. One of these is the interaction of small regulatory RNAs (sRNAs) with messenger RNAs of bacterial proteins that are important for antimicrobial resistance.

sRNAs are RNA molecules that control gene expression in bacteria mainly at a post-transcriptional level. These RNAs are typically 50 to 500 nucleotides long and act by base-pairing with target mRNAs, thereby altering their translation and stability [2]. There are different sRNAs that can collectively regulate the expression of many different genes, but for the purpose of this work, it is important to study those sRNAs that modulate the expression of genes contributing to resistance in bacteria.

Therefore, scientists from the Department of Biological DNA Modification performed RNA sequencing of *L. paracasei* RNA and identified the sRNAs whose expression was altered by the tested stress factors (NaCl, bile salt, H₂O₂, lactic acid, penicillin G). Eight sRNAs (sLCB2601+, sLCB649-, sLCB1691-, sLCB2636-, sLCB3045+, sLCB250-, sLCB457-, sLCB652-) were selected from the list to be further analysed in this study. Plasmids enhancing their expression were inserted into *L. paracasei*, the serial dilutions of which were spotted on stressor-supplemented agarose medium. The grown colonies were compared with control *L. paracasei* bacteria in which the sRNA-free plasmid was inserted.

In conclusion, this study focused on the effect of increased expression of sRNAs on bacterial resistance to various stressors. The results obtained may contribute to the understanding of the adaptation of *L. paracasei* to environmental conditions, which is important for the improvement of probiotic products.

[1] Hill, D., Sugrue, I., Tobin, C., Hill, C., Stanton, C., & Ross, R. P. (2018). The Lactobacillus casei Group: History and Health Related Applications. *Frontiers in Microbiology*, 9, 2107. <https://doi.org/10.3389/fmicb.2018.02107>

[2] Gottesman, S., & Storz, G. (2011). Bacterial Small RNA Regulators: Versatile Roles and Rapidly Evolving Variations. *Cold Spring Harbor Perspectives in Biology*, 3(12), a003798. <https://doi.org/10.1101/cshperspect.a003798>

ROLE OF SOLUBLE PD-1 AND PD-L1 IN PROSTATE CANCER

Žilvinas Survila^{1,2}, Margarita Žvirblė^{1,2}, Lukas Šimkus^{2,3}, Gintaras Zaleskis³, Vita Pašukonienė²

¹Institute of Biosciences, Life Sciences Center, Vilnius University, Vilnius, Lithuania

²Laboratory of Immunology, National Cancer Institute, Vilnius, Lithuania

³Department of Immunology, State Research Institute Centre for Innovative Medicine, Vilnius, Lithuania
zilvinas.survila@gmc.stud.vu.lt

The PD-1/PD-L1 axis regulates immune responses, and its dysregulation in cancer allows immune evasion and tumor progression [1]. Membranous PD-L1 is a potential biomarker for cancer, but its biopsy-based measurement is invasive [2]. In contrast, soluble forms of PD-1 and PD-L1, released into the bloodstream, present a non-invasive alternative for biomarker assessment and allows for a more convenient monitoring. Moreover, sPD-1 and sPD-L1 show promise in evaluating the aggressiveness of cancer. The concentrations of these soluble molecules may serve as indicative markers reflecting the tumor

's potential for progression and malignancy [3]. However, despite their potential significance, there is currently limited data available regarding the role of soluble PD-1 and PD L1 in the context of prostate cancer.

This study aims to explore the potential role of soluble PD-1 and PD-L1 as biomarkers for prostate cancer, evaluating their utility in both diagnosis and prognosis. To achieve this, we utilized a control group of 41 healthy male individuals and 88 prostate cancer patients determining their blood plasma concentrations of sPD-1 and sPD-L1 through a sandwich-type ELISA. The immunophenotype of prostate cancer patients, consisting of lymphocytes (different types of T cells, B cells, and natural killer (NK) cells), granulocytes, monocytes, and myeloid-derived suppressor cells (MDSC) was identified using immunostaining and flow cytometry techniques.

Our study findings indicate elevated blood plasma concentrations of sPD-1 and sPD-L1 in prostate cancer patients compared to healthy controls. Notably, we observe a significant correlation between increased sPD-L1 levels and higher Gleason scores. Additionally, there is improved disease-free survival within the patient group characterized by a low sPD-1/sPD-L1 ratio. Furthermore, concentrations of sPD 1 show a weak positive correlation with a higher percentage of immunosuppressive granulocytic and monocytic MDSC. These results underscore the potential of sPD-L1 and sPD-1 as a promising prognostic markers in prostate cancer.

[1] Han Y, Liu D, Li L. PD-1 and PD-L1 pathway: current researches in cancer. *Am J Cancer Res*. 2020.

[2] Vranic S, Gatalica Z. PD-L1 testing by immunohistochemistry in immuno-oncology. *Biomol Biomed*. 2023.

[3] Zhu X, Lang J. Soluble PD-1 and PD-L1: predictive and prognostic significance in cancer. *Oncotarget*. 2017.

ISOLATION AND EVALUATION OF MICROPLASTICS EXTRACTED FROM SEWAGE SLUDGE

Dovilė Motiejauskaitė¹, Karolina Barčauskaitė¹

¹Lithuanian Research Centre for Agriculture and Forestry, Institute of Agriculture Instituto Al. 1, Akademija, Kėdainiai distr, Lithuania
dovile.motiejauskaite@lammc.lt

Plastic is inseparable from everyday life. Being cheap, durable, light and easy to form, plastic has practically an unlimited number of possible applications. Despite the great joy of the industry, the public is facing an unexpected problem - plastic pollution. One of the biggest pollutants is microplastics (MP) – small synthetic water-insoluble solid particles ranging in size from 1µm to 5 mm[1]. It is of increasing concern due to the ecotoxicological risks it poses to aquatic and soil organisms and humans. MP research has gained more attention only in the last decade, but there is still no standardized methodology for its isolation and identification. Most of the research conducted so far focuses on water bodies and its organisms[3]. Nevertheless, microplastics in soil are a major problem, and due to the growing use of sewage sludge in agriculture, it is increasing.

Sewage sludge is a soil conditioner rich in organic matter and nutrients. In North America and Europe, about 50% of the generated sewage sludge is incorporated into the soil. However, despite its beneficial properties, sewage sludge, due to its poor treatment, accumulates many substances harmful to the environment – including MP[4]. There are very few studies covering MP in sewage sludge, and their comparability is poor due to the different methodology used. Therefore, it is extremely important to refine the methodology for the isolation of MP from highly complex matrixes, and to discover a fast and efficient method for its identification. Accordingly, the goal of this study was to determine the most effective conditions of the extraction method and to evaluate the quality of the isolated microplastics.

Sewage sludge was collected from a WWTP in Kaunas, Lithuania. Standard microplastic particles: polyamide, polypropylene, polyethylene – low and high density, were used. In case to remove organic matter (OM) from sewage sludge Fenton's reagent were used. Aqueous iron (II) sulfate solution concentration, reaction time, temperature, and the ratio of hydrogen peroxide to iron (II) sulfate solution were simulated to determine the optimal conditions. Electric stirrer were used to keep a constant temperature and mixing speed at 500rpm. After that, the sample was dried at 105 °C, burned for 4 hours at a temperature of 550 °C, and the OM removal efficiency was calculated. From the tests performed, the 5 best performing methods were selected and evaluated their impact on standard microplastic particles. Using the best-established method, microplastics were isolated from sewage sludge and their qualitative characteristics: size, shape and color were analyzed using a stereomicroscope. In order to evaluate the movement of microplastic in the environment density separation were performed using sodium bromide and distilled water.

The research results will be presented in a poster during the conference.

[1] R. Ahmed, A. K. Hamid, S. A. Krebsbach, J. He, and D. Wang, Critical review of microplastics removal from the environment, 2022

[2] A. L. Lusher, R. Hurley, C. Vogelsang, L. Nizzetto, and M. Olsen, Mapping microplastics in sludge, 55, 2017

[3] M. Dilara, H. Glu, and F. D. Sanin, Sewage sludge as a source of microplastics in the environment: A review of occurrence and fate during sludge treatment, J Environ Manage, vol. 295, p. 113028, 2021

METAGENOMIC ANALYSIS OF THE MICROBIOME COMPOSITION OF APHIDS ADELGES (APHRASTASIA) PECTINATAE (HEMIPTERA: ADELGIDAE)

Gustė Tamošiūnaitė¹, Jekaterina Havelka², Nomeda Kuisienė¹

¹Department of Microbiology and Biotechnology, Institute of Biosciences, Life Sciences Center, Vilnius University, Vilnius, Lithuania

²Department of Zoology, Institute of Biosciences, Life Sciences Center, Vilnius University, Vilnius, Lithuania
guste.tamosiunaite@gmc.stud.vu.lt

Aphids of the genus *Adelges* Vallot, 1836 are insects that feed by phloem sap sucking on host plant species of the conifer family Pinaceae, posing significant threats as pests. Bacteriocyte endosymbionts play a crucial role in the biology and ecology of these insects, residing within the host organism and participating in mutualistic relationships. Two classes of symbiotic bacteria are known in *Adelges* species: Betaproteobacteria and Gammaproteobacteria. In order to profile these symbiotic bacteria, total DNA was extracted from *Adelges* (*Aphrastasia*) *pectinatae* (Cholodkovsky, 1888) specimens, and subjected to next generation sequencing of 16S rRNA gene amplicon. Amplicon-based metagenomics targeted V3-V4 variable regions of bacterial 16S rRNA gene. It was determined that the representatives of the phylum Pseudomonadota were the most abundant (93.1% of all sequences) in the microbiome of *A. (A.) pectinatae*. 16S rRNA gene sequences of Gammaproteobacteria constituted 76.7% of all sequences, while only 0.3% of all sequences have been assigned to Betaproteobacteria. Unexpectedly, a significant portion of the analyzed sequences have been found to belong to the class Alphaproteobacteria in the phylum Pseudomonadota, namely to the orders Hyphomicrobiales (prev. Rhizobiales) (9.0% of all sequences) and Sphingomonadales (5.3% of all sequences). To the best of our knowledge, this is the first report about the quite abundant representatives of Alphaproteobacteria in the microbiome of aphids. Further analysis is needed to determine the role of these bacteria in the microbiome of *A. (A.) pectinatae*.

MOLECULAR DETECTION OF *BORRELIA* SPP. IN RED SQUIRREL (*SCIURUS VULGARIS*)

Ugnė Medikaitė¹, Indrė Lipatova¹, Justina Snegiriovaite¹, Jana Radzijeuskaja¹, Algimantas Paulauskas¹

¹Vytautas Magnus University
ugne.medikaite@vdu.lt

Lyme disease, caused by the spirochete bacteria *Borrelia burgdorferi* s.l., has emerged as a significant global health concern [1]. The incidence of Lyme disease has been increasing over the past few decades due to factors such as climate change, land-use patterns, and increasing migration of bacteria hosts and ticks [2]. The disease is most commonly reported in North America and Europe. High incidence rates have been recorded in Germany, Austria, Slovenia and Lithuania [3-5]. It is important to find out whether *Sciurus vulgaris* could be an important reservoir host of *Borrelia burgdorferi* s.l., as this wild rodent is also commonly found in peri-urban and urban areas and is constantly exposed to ticks as it moves through the ground. This study aimed to detect the presence of *Borrelia* spp. in red squirrels collected from the parks of Kaunas city. A total of 44 samples of red squirrel were tested by real-time PCR with the specific primers for *Borrelia*. Samples positive for *Borrelia* DNA were further analysed using a PCR targeting the *ospA* gene. Positive PCR products were selected for DNA sequencing. *Borrelia* species were detected in 31.8% (14/44) of squirrels. The pathogens were mostly found in the ear and lung tissues. The results of the study provide insight into the influence of squirrels on the spread of Lyme disease causative agents in urbanised areas.

ACKNOWLEDGMENTS. Part of this research was funded by European Social Fund under grant agreement P-ST-23-264 with the Research Council of Lithuania.

-
- [1] Radolf JD, Strle K, Lemieux JE, Strle F. Lyme Disease in Humans. *Curr Issues Mol Biol.* 2021;42:333-384.
 [2] Septfons A, Figoni J, Gautier A, Soullier N, de Valk H, Desenclos JC. Increased awareness and knowledge of Lyme Borreliosis and tick bite prevention among the general population in France: 2016 and 2019 health barometer survey. *BMC Public Health.* 2021;21:1808.
 [3] Marques AR, Strle F, Wormser GP. Comparison of Lyme Disease in the United States and Europe. *Emerg Infect Dis.* 2021;27(8):2017-2024.
 [4] Tilly K, Rosa PA, Stewart PE. Biology of infection with *Borrelia burgdorferi*. *Infect Dis Clin North Am.* 2008;22(2):217-v
 [5] WHO Regional Office for Europe and European Centre for Disease Prevention and Control. Lyme Borreliosis in Europe. WHO Regional Office for Europe in European Centre for Disease Prevention and Control. 2021

STUDY OF SOIL HEAVY METAL POLLUTION IMPACT ON THE ONION (*ALLIUM CEPA* L.) CIRCADIAN RHYTHM

Goda Petraitytė¹, Asta Stapulionytė²

¹Institute of Biosciences, Life Sciences Center, Vilnius University, Lithuania
goda.petraityte@gmc.stud.vu.lt

Soil is a loose, thin layer of the Earth's crust that is made up of organic matter, mineral matter, air, water and living organisms. However, in recent times, soil-related problems have grown up and become a serious problem around the world. Heavy metals are considered one of the most common soil pollutants, including cadmium (Cd), chromium (Cr), mercury (Hg), lead (Pb), copper (Cu), zinc (Zn), etc. Heavy metal contamination is characterized by its biological toxicity, wide distribution, and long-lasting presence in the soil [1]. The pollution caused by heavy metals restricts plant growth by affecting various aspects of the plant system, including seed germination, physiological processes, as well as genetic and biochemical elements [2].

For a plant to grow without harming its system, an endogenous regulatory network and mechanism are necessary. To achieve these objectives, plants utilize a circadian clock to anticipate daily changes. Circadian regulation is characterized by the crucial adaptation of plants to their changing environment. The circadian rhythm serves as a guide to regulate metabolic pathways and developmental processes in plants [3].

In this research, the common onion (*Allium cepa* L.) is employed as a standard model plant for circadian rhythm studies, owing to its simplicity and wide applicability in cytogenetic research. We aim to contribute to a better understanding of the impact of soil heavy metal pollution on plant growth by analyzing *Allium* circadian rhythm under heavy metal stress.

-
- [1] Zhao, H., Wu, Y., Lan, X., Yang, Y., Wu, X., & Du, L. (2022). Comprehensive assessment of harmful heavy metals in contaminated soil in order to score pollution level. *Scientific Reports*, 12(1). <https://doi.org/10.1038/s41598-022-07602-9>
- [2] Kiran, K., Bharti, R., & Sharma, R. (2022). Effect of heavy metals: An overview. *Materials Today: Proceedings*, 51, 880–885. <https://doi.org/10.1016/j.matpr.2021.06.278>
- [3] Venkat, A., & Muneer, S. (2022). Role of circadian rhythms in major plant metabolic and signaling pathways. *Frontiers in Plant Science*, 13. <https://doi.org/10.3389/fpls.2022.836244>

MICRORNA SIGNATURES AS PREDICTIVE TOOLS FOR NEOADJUVANT CHEMOTHERAPY RESPONSES IN TNBC

Domas Štītis^{1,3}, Adomas Vasiliauskas³, Linas Kunigėnas¹, Monika Drobniėnė^{1,2}, Eglė Strainienė^{1,3}, Kęstutis Sužiedėlis^{1,2}

¹National Cancer Institute

²Life Sciences Center

³Vilnius Gediminas Technical University
domas.stitis@gmail.com

Breast cancer is the most common type of cancer among women. Triple-negative breast cancer (TNBC) is a subtype that is particularly aggressive and has limited treatment options, resulting in poor outcomes. This study focuses on the role of specific miRNAs in the progression of triple-negative breast cancer. Bioinformatics analysis of The Cancer Genome Atlas (TCGA) data identified 195 miRNAs that impact 57 genes associated with resistance to platinum-based therapies. Thus, we selected a subset of miRNAs and determined their expression levels through RT-PCR in triple-negative breast cancer (TNBC) patient samples, both before and after neoadjuvant therapy. Finally, the patients were stratified into a high-risk group and a low-risk group according to the median expression level of each miRNA.

INVESTIGATION OF CHANGES IN OXIDATIVE STRESS BIOMARKERS: CATALASE ACTIVITY AND METALLOTHIONEIN LEVELS IN THE LIVER OF RAINBOW TROUT (*ONCORHYNCHUS MYKISS*) AFTER EXPOSURE TO MICROPLASTIC PELLETS

Vita Žvynakytė^{1,2}, Janina Pažusienė², Gintarė Sauliūtė², Milda Stankevičiūtė²

¹Vilnius University, Lithuania

²Laboratory of Ecotoxicology, Nature Research Centre, Lithuania
vita.zvynakyte@gmc.stud.vu.lt

Microplastics (MPs) pollution is one of the primary environmental challenges nowadays, although MPs were observed in the ecosystem almost 50 years ago [1]. Understanding the environmental impact of microplastics is very challenging as MPs have different physicochemical properties that make MPs multifaceted stressors [2]. It is known that MPs can cause changes in immune-related gene expression, antioxidant enzymes as well as antioxidant status in fish [2, 3]. In ecotoxicological studies antioxidant enzymes, metallothioneins are often chosen as biomarkers of oxidative stress, which reflect the response to environmental changes in fish [4].

The aim of this study was to determine the changes in catalase (CAT) activity and metallothionein (MT) level in the liver of rainbow trout (*Oncorhynchus mykiss*) after long-term exposure to different types of polymeric microplastic pellets. In homogenized liver of fish MT levels were determined according to the method of Viarengo et al. (1997) as modified by Peixoto et al. (2003). Catalase activity was measured according to Koroliuk et al. (1988) and Hadwan and Abed (2016) methods.

The experiment results showed a significant decrease in CAT activity in *O. mykiss* liver after exposure to the low-density polyethylene (LDPE) compared to the control (CTRL) group. In LDPE group also showed a significant decrease in CAT activity compared to the high-density polyethylene and polystyrene (PS) groups. Metallothionein level significantly decreased after exposure to LDPE and PS microplastic compared to the CTRL group. Initial analysis showed that the different types of MPs pellets induce CAT activity and MT level changes in rainbow trout. For this reason, it is important to continue the studies on oxidative stress biomarkers with the goal to characterise the harmful effects of microplastics on fish.

Acknowledgement

Study was funded by the Research Council of Lithuania through the project S-MIP-22-51, ARFA.

[1] M. Fiore, et al. Tackling Marine Microplastics Pollution: an Overview of Existing Solutions. *Water Air Soil Pollut* 233, 276 (2022)

[2] S. Yedier, S. K. Yalçınkaya, D. Bostancı, Exposure to polypropylene microplastics via diet and water induces oxidative stress in *Cyprinus carpio*. *Aquatic Toxicology* 259, 106540 (2023)

[3] Md. S. Bhuyan, Effects of Microplastics on Fish and in Human Health. *Frontiers in Environmental Science* 10, (2022)

[4] C. Campanale, C. Massarelli, I. Savino, V. Locaputo, ir V. F. Uricchio, A Detailed Review Study on Potential Effects of Microplastics and Additives of Concern on Human Health, *Int J Environ Res Public Health* (2020)

URBAN MICROBIOLOGY OF VILNIUS. BACTERIAL DIVERSITY IN STREET GREENERY

Viktorija Kalasinskaitė¹, Nomeda Kuisienė¹

¹Department of Microbiology and Biotechnology, Institute of Biosciences, Life Sciences Center, Vilnius University, Vilnius, Lithuania

viktorija.kalasinskaite@gmc.stud.vu.lt

Urban microbiology is a field of study that explores urban microorganism communities, their diversity, distribution, and functions in their habitat, as well as interactions with humans, animals, and plants. Like the human microbiome consists of microbial consortia inhabiting regions throughout the body, urban microbiomes are a collection of microbial communities that occupy diverse reservoirs throughout city landscapes, from the depths of sewers to the tops of buildings (Madeline Barron, 2021). Green infrastructure features have been built in urban areas as elements providing a range of benefits, e.g., processes that are mediated by microorganisms that improve air and water quality, in addition to the interactions with plant and tree rhizospheres. Investigation of microbiomes of the urban green infrastructure is one of the most important areas in urban microbiology research. In current study we present metagenomic urban microbiome analysis from 4 different locations of Vilnius. The objective of this study was to characterize the bacterial diversity of the street greenery in the streets of different activity. We have collected soil as well as wood chips samples from pedestrian and bicycle paths that are close or relatively close to the road from Shevchenkos, Gerosios vilties, Baltupiu and Antakalnio streets in Vilnius. We found that greenways in different streets have diverse bacterial communities, that were not associated with geographic locations. The most abundant bacterial phyla across all samples were Pseudomonadota, Actinobacteriota, Bacteroidota, and Acidobacteriota. The highest diversity across all samples has been determined in classes of Alphaproteobacteria, Actinobacteria, Gammaproteobacteria, and Bacteroidia. Unculturable bacteria have been detected in all samples. These Candidatus bacteria are commonly found in water deposits or water sediments samples and are known to belong to the phyla Pseudomonadota, Chloroflexota, and Acidobacteriota.

THE ROLE OF CAPSULAR POLYSACCHARIDES AND OUTER MEMBRANE VESICLES IN THE PATHOGENESIS OF OPPORTUNISTIC PATHOGEN ACINETOBACTER BAUMANNII

Meda Skinkytė¹, Laurita Klimkaitė¹, Jūratė Skerniškytė¹

¹Institute of Biosciences, Life Sciences Center, Vilnius University, Vilnius, Lithuania
meda.skinkyte@gmc.stud.vu.lt

Acinetobacter baumannii is considered one of the most crucial opportunistic pathogens, causing various medical-related infections worldwide. It commonly presents resistance to multiple antimicrobial agents, and hence, it is considered as a multidrug-resistant [1]. This opportunistic pathogen possesses multiple virulence factors, which contribute to the bacterial survival during the stress. *A. baumannii* ability to form biofilms on abiotic surfaces, such as catheters and endotracheal tubes, poses a great threat to the immunocompromised patients, therefore a better insight into *A. baumannii* pathogenesis could enhance the treatment of such individuals. Bacteria in biofilms can be 10–1,000 times less susceptible to various antimicrobial agents compared to planktonic bacteria [2]. The goal of this research is to investigate the impact of capsular polysaccharides and outer membrane vesicles produced by clinical *A. baumannii* isolates on biofilm formation and resistance under stress conditions, such as exposure to antimicrobial agents. The virulence properties of *A. baumannii* isolates and their $\Delta galU$ and $\Delta ompA$ mutants were assessed in this research. The deletion of *galU* gene provides capsule-less phenotype, whereas *ompA* knockout leads to a hyperproduction of outer membrane vesicles. Biofilm formation was evaluated by crystal violet staining, which revealed significant differences between mutant and wild-type isolates. The ability of various antimicrobial compounds to inhibit *A. baumannii* biofilms was tested. The results showed that the resistance of mutant isolates' biofilms was compromised in most cases compared to their wild-type isolates. Quantitative analysis demonstrated, that capsule production can alter the survival of *A. baumannii* in biofilms after exposure to antimicrobial agents.

[1] Michalopoulos, A. and Falagas, M. E. (2010). Treatment of Acinetobacter infections. Expert opinion on pharmacotherapy, 11(5), 779-788.
[2] Davies, D. (2003). Understanding biofilm resistance to antibacterial agents. Nature Reviews Drug Discovery 2, 114-122.

ANALYSIS OF PUTATIVE BETA-LACTAMASES FROM OPPORTUNISTIC PATHOGEN *STENOTROPHOMONAS MALTOPHILIA*

Edvard Romanovski¹, Laurita Klimkaitė¹, Ignas Ragaišis¹, Julija Armalytė¹

¹Institute of Biosciences, Department of Biochemistry and Molecular Biology, Life Sciences Center, Vilnius University, Lithuania
edvard.romanovski@gmc.stud.vu.lt

In recent decades rapidly increasing bacteria resistance to commonly used antibiotics has become an urgent healthcare challenge, especially affecting individuals with compromised immune system [1]. Opportunistic multidrug-resistant gram-negative bacterium *Stenotrophomonas maltophilia* has gained prominence due to challenging infections and resistance to commonly used antibiotics. Although *S. maltophilia* resistance to clinically important beta-lactam antibiotics is well-observed, only two beta-lactamases L1 and L2 are currently documented and described [2]. Initial research of beta-lactam resistant *S. maltophilia* SM3 strain indicated that other previously undescribed genes might code beta-lactamases.

The aim of this study is to analyse putative *S. maltophilia* beta-lactamases and evaluate their enzymatic activity. Putative beta-lactamases were bioinformatically analysed using Beta-Lactamase DataBase [3]. In order to test selected putative beta-lactamases function, analysed genes will be cloned into expression plasmid, functional activity will be examined in *Escherichia coli* expression strain using beta-lactamase activity specific nitrocefin test.

The bioinformatic analysis showed that ten analysed proteins are homologous to known beta-lactamases, proteins identity reaching 24.8% to 29.5%. The methodology for detecting enzymatic beta-lactamase activity was successfully tested on a known beta-lactamase L1 and functional activity of remaining putative beta-lactamases will be evaluated using the same approach.

[1] Antimicrobial Resistance Collaborators. (2022). Global burden of bacterial antimicrobial resistance in 2019: a systematic analysis. *The Lancet*; 399(10325): P629-655.

[2] Lin et al. (2009). The role of AmpR in regulation of L1 and L2 beta-lactamases in *Stenotrophomonas maltophilia*. *Research in Microbiology*, 160(2), 152–158.

[3] Naas et al., Beta-Lactamase DataBase (BLDB) - Structure and Function. *J. Enzyme Inhib. Med. Chem.* 2017, 32, 917-919.

THE IMPACT OF ELECTRIC FIELD-BASED ANTICANCER METHODS ON CELL VIABILITY WHEN 2D AND 3D CELL CULTURE MODELS ARE USED

Gabija Andreikė¹, Neringa Barauskaitė-Šarkiniene¹, Vitalij Novickij², Paulius Ruzgys¹

¹Faculty of Natural Sciences, Vytautas Magnus University, Kaunas, Lithuania

²VilniusTech, Naugarduko g. 41, 03227 Vilnius

gabija.andreike@vdu.lt

According to the World Health Organization, in 2020, 10 million people died from cancer. Therefore, there is a significant focus on improving treatment technologies and increasing the effectiveness of anticancer therapies in the scientific research field. One such technique is anticancer therapy involving the higher transfer of anticancer drugs to cancer cells affected by electric fields. This therapy is based on the process of electroporation, where the plasma membrane of a cell becomes temporarily permeable to hydrophilic molecules that normally cannot enter the cell. Electroporation occurs when an electric field increases the transmembrane potential of the affected cell to a poration threshold level. If the transmembrane potential is not too far from the threshold the reversible electroporation is obtained, hence cells do not die via necrosis. Nevertheless, the reversible electroporation is enough for anticancer drugs (e.g., bleomycin) to be delivered into the cell, leading to localized apoptotic cell death. This combination of applications to the cells to achieve cancer cell death is termed electrochemotherapy (ECT). Quite recently an alternative to bleomycin was proposed in ECT. Such alternative is Calcium ions that regulate many cellular functions, such as exocytosis, metabolism, gene expression, and the cell cycle. Apparently, once high enough concentrations of Calcium ions enter the cell with the help of electric fields the apoptotic cell death is triggered.

Another electric field-based method is irreversible electroporation (IE). The main difference is that if induced transmembrane potential greatly exceeds the electroporation threshold level, thus cells die due to the immense disruption of homeostasis. Alongside the ECT the IE is also considered as a good alternative to the conventional cancer treatment methods.

The majority of new anticancer therapy methods are being researched using a monolayer cell model (two-dimensional cell cultures). Unfortunately, such models often are too simplistic and do not permit observation of processes specific to more complex cancer tissue structures. This is why three-dimensional (3D) spheroid cell cultures are used. Such spheroids serve as an intermediate model between monolayer cell cultures and *in vivo* studies and can be an alternative to animal experiments. Although 3D cell cultures have been used more intensively in recent years, there are still too few studies to determine the effectiveness of electric field-based anticancer therapies. Therefore, the aim is to compare the impact of electric field-based anticancer methods on cell viability with 2D and 3D spheroid models.

Acknowledgment Nr. S-MIP-23-124 project.

PHYTOCHEMICAL ANALYSIS OF BEE POLLEN IN IMPACT OF DIFFERENT STORAGE CONDITIONS AND DURATION

Rosita Stebuliauskaitė¹, Sonata Trumbeckaitė¹, Mindaugas Liaudanskas^{1,2}, Vaidotas Žvikas², Neringa Sutkevičienė³

¹Department of Pharmacognosy, Faculty of Pharmacy, Lithuanian University of Health Sciences, Kaunas, Lithuania

²Institute of Pharmaceutical Technologies, Faculty of Pharmacy, Lithuanian University of Health Sciences, Kaunas, Lithuania

³Animal Reproduction Laboratory, Large Animal Clinic, Faculty of Veterinary Medicine, Kaunas, Lithuania
rosita.stebuliauskaite@stud.lsmu.lt

Background. Bioactive compounds found in bee pollen (BP) are essential for human health. Health benefits are related to unique chemical composition of BP. BP may be used as fresh and dried. Since the therapeutic effects depend on the quality of BP, preparation and storage conditions of BP are of great importance, as it may affect amount of bioactive compounds [1,2].

The aim. The aim of this study was to evaluate the influence of storage conditions and duration on amino acids (AA) amount, total phenolic content (TPC), total flavonoid content (TFC), as well as on the in vitro antioxidant activity of BP.

Methods. BP were collected from the apiary, Pasvalio district, Talkoniai (55.9598°N, 24.3422°E). Samples were dried or fresh-frozen (at -20°C or -80°C). TPC was evaluated by Folin-Ciocalteu method [2]. The reaction with AlCl₃ was used to determine the flavonoid content [3]. Antioxidant activity was evaluated by ABTS method [3]. Qualitative and quantitative analysis of AA was evaluated by UHPLC-MS/MS method [4]. Tests were carried out every 3 months (total duration of the study – 15 months). Means and standards deviations were calculated with SPSS 20.0.

Results. TPC, TFC and antioxidant activity were not affected up to 6 months of storage in dried and up to 9 months in frozen BP, but further decreased with storage time. After 15 months TPC in frozen (at -20°C and -80°C) BP decreased by 1.9 and by 1.5 times meanwhile in dried BP decreased by 2.5 times ($p < 0.05$). TFC in dried BP decreased by 3.1 times and in frozen BP by 1.9 and 1.7 times, respectively ($p < 0.05$). The antioxidant activity in vitro was decreased by 65% in dried BP after 15 months as compared to control. Frozen BP were much less affected ($p < 0.05$). After analysis, 17 AA were detected in both, dried and frozen BP. All of AA, except for cysteine, were well preserved for 6 months in both, dried and frozen samples. Amount of leucine, isoleucine, valine, histidine and arginine decreased over time in frozen samples, meanwhile amount of glycine, threonine, methionine, tyrosine, alanine and lysine was higher in frozen BP as compared to dried BP. Proline, aspartic acid, phenylalanine, glutamic acid and serine after 15 months storage were well preserved in both, frozen and dried samples.

Conclusions. In conclusion, the total phenolic content, the total flavonoids content, antioxidant activity in dried bee pollen gradually decreased during storage whereas frozen bee pollen were less affected. Quantitative composition of amino acids amount varies depending on storage conditions and duration.

[1] Sawicki T, Starowicz M, Kłębukowska L, Hanus P. The profile of polyphenolic compounds, contents of total phenolics and flavonoids, and antioxidant and antimicrobial properties of bee products. *Molecules*. 2022 Feb 15;27(4):1301.

[2] Anjos O, Paula VB, Delgado T, Estevinho LM. Influence of the storage conditions on the quality of bee pollen. 2019

[3] Chelucci E, Chiellini C, Cavallero A, Gabriele M. Bio-Functional Activities of Tuscan Bee Pollen. *Antioxidants*. 2023 Jan 3;12(1):115.

[4] Ares AM, Toribio L, Tapia JA, González-Porto AV, Higes M, Martín-Hernández R, Bernal J. Differentiation of bee pollen samples according to the apiary of origin and harvesting period based on their amino acid content. *Food Bioscience*. 2022 Dec 1;50:102092.

ESTABLISHMENT AND CHARACTERIZATION OF NEW ENDOMETRIAL CANCER CELL LINES

Aisté Avižaitė¹, Laura Marija Račytė¹, Veronika Dedonytė², Evelina Šidlovskā³, Margarita Montrimaitė⁴, Gediminas Januška⁴, Rūta Čiurlienė⁴, Eglė Žalytė¹

¹Department of Biochemistry and Molecular Biology, Institute of Biosciences, Vilnius University Life Sciences Center, Vilnius, Lithuania

²Department of Botany and Genetics, Institute of Biosciences, Vilnius University Life Sciences Center, Vilnius, Lithuania

³National Center of Pathology, Vilnius, Lithuania

⁴National Cancer Institute, Vilnius, Lithuania

aiste.avizaitė@chgf.stud.vu.lt

Endometrial cancer is the sixth most common cancer in the world, with Lithuania and Poland leading in Europe [1]. Common risk factors of endometrial cancer include older age, hormone therapy, obesity, hyperglycemia, diabetes, and some genetic disorders. Paclitaxel, cisplatin, and carboplatin are the first-line chemotherapy drugs that are used to treat endometrial cancer. However, new targeted therapy agents are constantly under development [2]. Cell lines are standard *in vitro* model systems of cancer. Unfortunately, most of the commercially available endometrial cancer cell lines are derived from the tumors of Asian patients. What is more, established lines that have been cultivated for a long time adapt to an artificial *in vitro* environment and lose their original phenotype due to genetic drift. Finally, each cancer patient and each disease is different and cannot be properly represented by a defined set of cell lines. Thus, we need new cancer cell lines to understand the causes of an increased predisposition to endometrial cancer among European women and to discover new effective treatments.

In this study, we present novel endometrial cancer cell lines, derived in 2023 from the tumor tissue of Lithuanian endometrial cancer patients. We characterized the cells by determining their growth rate, detecting the expression of cancer markers, analyzing colony-forming efficiency, karyotype and cell sensitivity to paclitaxel, cisplatin and carboplatin. We believe that these novel cell lines will be an effective tool for preclinical endometrial cancer studies in the future.

This work was funded by Vilnius University Science Promotion Fund (project no. MSF-JM-17/2022) and Future Biomedicine Fund (project no. (1.78) SU-442).

[1] R.L. Siegel, K.D. Miller, A. Jemal, Cancer statistics, 2020, CA: a cancer journal for clinicians 70(1) (2020) 7-30.

[2] M. Remmerie, V. Janssens, Targeted Therapies in Type II Endometrial Cancers: Too Little, but Not Too Late, International Journal of Molecular Sciences 19(8) (2018) 2380.

THE EFFECT OF MATERNAL HIGH-FAT DIET ON MORPHOLOGY AND INFLAMMATION OF OFFSPRING RETINA

Patricija Čepauskytė¹, Gintarė Urbonaitė¹, Neda Ieva Biliūtė¹, Guoda Laurinavičiūtė², Urtė Neniškytė^{1,3}

¹Institute of Biosciences, Life Sciences Center, Vilnius University, Lithuania

²Institute of Biomedical Sciences, Faculty of Medicine, Vilnius University, Lithuania

³VU-EMBL Partnership Institute, Life Sciences Center, Vilnius University, Lithuania
patricija.cepauskyte@gmc.stud.vu.lt

Aim: The standard diet in today's society consists of increased high fat content which contributes to the rising rates of obesity. Many studies indicate that maternal high-fat diet (mHFD) is the cause of systemic inflammation, potentially resulting in neurodevelopmental disorders of the offspring [1, 2, 3]. Female estrous cycle stages appeared to also have different response to inflammation [4, 5, 6]. In the context of inflammatory conditions, CD68 is used as a microglia activation marker that is often associated with immune cells of the central nervous system, including the retina [7]. Studies have shown that the retina is affected by diet consisting of high fat, however, there's little research done investigating its effects on the offspring retina [8]. This study aims to evaluate area changes of microglia and CD68 in the peripheral retina of mHFD offspring and assess how microglia and CD68 area depend on the stages of the estrous cycle.

Methods: Female C57Bl/6J mice from weaning to lactation were fed with control diet (CD, 10% fat) or high-fat diet (HFD, 60% fat). The offspring were weaned to CD. The eyeballs of the offspring were collected, fixed with 4% PFA, cryoprotected and sliced using cryotome. Microglia and activated microglia cells were labeled immunohistochemically using anti-RFP and anti-CD68 antibodies respectively, while cell nuclei were labeled with DAPI. The estrous cycle stages were determined by vaginal cytology in female offspring on the day of tissue collection (22 weeks old).

Results: We evaluated the area of microglia and CD68 in the peripheral retina and compared the measurements between the groups of offspring. mHFD significantly increased area of microglia and CD68 in female peripheral retina compared to maternal control diet offspring but had no significant effect on male retina. In addition, during evaluation of microglia area and CD68 area in microglia, alterations were observed in female offspring estrous cycle stages due to mHFD.

Conclusion: Our findings showed that mHFD had a gender-specific effect on the area of microglia and CD68 in offspring peripheral retina as well as revealed microglia and CD68 area changes in mHFD female offspring during estrous cycle stages.

Funding: This work was supported by the Science Promotion Fund of Vilnius University.

-
- [1] Maes M, Verkerk R, Bonaccorso S, Ombelet W, Bosmans E, Scharpé S. Depressive and anxiety symptoms in the early puerperium are related to increased degradation of tryptophan into kynurenine, a phenomenon which is related to immune activation. *Life Sci.* 2002 Sep 6;71(16):1837-48. doi: 10.1016/s0024-3205(02)01853-2. PMID: 12175700.
- [2] Oades RD, Myint AM, Dauvermann MR, Schimmelmann BG, Schwarz MJ. Attention-deficit hyperactivity disorder (ADHD) and glial integrity: an exploration of associations of cytokines and kynurenine metabolites with symptoms and attention. *Behav Brain Funct.* 2010 Jun 9;6:32. doi: 10.1186/1744-9081-6-32. PMID: 20534153; PMCID: PMC2900218.
- [3] Kang SS, Kurti A, Fair DA, Fryer JD. Dietary intervention rescues maternal obesity induced behavior deficits and neuroinflammation in offspring. *J Neuroinflammation.* 2014 Sep 12;11:156. doi: 10.1186/s12974-014-0156-9. PMID: 25212412; PMCID: PMC4172780.
- [4] Villa A, Vegeto E, Poletti A, Maggi A. Estrogens, Neuroinflammation, and Neurodegeneration. *Endocr Rev.* 2016 Aug;37(4):372-402. doi: 10.1210/er.2016-1007. Epub 2016 May 19. PMID: 27196727; PMCID: PMC4971309.
- [5] Chang RC, Shi L, Huang CC, Kim AJ, Ko ML, Zhou B, Ko GY. High-Fat Diet-Induced Retinal Dysfunction. *Invest Ophthalmol Vis Sci.* 2015 Apr;56(4):2367-80. doi: 10.1167/iovs.14-16143. PMID: 25788653; PMCID: PMC4407693.
- [6] Lee JJ, Wang PW, Yang IH, Huang HM, Chang CS, Wu CL, Chuang JH. High-fat diet induces toll-like receptor 4-dependent macrophage/microglial cell activation and retinal impairment. *Invest Ophthalmol Vis Sci.* 2015 May;56(5):3041-50. doi: 10.1167/iovs.15-16504. PMID: 26024088.
- [7] Choudhary M, Malek G. CD68: Potential Contributor to Inflammation and RPE Cell Dystrophy. *Adv Exp Med Biol.* 2023;1415:207-213.
- [8] Clarkon-Townsend DA, Douglass AJ, Singh A, Allen RS, Uwaifo IN, Pardue MT. Impacts of high fat diet on ocular outcomes in rodent models of visual disease. *Exp Eye Res.* 2021 Mar;204:108440. doi: 10.1016/j.exer.2021.108440. Epub 2021 Jan 11. PMID: 33444582; PMCID: PMC7946735.

FUNCTIONAL ANALYSIS OF HISTONE METHYLATION REGULATORY GENES IN PROSTATE CANCER CELL LINES

Marta Tamosiunaite¹, Ruta Maleckaite¹, Kristina Daniunaite¹

¹Institute of Biosciences, Life Sciences Center, Vilnius University, Vilnius, Lithuania
marta.tamosiunaite@gmc.stud.vu.lt

Prostate cancer (PCa) is the most commonly diagnosed malignancy in Europe and the 3rd leading cause of cancer related death among men [1]. The progression of this disease is known to be associated with various epigenetic mechanisms, one of them being gene expression alterations by microRNAs (miRNAs) [2]. They are small, non-coding RNAs which bind to their target mRNAs and decrease gene expression at the post-transcriptional level [3]. Understanding interactions between specific miRNAs and their target genes would help to find novel ways to treat PCa earlier.

In the present study, we focused on histone methylation regulating (HM) genes as potential miRNA targets. Nine HM genes were selected for the analysis based on our previous PCa studies [4; *Maleckaite et al., unpublished data*]. Based on the database search results, potential regulatory miRNAs of the HM genes were identified and the hypothesized regulatory network was created. After evaluating baseline miRNA and HM gene expression levels, two miRNAs – *miR-27a* and *miR-29a* – were selected for loss-of-function *in vitro* experiments in the PC-3 cell line.

Based on the formed miRNA-HM gene regulatory network, *miR-27a* had four potential targets (*KDM1A*, *KDM3A*, *KDM4B*, and *KDM5B*) and *miR-29a* – five targets (*KDM5A*, *KDM5B*, *KDM5D*, *KMT1E*, and *KMT5A*) with one overlapping gene. According to the preliminary data, inhibition of *miR-27a* resulted in increased expression of *KDM4B* and *KDM5B* as expected, while inhibition of *miR-29a* induced upregulation of all its targets except *KDM5D*. Surprisingly, inhibitors of both miRNAs caused downregulation of *KDM3A* indicating a more complex way of HM gene regulation mechanism.

In conclusion, our preliminary data revealed *miR-27a* and *miR-29a* as potential regulators of specific HM genes in PCa. Further experiments would follow to validate these findings, as well as to evaluate cellular effects of the inhibition of the two miRNAs. Satisfying results would lay the basis for the use of *miR-27a* and *miR-29a* inhibitors as prospective PCa therapeutics in the future.

[1] The European Cancer Information System (ECIS) (2023). Cancer cases and deaths on the rise in the EU. European Union. https://joint-research-centre.ec.europa.eu/jrc-news-and-updates/cancer-cases-and-deaths-rise-eu-2023-10-02_en

[2] Suzuki, H., Maruyama, R., Yamamoto, E., & Kai, M. (2012). DNA methylation and microRNA dysregulation in cancer. *Molecular Oncology*, 6(6), 567–578.

[3] Carthew, R. W., & Sontheimer, E. J. (2009). Origins and Mechanisms of miRNAs and siRNAs. *Cell*, 136(4), 642–655.

[4] Daniunaite, K., Dubikaityte, M., Gibas, P., Bakavicius, A., Rimantas Lazutka, J., Ulys, A., Jankevicius, F., & Jarmalaite, S. (2017). Clinical significance of miRNA host gene promoter methylation in prostate cancer. *Human Molecular Genetics*, 26(13), 2451–2461.

INVESTIGATION OF MITOCHONDRIAL NETWORK IN KERATINOCYTES WITH PSORIATIC PHENOTYPE

Martyna Ulduky¹, Gabrielė Kulkovienė^{1,2}, Zbigniew Balion³, Ramunė Morkūnienė¹, Aistė Jekabsone^{2,3}

¹Department of Drug Chemistry, Faculty of Pharmacy, Lithuanian University of Health and Sciences, Kaunas, Lithuania

²Laboratory of Pharmaceutical Sciences Institute of Pharmaceutical Technologies, Lithuanian University of Health and Sciences, Kaunas, Lithuania

³Preclinical Research Laboratory for Medicinal Products Institute of Cardiology, Lithuanian University of Health and Sciences, Kaunas, Lithuania
martyna.uldukyte@stud.lsmu.lt

Psoriasis is an inflammatory skin disease whose pathogenesis is driven by IL-17, IL-22, and TNF- α , which potently activate keratinocytes, causing hyperproliferation and abnormal differentiation [1]. Adaptive responses to psoriasis involve alterations in mitochondrial morphology, reflecting dynamic cellular adaptation based on external stimuli [2]. Therefore, mitochondrial dysfunction leads to inflammation and potential damage to the cell [3].

This study aims to investigate how the morphology of mitochondria in human keratinocytes (HaCaT) is affected by individual cytokines (IL-17, IL-22, and TNF- α) and cytokine mixture with 1, 3, and 24-hour stimulation time.

Two study groups of keratinocytes included treatment of individual cytokines and cytokine mixture. Mitochondrial morphology was analyzed using Live Mito Orange, STED nanoscopy, and fluorescence microscopy with Zeiss Axio Observer.Z1. A quantitative analysis of mitochondrial morphology was performed with the mitochondrial network analysis toolset (MiNA) in Fiji [4].

Cytokine mixture reduced mitochondrial area, branch lengths, and number of network branches, which is characteristic of mitochondrial fragmentation. Analysis of the impact of specific cytokines revealed IL-22 and TNF- α as the primary effectors in changing mitochondrial morphology. However, the cytokine mixture caused more pronounced changes, suggesting synergistic effects, that amplify the loss of network integrity. Furthermore, the most significant changes were seen after 1 hour of incubation, and although a significant decrease persisted after 24 hours, the trend indicated a restoration toward the baseline level.

The study results show that psoriatic phenotype-inducing cytokines cause the fragmentation of mitochondria in keratinocytes, where IL-22 and TNF- α play a crucial role. Further investigation of mitochondrial changes occurring in psoriasis under inflammatory conditions can offer valuable insights into the disease's pathogenesis.

[1] C. E. M. Griffiths, A. W. Armstrong, J. E. Gudjonsson et al., Psoriasis. *The Lancet*. 397, 1301-1315 (2021).

[2] C. A. Galloway, H. Lee, Y. Yoon, Mitochondrial morphology - emerging role in bioenergetics. *Free Radical Biology and Medicine*. 53, 2218-2228 (2012).

[3] J. van Horssen, P. van Schaik, M. Witte, Inflammation and mitochondrial dysfunction: A vicious circle in neurodegenerative disorders. *Neuroscience Letters*. 710, 132931 (2019).

[4] A. J. Valente, L. A. Maddalena, E. L. Robb et al., A simple ImageJ macro tool for analyzing mitochondrial network morphology in mammalian cell culture. *Acta Histochemica*. 119, 315-326 (2017).

OPTIMISATION OF THE EXTRACTION OF PHENOLIC COMPOUNDS FROM PLUM (PRUNUS DOMESTICA L.) FRUIT MESOCARPS USING RESPONSE SURFACE METHODOLOGY

Gabrielė Bočkutė¹, Mindaugas Liaudanskas^{1,2}, Kristina Zymonė^{1,3}, Jonas Viškelis⁴, Juozas Lanauskas⁴

¹Institute of Pharmaceutical Technologies, Faculty of Pharmacy, Lithuanian University of Health Sciences, Kaunas, Lithuania

²Department of Pharmacognosy, Faculty of Pharmacy, Lithuanian University of Health Sciences, Kaunas, Lithuania

³Department of Analytical and Toxicological Chemistry, Faculty of Pharmacy, Lithuanian University of Health Sciences, Kaunas, Lithuania

⁴Institute of Horticulture, Lithuanian Research Centre for Agriculture and Forestry, Babtai, Kaunas distr., Lithuania
gabriele.bockute@stud.lsmu.lt

Plums contain significant amounts of biologically active compounds which have hypoglycemic, laxative, hypotensive and hepatoprotective activity. Plums have large amounts of phenolic compounds, mainly neochlorogenic and chlorogenic acids, which may contribute to the laxative action and delay glucose absorption [1]. Extraction is the first and very important step of analytical determination of phenolic compounds, which plays a decisive role in the final result. Qualitative and quantitative studies of bioactive compounds from plant materials mainly depend on the selection of an appropriate extraction conditions [2].

The ultrasound-assisted extraction of phenolic compounds from plum samples was modelled using response surface methodology. A three-level-three-factor central composite design using the response surface methodology was employed to optimise three extraction variables, including ethanol concentration, extraction time and ultrasonic power, for the achievement of the highest extraction yield of the phenolic compounds from lyophilised plum samples. Six replicates were used to evaluate the pure error. Experimental data showed that response variables were fitted to a linear model. "Design-Expert® 6.0.8" software (Stat-Ease Inc., Minneapolis, Minnesota, USA) was used to analyse the data, develop models and optimise the extraction conditions. The total phenolic content was determined using Folin–Ciocâlțeu spectrophotometric assay and expressed as gallic acid equivalent (GAE) [3]. All data were recalculated for absolute dry weight of plant material.

The maximum experimental yield of phenolic compounds was 12.58 mg GAE/g which was close to the predicted yield (11.52 mg GAE/g DW). The optimised extraction conditions were 70% ethanol concentration, extraction time 60 min, and ultrasonic power 904 W. These optimised extraction conditions were applied for the analysis of plum samples of seven different cultivars.

[1] Trendafilova A, Ivanova V, Trusheva B, Kamenova-Nacheva M, Tabakov S, Simova S. Chemical Composition and Antioxidant Capacity of the Fruits of European Plum Cultivar Čačanska Lepotica Influenced by Different Rootstocks. *Foods*. 2022 Jan 1;11(18):2844

[2] Azmir J, Zaidul ISM, Rahman MM, Sharif KM, Mohamed A, Sahena F, et al. Techniques for extraction of bioactive compounds from plant materials: A review. *Journal of Food Engineering*. 2013 Aug;117(4):426–36

[3] Bobinaitė R, Viškelis P, Venskutonis PR. Variation of total phenolics, anthocyanins, ellagic acid and radical scavenging capacity in various raspberry (*Rubus* spp.) cultivars. *Food Chemistry*. 2012 Jun 1;132(3):1495–1501

SYNTHESIS AND CHARACTERISATION OF A MACROPHAGE-DERIVED HYBRID NANOSYSTEM FOR DOXORUBICIN DELIVERY TO GLIOBLASTOMA

Girstautė Dabkevičiūtė¹, Christian Celia², Vilma Petrikaitė^{1,3}

¹Life Sciences Center, Institute of Biotechnology, Vilnius University, Lithuania

²Department of Pharmacy, University of Gabriele d'Annunzio Chieti Pescara, Italy

³Laboratory of Drug Targets Histopathology, Lithuanian University of Health Sciences, Lithuania

girstaute.dabkeviciute@bti.stud.vu.lt

Glioblastoma (GBM), a highly aggressive brain cancer, has a median survival of 12-14 months with limited therapy options [1]. The challenging GBM microenvironment hinders conventional drug delivery, motivating nanoparticles (NPs) exploration. Liposomes (LPs), notable for their biocompatibility and targeted drug delivery capabilities, and naturally released extracellular vesicles (EVs), are promising drug carriers. Combining LPs and EVs creates a hybrid system with enhanced therapeutic properties [2]. Our study focuses on synthesising and characterising a LPs-EVs nanosystem for DOX delivery to GBM cells.

Two LP formulations, F1 and F2, were created via the thin layer evaporation (TLE) method, each with specific lipid molar ratios: 6:3:1 for DPPC:CHOL:DSPEmPEG2000 in F1 and 7:4:6:1 for DPPC:DPPS:CHOL:DSPEmPEG2000 in F2. Lipid films were hydrated with either a PBS solution (10 mM, pH 7.4), ammonium sulphate solution (250 mM, pH 5.5), or M0 macrophage-derived EVs in PBS, following extrusion through membrane filters (pore sizes: 800 to 100 nm). For therapeutic LPs, DOX was entrapped using a pH gradient and remote loading procedure, with entrapment efficiency determined by fluorescence. Size, polydispersity index (Pdl), and zeta potential (ZP) were assessed using dynamic light scattering. Long-term stability of empty, DOX-loaded, and hybrid NPs at 4°C was evaluated weekly for a month. Short-term stability of empty and DOX-loaded LPs in PBS and DMEM with 10% FBS at 37°C under stirring was assessed at various time points for 72 hours.

The average size of F1, F2, M0-F1 and M0-F2 NPs was below 136 nm, while DOX-loaded liposomes increased in diameter by up to 30 nm. The Pdl of empty NPs was lower than 0.14 and DOX loading increased it up to 0.18. ZP of empty NPs was -25.7 ± 1.5 mV (F1), -19.4 ± 1.9 mV (F2), -24.6 ± 2.4 mV (M0-F1), and -36.4 ± 3.9 mV (M0-F2), while DOX loading altered ZP from 3 to 6 mV. F1, F2, DOX-F2, M0-F1 and M0-F2 remained stable at 4°C for 4 weeks, showing no significant changes in size, Pdl, and ZP. However, DOX-F1 exhibited an increase in Pdl up to 0.3 after 17 days. Results showed that both empty and DOX-loaded NPs remained stable in PBS and DMEM with 10% FBS at 37°C under stirring for 72 hours.

To conclude, the F2 lipid formulation exhibited desirable properties as a base for the synthesis of hybrid macrophage-derived nanosystem, and M0-F2 NPs are worthy of further studies for DOX delivery to GBM cells.

[1] S. Bahadur et al. Current promising treatment strategy for glioblastoma multiform: A review. (Oncol. Rev. 2019)

[2] Z. Liu et al. Nanoscale drug delivery systems in glioblastoma (Nanoscale. Res. Lett. 2022)

ANTIMICROBIAL PROPERTIES OF BLACK SOLDIER FLY LARVAE PROTEIN EXTRACTS

Guoda Varnelytė^{1,2}, Bazilė Ravoitytė¹, Stanislavas Tracevičius³, Elena Servienė¹

¹Institute of Botany, Nature Research Centre, Akademijos 2, 08412 Vilnius, Lithuania

²Institute of Biosciences, Life Sciences Center, Vilnius University, Sauletekio 7, 10257 Vilnius, Lithuania

³UAB Insectum, P. Zadeikos 20, 06321, Vilnius, Lithuania

guoda.varnelyte@gmc.stud.vu.lt

In recent years, a lot of attention has been paid to the search for alternative sources of antimicrobial substances, as the irrational use of antibiotics in livestock production caused the spread of drug resistance among bacteria and decreased product quality. Industrial insect farming can be an alternative and sustainable source for the enrichment of animal feed as insects have a high nutritional value and low environmental footprint [1]. Among such insects are black soldier flies (*Hermetia illucens*), they are known for their ability to efficiently process organic waste and can have about 50% of crude protein in the larva stage. It is known that the amino acid composition is similar to fish meal which is often used in livestock production. Besides promoting animal growth, black soldier fly larvae (BSFL) have antibacterial activity provided by antimicrobial peptides (AMP). These AMPs can have biocidal activity against pathogenic bacteria, such as *Salmonella* sp. and methicillin-resistant *Staphylococcus aureus* [1, 2]. Antimicrobial peptides have great potential as an alternative to antibiotics due to their activity against a wide range of bacteria and a lower tendency to induce resistance. However, research on how AMPs can replace antibiotics is still in the preliminary stages.

The aim of this work is to produce extracts from the BSFL proteins and evaluate their antibacterial and antifungal properties. Two types of protein extracts were obtained using acetic acid extraction. The inhibitory and biocidal effects against bacteria and yeast cultures were evaluated using microbiological methods.

The results of this study showed that in most cases the BSFL protein extracts have a higher antimicrobial activity against bacteria than yeast. Potentially pathogenic microorganisms, such as *Staphylococcus aureus*, *Pseudomonas aeruginosa*, *Klebsiella pneumoniae*, *Sporobolomyces roseus*, and *Rhodotorula mucilaginosa*, are sensitive to tested protein extracts.

This study shows that BSFL protein extracts exhibit broad antimicrobial activity and may contribute to further research for alternative antimicrobial agents.

[1] Xia, J.; Ge, C.; Yao, H. Antimicrobial Peptides from Black Soldier Fly (*Hermetia illucens*) as Potential Antimicrobial Factors Representing an Alternative to Antibiotics in Livestock Farming. *Animals* 2021, 11, 1937.

[2] Lee, K.-S.; Yun, E.-Y.; Goo, T.-W. Evaluation of Antimicrobial Activity in the Extract of Defatted *Hermetia illucens* Fed Organic Waste Feed Containing Fermented Effective Microorganisms. *Animals* 2022, 12, 680.

THE EFFECTS OF HERBICIDE GLYPHOSATE ON THE NUTRITIONAL ECOLOGY OF CARABID BEETLES

Ieva Olechnavičiūtė^{1,2}, Norbertas Noreika^{1,2}

¹Laboratory of Entomology, Nature Research Centre, Vilnius 08412, Lithuania

²Chair of Plant Health, Institute of Agricultural and Environmental Sciences, Estonian University of Life Sciences, Tartu 51006, Estonia

olechnaviciute.ieva@gmail.com

Carabid beetles (Coleoptera: Carabidae) are important generalist predators in agroecosystems. They are known to effectively control various pests and weeds, but knowledge in principles and factors of their food preferences are limited. According to nutritional geometry concept, animals often are selective for foods of differing macronutritional composition to meet their specific nutritional requirements in order to achieve maximum fitness. However, such macronutrient selection can potentially be disturbed by various xenobiotics used in agriculture, e.g. pesticides. Glyphosate, the most widely used herbicide in the world, is known to affect insect behavior and gut microbiota which can likely change insect's macronutrient selection and lead to its reduced fitness.

The main aim of the current study was to investigate how carabid beetles balance macronutrients (proteins, lipids and non-structural carbohydrates) when treated with glyphosate. We hypothesized that glyphosate will cause higher carbohydrate consumption due to increased metabolic stress and that this consumption will increase with higher glyphosate concentration. As well, we expected glyphosate-treated beetles to lose weight and deplete their body lipids. Three different concentrations of pure glyphosate and a field relevant amount of commercial glyphosate-based product Roundup® Express were used mixed with mealworm powder and fed to *Pterostichus aethiops* beetles. After the pesticide treatment, beetles were served with three different uncontaminated food options: high in carbohydrates, lipids and protein for 24 hours. Carabids were offered the same three food options for 24 hours after a week. Served pesticide-treated and uncontaminated foods were weighted before and after to determine consumed amount. Beetles were weighted and their lipid and protein body content was measured after the experiment. Data analyses are currently being performed and the results will be presented.

ANALYSIS OF PAH METABOLITES AND ANTIOXIDANT CAPACITY IN MUSSELS (*Unio pictorum*) FROM NEMUNAS RIVER (LITHUANIA)

Reda Nalivaikienė¹, Virginija Kalcienė², Aleksandras Rybakovas¹, Dominykas Musneckis², Laura Butrimavičienė¹

¹Nature Research Centre

²Life Sciences Center, Vilnius University
reda.eglinskaite@gamtc.lt

The Rivers are under increasing constant threat of anthropogenic activities, most leading up to contamination. Various pollutants enter the aquatic environment and polycyclic aromatic hydrocarbonates (PAHs) are a significant part of it. The Nemunas is the fourth-largest river draining into the Baltic Sea and its basin covers the largest area in Lithuania. PAHs constantly contaminate the Nemunas River, a significant part of them produced during petrogenic and pyrogenic reactions [1]. Bivalves of the *Unionidae* family are distributed worldwide and are widely used as bioindicators in the determination of ecosystem status. Sensitivity and informativity of biochemical biomarkers assessed in mussels of the *Unionidae* family were demonstrated after exposure to various groups of pollutants *in situ* and under laboratory conditions [2]. Thus, the current study aimed to evaluate levels of PAH metabolites and antioxidant capacity in *Unio pictorum*. In this study, mussels were collected in the summer of 2020, 2021, and 2022 at 4 different Nemunas River sites. The first sampling site N1 was located upstream of the Alytus City industrial and municipal wastewater outlet. The other sites were located below the wastewater outlet – N2 at approximately 2 km distance, N3 – at a 30-32 km distance in Nemunas Loops Regional Park, and N4 – below the Birštonas and Prienai Cities. The naphthalene- type and benzo[a]pyrene-type PAH metabolites in *U. pictorum* haemolymph were analysed using a semi-quantitative fixed wavelength fluorescence method with the respective pairs of excitation and emission wavelengths [3]. The total antioxidant capacity of *U. pictorum* was evaluated using the ferric-reducing antioxidant power (FRAP) assay [4]. Analysis of study results showed that the levels of naphthalene-type and benzo(a)pyrene-type metabolites in the haemolymph of the mussels increased from 2020 at Nemunas sites N1 and N3, respectively. The antioxidant capacity of the bivalve mussels increased from 2020 to 2022 at all sites located downstream from site N1. Spearman rank correlation analysis revealed that there was no reliable relationship between the responses of the biomarkers in any of the studied years.

R-RAS-2 AS A POTENTIAL PREDICTIVE TARGET IN TRIPLE-NEGATIVE BREAST CANCER

Justas Burauskas^{1,2}, Agnė Šeštokaitė^{1,2}, Monika Drobnienė¹, Rasa Sabaliauskaitė^{1,2}

¹Vilnius university

²National Cancer institute
justasb18@gmail.com

Breast cancer is the most commonly diagnosed neoplasm worldwide and is the leading cause of cancer deaths amongst women. Triple-negative breast cancer (TNBC) is the most aggressive subtype with the lowest 5-year survival rates accounting for 12-18% of all breast cancers. TNBCs have a much higher recurrence and metastasis as a result of not being eligible for current treatment options due to the lack of estrogen, progesterone receptor, and human epidermal growth factor receptor 2. This aggressive cancer contributes to the overall shortened survival of patients diagnosed with TNBC.

Considering the absence of molecular targets, neoadjuvant chemotherapy (NAC) remains the standard of care for patient treatment. However, the effectiveness of treatment is unpredictable, as patients frequently develop resistance. For this reason, there is a growing need to develop novel non-invasive molecular predictive approaches for this disease. It has become evident that multiple signaling pathways are responsible for treatment resistance. Recent evidence from preclinical studies have marked a pivotal role of the R-RAS-2 gene which is involved in the STAT3 signaling pathway, in the progression, and chemoresistance of TNBC patients.

The aim of this study was to evaluate the expressions of STAT3, ALDH1A1, NFIB, UPF3A, BCL-2, and R-RAS-2 genes in serial plasma samples before and after NAC and determine their potential as predictive biomarkers.

In this study, we used reverse transcription quantitative PCR to determine gene expression in 81 TNBC patients

paired plasma samples before and after NAC. We determined that BCL-2, R-RAS-2, STAT3 and NFIB expression was higher after NAC (all $P < 0.005$, respectively). While R-RAS-2 higher expression of at least 10% was associated with partial response to NAC and residual disease ($P = 0.013$ and $P = 0.006$, respectively).

In conclusion, understanding how the multiple signaling pathways influence the course response to NAC in TNBC is important. To date, we found that R-RAS2 could be used as a predictive biomarker for monitoring TNBC patient response to chemotherapy and treatment effectiveness.

INACTIVATION OF ANTIBIOTIC-RESISTANT OPPORTUNISTIC PATHOGEN *STENOTROPHOMONAS MALTOPHILIA* BY CHLOROPHYLLIN-BASED ANTIMICROBIAL PHOTODYNAMIC THERAPY

Justė Tamulionytė¹, Irina Buchovec², Edita Sužiedėlienė¹

¹Institute of Biosciences, Department of Biochemistry and Molecular Biology, Life Sciences Center, Vilnius University, Lithuania

²Institute of Photonics and Nanotechnology, Faculty of Physics, Vilnius University, Lithuania
juste.tamulionyte@gmc.stud.vu.lt

Antimicrobial resistance is one of the most important current threats to global health [1]. *Stenotrophomonas maltophilia* is an emerging opportunistic pathogen responsible for highly lethal nosocomial infections among immunocompromised patients. Its ability to form biofilms as well as high-level intrinsic resistance to a wide range of antibiotics makes treatment of *S. maltophilia* infections very complicated, requiring alternative antimicrobial strategies [2]. One perspective method is antimicrobial photodynamic therapy (aPDT), which involves a photosensitizer, molecular oxygen and light to produce reactive oxygen species, causing oxidative stress, and killing bacterial cells.

The aim of this study was to analyse the efficacy of chlorophyllin-based aPDT (Chl-aPDT) inactivation against *S. maltophilia* when exposed to 402 nm light at different irradiances. Chl is a water-soluble chlorophyll derivative also known as a food colorant. Two multidrug-resistant biofilms forming clinical *S. maltophilia* isolates (SM3 and SM21) were used for Chl-aPDT. Bacterial cultures were suspended with 0.015 mM Chl in the dark. For inactivation, samples were exposed to 250 and 350 W/m² irradiance at different periods. The irradiation dose (J/m²) was calculated as irradiance (W/m²) multiplied by irradiation time (s). Bacterial viability was evaluated by colony-forming unit count (CFU/mL).

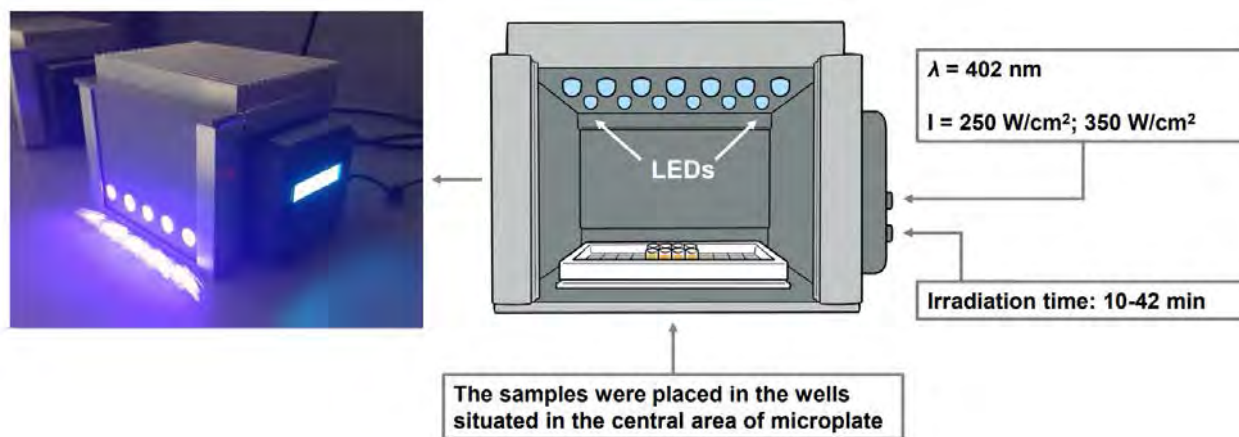


Fig. 1. The illumination system used in aPDT experiments.

The results showed that sensitivity to Chl-aPDT varies among both *S. maltophilia* isolates. SM3 was inactivated in a similar manner when exposed to the same irradiation dose at different irradiance. In contrast, the viability of SM21 after Chl-aPDT was more than 7-fold lower after irradiation at a dose of 31.5 J/cm² with 250 W/m² compared to 350 W/m², but almost 4-fold higher at a dose of 63 J/cm².

[1] Murray, Christopher J. L., et al. Global Burden of Bacterial Antimicrobial Resistance in 2019: A Systematic Analysis. *The Lancet*, vol. 399, no. 10325, Feb. 2022, pp. 629-55.

[2] Flores-Treviño, Samantha et al. *Stenotrophomonas maltophilia* biofilm: its role in infectious diseases. *Expert review of anti-infective therapy* vol. 17,11 (2019): 877-893.

DESIGN AND SYNTHESIS OF MUTANT VARIANTS OF THE ALLERGEN COMPONENT ART V 3 FROM ARTEMISIA VULGARIS

Eva Kupetytė¹, Laima Čepulytė¹, Rasa Petraitytė-Burneikienė¹

¹Department of Eukaryote Gene Engineering, Institute of Biotechnology, Life Sciences Center, Vilnius University, Lithuania
eva.kupetyte@gmc.stud.vu.lt

During the pollination season, airborne pollen and related allergies are significant public health issues. The World Health Organization has predicted that by the year 2050, one out of two people will suffer from allergy [1]. Allergen sources may vary: pollen, dust mites, food and pharmaceuticals, but the most common allergens are proteins. An allergen is described as any molecule that causes allergic responses and production of allergen-specific immunoglobulin E (IgE). Strong immune response caused by an allergen can contribute to the development of diseases such as asthma, allergic rhinitis and eczema [2]. Around the globe, allergies are a common health issue, although exact numbers are not accessible, estimates range from 20 % to 40 % [3]. Anti-inflammatory drugs and allergen avoidance are the most common recommendations to suppress allergic symptoms, but have no long-term effect and do not modulate the immune responses to allergens. In the future, development and application of hypoallergens in the personalized allergen immunotherapy could help to prevent adverse immune reactions. Molecules known as hypoallergens are less likely to induce allergen-specific IgE response but has the ability to elicit the T cell response, without causing allergic symptoms in the patient. Hypoallergens may eventually lead to more specialized, tailor-made allergen-specific immunotherapy [2].

In the present study, mutants of the *Artemisia vulgaris* allergen component Art v 3 were generated and analyzed. Amino acids that may be involved in IgE-binding epitope formation were identified based on the literature and bioinformatic analysis. Eleven different variants of Art v 3 protein mutants were selected for the research. Three of them were generated and experiments of their synthesis in *E. coli* were performed during this work. The results of these experiments provide an important findings towards elaboration of immunotherapeutic tools for allergen specific immunotherapy.

[1] T. Dbouk, N. Visez, S. Ali et al., Risk assessment of pollen allergy in urban environments. *Scientific reports*, 12(1), 21076 (2022)

[2] S. R. Durham, and M. H. Shamji, Allergen immunotherapy: past, present and future. *Nature reviews. Immunology*, 112. (Advance online publication 2022)

[3] D. Boehmer, B. Schuster, J. Krause et al., Prevalence and treatment of allergies in rural areas of Bavaria, Germany: a cross-sectional study. *The World Allergy Organization journal*, 11(1), 36 (2018)

MORPHOLOGICAL AND METABOLIC CHANGES IN BONE MARROW MESENCHYMAL STEM CELLS INDUCED BY HIF-1 ALPHA INHIBITOR LW6

Ignas Lebedis¹, Jolita Pachaleva¹, Eiva Bernotiene¹, Giedrius Kvedaras², Ilona Uzieliene¹

¹Department of Regenerative Medicine, State Research Institute Centre for Innovative Medicine, Lithuania

²The Clinic of Rheumatology, Traumatology Orthopaedics and Reconstructive Surgery, Institute of Clinical Medicine of the Faculty of Vilnius University, Lithuania
ignas.lebedis@gmc.stud.vu.lt

Human articular cartilage possesses weak regenerative capabilities after physical damage or age-related wear, making it susceptible to degenerative diseases such as osteoarthritis (OA). Cell based therapies using mesenchymal stem cells (MSCs) have shown promising results in cartilage regeneration due to their innate ability to stimulate tissue repair and effectively differentiate into chondrocytes. Research and clinical trials, however, often show varied results due to different cell culture conditions and models of differentiation [1].

Physiological conditions and physioxia are significant aspects of chondrogenesis, mainly due to hypoxia inducible factors (HIFs), which regulate cell metabolism, survival, gene transcription and in turn positively influence chondrogenic differentiation under low concentrations of oxygen in joints [2].

LW6, a novel inhibitor of hypoxia inducible factor 1 alpha (HIF-1 α) and its specific mechanisms of inhibition are not well understood, with potential targets or their combinations being HIF-1 α itself, the upregulation of Von Hippel-Lindau protein (VHL) or suppression of malate dehydrogenase 2 (MDH2) [3].

The aim of this study was to assess the morphological and metabolic changes in human bone marrow derived mesenchymal stem cells (BMMSCs), comparing them to human articular chondrocytes by proliferation assay, flow cytometry and metabolic analysis under normoxic (21% O₂) and hypoxic conditions (5% O₂) induced by the HIF-1 α inhibitor LW6.

Flow cytometry results suggest that LW6 causes morphological changes and increases cell granularity after 3, 7 and 21 days independent of physiological conditions, however a proliferation assay showed no significant impact on cell proliferation under the same culture conditions. A glycolytic rate assay showed that LW6 lowers the basal and maximal glycolytic capacity in BMMSCs in normoxic conditions but may otherwise have little effect to chondrocytes. Mitochondrial respiration was decreased by both hypoxic conditions and LW6 in BMMSCs and chondrocytes.

These results are an introductory investigation into the mechanisms of HIF-1 α inhibition by LW6 and the effects it may have on BMMSCs and chondrocytes during cell metabolism, growth and proliferation. These results show that LW6 affects cell morphology and cellular functions such as mitochondrial respiration and glycolysis. Future studies aim to investigate the molecular mechanisms that control these changes.

[1] Samal JRK, Rangasami VK, Samanta S, Varghese OP, Oommen OP. Discrepancies on the Role of Oxygen Gradient and Culture Condition on Mesenchymal Stem Cell Fate. *Adv Healthc Mater.* 2021;10(6):e2002058. doi:10.1002/adhm.202002058

[2] Di Mattia M, Mauro A, Citeroni MR, et al. Insight into Hypoxia Stemness Control. *Cells.* 2021;10(8):2161. Published 2021 Aug 22. doi:10.3390/cells10082161

[3] Naik R, Han S, Lee K. Chemical biology approach for the development of hypoxia inducible factor (HIF) inhibitor LW6 as a potential anticancer agent. *Arch Pharm Res.* 2015;38(9):1563-1574. doi:10.1007/s12272-015-0632-5

COMPARATIVE IMPACT OF β -CYCLODEXTRIN AND MUSTARD EXTRACT ON STABILITY IN RED CLOVER EXTRACT-LOADED MICROCAPSULES

Jurga Andreja Kazlauskaitė^{1,2}, Jurga Bernatoniene^{1,2}

¹Institute of Pharmaceutical Technologies, Lithuanian University of Health Sciences, Kaunas, Lithuania

²Department of Drug Technology and Social Pharmacy, Lithuanian University of Health Sciences, Kaunas, Lithuania
jurga.andreja.kazlauskaitė@lsmu.lt

Emulsion stability is crucial for microcapsule preparation, ensuring consistent encapsulation and release, so selecting appropriate emulsifiers is essential [1]. Mustard extract (ME) is a natural preservative and antiseptic agent, making it a promising option for improving emulsion stability [2]. β -cyclodextrin (CD), commonly used as a tablet excipient in the pharmaceutical industry, can also be an effective emulsifier due to its characteristics [3].

This study evaluated the emulsifying properties of CD and ME in O/W emulsions containing red clover extract and their impact on microcapsule parameters.

The emulsion formulations utilised a combination of 2% sodium alginate solution, sweet almond oil, CD or ME at varying concentrations as emulsifiers (2.5% to 10%), and xanthan. Emulsion stability was assessed through centrifugation, and particle size and distribution were analysed using Mastersizer. Microcapsules were formed using a 2% calcium chloride crosslinking agent, and their parameters were examined using a texture analyser and micrometre. Stability assessment showed that formulations reached maximum stability (100%) with the highest emulsifier percentages. At 7.5% ME, stability at 7000 rpm was 20%, while CD exhibited stability at 25%. Lower concentrations didn't form emulsions.

Particle size analysis of the most stable emulsions (10% ME/CD) revealed that 90% of ME particles were less than 0.744 μm ; CD particles were 0.981 μm . Microcapsules formed with 10% ME and CD had average sizes of 2.42 ± 0.02 and 2.56 ± 0.04 μm , respectively. Post-crushing, CD microcapsules exhibited superior strength at 858.40 ± 58.64 g compared to ME microcapsules at 803.60 ± 39.43 g. CD capsules also demonstrated higher swelling power at $287.01 \pm 14.24\%$ than ME capsules at $209.12 \pm 22.81\%$.

In conclusion, 10% concentrations of both emulsifiers provided optimal stability and particle size. Emulsions with CD had better parameters; however, ME also demonstrated effectiveness as a natural emulsifier.

[1] da Silva, L.C. et al., Methods of Microencapsulation of Vegetable Oil Principles Stability and Applications - A Minireview. Food Technol Biotechnol 60, 308-320, 2022.

[2] Wu., Y. et. al., Emulsifying Properties of Water Soluble Yellow Mustard Mucilage A Comparative Study with Gum Arabic and Citrus Pectin Food Hydrocoll. 47, 191-196, 2015.

[3] Matencio, A., et al., Applications of Cyclodextrins in Food Science: A Review. Trends Food Sci Technol. 104, 132-143, 2022.

FUNCTIONAL ANALYSIS OF ANTIVIRAL BREX PROTEINS

Aistė Petrauskaitė¹, Tomas Šinkūnas¹

¹Vilnius University

aiste.petrauskaite@gmc.stud.vu.lt

Bacteriophages are the most abundant biological entity in the biosphere, and they are responsible for the destruction of 20-40 % of bacterial cells every day [1]. This evolutionary pressure drives the emergence of diverse bacterial defence systems, one of which is the BREX (Bacteriophage Exclusion). This system is present in about 10 % of known prokaryotic genomes, yet its detailed defence mechanism remains to be elucidated [2]. Our study focuses on the type I BREX (BREX1) system, which is encoded by a cluster of six genes: *brxA-brxB-brxC-pglZ-brxL-pglX*. This system methylates host genomic DNA at specific sequences, thereby protecting it from autoimmunity. The non-methylated DNA of bacteriophages triggers BREX1, which blocks phage proliferation (Fig. 1).

We have previously shown that deletion of certain BREX1 genes results in cytotoxicity [3]. This suggests that some BREX1 proteins are involved in the autoregulation of the immune response, while others may act as effectors that interfere with the vital process of the cell. Here, we are analysing different compositions of BREX1 proteins to find a link to their function in the cell.

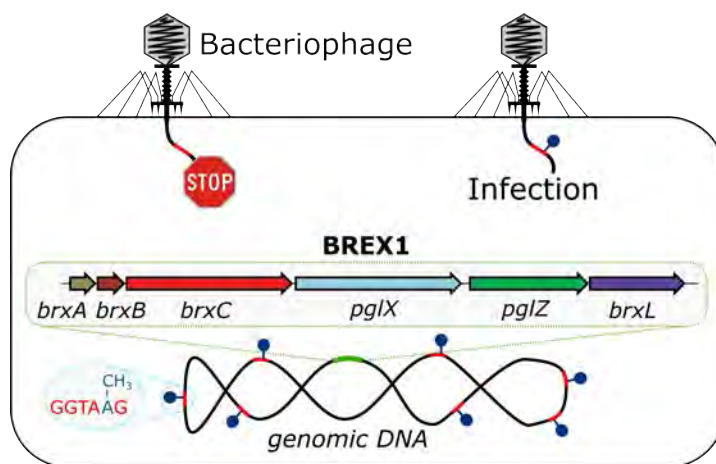


Fig. 1. The BREX1 defence system protects bacteria from bacteriophage infection.

[1] L.-C. Fortier, O. Sekulovic, Importance of prophages to evolution and virulence of bacterial pathogens

[2] T. Goldfarb et al., BREX is a novel phage resistance system widespread in microbial genomes

[3] J. Gordeeva et al., BREX system of Escherichia coli distinguishes self from non-self by methylation of a specific DNA site

ANALYSIS OF IN VITRO CYTOTOXICITY AND GENOTOXICITY OF POLYSTYRENE NANOPARTICLES IN HUMAN HEPATOMA CELL LINE (HEPG2)

Emilija Striogaitė¹, Milda Babonaitė¹, Jozas Rimantas Lazutka¹

¹Vilnius University

emilija.striogaitė@gmc.stud.vu.lt

Plastics are a major environmental concern as they can persist in the environment for hundreds of years. Plastic may be degraded into micro-particles < 5000 nm in diameter, and further into nanoparticles (NPs) < 100 nm in diameter. Among these, polystyrene nanoparticles (PS-NPs) are found to be the most represented NPs in the environment. In vivo and in vitro studies have suggested that PS-NPs may penetrate organisms through several routes i.e. skin, respiratory and digestive tracts, so it is essential to evaluate the safety and possible genotoxicity [1]. In this study, we evaluated the cytotoxicity and genotoxicity of PS-NPs in the human hepatoma cell line HepG2 in vitro. We comprehensively characterised the PS-NPs, assessed their cellular uptake, and measured the levels of reactive oxygen species by performing flow cytometry, evaluated cytotoxicity using AlamarBlue assay, and assessed genotoxicity through the alkaline comet assay [2, 3]. In this experiment, HepG2 cells were treated with PS-NPs at concentrations of 5-100 µg/mL. Flow cytometry results showed an efficient uptake of the nanoparticles into the cells and that an increase of PS-NPs leads to a rise in levels of reactive oxygen species. Tested concentrations were not cytotoxic in HepG2 cells, but an increase in DNA damage was found to be statistically significant at most concentrations. Besides, a very strong direct relationship was detected between the percentage of DNA damage and NP concentrations. These findings suggest the effective uptake and genotoxic potential of polystyrene nanoparticles and raise concern about the safety of plastics.

-
- [1] Kik, K., Bukowska, B., Sicińska, P. (2020). Polystyrene nanoparticles: Sources, occurrence in the environment, distribution in tissues, accumulation, and toxicity to various organisms. *Environmental Pollution*, 262, 114297.
- [2] Longhin, E. M., El Yamani, N., Rundén-Pran, E., Dusinska, M. (2022). The Alamar blue assay in the context of safety testing of nanomaterials. *Frontiers in Toxicology*, 4, 981701. <https://doi.org/10.3389/ftox.2022.981701>
- [3] Elespuru, R., et al. (2018). Genotoxicity assessment of nanomaterials: Recommendations on best practices, assays, and methods. *Toxicological Sciences*, 164(2), 391–416. <https://doi.org/10.1093/toxsci/kfy100>

THE SYNERGISTIC EFFECT OF TYROSINE KINASE INHIBITORS AND DOXORUBICIN IN TRIPLE-NEGATIVE BREAST CANCER

Ugnė Mekionytė¹, Vilma Petrikaitė¹

¹Laboratory of Drug Targets Histopathology, Institute of Cardiology, Lithuanian University of Health Sciences, Lithuania
ugne.mekionyte@lsmu.lt

Triple-negative breast cancer (TNBC) lacks chemotherapeutic targets, which makes it difficult to find alternative treatments. One of the drugs used in TNBC therapy is doxorubicin (DOX) also tyrosine kinase inhibitors (TKIs) are promising agents. Even though these compounds exhibit anti-cancer efficacy, drug resistance might develop due to efflux pump, cellular microenvironment and other mechanisms [1]. Synergistic effect of compounds acting by different pathways is one of the approaches to overcome drug resistance [2]. Therefore in this study we selected five most active sunitinib derivatives EMAC4001, 4006, 4007, 4008, 4017 synthesized at Cagliari University, Italy [3]. The aim of this study was to determine sunitinib and its analogues activity in combination with DOX on TNBC cells.

As a model cell lines for our research, human TNBC cell line MDA-MB-231 (WT) and DOX-resistant (DR) MDA-MB-231 were used. Compound effect on cell viability was measured using 3-(4,5-dimethylthiazol-2-yl)-2,5-diphenyltetrazolium bromide (MTT) assay after 72 h of incubation. The half-maximal effective concentrations (EC₅₀) were calculated using Hill equation. The activity of selected sunitinib and its derivatives in combination with DOX (1:1) was determined by calculating fraction affected (fa) versus combination index (CI) plots based on Chou-Talalay methodology [2]. MDA-MB-231 DR cell line was more resistant to all tested drugs than MDA-MB-231 WT. Sunitinib analogue EMAC4001 reduced cell viability the most among tested TKIs (EC₅₀ 105.7 ± 18.5 nM in MDA-MB-231 WT and 690.3 ± 158.9 nM in MDA-MB-231 DR). CI index showed that all combinations, except sunitinib and EMAC4007, had synergistic effect on MDA-MB-231 DR cells at fa = 0.5 (CI < 1).

Based on results, TKI and DOX combinations may be considered a promising chemotherapeutic agent against drug resistant TNBC.

-
- [1] V. Petrikaite, N. D'Avanzo, C. Celia, and M. Fresta, 'Nanocarriers overcoming biological barriers induced by multidrug resistance of chemotherapeutics in 2D and 3D cancer models', *Drug Resist. Updat.*, vol. 68, p. 100956, May 2023, doi: 10.1016/j.drug.2023.100956
- [2] T.-C. Chou, 'Drug Combination Studies and Their Synergy Quantification Using the Chou-Talalay Method', *Cancer Res.*, vol. 70, no. 2, pp. 440–446, Jan. 2010, doi: 10.1158/0008-5472.CAN-09-1947.
- [3] R. Meleddu et al., 'Investigating the Anticancer Activity of Isatin/Dihydropyrazole Hybrids', *ACS Med. Chem. Lett.*, vol. 10, no. 4, pp. 571–576, Apr. 2019, doi: 10.1021/acsmchemlett.8b00596.

DETERMINANTS OF INTRACELLULAR LOCALISATION OF NATIVE SACCHAROMYCES CEREVISIAE VIRUSES

Aušrinė Jašmontaitė¹, Gerda Skinderytė¹, Aleksandras Konovalovas¹, Saulius Serva¹

¹Life Sciences Center, Vilnius University, Vilnius, Lithuania
ausrine.jasmontaite@gmc.stud.vu.lt

Saccharomyces cerevisiae yeast are widely used in many industrial and scientific fields. Many natural and laboratory yeast strains contain native viruses which belong to *Totiviridae* family [1], including the satellite virus M and helper viruses ScV-LA (L-A) and ScV-LBC (L-BC). Totiviruses replicate inside of host cell and are only transmitted during reproduction and sporogenesis, therefore no extracellular state is detected [2]. Co-existence of M and L-A viruses determines the biocidal activity of yeast. However, it is often implied, that L-A (or L-BC) on its own has no significant impact on host cells [3]. Yet more detailed studies on native yeast viruses are relevant in order to assess their impact on yeast more accurately.

The aim of this research is to study localisation patterns and establish localisation determinants of native *S. cerevisiae* viruses. For this purpose, fluorescent proteins were used to mark endoplasmic reticulum of *S. cerevisiae* and Gag proteins of Totivirus capsid. Fluorescence microscopy demonstrated different localisation of L-A and L-BC viruses: L-A is found in nucleus, while L-BC is spread throughout cytosol. Although the structures of these viruses are very similar, some previous research suggest that the C terminal domain of L-A virus protein might determine the translocation to nucleus of host cell [4]. In addition, plasmids were constructed differing by -1 ribosomal frameshift, which is necessary for fused Gag-Pol viral protein synthesis. Different interactions with native viruses were observed: when proteins are translated without ribosomal frameshift, native L-A viruses are eliminated. Meanwhile, synthesis of full-length protein does not interfere with the replication of native L-A virus. Further research will be continued regarding the topic of localisation of native viruses in different strains of *S. cerevisiae* yeast, as well as determinants of localisation of these viruses.

[1] Smith, J., Petrovic, P., Rose, M., De Souza, C., Muller, L., Nowak, B., Martinez, J. (2021). Placeholder Text: A Study. The Journal of Citation Styles.

[2] Ghabrial, S. A., Castón, J. R., Jiang, D., Nibert, M. L., Suzuki, N. (2015). 50-plus years of fungal viruses. In *Virology* (Vols. 479-480, pp. 356-368). Academic Press Inc.

[3] Schmitt, M. J., Breinig, F. (2006). Yeast viral killer toxins: lethality and self-protection. In *Nature reviews. Microbiology* (Vol. 4, Issue 3, pp. 212-221).

[4] Konovalovas, A. (2018). Molecular determinants of *Totiviridae* family viruses of *Saccharomyces sensu stricto* clade [Dissertation]. Vilnius university.

ASSESSMENT OF PATHOGENIC OOMYCETES IMPACT ON *Salmosalar* L LARVAE USING OXIDATIVE STRESS BIOMARKERS

Eglė Gadeikytė^{1,2}, Gintarė Sauliūtė¹, Arvydas Markuckas², Milda Stankevičiūtė¹

¹Nature Research Centre, Akademijos St. 2, LT-08412 Vilnius, Lithuania

²Vilnius University, Life Sciences Center, Saulėtekio av. 7, 10223 Vilnius, Lithuania
egle.gadeikyte@gmc.stud.vu.lt

Freshwater fish are an important protein source for people in many countries, which is why aquaculture has now become a globally significant industry worldwide [1]. However, intensive aquaculture is related to the proliferation of parasites and other pathogenic organisms, posing a threat to biodiversity and food security worldwide [2]. One of these pathogens is oomycetes. Oomycetes, commonly known as water molds, are fungal-like microorganisms that can be parasitic towards a large number of plant and animal host species [3]. They cause one of the most destructive fish diseases in freshwater ecosystems – saprolegniasis [2]. Saprolegniasis is an infection that can develop at any stage of fish life [4] and is characterized mostly by a white or greyish cotton – wool like tuft found on infected skin, gills, or fish eggs. Due to the primary involvement of the skin in saprolegniasis, the disease is alternatively referred to as dermatomycosis.

Diseased fish in the most severe phase of infestation experience poor osmoregulation, respiratory failure, and, in certain cases, organ failure, which can lead to death [5]. It is critical to note that oomycete infections cause oxidative damage in fish, which contributes directly to disease pathogenesis [6]. Based on other research, *Saprolegnia parasitica* is the most important oomycete affecting freshwater fishes [6]. However, other oomycete species are also responsible for infestations, causing economically significant losses. For instance, *Saprolegnia australis*, acting as a pathogen on embryos and fry of salmonids, could colonize and cause their death [7].

The purpose of this research was to investigate the effects of *Saprolegnia* genus oomycetes on *Salmo salar* L. larvae. To achieve this aim, we evaluated the changes in enzyme glutathione S-transferases (GST) activity and levels of metallothionein (MTs). GST plays an important role in aquatic organisms protection from peroxidative damage [8]. MTs are metal-binding proteins with the ability to eliminate reactive oxygen species and maintain metal homeostasis in organisms [9]. Based on the results of present experiment, changes in GST activity were not detected. However, significant changes in MTs level were detected in oomycete-treated *S. salar* larvae compared with the control group.

Acknowledgments This research was funded by the Research Council of Lithuania, Project No. S-MIP-21-10, MULTIS.

-
- [1] Podeti. Koteswar Rao. Economically important freshwater fishes infected with fungi causes EUS. World J Adv Res Rev 2023; 17:605–609.
 [2] Pavić D, Grbin D, Hudina S, et al. Tracing the oomycete pathogen *Saprolegnia parasitica* in aquaculture and the environment. Sci Rep 2022; 12:16646.
 [3] Pavić D, Miljanović A, Grbin D, et al. Identification and molecular characterization of oomycete isolates from trout farms in Croatia, and their upstream and downstream water environments. Aquaculture 2021; 540:736652.
 [4] Barde RD. Clinical and pathological investigations in ulcer disease of *Cyprinus carpio* caused by *Aeromonas hydrophila*. ijhs 2022;3519–3526.
 [5] Lone SA, Manohar S. *Saprolegnia parasitica*, A Lethal Oomycete Pathogen: Demands to be Controlled. JIMB 2018; 6
 [6] Baldissera MD, Souza CF, Abbad LB, et al. Oxidative stress in liver of grass carp *Ctenopharyngodon idella* naturally infected with *Saprolegnia parasitica* and its influence on disease pathogenesis. Comp Clin Pathol 2020; 29:581–586.
 [7] Rezinciuc S, Sandoval-Sierra J-V, Diéguez-Urbeondo J. Molecular identification of a bronopol tolerant strain of *Saprolegnia australis* causing egg and fry mortality in farmed brown trout, *Salmo trutta*. Fungal Biology 2014; 118:591–600.
 [8] Park JC, Hagiwara A, Park HG, Lee J-S. The glutathione S-transferase genes in marine rotifers and copepods: Identification of GSTs and applications for ecotoxicological studies. Marine Pollution Bulletin 2020; 156:111080.
 [9] Kim J-H, Kang J-C. Oxidative stress, neurotoxicity, and metallothionein (MT) gene expression in juvenile rock fish *Sebastes schlegelii* under the different levels of dietary chromium (Cr6+) exposure. Ecotoxicology and Environmental Safety 2016; 125:78–84.

MYOGENIC AND EPITHELIOGENIC DIFFERENTIATION OF ADIPOSE AND BUCCAL MUCOSAL STEM CELLS FOR ARTIFICIAL URETHRA CONSTRUCTION

Andrius Buivydas¹, Povilas Barasa¹, Egidijus Šimoliūnas¹, Ieva Rinkūnaitė¹, Emilija Baltrukonytė¹, Virginija Bukelskienė¹

¹Department of Biological Models, Institute of Biochemistry, Life Sciences Center, Vilnius University, Lithuania
andrius.buivydas@gmc.stud.vu.lt

The urethra is crucial in the urinary system, facilitating urine flow from the bladder to the external environment. Repairing urethral damage is essential for restoring normal urinary functions and preventing long-term complications[1]. Current treatments typically involve surgical procedures that often require multiple interventions. Our goal is to enhance these treatments using 3D printing technology to create an artificial urethral tissue. This tissue aims to provide an ideal environment for cell expansion, migration, and differentiation into a functional tissue.

Our artificial tissue's foundation is a 3D scaffold composed of Gelatin Methacrylate (GelMA) and Silk Fibroin (SF). This scaffold forms a hydrogel with a firm structure when sonicated to denature the silk fibroin and exposed to UV to polymerize GelMA[2]. For the cellular aspect, it's necessary to mimic the urethra's natural structure, which consists of an epithelial wall surrounded by a muscular wall. Our previous work showed that rabbit adipose stem cells (RASC) are suitable for myogenic differentiation. And our recent findings indicate that RASC can effectively differentiate into myogenic-like cells in the GelMA-SF 3D environment as well. This was confirmed by measuring expressions of myogenic differentiation markers *Acta2* and *Cald1*, which showed increased expression levels in differentiated RASC within the GelMA-SF hydrogel. Additionally, alpha-SMA was immunocytochemically stained in RASC, showing higher protein expression in differentiated cells compared to undifferentiated ones. These results suggest successful myogenic-like cell differentiation of RASC cells hosted in a GelMA-SF hydrogel[3].

For epithelial differentiation, we selected rabbit buccal mucosa stem cells (RBMC). Their differentiation, conducted in 2D conditions, showed reduced *Ck14* gene expression and proliferation rates after 5 and 10 days, which is an indication of epithelial differentiation[4]. A cell morphology analysis of images, acquired by immunocytochemical staining of CK14, indicated that differentiated RBMC cells grew significantly larger which is consistent with epithelial differentiation progression. Additionally from the immunocytochemistry images cell density was evaluated, the results from these combined with the results of an MTT test showed a reduced proliferative rate of the differentiated cells. These findings suggest a successful transformation of RBMC cells into non-proliferative epithelial cells.

In summary, our research demonstrates that RASC in 3D GelMA-SF hydrogels can successfully differentiate into myogenic-like cells, and RBMC cells are capable of epithelial differentiation. Future studies will focus on combining these differentiated cell lines to replicate urethral tissues.

[1] Stein DM, et al. A geographic analysis of male urethral stricture aetiology and location. 2012 Dec 18

[2] Wenqian Xiao, et al. Cell-laden interpenetrating network hydrogels formed from methacrylated gelatin and silk fibroin via a combination of sonication and photocrosslinking approaches. 2019 Jun 1

[3] Helms F, et al. Complete Myogenic Differentiation of Adipogenic Stem Cells Requires Both Biochemical and Mechanical Stimulation. 2019 Feb 27

[4] Alam H, et al. Novel function of keratins 5 and 14 in proliferation and differentiation of stratified epithelial cells. 2011 Nov 1

DI(2-ETHYLHEXYL)PHTHALATE AND DIBUTYLPHTHALATE GENOTOXIC EFFECT ON RAT ERYTHROCYTES

Laurynas Orla¹, Edita Paulikaitė^{1,2}, Violeta Žalgevičienė², Rasa Aukštikalnienė¹, Vaidotas Valskys¹, Grita Skujienė¹

¹Institute of Biosciences, Life Sciences Center, Vilnius University, Lithuania

²Department of Anatomy, Histology and Anthropology, Institute of Biomedical Sciences, Faculty of Medicine, Vilnius University, Lithuania
laurynas.ora@gmc.stud.vu.lt

Phthalates are substances that have mutagenic and endocrine disrupting properties and tend to accumulate in the environment. Phthalates leach into water, both from wastewater and plastics, in small amounts, but this can have serious consequences for human health and the ecosystem. The aim of this project was to evaluate the effect of two types of phthalates (which consistently exceed the maximum allowable concentration in Lithuanian waters) in rat bone marrow cells using an in vivo micronucleus assay.

To find out the genotoxic effect, an analysis of micronuclei in polychromatic erythrocytes of rats was carried out. Female rats of Wistar strain, 5-8 weeks old, were divided into control and 5 experimental groups, which get standard food and additionally received a piece of ecological biscuit with different doses of phthalate dissolved in olive oil: 1) DEHP 200 µg/kg; 2) DEHP 1000 µg/kg; 3) DBP 100 µg/kg; 4) DBP 500 µg/kg; 5) mixture of phthalates (DEHP 200 µg/kg, DBP 100 µg/kg). Control animals received only a piece of the biscuit with olive oil. After 3 months, the rats were killed in a CO₂ chamber. Later, during the autopsy, femurs were dissected and bone marrow slides were prepared for the observation of micronuclei in polychromatic erythrocytes. Micronucleus analysis was performed by calculating 2000 PCE (polychromatic erythrocyte) and the ratio of PCE and NCE (normochromatic erythrocyte) and data were analysed using one-way ANOVA. Statistical analysis was performed using GraphPad Prism 9.0.0.

It was found that even small doses of phthalates during daily continuous consumption have a negative genotoxic effect on rats. All results were statistically significant ($p < 0.05$). Significantly more micronuclei were found in bone marrow preparations of rats exposed to DBP than to DEHP. The results of the study reveal that it is necessary to regulate the amount of phthalates in Lithuanian wellfields more effectively and to regulate wastewater treatment more strictly.

A MULTIPARAMETRIC ANALYSIS OF HUMAN MONOCYTE-DERIVED MACROPHAGE RESPONSE TO CARBON BLACK PARTICLES IN VITRO

Justina Pajarskienė¹, Ieva Uogintė², Steigvilė Byčenkienė², Rūta Aldonytė¹

¹Department of Regenerative Medicine, State Research Institute Centre for Innovative Medicine, Lithuania

²Department of Environmental Research, Center for Physical Sciences and Technology, Lithuania
justina.pajarskiene@imcentras.lt

Background. Macrophages as cells of the innate immune system and a first-line defense against various invading pathogens and other substances are responsible for phagocytosis. Phagocytosis is a process of particle elimination via ingestion and intracellular degradation and is widely studied in vitro. Most of the current quantitative phagocytosis assays consist of particles that are manufactured to have the same shape and size and are based on fluorescence or other types of dyes or biomarkers. These types of assays are useful but are lacking in variability, especially for the studies of phagocytosis of diverse environmental particles. One type of these particles is black carbon. Black carbon is a core component of air-polluting particulate matter and is associated with adverse health effects and increased susceptibility to respiratory infections, development of chronic obstructive pulmonary disease, and asthma. Lung-resident macrophages play a crucial role in the clearance and response to various inhaled particles, including black carbon. Phagocytosis by macrophages represents a fundamental process that determines the further fate of inhaled particles and the impact that they might have on human health.

Objectives. We aimed to investigate the interaction of BC particles and human monocyte-derived macrophages in vitro. The findings from this study open new insights into the role of macrophages in black carbon-exposed airways and lungs and have implications for the pathogenesis of many diseases.

Methods. We compared two types of commercially purchased black carbon particles by several physicochemical methods and by their biological effects on monocyte-derived macrophages. Confocal microscopy and CellProfiler, an open-source cell imaging tool, were employed for quantitative analysis of phagocytosis. Black carbon-induced changes in cell viability, morphology, and particle uptake/phagocytosis were quantified. Inflammation and oxidative stress biomarkers were assessed in parallel by Western blot (Nrf2, NQO1, HO-1, p62, p-p62, LC3A/B) and ELISA (IL-6, IL-8, IL-1B).

Results. We report significant and comparable monocyte-derived macrophage responses to both types of black carbon applied in terms of particle uptake, inflammatory cytokine production, and oxidative stress response-related protein expression. Our results show that black carbon particles induce innate immunity activation and oxidative stress in macrophages, potentially leading to the development of chronic inflammatory lung diseases.

Keywords. Monocyte / Macrophage; Phagocytosis; Particle analysis; Carbon black; CellProfiler;

INVESTIGATION OF THE PHOTOSTABILITY OF MAGNESIUMCHLOROPHYLLIN IN BACTERIAL SUSPENSIONS

Loreta Stankevičiūtė, Irina Buchovec^{1,2}

¹Institute of Biosciences, Department of Biochemistry and Molecular Biology, Life Sciences Center, Vilnius University, Lithuania

²Institute of Photonics and Nanotechnology, Faculty of Physics, Vilnius University, Lithuania
loreta.stankeviciute@chgf.stud.vu.lt

Bacterial resistance to antibiotics is a growing concern in the treatment of human infections caused by them. It has become a serious problem in hospitals as there are many opportunistic pathogens that are dangerous to immunocompromised patients. *Stenotrophomonas maltophilia* is a multidrug-resistant Gram-negative opportunistic pathogen that can infect immunocompromised individuals, as well as patients with severe burns or other injuries. The bacterium can cause a variety of infections, including respiratory, circulatory, and urinary tract infections, which are often fatal. [1] Antimicrobial photodynamic therapy (aPDT) is a photochemical antimicrobial method which is used as an alternative to antibiotics. aPDT is based on the interaction of the photosensitizer, molecular oxygen, and light of the appropriate wavelength. During this therapy the photosensitizer is excited by light and interacts with molecular oxygen to produce reactive oxygen species that can cause various cell damage or even death [2]. Natural photosensitizer Magnesium chlorophyllin (MgChl) is known as a water-soluble anionic chlorophyll derivative with a main absorption maximum at 405nm, that exhibits antimicrobial activity that generates ROS after exposure to visible light.

The aim of this study was to analyse the photostability of (MgChl) in the bacterial cell suspensions depending on the type of solution.

The optical absorption of MgChl is known to decrease after activation with visible blue light in phosphate-buffered saline (PBS) without bacterial cells [3]. These changes show the dose dependence of activation and can be used to compare the irradiation efficiency using different spectral components. We compared the absorption characteristics of 0.015 mM MgChl after irradiation (1.1 J/cm² to 31.5 J/cm².) at the optimum excitation wavelength of 402 nm in *S.maltophilia* cell suspension (10⁷ CFU/mL) in PBS (pH 7.4) and in a nutrient medium (tryptone soy broth, pH 7.2)

The results indicate that MgChl was more photostable in the PBS buffer than in the medium. This can be explained by the fact that the excitation of MgChl is inhibited by the lower penetration of light into the medium. The prospect of this research involves further investigating of antimicrobial effectiveness efficacy of MgChl by irradiating bacterial samples in a culture medium.

[1] Said, Mina S., et al. *Stenotrophomonas Maltophilia.*, StatPearls Publishing, 2023. ncbi.nlm.nih.gov

[2] Cieplik, Fabian, et al., Antimicrobial Photodynamic Therapy, What We Know and What We Dont. *Critical Reviews in Microbiology*, t. 44, nr. 5, 2018.

[3] Buchovec, I. et al. *J. Photochem. Photobiol. B, Biol.*, 2017, 172 10.

THE IMPACT OF AMINO AND CARBOXYL FUNCTIONAL GROUPS ON AMPEROMETRIC UREA BIOSENSOR AND POTENTIAL APPLICATIONS FOR AGRICULTURE

Gerda Šimėnaitė¹, Vidutė Gurevičienė¹, Marius Butkevičius¹

¹Department of Bioanalysis, Institute of Biosciences, Life Sciences Center, Vilnius University, Saulėtekio Av. 7, LT-10257 Vilnius, Lithuania
gerda.simenaite@gmc.stud.vu.lt

A graphene-based nanomaterials discovered to be promising for the development of amperometric biosensors. These biosensors have a lot of advantages such as large surface area, which is beneficial for the immobilization of enzymes, high electrical conductivity, conditionally low prices, and good biocompatibility. The synergistic effect of functional chemical groups influences biosensor's sensitivity, selectivity, and overall electrochemical performance.¹

Traditional methods for urea determination often involve complex procedures and time-consuming analyses. Amperometric urea biosensors offer an innovative and effective alternative to these challenges with the potential applications in the medicine, agriculture or fertilizer industry. Its high sensitivity and selectivity enable precise and real-time monitoring of urea levels in soil, contributing to efficient fertilizer management. This not only assists in preventing over-fertilization, reducing environmental impact, and minimizing resource wastage but also ensures optimal nutrient delivery to crops, thereby enhancing agricultural productivity.²

This study aimed to evaluate that the incorporation of positive amino or negative carboxyl functional groups into the reduced graphene oxide, in combination with urease, creates a mediator-free amperometric urea biosensor (Fig. 1). We demonstrated that the incorporation of amino functional group into the reduced graphene oxide positively influences biosensor's parameters and electrochemical performance. Therefore, biosensor with amino functional groups has been applied in practical applications. The urea levels in fertilisers were investigated and the uptake of plant fertiliser was observed by measuring the urea concentration in soils. Also, the performance of the amperometric urea biosensor has been verified with an analogue colorimetric method.

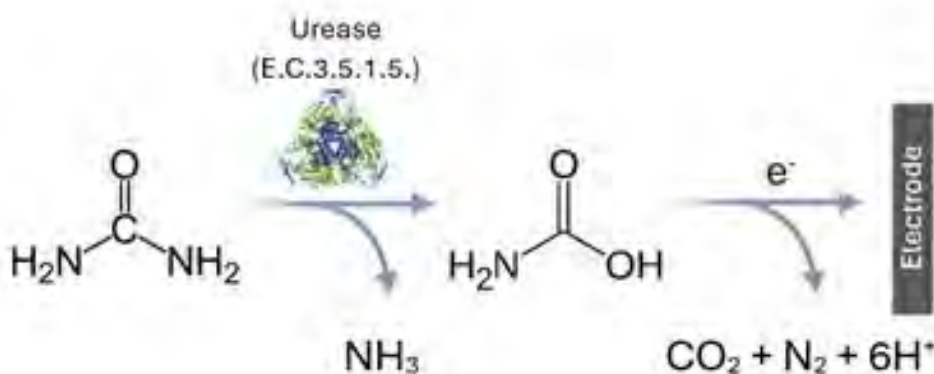


Fig. 1. The principle of direct carbamic acid oxidation.

[1] J.Razumiene, et al. The synergy of thermally reduced graphene oxide in amperometric urea biosensor: application for medical technologies. *Sensors*, 2020, 20.16: 4496.
 [2] S.N.Botewad, et al. Urea biosensors: A comprehensive review. *Biotechnology and Applied Biochemistry*, 2023, 70.2: 485-501.

TAU PROTEIN AND S100A9 CO-INTERACTION STUDIES

Lukas Krasauskas¹, Andrius Sakalauskas¹, Mantas Ziaunys¹, Vytautas Smirnovas¹

¹Amyloid Research Sector, Institute of Biotechnology, Life Sciences Center, Vilnius University, Lithuania
lukas.krasauskas@gmc.vu.lt

Neurodegenerative diseases are one of the most common disorders in the world. Unfortunately, despite intensive research, the understanding of the mechanism of these diseases is limited, and almost all existing treatments are symptomatic [1]. Alzheimer's disease has attracted the most attention from scientists because it is the most common neurodegenerative disease, affecting about 50 million people worldwide. In addition to amyloid plaques composed of amyloid-beta peptides, neurofibrillary tangles formed from the protein Tau are a hallmark of this disease and other tauopathies. Therefore, it is essential to understand the mechanisms at work in this process and determine the best way to curb them. Amyloid-beta aggregates (and alpha-synuclein aggregates in Parkinson's disease) have been shown to promote Tau aggregation [2]. It has also been observed that the aggregation of these two peptides involves the pro-inflammatory protein S100A9, whose elevated levels in the brain are recorded after various head injuries.

Furthermore, one other tauopathy – CTE (Chronic traumatic encephalopathy) – registers high levels of Tau aggregates, and the exact reasons for their formation are unknown. Researchers observed that this disease is quite prominent in contact sport players (e.g., American football) who experiences chronic head concussions [3]. There has been some speculation from the scientific community that neuroinflammation could induce Tau pathology; thus, it is feasible that S100A9 as a pro-inflammatory protein could be a culprit behind it or at least in part responsible. However, it is strange that there is not much information available or studies performed to confirm or rule out the potential of the S100A9 protein or its aggregates to participate directly in Tau aggregation. Therefore, we examined the ability of the S100A9 protein and its aggregates to promote Tau aggregation. We observed that Tau aggregation is dependent on S100A9 aggregate formation as S100A9 monomers alone do not induce Tau aggregation, while S100A9 aggregates induce notable fluorescence changes in the reaction mixture with Tau protein. Various conditions for S100A9 protein aggregation were examined in the study. Aggregation kinetics were recorded by fluorescence spectroscopy using the amyloidophilic dye thioflavin T. Atomic force microscopy was performed to analyze the morphology of the formed aggregates and FTIR spectroscopy was done to analyze secondary structure change in formed aggregates.

[1] Kametani, F., Hasegawa, M. (2018). Reconsideration of Amyloid Hypothesis and Tau Hypothesis in Alzheimer's Disease. *Frontiers in neuroscience*, 12, 25

[2] Nisbet, R. M., et al. (2015). Tau aggregation and its interplay with amyloid- β . *Acta neuropathologica*, 129(2), 207–220.

[3] Marklund, N., et al (2021). Tau aggregation and increased neuroinflammation in athletes after sports-related concussions and in traumatic brain injury patients – A PET/MR study. *NeuroImage: Clinical*, 30, 102665.

CHANGES IN ELECTROPHYSIOLOGICAL PROPERTIES OF MOUSE CA1 PYRAMIDAL NEURONS DURING EARLY POSTNATAL DEVELOPMENT

Emilija Kavalnytė¹, Kornelija Vitkutė¹, Daiva Dabkevičienė^{1,2}, Igor Nagula¹, Urtė Neniškytė^{1,3}, Aidas Alaburda¹

¹Institute of Biosciences, Life Sciences Center, Vilnius University, Vilnius, Lithuania

²National Cancer Institute, Vilnius, Lithuania

³VU-EMBL Partnership Institute, Life Sciences Center, Vilnius University, Vilnius, Lithuania
emilija.kavalnyte@gmc.stud.vu.lt

During the first weeks of postnatal development, neurons undergo morphological changes, and the number of ion channels in the membrane increases [1]. These changes affect neurons electrophysiological properties [2], which determine the ability to receive, process, and encode information. Most of the electrophysiological studies of hippocampal development have been performed with rats, and the electrophysiological maturation of mouse hippocampal CA1 pyramidal neurons remains unknown. Moreover, studies suggest that there are possible sex differences in brain development [3, 4], which may affect electrophysiological profiles as well. Our aim was to evaluate the electrophysiological properties of hippocampal CA1 pyramidal neurons during postnatal development in different sex mice.

Wild-type mice of different sexes and ages (5 to 21 postnatal days) were investigated in this study. Electrical activity of hippocampal CA1 pyramidal neurons in acute mouse brain slices was recorded using the patchclamp whole cell configuration method. From the recordings, passive and active membrane electrophysiological properties were evaluated.

Results of investigating passive membrane properties showed that during the first three postnatal weeks, in both females and males, the resting membrane potential of mice hippocampal CA1 pyramidal neurons did not change, while input resistance and membrane time constant decreased. There were changes in active properties as well: threshold of action potential hyperpolarized, width decreased and amplitude, maximal upstroke and downstroke velocities increased. Spike-frequency adaptation resulted in an increase of action potential width, a decrease of maximal upstroke and downstroke velocities, and a depolarization of the threshold in all age and sex groups. However, the changes of action potential width during spike-frequency adaptation became less pronounced with age.

In conclusion, our findings indicate that the passive and active electrophysiological properties of mouse hippocampal pyramidal neurons change during the first three weeks of postnatal development, resulting in a faster response to a stimulus and generation of action potential series of higher frequency. That may lead to more effective information processing in the mature brain.

-
- [1] Moody, W. J., and Bosma, M. M. (2005). Ion channel development, spontaneous activity, and activity-dependent development in nerve and muscle cells. *Physiological Reviews*, 85(3), 883–941.
- [2] Sanchez-Aguilera, A., Monedero, G., Colino, A., and Vicente-Torres, M. A. (2020). Development of Action Potential Waveform in Hippocampal CA1 Pyramidal Neurons. *Neuroscience*, 442, 151–167.
- [3] Weinhard, L., Neniškyte, U., Vadisiute, A., di Bartolomei, G., Aygun, N., Riviere, L., Zonfrillo, F., Dymecki, S., and Gross, C. (2018). Sexual dimorphism of microglia and synapses during mouse postnatal development: Sexual Dimorphism in Microglia and Synapses. *Developmental Neurobiology*, 78(6), 618–626.
- [4] Yagi, S., and Galea, L. A. M. (2019). Sex differences in hippocampal cognition and neurogenesis. *Neuropsychopharmacology*, 44(1), Article 1.

EVALUATION OF BIOFILM FORMATION AND BIOFILM-ASSOCIATED GENES DISTRIBUTION IN CLINICAL ISOLATES OF OPPORTUNISTIC PATHOGEN *STENOTROPHOMONAS MALTOPHILIA*

Dominykas Grigorjevas¹, Laurita Klimkaitė¹, Edita Sužiedėlienė¹, Julija Armalytė¹

¹Institute of Biosciences, Life Sciences Center, Vilnius University, Vilnius, Lithuania
dominykas.grigorjevas@gmc.stud.vu.lt

One of the biggest health problems in recent years is bacterial multidrug resistance to antibiotics. Almost 5 million deaths were associated with drug-resistant infections in 2019 and it is estimated that by 2050 this number will increase to 10 million per year [1]. *Stenotrophomonas maltophilia* is one of the rising multidrug-resistant opportunistic pathogens that has a mortality rate of up to 37.5% [2]. Infections caused by this pathogen are difficult to treat because of its multidrug resistance phenotype and ability to form biofilms [3]. Bacterial biofilms are complex microbial communities encased in extracellular polymeric substances [4]. This structure produced by bacteria helps them adhere to surfaces and protects them from unfavourable conditions (e.g. desiccation, antibiotics, immune system). *S. maltophilia* is a genetically diverse species and its ability to form biofilms can highly vary [5], therefore it is important to determine the biofilm-forming capability of *S. maltophilia* isolates collected from various sources.

This study aimed to evaluate biofilm formation and biofilm-associated gene distribution in 44 clinical isolates of *S. maltophilia* received from patients of Vilnius university hospital Santaros klinikos. Biofilm formation at 37 °C temperature was evaluated using crystal violet dye assay [5]. Gene prevalence in isolates was evaluated by performing PCR with gene-specific primers and visualizing results using agarose gel electrophoresis.

This study found that all analysed *S. maltophilia* isolates were able to form biofilms. Out of 44 analysed isolates, 14% were weak biofilm producers, 36% were moderate biofilm producers, and 50% were strong biofilm producers. The analysed biofilm-associated genes were highly abundant in all clinical isolates but could not be associated with biofilm production levels. This indicates that differences in gene expression could be responsible for the intensity of biofilm formation.

-
- [1] Salam MA, Al-Amin MY, Salam MT, Pawar JS, Akhter N, Rabaan AA, Alqumber MAA. Antimicrobial Resistance: A Growing Serious Threat for Global Public Health. Healthcare (Basel). 2023
- [2] Falagas, M.E.; Kastoris, A.C.; Vouloumanou, E.K.; Rafailidis, P.I.; Kapaskelis, A.M.; Dimopoulos, G. Attributable mortality of *Stenotrophomonas maltophilia* infections: A systematic review of the literature. *Future Microbiol.* 2009, 4, 1103–1109.
- [3] Brooke, J.S. *Stenotrophomonas maltophilia*: An Emerging Global Opportunistic Pathogen. *Clin. Microbiol. Rev.* 2012
- [4] Ailing Zhao, Jiazheng Sun, Yipin Liu. Understanding bacterial biofilms: From definition to treatment strategies. *Cell. Infect. Microbiol.*, 06 April 2023. Sec. Biofilms
- [5] Montoya-Hinojosa E, Bocanegra-Ibarias P, Garza-Gonzalez E, Alonso-Ambriz OM, Salazar-Mata GA. Discrimination of biofilm-producing *Stenotrophomonas maltophilia* clinical strains by matrix-assisted laser desorption ionization-time of flight. *PLoS One.* 2020

NEUROPROTECTIVE EFFECT OF PLANT DERIVED NANOVESICLES IN ISCHEMIA MODEL

Viktorija Kurmytė¹, Rokas Nekrošius², Zbigniew Balion¹

¹Preclinical Research Laboratory for Medicinal Products, Institute of Cardiology, Lithuanian University of Health Sciences, Kaunas, Lithuania

²Clinic of Cardiac, Thoracic and Vascular Surgery, Hospital of Lithuanian University of Health Sciences Kaunas Clinics, Kaunas, Lithuania
vikturm1023@kmu.lt

Neurological complications are one of the main causes of morbidity and mortality during cardiac surgery characterized by acute ischemic brain lesions, ischemic stroke and inflammation [1]. Existing prevention of ischemic damage (artificial oxygenation and cooling) are insufficient to prevent the damage. Extracellular vesicles (EVs) are nanosized double membraned particles containing cell metabolites, microRNAs, proteins and other substances found in the cells. They are involved in intracellular communication and can pass through blood-brain barrier. Although there is plenty of research done on mammalian EVs, plant derived extracellular vesicles (PDVs) are more scalable and sustainable in comparison [2]. PDVs also exert anti-inflammatory, anti-oxidant, anti-fungal and antimicrobial activity. They contain bioactive metabolites and microRNAs capable of cross-kingdom regulation of gene expression [3]. Unique biological cargo and permeability makes PDVs a good tool for medical applications and might be used during and after cardiac surgery to reduce cerebral damage caused by ischemia.

The aim of this research was to test the neuroprotective effects of PDVs in an ischemic model on mixed neuron-glia cell cultures. For this study, nanovesicles from *Rosa Damascena* rose buds, cranberries, blueberries, guelder rose, and nettle were isolated using the Exoplant-Lo kit (Exolitus). The Nanosight 300 was used to determine the size and concentration of nanovesicles (nanotracking analysis NTA). RNA concentration was determined using Trizol reagent. Protein concentration was determined using the Bradford method. Primary mixed neuron-glia cell culture was obtained from 5-7 days old Wistar rats. Cells were pretreated with PDVs for 24 hours and then transferred into hypoxic conditions (CO_2 5%, O_2 2%, N_2 95%) for 48h. The percentage of live cells was evaluated with fluorescence microscopy using live/dead fluorescent dyes.

Results indicated that size of obtained nanovesicles was in a range of 50 - 250 nm depending on source plant. PDVs contained significant concentrations of RNA and proteins complying with data found in literature. A range of nanovesicles derived from *Rosa Damascena* rose buds (1×10^{10} – 1×10^7 particles/ml) had neuroprotective effects on mixed neuronal-glia cell cultures in an ischemic model, while other PDVs had no or toxic effects at higher doses.

In summary, PDVs from *Rosa Damascena* rose buds prevented cell death in neuronal-glia cells during hypoxia, showing a potential use during cardiac surgeries in order to prevent neurological damage. Also the differences between plant source can highly impact effects of PDVs, as some plant PDVs can have adverse effects depending on concentration.

-
- [1] Lata AL, Hammon JW. Neurologic Complications of Cardiac Surgery [Internet]. In: Baumgartner WA, Jacobs JP, Darling GE, editors. Adult and Pediatric Cardiac Surgery. STS Cardiothoracic Surgery E-Book. Chicago: Society of Thoracic Surgeons; 2023. [cited 2024 January 10]. Available from: ebook.sts.org.
- [2] Lian MQ, Chng WH, Liang J, Yeo HQ, Lee CK, Belaid M, et al. Plant-derived extracellular vesicles: Recent advancements and current challenges on their use for biomedical applications. *J Extracell Vesicles*. 2022 Dec;11(12):12283.
- [3] Alfieri M, Leone A, Ambrosone A. Plant-Derived Nano and Microvesicles for Human Health and Therapeutic Potential in Nanomedicine. *Pharmaceutics*. 2021 Apr 6;13(4):498.

TOWARDS WHOLE-CELL BIOSENSOR DEVELOPMENT FOR MONITORING NATURALLY OCCURRING PHENOLIC ACIDS

Ernesta Augustiniene¹, Ingrida Kutraite¹, Ilona Jonuskiene^{1,2}, Naglis Malys^{1,2}

¹Bioprocess Research Centre, Faculty of Chemical Technology, Kaunas University of Technology, Radvilenu pl. 19, Kaunas LT-50254, Lithuania

²Department of Organic Chemistry, Faculty of Chemical Technology, Kaunas University of Technology, Radvilenu pl. 19, Kaunas LT-50254, Lithuania
ernesta.augustiniene@ktu.lt

Phenolic acids including hydroxybenzoic and hydroxycinnamic acids are important antioxidants and antimicrobial agents utilized in various industries, including food, pharmaceutical, cosmetics, and chemical[1]. They are usually synthesized chemically or extracted from plant biomass using physicochemical methods. However, these approaches have disadvantages, including the requirement of large amounts of solvent, the low recovery yield, and the consequent high cost that limits widespread use[2, 3]. The use of microbial cell factories based on *Escherichia coli*, *Streptomyces* sp., *Corynebacterium glutamicum*, *Pseudomonas* sp., *Bacillus* sp., *Amycolatopsis* sp., and *Klebsiella pneumonia* has come into focus as a sustainable alternative for phenolic acid production[4]. Inducible gene expression systems composed of chemical molecule-responsive transcription factor (TF) and inducible promoters have come into the focus as a platform for TF-based whole-cell biosensors and can be used as an *in vivo* analytical tool for extracellular and intracellular metabolite analysis. Previous studies have shown that this type of biosensors is adaptable to the design–build–test–learn cycle and has been successfully applied for high-throughput systems screening to study phenolic acids metabolism and forward engineering[5]. Here, by applying a multi-genome approach, we have identified phenolic acid-inducible gene expression systems composed of TF-inducible promoter pairs responding to different phenolic acids. Subsequently, they were used for the development of whole-cell biosensors based on model bacterial hosts, including *Escherichia coli*, *Cupriavidus necator* and *Pseudomonas putida*. The dynamics and range of the biosensors were evaluated by establishing their response to the primary inducer, while the specificity of biosensors was determined by screening twenty major phenolic acids. To exemplify applicability, we utilize a protocatechuic acid-biosensor to identify enzymes with enhanced activity for conversion of *p*-hydroxybenzoate to protocatechuate.

[1] Russell W and Duthie G. Plant secondary metabolites and gut health: the case for phenolic acids. *Proceedings of the Nutrition Society* 70, 2011.

[2] Li, M. et al. Enhancing isolation of *p* coumaric and ferulic acids from sugarcane bagasse by sequential hydrolysis. *Chemical Papers* 74, 2020.

[3] Zavala-López, M. and García-Lara, S. An improved microscale method for extraction of phenolic acids from maize. *Plant Methods* 13, 81, 2017.

[4] Huccetogullari D, Luo ZW, Lee SY. Metabolic engineering of microorganisms for production of aromatic compounds. *Microbial Cell Factories* 18, 41, 2019.

[5] Kaczmarek JA, Prather KLJ. Effective use of biosensors for high-throughput library screening for metabolite production. *Journal of Industrial Microbiology and Biotechnology* 48, 2021

CALCIUM-INDUCED HETERODIMERIZATION OF S100A8 WITH S100A1 TRIGGERS AMYLOID FIBRILLATION

Viktorija Karalkevičiūtė¹, Ieva Baronaitė¹, Darius Šulskis¹, Vytautas Smirnovas¹

¹Sector of Amyloid Research, Institute of Biotechnology, Life Sciences Centre, Vilnius University, Lithuania
viktorija.karalkeviciute@gmc.stud.vu.lt

S100 is a family of calcium-binding proteins, consisting of isoforms with structural similarity but functional diversity [1]. S100 proteins regulate various proteins involved in cellular functions like calcium homeostasis, cell growth, differentiation, cytoskeleton dynamics, and energy metabolism [2]. Several members are known to be important in neurodegeneration by signaling neuroinflammation and forming amyloid fibrils. One of them is S100A9, which is well-studied, but the roles of S100A1 and S100A8 remain relatively unexplored.

S100A1 is predominantly expressed in the brain, skeletal and cardiac muscles [3]. S100A1 interacts with tau, RAGE, and RyR - proteins that participate Alzheimer's disease (AD) cascade [4]. Another family member S100A8 is mostly found in neutrophils and monocytes [5] and plays a role in neurological disease pathology as well. S100A8 homodimers can independently induce neuroinflammation [6] and their overexpression in AD patients leads to activation of microglia [7, 8]. However, it is known that S100A8 can form a heterodimer with S100A9 called calprotectin [9], but interaction with S100A1 is still not investigated. Both S100A1 and S100A8 are expressed in the cerebral cortex as per the Human Protein Atlas (<https://www.proteinatlas.org/>) [10] and share structural similarities [1]. Thus, our main goal was to elucidate their potential complex formation.

To explore the aggregation kinetics of the S100A1/A8 complex, we employed the Thioflavin T Fluorescence Assay, unveiling calcium concentration-dependent amyloid formation. In addition, Atomic Force Microscopy (AFM) was used to visualize the S100A1/A8 fibrils and, Differential Scanning Fluorimetry (DSF) to quantify protein stabilities. In conclusion, our research contributes new findings to the understanding of S100A1 and S100A8 aggregation dynamics, offering valuable insights into their relevance to various diseases.

-
- [1] P. Singh and S. A. Ali, "Multifunctional Role of S100 Protein Family in the Immune System: An Update," *Cells*, vol. 11, no. 15, Jan. 2022.
 [2] R. Donato et al., "Functions of S100 Proteins," *Curr. Mol. Med.*, vol. 13, no. 1, pp. 24–57, Jan. 2013.
 [3] N. T. Wright et al., "S100A1: Structure, Function, and Therapeutic Potential," *Curr. Chem. Biol.*, vol. 3, no. 2, pp. 138–145, May 2009.
 [4] J. S. Cristóvão and C. M. Gomes, "S100 Proteins in Alzheimer's Disease," *Front. Neuroscience*, vol. 13, 2019.
 [5] K. Sunahori et al., "S100A8/A9 Heterodimer and Proinflammatory Cytokine Production in Rheumatoid Arthritis," *Arthritis Res. Ther.*, vol. 8, no. 3, p. R69, 2006.
 [6] T. Vogl et al., "Pro-Inflammatory S100A8 and S100A9 Proteins," *Int. J. Mol. Sci.*, vol. 13, no. 3, Mar. 2012.
 [7] M. Sidoryk-Wegrzynowicz et al., "Astrocytes in Mouse Models of Tauopathies," *Acta Neuropathol. Commun.*, vol. 5, no. 1, p. 89, Nov. 2017.
 [8] H. L. Weiner and D. Frenkel, "Immunology and Immunotherapy of Alzheimer's Disease," *Nat. Rev. Immunol.*, vol. 6, no. 5, May 2006.
 [9] I. P. Korndörfer et al., "Crystal Structure of the Human Calprotectin," *J. Mol. Biol.*, vol. 370, no. 5, pp. 887–898, Jul. 2007.
 [10] M. Uhlen et al., "Knowledge-based Human Protein Atlas," *Nat. Biotechnol.*, vol. 28, no. 12, pp. 1248–1250, Dec. 2010.

A COMPARATIVE STUDY OF ELECTROPORATION-INDUCED CELL DEATH IN SUSPENSION AND MONOLAYER CULTURES

Aras Rafanavičius¹, Ingrida Šatkauskienė², Saulius Šatkauskas²

¹Department of Biochemistry, Faculty of Natural Sciences, Vytautas Magnus University, Kaunas, Lithuania

²Cell and Tissue Biotechnology Research Group, Institute of Research of Natural and Technological Sciences, Vytautas Magnus University, Akademija, Lithuania
aras.rafanavicius@vdu.lt

Electroporation (EP) is a technique that uses short electric pulses to create pores in cell plasma membrane and has been utilized for malignant tissue ablation since 2005 [1]. If the amplitude of applied pulsation is sufficiently high, the cells eventually die due to homeostasis disruption and membrane damage. This process is called irreversible electroporation (IRE) and is used to target cancerous tumors and, as of recently, cardiac tissue, in order to treat certain types of arrhythmias [2, 3]. In the past years, many studies have evaluated the efficiency of IRE both *in vitro* and *in vivo*, however, these studies are not necessarily directly comparable, as different electrode configurations, medium compositions and electrical parameters are often used, and not all data is available publicly [3]. Thus, in this study, it was aimed to elucidate optimum conditions for IRE that would utilize lowest energy and achieve highest cell mortality rates.

Chinese hamster ovary cells were subjected to EP using stainless steel electrodes. During the evaluation of viability of electroporated suspended cells, the suspension was placed between parallelly-arranged electrode plates. The viability of the treated cells in suspension was evaluated by measuring their fluorescence after staining with propidium iodide, an otherwise membrane-impermeant dye, 20 min post-EP via flow cytometry. Clonogenic assay was also employed to assess cell survival. The same EP conditions were applied to cell monolayers, and the extent of electroporation was evaluated. The cells had been plated in the wells of 24-well plates 48 h prior to the experiment. Reversible and irreversible electroporation zones were identified using fluorescent microscopy. For imaging, the dead and permeable cells were stained with propidium iodide, and the viable cells were stained using calcein-AM.

The scope of irreversible electroporation was determined under varying electroporation parameters i.e., the number of pulses, pulse duration and amplitude while maintaining the same total single pulse energy. In cell suspensions, the decrease in cell viability is proportional to electric field strength, and ultimately plateaus after using a high number of pulses. The areas of reversible and irreversible cell monolayer electroporation were compared, and these results were contrasted with the results of viability of cells that were electroporated in suspension. Preliminary experiments show that irreversibly electroporated area grows more slowly than the area of reversible electroporation.

[1] Miller et al. (2005). Cancer cells ablation with irreversible electroporation. *Technology in cancer research and treatment*, 4(6), 699–705.

[2] Lavee et al. (2007). A novel nonthermal energy source for surgical epicardial atrial ablation: irreversible electroporation. *The heart surgery forum*, 10(2), E162–E167.

[3] Casciola et al. (2022). Human cardiomyocytes are more susceptible to irreversible electroporation by pulsed electric field than human esophageal cells. *Physiological reports*, 10(20), e15493.

DEVELOPMENT OF AN INNOVATIVE SCAFFOLD MADE FROM DECELLULARIZED CANINE BONE FOR USE IN VETERINARY DENTISTRY

Łukasz Młynarski¹, Julia Niegowska¹, Tomasz Gębarowski², Maciej Janeczek²

¹Students Scientific Society Department of Biostructure and Animal Physiology, Wrocław University of Environmental and Life Sciences, Poland

²Department of Biostructure and Animal Physiology, Wrocław University of Environmental and Life Sciences, Poland
123539@student.upwr.edu.pl

In canine veterinary medicine in the field of dentistry, doctors often encounter problems with bone defects. A common reason is trauma, but they can also arise from the formation of cysts. After tooth extraction, a defect in bone tissue is created, filling such a defect with a restorative explant significantly improves the degree of regeneration of the alveolar area. Our goal was to develop a method for decellularizing canine bone for use as allogeneic filling material. Usually, hydroxyapatite is used in the treatment of bone defects in the oral cavity, which is not always the optimal solution for bone healing. This is due to its brittleness, low resistance to stretching, fractures and unpredictable adaptability. Decellularized bone has been cleared of cells, preserving only its mineral and chemical composition. We have developed an effective method of cleaning the bone so that the result is an immunologically inert bone composite. We determined the composition and concentration of reagents, and their duration of action to achieve desired results. The research has allowed us to develop a decellularization method with satisfactory results. We hope that the developed product can be used for bone replacement in veterinary dentistry, especially in the extraction of canines.

THE SEA BUCKTHORN BERRY POMACE AND LEAF EXTRACTS: INVESTIGATION OF BIOLOGICALLY ACTIVE COMPOUNDS AND ANTIBACTERIAL PROPERTIES

Juozas Girtas¹, Natalja Makštutienė¹, Karolina Almonaitytė¹, Antanas Šarkinas¹

¹Food Institute, Kaunas University of Technology, Radvilenu Rd.19 C, Kaunas, Lithuania
juozas.girtas@ktu.edu

Plants are a rich source of biologically active compounds with various useful properties [1]. Sea buckthorn has a wide spectrum of useful compounds which are nutritious and can be found in berries, leaves, twigs and bark. The sea buckthorn industry is dependent on its berries, but there are almost no applications for its secondary biomass use, which alone reaches about 12–15% [2].

This study focused on the use of sustainable solvents for the sea buckthorn berry pomace and leaf extracts preparation. Biologically active compounds, such as phenolic and proanthocyanidins from the buckthorn berry pomace and leaf extracts were measured using spectrophotometric analysis. The extracts were used for anti-microbial activity against *Escherichia coli* ATCC 8739, *Staphylococcus aureus* ATCC 25923, *Salmonella typhimurium* ATCC 14028, *Bacillus cereus* ATCC 11778, *Listeria monocytogenes* ATCC 13932.

The highest concentration of phenolic compounds content in sea buckthorn berry pomace extract was determined 4.13 mg/g of dry material (DM) and in leaf extract 61.22 mg/g of DM. The highest concentration of proanthocyanidins in sea buckthorn leaf extract was determined 27.58 mg/g of DM. These identified concentrations are considered sufficient to exhibit measurable antibacterial activity against food spoilage microbes and food pathogens. The largest inhibition zone was determined in *S. aureus* ATCC 25923 (26.0 mm) and *B. cereus* ATCC 11778 (22.0 mm) bacterial strains where induced by leaves aqueous extract.

This research shows a potential of sea buckthorn berry pomace and leaves as a source of bioactive, anti-bacterial compounds, which can be used in various types of industries.

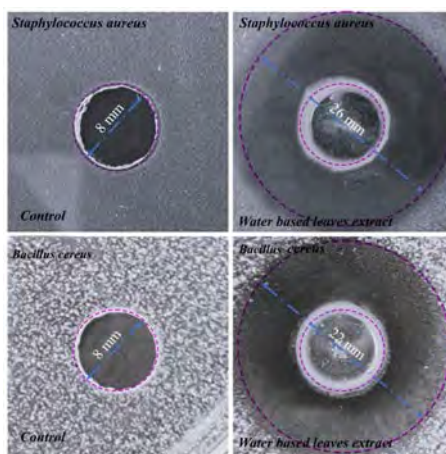


Fig. 1. Inhibition of bacteria *B.cereus* and *S.aureus* using water based leaf extracts.

Acknowledgements: This research was supported by Lithuanian Rural Development Program 2014- 2020 under activity “Support for the creation and development of EIP activity groups” project Circular manufacturing model for producing biologically active material No. 35BV-KK-22-1-05005-PR001

[1] TRITEAN, Naomi, et al. Cytocompatibility, Antimicrobial and Antioxidant Activity of a Mucoadhesive Biopolymeric Hydrogel Embedding Selenium Nanoparticles Phytosynthesized by Sea Buckthorn Leaf Extract. *Pharmaceuticals*, 2023, 17.1: 23.

[2] JANCEVA, Sarmite, et al. Sea buckthorn (*Hippophae rhamnoides*) waste biomass after harvesting as a source of valuable biologically active compounds with nutraceutical and antibacterial potential. *Plants*, 2022, 11.5: 642.

ADVANCING GGT RESEARCH WITH SECM AND NOVEL ELECTROCHEMICAL PROBES

Tomas Mockaitis¹, Sheng-Tung Huang², Inga Morkvėnaitė-Vilkončienė¹

¹Center for Physical Sciences and Technology, Department of Nanotechnology

²National Taipei University of Technology, Department of Chemical Engineering
tomas.mockaitis@ftmc.lt

γ-Glutamyl transpeptidase (GGT) is a crucial enzyme involved in the metabolism of glutathione (GSH) [1]. This enzyme is mostly found in the cellular membranes of many organs, with the highest concentrations observed in the liver, kidney, and pancreas. Increased levels of GGT have been found to be associated with various types of human tumors, including liver, cervical, ovarian, and breast cancers [2]. Elevated levels of GGT in the bloodstream can be utilized as a diagnostic indicator for assessing the functionality of the liver, bile ducts, the presence of pancreatitis, and cholestasis [3]. In addition, GGT is used as a biochemical marker for alcohol use because there is a direct relationship between the amount of alcohol consumed and the activity of GGT [4].

In clinical practice, GGT measurements are usually performed during liver function tests. GGT demonstrates potential as a therapeutic target for various disorders, in addition to its diagnostic usefulness. For instance, suppressing GGT activity in animal models of nonalcoholic fatty liver disease can enhance insulin sensitivity and decrease the accumulation of fat in the liver [3]. Therefore, it is imperative to assess GGT activity in the body and biological fluids for the immediate identification of diverse illnesses and the monitoring of therapy. Colorimetric measurement, electrochemical and luminescence analysis are some of the ways that the amount of GGT present can be found. Among these technologies, bioassays utilizing responsive probes have garnered significant interest. As a result, a number of responsive probes have been created in recent years to quantify GGT activity.

The signal intensity of an enzyme in an electrochemical system can be affected by whether the enzyme is immobilized on a surface or in a liquid state. The process of immobilizing on a surface is frequently utilized in bioelectrochemical devices, such as biosensors, to improve stability, expand the surface area, and enable electron transport. Enzymes can be immobilized on a surface to create a stable and regulated environment. It facilitates the effective flow of electrons to electrodes, hence improving the overall strength of the signal. The aim of our studies is to perform research on the enzyme GGT using scanning electrochemical microscopy (SECM) and a recently developed electrochemical probe [3].

Acknowledgements

The research was funded by Taipei Tech – VILNIUS TECH Joint Research Collaborative Seed Grant Program 2023. Project title: “Detection of biomarkers DPP-IV by electrochemical probes and scanning electrochemical microscope”.

-
- [1] H.Liu, F.Liu, et al., A novel mitochondrial-targeting near-infrared fluorescent probe for imaging γ-glutamyl transpeptidase activity in living cells, *Analyst*, 143(22), 5530-5535 (2018)
- [2] J.B.Whitfield, Gamma Glutamyl Transferase. In *Critical Reviews in Clinical Laboratory Sciences*, 38(4) (2001)
- [3] N.Kumaragurubaran et al., Development of an activity-based ratiometric electrochemical probe of the tumor biomarker γ-glutamyl transpeptidase. *Biosensors and Bioelectronics*, 248 (2024)
- [4] J.H.D.A.Van Beek et al., The association of alcohol intake with gamma-glutamyl transferase (GGT) levels: Evidence for correlated genetic effects, *Drug and Alcohol Dependence*, 134(1), 99-105 (2014)

POLYPYRROLE-MODIFIED SACCHAROMYCES CEREVISIAE USED IN MICROBIAL FUEL CELL

Domas Pirštelis¹, Kasparas Kižys¹, Inga Morkvėnaitė-Vilkončienė¹

¹Laboratory of Bioelectrochemical Technology, Center for Physical Sciences and Technology, Lithuania
kasparas.kizys@ftmc.lt

Microbial fuel cells (MFCs) have the potential to be utilized for water purification, energy generation, and as biosensors. However, their practical applicability is severely restricted due to their low current density. This study introduces an enhanced version of Bakers' yeast (*S. cerevisiae*) that incorporates MFC (Microbial Fuel Cell) modified with polypyrrole (pPy) in the presence of 9,10-phenanthrenequinone (PQ).

PQ functions as a redox mediator, facilitating the flow of electrons across the yeast membrane. This leads to an increased permeability of the membrane to electrical charge, while having a minor inhibitory effect on yeast growth [1]. To enhance MFC performance, yeast cells were genetically altered to incorporate a conductive polymer pPy, which was generated by leveraging the metabolic activities of the yeast cells themselves. pPy facilitates electrical charge transfer from the microbe to the electrode while also ensuring the yeast cell remains unharmed [2].

Three graphite electrodes coated with PQ, in their unmodified state, were tested. The electrodes were coated with yeast, and another set of electrodes were coated with yeast modified with pPy. Each set of electrodes was tested in PBS solution and a glucose/potassium hexacyanoferrate solution after 20 minutes of incubation. The electrodes were assessed using cyclic voltammetry. The unmodified electrode showed an oxidative peak of 165 mA in the glucose/potassium hexacyanoferrate solution. The yeast-covered electrode exhibited a significantly higher oxidative peak of 304 mA, which is 1.84 times greater than that of the unmodified electrode. The modified-yeast-covered electrode had the highest oxidative peak of 369 mA, which is 2.24 times greater than that of the unmodified electrode.

Based on the findings, it can be inferred that the current measured by graphite electrode is enhanced by 2.24 times when it is coated with PQ and pPy modified yeast. This results in greater potassium hexacyanoferrate oxidative peak currents compared to using PQ to cover the electrode. Therefore, the pPy modified yeast has a great potential to be used in microbial fuel cell for enhanced charge transfer.

[1] J. Rožėnė et al. *Electrochimica Acta* 373 p. 159-168 (2021)

[2] A. Kisieliute et al. *Chem. Eng.* 356 p. 1014–1021 (2019)

ADAPTABLE TARGET DNA LIBRARY CONSTRUCTION FOR BENCHMARKING PROGRAMMABLE NUCLEASES

Agata Kipran^{1,2}, Urtė Glibauskaitė^{1,2}, Rokas Grigaitis², Stephen Knox Jones Jr², Lina Krikščikaitė^{1,2}

¹Vilnius University

²VU LSC EMBL Partnership Institute

agata.kipran@gmc.stud.vu.lt

For practical application of programmable nucleases from microbial immune systems, a thorough knowledge of their processes is required. However, it might take years or decades because of the complexity of systems, current research methodologies, and resource constraints. Our approach is a plasmid-based target DNA library with a changeable target sequence with a Protospacer Adjacent Motif (PAM) flanked by barcode sequences for cleavage pattern analysis. We employ type IIS restriction endonucleases for PAM excision to change the constant PAM region while retaining variable targets and barcodes. The PAM exchange is accomplished by ligation with a short DNA sequence that matches the PAM of a different programmable nuclease. This allows for the quick adaptation of a single DNA library to test the specificity of numerous programmable nucleases. It also shortens the period between enzyme discovery and implementation.

COMPARATIVE STUDIES OF THE EFFECT OF LORATADINE AND DESLORATADINE ON NOVOCAINE HYDROLYSIS

Anastasiia Behdaj¹, Roman Smishko¹, Vadym Lisovyi^{1,2}, Volodymyr Bessarabov¹, Galina Kuzmina¹, Olha Syviuk¹

¹Department of Industrial Pharmacy, Kyiv National University of Technologies and Design, Ukraine

²Department of Chemical Technology and Resource Saving, Kyiv National University of Technologies and Design, Ukraine
a.behdaj@kyivpharma.eu

A local anesthetic is a drug used to temporarily numb a small part of the body before surgery. The target of local anesthetics is blockade of sodium channels, which transmit nerve impulses. Novocaine, a derivative of para-aminobenzoic acid, belongs to the ester group. Although novocaine is not a highly effective drug by modern standards, it is safe and readily available. Novocaine, are less likely to cause toxic reactions because they are rapidly destroyed in the body by butyrylcholinesterase. Butyrylcholinesterase is synthesized in the liver and is present in high concentrations in the blood plasma. Therefore, when a local anesthetic is injected into the tissue, it is rapidly hydrolyzed and inactivated, which stops the blockade of sodium channels.

Due to the short-term effect of novocaine, it is important to search for butyrylcholinesterase inhibitors that ensure the long-term effect of the drug. For this study, we selected loratadine and desloratadine, second- and third-generation antihistamine active pharmaceutical ingredients (APIs). The administration of local anesthetics often activates histamine receptors, so the additional use of antihistamine APIs can reduce side effects. Loratadine and desloratadine are safe to use and have several advantages. They do not cause sedation or affect attention levels. This is due to the fact that these compounds do not penetrate the blood-brain barrier.

It was found that the first-order rate constant of hydrolysis of novocaine in the system with human serum with the addition of 100 μM loratadine significantly decreases from $K_{H(0)}^1=0,85\pm0,07\times10^{-3} \text{ s}^{-1}$ to $K_{H(100)}^1=0,09\pm0,01\times10^{-3} \text{ s}^{-1}$, while the decomposition of novocaine decreases by 9.4 times. At concentrations of loratadine in the system of 25 μM and 50 μM , the rate constant significantly decreases by 2.9 and 5.6 times, respectively ($K_{H(25)}^1=0,29\pm0,02\times10^{-3} \text{ s}^{-1}$, $K_{H(50)}^1=0,15\pm0,01\times10^{-3} \text{ s}^{-1}$) ($p\leq 0,05$).

The studies also revealed that the third-generation antihistamine API, desloratadine, exhibits more potent inhibitory properties against butyrylcholinesterase. A decrease in the first-order rate constant is observed when 75 μM desloratadine is added to the system by 12.1 times from $K_{H(0)}^1=0,85\pm0,07\times10^{-3} \text{ s}^{-1}$ to $K_{H(75)}^1=0,07\pm0,01\times10^{-3} \text{ s}^{-1}$. At concentrations of 25 μM and 50 μM , the rate constant significantly decreases by 3.9 and 7.7 times, respectively ($K_{H(25)}^1=0,22\pm0,01\times10^{-3} \text{ s}^{-1}$ and $K_{H(50)}^1=0,11\pm0,02\times10^{-3} \text{ s}^{-1}$) ($p\leq 0,05$).

Therefore, it can be concluded that both loratadine and desloratadine possess inhibitory properties against the decomposition process of novocaine by human serum butyrylcholinesterase. New drugs for local anesthesia with prolonged effects may be developed by combining loratadine or desloratadine with novocaine in a single dosage form.

ENGINEERING DNMT1 FOR CATALYTIC ACTIVITY WITH SYNTHETIC ADOMET ANALOGS

Karina Račaitė¹, Aleksandras Čečkauskas¹, Vaidotas Stankevičius¹, Saulius Klimašauskas¹, Liepa Gasiulė¹

¹Department of Biological DNA Modification, Institute of Biotechnology, Life Sciences Center, Vilnius University, Lithuania
karina.racaitė@gmc.vu.lt

Cytosine methylation (5mC) is the most common epigenetic modification conserved in mammals. DNA methyltransferases use cofactor S-Adenosyl-L-methionine (AdoMet) as a methyl group donor to covalently modify genomic DNA [1]. In mammals, DNA methylation patterns are established by Dnmt3a and Dnmt3b and maintained by Dnmt1. DNA methylation is significant for embryonic development, gene regulation, suppression of transposable elements, genomic imprinting, and X chromosome inactivation. Regulation patterns of individual methyltransferases are still not clearly understood [2].

This study aimed to determine the ability of Dnmt1 to use synthetic AdoMet analogs, where the carboxyl group is changed into the hydroxyl group, *in vitro*. Hence, vectors containing mouse *Dnmt1* gene with desirable mutations were constructed and inserted into *Pichia pastoris* strain yeast cells by electroporation. Clones resistant to antibiotic G418 were selected and protein expression was induced using methanol. Dnmt1 mutants were purified from a soluble fraction of lysed *P. pastoris* cells via immobilized metal ion affinity chromatography. Purified proteins were used to label DNA using synthetic AdoMet analog SAMol-N₃ *in vitro* and click chemistry was applied to tag azidohex-2-ynyl groups with fluorescent dye. It has been confirmed that Dnmt1 mutants can use SAMol-N₃ to label DNA. Furthermore, HPLC-MS analysis revealed that purified Dnmt1 proteins were able to use synthetic AdoMet analogs (SAMol-N₃), although only in the absence of AdoMet.

[1] Lyko, F. (2018). The DNA methyltransferase family: A versatile toolkit for epigenetic regulation. *Nature Reviews Genetics*, 19(2), 81–92. <https://doi.org/10.1038/nrg.2017.80>

[2] Chen, T. (2011). Mechanistic and Functional Links Between Histone Methylation and DNA Methylation. *Progress in Molecular Biology and Translational Science* (T. 101, p. 335–348). Elsevier. <https://doi.org/10.1016/B978-0-12-387685-0.00010-X>

INHIBITION OF CRISPR-CAS DEFENCE BY ANTI-CRISPR PROTEINS

Melita Graužinytė¹, Tomas Šinkūnas¹

¹Department of Protein-DNA Interactions, Institute of Biotechnology, Life Sciences Center, Vilnius University
melita.grauzinyte@gmc.stud.vu.lt

Bacteriophages and bacteria are in a constant evolutionary arms race, developing a variety of attack, defence and counter-defence tactics. In the face of phage attacks, bacteria have evolved multiple defensive mechanisms, one of which is the CRISPR-Cas system. This system encodes a ribonucleoprotein complex that destroys the invading phages by targeting their genetic material.¹ To evade this defence strategy, phages employ anti-CRISPR (Acr) proteins that disrupt the functionality of the CRISPR-Cas system, typically by interfering with its DNA-binding or hydrolytic functions.² CRISPR-Cas systems are used as invaluable tools for genome editing.³ The ability of Acr proteins to modify the actions of CRISPR-Cas opens up new possibilities for their biotechnological applications.⁴ More than 100 Acr families have been identified, but the molecular mechanisms are only understood for a limited number of these proteins.⁴

In this study, we aim to elucidate the inhibition mechanisms of the type I-F CRISPR-Cas system by small AcrIF proteins. By combining *in vivo*, structural and biochemical methods, we analyse the molecular interplay between the components of the system and the AcrIF proteins.

-
- [1] Ishino, Y., Krupovic, M., Forterre, P. (2018). History of CRISPR Cas from Encounter with a Mysterious Repeated Sequence to Genome Editing Technology. *Journal of Bacteriology*, 200(7).
- [2] Bondy Denomy, J., Pawluk, A., Maxwell, K. L., Davidson, A. R. (2013). Bacteriophage genes that inactivate the CRISPR Cas bacterial immune system. *Nature*, 493(7432), 429.
- [3] Ran, F. A., Hsu, P. D., Wright, J., Agarwala, V., Scott, D. A., Zhang, F. (2013). Genome engineering using the CRISPR Cas9 system. *Nature Protocols*, 8(11), Article 11.
- [4] Kraus, C., Sontheimer, E. J. (2023). Applications of AntiCRISPR Proteins in Genome Editing and Biotechnology. *Journal of Molecular Biology*, 435(13), 168120.

THE QUANTITATIVE COMPOSITIONS OF MATRIX METALLOPROTEINASES IN BLOOD PLASMA OF DONOR GROUPS WITH VARIOUS TITERS OF ANTI-SARS-COV-2 IGG

Antonina Rachkovska¹, Vitaliy Karbovskiy², Maryna Kalashnikova¹

¹Taras Shevchenko National University of Kyiv, Ukraine

²LLC BIOPHARMA-PLASMA, Ukraine

tonia01128@gmail.com

Background. Matrix metalloproteinases (MMPs) play a key role in oxidative stress, circulatory metabolism, and pro- and anti-inflammatory conditions during the progression of SARS-CoV-2 infection. Protease activity dysregulation brought on by the inflammatory response could be connected to complications following COVID-19. Aberrant MMP function may show up in the blood and harm the blood's proteolytic processes in post-COVID-19 period.

The aim of our research to determine the quantitative levels MMP-1, -2, -3, -8, -9, -10 in blood plasma of donor groups depending on titers of anti-SARS-CoV-2 IgG.

Materials and methods. People who had suffered from COVID-19 agreed to be donors of blood plasma for biotechnological purposes at the "BIOPHARMA-PLASMA" company (Kyiv, Ukraine). Blood plasma was collected from donors who had recovered from COVID-19 3-6 months ago. We had donor groups with anti-SARS-CoV-2 IgG titers (20 donors in each group): 0, 10 ± 3 , 55 ± 5 , 65 ± 5 , 75 ± 5 , 85 ± 5 , 95 ± 5 , 125 ± 5 and 175 ± 5 Index (S/C). Levels of MMP-1, -2, -8, and -9 were determined using an enzyme-linked immunosorbent assay (ELISA).

Results. We established the quantitative amounts of gelatinases (MMP-2, MMP-9) and collagenases (MMP-1, MMP-8) in the blood plasma of donor groups depending on titers of anti-SARS-CoV-2 IgG. Here we have underlined the donor groups with maximum and minimum changes in MMP levels (among donor groups with titers of anti-SARS-CoV-2 IgG $\geq 10 \pm 3$ Index (S/C)) compared to the reference point (donor groups with titers of anti-SARS-CoV-2 IgG 0 Index (S/C)). The most statistically significant differences are the minimum (125 ± 5 Index (S/C)) and maximum (75 ± 5 Index (S/C)) levels of MMP-2 compared to the reference point; the maximum level of MMP-9 (10 ± 3 Index (S/C)) compared to the reference point; the maximum level of MMP-1 (175 ± 5 Index (S/C)) compared to the reference point; the minimum (10 ± 3 Index (S/C)) and maximum (65 ± 5 Index (S/C)) MMP-8 levels compared to the reference point. The results are presented in Figure 1.

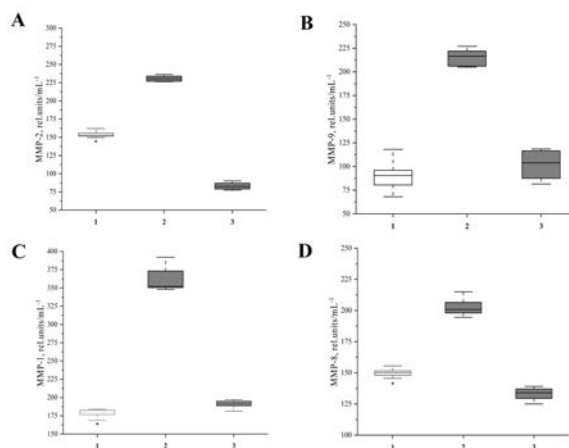


Fig. 1. A) The level of MMP-2 in donor groups with titers of anti-SARS-CoV-2 IgG: 1 – 0; 2 – 75 ± 5 ; 3 – 125 ± 5 ; B) The level of MMP-9 in donor groups with titers of anti-SARS-CoV-2 IgG: 1 – 0; 2 – 10 ± 3 ; 3 – 85 ± 5 ; C) The level of MMP-1 in donor groups with titers of anti-SARS-CoV-2 IgG: 1 – 0; 2 – 175 ± 5 ; 3 – 125 ± 5 ; D) The level of MMP-8 in donor groups with titers of anti-SARS-CoV-2 IgG: 1 – 0; 2 – 65 ± 5 ; 3 – 10 ± 3 .

Conclusion. We confirm the differences between MMP levels of reference point and donor groups with titers of anti-SARS-CoV-2 IgG $\geq 10 \pm 3$ Index (S/C). We underline that the presence of MMPs in blood plasma at various levels can lead to proteolysis destabilization. It may trigger metabolic dysfunctions and accompanying diseases in the post-COVID-19 period.

DEVELOPMENT OF A MOLECULARLY IMPRINTED POLYMER IMMUNOSENSOR FOR THE SEROLOGICAL DETECTION OF SARS-CoV-2 PROTEIN

Viktorija Liustrovaitė^{1,2}, Vilma Ratautaitė³, Arūnas Ramanavičius^{1,2,3}

¹NanoTechnas - Center of Nanotechnology and Materials Science, Institute of Chemistry, Faculty of Chemistry and Geosciences, Vilnius University

²Department of Physical Chemistry, Institute of Chemistry, Faculty of Chemistry and Geosciences, Vilnius University

³Department of Nanotechnology, State Research Institute Center for Physical and Technological Sciences
viktorija.liustrovaite@chgf.vu.lt

The current global health challenges, prompted by SARS-CoV-2, highlight the requirement for new diagnostic tools. The quick mutations of the virus underline the need for advanced analytical techniques to identify it precisely. Researchers have extensively explored the virus, including its protein structures, genome, and interactions with medications. However, traditional methods like reverse transcription polymerase chain reaction (RT-PCR) and enzyme-linked immunosorbent assay (ELISA) come with inherent limitations. Molecularly imprinted polymers (MIPs) are an attractive alternative to other detection techniques [1].

This study presents the development and characterisation of an immunosensor designed for the serological detection of the SARS-CoV-2 protein. The immunosensor employs a molecularly imprinted polymer (MIP) and integrates a self-assembled monolayer (SAM) on the gold interface. Electrochemical impedance spectroscopy (EIS) and square wave voltammetry (SWV) were utilised for the electrochemical characterisation of gold electrodes modified with MIP and non-imprinted polymer (NIP) layers. The use of screen-printed electrodes and electrochemical techniques ensures a cost-effective and reliable platform for developing of this biosensing technology [2].

The removal of the protein template from the MIP layer increase in the electron transfer rate and decreased the impedance. The MIP-based immunosensor exhibited higher sensitivity compared to the NIP counterpart, demonstrating its potential for selective protein detection. The limit of detection values obtained through SWV and EIS underscored the sensors capability to detect low concentrations of the target protein. Specificity tests confirmed minimal nonspecific binding, showing the reliability of the novel immunosensor. The findings highlight the potential of molecularly imprinted polymers for the creation of effective, sensitive, and selective biosensors, contributing to advances in the field of diagnostic technology for infectious diseases.

[1] V. Ratautaitė, et al. "Molecularly imprinted polypyrrole based sensor for the detection of SARS-CoV-2 spike glycoprotein." *Electrochimica acta* 403 (2022): 139581.

[2] M. Drobys, et al. "Determination of rSpike protein by specific antibodies with screen-printed carbon electrode modified by electrodeposited gold nanostructures." *Biosensors* 12.8 (2022): 593.

TRANSGLUTAMINASE APPLICATION FOR CARRIER-FREE ENZYME IMMOBILIZATION BY CLEA METHOD

Augustinas Vadeiša¹, Ieva Ožiūnaitė¹, Inga Matijošytė¹

¹Sector of Applied Biocatalysis, Institute of Biotechnology, Life Sciences Center, Vilnius University, Lithuania
augustinas.vadeisa@gmc.stud.vu.lt

Enzymes are widely used in industry, and they can be used in two different ways. The first approach involves using soluble enzymes, which are used only once and can be affected by environmental conditions such as temperature or pH, causing them to lose activity[1]. In addition, usually separating the enzymes from the reaction mixture is necessary. The second approach involves immobilization methods, which results in higher stability of the enzymes. There are two categories of enzyme immobilization methods: those involving support materials and carrier-free immobilization. Carrier-free immobilization, such as CLEA (cross-linked enzyme aggregates), is more attractive than immobilization with support materials because it is simple, cost-effective and does not require a matrix. Furthermore, pure enzymes are not necessary for CLEA.

The CLEA process consists of two phases: enzymes are first precipitated, and their aggregates are formed, and then these aggregates are cross-linked, typically using glutaraldehyde, a toxic and impure reagent[2]. Our project proposes using transglutaminase in CLEA preparation to eliminate the precipitation step and avoid using glutaraldehyde. Transglutaminase is an enzyme that catalyses the formation of cross-link isopeptide bonds between the glutamine γ -carboxyamide group and the lysine ϵ -amino group, which are highly resistant to proteolysis, preventing the loss of enzyme activity and leaching from CLEA derivatives[3].

To reach the project goal, considerable amounts of clean protein were needed. The initial investigation started from a desk study to identify the microorganisms that produce sufficient quantity of transglutaminase and found that *S. mobaraensis* is the bacterium capable of producing the highest amount of active enzyme. Four different growth media composition were tested to cultivate *S. mobaraensis*. The transglutaminase activity, protein concentration and specific activity were followed for 144 h. The influence of polypeptone, glucose and starch for transglutaminase expression were also examined. The output of transglutaminase production experiments will be presented in more detail during the poster session.

[1] Velasco-Lozano et al. Editorial: Designing Carrier-Free Immobilized Enzymes for Biocatalysis, *Front. Bioeng. Biotechnol.*, vol. 10, 2022.

[2] Z. Liu and S.R. Smith. Cross-Linked Enzyme Aggregate (CLEA) Preparation from Waste Activated Sludge, *Microorganisms*, vol. 11, 2023.

[3] K. Vasić et al. Transglutaminase in Foods and Biotechnology, *Int. J. Mol. Sci.*, vol 24, 2023.

INVESTIGATION OF LIPASE IMMOBILISATION BY CROSS-LINKED ENZYME AGGREGATE (CLEA) METHOD

Kristupas Valaitis¹, Justinas Babinskas¹, Inga Matijošytė¹

¹Sector of Applied Biocatalysis, Institute of Biotechnology, Life Sciences Center, Vilnius University, Lithuania
kristupas.valaitis@gmc.stud.vu.lt

Biocatalysts are a more environmentally friendly alternative to chemical catalysts with significantly higher reaction rates and substrate specificity. Some of the most employed biocatalysts in industrial applications are enzyme lipases, which catalyse a plethora of reversible carboxyl-nucleophile hydrolysis reactions. Nonetheless, free-state lipases exhibit limitations such as sensitivity to the reaction medium or low operational stability¹. Enzyme immobilisation extends the application of lipases by enhancing their stability and allows enzyme recycling. Yet, currently most applied immobilisation techniques for lipases (absorption or covalently binding to carriers) produce insufficient increase in stability, carriers are expensive and often make up most of enzyme-carrier mass². One of the strategies for solving these issues could be to use carrier-free enzyme immobilisation³.

One of the most promising carrier-free immobilisation methods is based on the cross-linking enzyme aggregates (CLEA). This method involves two steps: protein aggregation followed by cross-linking (Fig. 1).

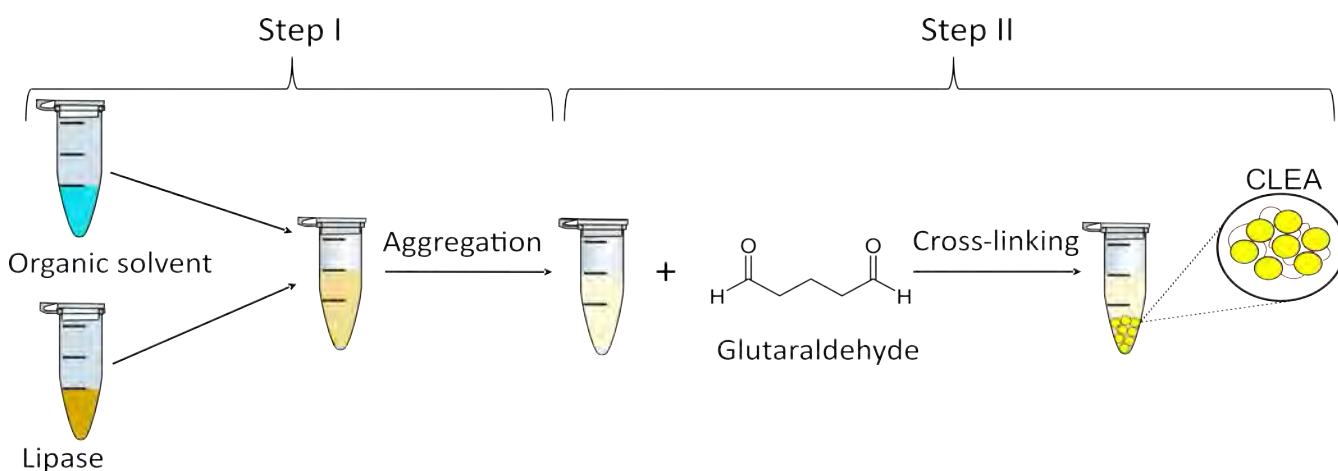


Fig. 1. Workflow of enzyme immobilisation by CLEA method.

First, enzyme aggregation is initiated by adding salts or organic solvents. Then, the enzyme aggregates are cross-linked with a bi-functional linking agent, i.e. glutaraldehyde⁴. It reacts with amino groups of lysine and arginine residues, forming imino groups. The main advantages of CLEA are that it is a relatively fast and straightforward method and does not require expensive reagents, carriers or purified enzymes. However, each step of the process must be optimised for the immobilised enzyme to retain its catalytic activity.

In this project, we investigated lipase Lipolase 100L (Novozymes) aggregation by different concentrations of four organic solvents (acetone, ethanol, isopropanol and 2-methoxyethyl ether) and optimised aggregation time. Furthermore, we optimised cross-linking reaction time and concentration of glutaraldehyde. The obtained results will be presented in more detail during the poster session.

[1] F. T. T. Cavalcante, A. L. G. Cavalcante, I. G. de Sousa, F. S. Neto, and J. C. S. dos Santos, "Current Status and Future Perspectives of Supports and Protocols for Enzyme Immobilization," *Catalysts*, vol. 11, no. 10, Art. no. 10, Oct. 2021

[2] D. Remonatto, R. H. Miotti Jr., R. Monti, J. C. Bassan, and A. V. de Paula, "Applications of immobilized lipases in enzymatic reactors: A review," *Process Biochem.*, vol. 114, pp. 1–20, Mar. 2022

[3] V. Chauhan et al., "An Insight in Developing Carrier-Free Immobilized Enzymes," *Front. Bioeng. Biotechnol.*, vol. 10, 2022

[4] C. S. Sampaio, J. A. F. Angelotti, R. Fernandez-Lafuente, and D. B. Hirata, "Lipase immobilization via cross-linked enzyme aggregates: Problems and prospects – A review," *Int. J. Biol. Macromol.*, vol. 215, pp. 434–449, Aug. 2022s: Problems and prospects – A review," *Int. J. Biol. Macromol.*, vol. 215, pp. 434–449,

APPLICATION AND OPTIMIZATION OF THE *ASPERGILLUS NIGER* EXTRACELLULAR ENZYME SYSTEM FOR THE DEGRADATION OF SUGAR BEET PULP (SBP)

Žydrūnė Gaizauskaitė¹, Renata Žvirdauskienė¹, Daiva Žadeikė¹

¹Department of Food Science and Technology, Kaunas University of Technology, Lithuania
zydrune.gaizauskaite@ktu.lt

One of the main challenges in agrofood sector waste is the lignocellulosic material and its environmental impact. Traditional disposal methods such as open burning or landfilling contribute to air and soil pollution [1]. Effective management of this waste stream is essential to minimize its negative impact on the environment. Long chain carbohydrates in lignocellulose can be broken down through enzymatic hydrolysis or thermochemical conversion to produce simple sugars and other bio-compounds. Sugar beets are one of the main crop for sugar production with approximately 260 Mt produced globally in 2022 with Europe contributing nearly 176 Mt of the global production. Sugar beet pulp (SBP) is a lignocellulosic by-product of the sugar industry that has traditionally been used for animal feed [2]. On a dry-weight basis, SBP consists primarily of polymeric carbohydrates (75–85% w/w), including 20–25% cellulose, 25–36% hemicelluloses, and 20–25% pectin, and low lignin content (1–3%) [3–5].

In this research *Aspergillus niger* extracellular enzyme system was explored for potential application in simple sugars production from SPB long chain carbohydrates and their further conversion into bioethanol. Using SPB biomass hydrolysis by inoculation with *A. niger* was carried out for 168 h at 20 °C–35 °C. A significant increase in the SBP degradation was noticed from 96 h of processing and reaching its highest at 132 h, e.g. the highest RS amounts were produced by *A. niger* at 25 °C (22.30–38.08 g/100 g d.w.). The fungi secreted large amounts of total cellulase, endoglucanase (131.56±2.11 EGU/100g d.w.), β -glucosidase (78.08±1.36 EGU/100g d.w.) activities in the SBP substrate. *A. niger* produced the highest total cellulase activity (212.33±2,09 FPU/100g d.w). These results suggest that SPB can be effectively utilized for the production of simple sugars through enzymatic hydrolysis by *A. niger*. SPB biomass conversion into simple sugars holds promising implications for bioethanol production in further steps of this research.

-
- [1] Fermanelli, Carla S., et al. Waste Management, 2020, 102: 362-370.
 [2] Marzo, C. et al Bioethanol Production from Food Crops; 2019; 61–79
 [3] Glaser, S.J et al. Biomass. Conv. Bioref. 2022.
 [4] Zheng, Yet al. Appl. Energy 2012, 93, 168–175.
 [5] Leijdekkers, A.G et al. Bioresour. Technol. 2013, 12, 518–525.

THE UTILISATION OF JUICE INDUSTRY WASTE FOR THE EXTRACTION OF ASCORBATE OXIDASE

Patrycja Kostiukevič¹, Yelyzaveta Gushchyna¹, Jolanta Sereikaitė¹

¹Vilnius Gediminas Technical University
patrycja.kostiukevic@stud.vilniustech.lt

Effective waste management and its use are a significant challenge in the implementation of zero-waste policies and the promotion of sustainable development. Approximately 44% of all waste comprises food and other green biomass residues, particularly from fruit and vegetable processing industries like juice production. Annually, the world generates about 4-5 million tons of apple pomace, with inefficient use [1]. Considering the circular economy principles, reusing these pomaces for high-value product manufacturing, such as extracting bioactive compounds, becomes of paramount importance. This waste management initiative not only aligns with global zero-waste goals, but also serves as an example of environmentally conscious practices. The study aims to extract ascorbate oxidase from apple pomace. An enzyme is important in the food industry and serves as an analytical reagent in the advancement of biosensor technologies [2]. For enzyme extraction, various methods were used, i.e., blending, mechanical stirring, and ultrasonic extraction. To determine the activity of ascorbate oxidase, two different substrates, such as L-ascorbic acid and catechol, were tested at different pH values. For further purification of the enzyme, chromatographic methods should be applied.

[1] Golebiewska E., Kalinowska M., Yildiz G. Sustainable use of apple pomace (AP) in different industrial sectors. *Materials*, 2022, 15, 1788.

[2] Wang X., Dong S., Wei H. Recent Advances on Nanozyme-based Electrochemical Biosensors. *Electroanalysis*, 2023, 35, e202100684

OPTIMISATION OF THE EXTRACTION OF PHENOCIL COMPOUNDS AND ORGANIC ACIDS FROM CONIFEROUS FOREST WASTE AND THEIR MICROBIOLOGICAL CHARACTERISTICS

Karolina Almonaitytė¹, Žydrūnė Gaižauskaitė¹, Juozas Girtas¹, Antanas Šarkinas¹, Sandra Kiseliovienė¹, Natalja Makštutienė¹, Alvija Šalaševičienė¹

¹Food Institute, Kaunas University of Technology, Radvilenu Rd.19 C, Kaunas, Lithuania
karolina.almonaityte@ktu.lt

After timber harvesting, approximately 30% of left unused the biomass consists of coniferous needles. However, through the extraction of valuable compounds such as proanthocyanidins (PA), phenolic compounds (PC), shikimic acid (SA), and others from these needles, we have the opportunity to purposefully utilise the by-products of forest biomass. Biologically active compounds like this, exhibit a broad spectrum of beneficial effects, including antioxidative, cardioprotective, antitumor, antibacterial, and antiviral effects [1,2,3].

This study focused on optimising the use of sustainable solvents for extraction process from coniferous needles through the application of Response Surface Methodology (RSM). Output data analysis was performed using analysis of variance (ANOVA). Aqueous extraction methods were selected to eliminate the need for additional solvent removal, thereby expanding the potential applications of the extracts.

Using RSM, the process was optimised of produce for an extract with the highest concentration of bioactive compounds. In this investigation, was achieved a maximum SA concentration of 32.4 ± 0.1 mg/g of d.w., PC 79.21 ± 0.21 mg/g of d.w. and PA 45.70 ± 0.24 mg/g of d.w. These identified concentrations are considered sufficient to exhibit measurable antibacterial activity against food spoilage microbes and food pathogens, specifically *Staphylococcus aureus* and *Bacillus cereus* (see Fig.1), in the context for application of new food production [4].

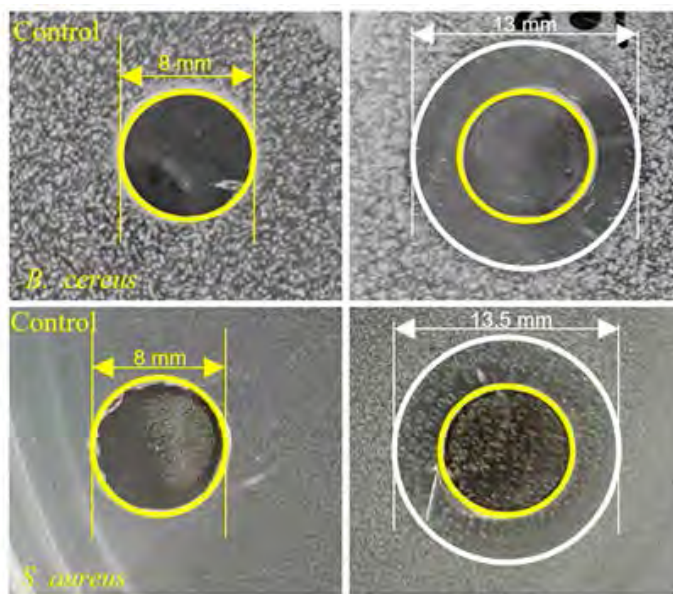


Fig. 1. Inhibition zones images of coniferous needles extracts

Acknowledgements This research was supported by the 2021-2027 Interreg Baltic Sea Region Programme project Innovation in forestry biomass residue processing: towards circular forestry with added value products(CEforestry) grant No. C023.

-
- [1] I. Lucinskaite et al., Wood Sci. Technol., 55, 1221-1235, 2021
 [2] J. Bai et al., LWT, 153, 112441, 2022
 [3] V. N. Burkova et al., Front. Chem., 2, 19-34, 2022
 [4] W. Thongphichai et al., Foods, 12, 2409, 2023

TOTAL INTERNAL REFLECTION ELLIPSOMETRY STUDY OF SARS-COV-2 OMICRON SPIKE PROTEIN AND POLYCLONAL ANTIBODIES INTERACTION

Mantvydas Usvaltas¹, Vincentas Mačiulis², Ieva Plikusienė^{1,2}

¹Faculty of Chemistry and Geosciences, Institute of Chemistry, Vilnius University

²State Research Institute Centre for Physical Sciences and Technology, Department of Nanotechnology
mantvydas.usvaltas@gmc.stud.vu.lt

It has been over two years since the detection of the SARS-CoV-2 Omicron variant, characterized by the highest number of mutations [1]. The vaccines provided a protection in the form of antibodies produced by the body against the original strain but understanding how the antibodies interact with other variants is of great importance. In this study, we investigated the interactions between specific polyclonal human antibodies and the Spike protein of SARS-CoV-2 Omicron variant. To assess whether the vaccines generated a higher amount of antibodies against this variant, we analyzed the blood serums of two individuals: one vaccinated against the wild-type SARS-CoV-2, and the other unvaccinated but recovered after the COVID-19 infection.

The use of total internal reflection ellipsometry provided a non-destructive, label-free, and highly sensitive approach [2]. This optical method employs surface plasmon resonance and allows real-time monitoring of interactions between molecules on the sensing surface of a biosensor and kinetics measurements. Such measurements were performed to determine the surface mass density formed on the sensing surface after the immunocomplex formation of specific polyclonal human antibodies to the Spike protein of SARS-CoV-2 Omicron variant by the use of mathematical modeling [3].

In this study, a self-assembling monolayer comprised of 11-mercaptopundecanoic acid molecules was utilized to immobilize the Spike protein onto the gold surface of a sensor disc. During the analysis, multiple dilutions of blood serums were prepared, and differences between the blood serums taken from vaccinated and unvaccinated individuals were observed. Notably, a higher amount of mass was formed on the sensing surface after the interaction between the SARS-CoV-2 Omicron Spike protein and the antibodies in blood serum taken from an individual who was vaccinated against the wild-type strain.

Acknowledgment: This project has received funding from the Research Council of Lithuania (LMTLT), agreement No [S-LZ-23-1]

[1] P. Mistry et al., 'SARS-CoV-2 Variants, Vaccines, and Host Immunity', *Front Immunol*, vol. 12, p. 809244, 2021, doi: 10.3389/fimmu.2021.809244.

[2] I. Plikusienė, V. Mačiulis, S. Juciute, A. Ramanavicius, and A. Ramanaviciene, 'Study of SARS-CoV-2 Spike Protein Wild-Type and the Variants of Concern Real-Time Interactions with Monoclonal Antibodies and Convalescent Human Serum', *Biosensors (Basel)*, vol. 13, no. 8, p. 784, Aug. 2023, doi: 10.3390/bios13080784.

[3] I. Plikusienė et al., 'Investigation of SARS-CoV-2 nucleocapsid protein interaction with a specific antibody by combined spectroscopic ellipsometry and quartz crystal microbalance with dissipation', *Journal of Colloid and Interface Science*, vol. 626, pp. 113–122, Nov. 2022, doi: 10.1016/j.jcis.2022.06.119.

APPLICATION OF SUSTAINABLE TECHNOLOGICAL SOLUTIONS FOR THE DEVELOPMENT OF FERMENTED PLANT PRODUCTS

Gabija Steigvilaitė¹, Lina Vaičiulytė²

¹Faculty of Chemical Technology, Kaunas University of Technology, Kaunas, Lithuania

²Food Institute, Kaunas University of Technology, Kaunas, Lithuania

gabija.steigvilaite@ktu.edu

As the human population continues to grow, the consumption of food products increases, which leads to the accumulation of organic waste and by-products of food processing industry. Berry pomace, including raspberry pomace, is a by-product of the berry processing industry, which has a limited application due to the high water content and the risk of microbiological spoilage. Commonly, raspberry pomace is thrown away as waste, composted or used in feed. In alignment with the principles of sustainability and the European Commission's Circular Economy Action Plan, this research aims to utilize the by-products of the food processing industry in the development of value-added products.

Raspberry pomace is rich in phytochemicals that exhibit antimicrobial and antioxidant properties [1]. These biologically active compounds can be applied as an alternative to pasteurization or chemical preservatives that can help to reduce the growth of technologically and nutritionally harmful microorganisms during fermentation process [2].

Low frequency (37 kHz) ultrasound at different intensities was applied to fresh raspberry pomace at 35 °C for 15, 30 and 45 min. Ultrasonication is an innovative and environmentally friendly method for pretreating raw materials and extracting biologically active compounds [3]. The efficiency of ultrasonication was characterized by the increase of total concentration of phenolic compounds, total concentration of anthocyanins and antioxidant activity of raspberry pomace water suspensions.

The production of fermented beverage involved the use of ultrasound pretreated raspberry pomace and symbiotic culture. To further enhance the microbial stability and probiotic effect of the beverage, additional lactic acid bacteria (LAB) were added at effective concentrations. It was found that the usage of pretreated raspberry pomace during fermentation process resulted in more microbiologically stable beverages compared to the control. In addition, it showed a significant increase in LAB and yeast concentration compared to the control. These findings suggest that the by-product of the berry processing industry may be a promising source of phytochemicals that could be used for the production of probiotic fermented beverages.

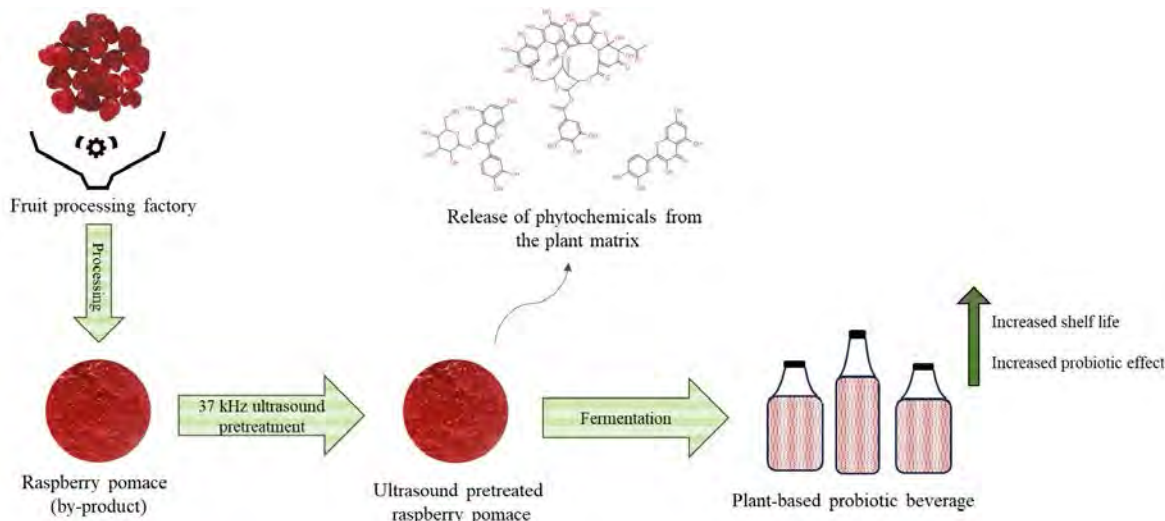


Fig. 1. Mechanism of raspberry pomace valorization strategy into a plant-based probiotic beverage

[1] Brodowska, A. J., Raspberry pomace - composition, properties and application, *European Journal of Biological Research*, 7, 86-96, 2017.

[2] Ejigayehu, T., et al., Potentials of Natural Preservatives to Enhance Food Safety and Shelf Life: A Review, *The Scientific World Journal*, 2022, 9901018, 2022.

[3] Xuan, Z., et al., Recovering high value-added anthocyanins from blueberry pomace with ultrasound-assisted extraction, *Food Chemistry: X*, 16, 100476, 2022.

CHANGES IN CYSTEINE PROTEASE ACTIVITY FROM ANANAS COMOSUS OVER TIME

Taisa Vashkevich¹, Vilma Kaškonienė¹, Audrius Sigitas Maruška¹

¹Instrumental Analysis Open Access Center, Vytautas Magnus University, Lithuania
taisa.vashkevich@stud.vdu.lt

Proteases are enzymes that break down proteins and peptides. They play important roles in physiological and pathological processes, such as digestion, blood clotting, and inflammation. Proteases can be derived from various sources, including fruits and vegetables, microorganisms, and even the digestive systems of animals. Depending on the protease's origin, different activities are observed, such as varying pH ranges and optimal temperatures. To our knowledge, there is a lack of literature data regarding changes in bromelain activity during the storage of both core and flesh juice. Bromelain is a cysteine protease found in pineapples, especially in the core. This enzyme is known for its proteolytic, anticoagulant, and anti-inflammatory properties and has applications in medicine, food science, and other fields [1]. This study aimed to compare and characterize protease activity between the juice of the core and flesh in the Golden Sweet pineapple (*Ananas comosus*) variety over time. Protease activity was measured using a casein digestion spectrophotometric assay adapted from Sigma's Non-specific Protease Activity protocol [2]. The activity of proteases from the fresh core appeared to be 29.24% higher than that from the flesh. These findings are consistent with existing studies of bromelain activity, which is higher in the core than in the flesh of pineapple [3]. During the conference, data describing bromelain activity between the core and flesh of the *Ananas comosus* measured every ten days will be presented.

-
- [1] Pavan, R., Jain, S., Shraddha, & Kumar, A. (2012). Properties and Therapeutic Application of Bromelain: A Review. *Biotechnology Research International*, 2012, 1–6. <https://doi.org/10.1155/2012/976203>
- [2] Cupp-Enyard, C. (2008). Sigma's Non-specific Protease Activity Assay - Casein as a Substrate. *Journal of Visualized Experiments*, 19. <https://doi.org/10.3791/899-v>
- [3] Huang, C. W., Lin, I. J., Liu, Y., & Mau, J. L. (2021). Composition, Enzyme and Antioxidant Activities of Pineapple. *International Journal of Food Properties*, 24(1), 1244–1251. <https://doi.org/10.1080/10942912.2021.1958840>

CHARACTERISATION OF FOUR ALPHA-L-FUCOSIDASES FROM ALPACA FECAL MICROBIOME METAGENOMIC LIBRARY

Pijus Serapinas¹, Rūta Stanislauškienė¹, Rasa Rutkienė¹, Renata Gasparavičiūtė¹, Agnė Krupinskaitė¹, Rolandas Meškys¹, Jonita Stankevičiūtė¹

¹Department of Molecular Microbiology and Biotechnology, Institute of Biochemistry, Life Sciences Center, Vilnius University, Lithuania
pijus.serapinas@gmc.stud.vu.lt

α -L-Fucose (Fuc), a unique carbohydrate with an L-configuration and lacking a C-6 hydroxyl group, is a key component of oligosaccharides and the predominant terminal sugar in glycoconjugates^[1]. Fucosylated glycoconjugates, which are vital to various organisms, play a crucial role in host-microorganism interactions, cell communication, neurological and immunological processes^[1,2].

α -L-Fucosidases, exo-acting glycoside hydrolases, catalyze the removal of α -L-fucose from oligosaccharides and glycoconjugates. The enzymes are widespread in organisms and tissues. They help gut microorganisms to colonize and adapt to the gut environment^[1]. Human α -L-fucosidase deficiency leads to fucosidosis and cancer. These enzymes have applications in medicine, research, and biotechnology, particularly in enzymatic oligosaccharide synthesis through transfucosylation^[2].

Four new fucosidases Fuc25A, Fuc25C, Fuc25D and Fuc25E were obtained screening metagenomic library from alpaca fecal microbiome. Most of their homologues are proteins from Clostridia class bacteria. Phylogenetic analysis revealed close relations between Fuc25A, Fuc25D, and Fuc25E, while Fuc25C was more distant. Recombinant proteins were synthesized in *Escherichia coli* and purified. Kinetic parameters determined using *p*-nitrophenyl-fucopyranoside as a substrate showed Fuc25D with the highest catalytic efficiency ($0,364 \mu\text{M}^{-1}\text{s}^{-1}$) and Fuc25C the lowest ($0,001 \mu\text{M}^{-1}\text{s}^{-1}$). We determined that all fucosidases are mesophilic with optimal activity at neutral pH. They were most stable in a slightly alkaline environment (pH 8) and 0 °C. All four fucosidases also demonstrated transfucosylation activity.

[1] Wu, Haiyang et al., Structure and function of microbial alpha-l-fucosidases: a mini review. *Essays in biochemistry* vol. 67,3 (2023): 399-414.

[2] Ma, Bing et al., Fucosylation in prokaryotes and eukaryotes. *Glycobiology* vol. 16,12 (2006): 158R-184R.

TRANSMISSION OF ACTION POTENTIALS THROUGH INTERNODAL CELLS OF NITELLOPSIS OBTUSA: INVESTIGATION OF THE EFFECT OF GLUTAMATE

Radvilė Janušauskaitė¹, Vilmantas Pupkis¹, Vilma Kisnierienė¹, Indrė Lapeikaitė¹

¹Department of Neurobiology and Biophysics, Life Sciences Center, Vilnius University, Lithuania
radvile.asar@gmail.com

Action potentials (APs) are inherent in both animals and plants and play a pivotal role in adaptive plant responses influencing changes in respiration, photosynthesis, and osmotic pressure. Glutamate (Glu), a key neurotransmitter, acts as a signalling molecule in plants, functioning both in the ambient environment and internally. For instance, an increase in external Glu levels increases the excitability of plant cells, resulting in APs with greater amplitude. The impact of these changes on AP transmission throughout the entire plant body is uncertain. Characean macroalgae offer a reliable model for studying cell-to-cell electrical signalling. The tandem of two cells in a thallus (internodal cell-multicellular node-internodal cell) offers a concise system for studying AP propagation in plants. This study focuses on the electrical signalling between tandem cells of *Nitellopsis obtusa* (Characeae) and aims to investigate the effect of external Glu on transmitting electrical signals locally. For this, intracellular glass electrodes were impaled in each internodal cell, and the two-electrode current-clamp technique was applied in each cell. The membrane potential in each cell was recorded, and three APs were elicited by increasing the current until the excitation threshold was reached, the process repeated every 5 minutes. This was iterated bidirectionally, signifying the initiation of APs in the apical cell and their transmission to the basal cell, and vice versa. This bidirectional process yields crucial insights into dynamic cellular communication within plants. Results indicate tendency that in standard conditions AP propagates to the apical direction at a higher velocity than the basal one. Exposing the tandem to 1 mM Glu after control measurements did not reveal a clear Glu effect: transmission between neighbouring cells was inconsistent, occurring at times and absent at others, although it appears that glutamate slows the transmission of action potentials to the neighbouring cells. More research is needed to fully explore Glu's impact on tandem cell AP transmission and its effects on electrophysiological parameters.

CHARACTERIZATION, DEVELOPMENT, AND APPLICATION OF GENTISIC ACID BIOSENSORS

Ingrida Kutraite¹, Ernesta Augustiniene¹, Naglis Malys^{1,2}

¹Bioprocess Research Centre, Faculty of Chemical Technology, Kaunas University of Technology, Radvilėnų pl. 19, LT-50254 Kaunas, Lithuania

²Department of Organic Chemistry, Faculty of Chemical Technology, Kaunas University of Technology, Radvilėnų pl. 19, LT-50254 Kaunas, Lithuania
ingrida.kutraite@ktu.lt

Gentisic acid is a secondary plant metabolite, known for its benefits to the human health. This compound alongside other phenolic acids has been recognized for its antioxidant, anti-inflammatory, anti-cancer, antimicrobial, cardioprotective, hepatoprotective, and neuroprotective activities. Gentisic acid is used in cosmetics industry, also for treatment of skin pigmentary disorders, it can be utilized as a marker for renal cell carcinoma, this acid itself and its derivatives are applied in pharmaceuticals synthesis. Conventionally, gentisic acid is produced chemically from hydroquinone or salicylic acid. With the increase in demand and the need of bio-sustainable production strategy, a microorganism-based production approach would benefit the industry and society. To expedite the enzyme and strain screening for the pathway engineering and production of gentisic acid, this study reports on the development and characterization of gentisic acid biosensor. Here, the transcription factor-based inducible gene expression system is identified, its genetics and mechanism of action are investigated. Moreover, the inducible system with metabolically associated genes is studied in *E. coli* developing it into a non-host whole-cell biosensor. We examine the biosensor's response to the extracellularly added gentisic acid and validate sensor's specificity. This is the first report of the gentisic acid-inducible biosensor.

STUDY OF NEW ANTI-PHAGE DEFENSE SYSTEMS

Viktorija Rainytė¹, Paulius Toliušis¹, Mindaugas Zaremba¹

¹Department of Protein - DNA Interactions, Vilnius University Life Sciences Center, Lithuania
viktorija.rainyte@gmc.vu.lt

The perpetual conflict between bacteria and bacteriophages has driven the evolution of intricate immune networks, shaping bacterial defense mechanisms against phage attacks. Historically, the exploration of bacterial defense systems emphasized well-established players like restriction-modification (RM), abortive infection systems (Abi), and CRISPR-Cas. However, recent studies are shedding light on the vast landscape of the bacterial pangenome, revealing previously unknown defence systems that are found on so-called defence islands[1,2].

This study focuses on newly identified bacterial defense systems featuring nucleases and ATPase domains, contributing to the growing understanding of bacterial defense strategies against bacteriophages. By analyzing how the catalytic domains of nucleases and ATPases interact, the study uncovers the molecular processes that control hydrolysis of DNA bonds.

Beyond fundamental insights into bacterial defense, our results hold potential applications in biotechnology, offering novel perspectives for the development of tools with practical implications across diverse industries.

-
- [1] Vassallo, C.N. et al. (2022) "A functional selection reveals previously undetected anti-phage defence systems in the E. Coli pangenome," *Nature Microbiology*, 7(10), pp. 1568–1579.
- [2] Millman, A. et al. (2022) "An expanded arsenal of immune systems that protect bacteria from phages," *Cell Host & Microbe*, 30(11).

COMPARING COPPER AND MAGNESIUM CHLOROPHYLLIN-CHITOSAN COMPLEXES

Gabrielė Vasiliauskaitė¹, Irina Buchovec²

¹Department of Neurobiology and Biophysics, Life Science Center, Vilnius University

²Institute of Photonics and Nanotechnology, Faculty of Physics, Vilnius University

gabriele.vasiliauskaite@gmc.stud.vu.lt

Food safety is a global concern, posing health risks to consumers and economic losses for the food industry due to potential contamination¹. Another noteworthy problem is the rising resistance of microorganisms to antibiotics and antimicrobial technologies. However, antimicrobial photodynamic inactivation (API) shows promising results in inactivating microorganisms². API uses photosensitizer (PS), light, and molecular oxygen. When PS absorbs a quantum of light it generates reactive oxygen species (ROS) through molecular interactions with oxygen in the surrounding environment³.

Microorganisms inactivation through ROS activity can be enhanced by change of charges. Natural PSs magnesium chlorophyllin (MgChl) and copper chlorophyllin (CuChl) are anionic compounds, which is why their binding or penetration to the cell is limited. When these PSs are combined with non-toxic cationic chitosan (CHS): MgChl-chitosan (MgChl-CHS) and CuChl-chitosan (CuChl-CHS) (Fig. 1. C, D) complexes can penetrate intracellular space easier and inactivate microorganisms more efficiently. The aim of this study is to compare MgChl-CHS and CuChl-CHS complexes photophysical properties to determine which one is more suitable for enhancing API technology effectiveness.

Initially, several primary solutions are prepared in deionized water: 0,01%MgChl-1%CHS and 0,01%CuChl-1%CHS, and for further experiments, these complexes are diluted with 0,9% NaCl and PBS solutions. The final working concentrations are 0,001%MgChl-1%CHS and 0,001%CuChl-1%CHS (Fig. 1. A, B).

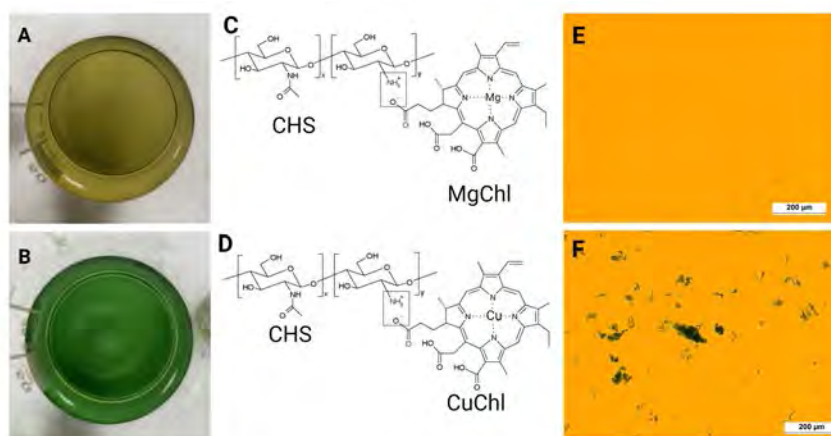


Fig. 1. (A) 0,01%MgChl-1%CHS solution; (B) 0,01%CuChl-1%CHS solution; electron microscope photo of: (C) 0,01%MgChl-1%CHS solution and (D) 0,01%CuChl-1%CHS solution.

This study showed that after combining CuChl-CHS precipitates fall out, whereas in the MgChl-CHS complex, no such precipitation is observed (fig.1. E, F). Also results showed that CuChl-CHS is more aggregated and more photostable than MgChl-CHS.

The prospect of this research involves further investigation of the properties of the MgChl-CHS and CuChl-CHS complexes and their antimicrobial effectiveness on microorganisms.

[1] FDA, Food and Drug Administration, 2020

[2] I. Buchovec et al. *Journal of Photochemistry and Photobiology* 172 p.1-10 (2017).

[3] Z. Luksiene et al. *Innovative Food Science and Emerging Technologies*, 463-472 (2019).

PREPERATION OF WATER-SOLUBLE BETA-CAROTENE-XYLAN COMPLEX

Elżbieta Karvovska¹, Rūta Gruškienė²

¹Vilnius Tech

elzbieta.karvovska@stud.vilniustech.lt

Beta-carotene the most widely distributed carotenoid is usually used as a colorant to field yellow-orange color in various foods and drinks. Also, it's a precursor of vitamin A and an excellent antioxidant, that scavenges free radicals in the human body and can help to prevent cancer, tumor metastasis, and cardiovascular diseases, and improve reproducibility [1]. However, due to its highly conjugated structure, beta-carotene is very unstable and can be easily degraded when opposed to oxygen or light during the storage or manufacture of foods. This can cause the loss of the nutritive and biologically desirable preparation as well as the production of on the side of flavor or aroma compounds. Furthermore, beta-carotene is soluble in oil, and organic solvents but not in water. These characteristics limit the use of beta-carotene in beverages and other applications.

Micro/nano encapsulation strategy can be used to overcome these drawbacks. Encapsulation entraps the sensitive bioactive ingredients in a coating material to protect its biological activity from environmental factors and enhance its physicochemical stability. Recently, different formulations of carotene with various macromolecules have received much attention. Macromolecules such as cyclodextrins, amylose, chitooligosaccharides, apoferritin, arabinogalactan, and others were studied [2,3].

There are studies demonstrating the successful application of xylan to encapsulate beta-carotene [3], this area of research can still be developed.

This study aims to prepare a water-soluble system of beta-carotene by applying the encapsulation technique. Xylan, derived from beechwood, was used as wall material. The complex was prepared by coprecipitation method by adding CAR solution in acetone to the aqueous xylan solvent heated to 65 C. In order to optimize the preparation of beta-carotene-xylan complexes, different ratios of compounds (carotene:xylan), i.e., 1:1, 1:3, 1:5, and 1:10 (w/w), were tested. It was found that the largest amount of carotene equal to 9,1014µg/mg of the complex is incorporated when a ratio of 1:5 is used. To check whether the carotene degradation process does not take place during the synthesis of the complexes, HPLC analysis was used. Also, the stability of entrapped CAR in the complexes was investigated. For this purpose, the complexes were kept in the dark for one nd the relative beta-carotene content was measured periodically to observe how it depends on the ratf components. Encapsulation of beta-carotene with xylan improves its solubility in water and provides new properties, and such systems may find applications in the food industry or other fields.

-
- [1] Li, X. et al. Microencapsulated beta-carotene preparation using different drying treatments. *J Zhejiang Univ Sci B*. 20, 901–909 (2019)
 [2] Celitan, E. et al. An Optimization Procedure for Preparing Aqueous CAR-HP-CD Aggregate Dispersions. *Molecules* 26, 7562 (2021)
 [3] Straksys, A. et al. New beta-carotene-xylan complexes: preparation and characterization. *Cellulose* 29, 8705–8718 (2022)

SURFACE PLASMON RESONANCE IMMUNOSENSOR FOR ACCURATE DETECTION OF ANTIBODIES AGAINST SARS-COV-2 NUCLEOCAPSID PROTEIN

Viktorija Lisyte¹, Almira Ramanaviciene¹, Anton Popov¹

¹NanoTechnas - Center of Nanotechnology and Materials Science, Institute of Chemistry, Faculty of Chemistry and Geosciences, Vilnius University
viktorija.lisyte@chgf.stud.vu.lt

SARS-CoV-2 virus continues to be a global challenge, impacting numerous countries [1]. As of March 2023, more than 760 million confirmed cases of COVID-19 and more than 6.8 million reported deaths have been reported to the World Health Organization (WHO) [2]. The evolution of the COVID-19 pandemic highlights a vital requirement for the development of rapid and precise tests to effectively manage disease spread and monitor illness advancement. Immunosensors appear to be the most appropriate type of sensor for this purpose, capable of identifying the SARS-CoV-2 virus to confirm the disease presence or monitoring antibodies against the virus to assess immunity [3]. Throughout the pandemic, numerous techniques were developed to detect SARS-CoV-2 virus and diagnose COVID-19 infection. These methods encompass various tests designed to detect viral antigens or specific antibodies. Microscale thermophoresis (MST), isothermal titration calorimetry (ITC), bilayer interferometry (BLI) and surface plasmon resonance (SPR) approaches have been widely used to investigate real-time biomolecule interactions, in particular the formation of antigen-antibody immune complexes [4]. The health challenges posed by the swift dissemination of Severe Acute Respiratory Syndrome SARS-CoV-2 have prompted thorough study of the SARS-CoV-2 nucleocapsid protein and specific antibodies against it. While much research has concentrated on the SARS-CoV-2 spike protein, exploring the nucleocapsid protein is equally significant because of its crucial role in the packaging of the coronavirus genomic RNA and viral replication [5]. This study introduces a direct, label-free method for sensitive detection of antibodies against SARS-CoV-2 nucleocapsid protein using a surface plasmon resonance device. Optimization of SARS-CoV-2 nucleocapsid protein immobilization and selection of regeneration solution were performed. The immunosensor, fabricated under optimal conditions demonstrated effective performance. The immunosensor exhibited a linear range from 0.5 to 50 nM for anti-SCoV2-rN, with a limit of detection of 0.057 nM and a limit of quantification of 0.19 nM. Notably, the immunosensor is also suitable for detecting multiple anti-SCoV2-rN antibodies.

Acknowledgments. This project has received funding from European Regional Development Fund (project No. 13.1.1-LMT-K-718-05-0033) under grant agreement with the Research Council of Lithuania (LMTLT). Funded as European Union's measure in response to Cov-19 pandemic.

-
- [1] Zukauskas, Sarunas, et al. Electrochemical biosensor for the determination of specific antibodies against SARS-CoV-2 Spike protein. *International journal of molecular sciences*, 2022, 24.1: 718.
 [2] Eltayeb, Ahmed, et al. Overview of the SARS-CoV-2 nucleocapsid protein. *International Journal of Biological Macromolecules*, 2024, 129523.
 [3] Drobysh, Maryia, et al. Determination of rSpike protein by specific antibodies with screen-printed carbon electrode modified by electrodeposited gold nanostructures. *Biosensors*, 2022, 12.8: 593.
 [4] Plikusiene, Ieva, et al. Study of SARS-CoV-2 spike protein wild-type and the variants of concern real-time interactions with monoclonal antibodies and convalescent human serum. *Biosensors*, 2023, 13.8: 784.
 [5] Plikusiene, Ieva, et al. Investigation of SARS-CoV-2 nucleocapsid protein interaction with a specific antibody by combined spectroscopic ellipsometry and quartz crystal microbalance with dissipation. *Journal of Colloid and Interface Science*, 2022, 626: 113-122.

THE FIRST STEP TOWARDS HUMANIZED RECOMBINANT TAU PROTEIN IN *P. PASTORIS* YEASTS

Airidas Jonušas^{1,2}, Lukas Krasauskas¹, Vytautas Smirnovas¹, Justina Versockienė², Eglė Lastauskienė²

¹Amyloid Research Sector, Institute of Biotechnology, Life Sciences Center, Vilnius University, Lithuania

²Laboratory of Molecular Microbiology of Eukaryotic Microorganisms, Institute of Bioscience, Life Sciences Center, Vilnius University, Lithuania

airidas.jonusas@gmc.stud.vu.lt

Neurodegenerative diseases are among the most common in the world. Despite intensive research, there are few treatment options available [1]. Many studies are done on disease-causing proteins, which are often produced in bacteria and differ from those in humans by post-translational modifications. Here, N-glycosylation is most interesting to us. By producing protein in a humanized expression system, we can glycosylate it similarly to humans [2]. Such proteins would enable more precise research and more effective drug discovery. Partially humanized *Pichia pastoris* M5 yeast, performing modified N-glycosylation, was chosen for our study. The goal of our project is to use gene engineering to change this N-glycosylation to be closer to the human system [3].

Using PCR, *TAU* gene was amplified with an additional sequence encoding 6xHis tag and restriction sites, cloned it into the integrating pPIC3.5K plasmid. Using the Sall REase, cutting the *HIS4* gene, Mut⁺ phenotype was obtained, which efficiently uses methanol, grows faster, and produces more proteins. For homologous recombination, digested plasmid was concentrated in 3 ways: column purification, organic DNA extraction, and magnetic particles (the best method). Yeast transformation was performed using chemical and electroporation methods. By the same scheme, the pPIC3.5K-Tau plasmid was cut with BglII, resulting in a Mut^S phenotype with the *AOX1* knocked out, having slower methanol catabolism, but if this will reduce the yield of protein will be checked in the future.

Pilot cultivation of *P. pastoris* M5 Mut⁺ was done, expression induction with methanol and SDS-PAGE was performed to check expression over time. To ensure having the target protein, western blot was done with anti-His monoclonal antibodies. To enhance gene expression a Kozak sequence will be inserted upstream of *TAU*, which should enhance gene expression. Using Mega primers, an Alpha mating factor signaling sequence will be inserted, which will direct protein for secretion into the medium, facilitating protein purification. From the available literature, Tau protein was obtained from partially humanized yeasts with modified N-glycosylation for the first time. This and further glycosylation modifications will allow to test whether these modifications change Tau protein aggregation and its structure.

[1] Chiti F, Dobson CM. Protein Misfolding, Amyloid Formation, and Human Disease: A Summary of Progress Over the Last Decade. *Annu Rev Biochem.* 2017 Jun 20;86:27-68.

[2] Jacobs PP, Geysens S, Verweken W, Contreras R, Callewaert N. Engineering complex-type N-glycosylation in *Pichia pastoris* using GlycoSwitch technology. *Nat Protoc.* 2009;4(1):58-70.

[3] Hamilton SR, Gerngross TU. Glycosylation engineering in yeast: the advent of fully humanized yeast. *Curr Opin Biotechnol.* 2007 Oct;18(5):387-92.

INHIBITION OF A BACTERIAL ANTIVIRAL BREX DEFENSE SYSTEM

Justė Adomaitytė¹, Tomas Šinkūnas¹

¹Department of Protein - DNA Interactions, Institute of Biotechnology, Life Sciences Center, Vilnius
juste.adomaityte@chgf.stud.vu.lt

Bacteriophages are viruses with the ability to infect and replicate in bacterial cells. Numerous bacteriophage species are virulent and therefore kill the infected cell. However, these organisms have a long history of coexistence. During their evolution, bacteria have been able to adapt by developing defense mechanisms that protect cells from the entry of bacteriophages and foreign nucleic acids. Although more than a hundred bacterial defense systems are currently known, bacteriophages can inhibit them by various mechanisms¹. Research of defense systems and their inhibitors is crucial not only for a better understanding of microbial evolution, but also as a resource for the development of various tools for biotechnology and biomedicine.

One of the bacterial antiviral defense systems is BREX (Bacteriophage Exclusion). It is present in about 10% of prokaryotic genomes. However, the mechanism of action is still undefined. BREX systems are divided into 6 types, with our research focusing on the predominant type 1 BREX system (BREX1), which consists of 6 genes: *brxA*, *brxB*, *brxC*, *pglZ*, *brxL*, *pglX*. The *pglX* gene encodes the m6A DNA methyltransferase, which methylates specific sequences in the host genomic DNA to distinguish itself from foreign DNA². Bacteriophages can evade the BREX1 system by two different mechanisms: (i) by epigenetically modifying (either by methylation or glycosylation) BREX1 recognition sequences in their genomes³, or (ii) by blocking the BREX1 system with their encoded protein inhibitors⁴. In this study, we analyse some phage-encoded proteins as potential inhibitors of the *Escherichia coli* HS BREX1 system in cells.

[1] Mayo-Munoz et al., (2023). A host of armor: Prokaryotic immune strategies against mobile genetic elements. *Cell reports*, 42(7), 112672.

[2] Goldfarb et al., (2015). BREX is a novel phage resistance system widespread in microbial genomes. *The EMBO journal*, 34(2), 169-183.

[3] Gordeeva et al., (2019). BREX system of *Escherichia coli* distinguishes self from non-self by methylation of a specific DNA site. *Nucleic acids research*, 47(1), 253-265.

[4] Isaev et al., (2020). Phage T7 DNA mimic protein Ocr is a potent inhibitor of BREX defence. *Nucleic acids research*, 48(10), 5397-5406.

S100A8 PROTEIN INTERACTION WITH LIPID MEMBRANES

Rimgailė Tamulytė¹, Darius Šulskis², Marija Jankunec¹

¹Institute of Biochemistry, Life Sciences Center, Vilnius University, Vilnius, Lithuania

²Institute of Biotechnology, Life Sciences Center, Vilnius University, Vilnius, Lithuania
rimgaile.tamulyte@bchi.stud.vu.lt

S100 proteins are calcium-binding proteins that regulate several processes associated with Alzheimer's disease (AD) but whose contribution and direct involvement in disease pathophysiology remains not fully established. Due to neuroinflammation in AD patients, the levels of several S100 proteins are increased in the brain and some S100s play roles related to the processing of the amyloid precursor protein, regulation of amyloid beta peptide levels and Tau phosphorylation [1]. The number of studies on the impact of S100 family proteins in co-aggregation processes with amyloid-like proteins is increasing. However, research has yet to unravel how S100 proteins interact with neuronal membranes. The present study is focused on the pro-inflammatory calcium-binding protein S100A8 of the S100 family. We employ various biomimetic membrane models such as solid supported lipid bilayers, tethered bilayer lipid membranes and liposomes to monitor the interaction between S100A8 protein and membrane surface. For this purpose, we employed high speed atomic force microscopy (HS-AFM), fluorescence spectroscopy and electrochemical impedance spectroscopy techniques. Our results indicate that the interaction between S100A8 and the membrane is lipid-charge sensitive. The greatest membrane disruptive effect is observed in negatively charged membranes. HS-AFM data reveals that the interaction of S100A8 with negatively charged bilayer leads to the rupture of the membrane by a detergent-like effect (Fig. 1). These results might broaden the understanding of S100A8 protein interactions with neuronal membranes and potentially affect the development of new diagnostic and therapeutic approaches for AD or other related diseases.

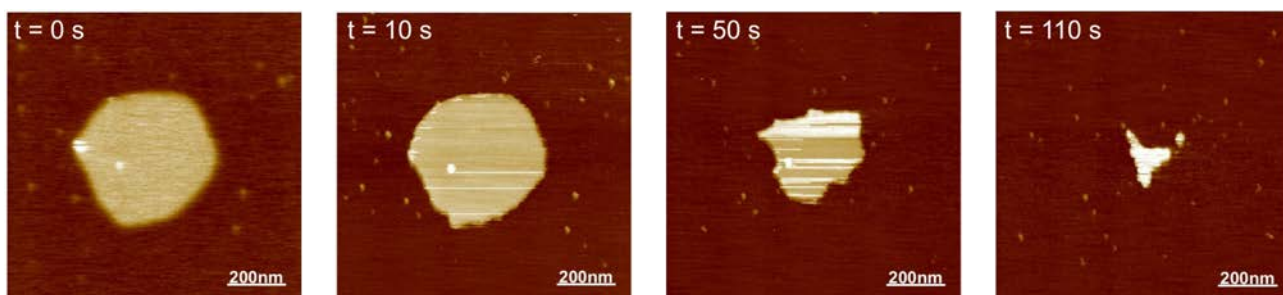


Fig. 1. HS-AFM images of S100A8 induced membrane dissolution. At $t = 0$, the protein was injected in the fluid cell during imaging. Interaction between S100A8 and negatively charged membrane leads to a detergent-like effect.

[1] J.S. Cristovao, C.M. Gomes. S100 Proteins in Alzheimers Disease. *Frontiers in neuroscience*, 2019, 13, 463.

STUDY OF THE OPTICAL AND FLUORESCENCE PROPERTIES OF THE COMPLEX OF CARBON QUANTUM DOTS AND COMPOUNDS WITH ANTICANCER PROPERTIES

Martynas Zalieckas^{1,2}, Katsiaryna Charniakova², Renata Karpicz²

¹Faculty of Fundamental Sciences, Vilnius Gediminas Technical University, Saulėtekio Ave. 11, LT-10223 Vilnius, Lithuania

²Center for Physical Sciences and Technology, Saulėtekio Ave. 3, LT-10257 Vilnius, Lithuania.
martynas.zalieckas@stud.vilniustech.lt

Quinone-based drugs such as doxorubicin (DOX), daunorubicin, etc. are widely used in cancer chemotherapy. Their use has adverse side effects such as dilated cardiomyopathy and heart failure. This has led to the development of controllable, nanocarrier-based drug delivery systems that allow the targeted release of drugs at specific locations. Potential candidates for the development of such systems, heavy metal-free carbon quantum dots (CQD), are receiving increasing attention.

Carbon quantum dots (CQDs), with advanced surface functionalization and luminescent properties that allow controlling the intracellular localization of nanocarrier-drug complexes, are a promising nanostructured material for theranostics, as they can simultaneously provide imaging and therapeutic effects. Theranostic agents must meet several requirements. The most important condition is that it delivers the medicine to the target. For this, it must be soluble in water and stable under physiological conditions. The nanocomplex must be biocompatible. It is highly desirable that it can be tracked optically to monitor its pharmacodynamics and accumulation in cancer tissue.

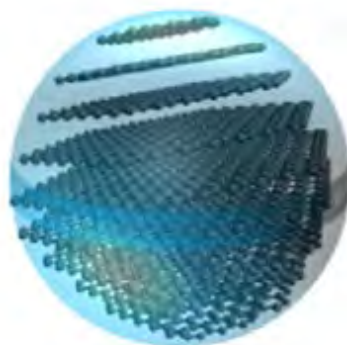


Fig. 1. Model structure of carbon quantum dots (CQD)

During this study, we intend to investigate the stability, optical and fluorescent properties of nanocomplexes of CQDs and compounds with anticancer properties using spectroscopic methods.

DEER SPECTROSCOPY OF S100A9 PROTEIN

Aistė Peštenytė¹, Gediminas Usevičius¹, Darius Šulskis², Ieva Baronaitė², Vytautas Smirnovas², Jūras Banys¹, Mantas Šimėnas¹

¹Faculty of Physics, Vilnius University, Saulėtekio al. 3, LT-10257, Vilnius, Lithuania

²Sector of Amyloid Research, Institute of Biotechnology, Life Sciences Centre, Vilnius University, LT-10257 Vilnius, Lithuania

aiste.pestenyte@ff.stud.vu.lt

Double electron-electron resonance (DEER) spectroscopy, a widely used tool in structural biology, explores biomolecules like proteins, RNA, and DNA by determining nanoscale distances between unpaired electron spins [1]. This pulsed electron paramagnetic resonance (EPR) technique utilizes microwave pulses of varying frequencies. In this process, one electron spin is detected through EPR, while the other one is excited by rotating its magnetization vector (Fig. 1) [2]. Throughout the experiment, we monitor the alterations in dipole interaction between the interacting unpaired electrons. DEER overcomes limitations in studying systems without unpaired electrons, such as biomolecules, by incorporating spin labels through site-directed spin-labeling (SDSL) [2]. Compared to other methods, DEER is not constrained by crystallized molecules or molecular weight limitations. The combination of SDSL with DEER emerges as a highly promising approach for structural analysis, enabling the observation of changes in local structure, interactions with other molecules, alterations in the distance between electron spins, and the visualization of conformational heterogeneity and dynamics [1].

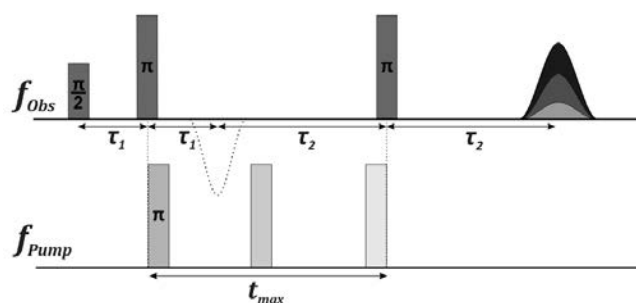


Fig. 1. Microwave pulse sequence of the DEER experiment.

To practically identify capabilities and limitations of DEER spectroscopy, we examined a calcium-binding protein S100A9, related to Alzheimer's and Parkinson's diseases. During this study, we determined the distance distribution (Fig. 2) between the two cysteine groups, utilizing the nitroxide radical as a spin label.

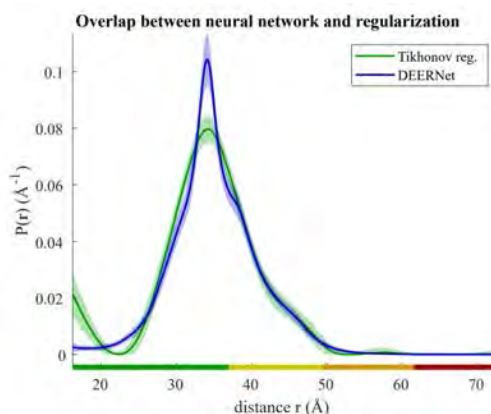


Fig. 2. Distance distribution between electron spins in the S100A9 protein.

[1] Indra D. et al., Use of electron paramagnetic resonance to solve biochemical problems, *Biochemistry* 2013.

[2] Jeschke G. DEER distance measurements on proteins. *Annual review of physical chemistry*. 2012 May.

DEVELOPMENT AND OPTIMIZATION OF A MONOCLONAL ANTIBODY-BASED SYSTEM FOR QUANTIFICATION OF hBiP

Gabija Klimavičiūtė¹, Evaldas Čiplys², Rimantas Slibinskas², Aurelija Žvirblienė¹, Martynas Simanavičius¹

¹Vilnius University, Life Sciences Center, Institute of Biotechnology, Department of Immunology

²Vilnius University, Life Sciences Center, Institute of Biotechnology, Department of Eukaryote Gene Engineering
gabija.klimaviciute@gmc.stud.vu.lt

hBiP (human binding immunoglobulin protein) is one of the most important endoplasmic reticulum (ER) chaperone proteins, which plays a key role in protein folding, export into the ER, assembly, signal transduction and calcium ion homeostasis^[1]. When ER stress occurs during cancer and neurodegenerative illnesses, hBiP appears to be involved in disease progression, tissue damage and autoimmune inflammation^{[2][3]}. Therefore, hBiP could be a potential biomarker for detecting and monitoring these diseases. Monoclonal antibodies are great biotechnological tools for investigation of various proteins and their roles^[4]. Antibodies could be used in the development of immunoassays for the quantification of their targets. In this study, we aim to develop and optimize the assay for hBiP detection and concentration determination while using monoclonal antibodies in the sandwich ELISA method. Test conditions were optimized, such as type of plate, immobilization and blocking solutions and monoclonal antibodies pair. It is important to develop a reliable test for quantification of hBiP to detect and monitor previously mentioned diseases, hence the accuracy of the test was evaluated. When developed, such a test can contribute to improve the understanding of the role of hBiP in disease pathogenesis and facilitate the development of personalized medicine approaches.

[1] Ni, M., Zhang, Y., Lee, A. S. Beyond the Endoplasmic Reticulum: Atypical GRP78 in Cell Viability, Signalling and Therapeutic Targeting. *Biochem J* 2011, 434 (2), 181-188.

[2] Zhang, L.-H., Zhang, X. Roles of GRP78 in Physiology and Cancer. *J Cell Biochem* 2010, 110 (6), 1299-1305.

[3] Gorbatyuk, M. S., Gorbatyuk, O. S. The Molecular Chaperone GRP78-BiP as a Therapeutic Target for Neurodegenerative Disorders: A Mini Review. *J Genet Syndr Gene Ther* 2013, 4 (2), 128.

[4] Zahavi, D. Weiner, L. Monoclonal Antibodies in Cancer Therapy. *Antibodies (Basel)* 2020, 9 (3), 34.

PREPARATION AND CHARACTERIZATION OF ENCAPSULATED MICROALGAE EXTRACT FROM *ARTHROSPIRA PLATENSIS*

Vesta Navikaite-Snipaitiene¹, Emilija Galkauskaite¹, Dovile Liudvinaviciute¹, Ramune Rutkaite¹, Vaida Kitryte-Syrpa¹, Michail Syrpas¹

¹Kaunas University of Technology
vesta.navikaite@ktu.lt

Microalgae have become very promising resources to obtain functional ingredients with added nutritional value in terms of high bioactivity and sustainability. Encapsulation is an effective solution in preservation of bioactive compounds against unsuitable environmental conditions and securing their bioavailability, stability and targeted release. Moreover, freeze-drying and spray-drying techniques are well suited for the production of solid micro- and nanoparticles with bioactive ingredients which have great potential in the development of nutraceutical products.

In this study, encapsulation of fermented and non-fermented microalgae extract (*Arthrospira platensis*) using polysaccharide derivatives and by employing freeze-drying and/or spray-drying techniques have been investigated. In the first step, the dispersions containing *Arthrospira platensis* extract and selected polysaccharides have been prepared and their properties as well as the stability of compositions have been assessed. Subsequently, the processing of the dispersions into dry particles by using various techniques have been investigated. The loading of bioactive substances such as phycocyanins in the particles have been varied and bioactive properties of the particles have been evaluated.

Acknowledgement. This project has received funding from the Research Council of Lithuania (LMTLT), agreement No S-MIP-23-78.

HYDROLYSIS OF ALKYL FUCOSIDES BY ALPHA-L-FUCOSIDASES

Daniel Parvicki¹, Rūta Stanislauskienė¹, Rasa Rutkienė¹, Agnė Krupinskaitė¹, Jonita Stankevičiūtė¹, Rolandas Meškys¹

¹Department of Molecular Microbiology and Biotechnology, Institute of Biochemistry, Life Sciences Center, Vilnius University, Lithuania
daniel.parvicki@gmc.stud.vu.lt

Fucosylated compounds are associated with a wide range of biological processes in different forms of life. In mammalian cells, they play an essential role in various biological and pathological processes (embryogenesis, cell adhesion, signaling, regulation of the immune response, etc.). Fucosylated human milk oligosaccharides (HMOs) offer benefits to infants by acting as prebiotics, preventing the attachment of pathogens and potentially providing protection against infections. Although there is a clear demand for fucosylated compounds, their availability is limited due to the difficult and expensive chemical synthesis. Therefore, enzymatic synthesis using α -L-fucosidases is considered a better alternative. These enzymes catalyse the removal of L-fucose from glycosides by the cleavage of O-glycosyl bonds. Moreover, under certain conditions, they can perform a transfucosylation reaction (the transfer of a fucosyl group from the donor to the acceptor molecule) [1, 2]. As methyl- α -L-fucopyranoside and 1-methoxyethyl- α -L-fucopyranoside could be potential fucosyl group donors, we aim to investigate whether α -L-fucosidases could hydrolyse these alkylated compounds and carry out trans-fucosylation.

We screened α -L-fucosidases from metagenomic libraries for their ability to hydrolyse methyl- α -L-fucopyranoside and 1-methoxyethyl- α -L-fucopyranoside. Several metagenomic fucosidases showed hydrolytic activity towards both compounds investigated. Few were chosen for further research. Recombinant proteins were successfully synthesised in *Escherichia coli* and purified. We showed that enzymes studied were also able to use methyl- α -L-fucopyranoside as fucosyl group donor in transfucosylation reactions. In our opinion, the alkyl fucosides studied could be potential novel substrates to be used by α -L-fucosidases as fucosyl group donors in the synthesis of fucosylated compounds.

[1] B. Zeuner and A. S. Meyer, Enzymatic transfucosylation for synthesis of human milk oligosaccharides. *Carbohydrate research* vol. 493 (2020): 108029.
[2] F. Guzmán-Rodríguez et al., Employment of fucosidases for the synthesis of fucosylated oligosaccharides with biological potential. *Biotechnology and applied biochemistry* vol. 66,2 (2019): 172-191.

TNPB-DNA INTERACTION STUDIES IN VITRO USING SINGLE-MOLECULE FLUORESCENCE MICROSCOPY

Monika Roliūtė¹, Aurimas Kopūstas^{1,2}, Marijonas Tutkus^{1,2}

¹Department of Protein-DNA Interactions, Institute of Biotechnology, Life Science Center, Vilnius University, Lithuania

²Center for Physical Sciences and Technology, Lithuania

monika.rolaute@gmc.stud.vu.lt

TnpB, derived from *Deinococcus radiodurans* ISDra2 transposon, is 408 amino acids long protein and together with an 150 nucleotides long RNA molecule forms a ribonucleoprotein (RNP) complex. It was experimentally shown that TnpB is an RNA dependent DNA nuclease and can be reprogrammed to cleave dsDNA *in vitro* and *in vivo*. Although TnpB protein function [1] and structure [2] were determined, TnpB binding lifetime to its substrate DNA, association constant (K_a), dissociation constant (K_d) remain unknown. Single molecule techniques can be adopted to measure kinetical and dynamical parameters of a biological system. Single molecule studies show a huge advantage over standard biochemical assays. It overcomes ensemble averaging over a heterogeneous population and allows to monitor protein-DNA interaction in real-time.

Here we use total internal reflection fluorescence (TIRF) microscopy technique to study TnpB RNP complex and DNA interaction *in vitro*. This is the first attempt to characterise kinetics of this recently discovered nuclease that has a huge potential for gene-editing. Since TnpB forms RNP complex inside the cell, it burdens its RNA efficient labelling with fluorophore. Therefore, we use a strategy to fluorescently label TnpB protein through streptavidin-biotin interaction, instead. Interaction between TnpB and DNA can be achieved through DNA or protein immobilization on the surface. We employed both of these approaches. All together, this study can give us fundamental insights about the biophysical properties of protein-DNA interaction, while data and results that we acquire are important for other researchers working with DNA-interacting proteins.

[1] Karvelis, T., et al. (2021). Transposon-associated TnpB is a programmable RNA-guided DNA endonuclease. *Nature*, 599(7886), 692-696.

[2] Sasnauskas, G., Tamulaitiene, G., Druteika, G. et al. (2023). TnpB structure reveals minimal functional core of Cas12 nuclease family. *Nature*, 616(7956), 384-389.

DEVELOPMENT OF THE SCREENING SYSTEM FOR TRANSPOSABLE ELEMENTS

Bartė Žiliukaitė¹, Gytis Druteika¹, Tautvydas Karvelis¹

¹Department of Protein-DNA Interactions, Institute of Biotechnology, Life Sciences Center, Vilnius University, Lithuania
barte.ziliukaite@chgf.stud.vu.lt

Prokaryotic CRISPR-Cas systems are responsible for the adaptive immunity against foreign DNA, which is based on guide RNA-dependent DNA or RNA nuclease activity. Nowadays, these systems are adapted and widely used for genome editing; however, they are inefficient, prone to off-target activity, and require PAM sequences that may greatly limit possible targets in the genome. In addition, gene editing with Cas proteins relies on homologous recombination repair, which is tied to active cell division and, therefore, is not applicable to some cell types [1]. All these limitations of CRISPR-Cas systems raise demand for novel genome editing tools. Recent studies and bioinformatic analysis show that Cas12 nucleases may have evolved from TnpB – proteins encoded by IS200/IS605 family insertion sequences (IS) [2]. IS, as well as plasmids, bacteriophages, and transposons, are mobile genetic elements (MGE) that are abundant in both prokaryotes and eukaryotes and play an important role in the evolution and expression of the host genome [3]. The wide variety and evolutionary proximity of IS to Cas proteins make IS a potential source of novel genome editing tools. This study aimed to develop a screening system for transposable elements. Based on the previously described work [4,5], we constructed vectors, which contain an active transposase and an antibiotic resistance gene-carrying minimal transposable element (mini-Tn). We conducted experiments to select bacterial strains that are most suitable for transposition assay, optimized bacterial conjugation conditions, and determined the best conditions for transposase expression. These results contribute to the development of a robust IS screening system, which will facilitate the detection of new IS that could lead to novel genome editing tools.

-
- [1] Strecker J, Ladha A, Gardner Z, et al. RNA-guided DNA insertion with CRISPR-associated transposases. *Science*. 2019;365(6448):48-53. doi:10.1126/science.aax9181
- [2] Sasnauskas G, Tamulaitiene G, Druteika G, et al. TnpB structure reveals minimal functional core of Cas12 nuclease family. *Nature*. 2023;616(7956):384-389. doi:10.1038/s41586-023-05826-x
- [3] Siguier P, Gourbeyre E, Chandler M. Bacterial insertion sequences: their genomic impact and diversity. *FEMS Microbiol Rev*. 2014;38(5):865-891. doi:10.1111/1574-6976.12067
- [4] Kaczmarek Z, Czarnocki-Cieciura M, Górecka-Minakowska KM, et al. Structural basis of transposon end recognition explains central features of Tn7 transposition systems. *Mol Cell*. 2022;82(14):2618-2632.e7. doi:10.1016/j.molcel.2022.05.005
- [5] Meers C, Le HC, Pesari SR, et al. Transposon-encoded nucleases use guide RNAs to promote their selfish spread. *Nature*. 2023;622(7984):863-871. doi:10.1038/s41586-023-06597-1

FTIR-ATR ANALYSIS FOR THE OPPORTUNISTIC YEASTS GROWN IN SIMULATED MICROGRAVITY AND RESISTANCE TO PHYSICAL AGENTS

Irmantas Čiužas¹, Gerda Anužienė², Justina Versockienė¹, Eglė Lastauskienė¹

¹Institute of Biosciences, Life Sciences Center, Vilnius University, Saulėtekio Av. 7, LT-10257 Vilnius, Lithuania

²Chemical Physics Institute, Faculty of Physics, Vilnius University, Saulėtekio Av. 3, LT-10257 Vilnius, Lithuania
irmantas.ciuzas@gmc.stud.vu.lt

Yeasts grown in space experience a unique physiological response, starting from modified cell morphology and growth dynamics to increased resistance for antimicrobial compounds [1]. Yeast morphogenic changes have been observed, which occur in response to a cell's environmental stressors and contribute to the virulence of an opportunistic pathogen [2]. In this work, the effect of microgravity on the resistance of *Candida guilliermondii* to physical agents was measured by comparing cells grown under normal gravity and simulated microgravity.

The study attempted to evaluate physical factors such as resistance to electric shock. Microgravity was simulated using a rotary cell culture system, cells were exposed to an electric shock by a pulsed electric field generator. The method of an attenuated total reflection of infrared radiation (ATR IR) spectroscopy was applied for the analysis. ATR IR absorption spectra of 14 samples of 7 grown in gravity and 7 in simulated microgravity were analyzed.

The obtained results show a significant difference between *C. guilliermondii* grown under normal gravity and microgravity treated with electric shock. Cells grown in microgravity showed a 16.2-fold increase in resistance to electric shock. The main difference between ATR IR absorbance spectra of *C. guilliermondii* yeast grown in gravity and microgravity were observed at 1374 cm^{-1} (nucleobases $\nu(\text{C-N})$) and 1744 cm^{-1} (lipid $\nu(\text{C=O})$) spectral bands [3-4]. Both mentioned spectral bands are more intense in the ATR IR absorbance spectra of *C. guilliermondii* yeast grown in gravity.

To conclude, yeast cells grown in microgravity can be differently affected by physical agents. For better understanding of microgravity's effects, it is important to carry out more studies with different types of cells and prolonged exposure to microgravity.

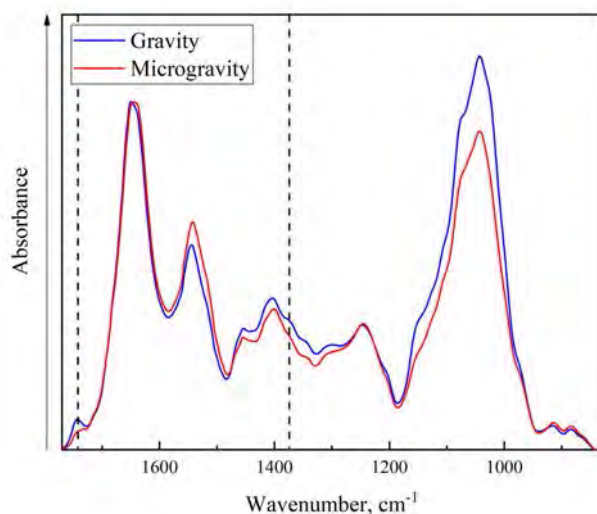


Fig. 1. ATR IR absorbance spectra of *C. guilliermondii* grown in gravity and microgravity

-
- [1] Milojevic, T., & Weckwerth, W. (2020). Molecular Mechanisms of Microbial Survivability in Outer Space: A Systems Biology Approach. *Frontiers in Microbiology*, 11
- [2] Altenburg, S., Nielsen-Preiss, S. M., & Hyman, L. E. (2008). Increased Filamentous Growth of *Candida albicans* in Simulated Microgravity. *ScienceDirect*, 6(1), 42–50
- [3] A. Salman, L. Tsrar, A. Pomerantz, R. Morehc, S. Mordechai, M. Huleihel. (2010). FTIR spectroscopy for detection and identification of fungal phytopathogens. *Spectroscopy* 24, 261–267
- [4] Z. Movasaghi, S. Rehman, and I. Rehman. (2008.) Fourier Transform Infrared (FTIR) Spectroscopy of Biological Tissues, *Applied Spectroscopy Reviews* 43, 134–179 (2008)

DISINFECTION OF MICROORGANISMS WITH FAR-UVC 222 NM IRRADIATION

Simona Jaseliunaite^{1,2}, Dovile Cepukoit¹, Daiva Burokiene¹

¹Nature Research Center

²Vilnius University

dovile.cepukoit@gamtc.lt

The use of ultraviolet C (UVC) irradiation is an effective method of controlling microorganisms. This control strategy is used to disinfect surfaces, air and water. The most commonly used type of UVC is 254nm, unfortunately this radiation is harmful to humans and can cause skin cancer, dermatitis and other diseases [1]. It is known that FAR-UVC 222 nm irradiation has a disinfectant effect on microorganisms and that it is not harmful to human health. This study was designed to investigate the effects of FAR-UVC 222nm irradiation on a range of microorganisms including *B. subtilis*, *P. aeruginosa*, *Rouxiela* sp., *A. flavus*, *B. cinerea*, *Cladosporium sphaerospermum* and *P. commune*. To completely inhibit the growth of microorganisms, the exposure time and distance between the object and the lamp were determined. The results indicate that *B. subtilis* bacteria can be effectively destroyed by FAR-UVC 222 nm irradiation at a distance of 10 cm for 187 seconds. Thus, the initial findings of this study indicate that FAR-UVC 222 nm could be a feasible approach for pathogen biocontrol. Further studies will determine the exposure time and distance required for FAR-UVC 222 nm irradiation to inhibit the germination of fungal conidia and formation of bacterial colonies.

[1] K. Narita, et al., Chronic irradiation with 222-nm UVC light induces neither DNA damage nor epidermal lesions in mouse skin, even at high doses, 2018.

CONSTRUCTION OF BACTERIOPHAGES GENOMIC LIBRARY

Migle Plioplyte¹, Jonas Juozapaitis¹, Giedrius Sasnauskas¹

¹Department of Protein - DNA Interactions, Vilnius University Life Sciences Center, Lithuania
migle.plioplyte@gmc.stud.vu.lt

Bacteria have developed a wide range of antiviral defenses to protect themselves from infection by their own viruses (bacteriophages). One of the defense strategies that bacteria use against their viruses is abortive infection (Abi). The Abi system acts as a cellular response to viral infection, with virus-infected cells dying or slowing down their metabolism, thereby limiting further phage multiplication in the population [1].

Although the understanding of bacterial defense mechanisms has increased considerably, one of the main unanswered questions is how the Abi system is activated in the event of phage infection. So far, in the study of bacterial defense systems, one approach to finding factors that activate bacterial defense systems has been to study bacteriophage mutants that evade bacterial defense systems, but this approach has drawbacks [2].

Our work aims to address the shortcomings of phage mutant assays and to propose a new, faster method to simultaneously screen more bacterial defense systems for their activating factors. This will be done using libraries of random genomic DNA fragments from bacteriophages.

[1] Bernheim A, Sorek R. The pan-immune system of bacteria: antiviral defence as a community resource. *Nat Rev Microbiol*. 2020 Feb;18(2):113-119. doi: 10.1038/s41579-019-0278-2. Epub 2019 Nov 6. PMID: 31695182.

[2] Stokar-Avihail A, Fedorenko T, Hör J, Garb J, Leavitt A, Millman A, Shulman G, Wojtania N, Melamed S, Amitai G, Sorek R. Discovery of phage determinants that confer sensitivity to bacterial immune systems. *Cell*. 2023 Apr 27;186(9):1863-1876.e16. doi: 10.1016/j.cell.2023.02.029. Epub 2023 Apr 7. PMID: 37030292.

STABILITY OF L-A1 VIRUS-LIKE PARTICLES PURIFIED FROM SACCHAROMYCES CEREVISIAE

Kamilė Vaišaitė¹, Enrika Celitan¹, Saulius Serva¹

¹Vilnius University, Life Sciences Center, Vilnius, Lithuania
kamile.vaisaite@chgf.stud.vu.lt

ScV-L-A1, a member of the virus family *Totiviridae*, is a double-stranded RNA virus often associated with a phenomenon referred to as the killer yeast phenotype. Although this infectious element is known to lack an extracellular phase, it was found to be stably maintained in 15 out of 70 wild *Saccharomyces cerevisiae* strains by transmission through cell-cell mating [1]. The genome of L-A1 virus is shielded and delivered from cell to cell by a capsid composed of 60 asymmetric homodimers of single major capsid protein Gag. The pores in the capsid serve as a molecular sieve, allowing transcripts and metabolites to pass through while retaining dsRNA and blocking entry for degradative enzymes [2]. In this sense, L-A1 virus, as well as any other virus, may be considered a natural nano-delivery system.

Synthesis of virus-like particles is an approach to take advantage of viruses' innate capacity to protect and transport cargo to their intended destination. These are nanoparticles self-assembled from viral capsid proteins, yet incapable of replication due to the lack of genetic material [3]. Therefore, VLPs have been used for the delivery of drugs, nucleic acids, peptides, and proteins [4]. Although a broad range of host cells can be cultivated for the production of VLPs, yeast expression systems – particularly *S. cerevisiae* – are prevalent for this purpose due to inexpensive culturing, rapid cell growth, effective protein expression, scalability and native post-translational protein modifications [3].

The main goal of this study was to examine the stability of L-A1 VLPs purified from *S. cerevisiae*. The synthesis of recombinant major capsid protein of L-A1 in *S. cerevisiae* was induced, and the self-assembled nanoparticles were consequently purified by ultracentrifugation of the yeast lysate through sucrose cushion and cesium chloride density gradient. Transmission electron microscopy (TEM) and dynamic light scattering (DLS) techniques were used to demonstrate the formation of 41.3 ± 1.6 nm L-A1 VLPs, corresponding the size of the native L-A1 virus (40.0 nm) [2]. Since evaluation of the particle stability in different conditions is valuable for the development of nano-delivery systems, the effects of temperature, buffer identity, ionic strength, pH, and Mg^{2+} ions on the VLP size stability were assessed. After the monitoring of the particle size by DLS method for 4 weeks, substantial change in size (aggregation) was observed only at the end of the experiment in Tris-HCl-based buffer at 37°C. Although the purified VLPs can be regarded as fairly stable, additional investigation into their cytotoxicity and cargo encapsulation is necessary prior to applying them for nano-delivery.

[1] Wickner, R.B., *et al.* (2013). Viruses and prions of *Saccharomyces cerevisiae*. *Advances in Virus Research* 86(1).

[2] Naitow, H., *et al.* (2002). L-A virus at 3.4 Å resolution reveals particle architecture and mRNA decapping mechanism. *Nature Structural & Molecular Biology* 9, 725-728.

[3] Nooraei, S., *et al.* (2021). Virus-like particles: preparation, immunogenicity and their roles as nanovaccines and drug nanocarriers. *Journal of Nanobiotechnology* 19(1), 1-27.

[4] Chung, Y.H., *et al.* (2020). Viral nanoparticles for drug delivery, imaging, immunotherapy, and theranostic applications. *Advanced Drug Delivery Reviews* 156, 214-235.

FUNCTIONAL ANALYSIS OF CRISPR-CAS TYPE I-D SYSTEM AND WYL DOMAIN-CONTAINING PROTEIN

Gabija Naujokaitė¹, Jonas Juozapaitis¹, Arūnas Šilanskas¹, Tomas Šinkūnas¹, Virginijus Šikšnys¹, Inga Songailienė¹

¹Department of Protein - DNA Interactions, Institute of Biotechnology, Life Sciences Center, Vilnius University, Lithuania
gabija.naujokaite@chgf.stud.vu.lt

The research of arms race between viruses and bacteria resulted in many molecular tools that are now successfully used in genetic engineering. One of the most popular examples is the CRISPR-Cas system - an adaptive immunity found in bacteria and archaea. It can be easily reprogrammed to target different DNA sequences and therefore used to regulate gene expression or edit genomes [1].

The most widespread class 1 type I systems consist of multiprotein crRNA-guided effector (Cascade). It binds dsDNA target distinguished by a short sequence (PAM) only found in the foreign DNA. Once R-loop is formed the Cas3 helicase-nuclease degrades the target DNA [1]. The subtype I-D carries a type III like large subunit Cas10d which encodes a HD-nuclease domain and is considered an evolutionary intermediate between type I and type III systems [2]. This complex itself might perform the initial target nicking, while Cas3 acts as a helicase. Currently published results about type I-D CRISPR-Cas system are contradictory, one side claims the discovery PAM-dependent dsDNA and PAM-independent ssDNA cleavage [2], while the other denies the ssDNA cleavage and observes a ssRNA binding activity [3].

WYL domain-containing proteins can interact with DNA and are often described as transcription factors, but their function is not yet fully understood. Many of them are linked with antiviral defense systems and their genes are often found near CRISPR-Cas, BREX and other systems [4]. In our case, the WYL gene is in the same operon as type I-D system and could possibly regulate its transcription or cleavage activity. Therefore, we aim to determine the mechanism of type I-D CRISPR-Cas system and the possible interaction with WYL protein by utilizing *in vivo* phage and plasmid interference assays and *in vitro* DNA cleavage methods.

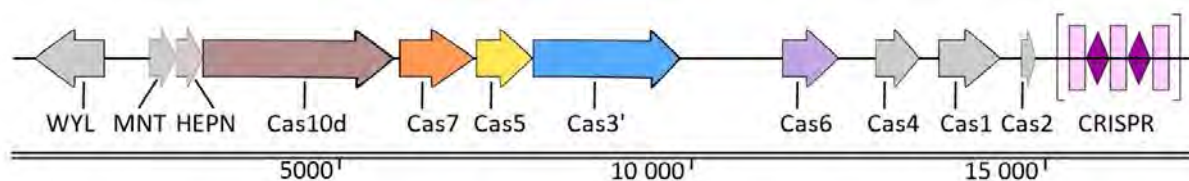


Fig. 1. *A. flos-aquae* genome operon carrying WYL and type I-D CRISPR-Cas.

- [1] T. Y. Liu and J. A. Doudna, Chemistry of Class 1 CRISPR-Cas effectors Binding, editing, and regulation, *J. Biol. Chem.*, vol. 295, no. 42, pp. 14473–14487, Oct. 2020.
- [2] J. Lin, A. Fuglsang, A. L. Kjeldsen, K. Sun, Y. Bhoobalan-Chitty, and X. Peng, DNA targeting by subtype I-D CRISPR-Cas shows type I and type III features, *Nucleic Acids Res.*, vol. 48, no. 18, pp. 10470–10478, Sep. 2020.
- [3] E. A. Schwartz et al., Structural rearrangements allow nucleic acid discrimination by type I-D Cascade, *Nat. Commun.*, vol. 13, no. 1, Art. no. 1, May 2022.
- [4] L. M. Keller and E. Weber-Ban, An emerging class of nucleic acid-sensing regulators in bacteria WYL domain-containing proteins, *Curr. Opin. Microbiol.*, vol. 74, p. 102296, Apr. 2023.

UPCONVERTING NANOPARTICLES AND PHOTSENSITIZER CHLORIN E6 COMPLEX FOR CANCER THERANOSTICS

Emilė Pečiukaiytė^{1,2}, Simona Steponkienė¹, Eglė Ežerskytė^{1,3}, Vaidas Klimkevičius^{1,3}, Vitalijus Karabanovas^{1,4}

¹Biomedical Physics Laboratory of National Cancer Institute, Baublio 3B, LT-08406, Vilnius, Lithuania

²Life Sciences Center, Vilnius University, Saulėtekio av. 7, LT-10257, Vilnius, Lithuania

³Institute of Chemistry, Faculty of Chemistry and Geosciences, Vilnius University, Naugarduko 24, LT-03225, Vilnius, Lithuania

⁴Department of Chemistry and Bioengineering, Vilnius Gediminas Technical University, Sauletekio av. 11, LT-10223, Vilnius, Lithuania
emile.peciukaiyte@nvi.lt

A growing field of biomedical studies involves employing nanoparticles (NPs) for theranostics, a combination of therapy and diagnostics. Surface modifications, enabled by diverse ligands such as phospholipids (PLs), enhance functionality, due to PLs similarity to the cell membrane. Conjugating phospholipids with polyethylene glycol (PEG) acts as a shielding mechanism, extending NPs circulation lifetime. Among therapeutic methods, photodynamic therapy (PDT) requires only three components for effectiveness: light, photosensitizer (PS), and oxygen. However, the primary challenge lies in the limited deep tissue penetration of red light, impeding the advantages of PDT [1].

Rare earth-doped upconverting nanoparticles (RENPs) excel among NPs due to narrow emission peaks, notable biocompatibility, and the conversion of near-infrared light to visible or UV light. This conversion is beneficial for enhanced tissue penetration within the biological optical transparency window (600 nm to 1200 nm). Moreover, the increased converted energy serves as an energy donor for photosensitizer (PS) excitation. Among the PS used in research, Chlorin e6 (Ce6) stands out as a clinically approved PS with a high tendency to produce reactive oxygen species and exhibit anticancer potential. In this context, the complex of RENPs and Ce6 can be used for the development of multifunctional nanopatform tailored for cancer theranostics [2].

The aim of the study was to perform NaGdF₄:Yb³⁺,Er³⁺@NaGdF₄:Yb³⁺,Nd³⁺ RENPs surface modifications with different ratios of PLs, to form PLs modified RENPs-Ce6 complexes with efficient singlet oxygen generation, and to assess surface-modified RENPs and RENPs-Ce6 accumulation in MDA-MB-231 breast cancer cells in different mediums. Spectroscopic properties, optical stability, hydrodynamic diameter, and singlet oxygen generation efficiency were determined. The obtained results revealed that PLs surface-modified RENPs retained emission peaks, remained stable in a water medium for 7 days, and exhibited hydrodynamic diameters ranging from 37 nm to 55 nm. RENPs-Ce6 complexes were formed, with the hydrodynamic diameter strongly corresponding to the presence or absence of the PEG molecule. Singlet oxygen generation results showed no effect in PLs modified RENPs, while RENPs-Ce6 complexes manifested a positive effect. However, phospholipids modification with a ratio of 2:1 excelled with the greatest outcome. Both PLs modified RENPs and RENPs-Ce6 complexes accumulated in breast cancer cells; nevertheless, the nature of accumulation was dependant on the cell culture medium.

This study was supported by the funds of Lithuania. Grant No. S-MIP-22-31 and Grant No. P-ST-23-224.

[1] Liang, G., Wang, H., Shi, H., Wang, H., Zhu, M., Jing, A., Li, J., I & Li, G. (2020). Recent progress in the development of upconversion nanomaterials in bioimaging and disease treatment. In *Journal of Nanobiotechnology* (Vol. 18, Issue 1). Springer Science and Business Media LLC.

[2] Skripka, A., Karabanovas, V., Jarockyte, G., Marin, R., Tam, V., Cerruti, M., Rotomskis, R., I & Vetrone, F. (2019). Decoupling Theranostics with Rare Earth Doped Nanoparticles. In *Advanced Functional Materials* (Vol. 29, Issue 12, p. 1807105). Wiley.

INTERACTION OF ALKYLPHOSPHOLIPIDS WITH TETHERED BILAYER LIPID MEMBRANES

Rūta Bagdonaitė¹, Artūras Polita¹

¹Institute of Biochemistry, Life Sciences Center, Vilnius University, Saulėtekio av. 7, Vilnius, LT-10257, Lithuania
ruta.bagdonaitė@bchi.stud.vu.lt

Synthetic alkylphospholipids (APLs) are stable analogs of lysophosphatidylcholine, which are being investigated as potential antitumor agents. APLs exert their activities by acting on cell membranes [1], however understanding of their interaction with lipid bilayers is still lacking. In this work we investigated three APLs differing in hydrocarbon chain length and headgroup composition – miltefosine (hexadecylphosphocholine), edelfosine (1-O-octadecyl-2-O-methyl-sn-glycero-phosphocholine) and perifosine (Octadecyl-(1,1-dimethyl-4-piperidyl) phosphate). We used tethered bilayer lipid membranes (tBLMs) formed on self-assembled monolayer modified gold surface as an artificial membrane model [2] and measured its interaction with APLs. We employed electrochemical impedance spectroscopy (EIS) to assess defect formation and fluorescence lifetime imaging microscopy (FLIM) to observe membrane structural changes through microviscosity measurements. Incubation of APLs with tBLMs composed of dopc and cholesterol induced dielectric membrane damage in a time and concentration-dependent manner, with miltefosine being less damaging compared to edelfosine and perifosine at the same concentrations. APLs' induced damage was also demonstrated to be partially reversible at moderate concentrations, reaching a point in EIS spectra after which it shifts back towards lower defect densities. FLIM measurements showed that besides defect formation APLs also induce changes in membrane organization and form mobile micron-scale cholesterol-rich domains.

[1] W.J.vanBlitterswijk, M.Verheij, AnticancerMechanismsAndClinicalApplicationOfAlkylphospholipids (Biochim. Biophys. Acta - Mol. Cell Biol. Lipids, 2013)
[2] T.Penkaukas, G.Preta, BiologicalApplicationsOfTetheredBilayerLipidMembranes (Biochimie, 2019)

CHANGES OF PHOTOSYNTHETIC PARAMETERS IN MICROALGAE INDUCED BY PHOTOOXIDATIVE STRESS

Rasa Miliukaitė¹, Agnė Kalnaitytė-Vengeliienė¹

¹Biophotonics Group of Laser Research Centre, Vilnius University, Saulėtekio ave. 9, III bld. LT-10222, Vilnius, Lithuania
rasa.miliukaite@ff.stud.vu.lt

Oxidative stress in algae could be caused by abiotic stressors, e.g. exposure to heavy metals, chemicals, light and heat stress, thus acting as nonspecific response to harmful factors. Although, because of their sensitive response algae and other photosynthetic microorganisms are used as natural indicators in environmental studies, there is still a lack of complex knowledge of whether the responses elicited by different factors would have common features. As photosynthetic activity is highly associated with physiological state of the plant, non-invasive tools, such as spectroscopy and microscopy, application *in vivo* are preferred.

In this study oxidative stress was caused by different stressors on *Desmodesmus communis* freshwater microalgae. To determine physiological responses induced by H₂O₂, white and violet light (829 μmol photons/(m²s) irradiation for 90 min and 1012 μmol photons/(m²s) for 30 min respectively), steady-state fluorescence and photosynthetic parameters measured by pulsed amplitude modulated fluorometer as well as microscopic images of algae were analysed. A ratio of autofluorescence (at 683 nm) excitation intensities at 484 nm and 435 nm (Fig. 1 a), as well as electron transport rate through PSII (Fig. 1 b) decreased immediately after algae exposure, although, depending on stressor, after 24 hours parameters tend to approach control values. Furthermore, the effects of chlorophyllin as a photosensitizer has also been studied with these algae.

Acknowledgements. This research is funded by Research Council of Lithuania, agreement No. P-ST-23-111.

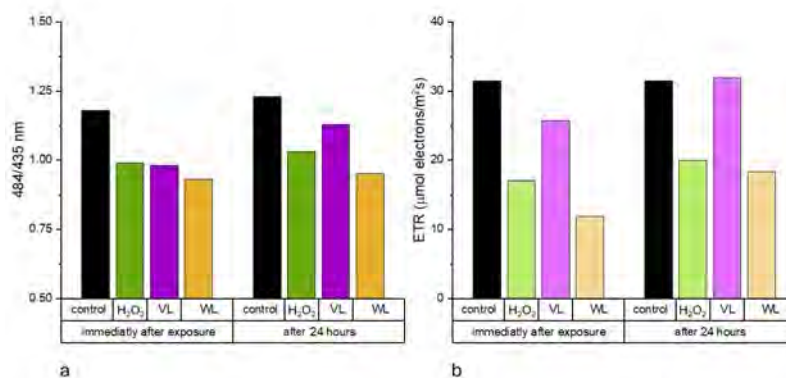


Fig. 1. The rate of excitation at 484 nm and 435 nm of autofluorescence intensities at 683 nm (a) and electron transport rate (b) of algae immediately after exposure with hydrogen peroxide (H₂O₂), violet light (VL) and white light (WL).

OPTIMAZING LINKER PEPTIDE FOR EFFECTIVE PRESENTATION OF Aga2 AND A. *baumannii* Blp1 C-TERMINAL FRAGMENT FUSION PROTEIN ON THE SURFACE OF *S. cerevisiae*

Arūnė Verbickaitė¹, Ieva Šapronytė¹, Rasa Petraitytė Burneikienė¹

¹Institute of Biotechnology, Department of Eukaryote Gene Engineering, Life Sciences Center, Vilnius University, Lithuania
arune.verbickaite@gmc.vu.lt

Yeast display (or yeast surface display), a protein engineering technique that involves the expression of recombinant proteins incorporated into the yeast cell wall, offers a versatile platform for expanding the applications of *Saccharomyces cerevisiae* in various scientific, biotechnological, and biomedical applications. This technique leverages yeast cell wall proteins to anchor target proteins onto the cell surface [1]. The yeast display technique was first published in 1997 [2], and until now, there is no data that it has been used in Lithuania. The display of proteins on yeast cell surfaces is facilitated by wall protein a-agglutinin, which mediates cell-cell contacts during yeast cell mating. A-agglutinin consists of an Aga1 subunit linked to an Aga2 subunit by two disulfide bridges. Genetic fusion of the target protein with the Aga2 subunit enables its display on the cell surface through interaction with the Aga1 subunit, which is directly anchored to the cell wall [1].

Concerning the immunostimulatory properties of the yeast wall and GRAS status, yeast surface display technology is a promising tool for developing oral vaccines [3]. In this study, we used a protein from the opportunistic bacterium *Acinetobacter baumannii* as the target antigen. The C-terminal 163 amino acid fragment of Blp1 exhibits conservation among clinically isolates, including those resistant to antibiotics, making it an ideal candidate for vaccine development [4].

In the initial phase of this study, the Aga2 subunit was linked to the C-terminal 163 amino acid fragment of Blp1 via a flexible linker composed of glycine and serine amino acids. The aim of this study was to investigate the feasibility of displaying the C-terminal 163 amino acid fragment of the Blp1 protein on the surface of *S. cerevisiae* yeast cells using different linker peptides. The Aga2 subunit was linked to the target fragment by a double extension of the original linker sequence consisting of glycine and serine amino acids, also by a single and double alpha-helix-forming sequence, and by an alpha-helix-forming sequence with serine and glycine amino acid termini. All constructed fusion proteins were successfully displayed on the surface of yeast cells. The results demonstrated that altering the linker sequence had a positive effect and increased the efficiency of the fusion protein display. Among the tested linker variants, the single alpha-helix-forming sequence exhibited the most pronounced effect, with the greatest effect on anchoring the target protein to the yeast cell surface.

-
- [1] Ueda, M., 2019. Principle of cell surface engineering of yeast. In *Yeast Cell Surface Engineering: Biological Mechanisms and Practical Applications*. Springer Singapore, pp. 3–14.
 [2] Boder, E.T., Wittrup, K.D., 1997. Yeast surface display for screening combinatorial polypeptide libraries. *Nature Biotechnology*, 15(6), pp.553–557.
 [3] Shibasaki, S., Ueda, M., 2023. Progress of Molecular Display Technology Using *Saccharomyces cerevisiae* to Achieve Sustainable Development Goals. *Microorganisms* 2023, Vol. 11, Page 125, 11(1), p.125
 [4] Skemiškytė, J., Karazijaitė, E., Deschamps, J., Krasauskas, R., Armalytė, J., Briandė, R., Sužiedėlienė, E., 2019. Blp1 protein shows virulence-associated features and elicits protective immunity to *Acinetobacter baumannii* infection. *BMC Microbiology*, 19(1), pp.1–12.

ANTIOXIDANT PROPERTIES OF THE SOLID DISPERSION SYSTEM OF HESPERIDIN OBTAINED BY THE CENTRIFUGAL FIBER FORMATION METHOD

Vadym Lisovyi^{1,2}, Viktoriia Lyzhniuk¹, Volodymyr Bessarabov¹, Andriy Goy¹, Galina Kuzmina¹, Olga Kovalevska¹

¹Department of Industrial Pharmacy, Kyiv National University of Technologies and Design, Ukraine

²Department of Chemical Technology and Resource Saving, Kyiv National University of Technologies and Design, Ukraine
v.lisovyi@kyivpharma.eu

In recent years, there has been increasing evidence that oxidative stress plays a key role in the pathophysiology of many diseases, including neurodegenerative disorders, inflammation, atherosclerosis and even cancer. The current pharmacotherapy for oxidative stress and related diseases involves the use of antioxidants. Phenolic compounds, particularly bioflavonoids, represent one of the largest classes of antioxidants. Among the many members of this class of biologically active substances, a well-known representative is hesperidin. However, the use of this bioflavonoid is limited by its low solubility. A promising approach for improving the solubility of many poorly water-soluble bioflavonoids, particularly hesperidin, is the formation of solid dispersed systems (SDS). This confirms the prospect of developing solid dispersions of hesperidin and studying their antioxidant properties.

The present study examines the influence of a polymer solid dispersion system based on hesperidin on the lipids peroxidation process. An innovative technology of centrifugal fiber formation was used to prepare a solid dispersion system of hesperidin. Polyvinylpyrrolidone K-17 (PVP K-17) was chosen as the polymer carrier for the preparation of SDS.

The influence of the polymeric SDS of hesperidin on the process of lipid peroxidation was studied using a standard determination with thiobarbituric acid (TBA). The method is indirect and is based on the ability of TBA to react with malondialdehyde (MDA), an intermediate product of the enzymatic oxidation of arachidonic acid and the final product of lipid oxidative degradation. The result of the reaction is a trimethine complex which has a characteristic absorption spectrum with a maximum at a wavelength of 535 nm [1].

As a result of the conducted research, it was established that the addition SDS of hesperidin, to the model biological system, leads to a decrease in the amount of the formed trimethine complex. Accordingly, the number of products of lipid peroxidation significantly decreases. The number of products of lipid peroxidation when adding SDS hesperidin at a concentration of 25 μM decreases by 1.4 times, at a concentration of 50 μM – by 2.1 times, and at a concentration of 100 μM – by 3.6 times ($C_{(0)} = 14.73 \pm 0.43 \text{ mM}$; $C_{(25)} = 10.84 \pm 0.43 \text{ mM}$; $C_{(50)} = 6.89 \pm 0.11 \text{ mM}$; $C_{(100)} = 4.14 \pm 0.33 \text{ mM}$).

Thus, it has been confirmed that hesperidin in the composition of a solid dispersion system with PVP K-17, obtained by the method of centrifugal fiber formation, effectively inhibits the process of oxidative destruction of lipids in a dose-dependent manner. Therefore, the studied polymeric SDS of hesperidin can potentially be used as an active pharmaceutical ingredient for the production of medicinal products with antioxidant effect.

[1] J. Aguilar Diaz De Leon, C. R. Borges. Evaluation of Oxidative Stress in Biological Samples Using the Thiobarbituric Acid Reactive Substances Assay. Journal of visualized experiments : JoVE, (159), 10.3791/61122 (2020). <https://doi.org/10.3791/61122>

ACTIVATION AND REGULATION OF THE TYPE-III CRISPR-CAS ASSOCIATED SIGNALING CASCADE

Dalia Smalakyte¹, Audrone Ruksenaite¹, Giedrius Sasnauskas¹, Giedre Tamulaitiene¹, Gintautas Tamulaitis¹

¹Institute of Biotechnology, Life Sciences Center, Vilnius University, Lithuania
dalia.smalakyte@bti.vu.lt

Prokaryotes employ various defense mechanisms to protect themselves against foreign nucleic acids, including viruses. Several of these mechanisms rely on a signaling pathway that uses cyclic nucleotide derivatives to activate specific effectors. Examples of such defense systems include CBASS [1], Thoeris [2], Pycsar [3], and the type III CRISPR-Cas system [4]. In the latter, upon detecting viral RNA, the interference complex generates cyclic oligoadenylates (cA_n), which activate effector proteins through a sensory CARF or SAVED domain [5]. To date, predominantly single-protein CARF effectors have been characterized [6]. However, the existence of type III CRISPR-Cas-associated multi-component effector systems that can function as CRISPR-activated signaling cascades has been proposed [7-9].

This study focuses on the type III-A CRISPR-Cas-associated tripartite CalpL-CalpT-CalpS effector system from *Candidatus Cloacimonas acidaminovorans* strain Evry. CalpS, which functions as an ECF-like sigma-factor, forms a stable heterodimer with its anti-sigma factor CalpT. When activated by cA₄, the SAVED-Lon protease fusion protein CalpL specifically cleaves CalpT, releasing CalpS for gene expression regulation. In this study, we used structural and biochemical assays and experiments in *E. coli* to elucidate the molecular mechanism of the activation and regulation of the CRISPR-Cas-activated CalpL-CalpT-CalpS signaling cascade.

-
- [1] Slavik KM, Kranzusch PJ. CBASS to cGAS-STING: the origins and mechanisms of nucleotide second messenger immune signaling. *Annual Review of Virology*. 2023 Sep 29;10:423-53.
- [2] Ofir G, Herbst E, Baroz M, Cohen D, Millman A, Doron S, Tal N, Malheiro DB, Malitsky S, Amitai G, Sorek R. Antiviral activity of bacterial TIR domains via immune signalling molecules. *Nature*. 2021 Dec 2;600(7887):116-20.
- [3] Tal N, Morehouse BR, Millman A, Stokar-Avihail A, Avraham C, Fedorenko T, Yirmiya E, Herbst E, Brandis A, Mehlman T, Oppenheimer-Shaanan Y. Cyclic CMP and cyclic UMP mediate bacterial immunity against phages. *Cell*. 2021 Nov 11;184(23):5728-39.
- [4] Kazlauskienė M, Kostiuik G, Venclovas Č, Tamulaitis G, Siksnys V (2017) A cyclic oligonucleotide signaling pathway in type III CRISPR-Cas systems. *Science*, 357(6351), 605-609.
- [5] Makarova KS, Timinskas A, Wolf YI, Gussow AB, Siksnys V, Venclovas Č, Koonin EV. Evolutionary and functional classification of the CARF domain superfamily, key sensors in prokaryotic antiviral defense. *Nucleic acids research*. 2020 Sep 18;48(16):8828-47.
- [6] Stella G, Marraffini L. Type III CRISPR-Cas: beyond the Cas10 effector complex. *Trends in Biochemical Sciences*. 2023 Nov 8.
- [7] Rouillon C, Schneberger N, Chi H, Blumenstock K, Da Vela S, Ackermann K, Moecking J, Peter MF, Boenigk W, Seifert R, Bode BE. Antiviral signalling by a cyclic nucleotide activated CRISPR protease. *Nature*. 2023 Feb 2;614(7946):168-74.
- [8] Strecker J, Demircioglu FE, Li D, Faure G, Wilkinson ME, Gootenberg JS, Abudayyeh OO, Nishimasu H, Macrae RK, Zhang F. RNA-activated protein cleavage with a CRISPR-associated endopeptidase. *Science*. 2022 Nov 25;378(6622):874-81.
- [9] Altae-Tran H, Kannan S, Suberski AJ, Mears KS, Demircioglu FE, Moeller L, Kocalar S, Oshiro R, Makarova KS, Macrae RK, Koonin EV., Zhang F. Uncovering the functional diversity of rare CRISPR-Cas systems with deep terascale clustering. *Science*. 2023 Nov 24;382(6673):ead11910.

FTDMP: A FRAMEWORK FOR PROTEIN-PROTEIN, PROTEIN-DNA AND PROTEIN-RNA DOCKING AND SCORING

Rita Banciul¹, Kliment Olechnovič^{1,2}, Justas Dapkūnas¹, Česlovas Venclovas¹

¹Institute of Biotechnology, Life Sciences Center, Vilnius University

²CNRS Laboratoire Jean Kuntzmann, Grenoble

rita.banciul@gmc.vu.lt

Knowledge of the 3D structure of protein-protein and protein-nucleic acid complexes is crucial for understanding the molecular mechanisms that govern essential cellular processes. Experimental methods such as X-ray crystallography, NMR, and CryoEM provide high-quality structures, but are expensive and time consuming. Thus, there is a need for computational structure prediction. While the AI-based method AlphaFold has revolutionized single chain protein structure prediction, challenges remain, particularly in modeling antibody-antigen interactions, protein-nucleic acid complexes, and proteins lacking close homologs. In these cases, docking can be employed to generate structure models. As a result, effective methods for selection of the most accurate models are necessary.

Here we present FTDMP, a newly developed framework for protein-protein and protein-nucleic acid docking and scoring. The framework can be used in two ways: to perform docking and subsequent scoring, or to evaluate and rank user provided models coming from various sources (AlphaFold, RoseTTAFold, docking, etc.). The full FTDMP docking and scoring framework was tested on protein-protein, protein-DNA, and protein-RNA docking benchmarks [1-3]. Compared to currently available docking systems, FTDMP demonstrated improved results of the free unbound-unbound docking when the top-ranked model was considered, and very high rates for bound-bound docking (up to 83% for the top prediction). The ranking in FTDMP is done by a newly developed method, VorolF-jury [4]. The protocol based on this method obtained top results in the community-wide CASP15-CAPRI scoring experiment [5]. FTDMP can be used not only with the built-in, but also with external scoring methods. Thus, the framework can be employed for fast and straightforward evaluation of new scoring functions.

FTDMP, docking benchmarks and docking results are available at <https://github.com/kliment-olechnovic/ftdmp>.

[1] van Dijk, M., Bonvin, A.M. (2008). A protein-DNA docking benchmark. *Nucleic Acids Res*, 36, e88.

[2] Guest, J. D., et al. (2021). An expanded benchmark for antibody-antigen docking and affinity prediction reveals insights into antibody recognition determinants. *Structure*, 29(6), 606-621.e5.

[3] Zheng, J., et al. (2020). P3DOCK: a protein-RNA docking webserver based on template-based and template-free docking. *Bioinformatics*, 36(1), 96-103.

[4] Olechnovič, K., et al. (2023). Prediction of protein assemblies by structure sampling followed by interface-focused scoring. *Proteins*, 91(12), 1724-1733.

[5] Lensink, M.F., et al. (2023). Impact of AlphaFold on structure prediction of protein complexes: The CASP15-CAPRI experiment. *Proteins*, 91(12), 1658-1683.

The ASCH domain-containing protein from *Thermus thermophilus* acts as a tRNA deacetylase

Greta Gakaite¹, R Statkevičiūtė¹, R Meškys¹

¹Department of Molecular Microbiology and Biotechnology, Institute of Biochemistry, Life Science Centre, Vilnius University, Vilnius, Lithuania
greta.gakaite@chgf.stud.vu.lt

Proteins containing the ASC-1 homology (ASCH) domain are present in all domains of life, including several prokaryotic viruses. It is suggested that these 103–120 amino acid long domains could have functions in transcription co-activation, RNA metabolism, and translation regulation in prokaryotes. However, despite their high abundance in nature, most proteins of the ASCH superfamily are considered hypothetical due to a lack of experimental data. One of the well-characterized proteins containing the ASCH domain is an amidohydrolase YqfB from *Escherichia coli*. The primary substrate of YqfB is the modified nucleoside N4-acetylcytidine (ac4C), which is highly abundant in both eukaryotic and prokaryotic RNA molecules. Recently, we identified a novel RNA-binding ASCH domain-containing protein TthASCH from the thermophilic bacterium *Thermus thermophilus*, which was shown to be active towards ac4C *in vitro*. This study aimed to investigate the catalytic mechanism of enzymatic ac4C hydrolysis and to confirm whether TthASCH can act as an eraser of the ac4C modification of tRNA. To reveal the amino acids that may be crucial for its catalytic activity of TthASCH, we purified 13 mutants of TthASCH and determined their amidohydrolase activity towards ac4C by using thin-layer chromatography. The results suggested a catalytic dyad (Lys-Glu) and Arg acting as an oxyanion hole, hence, TthASCH forms an active center different compared to YqfB. Furthermore, we present experimental evidence that the synthesis of TthASCH in *E. coli* leads to decreased ac4C levels in tRNA molecules. This study expands the knowledge of the possible functional diversity of proteins belonging to the ASCH superfamily, as no tRNA ac4C erasers have been reported to date.

QUANTITATIVE AND QUALITATIVE ANALYSIS OF MONOTERPENES AND SESQUITERPENES IN INDUSTRIAL HEMP BIOMASS

Algimanta Kundrotaitė¹, Karolina Barčauskaitė¹

¹Lithuanian Research Centre for Agriculture and Forestry
algimanta.kundrotaite@gmail.com

Fibrous hemp essential oil is a complex mixture of many volatile organic compounds (VOCs). The main chemical components of essential oils are compounds belonging to monoterpenes and sesquiterpenes: myrcene, beta-caryophyllene, limonene, alpha-pinene, beta-pinene, alpha-humulene. Monoterpenes have antifungal, antibacterial, antiviral, antioxidant, anticancer, anti-inflammatory effects. Sesquiterpenes have anti-carcinogenic, anti-inflammatory, antiseptic and oxidative stress-reducing effects. VOCs can act both as direct inhibitors of bacterial growth by activating defense signaling pathways and thus making plants more resistant to pathogens, and as repellents that reduce the number of herbivores, especially insects and larvae. In order to implement the European Green Course strategy and achieve the goal of reducing the use of chemical plant protection products by 50 percent by 2030, it is necessary to look for alternative measures that ensure plant health and to study the chemical composition of plant essential oils, as it is believed that the organic compounds found in plant essential oils can at least partially replace synthetic pesticides, which would reduce the use of chemical plant protection products.

In this study fibrous hemp essential oils were obtained by hydrodistillation method. Above Ground industrial hemp biomass excluding stems was collected, air-dried, homogenized and used to recover mono and sesquiterpenes. Different amounts of dried plant material (1, 2, 3, 4 and 5 grams) were hydrodistilled for different time periods (5, 10, 20, 30, 60, 90 and 120 minutes). Essential oils were examined using gas chromatography – mass spectrometry system.

Results show that most of the detected terpenes belonged to sesquiterpenes and quantity and quality varied depending on the amount of material and extraction time.

Acknowledgement: The performed study received financial support from the Research Council of Lithuania project No. P-ST-23-374.

[1] Picazo-Aragonés, J., et al. 2020. Plant Volatile Organic Compounds Evolution: Transcriptional Regulation, Epigenetics and Polyploidy. *International Journal of Molecular Sciences*. 21(23): 8956.

MECHANISM OF CRISPR-CAS3 HELICASE USING MAGNETIC TWEEZERS

Miglė Šarpilo^{1,2}, Algirdas Toleikis^{1,2}

¹Vilnius University

²Institute of Biotechnology

migle.sarpilo@gmc.vu.lt

CRISPR-Cas provides RNA-guided adaptive immunity against invading genetic elements. CRISPR systems consist of multiple Cas proteins responsible for CRISPR-dependent cell immunity mechanisms. The effector complex in CRISPR I-E consists of Cascade and Cas3. Cascade is responsible for foreign DNA targeting. Meanwhile, Cas3, which possesses helicase and nuclease activity, is a key system protein, necessary for crRNA-guided interference of virus proliferation. Although single-component Class 2 CRISPR systems, such as type II Cas9 are widely used for genome editing, the research on multi-component Class 1 proteins of the same system has been less developed. Components of the I-E CRISPR system have already been used as a genome-editing tool to generate big deletions. However, the detailed mechanism by which Cas3 achieves its function is not well understood. This study aims to elucidate the mechanism of Cas3 unwinding. We are using single-molecule force microscopy, namely, magnetic tweezers, to probe the mechanical aspects of Cas3 unwinding activity. Greater knowledge of the Cas3 mechanism of action would improve the application of Cas3 as a tool for genome editing.

ANALYSIS OF FLUORESCENCE SPECTRA OF COPPER CHLOROPHYLLIN SOLUTIONS

Laura Kaziūnaitė¹, Irina Buchovec²

¹Institute of Biosciences, Life Sciences Center, Vilnius University, Saulėtekis ave. 7, LT-10257, Vilnius, Lithuania.

²Institute of Photonics and Nanotechnology, Faculty of Physics, Vilnius University, Saulėtekis ave. 3, LT-10257, Vilnius, Lithuania.

laura.kaziunaite@gmc.stud.vu.lt

Antimicrobial photodynamic inactivation (API) is a modern biophotonic technology that can fight a wide range of microorganisms. API requires three components: molecular oxygen, a photosensitizer (PS), and light with a wavelength in the absorption region of the PS. The interaction between PS and light in an oxygenated environment leads to photo-oxidative reactions, the formation of reactive oxygen species, and damage to bacterial cells. This versatile mechanism of action makes API a very widely used technique [1].

The antibacterial efficacy of API depends on the photophysical properties of the PS chosen. Desirable properties of PS include water solubility, photostability, minimal aggregation tendency, and a broad spectrum of antimicrobial activity at relatively low PS concentrations and light doses.

Chlorophyllin molecules are macrocyclic organic tetrapyrrole compounds in the class of porphyrins that exhibit large optical nonlinearities, making them a great candidate to be applied as PSs for API. It is known that porphyrins can form aggregates in aqueous media and that aggregation can affect physical properties such as fluorescence emission [2]. One method to determine the formation of aggregates in solution is the use of the aggregate-degrading agent Triton X-100. The main goal of this study is to investigate the physical properties of Cu-Chl by measuring its excitation and emission spectra.

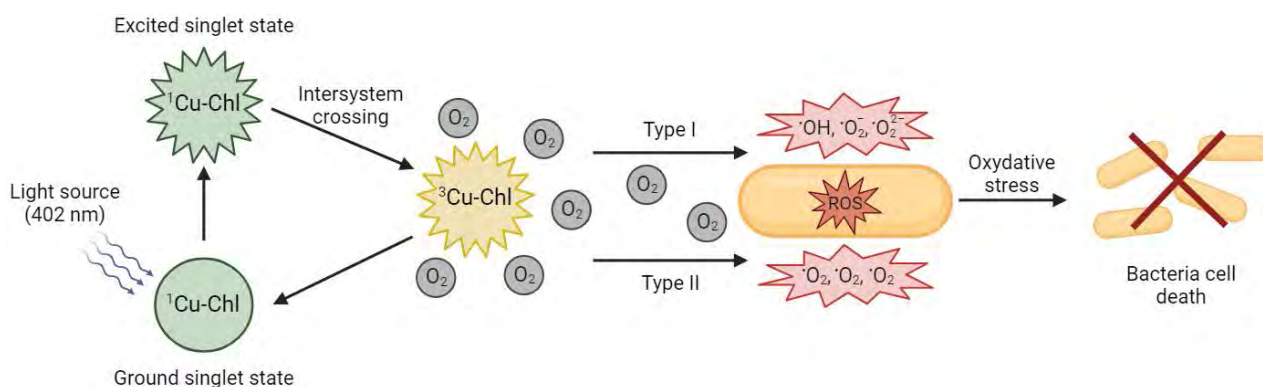


Fig. 1. Mechanism of API

In order to assess the intensity, shape and lifetime of the Cu-Chl fluorescence spectra, measurements of the fluorescence emission and excitation spectra of different concentrations of Cu-Chl in distilled water and phosphate-buffered saline (PBS) were performed. The excitation spectra of both solutions showed a maximum at 402 nm. Therefore, 402 nm was chosen as the excitation maximum for Cu-Chl emission. From the results of the fluorescence emission spectra, the fluorescence of Cu-Chl in PBS buffer is more intense than in distilled water. On the other hand, the addition of the monomeriser Triton X-100 resulted in higher fluorescence.

The prospect of this research involves further investigating the properties of Cu-Chl and antimicrobial effectiveness against plant pathogens.

[1] Buchovec, I. et al. *International Journal of Molecular Sciences*, 2020, 21(18), p. 6932. DOI: 10.3390/ijms21186932.

[2] Karolczak, J. et al. *The Journal of Physical Chemistry A*, 2004, 108(21), p. 4570-4575. DOI: 10.1021/jp049898v.

PHOTOSENSITIZER TPPS₄ AGGREGATION AND AGGREGATE TYPE SPECTROSCOPIC STUDIES IN NEUTRAL AND HIGHLY ACIDIC PH ENVIRONMENTS

Greta Tamoliūnaitė^{1,2}, Vilius Poderys¹, Ričardas Rotomskis^{1,3}

¹Biomedical Physics Laboratory of National Cancer Institute, Vilnius, Lithuania

²Faculty of Chemistry and Geosciences, Vilnius University, Vilnius, Lithuania

³Faculty of Physics, Vilnius University, Vilnius, Lithuania

greta.tamoliunaite@chgf.stud.vu.lt

Cancer development in patients is at an utmost high. A progressive cancer treatment is photodynamic therapy (PDT), that utilizes photosensitizer, light and molecular oxygen to initiate selective cancer cells death by singlet oxygen, produced by the long lived triplet state of the photosensitizer.

The absorption spectra changes of 5,10,15,20-Tetrakis(4-sulfonatophenyl)porphyrin (TPPS₄), a photosensitizer proposed for PDT, were measured with Varian Cary 50 spectrophotometer in spectral region 350 nm - 750 nm, in deionized water at different pH (achieved by adding into the aqueous solution HCl (1M) and NaOH(1M)) and different concentrations ($1 \times 10^{-2} \text{M}$ - $1 \times 10^{-6} \text{M}$). It is well known that in acidic environment TPPS₄ molecules can form J-aggregates, that exhibit characteristic absorption bands at 490 nm and 709 nm. These aggregates are formed because negatively charged SO₃⁻ group interacts with the positively charged core of protonated porphyrin ring [1]. At neutral pH, the TPPS₄ core is neutral, therefore J-aggregates are unable to form, but spectral changes were detected at high TPPS₄ concentrations. A significant Red-shift of Q₁ and Q₄ absorption bands and the intensity redistribution of central Q₂ and Q₃ bands show a new type of aggregate, possibly face-to-face, formation.

At very acidic pH=-1 all SO₃⁻ are protonated, therefore there are no electrostatic interactions of the positively charged core of porphyrin ring and neutral SO₃⁻, but, with increasing TPPS₄ concentration, absorption spectrum changes were detected, which are slightly similar to J-aggregate formation. Our studies have shown that, regardless of the pH of the solution, TPPS₄ form aggregates at high concentrations, that are characterized by a lower quantum efficiency of singlet oxygen generation, therefore it is necessary to control the concentration of TPPS-based photodrugs, injected into the patient, because a too high dose of a photosensitizer can lead to aggregation and, as a result, the decrease in singlet oxygen generation, which will determine the lower efficiency of PDT.

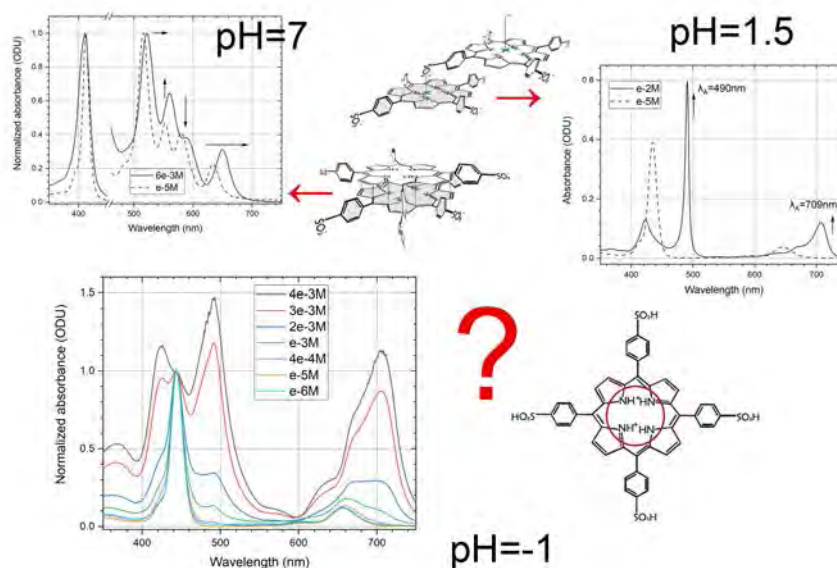


Fig. 1. TPPS₄ aggregation and aggregate types in different pH environments.

[1] Rotomskis R, Augulis R, Snitka V, Valiokas R, Liedberg B, Hierarchical Structure of TPPS₄ J-Aggregates on Substrate Revealed by Atomic Force Microscopy, J. Phys. Chem. B 2004 108(9), 2833-2838. DOI: 10.1021/jp036128v

MAMMALIAN CELLS ELECTROPORATION IN THE MICROFLUIDIC CHIP

Agne Damarackaite^{1,2}, Neringa Bakute¹, Arunas Stirke¹

¹Center for Physical Science and Technology, Department of Functional Materials and Electronics, Sauletekio av. 3, LT-10257 Vilnius

²Life Sciences Center, Vilnius University, Sauletekio av. 7, LT-10257 Vilnius
neringa.bakute@ftmc.lt

Electroporation is a technique to increase cell permeability by applying pulsed electric field (PEF) on cells. Electroporation is typically performed using commercially available cuvettes, nevertheless, it can also be performed at the microscale using a microfluidic chip. In this way, cells are exposed to more uniform electric field, favorable chemical environment, heat dissipates faster [1]. Microfluidic chips are usually fabricated using soft-lithography technique with polydimethylsiloxane (PDMS) as a polymer. Though PDMS is biocompatible and has good optical transparency, its main disadvantages are small molecule adsorption and susceptibility to mechanical stress [2]. Off-stoichiometry thiol-ene (OSTE) can be used as an alternative polymer in microchip fabrication overcoming those disadvantages and retaining the advantages of PDMS [3].

Our laboratory has fabricated the OSTE-based microfluidic chip (Fig. 1). Our goal is to test if the microchip is suitable for mammalian cells electroporation. We performed stop-flow and continuous flow electroporation of rat glioma C6 cell line in the microchip. Cell permeability and viability were evaluated using fluorescent spectrophotometry with DAPI and trypan blue test, respectively. Stop-flow electroporation showed an increase of cell permeability to DAPI with increasing electric field from 1.8 kV/cm to 10 kV/cm with 8 pulses, meanwhile with 16 pulses cell permeability has reached the maximum at 1.8 kV/cm. (Fig. 2 (a)). The viability was not influenced with 8 pulses at all tested electric field strengths. In continuous flow electroporation at 1.8 kV/cm, the same permeability increase was reached with 64 and 128 pulses per cell (Fig. 2 (b)). To conclude, the fabricated microchip is suitable for the PEF treatment of mammalian cells.

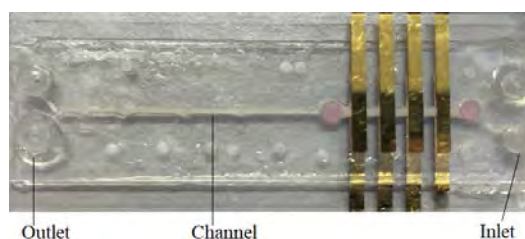


Fig. 1. Microfluidic chip for cell electroporation.

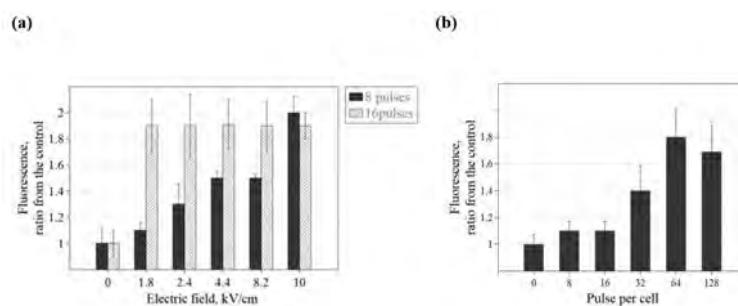


Fig. 2. Permeability to DAPI after (a) stop-flow electroporation with different electric fields, 8 or 16 pulses, and (b) continuous flow electroporation with the electric field of 1.8 kV/cm. In (a) and (b) electroporation is performed with 100 μ s pulse length and 1 Hz frequency. Fluorescence is expressed as ratio from the non-electroporated control. Error bars show standard deviation.

- [1] Campelo, S.N. et al. (2023) 'Recent advancements in electroporation technologies: From bench to Clinic', Annual Review of Biomedical Engineering, 25(1), pp. 77–100. doi:10.1146/annurev-bioeng-110220-023800.
- [2] Wong, I. and Ho, C.-M. (2009) 'Surface molecular property modifications for Poly(dimethylsiloxane) (PDMS) based microfluidic devices', Microfluidics and Nanofluidics, 7(3). doi:10.1007/s10404-009-0443-4.
- [3] Carlborg, C.F. et al. (2011) 'Beyond PDMS: Off-stoichiometry thiol-ENE (OSTE) based soft lithography for rapid prototyping of microfluidic devices', Lab on a Chip, 11(18), p. 3136. doi:10.1039/c1lc20388f.

ORGANIZERS



Faculty of
Physics



CENTER
FOR PHYSICAL SCIENCES
AND TECHNOLOGY

OPTICA
Advancing Optics and Photonics Worldwide

STUDENT CHAPTER
VILNIUS UNIVERSITY

SPIE. STUDENT
CHAPTER
VILNIUS
UNIVERSITY



SPONSORS



EVENT FRIEND



MEDIA PARTNER

